

VOL. 471 JUNE 2, 1989
COMPLETE IN ONE ISSUE

R. P. W. Scott Honour Volume

OF

CHROMATOGRAPHY

INTERNATIONAL JOURNAL ON CHROMATOGRAPHY, ELECTROPHORESIS AND RELATED METHODS

EDITORS

R. W. Giese (Boston, MA)
J. K. Haken (Kensington, N.S.W.)
K. Macek (Prague)
L. R. Snyder (Orinda, CA)

EDITOR, SYMPOSIUM VOLUMES, E. Heftmann (Orinda, CA)

EDITORIAL BOARD

D. W. Armstrong (Rolla, MO)
W. A. Aue (Halifax)
P. Boček (Brno)
A. A. Boulton (Saskatoon)
P. W. Carr (Minneapolis, MN)
N. H. C. Cooke (San Ramon, CA)
V. A. Davankov (Moscow)
Z. Deyl (Prague)
S. Dilli (Kensington, N.S.W.)
H. Engelhardt (Saarbrücken)
F. Erni (Basle)
M. B. Evans (Hatfield)
J. L. Glajch (N. Billerica, MA)
G. A. Guiochon (Knoxville, TN)
P. R. Haddad (Kensington, N.S.W.)
I. M. Hais (Hradec Králové)
W. S. Hancock (San Francisco, CA)
S. Hjerten (Uppsala)
Cs. Horváth (New Haven, CT)
J. F. K. Huber (Vienna)
K.-P. Hupe (Waldbrunn)
T. W. Hutchens (Houston, TX)
J. Janák (Brno)
P. Jandera (Pardubice)
B. L. Karger (Boston, MA)
E. sz. Kováts (Lausanne)
A. J. P. Martin (Cambridge)
L. W. McLaughlin (Chestnut Hill, MA)
R. P. Patience (Sunbury-on-Thames)
J. D. Pearson (Kalamazoo, MI)
H. Poppe (Amsterdam)
F. E. Regnier (West Lafayette, IN)
P. G. Righetti (Milan)
P. Schöenmakers (Eindhoven)
G. Schonburg (Mülheim/Ruhr)
P. Schwarzenbach (Dübendorf)
R. E. Shoup (West Lafayette, IN)
A. M. Sioffi (Marseille)
D. J. Snydon (Boston, MA)
K. K. Unger (Mainz)
J. T. Watson (East Lansing, MI)
B. D. Westerland (Uppsala)

EDITORS, BIBLIOGRAPHY SECTION

Z. Deyl (Prague), J. Janák (Brno), V. Schwarz (Prague), K. Macek (Prague)

ELSEVIER

JOURNAL OF CHROMATOGRAPHY

Scope. The *Journal of Chromatography* publishes papers on all aspects of chromatography, electrophoresis and related methods. Contributions consist mainly of research papers dealing with chromatographic theory, instrumental development and their applications. The section *Biomedical Applications*, which is under separate editorship, deals with the following aspects: developments in and applications of chromatographic and electrophoretic techniques related to clinical diagnosis or alterations during medical treatment; screening and profiling of body fluids or tissues with special reference to metabolic disorders; results from basic medical research with direct consequences in clinical practice; drug level monitoring and pharmacokinetic studies; clinical toxicology; analytical studies in occupational medicine.

Submission of Papers. Papers in English, French and German may be submitted, in three copies. Manuscripts should be submitted to: The Editor of *Journal of Chromatography*, P.O. Box 681, 1000 AR Amsterdam, The Netherlands, or to: The Editor of *Journal of Chromatography, Biomedical Applications*, P.O. Box 681, 1000 AR Amsterdam, The Netherlands. Review articles are invited or proposed by letter to the Editors. An outline of the proposed review should first be forwarded to the Editors for preliminary discussion prior to preparation. Submission of an article is understood to imply that the article is original and unpublished and is not being considered for publication elsewhere. For copyright regulations, see below.

Subscription Orders. Subscription orders should be sent to: Elsevier Science Publishers B.V., P.O. Box 211, 1000 AE Amsterdam, The Netherlands, Tel. 5803 911, Telex 18582 ESPA NL. The *Journal of Chromatography* and the *Biomedical Applications* section can be subscribed to separately.

Publication. The *Journal of Chromatography* (incl. *Biomedical Applications*) has 37 volumes in 1989. The subscription prices for 1989 are:

J. Chromatogr. + Biomed. Appl. (Vols. 461–497):

Dfl. 6475.00 plus Dfl. 999.00 (p.p.h.) (total ca. US\$ 3737.00)

J. Chromatogr. only (Vols. 461–486):

Dfl. 5200.00 plus Dfl. 702.00 (p.p.h.) (total ca. US\$ 2951.00)

Biomed. Appl. only (Vols. 487–497):

Dfl. 2200.00 plus Dfl. 297.00 (p.p.h.) (total ca. US\$ 1248.50).

Our p.p.h. (postage, package and handling) charge includes surface delivery of all issues, except to subscribers in Argentina, Australia, Brasil, Canada, China, Hong Kong, India, Israel, Malaysia, Mexico, New Zealand, Pakistan, Singapore, South Africa, South Korea, Taiwan, Thailand and the U.S.A. who receive all issues by air delivery (S.A.L. — Surface Air Lifted) at no extra cost. For Japan, air delivery requires 50% additional charge; for all other countries airmail and S.A.L. charges are available upon request. Back volumes of the *Journal of Chromatography* (Vols. 1–460) are available at Dfl. 195.00 (plus postage). Claims for missing issues will be honoured, free of charge, within three months after publication of the issue. Customers in the U.S.A. and Canada wishing information on this and other Elsevier journals, please contact Journal Information Center, Elsevier Science Publishing Co. Inc., 655 Avenue of the Americas, New York, NY 10010. Tel. (212) 633-3750.

Abstracts/Contents Lists published in Analytical Abstracts, ASCA, Biochemical Abstracts, Biological Abstracts, Chemical Abstracts, Chemical Titles, Chromatography Abstracts, Current Contents/Physical, Chemical & Earth Sciences, Current Contents/Life Sciences, Deep-Sea Research/Part B: Oceanographic Literature Review, Excerpta Medica, Index Medicus, Mass Spectrometry Bulletin, PASCAL-CNRS, Referativnyi Zhurnal and Science Citation Index.

See inside back cover for Publication Schedule, Information for Authors and information on Advertisements.

© ELSEVIER SCIENCE PUBLISHERS B.V. — 1989

0378-4347/89/\$03.50

All rights reserved. No part of this publication may be reproduced, stored in a retrieval system or transmitted in any form or by any means, electronic, mechanical, photocopying, recording or otherwise, without the prior written permission of the publisher, Elsevier Science Publishers B.V., P.O. Box 330, 1000 AH Amsterdam, The Netherlands.

Upon acceptance of an article by the journal, the author(s) will be asked to transfer copyright of the article to the publisher. The transfer will ensure the widest possible dissemination of information.

Submission of an article for publication entails the authors' irrevocable and exclusive authorization of the publisher to collect any sums or considerations for copying or reproduction payable by third parties (as mentioned in article 17 paragraph 2 of the Dutch Copyright Act of 1912 and the Royal Decree of June 20, 1974 (S. 351) pursuant to article 16 b of the Dutch Copyright Act of 1912) and/or to act in or out of Court in connection therewith.

Special regulations for readers in the U.S.A. This journal has been registered with the Copyright Clearance Center, Inc. Consent is given for copying of articles for personal or internal use, or for the personal use of specific clients. This consent is given on the condition that the copier pays through the Center the per-copy fee stated in the code on the first page of each article for copying beyond that permitted by Sections 107 or 108 of the U.S. Copyright Law. The appropriate fee should be forwarded with a copy of the first page of the article to the Copyright Clearance Center, Inc., 27 Congress Street, Salem, MA 01970, U.S.A. If no code appears in an article, the author has not given broad consent to copy and permission to copy must be obtained directly from the author. All articles published prior to 1980 may be copied for a per-copy fee of US\$ 2.25, also payable through the Center. This consent does not extend to other kinds of copying, such as for general distribution, resale, advertising and promotion purposes, or for creating new collective works. Special written permission must be obtained from the publisher for such copying.

No responsibility is assumed by the Publisher for any injury and/or damage to persons or property as a matter of products liability, negligence or otherwise, or from any use or operation of any methods, products, instructions or ideas contained in the materials herein. Because of rapid advances in the medical sciences, the Publisher recommends that independent verification of diagnoses and drug dosages should be made. Although all advertising material is expected to conform to ethical (medical) standards, inclusion in this publication does not constitute a guarantee or endorsement of the quality or value of such product or of the claims made of it by its manufacturer.

This issue is printed on acid-free paper

Printed in The Netherlands

For contents see p. VII

JOURNAL OF CHROMATOGRAPHY

VOL. 471 (1989)

JOURNAL *of* CHROMATOGRAPHY

INTERNATIONAL JOURNAL ON CHROMATOGRAPHY,
ELECTROPHORESIS AND RELATED METHODS

EDITORS

R. W. GIESE (Boston, MA), J. K. HAKEN (Kensington, N.S.W.), K. MACEK (Prague),
L. R. SNYDER (Orinda, CA)

EDITOR, SYMPOSIUM VOLUMES

E. HEFTMANN (Orinda, CA)

EDITORIAL BOARD

D. W. Armstrong (Rolla, MO), W. A. Aue (Halifax), P. Boček (Brno), A. A. Boulton (Saskatoon), P. W. Carr (Minneapolis, MN), N. H. C. Cooke (San Ramon, CA), V. A. Davankov (Moscow), Z. Deyl (Prague), S. Dilli (Kensington, N.S.W.), H. Engelhardt (Saarbrücken), F. Erni (Basle), M. B. Evans (Hatfield), J. L. Glajch (N. Billerica, MA), G. A. Guiochon (Knoxville, TN), P. R. Haddad (Kensington, N.S.W.), I. M. Hais (Hradec Králové), W. S. Hancock (San Francisco, CA), S. Hjertén (Uppsala), Cs. Horváth (New Haven, CT), J. F. K. Huber (Vienna), K.-P. Hupe (Waldbronn), T. W. Hutchens (Houston, TX), J. Janák (Brno), P. Jandera (Pardubice), B. L. Karger (Boston, MA), E. sz. Kováts (Lausanne), A. J. P. Martin (Cambridge), L. W. McLaughlin (Chestnut Hill, MA), R. P. Patience (Sunbury-on-Thames), J. D. Pearson (Kalamazoo, MI), H. Poppe (Amsterdam), F. E. Regnier (West Lafayette, IN), P. G. Righetti (Milan), P. Schoenmakers (Eindhoven), G. Schomburg (Mülheim/Ruhr), R. Schwarzenbach (Düben-dorf), R. E. Shoup (West Lafayette, IN), A. M. Siouffi (Marseille), D. J. Strydom (Boston, MA), K. K. Unger (Mainz), J. T. Watson (East Lansing, MI), B. D. Westerlund (Uppsala)

EDITORS, BIBLIOGRAPHY SECTION

Z. Deyl (Prague), J. Janák (Brno), V. Schwarz (Prague), K. Macek (Prague)



ELSEVIER

AMSTERDAM — OXFORD — NEW YORK — TOKYO

J. Chromatogr., Vol. 471 (1989)

All rights reserved. No part of this publication may be reproduced, stored in a retrieval system or transmitted in any form or by any means, electronic, mechanical, photocopying, recording or otherwise, without the prior written permission of the publisher, Elsevier Science Publishers B.V., P.O. Box 330, 1000 AH Amsterdam, The Netherlands.

Upon acceptance of an article by the journal, the author(s) will be asked to transfer copyright of the article to the publisher. The transfer will ensure the widest possible dissemination of information.

Submission of an article for publication entails the authors' irrevocable and exclusive authorization of the publisher to collect any sums or considerations for copying or reproduction payable by third parties (as mentioned in article 17 paragraph 2 of the Dutch Copyright Act of 1912 and the Royal Decree of June 20, 1974 (S. 351) pursuant to article 16 b of the Dutch Copyright Act of 1912) and/or to act in or out of Court in connection therewith.

Special regulations for readers in the U.S.A. This journal has been registered with the Copyright Clearance Center, Inc. Consent is given for copying of articles for personal or internal use, or for the personal use of specific clients. This consent is given on the condition that the copier pays through the Center the per-copy fee stated in the code on the first page of each article for copying beyond that permitted by Sections 107 or 108 of the U.S. Copyright Law. The appropriate fee should be forwarded with a copy of the first page of the article to the Copyright Clearance Center, Inc., 27 Congress Street, Salem, MA 01970, U.S.A. If no code appears in an article, the author has not given broad consent to copy and permission to copy must be obtained directly from the author. All articles published prior to 1980 may be copied for a per-copy fee of US\$ 2.25, also payable through the Center. This consent does not extend to other kinds of copying, such as for general distribution, resale, advertising and promotion purposes, or for creating new collective works. Special written permission must be obtained from the publisher for such copying.

No responsibility is assumed by the Publisher for any injury and/or damage to persons or property as a matter of products liability, negligence or otherwise, or from any use or operation of any methods, products, instructions or ideas contained in the materials herein. Because of rapid advances in the medical sciences, the Publisher recommends that independent verification of diagnoses and drug dosages should be made.

Although all advertising material is expected to conform to ethical (medical) standards, inclusion in this publication does not constitute a guarantee or endorsement of the quality or value of such product or of the claims made of it by its manufacturer.

This issue is printed on acid-free paper

Printed in The Netherlands

SPECIAL VOLUME



HONOUR VOLUME
on the occasion of the 65th birthday of

R. P. W. SCOTT

Guest Editor
J. JANÁK
(Brno)

CONTENTS

HONOUR VOLUME ON THE OCCASION OF THE 65TH BIRTHDAY OF R. P. W. SCOTT

Historical

- Profile of R. P. W. Scott
by D. E. Martire 1

Critical reviews

- Ribonucleoside analysis by reversed-phase high-performance liquid chromatography
by C. W. Gehrke and K. C. Kuo (Columbia, MO, U.S.A.) 3
- Gas-solid chromatography on open-tubular columns: an isotope effect
by M. Mohnke and J. Heybey (Leipzig, G.D.R.) 37
- Basic equations in continuous gas extraction and their application to headspace analysis
by A. G. Vitenberg and B. V. Ioffe (Leningrad, U.S.S.R.) 55

Theory

- Theory of open-tube chromatography: and exact proof of Golay's equations
by A. A. Clifford (Leeds, U.K.) 61
- Application of a unified molecular theory to gas-liquid chromatography
by D. E. Martire (Washington, DC, U.S.A.) 71
- Comparison between the conditions for solute focussing by the static and dynamic solvent effects
under ideal conditions
by P. J. Apps and V. Pretorius (Pretoria, South Africa) 81

Gas chromatography

- Comparison of solvent models for characterizing stationary phase selectivity in gas chromatography
by S. K. Poole, B. R. Kersten and C. F. Poole (Detroit, MI, U.S.A.) 91
- Determination of the gas chromatographic performance characteristics of several graphitized carbon
blacks
by W. R. Betz and W. R. Supina (Bellefonte, PA, U.S.A.) 105
- Characteristics of glass based packings as a support in chromatography
by L. S. Green and W. Bertsch (Tuscaloosa, AL, U.S.A.) 113
- New method for measuring obstructive factors and porosity using gas chromatographic instrumenta-
tion
by N. A. Katsanos and Ch. Vassilakos (Patras, Greece) 123
- Use of gas chromatography for a study of crown ethers
by A. Kohoutová, E. Smolková-Keulemansová and L. Feltl (Prague, Czechoslovakia) . . . 139
- Isomerization of propyne to propadiene. Studies by gas chromatography
by P. M. Lyne and C. S. G. Phillips (Oxford, U.K.) 145
- Sample preparation by means of a supported liquid membrane for the determination of chloro-
phenoxyalkanoic acids
by G. Nilvé, G. Audunsson and J. Å. Jönsson (Lund, Sweden) 151
- Quantitative high-resolution gas chromatography and mass spectrometry of toxaphene residues in
fish samples
by F. I. Onuska and K. A. Terry (Burlington, Canada) 161

Determination of sensorial active trace compounds by multi-dimensional gas chromatography combined with different enrichment techniques by S. Nitz, H. Kollmannsberger and F. Drawert (Freising-Weihenstephan, F.R.G.)	173
Relative gas-liquid chromatographic retention factors of trimethylsilyl ethers of diradylglycerols on polar capillary columns by J. J. Myher and A. Kuksis (Toronto, Canada)	187
Gas chromatographic retention of carbohydrate trimethylsilyl ethers. III. Ketoheoses by A. Garcíá-Raso (Palma de Mallorca, Spain), and M. Fernández-Díaz, M. I. Páez, J. Sanz and I. Martínez-Castro (Madrid, Spain)	205
Dispersion and selectivity indices in gas chromatography. Part II. Studies of homologous carbonyl and carboxyl compounds by M. B. Evans (Hatfield, U.K.) and J. K. Haken (Kensington, Australia)	217
Quantitative relationships between the structure of alkylbenzenes and their gas chromatographic retention on stationary phases with different polarity by N. Dimov (Sofia, Bulgaria) and Ov. Mekenyan (Burgas, Bulgaria)	227
Effect of repeated cross-linking of SE-54 stationary phase film on the chromatographic properties of capillary columns by K. Janák, M. Horká and K. Tesařík (Brno, Czechoslovakia)	237
Non-linearity of the plot of log (adjusted retention time) <i>versus</i> carbon number of <i>n</i> -alkanes in series-coupled gas chromatographic columns by T. Maurer, Th. Welsch and W. Engewald (Leipzig, G.D.R.)	245
Interface adsorption and reproducibility of retention indices in glass capillary columns with dimethylpolysiloxane stationary phases cross-linked by γ -irradiation by P. Farkaš, L. Soják and M. Kováč (Bratislava, Czechoslovakia) and J. Janák (Brno, Czechoslovakia)	251
<i>Liquid chromatography</i>	
Determination of the enantiomers of α -H- α -amino acids, α -alkyl- α -amino acids and the corresponding acid amides by high-performance liquid chromatography by A. Duchateau, M. Crombach, J. Kamphuis, W. H. J. Boesten, H. E. Schoemaker and E. M. Meijer (Geleen, The Netherlands)	263
Improved chiral stationary phase for the separation of the enantiomers of chiral acids as their anilide derivatives by W. H. Pirkle and J. E. McCune (Urbana, IL, U.S.A.)	271
Chromatographic evaluation of oligomeric C ₈ reversed phases for the use in high-performance liquid chromatography by S. O. Akapo, A. Furst, T. M. Khong and C. F. Simpson (London, U.K.)	283
Mass detection limits achieved with a commercially available fluorimeter in micro high-performance liquid chromatography by T. Takeuchi, T. Asano and D. Ishii (Nagoya, Japan)	297
Simultaneous photometric and conductivity detection for microcolumn liquid chromatography by M. Janeček and K. Šlais (Brno, Czechoslovakia)	303
Effect of the position of the laser beam focal point on a capillary flow-through cell on the signal-to-noise ratio for a fluorimetric detector in capillary column liquid chromatography by T. Tsuda (Nagoya, Japan) and H. Noda (Kyoto, Japan)	311
Trace enrichment of pyrimidine nucleobases, 5-fluorouracil and bromacil on a silver-loaded thiol stationary phase with on-line reversed-phase high-performance liquid chromatography by C. Lipschitz, H. Irth, G. J. de Jong, U. A. Th. Brinkman and R. W. Frei (Amsterdam, The Netherlands)	321

Quantitative microscale liquid chromatography of piperine in pepper and pepper extracts by M. Verzele, F. Van Damme and G. Schuddink (Ghent, Belgium) and P. Vyncke (Eke, Belgium)	335
<i>Supercritical fluid chromatography</i>	
Effect of pressure drop across the column on average densities and capacity factors in supercritical fluid chromatography by K. D. Bartle, T. Boddington, A. A. Clifford and G. F. Shilstone (Leeds, U.K.)	347
Adsorption isotherms on silica for methanol and 1-hexanol modifiers from supercritical carbon dioxide by C. H. Lochmüller and L. P. Mink (Durham, NC, U.S.A.)	357
<i>Other chromatographic techniques and combinations</i>	
Aqueous size-exclusion chromatography of anionic and non-ionic water-soluble polymers on silica gel with bonded hydrophilic groups by S. Mori (Mie, Japan)	367
Overpressured multi-layer chromatography by E. Tyihák, E. Mincsovics and T. J. Székely (Budapest, Hungary)	375
Laser microprobe mass spectrometry of selected compounds directly from normal phase high-perfor- mance thin-layer plates by R. W. Finney and H. Read (Sunbury-on-Thames, U.K.)	389
Determination of free and esterified sterols and of wax esters in oils and fats by coupled liquid chromatography-gas chromatography by K. Grob and M. Lanfranchi (Zürich, Switzerland) and C. Mariani (Milan, Italy)	397
Retention behaviour of β -carbolines in normal-phase chromatography. Silica and amino phases in high-performance and thin-layer chromatography by M. C. Pietrogrande, F. Dondi, P. A. Borea and C. Bigli (Ferrara, Italy)	407
<i>Capillary electrophoresis</i>	
Zone broadening due to sample injection in capillary zone electrophoresis by E. Grushka and R. M. McCormick (Wilmington, DE, U.S.A.)	421
Capillary zone electrophoretic separations of proteins in polyethylene glycol-modified capillaries by G. J. M. Bruin, J. P. Chang, R. H. Kuhlman, K. Zegers, J. C. Kraak and H. Poppe (Amsterdam, The Netherlands)	429
<i>Research notes</i>	
Picolinic acid: a mobile phase additive for improved chromatography of metal-chelating heterocyclic acids and β -diketones by D. W. Roberts, R. J. Ruane and I. D. Wilson (Macclesfield, U. K.)	437
Trace/ultratrace analyses of unstable compounds. Investigations on hydrazobenzene and azobenzene by S. Ahuja, G. Thompson and J. Smith (Suffern, NY, U.S.A.)	443
<i>Letter to the Editor</i>	
On some nomenclature in chromatography by O. K. Guha (Bihar, India)	447
<i>Author Index</i>	449

PROFILE OF R. P. W. SCOTT

RAYMOND PETER WILLIAM SCOTT was born on June 20, 1924 in Erith, Kent, U.K. He studied at the University of London, obtaining his B.Sc. degree in 1946 and his D.Sc. degree in 1960. After spending more than a decade at Benzole Producers, Ltd., where he became head of the Physical Chemistry Laboratory, he joined W. G. Pye in 1960. In 1961 he moved to Unilever Research Laboratories as manager of the Physical Chemistry Department. In 1969 he became Director of Physical Chemistry at Hoffmann-La Roche Inc., Nutley, NJ, U.S.A. and subsequently accepted the position of Director of the Applied Research Department at the Perkin-Elmer Corporation, Norwalk, CT, U.S.A. in 1980.

In 1986 he became an independent consultant and was appointed Visiting Professor at Georgetown University, Washington, DC, U.S.A. and Birbeck College of the University of London. He now resides in Avon, CT, U.S.A. and Sedlescombe, East Sussex, U.K. with his wife Barbara ("Bunny"), whom he married in 1946. Their son Kevin is both a scientist (D. Phil. from Oxford University, working with Professor Courtenay Phillips) and an ordained minister, and is currently plying his trades in Edinburgh where he has a research fellowship at the University. Their other son, Kerry, is Director of Music at a school in Sussex.

Dr. Scott is the author or co-author of over 120 scientific papers, largely involving the practice and theory of both gas and liquid chromatography. He edited the proceedings of the *1960 Gas Chromatography Symposium* which was held in Edinburgh and, more recently, a book entitled *Small Bore Liquid Chromatography Columns*. He is author of two books, *Contemporary Liquid Chromatography* and *Liquid Chromatography Detectors*, the second edition of which has recently been published. Dr. Scott was a founding member of the Gas Chromatography Discussion Group (U.K.) and exhibited high-speed columns at the Royal Society Tercentary Exhibition in 1961. He received the American Chemical Society Award in Chromatography (1977), the M.S. Tswett Chromatography Medal (1978), the Tswett Medal of the U.S.S.R. (1979), the A.J.P. Martin Chromatography Award (1982) and the Royal Society of Chemistry Award in Analysis and Instrumentation (1988). He has taken part in teaching several courses in liquid chromatography in the U.S.A., U.K. and Australia, and has presented many invited lectures in Europe and the U.S.A. He is a member of the editorial boards of the *Journal of Chromatographic Science* and the *Journal of Liquid Chromatography*.

Dr. Scott's activities in gas chromatography started practically at the inception of the technique. He pioneered the development of high-resolution columns, high-sensitivity detectors and presented fundamental treatments of the relationship between the theory and practice of the technique. He joined those early chromatographers who became involved in the development of modern, high-performance liquid chromatography, invented the wire-transport liquid chromatography detector, and pioneered in many of the achievements which are today routinely utilized by many analytical laboratories. He was the first to introduce a suitable liquid chromato-

graphy-mass spectrometry interface to provide electron impact spectra. More recently, he introduced microbore columns to liquid chromatography, has constructed columns having efficiencies of three-quarters of a million theoretical plates and has achieved liquid chromatographic separations in less than a second. He has also developed and remains a proponent of low-cost, high-quality instrumentation.

Despite heavy administrative duties throughout his career, Dr. Scott never lost touch with the laboratory. He is a "hands-on" scientist with a remarkable record of accomplishments in chromatography, ranging from hardware design and development to fundamental theory. He has not shied away from questioning the "conventional wisdom", and his original approach to problems has produced significant breakthroughs. He has retained a boyish enthusiasm and energy for research, stimulating those with whom he interacts.

In recognition of his many important contributions to chromatography and in appreciation of his personal qualities, his colleagues, collaborators and friends are pleased and honored to dedicate the papers in this volume to Dr. R. P. W. Scott on the occasion of his sixty-fifth birthday.

Washington, DC (U.S.A.)

DANIEL E. MARTIRE

CHROM. 21 402

RIBONUCLEOSIDE ANALYSIS BY REVERSED-PHASE HIGH-PERFORMANCE LIQUID CHROMATOGRAPHY

CHARLES W. GEHRKE* and KENNETH C. KUO

Department of Biochemistry, University of Missouri-Columbia and Cancer Research Center, Columbia, MO 65201 (U.S.A.)

SUMMARY

Over the past fifteen years we have developed and refined the analytical chromatographic methodologies using reversed-phase high-performance liquid chromatography and UV-photodiode array detection (RPLC-UV) for the detection and measurement of the major and modified nucleosides in nucleic acids and biological fluids. RPLC-UV nucleoside analysis as it has now evolved is a powerful new research tool to aid investigators in the fields of biochemical and biomedical research. This RPLC-UV nucleoside method can resolve more than 65 nucleosides in a single analysis with "run-to-run" peak retention variations of less than 1%. A complete nucleoside composition can be obtained from as little as 0.5 μg RNA. Identification and confirmation of nucleosides can be made from the highly reproducible retention times and from the characteristic UV spectrum from a few picomoles (*ca.* 1 ng) of nucleoside.

In this paper we introduce standard RPLC-UV methodologies for the analysis of nucleosides and nucleoside composition of RNAs. The chromatographic protocols and standard nucleoside columns are presented and the essential requirements necessary in the HPLC instrumentation are described. Three optimized RPLC systems were developed, each with particular emphasis placed on resolution, speed, or sensitivity. In addition, three unfractionated tRNAs were selected as sources of reference nucleosides and for assessment of the performance of the chromatography. From these tRNAs, a large array of nucleosides were characterized which are used in standardization and calibration of the method. Also discussed is the use of a diode-array detector for enhancement of the reliability of nucleoside identification and accuracy of measurement. An extended enzymatic hydrolysis protocol for the liberation of exotically modified nucleosides in tRNAs is also described. Chromatographic retention times and UV spectra for a large number of ribonucleosides are tabulated.

The RPLC-UV ribonucleoside analytical protocols are capable of quantifying 31 nucleosides. Approximately 1 μg of an isoaccepting tRNA, or 20 μg of unfractionated tRNA are needed for quantitative analysis. With this amount of tRNA, the percent relative error of measurement of the four major nucleosides is less than 2%, and for the modified nucleosides about 5%. As little as 0.2 μg of pure isoaccepting tRNA can be analyzed, but at the expense of precision as at this low sample size a 20-30% relative error for modified nucleosides is to be expected.

For quantitation of the modified nucleosides in rRNA, which contains much less modification than tRNAs, 10–100 μg of sample are needed per injection. This amount is within the loading capacity of a regular analytical column (25 cm \times 4.6 mm silica based C_{18} column). However, with this quantity injected, caution is required to ensure that the response for the four major nucleosides is within the linear range of the detector and data reduction system. Quantitative data from the analysis of 16S and 23S rRNA are given.

Examples are presented of some unique and interesting applications of this nucleoside methodology to biochemical and biomedical investigations.

INTRODUCTION

Research directions in nucleic acid biochemistry are toward a better understanding of how the chemical structure of nucleic acids is correlated with their unique biological function. This information can be used to gain a deeper insight into how cells normally regulate their metabolic activities, allows speculation on how they evolved their respective biological role(s), and potentially permits correlation of the altered structures of nucleic acids in abnormal or diseased states to biological function. An understanding of how cells behave normally and in the diseased state provides the basis for the development of rational therapeutics and improved diagnostic tools. As in any field of scientific research, methodological limitations have hampered the advancement and exploitation of modified nucleosides as signals in routine tests in clinical chemistry, and in biochemical research generally. The development of nucleoside analytical methodologies will allow a better understanding of the action of living processes at the molecular level. Studies are now being undertaken in many laboratories on nucleic acid metabolites as cancer markers, and of chemical carcinogens and mutagens adducted to nucleic acids for assessment of human exposure. On the other hand, research on the metabolic activities of nucleic acids related to human health and nutrition is still in its relative infancy. Professor Gerhard Schöch of Dortmund has pioneered studies on whole body RNA turnover and investigated RNA metabolism as an indicator of nutritional status^{1,2}. This research will have an important impact and benefit to human health.

The development of high-resolution chromatographic methodology for qualitative identification and quantitative measurement of an array of nucleosides has been a challenge for analytical biochemists.

Randerath's group developed two sensitive methods for tRNA composition analysis from low microgram amounts of tRNAs. In these methods, radioactive labels, ^3H and ^{32}P , are introduced chemically or enzymatically into the ribonucleosides and 3'-nucleotides, respectively, followed by thin-layer chromatography. Autoradiography and off-line activity counting are used for the detection and quantitation of the labelled nucleosides³. Both methods have been used in many applications since the late 1960s. However, the tritium derivative method cannot detect 2'-O-methylated nucleosides because the methyl group at the 2'-O-position prevents formation of a dialdehyde by sodium metaperiodate. In addition alkali-labile modified nucleosides such as 1-methyladenosine (m^1A), 7-methylguanosine (m^7G), and 4-acetylcytidine (ac^4C) are partially or completely destroyed by this method. Also, modified

nucleosides sensitive to oxidation or borohydride concentration such as thiolated nucleosides, dihydrouridine (hU), and pseudouridine (Ψ) are either destroyed or produce multiple peaks. Further, the base specificity of T_4 polynucleotide kinase causes non-uniform labeling of some modified nucleotides which limits the quantitative application of the 3H and ^{32}P derivative methods⁴.

The first introduction of reversed-phase liquid chromatographic (RPLC) nucleoside analysis was from Gehrke and Kuo's^{5,6} group and Brown's laboratory^{7,8}, with these methods primarily aimed at analysis of RNA metabolites in body fluids for biomedical research. Later, the development of RPLC methodology by Ames' group⁹, and McCloskey and Vestal's work^{10,11} using LC thermal spray mass spectrometry on the structure elucidation of nucleosides were important contributions to tRNA composition analysis and structure identification of modified nucleosides.

During the past fifteen years we have continued our investigations on RPLC nucleoside analysis and have developed a quantitative enzymatic RNA hydrolysis procedure¹², and comprehensive chromatography protocols¹³⁻¹⁵. We have also established a database of chromatographic and UV-spectral data on more than 80 nucleosides. At least 35 known nucleosides can be identified or quantified directly from an enzymatic hydrolysate of tRNA in a single chromatographic run with high precision and accuracy. Also, total nucleoside composition can be obtained from as little as 0.5 μg (0.01 A_{260}) of tRNA using the regular analytical column, and from 0.2 μg of a single species tRNA with a microbore (2 mm I.D.) column. Using our developed methods, we determined the nucleoside compositions of tRNA, rRNAs, cell cultures, tissues, urine, serum and other body fluids. In collaboration with scientists across the world we studied the modifications in tRNAs to complement tRNA sequence work; investigated the relationships of modification and functions of RNAs; searched for modification defects in tRNAs from yeast mutants; compared the modified nucleoside profiles of tRNAs in normal and cancer in human tissues, and studied nucleosides in serum and urine of normal human populations and made comparative studies on several types of cancers¹⁶⁻²¹.

The scientists that we have collaborated with, exchanged scientific information, and obtained precious RNA samples and reference nucleosides are: Dr. P. Agris, Dr. S. Altman, Dr. G. Björk, Dr. E. Borek, Dr. J. Cannon, Dr. G. Chheda, Dr. J. Desgrès, Dr. G. Dirheimer, Dr. J. Ebel, Dr. H. Gauss, Dr. H. Grosjean, Dr. T. Heyman, Dr. J. Hoffman, Dr. J. Horowitz, Dr. R. Hutter, Dr. J. Katze, Dr. G. Keith, Dr. H. Kersten, Dr. W. Kersten, Dr. J. Kohli, Dr. G. Krupp, Dr. E. Kubli, Dr. J. McEntire, Dr. M.-D. Morch, Dr. G. Mills, Dr. P. Niederburger, Dr. K. Nishikawa, Dr. K. Nishimura, Dr. B. Orthwerth, Dr. Salvatore, Dr. E. Schlimme, Dr. O. Sharma, Dr. D. Söll, Dr. M. Sprinzl, Dr. P. Staheli, Dr. R. Trewyn, Dr. R. Valle, Dr. T. P. Waalkes, Dr. K. Watanabe, and Dr. T.-W. Wong. Their generosity and collaboration have made this research possible.

In this paper we address the RP-HPLC protocols for chromatography of ribonucleosides in biological samples and present some interesting applications of the method. The following topics are discussed:

- (i) basic HPLC instrumental component requirements,
- (ii) chemical nature, efficiency, and selectivity of the "nucleoside column",
- (iii) chromatographic parameters,
- (iv) optimization of the nucleoside separation to provide high-resolution, high-speed, and high-sensitivity chromatographic systems,

- (v) introduction of nucleoside reference standards of unfractionated tRNA (*E. coli*, brewer's yeast, and calf liver) for transfer of this technology to other laboratories,
- (vi) HPLC-UV characterization of 67 ribonucleosides,
- (vii) applications of RPLC-UV nucleoside analysis to biochemical and biomedical investigations.

Earlier we published on methods for determining mRNA cap structures and its internal modifications²¹. Our chromatographic methods for nucleosides in DNA, RNAs and metabolites in body fluids are reported separately.

EXPERIMENTAL

Chromatography

HPLC instruments. A completely automated LC system, HP 1090M from Hewlett-Packard (Palo Alto, CA, U.S.A.), was used for almost all the investigations presented in this paper. The HP-1090M system consisted of a DR5 ternary solvent delivery system, variable-volume auto-injector, autosampler, diode-array detector, and heated-column compartment. The liquid chromatography work station is composed of an HP Model 310 computer, supported by Rev. 4.05 operation software, HP-HIL 512 × 400 color monitor with bit-mapped display, and HP-9133H 20 mb Winchester disc drive with 710 kb micro floppy disk. A Think-Jet printer and HP 7475A plotter were used for hard copy data presentation. The cooling coil of the heated column compartment was cooled by circulation of refrigerated ethylene glycol based anti-freeze by a Haake Model FJ circulating bath (Saddle Brook, NJ, U.S.A.). The cooling bath was positioned inside a small refrigerator and the anti-freeze was also circulated through a 3 m × 10 mm copper tubing coil which was positioned inside the freezer compartment for additional cooling. Some initial developmental chromatography was performed on a manual system which consisted of a Series 4 liquid chromatograph (Perkin Elmer, Norwalk, CT, U.S.A.), U6K universal injector (Waters Assoc., Milford, MA, U.S.A.) and a diode-array detector HP-1040A HPLC detection system (Hewlett-Packard).

Chemicals and solvents. The methanol and acetonitrile used were RPLC grade, either of B & J from American Scientific Products (McGaw Park, IL, U.S.A.) or OmniSolv from EM Chemicals (Cherry Hill, NJ, U.S.A.).

RPLC water was obtained through a three-step purification process. The first step was reversed osmosis using an RO-Pure apparatus (Model D0640, Barnstead Company, Boston, MA, U.S.A.). The second step of purification was accomplished with a Nanopure four-cartridge system (Model D1794, Barnstead) composed of one charcoal cartridge for adsorption of organics, two mixed bed ion-exchange cartridges for removal of anions and cations, and one filtration cartridge capable of removing particulates larger than 0.22 μm. In the third step, the Nanopure water was distilled in an all glass still with PTFE tubing connections (Model AG-11, Corning Glass Works, Corning, NY, U.S.A.).

Ammonium phosphate, zinc sulfate, and sodium acetate were purchased from J. T. Baker (Phillipsburgh, NJ, U.S.A.). Ammonium hydroxide and phosphoric acid were from Mallinckrodt (St. Louis, MO, U.S.A.).

The modified ribonucleoside reference standard compounds used were from several sources; Sigma (St. Louis, MO, U.S.A.), Mann Research Labs. (New York, NY, U.S.A.), and Vega Biochemicals (Tucson, AZ, U.S.A.).

Nuclease P1 was purchased from Boehringer Mannheim Biochemicals (Indianapolis, IN, U.S.A.). Bacterial alkaline phosphatase (BAP) from *E. coli* Type III was purchased from Sigma, product No. P-4252. The bacterial alkaline phosphatase must be pretested for possible contamination with adenosine deaminase. The above enzymes are the only sources that we have tested which are free of adenosine deaminase activity under our hydrolysis protocol. An enzymes blank must be run for each newly purchased enzyme lot to observe possible RNA and DNA contamination.

All the transfer ribonucleic acids (tRNAs) were purchased from Boehringer Mannheim Biochemicals and included unfractionated tRNAs from brewer's yeast (Cat. No. 109 517), unfractionated tRNAs from calf liver (Cat. No. 647 576), unfractionated tRNAs from *E. coli* MRE 600 RNase negative (Cat. No. 109 541); amino acid specific tRNAs from *E. coli* MRE 600, were N-formylmethionine-specific (Cat. No. 109 584), glutamic acid-specific II (Cat. No. 109 609), phenylalanine-specific (Cat. No. 109 673), tyrosine-specific (Cat. No. 109 703) and valine-specific I (Cat. No. 109 720). tRNA phenylalanine-specific was from brewer's yeast (Cat. No. 109 657).

Columns. Nucleoside columns (Supelcosil LC-18S; 25 cm × 4.6 mm, 15 cm × 4.6 mm, and 20 cm × 2.0 mm) were obtained from Supelco (Bellefonte, PA, U.S.A.).

Elution buffers. The composition of the HPLC elution buffers were as follows: (A) 2.50% methanol in 0.010 M $\text{NH}_4\text{H}_2\text{PO}_4$; pH 5.3, (B) 20.0% methanol in 0.010 M $\text{NH}_4\text{H}_2\text{PO}_4$; pH 5.1, (C) 35.0% acetonitrile in 0.010 M $\text{NH}_4\text{H}_2\text{PO}_4$; pH 4.9.

The buffer salt stock solution ($\text{NH}_4\text{H}_2\text{PO}_4$ buffer, 1.00 M) should be prepared using HPLC water, and the solution should be filtered through a 0.2- μm Nylon-66 membrane filter (Rainin Instrument, Woburn, MA, U.S.A.) and stored at 4°C.

The buffers were made by adding the appropriate volumes of buffer salt stock solution and organic solvent into a volumetric flask, then adjusting to volume with freshly filtered HPLC water.

All glassware used for preparing buffers should be used exclusively for that purpose. Also, separate pH electrodes should be reserved and used only for buffer preparation. Buffers should be made to final volume in volumetric flasks and aliquots should be taken with volumetric pipets. pH adjustment of buffers A and B are made using dilute solutions of NH_4OH or H_3PO_4 . No pH adjustment is needed for buffer C.

After the buffers are prepared, they should not be filtered as filtration will lower the concentration of organic solvent in the buffer due to evaporation. Filter only the HPLC water and the buffer salt stock solution. In general, HPLC grade organic solvents are prefiltered by the manufacturer; if they are not, they should be filtered with a 0.2- μm PTFE or nylon filter. Buffer A may be kept at room temperature for 48 h, and can be maintained in a freezer for several months. Buffers B and C can be stored at room temperature for a week. If the buffers are continuously degased with helium, then the buffers should be replaced every two days to avoid concentration changes as a result of evaporation of the organic solvents.

Gradient elution. The HPLC conditions for high-resolution chromatography, high-speed chromatography, and high-sensitivity chromatography are presented in Tables I-III.

Enzymatic hydrolysis

Analytical scale enzymatic hydrolysis procedure (0.5–250 μg of RNA). (1) Aliquot 0.5–250 μg of RNA in 50 μl of water into a 1.5-ml or 400- μl polypropylene

TABLE I

HPLC CONDITIONS FOR HIGH-RESOLUTION GRADIENT ELUTION CHROMATOGRAPHY

Column: Supelcosil LC-18S 250 × 4.6 mm, flow-rate: 1.0 ml/min, temperature: 26°C.

Step (No)	Step time (min)	Buffer composition (%)			Gradient type
		A	B	C	
1	12.0	100.0	0.0	0.0	Isocratic
2	8.0	90.0	10.0	0.0	Linear
3	5.0	75.0	25.0	0.0	Linear
4	7.0	40.0	60.0	0.0	Linear
5	4.0	38.0	62.0	0.0	Linear
6	9.0	0.0	100.0	0.0	Linear
7	35.0	0.0	0.0	100.0	Linear
8	10.0	0.0	0.0	100.0	Isocratic

TABLE II

HPLC CONDITIONS FOR HIGH-SPEED GRADIENT ELUTION CHROMATOGRAPHY

Column: Supelcosil LC-18S 150 × 4.6 mm, flow-rate: 1.0 ml/min, temperature: 26°C.

Step (No)	Step time (min)	Buffer composition (%)			Gradient type
		A	B	C	
1	7.2	100.0	0.0	0.0	Isocratic
2	4.8	90.0	10.0	0.0	Linear
3	3.0	75.0	25.0	0.0	Linear
4	4.2	40.0	60.0	0.0	Linear
5	2.4	38.0	62.0	0.0	Linear
6	5.4	0.0	100.0	0.0	Linear
7	21.0	0.0	0.0	100.0	Linear
8	7.0	0.0	0.0	100.0	Isocratic

TABLE III

HPLC CONDITIONS FOR HIGH-SENSITIVITY GRADIENT ELUTION CHROMATOGRAPHY

Column: Supelco LC-18S 150 × 2.1 mm, flow-rate: 0.21 ml/min, temperature: 26°C.

Step (No)	Step time (min)	Buffer composition (%)			Gradient type
		A	B	C	
1	7.2	100.0	0.0	0.0	Isocratic
2	4.8	90.0	10.0	0.0	Linear
3	3.0	75.0	25.0	0.0	Linear
4	4.2	40.0	60.0	0.0	Linear
5	2.4	38.0	62.0	0.0	Linear
6	5.4	0.0	100.0	0.0	Linear
7	21.0	0.0	0.0	100.0	Linear
8	7.0	0.0	0.0	100.0	Isocratic

micro-centrifuge tube, and heat for 2 min in a boiling water bath. Rapidly cool in an ice water bath. (2) Add 5 μ l of 10 mM ZnSO₄ solution, 10 μ l of nuclease P1 (200 units per ml, in 30 mM sodium acetate, pH 5.4). (3) Incubate at 37°C in a water bath for 16 h (overnight). (4) Add 10 μ l of 0.5 M Tris buffer, pH 8.3, and 10 μ l of bacterial alkaline phosphatase (BAP) (100 units per ml, in 2.5 M ammonium sulfate). (5) Incubate at 37°C in a water bath for 2 h.

Semi-preparative enzymatic hydrolysis procedure (mg quantities of RNA). (1) Take a ca. 2–5 μ g portion of the sample and perform an analytical scale enzymatic hydrolysis and RPLC analysis as described above to establish the RPLC profile of the nucleosides in the sample. (2) Dissolve the remaining RNA sample (mg quantities) in a minimum amount of water (0.5–1.0 ml) and heat in a boiling water bath for 2 min. Rapidly cool in an ice water bath. (3) Add 25 μ l of 10 mM ZnSO₄ solution and 50 μ l of nuclease P1 (200 units per ml, in 30 mM sodium acetate, pH 5.4). (4) Incubate at 37°C for 16 h in a water bath. (5) To check the completeness of the nuclease P1 hydrolysis, take an aliquot of the hydrolysate which contains 2–5 μ g of RNA and proceed to step 6. (6) Add 10 μ l 0.5 M Tris pH 8.3 and 10 μ l of BAP (100 units per ml, in 2.5 M ammonium sulfate) to the aliquot. (7) Incubate at 37°C for 2 h in a water bath. (8) Analyze this hydrolysate by RPLC and compare the nucleoside profile with the analytical hydrolysate (step 1) to determine the completeness of nuclease P1 hydrolysis of the mg quantity of RNA. If the chromatogram of the semi-preparative hydrolysate shows certain modified nucleosides are either missing or present at lower amounts, especially the 2'-O-methylated or exotic nucleosides, this indicates incomplete enzymatic hydrolysis of the preparative scale RNA by nuclease P1. (9) After ensuring that the nuclease P1 hydrolysis (step 4) has reached completion, add 100 μ l of 0.5 M Tris buffer, pH 8.3 and 100 μ l of BAP (100 units per ml, in 2.5 M ammonium sulfate). (10) Incubate at 37°C in a water bath for 2 h. (11) Analyze ca. 2–5 μ g of the hydrolysate by RPLC. If 5'-nucleoside monophosphates of cytidine, uridine, guanosine or adenosine are observed, repeat step 10. The elution positions of the four nucleotides are shown in Fig. 1.

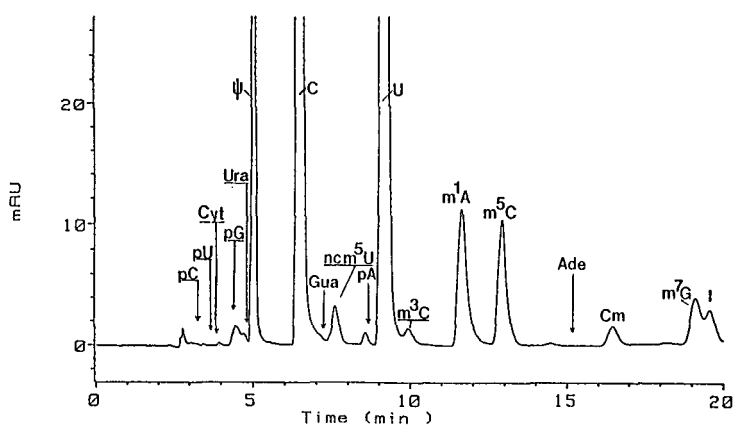


Fig. 1. Elution positions of major nucleobases and 5'-nucleoside monophosphates. For all experimental details refer to the Experimental section and for symbols refer to Table IV.

Notes. (1) The BAP is in suspension, mix well before using. (2) Vortex mix for a few seconds to mix the solutions at each addition step and follow with brief centrifugation to avoid drops adhering on the cap or the walls of the centrifuge tube. (3) Briefly centrifuge the sample hydrolysate to remove suspended protein before transfer of the hydrolysate to the RPLC sample vial or injection onto the RPLC column.

RESULTS AND DISCUSSION

RPLC coupled with a diode-array detector is a powerful combination for the chromatographic analysis of modified nucleosides. The high selectivity and efficiency of the reversed-phase column is essential for the separation of a large number of modified nucleosides which often differ only slightly in structure. The electronic structures of purine and pyrimidine rings give very high molar absorptivities in the UV range (*ca.* 5000–20 000), and in most cases the λ_{max} is in the range 260–280 nm. With an optimized RPLC–UV system, low picomole levels (*ca.* 1 ng or less) of a nucleoside can be detected with ease. Thus, the combination of RPLC with UV detection provides exceedingly high chromatographic selectivity and sensitivity for nucleoside analysis.

Transfer RNA nucleoside analysis

Transfer RNA is one of the most heterogeneous biopolymers known. It is a relatively small polymer, ranging in length from 73 to 94 nucleosides, and contains a large number of modified nucleosides. Nishimura²² identified 47 naturally occurring nucleosides in tRNAs, and Dunn and Hall²³ compiled a list of 79 natural and synthetic nucleosides. In our laboratory we have separated and identified more than 80 nucleosides in tRNAs from a wide variety of sources. Sixty-seven of these ribonucleosides have been identified by comparison of their chromatographic and/or absorbance spectral properties with known reference compounds. New, unknown nucleosides are still being identified and reported. For example, at the 12th International tRNA Workshop (Umea, Sweden) in 1987; 2'-O-ribosyladenosine was reported at position 64 in Met-tRNA initiator of yeast by our group²⁴. 5-Carboxymethylaminomethyl-2'-O-methyluridine was identified by Yokoyama and his group²⁵ in the first position of the anticodon of Leu-4 tRNA of *E. coli*. Four new modified nucleosides, 5,2'-O-dimethylcytidine, N⁴-acetyl-2'-O-methylcytidine, 2-thio-2'-O-methyluridine, and N²,N²-2'-O-trimethylguanosine were reported by McCloskey's group²⁶ from hyperthermophilic archaeobacteria tRNAs. In our recent collaborative investigations with Drs. Lagerkvist and Samuelsson of the University of Gothenburg we have found six unknown nucleosides in tRNAs from *Mycoplasma mycoides*²⁷, and confirmed the presence of eight known modified nucleosides reported in sequence studies.

It is a challenge to the analytical biochemist to simultaneously chromatograph and measure such a large number of nucleosides in a complex biological matrix. Further, the lack of pure, authentic nucleosides to serve as analytical reference standards presents a major problem. Currently, only about twenty modified ribonucleosides can be obtained through commercial suppliers. Fortunately, we have been supported by the generosity of many scientists from many parts of the world. They provided us with a few micrograms of their precious nucleoside reference compounds

and isoaccepting tRNAs which allowed us to establish the identity of 67 reference ribonucleosides.

Ribonucleoside reference standards

We have standardized the chromatographic retention times, obtained RPLC-UV spectra, and established molar response factors for a large number of ribonucleosides. However, the nucleosides we have are insufficient in number and in amount for the transfer of this technology to other laboratories. Scientists at other laboratories need to standardize and calibrate their analytical systems for analysis of modified nucleosides in a broad range of biological matrices. To overcome the limitation of insufficient reference nucleosides, we selected three unfractionated tRNAs, *E. coli*, brewer's yeast, and calf liver, as reference sources of modified nucleosides. Each of these tRNAs contain unique as well as common nucleosides and provide an array of modified nucleosides that are often encountered by researchers. Some minor differences in the modified nucleosides might be observed in these three tRNAs from different commercial sources, especially for *E. coli* tRNAs. This problem can be resolved by using a reliable supplier or by standardization of a selected lot of tRNAs obtained in large quantity and of good homogeneity. During the last five years we have not encountered problems of variability in tRNAs from the suppliers that we use.

Fig. 2 presents chromatograms from the high-resolution separation of the nucleosides in the three reference tRNAs with detection at 254 nm. The nucleoside peaks are identified by an assigned index number which essentially corresponds to their respective elution order. Table IV gives the IUPAC names, one letter symbol, and the index number of the nucleosides that were characterized by RPLC-UV. Other ribonucleosides which are not yet characterized by our RPLC-UV system are also included in this table.

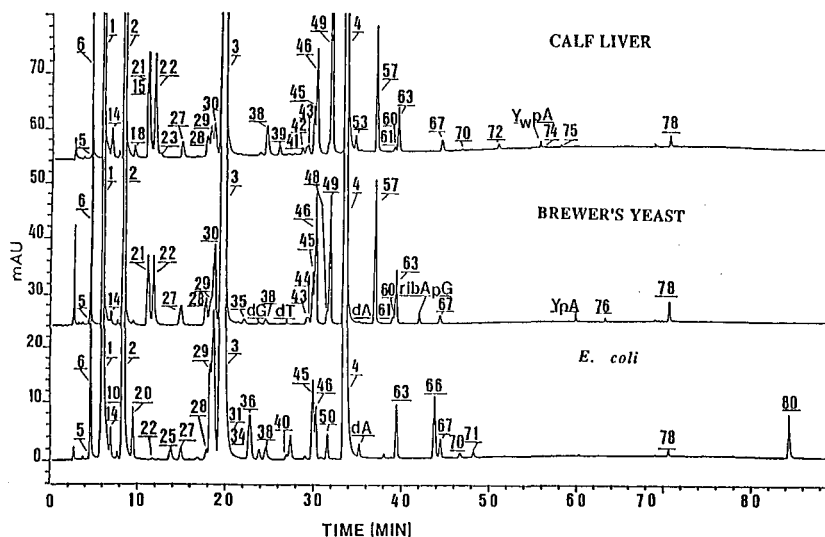


Fig. 2. HPLC chromatography of reference nucleosides from unfractionated calf liver, brewer's yeast, and *E. coli* tRNAs.

TABLE IV
NOMENCLATURE OF RIBONUCLEOSIDES AND INDEX NUMBERS

<i>IUPAC name</i>	<i>One-letter symbol</i>	<i>Index number</i>
<i>Adenosines</i>		
Adenosine	A	4
2'-O-Methyladenosine	Am	61
1-Methyladenosine	m ¹ A	21
1-Methyl-2'-O-methyladenosine	m ¹ Am	
2-Methyladenosine	m ² A	66
2-Methylthioadenosine	ms ² A	
3-Methyladenosine	m ³ A	
1,3-Dimethyladenosine	m ¹ m ³ A	
5'-Methylthioadenosine	ms ^{5'} A	
1,N ⁶ -Dimethyladenosine	m ¹ m ⁶ A	
N ⁶ -(N-Formyl- α -aminoacyl)adenosine	f ⁶ A	
N ⁶ -Methyladenosine	m ⁶ A	67
N ⁶ -Methyl-2-methylthioadenosine	ms ² m ⁶ A	
N ⁶ ,N ⁶ -Dimethyladenosine	m ⁶ Am	74
N ⁶ -Methyl-2'-O-methyladenosine	m ⁶ Am	71
2-Hydroxyadenosine	o ² A (isoG)	
N ⁶ -Carbamoyladenosine	nc ⁶ A	
N ⁶ -Threoninocarbonyladenosine	tc ⁶ A (t ⁶ A)	63
N ⁶ -Methyl-N ⁶ -threoninocarbonyladenosine	mtc ⁶ A (mt ⁶ A)	70
N ⁶ -Threoninocarbonyl-2-methylthioadenosine	ms ² tc ⁶ A (ms ² t ⁶ A)	72
N ⁶ -Glycinocarbonyladenosine	gc ⁶ A (g ⁶ A)	50
N ⁶ -Methyl-N ⁶ -glycinocarbonyladenosine	mgc ⁶ A (mg ⁶ A)	
N ⁶ -(Δ^2 -Isopentenyl)adenosine	i ⁶ A	78
N ⁶ -(Δ^2 -Isopentenyl)-2-methylthioadenosine	ms ² i ⁶ A	80
N ⁶ -(cis-4-Hydroxyisopentenyl)adenosine	cis oi ⁶ A	
N ⁶ -(4-Hydroxyisopentenyl)-2-methylthioadenosine	ms ² oi ⁶ A	79
9-(2'-O-Ribosyl- β -D-ribofuranosyl)adenine	rA	
<i>Inosines</i>		
Inosine	I	29
1-Methylinosine	m ¹ I	43
2-Methylinosine	m ² I	
7-Methylinosine	m ⁷ I	16
9- β -D-Ribofuranosylpurine (Nebularine)	neb	
7- β -D-Ribofuranosylhypoxanthine		
<i>Cytidines</i>		
Cytidine	C	1
2'-O-Methylcytidine	Cm	27
2-Thiocytidine	s ² C	20
3-Methylcytidine	m ³ C	18
N ⁴ -Methylcytidine	m ⁴ C	22
N ⁴ -Methyl-2'-O-methylcytidine	m ⁴ Cm	
N ⁴ -Methyl-2-thio-2'-O-methylcytidine	m ⁴ s ² Cm	
N ⁴ -Acetylcytidine	ac ⁴ C	48
5-Methylcytidine	m ⁵ C	23
5-Methyl-2'-O-methylcytidine	m ⁵ Cm	
5-Hydroxymethylcytidine	om ⁵ C	12

TABLE IV (continued)

<i>IUPAC name</i>	<i>One-letter symbol</i>	<i>Index number</i>
<i>Guanosines</i>		
Guanosine	G	3
2'-O-Methylguanosine	Gm	45
1-Methylguanosine	m ¹ G	46
N ² -Methylguanosine	m ² G	49
3-Methylguanosine	m ³ G	
7-Methylguanosine	m ⁷ G	28
N ² ,N ² -Dimethylguanosine	m ² ₂ G	57
N ² ,N ² -Dimethyl-2'-O-methylguanosine	m ² ₂ Gm	
N ² ,N ² ,7-Methyltrimethylguanosine	m ² ₂ m ⁷ G	
Queuosine	Q	40
β-D-Mannosylqueuosine	manQ	41
β-D-Galactosylqueuosine	galQ	42
Xanthosine	X	32
1-Methylxanthosine	m ¹ X	
7-Methylxanthosine	m ⁷ X	
<i>Uridines</i>		
Uridine	U	2
2-Thiouridine	s ² U	33
2-Thio-2'-O-methyluridine	s ² Um	
2-Selenouridine	Se ² U	
3-(3-Amino-3-carboxypropyl)uridine	acp ³ U, (nbt ³ U)	32
3-Methyluridine	m ³ U	37
4-Thiouridine	s ⁴ U	36
2,4-Dithiouridine	s ² s ⁴ U	
4-Thiouridine disulphide	(s ⁴ U) ²	
5-(β-D-Ribofuranosyl)uracil (pseudouridine)	Ψ	6
5-(2'-O-Methyl-β-D-ribofuranosyl)uracil	Ψm	39
5-(β-D-Ribofuranosyl)-N ¹ -methyluracil	m ¹ Ψ	17
5-(2'-O-Methyl-β-D-ribofuranosyl)-N ¹ -methyluracil	m ¹ Ψm	
5,6-Dihydrouridine	hU (D)	5
5-Methyl-5,6-dihydrouridine	m ⁵ hU (m ⁵ D)	
5-Methyluridine	m ⁵ U(T)	30
5-Methyl-2'-O-methyluridine	m ⁵ Um (Tm)	53
5-Methyl-2-thiouridine	m ⁵ s ² U (s ² T)	52
5-Hydroxyuridine	o ⁵ U	11
5-Carboxyhydroxymethyluridine	com ⁵ U	
5-Carboxymethyluridine	cm ⁵ U	7
5-Carboxymethyl-2-thiouridine	cm ⁵ s ² U	
5-Methoxyuridine	mo ⁵ U	34
5-Methoxy-2-thiouridine	mo ⁵ s ² U	55
5-Aminomethyluridine	nm ⁵ U	
5-Aminomethyl-2-thiouridine	nm ⁵ s ² U	
5-Methylaminomethyluridine	mnm ⁵ U	9
5-Methylaminomethyl-2'-O-methyluridine	mnm ⁵ Um	
5-Methylaminomethyl-2-thiouridine	mnm ⁵ s ² U	25
5-Methylaminomethyl-2-selenouridine	mnm ⁵ Se ² U	
5-Carboxymethylaminomethyluridine	cmnm ⁵ U	8
5-Carboxymethylaminomethyl-2'-O-methyluridine	cmnm ⁵ Um	

(continued on p. 14)

TABLE IV (continued)

IUPAC name	One-letter symbol	Index number
5-Carboxymethylaminomethyl-2-thiouridine	cmnm ⁵ s ² U	24
5-Carbamoylmethyluridine	ncm ⁵ U	14
5-Carbamoylmethyl-2'-O-methyluridine	ncm ⁵ Um	
5-Carbamoylmethyl-2-thiouridine	ncm ⁵ s ² U	
5-Methoxycarbonylmethyluridine	mcm ⁵ U	44
5-Methoxycarbonylmethyl-2-thiouridine	mcm ⁵ s ² U	60
5-Methylcarboxymethoxyuridine	mcmo ⁵ U	54
5-Methylcarboxymethoxy-2-thiouridine	mcmo ⁵ s ² U	68
6-Carboxyuridine (Oridine)	c ⁶ U (O)	
Hydroxywybutosine	Y _{OH}	75
Wybutosine	Y _i	76
Wyosine	Y	77

A total of 67 ribonucleosides have been chromatographically and spectrometrically characterized. Their elution time and HPLC-UV spectra are given in Table V, and Fig. 3. With the continuing efforts of scientists in tRNA research we

TABLE V

HIGH-RESOLUTION RPLC ELUTION SEQUENCE OF RIBONUCLEOSIDES

The number below each nucleoside indicates retention time in minutes under our standard chromatographic conditions.

hU, ψ , cm ⁵ U, cmnm ⁵ U, mnm ⁵ U, C, cmo ⁵ U, o ⁵ U, om ⁵ C, ncm ⁵ U, U, m ⁷ I, m ¹ ψ , m ³ C,	4.4	4.6	5.0	5.1	5.4	5.9	6.1	6.4	6.7	7.2	8.4	8.6	9.2	9.4	
om ⁵ U, s ² C, m ¹ A, m ⁵ C, m ⁴ C, cmnm ⁵ s ² U, mnm ⁵ s ² U, 2,5-PCNR, 4,3-PCNR, C _m , m ⁷ G,	9.5	9.6	10.6	11.4	11.9	12.1	12.6	14.6	14.8	15.5	18.0				
I, m ⁵ U, G, acp ³ U, X, s ² U, mo ⁵ U, s ⁴ U, m ³ U, U _m , ψ _m , Q, ^{man} Q, ^{gat} Q, m ¹ I,	18.5	19.8	19.0	20.1	20.4	21.1	21.6	24.0	24.5	25.3	26.9	27.4	28.1	28.7	29.4
mcm ⁵ U, G _m , m ¹ G, ac ⁴ C, m ² G, g ⁶ A, A, m ⁵ s ² U, m ⁵ U _m , mcmo ⁵ U, mo ⁵ s ² U, rA,	29.8	30.4	31.0	32.0	32.4	32.6	33.5	34.4	34.8	35.0	35.8	37.0			
m ² m ² G, mcm ⁵ s ² U, A _m , t ⁶ A, m ² A, m ⁶ A, mcmo ⁵ s ² U, mt ⁶ A, m ⁶ A _m , ms ² t ⁶ A, m ⁶ m ⁶ A,	37.8	39.7	40.1	41.6	45.2	46.2	47.4	48.3	49.4	51.9	56.3				
Y _{OH} , Y _w , cis io ⁶ A, i ⁶ A, cis ms ² io ⁶ A, ms ² i ⁶ A	59.0	65.0	70.0	84.6											

Total: 69 molecules

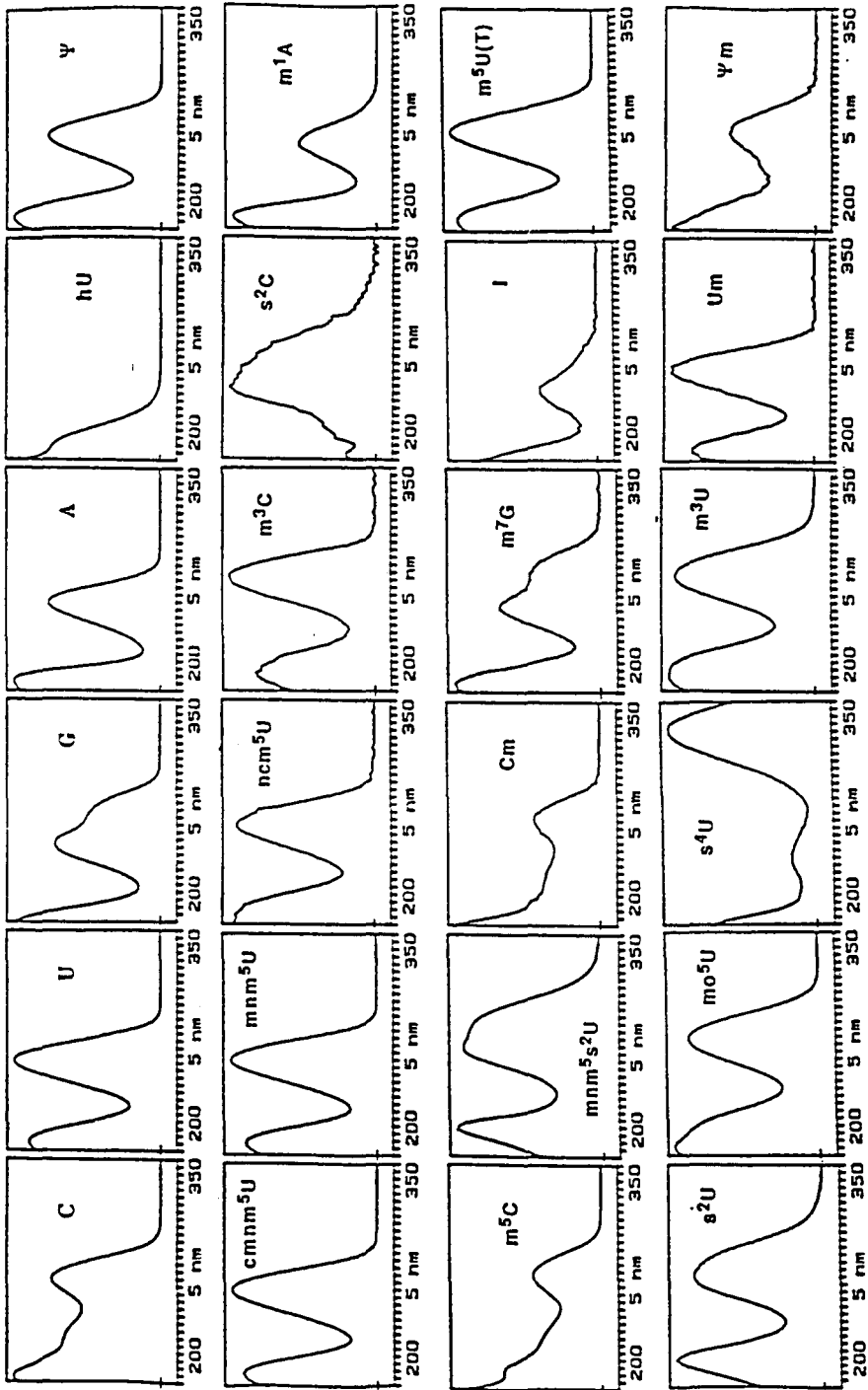
2,5-PCNR is 2-pyridone-5-carboxamide-N¹-ribofuranoside

4,3-PCNR is 4-pyridone-3-carboxamide-N¹-ribofuranoside

Ribonucleosides with elution times not assigned

m¹Am, ms²A, m³A, m¹m³A, ms²m⁶A, o²Am, nc⁶A, mg⁶A, m⁴Cm, s²m⁴Cm, m⁵Cm, om⁴C, m²m²m⁷G, m²I, m¹X, m⁷X, m¹ ψ _m, s²Um, Se²U, s²s⁴U, (s⁴U)², m⁵hU, com⁵U, cm⁵s²U, nm⁵U, nm⁵s²U, mnm⁵Um, mnm⁵Se²U, cmnm⁵Um, ncm⁵Um, c⁶U, 2-ribosylguanine, and 2,4-diaminopyrimidine nucleoside

Total: 33 molecules



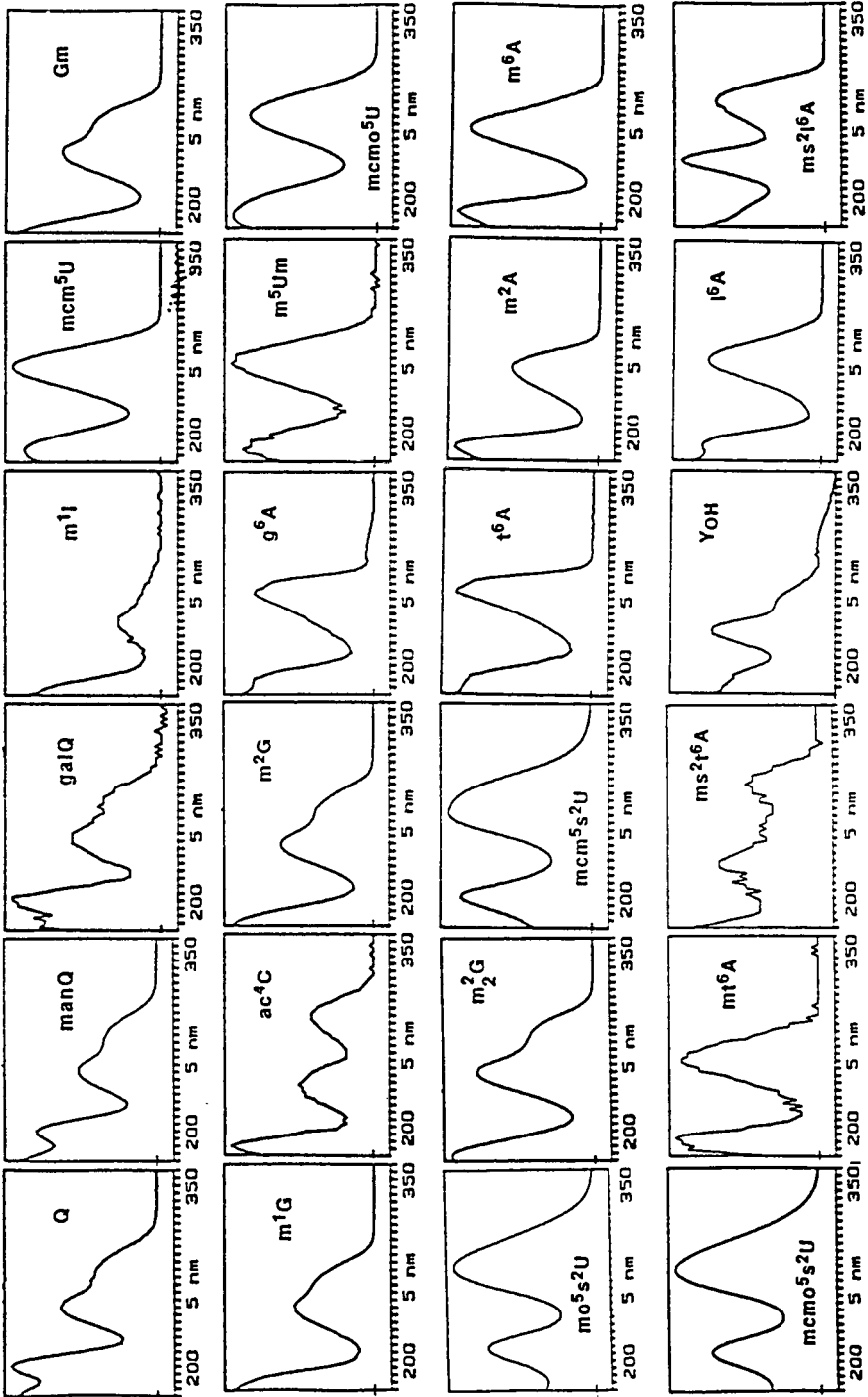


Fig. 3. HPLC-UV spectra of reference nucleosides.

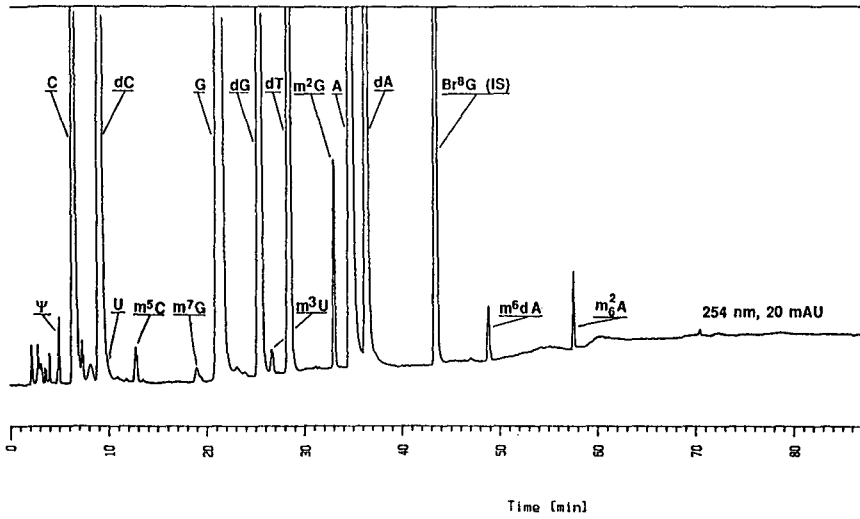


Fig. 4. HPLC of nucleosides in *E. coli* 16S ribosomal RNA.

believe that most of the remaining nucleosides will soon be identified and characterized.

Ribosomal RNA nucleoside analysis

Ribosomal RNA (rRNA) is a high-molecular-weight RNA. In *E. coli*, 70S rRNA has a molecular weight of $2.75 \cdot 10^6$ a.m.u. and the small subunits, 16S rRNA, and 23S rRNA have 1542 residues and 4718 residues, respectively. Only ten methylated nucleosides have been identified in the 16S and 23S rRNAs²⁸⁻³⁰. For composition analysis of rRNA it is necessary to separate and measure one modified

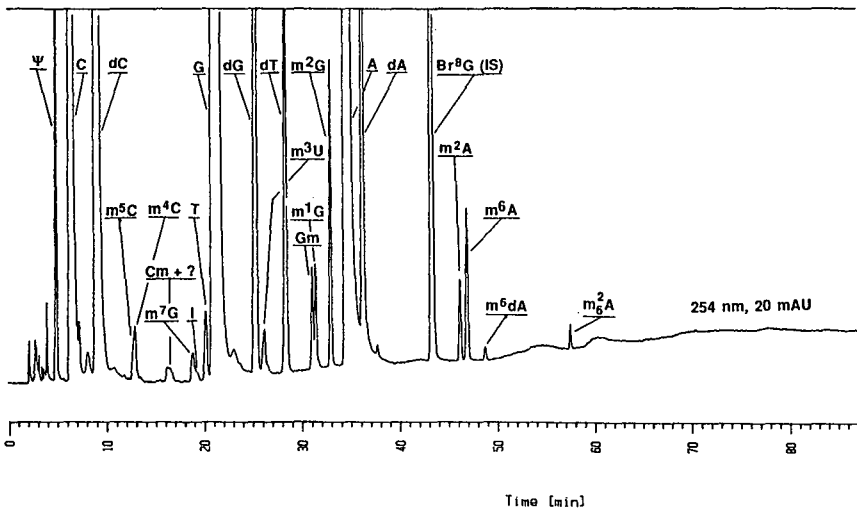


Fig. 5. HPLC of nucleosides in *E. coli* 23S ribosomal RNA.

nucleoside residue in *ca.* 5000 nucleotides. This demands high chromatographic column capacity for rRNA composition analysis, in order that a large amount of sample (100 μ g or more) can be injected without loss of chromatographic resolution. The chromatographic protocol we have described for tRNA nucleoside composition analysis has an adequate capacity range to meet this requirement for rRNA analysis.

Samples of 16S and 23S rRNA were obtained from Drs. Ebel and Ehresmann (IBMC, Strasbourg, France) and analyzed by RPLC in our laboratory. The chromatograms are presented in Figs. 4 and 5, and the quantitative results are presented in Table VI. Deoxyribonucleosides were found in the enzymatic hydrolysates of both of the rRNA samples, however their presence does not interfere in the measurement of any known modified ribonucleoside. Some interesting observations were noted, in that by RPLC we found qualitative and quantitative differences of modification in both 16S rRNA and 23S rRNA as compared to the literature values. In 16S rRNA we found one additional residue of Ψ , m⁵C, and m²G; and two nucleosides, Gm and m⁴Cm, were not found by RPLC. From 23S rRNA, four additional Ψ , two of m⁴C, one of m⁵U, two of m²G, and one of m²A were found by RPLC. A number of other modifications as shown in Table VI were in agreement with the literature values.

TABLE VI
HPLC QUANTITATION OF NUCLEOSIDES IN *E. coli* 16S AND 23S RIBOSOMAL RNA

	16S rRNA		23S rRNA	
	HPLC	Lit. ^a	HPLC	Lit. ^b
<i>Nucleosides (mol-%)</i>				
C	23.0	22.8	22.2	
U	20.9	20.4	20.4	
G	30.4	31.6	30.7	
A	25.1	25.2	26.0	
	99.4	100.0	99.3	
<i>Residues/mol</i>				
ψ	1.3	0.0	7.8	3.0
m ⁵ C	2.0	1.0		
m ⁴ C			1.9	0.0
m ⁷ G	0.5 ^c	1.0	0.7 ^c	1.0
Cm+?			0.9	1.0
T			1.7	1.0
m ³ U	0.8	1.0	0.9	1.0
Gm	0.0	1.0	0.9	1.0
m ⁴ Cm	0.0	1.0		
m ¹ G			0.8	1.0
m ² G	2.9	2.0	2.3	0.0
m ² A			0.9	0.0
m ⁶ A			2.1	2.0
m ² ₂ A	1.6	2.0	0.2	0.0

^a Literature values from ref. 29.

^b Literature values obtained from ref. 30.

^c m⁷G is partially lost during hydrolysis (a sensitive molecule).

^d The 210-nm signal was examined; no hU was observed.

Applications of RPLC-UV nucleoside analysis to biochemical and biomedical investigations

We have applied the RPLC-UV nucleoside methodology to many interesting research investigations. Some examples are presented with detailed information described in the cited references. The high-sensitivity and selectivity of RPLC of nucleosides allows detection of a change of a single modification in a mixture of unfractionated tRNAs. Thus, this technique is a very powerful research tool for detection of modification differences in parental-mutant tRNAs. In collaboration with Professor J. Kohli at the University of Bern, a set of antisuppressor mutants of *S. pombe* were investigated; these mutants have been assigned to different non-tRNA genes which are candidates for defects in tRNA modification. This set of mutants was subjected to an extensive tRNA screen by the laborious RPC-5 chromatography which resulted in the identification of only a single modification defect (deficiency of isopentenyladenosine). A new search was conducted in our laboratory on the same set of mutants with the RPLC-UV method which revealed altered tRNA modification patterns in five additional strains. Most interesting was the antisuppressor mutant *sin3*, in which the tRNA is devoid of 5-methoxycarbonylmethyl-2-thiouridine (mcm^5s^2U). This modification change in the tRNA indicates a defect in the sulfur transferase enzyme that introduces the 2-thio group in this hypermodified uridine which is often found in the wobble position of anticodons^{31,32}.

The effect of physiological stresses on post-transcriptional modification changes in tRNAs was studied with Drs. P. Staheli and R. Hutter of the Microbiology Institute in Zurich. From the results of RPLC nucleoside analysis, a 2'-O-methylguanosine (Gm)-deficient tRNA^{Trp} was identified in tryptophan-limited *Saccharomyces cerevisiae*³³.

In another study with Dr. P. Agris of the University of Missouri, we measured the *in vivo* incorporation of [¹³C₂]adenine, and [¹³C₂]uracil in RNA using RPLC and mass spectrometry. This study demonstrated that the position and amount of incorporation of ¹³C from specific nucleic acid precursors could be identified using only micrograms of RNA. The information is important in NMR studies of nucleic acid conformation and biosynthesis³⁴.

Using the RPLC-UV method, we determined the precise nucleoside composition of a wide range of purified tRNAs. The nucleoside composition data were used to complement and confirm tRNA sequence results. We have analyzed tRNAs from many researchers, especially a large number of bacterial, yeast, and mammalian isoaccepting tRNAs provided by Dr. G. Keith of the Institut de Biologie Moleculaire et Cellulaire, Strasbourg³⁵. New information on a number of known and unknown modified nucleosides were obtained (Figs. 6-8 and Table VII). In collaboration with Dr. T.-W. Wong of the University of Illinois on a study of tRNA thiolation in normal and cancer mammalian cells, two new tRNAs, a glutamate tRNA and a glutamine tRNA, both containing a large number of modifications were sequenced with the aid of our RPLC composition data^{36,37}.

The high-resolution, high-speed, and non-destructive nature of the RPLC-UV nucleoside method have been widely applied in the isolation of unknown modified nucleosides in RNAs and body fluids for structure elucidation³⁸⁻⁴⁰. In a collaborative study with Dr. G. Dirheimer of Strasbourg and Dr. J. McCloskey of the University of Utah, 5-carboxymethylaminomethyluridine ($cmnm^5U$) was identified in mito-

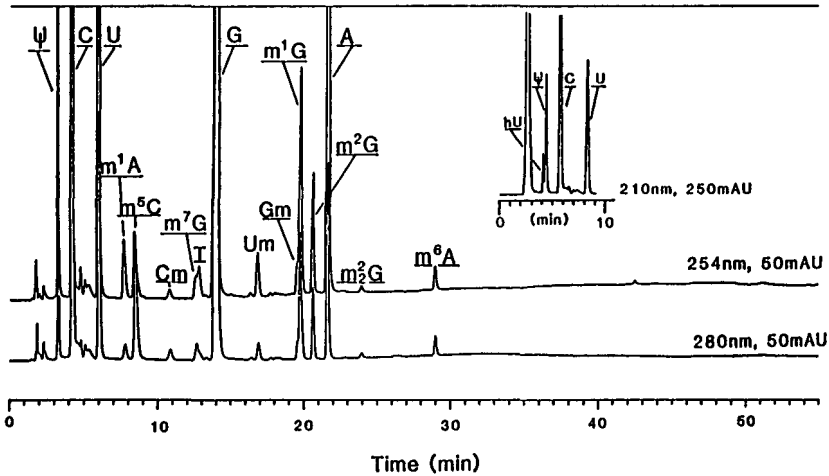


Fig. 6. HPLC of nucleosides in tRNA^{Pro} from bovine.

chondrial tRNA^{L^{eu}}. In studies with Dr. M. Ehrlich of Tulane University, N⁴-methyldeoxycytidine was identified in thermophilic bacteria⁴¹. With Dr. J. Desgrès of the University of Dijon and Dr. G. Keith of Strasbourg, several modified nucleosides were identified in tRNAs and body fluids; in particular, 5-carbamoylmethyluridine (ncm⁵U) in yeast and bovine prolyl tRNA_(U*GG)³⁵, also, a new major RNA metabolite, 5-hydroxymethylcytidine (om⁵C) was found in canine serum⁴².

A most unique and interesting new identification is a dinucleoside N₁pN₂ located at positions 64 and 65 in the T-Ψ stem of yeast methionine initiator tRNA and which is resistant to hydrolysis by nuclease P1 and T₂-RNase. We confirmed the structure of the N₂ nucleoside by RPLC retention and the UV spectrum as guanosine.

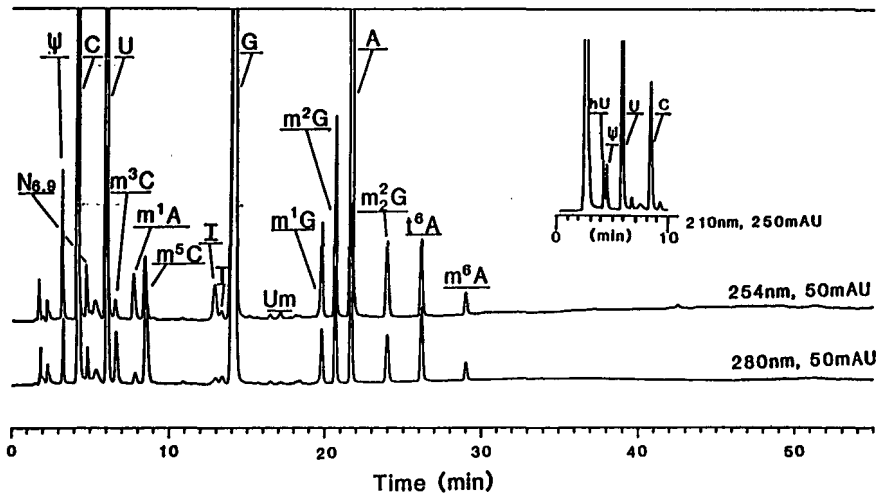


Fig. 7. HPLC of nucleosides in tRNA^{Thr} from bovine.

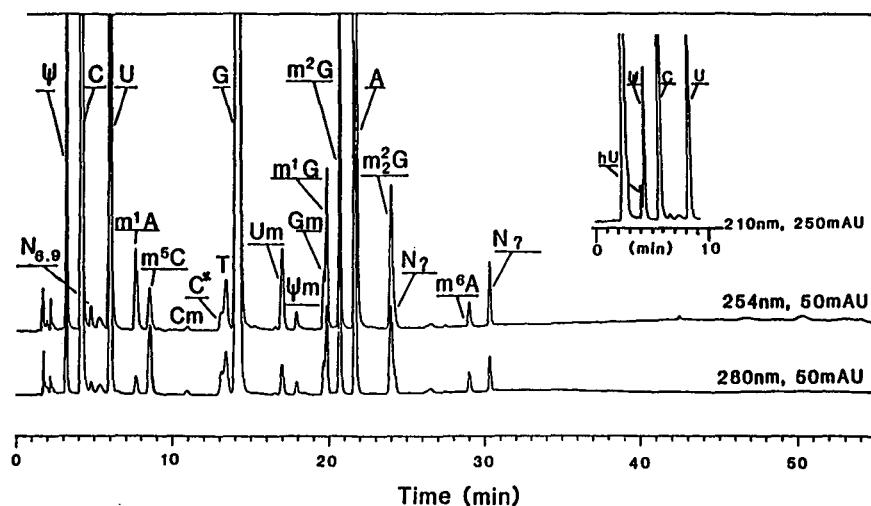


Fig. 8. HPLC of nucleosides in tRNA^{Leu} from bovine.

The structure of the N₁ nucleoside was characterized as a phosphorylated 9-(2'-O-ribose-β-D-ribofuranosyl)-adenine by RPLC-UV, mass spectrometry and on comparison with O-riboseadenosine obtained from biosynthetic poly-adenosine diphosphate ribose. The exact position of the phosphate group is not known and still under our investigation^{24,42}.

In research with Dr. T. Heyman of the Institut Curie, and Drs. F. Salvatore and F. Esposito of the University of Naples⁴², we found the mole percent values of nucleobase-methylated nucleosides in the tRNAs from Rous sarcoma virus-transformed chicken embryonic fibroblast cells (RSV-CEF) were 50–120% higher than in the tRNAs from non-transformed chicken embryonic fibroblast (CEF) cells. In addition, the amount of 2'-O-methylated nucleosides and threoninocarbonylated modified adenosine were only elevated about 10% in RSV-CEF cells over the CEF cells. Experiments are underway to study the tRNA turnover rates in CEF and RSV-CEF cells. It would also be interesting and important to see the changes in modified nucleosides that are related to the changes in the distribution of isoaccepting tRNAs in the CEF and RSV-CEF cells.

We have studied the modification differences in human normal tissue and cancer tissue tRNAs in collaboration with Dr. R. Trewyn of the Ohio State University⁴². Transfer RNAs from normal and cancerous human breast, stomach, and colon tissues were extracted and twenty nucleosides in each tRNA were quantified by our RPLC-UV method. The nucleobase-modified nucleosides in the tRNAs from cancerous breast and stomach tissues were *ca.* 40–100% higher than in the tRNAs from the respective adjacent normal tissues. Further, the mol-% values for the four 2'-O-methylated nucleosides were *ca.* 40–60% lower in the tRNA of the cancerous tissue. In a comparison of tRNAs from normal and cancerous colon tissue, no significant differences were observed in the mol-% values of all the modified nucleosides. The observed increase in nucleobase-modified nucleosides in tRNAs from cancerous breast and stomach tissues are in agreement with the results observed in

TABLE VII
HPLC OF NUCLEOSIDE COMPOSITION IN BOVINE ISOACCEPTING tRNAs

nd = Not detected. nc = not calculated.

Nucleoside	Mol-% of nucleosides			
	<i>Pro-tRNA</i>	<i>Lys-tRNA</i>	<i>Thr-tRNA</i>	<i>Leu-tRNA</i>
C	24.1	25.0	23.4	23.6
U	12.8	10.9	14.1	14.8
G	27.6	27.8	24.7	22.9
A	14.9	15.9	16.1	17.6
hU	3.08	3.97	4.21	nc
ψ	5.92	6.35	2.46	4.98
ncm ⁵ U ^a	nd	nd	nd	2.84
m ³ C	nd	1.36	1.05	nd
m ¹ A	1.07	0.94	0.94	1.12
m ⁵ C	3.48	0.32	3.31	1.19
Cm	0.35	0.05	0.90	nd
m ⁷ G	0.39	0.05	0.01	nd
I	0.73	0.01	0.95	1.30
m ⁵ U(T)	nd	1.21	0.04	1.20
Um	0.99	0.11	0.04	1.19
Gm	0.38	0.01	1.10	0.43
m ¹ G	2.65	1.30	1.17	1.12
ac ⁴ C	nd	nd	nd	0.82
m ² G	1.13	1.97	2.33	2.35
m ₂ ² G	0.08	0.15	1.11	1.19
t ⁶ Ä	nd	2.00	2.17	nd
m ⁶ A	0.42	0.42	0.44	0.10
N ₁ ^b				0.60
N ₂ ^c				nc
Total	100.5	99.72	100.5	99.33

^a ncm⁵U was calculated using factor of U.

^b N₁ is an unknown nucleoside. Probably a modified A.

^c N₂ is an unknown nucleoside. Probably a modified C.

collaborative studies with Dr. T. Heyman at the Curie Institute of tRNAs from CEF and RSV-CEF cells⁴³. In the experiment with Dr. Heyman, the purine and pyrimidine bases in the RSV-CEF cells were highly modified as compared to the CEF cells from lymphomatosis-free embryos of brown leghorn, Edinburgh strain. This may imply that the tRNA differences observed in normal and diseased breast and stomach tissues is related to the cancer and not to different cell types. The lower ribomethylated nucleoside levels observed in the tRNAs in cancerous breast and stomach tissue and not observed in transformed cells in culture may be due to insufficient methyl donor in the tissues, which was in excess in the cell culture medium⁴³. The altered levels of modified nucleosides observed in tRNAs from cancerous breast and stomach tissues but not in tRNA from colon tissue, can perhaps be explained by the rate of cell growth. In breast and stomach tissue the respective cancer cells have a much higher rate of division as compared to normal cells; whereas, in colon tissue the normal and cancer cells are both rapidly dividing.

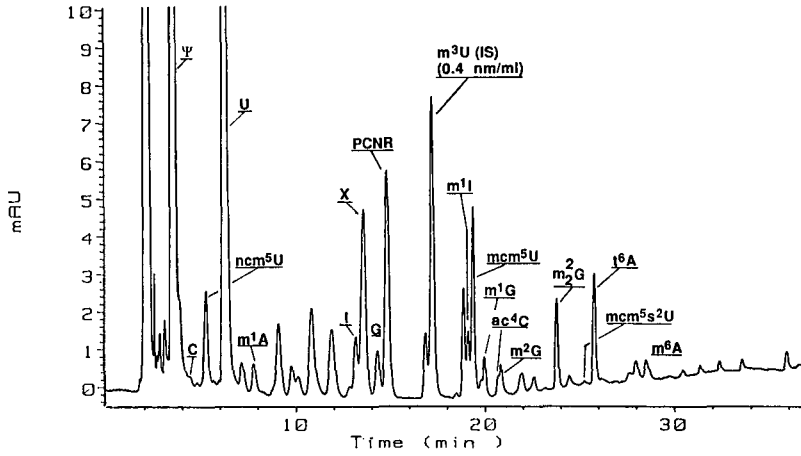


Fig. 9. RPLC separation of nucleosides in serum from patient with acute myelogenous leukemia (ref. 20).

Quantitative analysis for ribonucleosides in urine and serum is one of the major research areas in our laboratory. Only nine modified nucleosides were quantitatively analyzed by the RPLC method that we published in the late 70's^{5,6,45}. At the conference on modified nucleosides and cancer at Freiburg¹³, we reported on the RPLC analysis of six nucleosides from pooled normal serum. In 1986, we improved the methodology for modified nucleosides in serum and urine and with this new method more than 35 known nucleosides and unidentified nucleosides can be measured in 35 min (Figs. 9 and 10). We have used this new method in a number of studies^{20,44,46-49}.

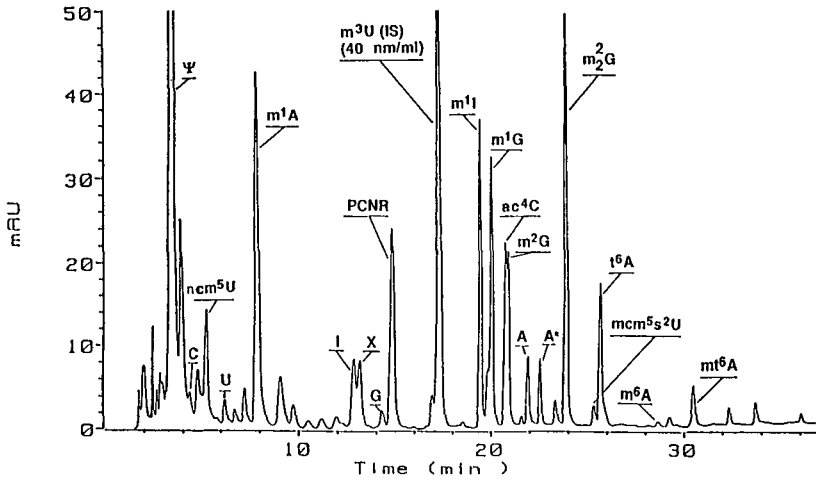


Fig. 10. RPLC separation of nucleosides in normal human urine (ref. 20).

Instrumentation

The advantages of HPLC are not solely determined by the high-performance of the column and separation parameters, as the specifications and limitations of the instrumentation is an integral part of HPLC. In the following section the requirements of basic instrumental components that are needed for nucleoside analysis are discussed. Several companies manufacture high quality HPLC instruments but there are some significant differences among them. The user should be aware of the specifications, limitations, and performance of the commercial instruments for nucleoside analysis so that proper selections can be made.

Injector. A variable-volume injector capable of injecting sample volumes from 5 to 200 μl with high precision and accuracy should be used. Although a manual injector may be used, an automated injector is much preferred, as automated recycling of the chromatographic system is not only more efficient, but also improves the precision of analysis.

Solvent delivery system. A ternary solvent delivery system capable of generating at least eight linear multi-gradient steps is necessary. Accurate flow-rate, low pulsation, and low dispersion volume are essential. At a flow-rate of 1.0 ml/min the gradient delay time should not be more than 1.5 min. Otherwise, the time for each of the gradient steps will require readjustment. The gradient delay time (which can be empirically determined) is defined as the time required from the formation of the elution gradient, before or after the pump, to traverse the injector, connecting tubing (not including the column) and to be observed by the detector.

Temperature-controlled column oven. It is essential to have a temperature controlled column oven which is capable of maintaining a constant temperature at $26 \pm 0.2^\circ\text{C}$. Most commercially available ovens have difficulty in controlling the temperature at this setting, with the exception of those ovens which have a cooling device. Ovens using contact heating and operated in an air conditioned room where the temperature is maintained at lower than 22°C can also be used. A column temperature of 26°C is needed for the separation of the thymidine (T) and guanosine (G) peaks. The narrow ($\pm 0.2^\circ\text{C}$) temperature range is necessary to achieve reproducibility of retention times. Also, preheating the elution solvent is recommended.

Detector. A photodiode-array detector is highly recommended; however, a dual-wavelength UV detector will suffice. The ability to monitor at 254 and 280 nm simultaneously is important for highly accurate analyses.

Computer. The computer controls the injector, solvent delivery system, and detector, thus allowing the integral components to function as a unitized system. It should be able to collect, integrate, and store data as well as provide hard copies of reports and graphics. The computer should be capable of performing post-run integration which is one of the very important requirements for quantitative analysis.

Several commercial companies manufacture instruments capable of meeting the requirements for the HPLC of nucleosides. Although these instrument are capable of performing nucleoside analysis, there are some significant differences among them. The user needs to know the specifications, performance, and limitations of the instruments so that the proper selection can be made to meet the user's need and above recommendations.

It is suggested that the user analyze a performance sample of reference unfractionated tRNAs from *E. coli*, yeast or calf liver and compare that separation and

sensitivity with our chromatography. In a broader perspective (and in AOAC terms) this is defined as “proficiency testing”, or as a systematic testing program in which uniform known samples are analyzed in different laboratories, or a random series of uniform samples are analyzed to assess the accuracy of an analytical method in measuring the analyte(s).

We propose and recommend an interlaboratory sample testing program to: (i) provide a measure of the precision and an estimation of the accuracy of the nucleoside chromatographic method in other laboratories, (ii) identify weak procedural steps, poor instrumentation performance and chromatography, (iii) detect and provide training needs, and (iv) upgrade the overall quality of laboratory performance.

Chromatographic columns

The chemical nature of the bonded phase, the percent carbon loading, type of silica, silica particle size, porosity, silanol surface deactivation and column packing technique are all significant factors affecting the capacity factor, efficiency and selectivity of the chromatography. For nucleoside separation, a column with C₁₈ (ODS) bonded to 5 μm spherical silica beads is the most suitable for high column efficiency and capacity.

To ensure that columns from different production lots have the required repeatability, reproducibility, selectivity, and resolution, we have developed a “nucleoside column” (Supelcosil LC18S) in collaboration with Supelco. This column has excellent efficiency and selectivity for nucleosides; also it is surface deactivated and gives the needed separation and peak symmetry for the basic nucleosides. The effective column efficiency, N_{eff} , was calculated from $N_{\text{eff}} = 5.5(t'/w)^2$ for four randomly selected nucleoside columns using uridine (U) and guanosine (G) as the test compounds. The average column efficiency was 4800 ± 700 plates per column (19 000 plates/m) for U, and 7700 ± 1100 plates per column for G (31 000 plates/m). The height equivalent for a theoretical plate (HETP) was 0.052 mm and 0.033 mm for U and G, respectively. Compared to our previously reported values⁴⁵ using a very popular other commercial source ODS column, the HETP obtained was 0.105 mm for U and 0.102 mm for G. Thus, our “nucleoside column” displays more than a two-fold increase in efficiency as compared to the column that we reported earlier.

The repeatability and reproducibility of nucleoside retention times on the nucleoside columns were evaluated on a “run-to-run” and “column-to-column” basis (Table VIII). The relative standard deviation (R.S.D.) of the retention time for each of 26 nucleosides in a hydrolysate of unfractionated calf liver tRNAs were calculated from five runs on one column, and from one run each on ten columns. Excluding three positively charged nucleosides, m³C, m¹A and m⁷G, the range of retention R.S.D. is 0.120–0.556% for “run-to-run” and 0.549–1.02% for “column-to-column”. The positively charged nucleosides, m³C, m¹A and m⁷G give higher R.S.D. as the retention of these three nucleosides are subjected to two types of retention mechanisms, hydrophobic and ionic interaction. Their retention is very sensitive and subject to surface deactivation and equilibration of the column between runs.

Chromatographic parameters

Controlled ionization of the nucleosides in the mobile phase is the most important factor in determining the separation of the large number of chemically

TABLE VIII
REPEATABILITY AND REPRODUCIBILITY OF THE NUCLEOSIDE COLUMNS

Nucleoside	Relative standard deviation (%) ^a	
	Run-to-run ^b	Column-to-column ^c
hU	0.282	1.021
ψ	0.388	0.999
C	0.419	1.149
ncm ⁵ U	0.463	1.475
U	0.387	1.893
m ³ C	1.594	1.760
m ¹ A	1.619	1.867
m ⁵ C	0.494	1.687
Cm	0.503	1.664
m ⁷ G	1.544	1.685
T	0.420	1.590
G	0.520	1.586
Um	0.335	1.142
ψm	0.312	0.906
Q1	0.508	0.769
Q2	0.556	0.946
m ¹ I	0.248	0.853
Gm	0.208	0.803
m ¹ G	0.211	0.766
m ² G	0.192	0.683
A	0.155	0.700
Tm	0.122	0.632
m ² G	0.120	0.713
mcm ⁵ s ² U	0.324	0.765
t ⁶ A	0.233	0.767
m ⁶ A	0.144	0.549

^a R.S.D. (%) for retention time of each nucleoside in minutes.

^b Five runs from one column.

^c One run each from ten columns.

diverse nucleosides. This requires the use of secondary chemical equilibria of the nucleosides in the mobile phase to achieve the desired chromatographic selectivity. Thus, factors affecting ionization such as mobile phase pH, type and concentration of organic modifier, type and concentration of buffer salts, and column temperature were investigated and are discussed^{45,50}.

Mobile phase pH. Changes in the pH of the mobile phase gave predictable variation in the RPLC retention of organic acids as reported by Horváth *et al.*⁵¹. Also, changes in pH give predictable variations in retention of nucleosides. At a given pH, the nucleosides behave as either weak acids, weak bases, or neutral molecules. A slight change in pH will cause characteristic changes in their retention times. An increase in the pH of the mobile phase reduces the positive charge on the basic nucleosides and increases the negative charge on acidic nucleosides. Thus, the basic nucleosides become less ionic, the retention time is increased, and the acidic nucleosides become more ionic, and the retention time is decreased, whereas the neutral nucleosides will elute at the

same time. A slight decrease in pH will cause the opposite effect. The magnitude of the change in the retention time is directly proportional to the degree of acidity or basicity of the molecule⁵¹. The change in retention can be quite large when the pH of the buffer is near the pK_b value of the nucleoside. Changing the pH of the elution buffers is one of the most useful approaches to search for small quantities of modified nucleosides co-eluting with one of the major nucleosides. In this case the use of peak convolution software does not work well when the ratio of the two co-eluted peaks is 20 to 1 and the differences in their spectra are not sufficiently large. In many cases, by making a slight change in the pH of the elution buffer, the co-eluted modified nucleosides often can be separated. As example, in the analysis of *E. coli* tRNA^{val}, the co-eluted peaks of 5-carboxymethoxyuridine (cmo⁵U) and cytidine (C) did not separate at pH 5.3 (Fig. 11a) but when the pH was decreased to 4.0 the more acidic cmo⁵U eluted later and gave baseline separation from C (Fig. 11b).

Organic modifiers. We have studied methanol and acetonitrile as organic modifiers. Compared to methanol, acetonitrile offers approximately twice the elution power for nucleosides, but there is not a significant difference in selectivity for separation of the nucleosides. The higher elution power of acetonitrile for nucleosides

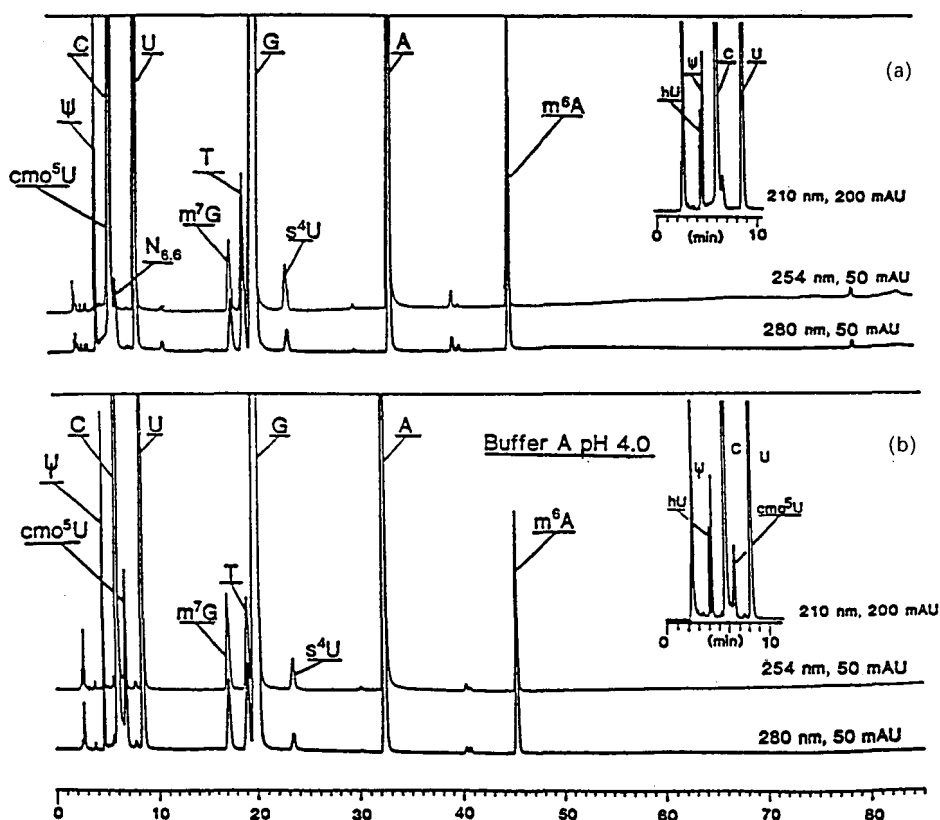


Fig. 11. HPLC of *E. coli* tRNA^{val}, pH 5.3 (a) and 4.0 (b). The effect of mobile phase pH on the RPLC selectivity of nucleosides.

is due to its competition for hydrogen bond formation with column silanol groups. The solvent selectivity of methanol–water *vs.* acetonitrile–water was studied by Tanaka *et al.*⁵² and Bakalyar *et al.*⁵³. Our findings with modified nucleosides agree with their reported results, that hydroxy, methoxy, ketone, and methyl ester-substituted aromatics have little or no difference in selectivity when using methanol–water or acetonitrile–water. We used methanol as the organic modifier in the first two elution buffers as methanol is inexpensive, can be purchased in a highly purified grade, and has a long shelf-life. For the third eluting buffer we chose acetonitrile as the organic modifier taking advantage of its low UV cut-off and high-elution power, minimizing a rising baseline in the latter part of the chromatographic analysis. The highest purity grade of methanol and acetonitrile should be used, and the acetonitrile should be stored no more than two to three months. On longer storage, acetonitrile forms a low level of polymers that causes pump check valves to stick and not function properly. We have examined the residue after evaporating aged acetonitrile by direct probe electron impact–mass spectrometry (EI–MS), and the residue appears to be a high-molecular-weight acrylic-type polymer.

The chromatographic selectivity of nucleosides as a function of methanol concentration was first reported by us⁴⁵. The retention of nucleosides decreased with an increase in concentration of methanol. Of the seventeen nucleosides we investigated, the rates of decrease of the retention of nucleosides can be placed into three groups. The decreased retention of the nucleosides were all in a semi-logarithmic relationship with an increase in concentration of methanol. These data facilitated our selection of the gradient step times and gradient ramp slopes to achieve effective separation of a large number of modified nucleosides that are difficult to separate. The concentration of methanol changes the partition distribution and ionic equilibrium of the nucleosides; it also alters the hydrophobic interaction of the nucleosides in the C_{18} phase and/or the solvation of the nucleoside in the mobile phase. In general, methanol selectivity is seen within each of four major nucleoside families. (*i.e.* each major nucleoside and all of its respective modifications).

In our studies on capacity factors as a function of methanol concentration it was found that in most cases, purines have a larger $-[dk'/d(\text{CH}_3\text{OH}\%)]$ than the pyrimidines. Those nucleosides with more methyl modification or less hydroxyl functional groups will also have a larger $-[dk'/d(\text{CH}_3\text{OH}\%)]$. The methanol selectivity is illustrated in Fig. 12 which shows the separation of m^1G , G_m , and m^2G using 5 and 15% methanol in the elution buffer consisting of 0.01 M $\text{NH}_4\text{H}_2\text{PO}_4$ (pH 5.1) in an isocratic mode. The elution order of G_m , m^1G and m^2G is changed to m^1G , G_m and m^2G when the methanol concentration of the elution buffer is increased from 5 to 15%. The difference between these three modified guanosines is the position of the methyl group, with G_m less polar than m^1G and m^2G . Increasing the methanol concentration in the elution buffer from 5 to 15% inverts the elution order of G_m and m^1G and keeps the relative elution position of m^1G and m^2G essentially the same. This indicates that m^1G and m^2G have larger $-[dk'/d(\text{CH}_3\text{OH}\%)]$ values than G_m . This observation is generally true in reversed-phase separation; for example, Colin and Guiochon⁵⁴ reported that with a C_{18} column the retention of benzene relative to the retention of phenol was increased from 3 to 5 when the methanol concentration in the eluent was increased from 20 to 50%. Under our standard separation conditions we compromise the separation between G_m and m^1G so that we can obtain the separation

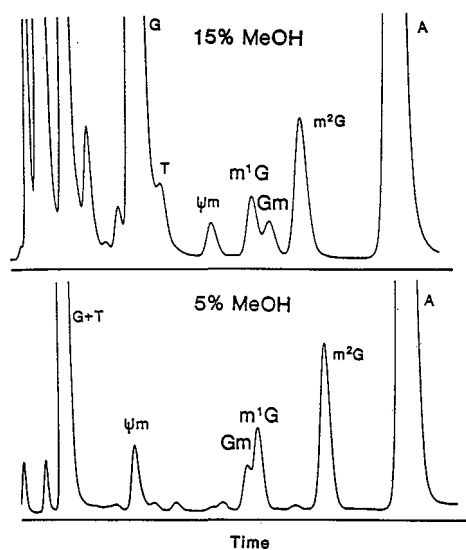


Fig. 12. Methanol (MeOH) selectivity in HPLC nucleoside separation.

of ac^4C and m^2G . If the separation of ac^4C and m^2G is not of concern, then separation of G_m and m^1G can be improved by increasing the slope of the gradient ramp between 20 and 36 min.

Buffer salts. $NH_4H_2PO_4$ was used as buffer salt based on its low UV cut-off (molar absorptivity <0.01 at 195 nm) and its higher solubility as compared to the potassium or sodium salts. The low molarity (0.01 M) solution that we selected was to minimize the UV interference from possible contaminants in the salt and to reduce instrument down time. Buffers with high salt concentrations will decrease the column longevity and shorten the life of the pump parts, thus requiring more frequent repairs of the pump seals, plunger, and valves. The ammonium phosphates have very low buffer capacity between pH 4 and 6. Our chromatography protocols which give the narrow nucleoside peaks with good peak symmetry indicates that pH is of major importance, but that a large buffer capacity is not required. The use of higher concentrations (0.05–0.20 M) of other salts, such as ammonium acetate or ammonium formate, improves the peak symmetry and retention time reproducibility for the basic nucleosides by masking the active sites on the column packing. These organic salts are also volatile and can be removed by vacuum evaporation to obtain a salt-free nucleoside in the eluate. However, in general, phosphate buffers provide superior column efficiency as compared to acetate buffers, and the UV absorptivity of acetate and formate buffers are much greater than the phosphate buffers. The high UV absorption gives high chromatographic background, thus causing an unstable baseline resulting in poor precision and accuracy of measurement and a decrease in sensitivity of detection.

Column temperature. Column temperature is a very important parameter, as increasing column temperature reduces the retention time and column pressure. More important, a higher temperature will increase column efficiency due to an increase in the diffusivity of the solutes and an increase in the rate of mass transfer. A constant

column temperature is essential to maintaining reproducibility of retention time, and an optimum column temperature is needed to achieve the best separation. In our studies on the relationship of column temperature *versus* elution of nucleosides we found a temperature-dependent selectivity and a linear relationship of $\log k'$ *versus* temperature⁴⁵. In a study of seventeen nucleosides, we found that the nucleosides fall into one of three different $-(dk'/dT)$ groups. In general, a larger solute molecular weight results in a greater $-(dk'/dT)$. Purines, in general, have larger $-(dk'/dT)$ values than pyrimidines. The nucleosides inosine, ribothymidine, and guanosine represent a group that is very difficult to separate. As we have demonstrated in Fig. 13, the relative elution positions of these three nucleosides can be achieved by simply changing the column temperature.

Optimized chromatographic separation systems

Three RPLC separation methods have been developed to accommodate most of the needs for major and modified ribonucleoside analysis with respect to resolution, speed, and sensitivity. Columns with different dimensions (length and inside diameters) are used for each method. Other chromatographic parameters as elution buffers and temperature are unchanged. When columns of different inside diameters are used, the volumetric flow-rate is adjusted proportionally to maintain an identical linear flow-rate. When the column length was changed, the gradient step times were changed in direct proportion to the length of the columns. The details of the three chromatography systems are as follow.

High-resolution chromatography method. A 250×4.6 mm Supelcosil LC-18S "nucleoside column" is used. This system is used either for RNA samples that have a larger number of modified nucleosides, or to separate nucleosides with similar

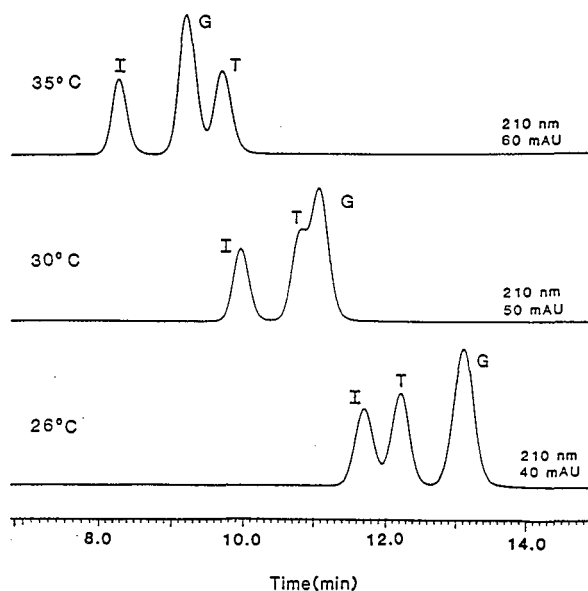


Fig. 13. Temperature selectivity in HPLC nucleoside separation.

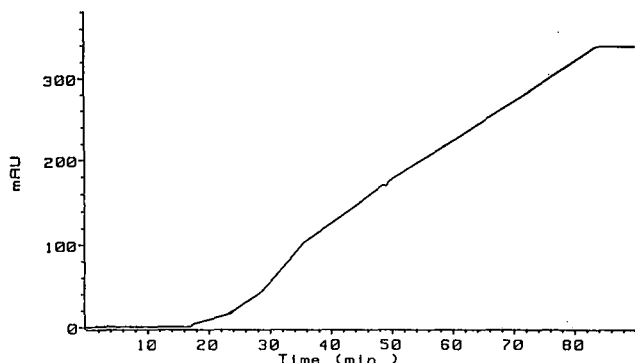


Fig. 14. Simulated high-resolution chromatography elution-gradient curve monitored after the column.

separation factors. A large sample (more than 100 μg) is needed for composition analysis of rRNAs, thus analyses of RNA are made using this system because of the need for high column-loading capacity. Also, because of its high-resolving power, this system was used for the characterization of the nucleosides in the three unfractionated reference tRNAs. Table I presents the detailed gradient steps and compositions of the three elution buffers used, and Fig. 14 shows the actual gradient obtained after the column. To determine the actual gradient, we used 100% methanol, 0.25% acetone in methanol, and 0.75% acetone in methanol, in place of buffers A, B, and C and monitored the eluate at 254 nm signal. In this way, the HPLC system can be monitored with respect to the true gradient delay time, slope of gradient ramps, pulsation of the pump, and mixing of the buffer: all can be detected by this test. Fig. 15 demonstrates the high-resolving power of this system for an enzymatic hydrolysate of unfractionated calf liver tRNA.

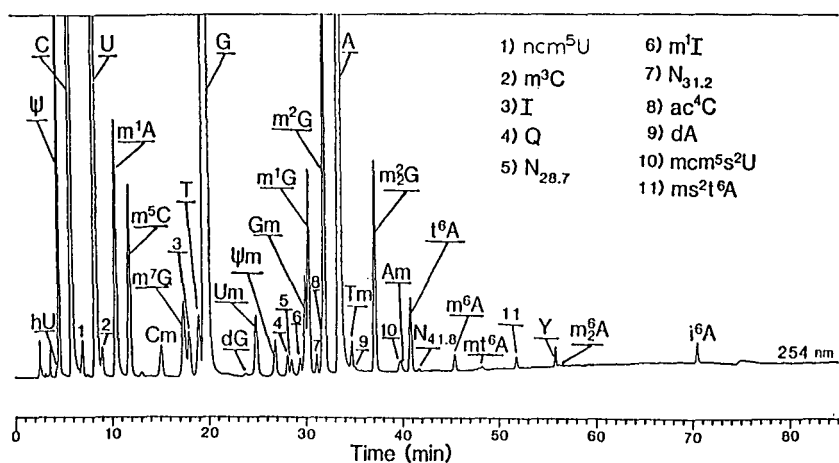


Fig. 15. HPLC of nucleosides in unfractionated calf liver tRNAs using high-resolution chromatography.

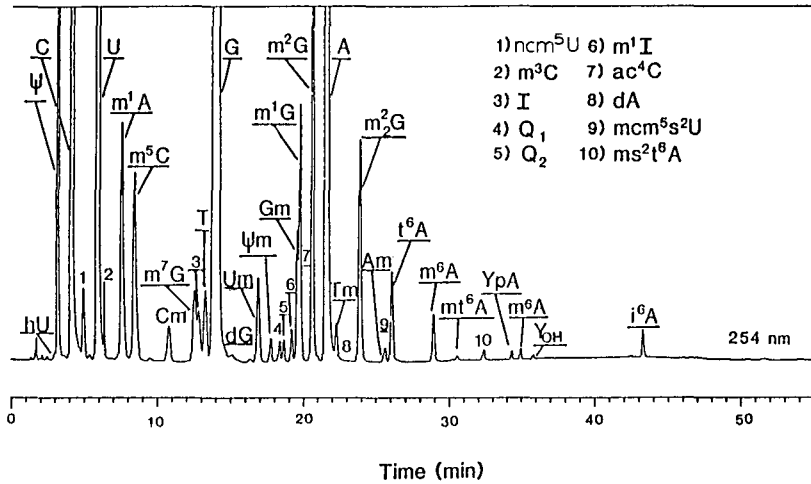


Fig. 16. HPLC of nucleosides in unfractionated calf liver tRNAs using high-speed chromatography.

High-speed chromatography method. This separation method is well suited to separate partially purified tRNAs, single species pure isoaccepting tRNAs, and ribonucleosides that have been isolated from physiological fluids by boronate affinity gel. This system has two distinct advantages. The run time is 35 min less than the high-resolution method and the sensitivity (signal-to-noise ratio S/N) is increased by 170% over the high-resolution method. A 150×4.6 mm Supelcosil LC-18S column is used, this is the most frequently used method in our laboratory. The only difference in the chromatographic parameters of the high-speed method as compared to the high-resolution method is that the gradient step times are proportionally reduced by a column length ratio of 17/27 for the high-speed method. The total column length of

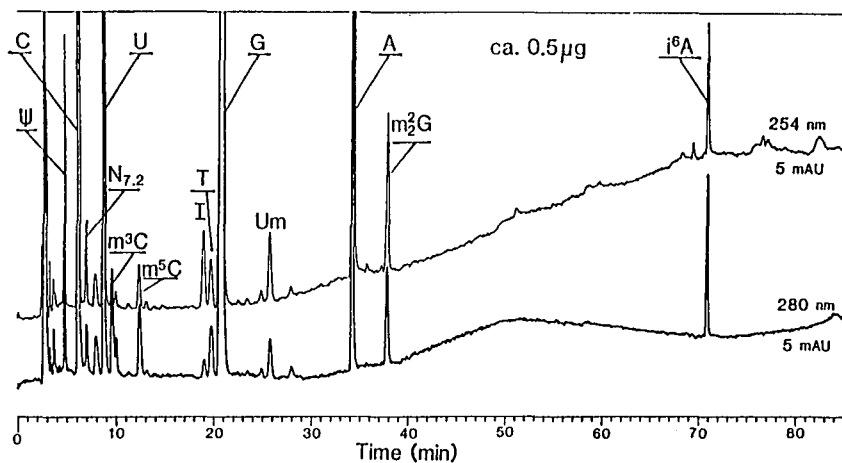


Fig. 17. HPLC of nucleosides in yeast tRNA^{Ser} using high-speed chromatography.

the high-speed column is 170 mm (150 mm plus 20 mm for the guard column), and the total length of the high-resolution column is 270 mm (250 mm plus 20 mm for the guard column). The gradient step times presented in Table I are multiplied by 17/27 for the gradient times used in the high-speed chromatographic method. Fig. 16 presents the same hydrolysate of unfractionated calf liver tRNAs separated on the 150-mm column as seen in Fig. 15 on the 250-mm column. An essentially identical separation was obtained from both columns. A slight difference that was observed is the separation of the very closely eluted nucleoside pairs such as m^7G and I, or ac^4C and m^2G , which are slightly compromised in the high-speed method. When speed or sensitivity, not resolution, is needed, this system is preferable to the high-resolution system. Fig. 17 demonstrates the sensitivity of this method showing the quantitative measurement of nucleosides in 0.5 μg of an isoaccepting yeast tRNA^{Ser} hydrolysate.

High-sensitivity chromatography method. This method is used for samples that contain only very small amounts of nucleosides. At the present time, microbore HPLC columns (1–2 mm I.D.) are not as widely used as regular bore analytical (4–6 mm I.D.) columns. This is partially because microbore column chromatography requires special instrumentation with a very low dispersion volume, and also because the columns have low column loading capacities and are somewhat inconsistent in performance from column to column. Often only picomole amounts of nucleosides are available in research samples, thus microbore columns are the simplest solution to obtain the

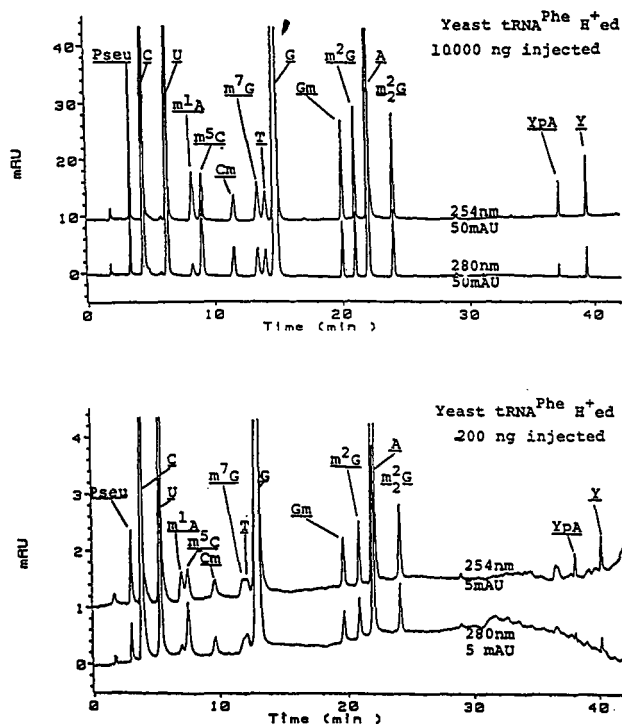


Fig. 18. Comparison of high-speed (top) and high-sensitivity (bottom) chromatography of nucleosides in yeast tRNA^{Phe}.

needed sensitivity. We use a 15 cm \times 2.1 mm I.D., 5- μ m spherical silica ODS column using experimental parameters identical to those used in the high-speed chromatography method, except that the volumetric flow-rate was reduced from 1.0 to 0.21 ml/min in order to maintain the same linear flow-rate. A yeast tRNA^{Phe} hydrolysate was chromatographed on both the 150 \times 4.6 mm regular-bore high-speed column (Fig. 18a) and 150 \times 2.1 mm high-sensitivity microbore column (Fig. 18b), 10 000 ng and 200 ng of the tRNA hydrolysate were injected, respectively on each column. The attenuation of each run was 50 mAU for the regular-bore column and 5 mAU for the microbore column. The microbore column gave four-fold higher sensitivity (peak height per ng) than the regular-bore column. The modified nucleoside peaks in Fig. 18b are about 1.5 ng each. Serious peak tailing of the basic nucleosides m¹A and m⁷G was observed in the microbore analysis. We believe this problem can be corrected with another pre-tested column or by increasing the concentration of buffer salts to provide a greater masking effect of the exposed silanol active sites.

CONCLUSION

A new RPLC-UV photo-diode-array technology is presented for the simultaneous measurement and identification of a large number of nucleosides in complex biological matrices. The new nucleoside methods have broad application to biochemical and biomedical investigations, and present a new research tool to advance studies in molecular biology.

ACKNOWLEDGEMENTS

The authors wish to acknowledge the valuable suggestions and technical support of: Dr. G. Davis, Mr. R. Suits, Mr. K. Leimer, Mr. R. McCune, Mr. D. Kirk, Mr. D. Phan, Mr. N. Williams, Mr. R. Merritt, Mr. J. Pautz, Mr. F. Davis, Mr. K. Barnes, and in particular the professors and scientists whom we collaborated with and cited in the introduction section for their stimulating discussions, valuable suggestions, generous gifts of RNAs, and reference modified nucleosides. Without their help and excellent support of their laboratories this research would not have been possible.

This research was supported by the University of Missouri-Columbia, Marion Laboratories (Kansas City, MO, U.S.A.); Supelco, Inc. (Bellefonte, PA); and the Higher Education Research Assistance Act of the State of Missouri. The financial support of these institutions is gratefully acknowledged.

REFERENCES

- 1 G. Schöch, G. Heller-Schöch, J. Muller, M. Heddich and R. Gruttner, *Klin. Padiatr.*, 194 (1982) 317-319.
- 2 G. Sander, H. Topp, G. Heller-Schöch, J. Weiland and G. Schöch, *Clin. Sci.*, 71 (1986) 367-374.
- 3 K. Randerath, R. C. Gupta and E. Randerath, *Methods Enzymol.*, 65 (1980) 638-680.
- 4 M. Silberklang, A. M. Gium and U. L. RajBhandary, *Methods Enzymol.*, 59 (1979) 58-109.
- 5 G. E. Davis, R. S. Suits, K. C. Kuo, C. W. Gehrke, T. P. Waalkes and E. Borek, *Clin. Chem.*, 23 (1977) 1427-1435.
- 6 C. W. Gehrke, K. C. Kuo, G. E. Davis, R. D. Suits, T. P. Waalkes and E. Borek, *J. Chromatogr.*, 150 (1978) 455-476.
- 7 R. A. Hartwick and P. R. Brown, *J. Chromatogr.*, 126 (1976) 679-691.

- 8 M. Zakaria and P. R. Brown, *J. Chromatogr.*, 226 (1981) 267–290.
- 9 M. Buck, M. Connick and B. N. Ames, *Anal. Biochem.*, 129 (1983) 1–13.
- 10 N. C. De, A. Mittelman, S.P. C. G. Edmonds, E. E. Jenkins, J. A. McCloskey, C. R. Blakeley, M. L. Vestal and G. B. Chheda, *J. Carbohydr. Nucleosides Nucleotides*, 8 (1981) 363–389.
- 11 C. R. Blakeley and M. L. Vestal, *Anal. Chem.*, 55 (1983) 750–754.
- 12 C. W. Gehrke, K. C. Kuo, R. A. McCune, K. O. Gerhardt and P. F. Agris, *J. Chromatogr.*, 230 (1982) 297–308.
- 13 C. W. Gehrke, R. W. Zumwalt, R. A. McCune and K. C. Kuo, *Recent Results Cancer Res.*, 84 (1983) 344–459.
- 14 C. W. Gehrke and K. C. Kuo, *Bull. Mol. Biol. Med.*, 10 (1985) 119–142.
- 15 C. W. Gehrke and K. C. Kuo, in F. Cimino, G. Birkmayer, J. Klavins, E. Pimentel and F. Salvatore (Editors), *Human Tumor Markers*, Walter de Gruyter, New York, 1987, pp. 475–502.
- 16 T. P. Waalkes, C. W. Gehrke, W. A. Blyer, R. W. Zumwalt, C. L. M. Olweny, K. C. Kuo, D. B. Lakings and S. Jacobs, *Cancer Chemother. Rep.*, 59 (1975) 721–727.
- 17 C. W. Gehrke, K. C. Kuo, T. P. Waalkes and E. Borek, in R. W. Ruddon (Editor), *Biological Markers Neoplasia: Basic Appl. Aspects*, (1978) 559–567.
- 18 T. P. Waalkes, M. D. Abeloff, D. S. Ettinger, K. B. Woo, C. W. Gehrke, K. C. Kuo and E. Borek, *Cancer*, 50 (1982) 2457–2464.
- 19 J. E. McEntire, K. C. Kuo, M. E. Smith, D. L. Stalling, J. W. Richens, Jr., C. W. Gehrke and B. W. Papermaster, *Cancer Res.*, 49 (1989) 1057–1062.
- 20 K. C. Kuo and C. W. Gehrke, in preparation.
- 21 K. C. Kuo, C. E. Smith, Z. Shi, P. F. Agris and C. W. Gehrke, *J. Chromatogr.*, 378 (1986) 361–374.
- 22 S. Nishimura, in P. R. Schimmel, D. Söll and J. N. Abelson (Editors), *Transfer RNA: Structure, Properties, and Recognition*, Cold Spring Harbor Laboratory, Cold Spring Harbor, NY, 1979, pp. 59–79.
- 23 D. B. Dunn and R. H. Hall, *Purines, Pyrimidines, Nucleosides, and Nucleotides; Physical Constants and Spectral Properties, Handbook of Biochemistry and Molecular Biology, Nucleic Acids*, Vol. 1, 3rd ed., 1975, CRC Press, Boca Raton, FL.
- 24 J. Desgres, G. Keith, K. C. Kuo and C. W. Gehrke, *Nucleic Acids Res.*, 17 (1989) 865–882.
- 25 S. Yokoyama, T. Muramatsu, G. Kawai, N. Horie, Z. Yamaizumi, Y. Kuchino, S. Nishimura, E. Goldman and T. Miyazawa, presented at the *12th International Workshop on tRNA, July, 1987, Umea*.
- 26 C. G. Edmonds, P. F. Crain, T. Hashizume, R. Gupta, K. O. Stetter and J. A. McClosky, presented at the *12th International Workshop on tRNA, July, 1987, Umea*.
- 27 C. W. Gehrke, unpublished data.
- 28 H. F. Noller, *Annu. Rev. Biochem.*, 53 (1984) 119–162.
- 29 R. R. Gutell, B. Weiser, C. R. Woese and H. F. Noller, *Prog. Nucleic Acids Res. Mol. Biol.*, 32 (1985) 155–216.
- 30 C. Branlant, A. Krol, M. A. Machatt, J. Pouyet and J. Ebel, *Nucleic Acids Res.*, 9 (1981) 4303–4324.
- 31 W. D. Heyer, P. Thuriaux, J. Kohli, P. Ebert, H. Kersten, C. W. Gehrke, K. C. Kuo and P. F. Agris, *J. Biol. Chem.*, 259 (1985) 2856–2862.
- 32 A. M. Grossenbacher, B. Stadelmann, W. D. Heyer, P. Thuriaux, J. Kohli, C. Smith, P. F. Agris, K. C. Kuo and C. W. Gehrke, *J. Biol. Chem.*, 261 (1987) 16351–16355.
- 33 P. Staheli, P. F. Agris, P. Niederberger, C. W. Gehrke and R. Hutter, *J. Gen. Microbiol.*, 128 (1982) 2591–2600.
- 34 P. F. Agris, J. G. Tompson, C. W. Gehrke, K. C. Kuo and R. H. Rice, *J. Chromatogr.*, 194 (1980) 205–212.
- 35 G. Keith, presented at the *11th International tRNA Workshop, Banz., 1985*, Abstract.
- 36 J. C. Chan, J. A. Yang, M. J. Dunn, P. F. Agris and T.-W. Wong, *Nucleic Acids Res.*, 10 (1982) 4605–4508.
- 37 J. A. Yang, L. W. Tai, P. F. Agris, C. W. Gehrke and T.-W. Wong, *Nucleic Acids Res.*, 11 (1983) 1991–1993.
- 38 M. Buck, J. A. McCloskey, B. Basile and B. N. Ames, *Nucleic Acids Res.*, 10 (1982) 5649–5662.
- 39 G. B. Chheda, H. A. Tworek, A. K. Bhargava, J. G. Angkowiak, S. P. Dutta and H. B. Patrzyk, *36th ASMA Conference on Mass Spectrometry and Allied Topics*, San Francisco, CA, June 1988.
- 40 N. Yamamoto, Z. Yamaizumi, S. Yokoyama, T. Miyazawa and S. Nishimura, *J. Biochem. (Tokyo)*, 97 (1985) 361–364.
- 41 M. Ehrlich, M. A. Gama-Sosa, L. H. Carreir, L. G. Ljungdahl, K. C. Kuo and C. W. Gehrke, *Nucleic Acids Res.*, 13 (1985) 1339–1412.

- 42 Unpublished data.
- 43 T. Heyman, personal communication.
- 44 F. Salvatore, L. Sacchetti, F. Pane, K. C. Kuo and C. W. Gehrke, in preparation.
- 45 C. W. Gehrke, K. C. Kuo and R. W. Zumwalt, *J. Chromatogr.*, 188 (1980) 129–147.
- 46 K. C. Kuo, C. W. Gehrke, R. A. McCune, T. P. Waalkes and E. Borek, *J. Chromatogr.*, 145 (1978) 383–392.
- 47 C. W. Gehrke and K. C. Kuo, F. Cimino *et al.* (Editors), *Human Tumor Markers*, Walter de Gruyter, New York, 1987, pp. 475–502.
- 48 K. C. Kuo, F. Esposito, J. E. McEntire and C. W. Gehrke, in F. Cimino *et al.* (Editors), *Human Tumor Markers*, Walter de Gruyter, New York, 1987, pp. 503–519.
- 49 K. C. Kuo, F. Salvatore, L. Sacchetti, F. Pane and C. W. Gehrke, in preparation.
- 50 B. L. Karger, J. N. LePage and N. Tanaka, in Cs. Horváth (Editor), *High-Performance Liquid Chromatography Advances and Perspectives*, Vol. 1, Academic Press, NY, 1980, pp. 113–207.
- 51 Cs. Horváth, W. Melander and I. Molnar, *Anal. Chem.*, 49 (1977) 142–154.
- 52 N. Tanaka, H. Goodell and B. L. Karger, *J. Chromatogr.*, 158 (1978) 233–248.
- 53 S. R. Bakalyar, R. McIlwrick and E. Roggendorf, *J. Chromatogr.*, 142 (1977) 353–365.
- 54 H. Colin and G. Guiochon, *J. Chromatogr.*, 158 (1978) 183–205.

CHROM. 21 286

GAS-SOLID CHROMATOGRAPHY ON OPEN-TUBULAR COLUMNS: AN ISOTOPE EFFECT

MANFRED MOHNKE*

Forschungsstelle für chemische Toxikologie der Akademie der Wissenschaften der DDR, Permoserstrasse 15, 7050 Leipzig (G.D.R.)

and

JÜRGEN HEYBEY

Zentralinstitut für Isotopen- und Strahlenforschung der Akademie der Wissenschaften der DDR, Permoserstrasse 15, 7050 Leipzig (G.D.R.)

SUMMARY

Attempts to provide porous-layer open-tubular (PLOT) columns with Chromosorb 102, molecular sieve 5A, molecular sieve 13X and activated charcoal are described. The high separation performance of these PLOT columns at relatively high separation temperatures and shorter separation times is demonstrated by the example of the separation of low-boiling gases and isotope molecules. Precise measurements of the temperature dependence of separation factors and specific retention volumes supply the basis for the calculation of differences in the enthalpy and entropy of adsorption. A model of a molecular size isotope effect is proposed and validated experimentally.

INTRODUCTION

Isotope effects in adsorption are now generally understood, but there is no analytic expression for the interaction of each kind of gas with particular adsorbents. One of the main difficulties in this connection is the absence of spectroscopic methods for the detection of molecular physical changes in chemical compounds in the adsorption state. Therefore, it is necessary to establish isotope effects in model tests simulating the various special interactions and to interpret them theoretically.

One of the possible model situations for the investigation of isotope effects in adsorption is gas chromatography, which permits the determination of physico-chemical quantities such as enthalpy of adsorption and separation factors from measurable quantities such as retention times as a function of test parameters such as temperature. Consequently, it was the aim of this study to produce appropriate separation columns that might provide information on isotope effects by enabling the required quantities to be determined experimentally. The main field of application of gas chromatography is, of course, analytical chemistry. Hence insights gained from

this study into adsorption and isotope effects occurring on adsorption may also provide important conclusions for isotope gas chromatography.

The high separation efficiency of capillary columns allows separations that are not practicable with packed columns. We therefore attempted to use capillaries to test the separation of isotope molecules, which is one of the most difficult tasks.

For the gas chromatographic separation of isotope systems of low-boiling substances such as $^1\text{H}_2$ - $^2\text{H}_2$ - $^3\text{H}_2$, $^{16}\text{O}_2$ - $^{18}\text{O}_2$, $^{14}\text{N}_2$ - $^{15}\text{N}_2$, ^{20}Ne - ^{22}Ne , ^{36}Ar - ^{40}Ar , ^{82}Kr - ^{86}Kr , ^{12}CO - ^{13}CO and $^{12}\text{CH}_4$ - $^{13}\text{CH}_4$, no suitable liquid stationary phase has been found so far. On the one hand, a suitable stationary phase should be applicable at room temperature so that the columns are durable, and on the other it ought to provide a sufficient solvent power for different substances and a sufficiently large separation factor for isotope systems. As the physical condition of the stationary phase may be either liquid or solid, only those solids that are durable when applied on the inner wall of a capillary column for high quality separation are applicable.

So far, only silica gels produced by alkaline corrosion of glass have been used as sorbents in gas-solid chromatographic capillaries¹⁻⁵. Such columns provide high capacity ratios and high performance only at low temperatures. Possibilities of coating them with adsorbents such as molecular sieves, carbon molecular sieve, activated charcoal, porous polymers or alumina were lacking. However, the application of such stationary phases permits work at high temperature and high capacity ratio, if it is possible to produce thick coatings (about 30 μm). Sharp, symmetrical peaks would be achieved within short separation times.

For the CH_4 - C^2H_4 separation, for example, the separation factor inverts with temperature. For the logarithm of the retention volumes of methane and deuteromethane, Bruner *et al.*² found

$$\ln \left[\frac{V_{\text{R}}(\text{CH}_4)}{V_{\text{R}}(\text{C}^2\text{H}_4)} \right] = \frac{A}{T^2} - \frac{B}{T} \quad (1)$$

an expression having the same analytical form as the logarithm of the vapour pressure ratio of the two isotope-substituted substances. The isotope effect results from the sum of two constituents with opposite signs, and with increasing temperature a positive "normal" isotope effect may turn into a negative "inverse" effect. The plot of the expression $T \ln[V_{\text{R}}(\text{CH}_4)/V_{\text{R}}(\text{C}^2\text{H}_4)]$ vs. $1/T$ provides straight lines that intersect the abscissa at the so-called inversion point, from which the constants A and B can easily be determined. The result is inversion of the peak sequence. At high temperatures (*e.g.*, room temperature) first C^2H_4 then CH_4 is eluted. This is important for the determination of traces of CH_3^2H in CH_4 as main component, as the demands on the separation performance in the reverse case are considerably higher. A column that separates the deuteromethanes is also applicable to studies of the deuterium isotope effect of methane.

The only possibility for the high-performance separation of low-boiling isotopic species seems to be to use capillaries with a thick coating of suitable adsorbents. For this purpose, the development of a coating method for providing high-performance columns of high permeability and great length is necessary. Glass or fused silica should be used as the capillary material for reasons of low surface activity and transparency.

EXPERIMENTAL

Coating experiments

For making pure adsorption capillaries only the corrosion techniques mentioned were successful. A static method has been suggested by Halasz and Horváth⁶⁻⁸ and used successfully for many separations. They filled long steel capillaries (up to 50 m) with stable suspensions of many solids and liquid stationary phases, closed the capillaries at one end and passed them through a micro-furnace, where the solvent evaporated through the open end, then into a large furnace to prevent recondensation of the solvent. In this process the solid that settles on the capillary wall is retained, while the solvent vapour flowing continuously over the already settled solid coating has a smoothing effect. The same technique was used by Ettre and co-workers^{9,10} to produce 45-m separation columns with 57 000 plates. For this purpose, stable suspensions with particle sizes between 1 and 10 μm are necessary.

Adhesiveness of dispersed adsorbents

The greatest problem encountered in the production of sorbent-coated capillary columns is the durability of the solid coatings on smooth walls. The adhesiveness of these solid particles is partly based on adhesion between the particles and the surface to be coated, and partly on cohesion between the particles themselves. It is known from experience that adhesion is lower with larger particles. With finely dispersed substances, effectively adhering coats are obtained, as in thin-layer chromatography. According to Patat and Schmid¹¹, the binding between the particles results from Van der Waals forces, whose influence decreases with the sixth power of distance. Further, according to Cremer¹², adhesiveness depends on the kind and pretreatment of the dispersed solid, its grain size and the pretreatment of the supporting surface. Rumpf¹³ found that tensile strengths up to 1 MPa result from Van der Waals forces at particle sizes between 0.01 and 1 μm and at a grain distance of 0.01 μm . Compact solids have tensile strengths of more than 100 MPa. The durability of a settled layer of finely dispersed particles depends largely on the radius of curvature of the support surface. As the radius of curvature is very small in capillary columns, a highly curved ring of high stability is produced, comparable to an arched bridge under load. This ring will break down only if sections are removed from inside.

Layer thickness

The thickness of the adsorbent layer in porous-layer open-tubular (PLOT) columns must be suitable for the particular task to be fulfilled. The minimum layer thickness required depends mainly on the distribution coefficient of the components to be separated and hence on the kind of adsorbent and on the separation temperature. On the other hand, the layer must not be too thick, otherwise diffusion in its stationary phase will contribute to peak broadening, *i.e.*, increase the height equivalent to a theoretical plate (HETP). Hence it is an optimization problem to find the correct layer thickness. The layer thickness may be controlled with the help of the concentration of the solid in the suspension. In addition, it is possible to vary the radius of the uncoated capillary, R_K , as the column diameter influences the loading capacity.

From the relationship

$$\frac{R_K^2 \pi}{100} = \frac{(R_K^2 - r^2) \pi}{c} \quad (2)$$

where c is the solid concentration (vol.-%) the free radius r of the coated capillary is calculated as

$$r = R_K \sqrt{1 - \frac{c}{100}} \quad (3)$$

As $R_K = r + d_s$ where d_s is the layer thickness, we obtain

$$d_s = R_K \left(1 - \sqrt{1 - \frac{c}{100}} \right) \quad (4)$$

Fig. 1A shows the layer thickness as a function of the solid concentration for the radii $R_K = 125, 160$ and $265 \mu\text{m}$. The ratio between the gas volume and the volume of

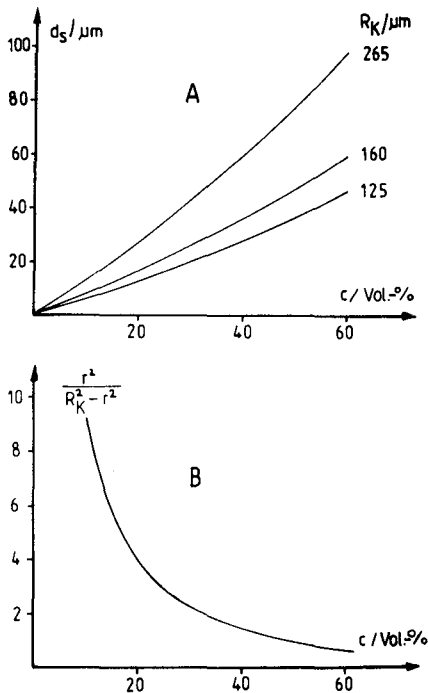


Fig. 1. (A) Layer thickness (d_s) as a function of the concentration of adsorbent (c) in the suspension. (B) Cross-sectional area ratio (gas/adsorbent) as a function of the content of adsorbent in suspensions.

the stationary phase is proportional to the value $r^2/(R_K^2 - r^2)$. From eqn. 3, the cross-section ratio may be calculated:

$$\frac{r^2}{R_K^2 - r^2} = \frac{100}{c} - 1 \quad (5)$$

Fig. 1B shows the plot of this function against c . The large increase in the cross-section ratio with decrease in the amount of solid in the suspension indicates that the application of high solid concentrations, e.g., 20–50 vol.-%, will be necessary. From eqn. 5,

$$c = 100 \left(1 - \frac{r^2}{R_K^2} \right) \quad (6)$$

and, as $r = R_K - d_s$,

$$c = 100 \left[1 - \frac{(R_K - d_s)^2}{R_K^2} \right] \quad (7)$$

Preparation of suspensions

It was observed in all coating experiments that the suspension must meet the highest demands. This holds, in particular, for the mentioned tendency for sedimentation, the evaporation behaviour and the filling capacity of the capillaries. It was observed with all suspensions that even fine solids, owing to their high surface energy and the high collision density of the particles, produce particle enlargement and consequently sedimentation at high solid concentrations after various times. Particle enlargement before evaporation results in solid layers with low packing densities and hence produces loose layers of low durability. As during evaporation of the dispersion medium linear vapour flow-rates amounting to a few metres per second occur in the capillary, clogging of the inside is a frequent consequence. To prevent particle enlargement due to movement of particles and consequences such as sedimentation, clogging, non-uniform layer thickness and poor durability of the layers, it is advantageous to add thickeners to the suspensions. These greatly reduce the translation movements of the particles.

The thickener should meet the following demands: it must be soluble in the dispersion medium or able to swell; the necessary concentration must be as low as possible; the micropores of the adsorbent must not be clogged; when the adsorbent is activated (200–500°C), decomposition products must not affect the surface, or there must be no decomposition; and it should not have a tendency to foam during evaporation. Suitable substances are colloids, which in addition should be thixotropic. They make the filling of very long capillaries feasible.

The dispersion medium must also meet certain demands: viscosity, density and polarity greatly influence the sedimentation tendency; low boiling point and high evaporation speed simplify evaporation; and low surface tension and low foaming tendency prevent clogging. Many empirical experiments are necessary in order to select a suitable dispersion medium for a given solid, as little experience has been

gained in this field so far. In fact, the preparation of the suspension decides the success of the coating procedure.

RESULTS AND DISCUSSION

Separation with Chromosorb 102

A glass capillary (15 m \times 0.30 mm I.D.) was coated with Chromosorb 102 using the static method. The layer thickness was about 25 μm . For activating the stationary phase, a heating rate of 2°C min^{-1} from 20 to 190°C was used under a stream of pure hydrogen. After an activation period of 3 h at 190°C it was just possible at -46°C to separate C^2H_4 from CH_4 in this sequence with a resolution of about 10%. The capacity ratio for CH_4 was 1.06 and the separation factor $\alpha(\text{CH}_4/\text{C}^2\text{H}_4)$ could be determined, in good agreement with Czubryt and Gesser¹⁴, to be 1.065. The separation time was about 2.5 min. An attempt to determine the function $\log \alpha$ versus $1/T$ for this system failed owing to poor separation at both lower and higher temperatures.

For substances having a higher value of k from the beginning, e.g., water, this separation column is possibly appropriate. Considering that the vapour pressure ratio is $p_{\text{H}_2^{16}\text{O}}/p_{\text{H}_2^{18}\text{O}} = 1.062$ at 46°C , then 13 000 theoretical plates would be sufficient for the complete separation of these molecules for $k = 10$. Later, De Zeeuw^{15,16} succeeded in coating fused-silica PLOT columns with Porapak Q for the separation of gases and low-boiling polar and non-polar liquids. Such columns are now available from Chrompack as PoraPLOT Q.

Separation with molecular sieve 5A

By applying an aqueous suspension containing molecular sieve crystals about 1 μm in size at a concentration of 35 vol.-%, a capillary column was coated with a uniform, thick porcelain-like rigid layer of 30 μm thickness with good adhesiveness using the static method. A typical cross-section is shown (1:100) in Fig. 2. Even at gas speeds of 1 m s^{-1} , blow-out of molecular sieve was not observed. Glass capillaries having a molecular sieve layer may be straightened, and column parts may be assembled manually. As the molecular sieve contains a lot of water in the micropores and hollow spaces, heating must begin carefully. Heating proceeded at a rate of 1°C min^{-1} from 20 to 100°C and was kept at the latter value for 8 h. Then the column was heated at the same rate to 350°C and subsequently activated for 2 h, always under a flow of pure hydrogen. Fast heating of the newly prepared column with a high water content may easily produce considerable hydrolysis of the molecular sieve and lead to its destruction.

For checking and optimizing the separation efficiency, chromatograms were obtained at gas speeds between 22.4 and 61.5 cm s^{-1} for samples containing He, Ar, O_2 , N_2 , C^2H_4 and CH_4 . Fig. 3 shows a typical chromatogram. At room temperature all the components mentioned were completely separated. It should be noted that the whole chromatogram takes only about 25 min to acquire and for methane at the peak width at half-height is only 10 s. The peak symmetry is good; the tailing of the C^2H_4 peak is due to CH^2H_3 still contained in the sample, produced during the formation of C^2H_4 from aluminium carbide and $^2\text{H}_2\text{O}$. Even Ar and O_2 are completely separated. The optimum mean linear velocity for hydrogen is 31.3 cm s^{-1} measured with CH_4 .

Table I gives the separation factors and their logarithms calculated for the pairs

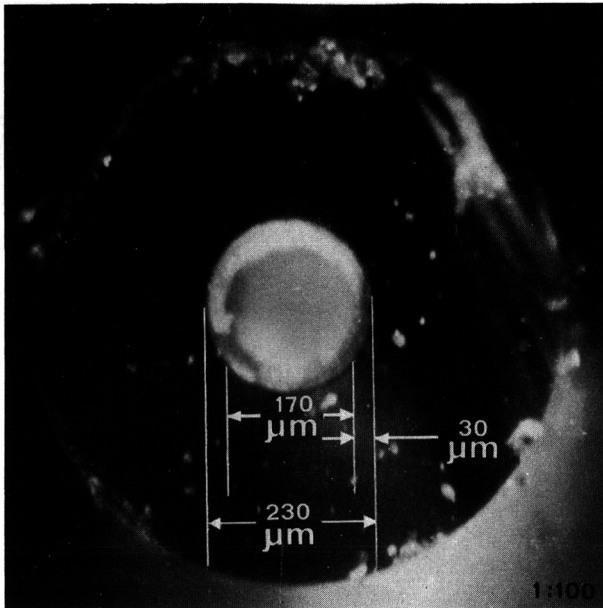


Fig. 2. Cross-section of a molecular sieve 5A capillary (1:100). Capillary I.D. = 230 μm; layer thickness = 30 μm.

O₂-Ar, N₂-O₂, CH₄-N₂ and CH₄-C²H₄, positioned close to each other in the chromatogram. Fig. 4 shows that the separation factor for N₂-O₂ increases strongly and that for Ar-O₂ increases slightly in a linear fashion with 1/T. Over the whole temperature range, however, α remains constant, within experimental error, for CH₄-C²H₄ (the error is smaller than ±0.1%). It must be added that above 50°C separation is no longer complete, which leads to errors in retention time determina-

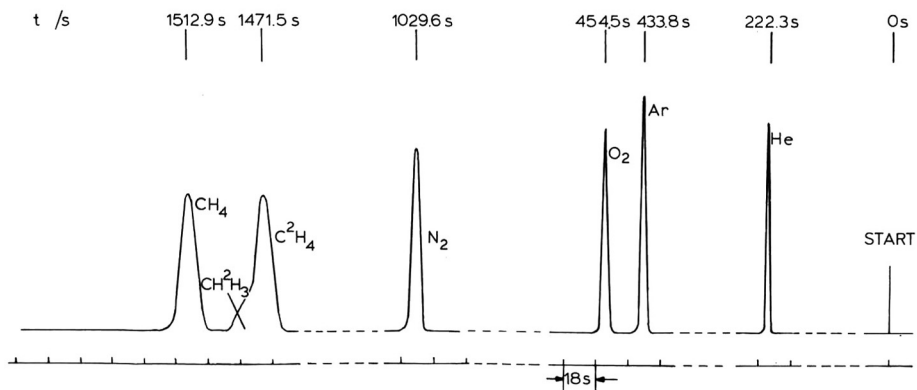


Fig. 3. Molecular sieve 5A PLOT column. I.D. = 330 μm; layer thickness = 30 μm; length = 67 m; temperature = 22.3°C; 1.4 bar H₂; microthermal conductivity detector; HETP_{eff.} = 0.71 mm; effective plate number = 94 150; capacity ratio (CH₄) = 5.8; α_{CH₄/C²H₄} = 1.0336.

TABLE I
DEPENDENCE OF RELATIVE RETENTION (α) AND LN α ON THE SEPARATION TEMPERATURE

Temperature		$10^3/T$ (K^{-1})	$\alpha_{O_2/Ar}$	$\ln \alpha$	α_{N_2/O_2}	$\ln \alpha$	α_{CH_4/N_2}	$\ln \alpha$	α_{CH_4/C^2H_6}	$\ln \alpha$
$^{\circ}C$	K									
-45	228.2	4.38	1.21	0.191	11.04	2.40	1.19	0.17	1.03185	0.031
-24	249.2	4.01	1.18	0.166	6.36	1.85	1.35	0.30	1.03374	0.033
- 5.0	268.2	3.73	1.12	0.113	4.44	1.49	1.49	0.40	1.03407	0.034
0.0	273.2	3.66	1.12	0.113	4.55	1.52	1.49	0.40	1.03359	0.033
10.0	283.2	3.53	1.11	0.104	4.02	1.39	1.53	0.425	1.03446	0.034
30.3	303.5	3.30	1.09	0.086	3.28	1.19	1.62	0.48	1.03414	0.034
30.3	303.5	3.30	1.10	0.095	3.26	1.18	1.62	0.48	1.03279	0.032
40.2	313.4	3.19	1.08	0.077	3.00	1.10	1.65	0.50	1.03392	0.033
50.2	323.4	3.09	1.08	0.077	2.77	1.02	1.68	0.52	1.03390	0.033
60.0	333.2	3.00	1.06	0.058	2.59	0.95	1.71	0.54	1.03015	0.030
70.2	343.4	2.91	1.05	0.049	2.43	0.89	1.73	0.55	1.03198	0.031
80.1	353.3	2.83	-	-	-	-	1.74	0.55	1.03053	0.030
95	368.2	2.72	-	-	-	-	1.75	0.56	-	-

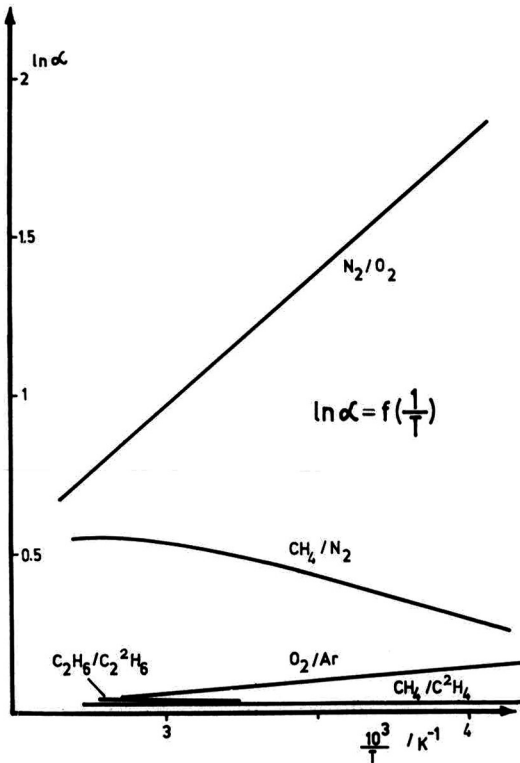


Fig. 4. Plots of $\ln \alpha$ versus $1/T$.

TABLE II

DIFFERENTIAL ENTHALPIES OF ADSORPTION (ΔH_{GC}) CALCULATED FROM LINEAR PLOTS OF $\ln V_g$ VERSUS $1/T$ m = slope, b = intercept on the ordinate, r^2 = regression coefficient.

Gas	m	b	r^2	ΔH_{GC} (kcal mol ⁻¹)
Ar	547.57	-1.311	0.9996	-2.505
O ₂	583.70	-1.393	0.9998	-2.670
N ₂	964.57	-2.125	0.9996	-4.413
C ² H ₄	869.41	-1.621	0.9998	-3.978
CH ₄	868.26	-1.602	0.9996	-3.972

tions. The constancy of the α value, which seems surprising, indicates an abnormal behaviour of methane towards the adsorbent, as can also be seen from the plot for CH₄-N₂. For this pair, the separation factor even decreases with decreasing temperature. That the separation of argon and oxygen is almost as difficult as the separation of isotope molecules is shown by the separation factors at room temperature.

Evaluation of separation factors for the system CH₄-C²H₄ between 228.2 and 323.4 K results in a mean value of $\alpha = 1.0336 \pm 0.0008$. At this separation factor and a value of $k = 5.75$ (measured at 22.3°C), complete separation requires 47 000 plates; the performance of a 67-m capillary is more than twice as efficient.

From the slopes of the straight lines of $\log V_g^{PT}$ versus $1/T$ (where V_g^{PT} is the corrected specific retention volume), the differential enthalpies of adsorption, ΔH_{GC} , can be calculated. In order to achieve the highest possible precision, linear regression calculations were carried out. The results are given in Table II. The parallel course of

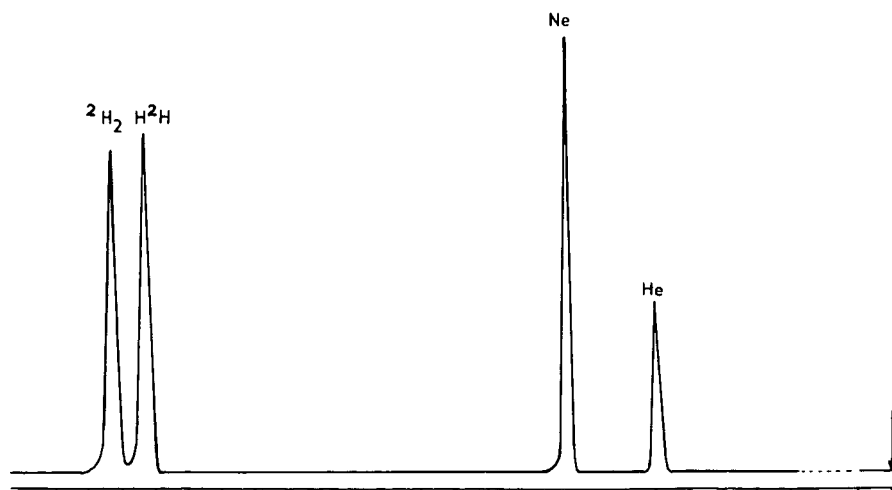


Fig. 5. Separation of H²H and ²H₂. PLOT column (see Fig. 3). Temperature = -78.5°C; $\alpha_{2H_2/H^2H} = 1.0622$; capacity ratio (²H₂) = 0.574; separation time = 4.6 min (1 cm = 6 s).

the straight lines for CH_4 and C^2H_4 shows that the ΔH values are identical for both substances (the slight difference of $0.006 \text{ kcal mol}^{-1}$ is within the measurement tolerance).

The high separation efficiency of the molecular sieve 5A PLOT column may also be demonstrated by the complete separation of H^2H and $^2\text{H}_2$ (Fig. 5) in an extremely short time and at a high separation temperature that was previously impossible. Recently, molecular sieve PLOT columns have been successfully produced with fused silica^{17,18} and are now available in high quality.

The constancy of the separation factor α in the molecular sieve 5A column for CH_4 and C^2H_4 over a wide range of temperatures is at first glance an unexpected result. All previous gas chromatographic work on these isotopic species^{4,14,19-22} yielded a distinctive dependence of the relative retention on temperature. In the usual representation,

$$\ln \alpha = \ln\left(\frac{K}{K'}\right) = \ln\left(\frac{k}{k'}\right) = \ln\left(\frac{t_R}{t'_R}\right) = -\frac{\Delta(\Delta H)}{RT} + \frac{\Delta(\Delta S)}{R} \quad (8)$$

where K = distribution coefficient, k = capacity ratio, t_R = net retention time, the quantity $\Delta(\Delta H) = \Delta H - \Delta H'$ is assigned to the difference in the changes in enthalpy of the isotopic species passing from the mobile to the stationary phase and the quantity $\Delta(\Delta S) = \Delta S - \Delta S'$ to the difference in the changes in entropy; the primed symbols apply to the heavier isotope. Lack of temperature dependence of the separation factor α ,

$$\ln \alpha = \ln\left(\frac{K_{\text{CH}_4}}{K_{\text{C}^2\text{H}_4}}\right) = \ln\left(\frac{t_{R \text{ CH}_4}}{t_{R \text{ C}^2\text{H}_4}}\right) = \frac{\Delta(\Delta S)}{R} \quad (9)$$

means that no difference in the enthalpy of adsorption of the isotopic species can be observed and that an entropic term, perhaps purely steric in nature, is responsible for the fractionation. The gas chromatographic process comprises not only the establishment of a local thermodynamic equilibrium but also a kinetic process, in our case the movement of the molecules to be separated through the framework of the molecular sieve, that is, through the windows, channels and cavities of the zeolite. Therefore, $\Delta(\Delta S)$ need not be an entropic difference in the common thermodynamic sense. We suggest that the difference in the retention times of methane and methane- d_4 can be explained by means of the difference in the molecular sizes of the two isotopic species.

Kuchitsu and Bartell²³ investigated the effect of the anharmonicity of the internal vibrations on the bond length of polyatomic molecules and showed that the molecular dimensions of C^2H_4 must be some thousandth parts smaller than those of CH_4 . The theoretical analysis was supported by experimental spectroscopic constants, diffraction data and scattering experiments. Grigor and Steele²⁴ explained the differences in the physical properties of liquid methane and methane- d_4 (including the vapour pressure isotope effect) by means of the assumption that the C^2H_4 molecule is 0.4% smaller than that of CH_4 . In the same way, Gainar *et al.*²⁵ succeeded in interpreting the isotope effect on the virial coefficient. The diameter of the CH_4 molecule, estimated at $4.0 \cdot 10^{-8} \text{ cm}$, is nearly as the pore width of molecular sieve 5A

($5.0 \cdot 10^{-8}$ cm). The difference of $0.016 \cdot 10^{-8}$ cm between the diameters of CH_4 and C^2H_4 probably leads to a sieve effect. This may be shown by the following simple consideration.

The entrance windows of the zeolite should be nearly circular openings of diameter D . The nearly spherical CH_4 molecule of diameter σ and the C^2H_4 molecules with a smaller diameter $\sigma - \Delta\sigma$ must pass through. For this the centres of the molecules have to go through a circular area of diameter $D - \sigma$ or $D - (\sigma - \Delta\sigma)$, respectively (Fig. 6, dotted areas). The probability of passing through the windows is proportional to these areas, and if this quantity controls the stay in the zeolite framework, the ratio of the retention times of the isotopic species must be the reciprocal of the ratio of these areas. Hence

$$\alpha = \frac{t_{R \text{CH}_4}}{t_{R \text{C}^2\text{H}_4}} = \frac{F_{\text{C}^2\text{H}_4}}{F_{\text{CH}_4}} = \frac{\frac{\pi}{4}[D - (\sigma - \Delta\sigma)]^2}{\frac{\pi}{4}(D - \sigma)^2} \quad (10)$$

The heavier isotopic molecule has the greater chance of passing through the pores and therefore has the shorter retention time. Simple mathematical operations yield

$$\ln \alpha = \frac{2\Delta\sigma}{D - \sigma} = \frac{\Delta(\Delta S)}{R} \quad (11)$$

(valid for $|\Delta\sigma| \ll |D - \sigma|$).

Fig. 7 shows the strong dependence of the separation factor on the quantity $D - \sigma$; the difference in molecular diameters is assumed to be $\Delta\sigma = 0.016 \cdot 10^{-8}$ cm. The separation factor $\alpha = 1.0336 \pm 0.0008$ for methane and methane- d_4 in the 5A column corresponds to $D - \sigma = (0.97 \pm 0.1) \cdot 10^{-8}$ cm (see Fig. 7). Hence we obtain a pore

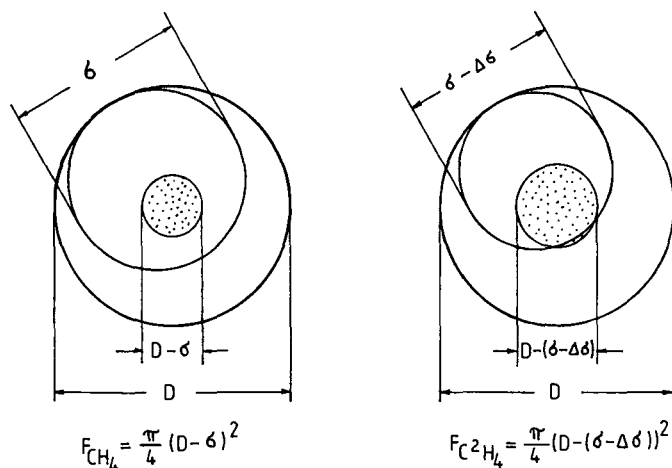


Fig. 6. Comparison of the available areas (dotted circles) for CH_4 and C^2H_4 to pass through pore openings.

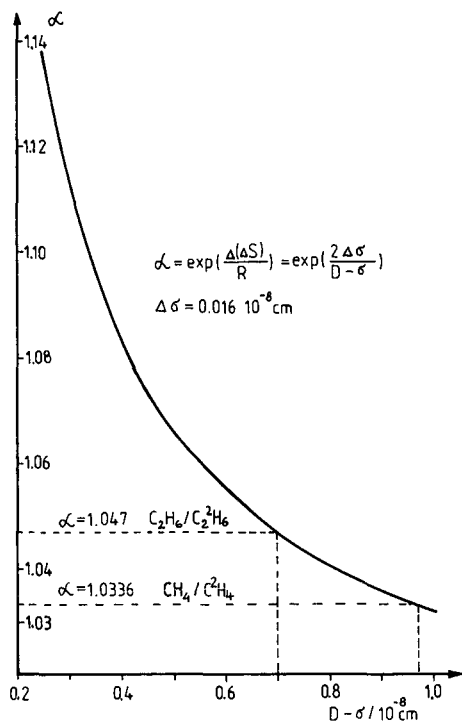


Fig. 7. Increase in separation factor α with diminishing difference between pore width and molecular diameter.

width of $(4.97 \pm 0.1) \cdot 10^{-8}$ cm for molecular sieve 5A. This value demonstrates consistency with the common picture of 5A zeolite. Eqn. 11 gives $\Delta(\Delta S) = R \ln \alpha = 0.0657 \text{ cal mol}^{-1} \text{ K}^{-1}$, which is a reasonable value for the differential entropy of adsorption for the $\text{CH}_4\text{-C}^2\text{H}_4$ separation.

In order to check our explanation of the abnormal isotope fractionation in zeolites, we tried to reduce the difference $D - \sigma$ by choosing isotopic molecules with a greater diameter. The pair $\text{C}_2\text{H}_6\text{-C}_2^2\text{H}_6$ seemed to be suitable; gas chromatographic conditions allowed evaluations in a high temperature range, from 44.5 to 80°C. The observed separation factor decreases only insignificantly with increasing temperature (see Fig. 4), which may result from the non-spherical form or (in comparison with the CH_4 molecule) additional intermolecular motions of the C_2H_6 molecule. Inserting the measured isotope separation factor $\alpha = 1.047$ at 44.5°C and the value $\Delta\sigma = 0.016 \cdot 10^{-8}$ cm (which seems reliable²⁶ also for the difference in the mean diameters of the C_2H_6 and C_2^2H_6 molecules) into eqn. 11, one obtains $D - \sigma = 0.7 \cdot 10^{-8}$ cm. This corresponds to an effective diameter $\sigma = 5.0 - 0.7 = 4.3 \cdot 10^{-8}$ cm of the C_2H_6 molecule, which is in good accord with the common value obtained, e.g., from the transport properties of C_2H_6 .

The gas chromatographic separation of isotopic compounds in connection with the very simple model of a molecular sieve has served as a means of determining effective pore widths from known effective molecule diameters and *vice versa*. Of

course, the reliability and range of applicability of the model should be investigated. With the estimated separation factor $\alpha_{\text{C}_2\text{H}_6/\text{C}_2^2\text{H}_6} = 1.047$ and a value $k = 49.3$, complete separation should require 19 000 plates. The column had a length of 18.8 m and for C_2^2H_6 an effective performance of 29 500 plates at 44.5°C. Therefore, complete separation was easily obtained (Fig. 8). In spite of the relatively high temperature, the separation of argon and oxygen is also complete, in a separation time of less than 3 min. The same effect was achieved by Heylmun²⁷ with a 4.5-m column packed with 5A molecular sieve at -72°C and a separation time of 30 min. Our capillary separates N_2 and Kr in less than 6 min.

Methane and methane- d_4 on a zeolite 13X capillary

In order to avoid the limiting influence of steric hindrance to the movement of methane molecules in zeolite 5A on the isotope fractionation, a zeolite 13X capillary column of length 53 m was prepared using an aqueous suspension. It should utilize the well known differences in polarizability of isotopic compounds²⁰. In order to use eqn. 8 for a rough calculation of the expected separation factor for $\text{CH}_4/\text{C}^2\text{H}_4$, the zeolite 13X was modelled by an adsorbing area, which could be the surface of the supercages. The smaller C^2H_4 molecules take up slightly less area than the larger CH_4 molecules, so the probability of settling on the surface is greater for C^2H_4 than for CH_4 molecules. This leads to a contribution to the entropic term:

$$\frac{\Delta(\Delta S)}{R} = \ln \left[\frac{(\sigma - \Delta\sigma)^2}{\sigma^2} \right] = -2 \cdot \frac{\Delta\sigma}{\sigma} \quad (12)$$

On the other hand, the relative differences in the polarizability, $\Delta a = a - a'$, of isotopic pairs are connected with the relative differences in the adsorption energies²⁸. The equation

$$\frac{\Delta(\Delta H)}{\Delta H} = \frac{\Delta a}{a} - f \left(\frac{\Delta\sigma}{\sigma} \right) \quad (13)$$

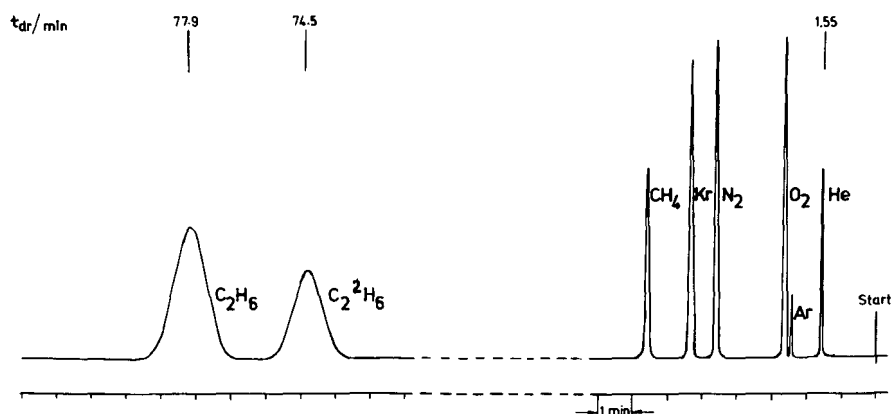


Fig. 8. Separation of C_2H_6 - C_2^2H_6 . Molecular sieve PLOT column (18.8 m \times 0.31 mm I.D.); layer thickness = 30 μm ; temperature = 44.5°C; effective plate number = 29 500; capacity ratio (C_2H_6) = 49.3; $\alpha_{\text{C}_2\text{H}_6/\text{C}_2^2\text{H}_6} = 1.047$.

takes account of the fact that the distances of the centres of isotopic molecules from the adsorbing surface are different. The enthalpy of adsorption is related to the minimum value φ_0 of the potential function of the interaction of a molecule with the surface²⁸. This quantity is proportional to a and mostly in a good approximation to a negative power of the equilibrium distance z_0 . Analogously to that power exponent the factor f depends on the structure of the surface, ranging from *ca.* 0.5 to *ca.* 3; in our case, $f = 3$ is suggested by theoretical reasons (London dispersion theory²⁶) but $f = 2$ fit better the experimental results. For the pair $\text{CH}_4\text{-C}^2\text{H}_4$ we have $\Delta\sigma/\sigma = 0.004$ and $\Delta a/a = 0.014$ and $-\Delta H \approx 4 \text{ kcal mol}^{-1}$. Eqns. 13 and 8 yield

$$-\Delta(\Delta H) \approx 24 \text{ cal mol}^{-1} = 0.012R \cdot 10^3 \text{ K}$$

and

$$\ln \alpha = -0.008 + \frac{0.012}{T/10^3} \quad (14)$$

The study of the fractionation of isotopic methanes by means of zeolite 13X capillary shows a completely unexpected result (Fig. 9, Table III). Above 20°C the separation factor decreases, corresponding to the difference in adsorption energies of the isotopes, but below 20°C the separation factor remains constant at a value that is nearly the same as that with zeolite 5A. There must be a change in the state of adsorbed molecules in the zeolite 13X at 20°C. Below this characteristic temperature, the large adsorbing cavities (supercages) could be filled with a kind of scarcely moveable (condensed) molecules or the larger openings are in some sense rimmed with them, so that only windows of dimensions similar to those in zeolite 5A are available for the isotopic methane species to pass.

Deuterated methanes on an activated charcoal PLOT column

Gant and Yang¹⁹ tried to separate the different deuterated methane species by means of a 15.3 m \times 0.152 cm I.D. packed charcoal column. Although they did not succeed in achieving a complete separation, they were able to determine the

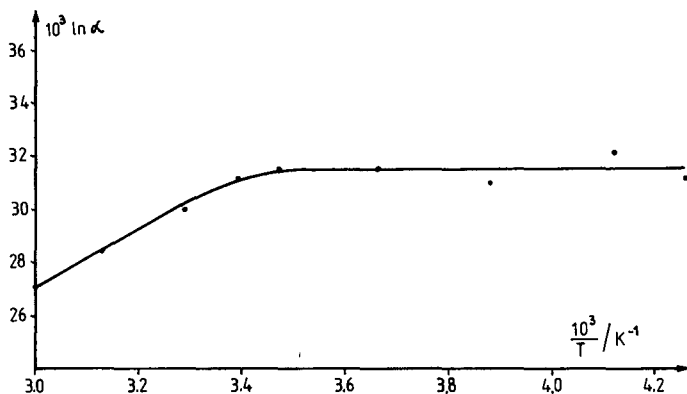


Fig. 9. Separation factor for $\text{CH}_4/\text{C}^2\text{H}_4$ on zeolite 13X column as a function of temperature.

TABLE III

SEPARATION FACTORS FOR $\text{CH}_4\text{-C}^2\text{H}_4$ ON THE CHARCOAL COLUMN: COMPARISON BETWEEN EXPERIMENTAL VALUES AND VALUES GIVEN BY A ROUGH CALCULATION VIA EQN. 14

Temperature (°C)	$10^3/T$ (K^{-1})	$10^3 \ln \alpha$ (calc.) (eqn. 14)	$10^3 \ln \alpha$ (meas.) (Fig. 9)
60	3.001	28.0	27.0
40	3.193	30.3	29.2
20	3.411	32.9	31.4
0	3.660	36.0	31.6
-20	3.950	39.4	31.5
-40	4.307	43.7	31.6

dependence of the separation factor on temperature for the system $\text{CH}_4\text{-C}^2\text{H}_4$. A measurable difference in the enthalpies of adsorption of the isotopic compounds was found, indicating that wide pores must exist. The separation factor for the pair $\text{CH}_4\text{-CH}_3^2\text{H}$ was calculated to be 1.016 at 280 K¹⁹. The reported values encouraged us to work with charcoal-coated capillaries.

In order to remove remaining metal oxides and sulphides, technical charcoal was boiled several times with concentrated hydrochloric acid, washed until neutral and dried. After crushing by hand, the charcoal was dried for 24 h and pulverized in a vibration mill to a grain size of 1–3 μm . It was difficult to prepare stable suspensions. Aqueous systems also with addition of wetting agents failed. Organic solvents, *e.g.*, cyclohexanone led to stable suspensions but not to layers that adhered durably to the capillary. Good results were obtained by means of ethanol–water (4:1). We succeeded in coating about 30-m PLOT columns with a stable 30- μm layer. Several sections of this type were joined manually under the microscope by fusing. Fig. 10 shows that the separation of the single partially deuterated methanes is nearly complete at -9.5°C .

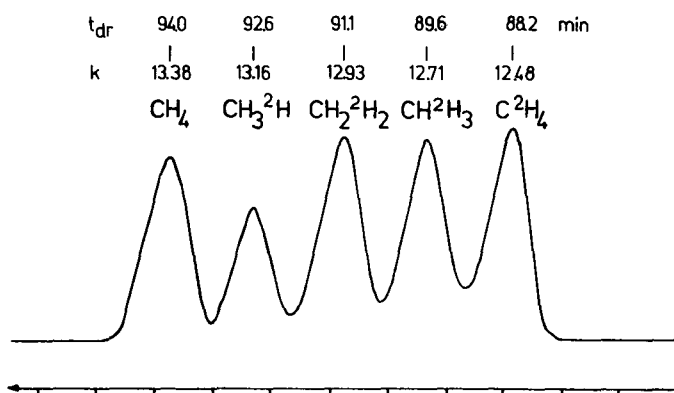


Fig. 10. Separation of deuterated methanes. Active charcoal PLOT column (98 m \times 0.28 mm I.D.); layer thickness \approx 30 μm ; temperature = -9.5°C ; effective plate number = 66 500.

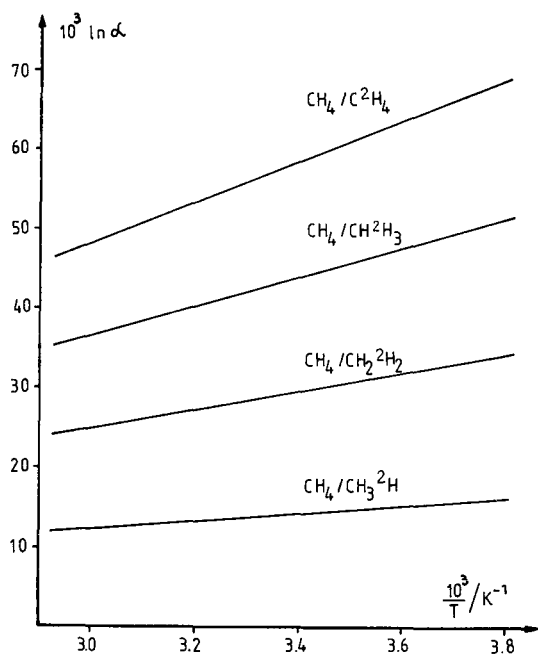


Fig. 11. Separation factor for different deuterated methanes as a function of temperature (-9.5 to 74.7°C).

The separation factor for the pair $\text{CH}_4\text{-C}^2\text{H}_4$ is given by

$$\ln \alpha = -0.0284 + \frac{0.0256}{T/10^3} \quad (15)$$

This gives $\Delta(\Delta S) = -0.056 \text{ cal mol}^{-1} \text{ K}^{-1}$ and $\Delta(\Delta H) = 50.8 \text{ cal mol}^{-1}$. ΔH_{CH_4} was calculated to be $4.32 \text{ kcal mol}^{-1}$. These values correspond fairly well with differential thermodynamic properties found by other workers^{20,21}. We again see that according to eqn. 13 the relative difference of 1.17% in the enthalpies of adsorption is smaller than the relative difference in the polarizabilities. Fig. 11 demonstrates the validity of the law of the mean also for the fractionation of the partially deuterated methanes:

$$\ln \alpha(\text{CH}_4/\text{CH}_{4-n}\text{H}_n) = \frac{n}{4} \ln \alpha(\text{CH}_4/\text{C}^2\text{H}_4) \quad (16)$$

(n = number of H nuclei in CH_4 which are replaced with ^2H). Only the species CH_3^2H shows a very slightly deviation in the lower temperature range. Such a behaviour was also observed by Fang and Van Hook²⁹ for isotope effects on the vapour-phase second virial coefficients of the deuterated methanes and may be connected with the quantum effects on the rotational degrees of freedom.

REFERENCES

- 1 M. Mohnke and W. Saffert, *Kernenergie*, 4/5 (1962) 434.
- 2 F. A. Bruner, G. P. Cartoni and A. Liberti, *Anal. Chem.*, 38 (1966) 298.

- 3 G. P. Cartoni and M. Possanzini, *J. Chromatogr.*, 39 (1969) 99.
- 4 F. A. Bruner, G. P. Cartoni and M. Possanzini, *Anal. Chem.*, 41 (1969) 1122.
- 5 A. Purer, R. L. Kaplan and D. R. Smith, *J. Chromatogr. Sci.*, 7 (1969) 504.
- 6 Cs. Horváth, *Inaugural Dissertation*, Universität Frankfurt, 1963.
- 7 I. Halasz and Cs. Horváth, *Nature (London)*, 197 (1963) 71.
- 8 I. Halasz and Cs. Horváth, *Anal. Chem.*, 35 (1963) 499.
- 9 L. S. Ettre, J. E. Purcell and S. D. Norem, *J. Gas Chromatogr.*, 3 (1965) 181.
- 10 J. E. Purcell and L. S. Ettre, *J. Gas Chromatogr.*, 6 (1968) 18.
- 11 F. Patat and W. Schmid, *Chem.-Ing.-Tech.*, 32 (1960) 8.
- 12 E. Cremer, "Adhesion of Powders", in *Proceedings of the International Symposium on the Reactivity of Solids, Gothenburg, 1952*, published in 1954, pp. 1043–1049; *C.A.*, 48 (1954) 7512i.
- 13 H. Rumpf, *Chem.-Ing.-Tech.*, 30 (1958) 144 and 329.
- 14 J. J. Czubryt and H. D. Gesser, *J. Gas Chromatogr.*, 6 (1968) 41.
- 15 J. de Zeeuw, R. C. M. de Nijs, J. C. Buyten, J. A. Peene and M. Mohnke, *Int. Lab.*, December (1987) 52.
- 16 J. de Zeeuw, R. C. M. de Nijs, J. C. Buyten, J. A. Peene and M. Mohnke, *J. High Resolut. Chromatogr. Chromatogr. Commun.*, 11 (1988) 162.
- 17 J. de Zeeuw and R. C. M. de Nijs, *Chrompack News*, 12 (1985) 1.
- 18 J. de Zeeuw, R. C. M. de Nijs and L. Henrich, *J. Chromatogr. Sci.*, 25 (1987) 81.
- 19 P. L. Gant and K. Yang, *J. Am. Chem. Soc.*, 86 (1964) 5063.
- 20 A. Di Corcia and A. Liberti, *Trans. Faraday Soc.*, 66 (1970) 967.
- 21 P. Pareja and H. Amariglio, *J. Chim. Phys.*, 67 (1970) 938.
- 22 J. T. Phillips and W. A. Van Hook, *J. Phys. Chem.*, 71 (1967) 3276.
- 23 K. Kuchitsu and L. S. Bartell, *J. Chem. Phys.*, 36 (1962) 2460 and 2481.
- 24 A. F. Grigor and W. A. Steele, *J. Chem. Phys.*, 48 (1968) 1032 and 1038.
- 25 I. Gainar, K. Strein and B. Schramm, *Ber. Bunsenges. Phys. Chem.*, 76 (1972) 1242.
- 26 I. Gainar, K. Schäfer, B. Schmeiser, B. Schramm and K. Strein, *Ber. Bunsenges. Phys. Chem.*, 77 (1973) 372.
- 27 G. W. Heylman, *J. Gas Chromatogr.*, 3 (1965) 82.
- 28 D. P. Poshkus, *J. Chromatogr.*, 49 (1970) 146.
- 29 A. Y. Fang and W. A. Van Hook, *J. Chem. Phys.*, 60 (1974) 3513.

CHROM. 21 300

BASIC EQUATIONS IN CONTINUOUS GAS EXTRACTION AND THEIR APPLICATION TO HEADSPACE ANALYSIS

A. G. VITENBERG* and B. V. IOFFE

Chemical Faculty, Leningrad State University, 199034 Leningrad (U.S.S.R.)

SUMMARY

The evolution of ideas on the rules of continuous gas extraction based on dynamic headspace analysis is outlined. The application of a simpler exponential equation that describes well the course of gas extraction under the conditions of a sufficiently small volume of the vapour phase is recommended for practical purposes. The possibility of performing under non-equilibrium conditions not only stripping but also variants of the analysis that do not require full extraction of the sample components is considered. The expediency of the application of continuous gas extraction is demonstrated by the determination of volatile substances with low liquid-gas partition coefficients, where high sensitivity can be achieved by direct headspace analysis under static conditions.

INTRODUCTION

Dynamic variants of headspace analysis, allowing the limit of determination of comparatively low-volatile substances to be decreased, are finding widespread application. These methods are based on continuous gas extraction, *i.e.*, on the transfer of vapours of components from the condensed phase by a stream of gas passing through the bulk of a liquid or above the surface of a solid compound. Dynamic variants were not discussed in the first book on headspace analysis¹ and the usability of the method itself was limited to closed systems in thermodynamic equilibria. However, already in the early 1960s, at the outset of headspace analysis, work was reported in which continuous gas extraction of solutions was studied in order to determine and concentrate volatile admixtures, to measure partition coefficients and to calibrate gas chromatographic detectors. Such studies were performed independently and have remained little known for years. Information on this subject, collected together about 5 years ago², now requires the addition of the results of more recent studies. This paper is aimed at the generalization and classification of the rules based on dynamic headspace analysis. The use of headspace analysis for non-equilibrium systems, from which full extraction of sample component is difficult or impossible, is considered.

BASIC EQUATIONS OF CONTINUOUS GAS EXTRACTION UNDER EQUILIBRIUM CONDITIONS

In 1961, for the measurement of liquid-gas partition coefficients and hence also for analytical purposes, Wahlroos^{3,4} proposed the equation

$$C_G = C_G^0 \exp\left(-\frac{V_g}{KV_L + V_G}\right) \quad (1)$$

describing the changes in the concentrations, C_G , of vapours at the outlet from the vessel with an initial value C_G^0 as a function of the volume of the extracting gas passed, V_g ; V_L and V_G are the volumes of the liquid and the gas in the saturator, respectively, and K is the partition coefficient, $K = C_L/C_G$, where C_L is the concentration of the volatile compound in the liquid phase.

In 1963 the same equation was derived by Fowles and Scott⁵ in connection with the development of a new procedure for the calibration of chromatographic detectors. At the same time, in order to describe a similar gas extraction process, Burnett⁶ published another equation, used for the determination of partition coefficients. With our system of symbols it has the following form:

$$C_G = \frac{C_L^0}{K[1 - (V_g/KV_L)]} \cdot \exp(-V_g/V_L K) - \exp(-V_g/V_G) \quad (2)$$

where C_L^0 is the initial concentration of the volatile compound in the solution.

The above work preceded the development of headspace analysis, as continuous gas extraction gained widespread use in the 1970s. The reasons for the differences between eqns. 1 and 2 were then clarified. It was demonstrated⁷ that eqn. 1 concerns the situation where thermodynamic equilibrium between the liquid and the gas is established virtually instantly in all stages of the process, i.e., among gas bubbles passing through the solution and also between the solution and the gas enclosed above this solution. Under these conditions, a bubble of the gas leaving the solution and the gas leaving the vessel have the same composition. Eqn. 2 corresponds to a model in which the exchange between the liquid and the gas proceeds only during the passage of the bubble through the bulk of the liquid. In such a situation, the concentration of the compound in the stream of gas at the outlet from the vessel differs markedly from that in the gas bubble leaving the solution. Hence eqns. 1 and 2 describe two different models of the process; one of them assumes equilibrated exchange between the liquid and the gas in the volume V_G above the liquid layer in a closed vessel and the other one excludes it entirely.

The situation in which the exchange between the liquid and the gaseous phases in the vessel proceeds under static conditions only until the beginning of the flow of the gas through the solution is also possible. This is described by the equation

$$C_G = \frac{C_L^0}{K[1 - (V_g/KV_L)^2]} \left[\exp\left(-\frac{V_g}{KV_L}\right) - \frac{V_g}{KV_L} \exp(-V_g/V_G) \right] \quad (3)$$

Experimental testing showed that real continuous gas extraction process is accomplished under intermediate conditions. Calculations based on eqns. 1–3 can be derived if the conditions for the realization of the corresponding models are provided. For the use of eqn. 1 it is essential to ensure intense mixing of the gaseous phase. Eqn. 2 can be used with sufficiently high (but compatible with the demands on equilibrium mass transfer) flow-rates of the gas, provided that the mass transfer above the solution with the solution itself is minimized or excluded. All of the above require the construction of complicated devices, which is not always feasible. It is much simpler to select for the performance of the experiment conditions under which the role of the gas in the vessel can be neglected. This can easily be achieved if considerable “dead” volumes of the gas above the solutions are eliminated, *i.e.*, if vessels having negligibly small values of V_G are used. Inserting $V_G/KV_L = 0$, eqns. 1–3 are simplified to

$$C_G = \frac{C_L^0}{K} \cdot \exp(-V_g/KV_L) \quad (4)$$

A criterion for the usability of eqn. 4 is the condition that the differences in the results obtained by calculations with eqns. 1–3 must not exceed the error of the setting or the determination of the concentration of the compound in the gaseous stream. Substantially it is controlled by the value of V_G/KV_L . For instance, with $V_G/KV_L = 0.02$ and $V_g = 350$ ml, the differences between the values of C_G calculated according to eqn. 4 and eqns. 1–3 are 7.6, 0.1 and 2.1%, respectively, and with an increase in V_G/KV_L to 0.45, the differences become intolerable (344, 80 and 83%, respectively).

Even though the relationships among the different models of continuous gas extraction had been explained in 1979, we can still come across applications of eqn. 1 under conditions that do not guarantee its validity. In a paper on the enrichment of volatile admixtures⁸, the theory of the method is presented on the basis of eqn. 1 without any comments concerning the constraints on its application. In a review⁹ the description of dynamic variants of headspace analysis is also based only on eqn. 1.

Eqns. 1–4 characterize the process of continuous gas extraction of volatile compounds from a non-volatile solvent under experimental conditions. The extension of gas extraction to solutions in volatile solvents can make the scope of practical applications considerably wider. In 1978, we investigated the general case of the continuous gas extraction of binary systems without restrictions on the volatility of their components, which can be described by the equation

$$C_L = C_L^0 \left(\frac{V_L^0 - FV_g}{V_L^0} \right)^{(1-FK)/FK} \quad (5)$$

where F is a measure of the volatility of the solvent at a vapour pressure P_L , density δ_L and molecular mass M at temperature T ($F = P_L M / RT \delta_L$). The physical meaning F is the volume of the solvent in unit volume saturated with it.

The assumptions of ideality of phases, distribution of linear isotherms and character of the extraction process equilibrium are common to all the above cases. For solutions of finite dilution the first two assumptions are sufficiently justified (in the determination of admixtures), but the last factor mostly depends on the conditions under which the extraction is performed and needs particular investigation.

DYNAMIC HEADSPACE ANALYSIS UNDER NON-EQUILIBRIUM CONDITIONS

For aqueous solutions and solutions in organic liquids of low viscosity, thermodynamic equilibrium is virtually achieved by bubbling with small gas bubbles at a speed of the order of tens of ml/min. This can be partially verified by the correspondence of the results of measurements of partition coefficients by static and dynamic methods (see ref. 2, Tables 1.1 and 1.2). However, in viscous liquids and in elastic and solid particles, the mass transfer is difficult and establishment of the equilibrium is slowed and restricted by diffusion processes. In stripping gas extraction it is obviously not important whether or not the process is an equilibrium one, as only the components to be determined need to be extracted completely. In any variants of dynamic headspace analysis with incomplete extraction of components it is necessary that non-equilibrium of the processes be taken into consideration.

As already observed in the evaluation of discrete gas extraction under non-equilibrium conditions¹⁰, the amount of the volatile component, m_t , that has diffused into the gas phase within a time τ comprises a portion of this quantity, m_∞ , which would evaporate within the infinite time required for the establishment of true equilibrium. The ratio m_t/m_∞ characterizes the degree of the approximation towards equilibrium so that under stable conditions of mass transfer (form and surface area of the interphase, particle size, values of the diffusion coefficients and concentration gradients) the degree of approximation to an equilibrium separation will be determined by the duration of contact of the gas with the condensed phase. With a fixed time τ , the gas extraction process under non-equilibrium conditions can be described by equations of the same form as for equilibrium conditions. The only difference is that in place of the partition coefficients K the equations will involve parameters k that depend on τ and conditions of the mass transfer that characterize non-equilibrium ratios of the concentrations of the sample components in co-existing phases.

It follows from the above considerations that in continuous gas extraction with instantaneous concentration under non-equilibrium conditions, which is based on the analysis of concentrates or condensates of the components of the gaseous phase that was blown through the sample for identical time interval, the same equations can be used for the calculation as in discrete gas extraction, provided that the conditions of the process and the time of the collection of fractions are strictly controlled.

Such an approach was applied to the determination of trace amounts of interfering admixtures in electrolytes of lithium galvanic elements¹¹. Propyl carbonate, serving as a solvent, can contain undesirable contamination with propylene oxide, propanal, acetone and chloropropanols, which possess extremely high partition coefficients. Total extraction of these contaminants is difficult and the use of stripping is expedient, but direct headspace analysis when their concentrations are less than 100 mg/l is impossible. By repeating bubbling of the electrolyte with nitrogen for 30 min and analysing the contents of the cryogenic trap on the chromatograph each time, it was possible to determine the content of contaminants (with a relative standard deviation of 10%) from the ratio of the areas A (or heights) of the corresponding peaks on the chromatograms:

$$S_i = f_i A_i / (1 - A_2/A_1) \quad (6)$$

where f_i is calibration factor for each component i .

Eqn. 6 is analogous to the equations for calculation in multiple gas extraction under static equilibrium conditions. Non-equilibrium of the process leads only to a slight increase in the ratio A_2/A_1 and to a corresponding decrease in the precision of the analysis.

As the ratio A_{n+1}/A_n remains constant with increasing number of multiple extractions n , it can serve as an objective criterion of the possible application of such an approach to the determination of volatile components. However it is necessary to consider that a substantial increase in the number of extractions or in the volume of gas bubbled through can lead to the appearance of apparatus memory effects¹², which will cause a deviation from linearity of the function $\log A(n)$. However, these comments are associated with the question of applicability limits and with the field of most expedient applications of continuous gas extraction.

APPLICATIONS OF DYNAMIC HEADSPACE ANALYSIS

Extraction of volatile components of solutions with a stream of inert gas has been widely used in analytical practice for the determination of contaminants. The most popular variant is the purge and trap technique, which makes it possible to set the limits of the determinations of volatile components in solutions at units of parts per 10^9 with enrichment of the determined contaminants in cryogenic, adsorption or absorption traps. The possibilities of the method were found to be so attractive that most of the companies manufacturing gas chromatographic instrumentation supply their products with equipment for dynamic headspace analysis. However, the use of dynamic headspace analysis for the enrichment and determination of volatile contaminants is not always justified. First, this is connected with the complexity of the technical performance of the analysis, with the possibility of forming fog and with mechanical delivery of the condensed phase in a gas stream. In a number of instances, particularly in the determination low-volatile and poorly soluble compounds, the use of direct static headspace analysis appears more appropriate as it makes it possible, without any concentration, to decrease the limit of determination of the components, with low partition coefficients ($K < 10$) by gas chromatography by 2–3 orders of magnitude² to the level of units of parts per 10^9 . An exception to this rule arises in instances where the concentrations of volatile compounds in the sample material are very low (parts per 10^9 and below) and the concentrations of the components to be determined in the extracting gas are at the same level as those of impurities present in the gas. In such instances it is appropriate to use the circular version of dynamic headspace analysis¹³, which avoids the accumulation of contaminants of the carrier gas in the concentrator.

When the sensitivities of static and dynamic headspace analyses are the same, the static variants, the reproducibility and accuracy of which are better, are to be preferred. Regardless of evidence for this aspect, descriptions can be found in the literature of applications of the purge and trap technique to situations where it need not have been used and where static headspace analysis could have readily provided the required sensitivity. The determination of halocarbons in water represents the best example. The importance of the solution of this problem, particularly for drinking water, stimulated a number of studies in which dynamic headspace analysis was mainly

used (e.g., refs. 14–17) and static variants for the same purposes were hardly mentioned. The required limit of determination of halocarbons, of the order of micrograms per litre, can also be achieved by direct headspace analysis under static conditions as the partition coefficients of the simplest halocarbons differ only slightly from unity¹⁸ at about room temperature.

The use of dynamic headspace analysis is suitable only in the determination of compounds with high partition coefficients ($k > 10^3$), where the volume of the gaseous phase must be increased considerably in order to extract an amount of the compound sufficient for the determination. Under static conditions the ratio of the volume of the extracting gas to that of the condensed phase usually seldom exceeds 10–20. In a dynamic version this ratio is limited by the volatility of the condensed phase only and values of 10^3 and higher can be achieved.

The higher efficiency of dynamic headspace analysis is an advantage over static variants as, with the use of the same volume of gas, continuous gas extraction extracts larger amounts of a compound. In addition, a higher degree of enrichment can be achieved by headspace concentration at the expense of using a larger volume of the extracting gas. However, regardless of the higher efficiency of continuous gas extraction, static conditions for the determination of compounds with high partition coefficients are sometimes preferred owing to difficulties with the reproducibility of the conditions of the dynamic versions.

REFERENCES

- 1 H. Hachenberg and A. P. Schmidt, *Gas Chromatographic Headspace Analysis*, Heyden, London, 1977.
- 2 B. V. Ioffe and A. G. Vitenberg, *Head-Space Analysis and Related Method in Gas Chromatography*, Wiley, New York, 1984.
- 3 Ö. Wahlroos, *Acta Chem. Scand.*, 15 (1961) 2053.
- 4 Ö. Wahlroos, *Acta Chem. Scand.*, 20 (1966) 197.
- 5 I. A. Fowles and R. P. W. Scott, *J. Chromatogr.*, 11 (1963) 1.
- 6 M. G. Burnett, *Anal. Chem.*, 35 (1963) 1567.
- 7 A. G. Vitenberg and M. I. Kostkina, *Zh. Anal. Khim.*, 34 (1979) 1800.
- 8 J. Curvers, Th. Noy, C. Cramers and J. Rijks, *J. Chromatogr.*, 289 (1984) 171.
- 9 J. Drozd and J. Novák, *J. Chromatogr.*, 165 (1979) 141.
- 10 B. V. Ioffe and T. L. Reznik, *Zh. Anal. Khim.*, 36 (1981) 2191.
- 11 B. V. Ioffe, G. N. Bystrova and I. G. Zenkevich, *Zh. Anal. Khim.*, 40 (1985) 306.
- 12 B. V. Ioffe, A. G. Vitenberg and T. L. Reznik, *Zh. Anal. Khim.*, 37 (1982) 902.
- 13 J. Drozd, Z. Vodáková and J. Novák, *J. Chromatogr.*, 354 (1986) 47.
- 14 E. Kozłowski, E. Slenkowska-Zyskowska and M. Biznik, *Chem. Anal. (Warsaw)*, 28 (1983) 817.
- 15 T. Wang and R. Lenahan, *Bull. Environ. Contam. Toxicol.*, 32 (1984) 429.
- 16 R. Otson and D. T. Williams, *Anal. Chem.*, 54 (1982) 942.
- 17 G. Castello, T. C. Gerbino and S. Kanitz, *J. Chromatogr.*, 247 (1982) 263.
- 18 L. E. Kaiser and B. G. Oliver, *Anal. Chem.*, 48 (1976) 2207.

CHROM. 21 288

THEORY OF OPEN-TUBE CHROMATOGRAPHY: AN EXACT PROOF OF GOLAY'S EQUATIONS

A. A. CLIFFORD

Department of Physical Chemistry, University of Leeds, Leeds LS2 9JT (U.K.)

SUMMARY

A proof is given of Golay's equations for chromatography in an uncoated (or thinly coated), open-tubular column. The new derivation is exact and it is thus shown that it is not necessary to neglect some terms in the appropriate equations, as has been done in previous proofs. Furthermore, the proof is given for the situation where the rate of adsorption on to and desorption from the tube walls is not considered to be infinitely fast as was previously discussed. The effect of comparatively slow equilibration of material between the flowing medium and the tube wall is to increase the width of a peak, but not to change the average degree of retention.

INTRODUCTION

The theory of chromatography in an open tube was considered by Golay in 1958¹ and his proof is reproduced in many textbooks on chromatography. The problem is a special case of the theory of dispersion of material in a medium flowing in a tube which has been studied for a variety of circumstances; originally by Westhaver² for the concentration of a potassium isotope by countercurrent electromigration and later by a number of authors whose papers have been reviewed recently³.

In Golay's treatment, the appropriate differential equation and boundary condition are manipulated and it is then asserted that certain terms are comparatively small and they are therefore neglected. While investigating a related but more complex problem⁴ (the dispersion and chromatography of hydrogen atoms in a flown gas⁵) it has been found that it is not necessary to make these approximations and that Golay's ultimate equations can be proved exactly. This paper sets out the exact proof with one additional complication. In the proof below we do not assume, as did Golay, that the equilibration of material between the carrier and the stationary walls is instantaneous, but allow it to occur at a finite rate. This adds an extra term to Golay's equation for the peak width, which tends to zero as the rate of equilibration tends to infinity.

The equation which governs this problem, and from which Golay begins his treatment, is the general diffusion equation

$$\frac{\partial f}{\partial t} = \nabla \cdot (D \nabla f) - v \cdot \nabla f, \quad (1)$$

where ∇ is the differential operator, f is the local and instantaneous concentration of the material being transported, D is the diffusion coefficient, and v the velocity of the medium at the particular point in the column. In the present paper, as in Golay's treatment, we consider a circular column in which there is streamline (Pouisseulle or laminar) flow with no "slip" of the boundary layer along the tube wall.

We also assume, as did Golay, that the pressure is constant along the column (*i.e.* the gas viscosity coefficient is tending to zero) and consequently the diffusion coefficient and average velocity of the carrier is constant. This will certainly not be the case in open-tube chromatography, where a drop of one atmosphere pressure across a long column of 100 m is common. But, because the fractional drop in pressure over a one metre length of the column is small, it is believed that the results for a constant pressure model can be applied to the situation of a pressure drop with good approximation.

The column is a cylinder, and the cylindrical coordinates r , θ and z are used. It is assumed from the outset that the concentration of material is independent of the azimuthal angle θ . It can be shown⁴ that, if this is not the case initially it will rapidly become so. Thus, $f \equiv f(r, z, t)$. In the new coordinates and making all the assumptions given above eqn. 1 becomes

$$\frac{\partial f}{\partial t} = D \frac{\partial^2 f}{\partial z^2} + D \frac{1}{r} \frac{\partial}{\partial r} \left(r \frac{\partial f}{\partial r} \right) - 2v_o \left(1 - \frac{r^2}{r_o^2} \right) \frac{\partial f}{\partial z}, \quad (2)$$

where r_o is the column radius, and v_o is the average velocity of the carrier. The expression $2v_o [1 - (r^2/r_o^2)]$ gives the variation of velocity across the column from zero at the walls to $2v_o$ at the centre.

This differential equation has to be solved in conjunction with a boundary condition which for Golay's treatment, assuming rapid equilibration, was

$$-D \frac{\partial f}{\partial r} = \frac{r_o k'}{2} \frac{\partial f}{\partial t}, \quad (3)$$

where k' is a constant which was assumed to be the ratio of the amount of material on the tube wall to that in the carrier. Golay solved eqn. 2 with the condition given in eqn. 3 by manipulating the equations and using his insight into the problems to neglect certain terms, which he asserted were small. He finally obtained the correct results that the average velocity (v_{av}) of the material is given by

$$v_{av} = \frac{v_o}{1 + k'} \quad (4)$$

and the rate of increase of the mean-squared width of the peak of material is equal to

$$\frac{2D}{1 + k'} + \frac{r_o^2 v_o^2}{24D} \cdot \frac{1 + 6k' + 1(k')^2}{(1 + k')^3} \quad (5)$$

BOUNDARY CONDITION FOR FINITE RATES OF EQUILIBRATION

It is first necessary to obtain the boundary condition that is appropriate when adsorption and desorption are not fast. Let k_a be the rate of adsorption per unit area per unit concentration in the carrier near the surface, k_d the rate of desorption per unit area per unit surface concentration, and f_s the surface concentration. By Fick's law the flux of molecules near the surface is equal to $-D(\partial f/\partial r)$ and so at $r = r_o$

$$-D \frac{\partial f}{\partial r} = k_a f - k_d f_s. \quad (6)$$

The change of surface concentration will be equal to the same quantity;

$$\frac{\partial f_s}{\partial t} = k_a f - k_d f_s \quad (7)$$

Elimination of f_s from eqns. 6 and 7 gives

$$D \frac{\partial^2 f}{\partial r \partial t} + k_a \frac{\partial f}{\partial t} + k_d D \frac{\partial f}{\partial r} = 0. \quad (8)$$

This is the boundary condition that we seek. As will be shown later this boundary condition becomes identical to that used in Golay's derivation and eqn. 8 becomes eqn. 3 as k_a and k_d become large in the rapid equilibration limit.

EQUATIONS FOR THE MOMENTS

Eqn. 2 is difficult to solve because the variables are not separable. We therefore turn to the method of moments, first used by Aris⁶ in this context for a similar but simpler problem. We define the p th moment of the distribution of the injected material, c_p , by

$$c_p(r, t) = \int_{-\infty}^{\infty} f(r, z, t) z^p dz \quad (9)$$

We will be interested in the zeroth, first and second moment given by $p = 0, 1$ and 2 in eqn. 9. These will respectively give information about the total amount of material, its average flow-rate, and its average width. It should be noted that the moments, c_p , depend on the radial coordinate r . They refer to the distribution of material in longitudinal elemental filaments inside the column.

We also define moments averaged over the column cross-section, m_p by

$$m_p(t) = 2\pi \int_0^r c_p(r, t) r dr \quad (10)$$

m_0 will be the total amount of material in the column, which will expect to be constant. m_1/m_0 will give the average distance of the material along the tube and will give information about chromatographic retention. m_2/m_0 will give the mean-squared distance of the material from the beginning of the column and thus $[m_2/m_0 - (m_1/m_0)^2]$ will give the mean-squared distance of the material from its average position, *i.e.* the mean-squared width of the peak.

The calculation is carried out as follows. Equations are obtained for the moments c_p and solutions for c_0 , c_1 and c_2 are found. The moments m_0 , m_1 and m_2 are then calculated from the solutions for c_0 , c_1 and c_2 . To obtain equations for the moment c_p , both the differential eqn. 2 and its boundary condition (eqn. 8) are multiplied by $z^p dz$ and integrated from $-\infty$ to $+\infty$ to give, respectively

$$\frac{\partial c_p}{\partial t} = D \frac{1}{r} \frac{\partial}{\partial r} \left(r \frac{\partial c_p}{\partial r} \right) + 2v_0 \left(1 - \frac{r^2}{r_0^2} \right) p c_{p-1} + D p (p-1) c_{p-2} \quad (11)$$

and

$$D \frac{\partial^2 c_p}{\partial r \partial t} + k_a \frac{\partial c_p}{\partial t} + k_d \frac{\partial c_p}{\partial r} = 0 \quad (12)$$

Eqn. 11 was obtained using integration by parts and also assuming that $f(r, z, t) \rightarrow 0$ as $z \rightarrow \pm \infty$. Equation 11 is a general equation for the moments c_p , which must be solved in conjunction with its boundary condition¹³. The most general solutions are quite complex, but a full analysis shows that only parts of the solutions are important even a very short time after injection of the material on to the column⁵. These are the solutions that are practically important and that are given below.

SOLUTIONS FOR THE MOMENTS c_0 AND m_0

The equation for c_0 is (eqn. 11)

$$\frac{\partial c_0}{\partial t} = D \frac{1}{r} \frac{\partial}{\partial r} r \frac{\partial c_0}{\partial r} \quad (13)$$

and its boundary condition (eqn. 12), at $r = r_0$, is

$$D \frac{\partial^2 c_0}{\partial r \partial t} + k_a \frac{\partial c_0}{\partial t} + D k_d \frac{\partial c_0}{\partial r} = 0 \quad (14)$$

These equations are satisfied by

$$c_0 = A \quad (15)$$

where A is a constant, independent of r and t . This shows that there is a solution where the total amount of material in a longitudinal filament in the open-tube column is constant and the same in all filaments of the same cross-sectional area. There is

therefore a steady-state solution where there is no net radial flow of material (although there is in fact radial flow at particular points in the column which averages to zero).

Application of eqn. 10 to the solution (eqn. 15) gives also

$$m_o = \pi r_o^2 A \quad (16)$$

and m_o , the total amount of material in the tube, is also as expected, a constant, independent of time.

SOLUTIONS FOR THE MOMENTS c_1 AND m_1

The equation for c_1 , obtained from eqn. 11 after substituting for c_o , is

$$\frac{\partial c_1}{\partial t} = D \frac{1}{r} \frac{\partial}{\partial r} \left(r \frac{\partial c_1}{\partial r} \right) + 2A v_o \left(1 - \frac{r^2}{r_o^2} \right) \quad (17)$$

and its boundary condition (eqn. 12), at $r = r_o$, is

$$D \frac{\partial^2 c_1}{\partial r \partial t} + k_a \frac{\partial c_1}{\partial t} + D k_a \frac{\partial c_1}{\partial r} = 0 \quad (18)$$

As can be shown by substituting into both equations, a solution for c_1 is

$$c_1 = B + A \frac{v_o r_o^2}{8D} \left[\frac{r^4}{r_o^4} - 2 \left(\frac{1 + 2k'}{1 + k'} \right) \frac{r^2}{r_o^2} \right] + A \frac{v_o}{1 + k'} t \quad (19)$$

where B is another constant and k' is defined by

$$k' = 2k_a / r_o k_a \quad (20)$$

We shall show later that k' is identical to the normal chromatographic retention coefficient.

The moment m_1 can then be calculated using eqn. 10 to be

$$\frac{m_1(t)}{\pi r_o^2} = B - \frac{A v_o r_o^2}{24D} \cdot \frac{2 + 5k'}{1 + k'} + \frac{A v_o}{1 + k'} t \quad (21)$$

Using the boundary condition that $m_1 = 0$ at $t = 0$, then

$$B = \frac{A v_o r_o^2}{24D} \cdot \frac{2 + 5k'}{1 + k'} \quad (22)$$

and

$$m_1(t) = \pi r_o^2 \frac{A v_o}{1 + k'} t \quad (23)$$

and hence

$$m_1(t)/m_o = \frac{v_o}{1+k'} t \quad (24)$$

as obtained by Golay. Using this value of B , the equation for c_1 becomes

$$c_1 = \frac{Av_o r_o^2}{24D} \left[3 \frac{r^4}{r_o^4} - 6 \left(\frac{1+2k'}{1+k'} \right) \frac{r^2}{r_o^2} + \left(\frac{2+5k'}{1+k'} \right) \right] + \frac{Av_o}{1+k'} t \quad (25)$$

SOLUTIONS FOR THE MOMENTS c_2 AND m_2

The equation for c_2 , obtained from (eqn. 11) after substituting for c_o and c_1 , is

$$\begin{aligned} \frac{\partial c_2}{\partial t} = D \frac{1}{r} \frac{\partial}{\partial r} r \frac{\partial c_2}{\partial r} + \\ + 4v_o \left(1 - \frac{r^2}{r_o^2} \right) \left\{ \frac{Av_o r_o^2}{24D} \left[3 \frac{r^4}{r_o^4} - 6 \left(\frac{1+2k'}{1+k'} \right) \frac{r^2}{r_o^2} + \frac{2+5k'}{1+k'} \right] + \frac{Av_o}{1+k'} t \right\} + 2AD \end{aligned} \quad (26)$$

and its boundary condition, at $r = r_o$, is

$$D \frac{\partial^2 c_2}{\partial r \partial t} + k_d \frac{\partial c_2}{\partial t} + Dk_d \frac{\partial c_2}{\partial r} = 0 \quad (27)$$

As can be shown by substitution, a solution for c_2 is the following

$$\begin{aligned} c_2 = C + A \left\{ \left(-\frac{1}{2} \frac{k'}{1+k'} + \frac{v_o^2}{2Dk_d} \cdot \frac{k'}{(1+k')^3} - \frac{v_o^2 r_o^2}{96D^2} \cdot \frac{3+16k'+27(k')^2+20(k')^3}{(1+k')^3} \right) r^2 + \right. \\ + \left(\frac{v_o^2}{96D^2} \cdot \frac{5+19k'+17(k')^2}{(1+k')^2} \right) r^4 - \left(\frac{5v_o^2}{144D^2 r_p^2} \cdot \frac{1+2k'}{1+k'} \right) r^6 + \left(\frac{v_o^2}{128r_o^4 D^2} \right) r^8 + \\ + \left(\frac{2D}{1+k'} + \frac{2v_o^2}{k_d} \cdot \frac{k'}{(1+k')^3} + \frac{r_o^2 v_o^2}{24D} \cdot \frac{5+20k'+21k'^2}{(1+k')^3} \right) t - \\ \left. - \left(\frac{v_o^2}{2D} \cdot \frac{1+2k'}{(1+k')^2} \right) r^2 t + \left(\frac{v_o^2}{4Dr_o^2} \cdot \frac{1}{1+k'} \right) r^4 t + \frac{v_o^2}{(1+k')^2} t^2 \right\} \end{aligned} \quad (28)$$

This is a complex function of both r and t , but m_2 can be calculated from it using eqn. 10 to be

$$m_2(t) - m_2(o) = \pi r_o^2 A \left[\frac{2D}{1+k'} + \frac{2v_o^2}{k_d} \cdot \frac{k'}{(1+k')^3} + \frac{r_o^2 v_o^2}{24D} \cdot \frac{1+6k'+11(k')^2}{(1+k')^3} \right] t + \frac{Av_o^2}{(1+k')^2} t^2 \quad (29)$$

In this equation, all the constants independent of time have been lumped together in $m_2(0)$, the second moment of the peak when injected. The quantity $m_2/m_o - (m_1/m_o)^2$, which gives the mean squared width of the pulse is thus given by its initial value plus the quantity

$$\left[\frac{2D}{1+k'} + \frac{2v_o^2}{k_d} \cdot \frac{k'}{(1+k')^3} + \frac{r_o^2 v_o^2}{24D} \cdot \frac{1+6k'+11(k')^2}{(1+k')^3} \right] t \quad (31)$$

Of the three terms in the square brackets, the first and last are identical to those obtained by Golay and given by eqn. 5.

THE CHROMATOGRAPHIC RETENTION COEFFICIENT, k'

So far the quantity k' has been defined by eqn. 20 in terms of k_a and k_d . In this section it will be proved that in a chromatography column k' is equal to the ratio of the amount of material adsorbed on the walls to that in the carrier. For a stationary gas in a closed tube, which has reached equilibrium it is easy to see that this is the case. The concentration will be uniform throughout the tube and the rates of adsorption will be equal at equilibrium and

$$k_a f = k_d f_s \quad (31)$$

In a column of length l the ratio of the total amount of material on the wall to that in the gas will be given by

$$2\pi r_o l f_s / \pi r^2 l f \quad (32)$$

which from eqns. 31 and 20 is equal to k' .

For a moving carrier we need to investigate the surface concentration as a function of z and t . It is given by eqn. 6 as

$$f_s = \frac{k_a}{k_d} f(r_o) - \frac{D}{k_d} \left(\frac{\partial f}{\partial r} \right)_{r=r_o} \quad (33)$$

Multiplying by dz and integrating between $\pm \infty$ gives

$$\int_{-\infty}^{\infty} f_s(z,t) dz = \frac{k_a}{k_d} c_o(r_o,t) - \frac{D}{k_d} \left[\frac{c_o(r,t)}{\partial r} \right]_{r=r_o} \quad (34)$$

The total amount of material on the surface is therefore given by

$$2\pi r_o \int_{-\infty}^{\infty} f_s(z,t) dz = 2\pi r_o \frac{k_a}{k_d} A \quad (35)$$

since $c_o = A$ is a constant. The ratio of this to the total amount of material in the carrier, m_o , (given by eqn. 16) is therefore $2k_a/r_o k_d = k'$, in a moving carrier also.

DISCUSSION

The equations for open-tube chromatography at constant pressure have been solved without approximation. The solution given is not the most general one, but it has been shown elsewhere⁴ that it is the only solution that is stable. The final expressions obtained both for the rate of elution and for the dispersion of material are basically those given correctly some time ago by Golay using an approximation method.

In this treatment, however, it has not been assumed that the rate of equilibration of material between the carrier and the surface is infinitely rapid. This has been found not to affect the degree of chromatographic retention, but increases the rate of dispersion (or spreading) of the peak. The rate of dispersion is given by eqn. 31 and contains three terms. The first, $2D/(1 + k')$, arises from longitudinal diffusion. The third term,

$$\frac{r_o^2 v_o^2}{24D} \cdot \frac{1 + 6k' + 11(k')^2}{(1 + k')^3} \quad (36)$$

represents dispersion due to the variation of velocity across the column, which is reduced by radial diffusion. The second term is a new one due to the finite rate of adsorption and is equal to

$$\frac{2v_o^2}{k_a} \cdot \frac{k'}{(1 + k')^3} = \frac{v_o^2 r_o}{k_a} \cdot \frac{(k')^2}{(1 + k')^3} \quad (37)$$

The effect arises from the variance of the time spent by molecules of the material on the surface. The more rapid absorption and desorption is for a given k' , the more times a molecule absorbs and desorbs as it passes through the column, and the closer is the time spent by that molecule on the surface to the average. Thus for rapid equilibration the term in eqn. 37 will disappear and eqn. 31 will resemble Golay's original expression (eqn. 5). At the same time the boundary condition given in eqn. 8 will reduce to Golay's boundary condition (eqn. 3).

Finally, it was shown that the ratio of the total amounts of material on the surface to that in the carrier is given by

$$k' = 2k_a/r_o k_d$$

for a moving carrier where k_a and k_d , the rate constants for adsorption and desorption, are defined in the section boundary condition for finite rates of equilibrium. This is in spite of the fact that the longitudinal distribution in the carrier varies with the radial parameter and is, in general, different again from that on the surface.

ACKNOWLEDGEMENTS

The author would like to thank Professor P. Gray, Dr. K. D. Bartle and Dr. T. Boddington for helpful discussions and S.E.R.C. for financial support.

REFERENCES

- 1 M. J. E. Golay, in D. H. Desty (Editor), *Gas Chromatography*, Butterworths, London, 1958, pp. 36–55.
- 2 J. W. Westhaver, *J. Res. Nat. Bur. Stand.*, 38 (1947) 169–183.
- 3 R. Aris, in W. E. Stewart, W. H. Harmon and C. C. Conley (Editors), *Dynamics and Modelling of Reactive Systems*, Academic Press, New York, 1980, pp. 1–35.
- 4 T. Boddington and A. A. Clifford, *Proc. R. Soc. London*, A389 (1983) 179–196.
- 5 A. A. Clifford, P. Gray, R. S. Mason and J. I. Waddicor, *Faraday Disc. R. Soc. Chem.*, 15 (1980) 155–160.
- 6 R. Aris, *Proc. R. Soc. London*, A235 (1956) 67–77.

CHROM. 21 307

APPLICATION OF A UNIFIED MOLECULAR THEORY TO GAS-LIQUID CHROMATOGRAPHY

DANIEL E. MARTIRE

Department of Chemistry, Georgetown University, Washington, DC 20057 (U.S.A.)

SUMMARY

A novel, unified molecular theory of chromatography is applied to derive equations for gas-liquid chromatography (GLC) and to treat representative GLC problems involving the interpretation and prediction of absolute retention (partition coefficients), the effect of the molecular weight of the stationary liquid phase on relative retention, and the isolation and quantitation of functional-group (energetic) contributions to retention. The utility and efficacy of this new theoretical approach to GLC are thereby demonstrated.

INTRODUCTION

A unified molecular theory of fluid-liquid (absorption) chromatography, encompassing gas, liquid and supercritical-fluid mobile phases, has recently been developed¹. This comprehensive theory, which is based on a lattice-fluid (or Ising-fluid) model and statistical thermodynamics is applied in the present paper to treat more rigorously several representative problems in gas-liquid chromatography (GLC) with a single-component stationary liquid phase (solvent): (1) the interpretation and prediction of absolute retention for simple, alkane solute plus alkane solvent systems; (2) the effect of the molecular weight (or chain length) of the solvent on solute relative retention and, cognately, the use of GLC for the determination of solvent molecular weight; (3) the isolation and quantitative assessment of functional-group (energetic) contributions to solute retention. The following derivations and analyses are intended to be indicative rather than exhaustive.

THEORY

In the lattice-fluid model^{1,2}, expansion (compression) effects, configurational entropy, and attractive and repulsive interactions are rigorously taken into account using the Bragg-Williams (random-mixing) approximation. In this model a molecule of component i is taken to consist of r_i segments, where r_i is proportional to the hard-core or van der Waals volume of the molecule. The attractive interaction energy between nearest-neighbor segments on molecules i and j is designated by ε_{ij} , where, adopting the Sanchez-Lacombe (SL) convention² here, $\varepsilon_{ij} > 0$. Also, for a given pure

component ($j = i$), the segmental pair interaction energy, ε_{ii} , is related to the SL reduced temperature of that component, \tilde{T}_i , by^{1,2}

$$z\varepsilon_{ii}/2k_{\text{B}}T = \tilde{T}_i^{-1} = T_i^*/T \quad (1)$$

where z is the coordination number of the lattice, k_{B} is the Boltzmann constant, T is the absolute temperature, and T_i^* , the characteristic temperature of component i (a scale parameter, not to be confused with the critical temperature), is proportional to ε_{ii} . Similarly, the SL reduced density of pure component i , $\tilde{\rho}_i$, is related to the experimental, pure-component density, ρ_i^0 , by^{1,2}

$$\tilde{\rho}_i = \rho_i^0/\rho_i^* = \theta_i^0 \quad (2)$$

where ρ_i^* is the characteristic density of component i (the close-packed density; another scale parameter, not to be confused with the critical density) and θ_i^0 is the occupied volume fraction of pure i .

In the following treatment, the subscripts a, b, c and d denote, respectively, solute molecules containing other functional groups in addition to paraffinic ones (a = "active" solute), paraffinic solute molecules (b = "reference" solute), solvent molecules containing other functional groups in addition to paraffinic ones (c = "active" solvent), and paraffinic solvent molecules (d = "reference" solvent). Eqn. 39 (or 40) in ref. 1 describes the distribution constant (partition coefficient), K , for ideal GLC (strictly, the value obtained by extrapolation to zero column pressure). Substituting $\tilde{\rho}_i$ for θ_i^0 and using the convention $\varepsilon_{ij} > 0$ [rather than $\varepsilon_{ij} < 0$ (ref. 1)], the equation for the reference system (solute b + solvent d) becomes

$$\ln K_{\text{b(d)}} = r_{\text{b}}[(z\varepsilon_{\text{bd}}/k_{\text{B}}T)\tilde{\rho}_{\text{d}} - (z\varepsilon_{\text{dd}}/2k_{\text{B}}T)\tilde{\rho}_{\text{d}}^2 - (1 - r_{\text{d}}^{-1})\tilde{\rho}_{\text{d}}] \quad (3)$$

It sensibly predicts that K , hence the specific retention volume, will increase with increasing r_{b} , increasing ε_{bd} and decreasing ε_{dd} , and clearly shows that K depends on both T and $\tilde{\rho}_{\text{d}}$, where the latter governs the average distance between molecules (and non-bonded molecular segments) in the stationary phase. Note that the last term, $-r_{\text{b}}(1 - r_{\text{d}}^{-1})\tilde{\rho}_{\text{d}}$, is the configuration entropy contribution to $\ln K$.

Introducing eqn. 1 into eqn. 3, one obtains an expression in terms of the reduced variables of the solvent component:

$$\ln K_{\text{b(d)}} = r_{\text{b}}[2(\varepsilon_{\text{bd}}/\varepsilon_{\text{dd}})(\tilde{\rho}_{\text{d}}/\tilde{T}_{\text{d}}) - (\tilde{\rho}_{\text{d}}^2/\tilde{T}_{\text{d}}) - (1 - r_{\text{d}}^{-1})\tilde{\rho}_{\text{d}}] \quad (4)$$

Allowing for a deviation from the geometric-mean approximation for ε_{bd} , one has

$$\varepsilon_{\text{bd}} \approx (\varepsilon_{\text{bb}}\varepsilon_{\text{dd}})^{1/2}(1 + \eta_{\text{bd}}) \quad (5)$$

where η_{bd} , which reflects the deviation, is expected to be small with respect to unity. Substituting eqns. 1 and 5 into eqn. 4, one obtains

$$\ln K_{\text{b(d)}} = r_{\text{b}}[(2/\tilde{T}_{\text{b}}^{1/2})(1 + \eta_{\text{bd}})(\tilde{\rho}_{\text{d}}/\tilde{T}_{\text{d}}^{1/2}) - (\tilde{\rho}_{\text{d}}^2/\tilde{T}_{\text{d}}) - (1 - r_{\text{d}}^{-1})\tilde{\rho}_{\text{d}}] \quad (6)$$

which may be written as follows:

$$\ln K_{b(d)} = r_b \{ A[(1 + \eta_{bd})/\tilde{T}_b^{1/2}] - B \} \quad (7)$$

where

$$A = (2\rho_d/\tilde{T}_d^{1/2}) \quad (8)$$

$$B = (\tilde{\rho}_d^2/\tilde{T}_d) + (1 - r_d^{-1})(\tilde{\rho}_d) \quad (9)$$

Note that A and B depend only on properties of the pure solvent. Therefore, if the molecular-size parameters r_b and r_d , and the reduced variables $\tilde{\rho}_d$, \tilde{T}_d and \tilde{T}_b are known, and the binary molecular parameter η_{bd} can be determined, then it should be possible to utilize eqn. 6 (or eqns. 7–9) for the prediction of absolute partition coefficients of alkane solutes in alkane solvents. The feasibility of this approach will be investigated in the next section.

It follows from eqn. 4 that, for the system (solute a + solvent d), one can write

$$\ln K_{a(d)} = r_a [2(\varepsilon_{ad}/\varepsilon_{dd})(\tilde{\rho}_d/\tilde{T}_d) - (\tilde{\rho}_d^2/\tilde{T}_d) - (1 - r_d^{-1})\tilde{\rho}_d] \quad (10)$$

If one now chooses a and b such that $r_a \approx r_b$ (*vide infra*), then eqns. 4 and 10 give

$$\ln[K_{a(d)}/K_{b(d)}] = \ln R_{(a/b)(d)} \approx 2r_b [(\varepsilon_{ad}/\varepsilon_{dd}) - (\varepsilon_{bd}/\varepsilon_{dd})] [\tilde{\rho}_d/\tilde{T}_d] \quad (11)$$

where $R_{(a/b)(d)}$ is the relative retention of solutes a and b in solvent d. Note that eqn. 11 predicts that R will increase with increasing r_b , increasing ε_{ad} , decreasing ε_{bd} , increasing $\tilde{\rho}_d$ and decreasing \tilde{T}_d . Also, a modified geometric-mean expression, similar to eqn. 5, can be written for ε_{ad} :

$$\varepsilon_{ad} \approx (\varepsilon_{aa}\varepsilon_{dd})^{1/2}(1 + \eta_{ad}) \quad (12)$$

Applying eqns. 1, 5 and 12 to eqn. 11 yields

$$\ln R_{(a/b)(d)} \approx 2r_b \{ [(1 + \eta_{ad})/\tilde{T}_a^{1/2}] - [(1 + \eta_{bd})/\tilde{T}_b^{1/2}] \} (\tilde{\rho}_d/\tilde{T}_d^{1/2}) \quad (13)$$

Eqn. 13 describes, in terms of the reduced temperatures of the pure components, the reduced density of the solvent component and three molecular parameters, r_b , η_{ad} and η_{bd} , the relative retention of an “active” solute and a “reference” solute in a given “reference” solvent. It will be applied in the next section to examine the dependence of this relative retention on the molecular weight (or chain length) of n -alkane solvents.

From eqns. 1 and 11:

$$\ln R_{(a/b)(d)} \approx r_a (z/k_B T) (\varepsilon_{ad} - \varepsilon_{bd}) (\tilde{\rho}_d) \quad (14)$$

where r_b has now been replaced by r_a ($\approx r_b$). Similarly, the relative retention of solutes a and b in an “active” solvent (c), $R_{(a/b)(c)}$, is given by

$$\ln R_{(a/b)(c)} \approx r_a(z/k_B T)(\varepsilon_{ac} - \varepsilon_{bc})(\tilde{\rho}_c) \quad (15)$$

If one chooses solvents c and d such that $\tilde{\rho}_c \approx \tilde{\rho}_d$ [solvents having comparable chain lengths ($r_c \approx r_d$) and expansion coefficients^{1,2}], then subtracting eqn. 14 from eqn. 15 yields

$$\ln[R_{(a/b)(c)}/R_{(a/b)(d)}] = \ln Q \approx r_a(z/k_B T)(\varepsilon_{ac} - \varepsilon_{bc} - \varepsilon_{ad} + \varepsilon_{bd})(\tilde{\rho}_d) \quad (16)$$

where Q is the ratio of two relative retention quantities.

Recalling the nature of molecules a, b, c and d, and assuming that the “active” solute molecules (a) consist of type-p (paraffinic) and type-x chemical groups and the “active” solvent molecules (c) consist of type-p and type-y chemical groups, while the “reference” molecules (b and d) consist only of type-p groups, the ε_{ij} values in eqn. 16 may be decomposed as follows^{3,4}:

$$\varepsilon_{bd} = \varepsilon_{pp} \quad (17a)$$

$$\varepsilon_{ad} = f_{ap}\varepsilon_{pp} + f_{ax}\varepsilon_{px} \quad (17b)$$

$$\varepsilon_{bc} = f_{cp}\varepsilon_{pp} + f_{cy}\varepsilon_{py} \quad (17c)$$

$$\varepsilon_{ac} = f_{ap}f_{cp}\varepsilon_{pp} + f_{ap}f_{cy}\varepsilon_{py} + f_{ax}f_{cp}\varepsilon_{px} + f_{ax}f_{cy}\varepsilon_{xy} \quad (17d)$$

where ε_{kl} ($k, l = p, x, y$) now denotes the attractive interaction energy, per unit segment, between type- k and type- l moieties on adjacent molecules, and f_{jk} ($j = a, b, c, d$; $k = p, x, y$) denotes the fraction of a molecule of type- j that contains type- k functional groups. Note that the number of segments on molecule j containing type- k moieties, r_{jk} , is related to f_{jk} by

$$r_{jk} = f_{jk}r_j \quad (18a)$$

$$\sum_k r_{jk} = \sum_k f_{jk}r_j = r_j \quad (18b)$$

where $f_{ap} + f_{ax} = 1$, $f_{cp} + f_{cy} = 1$, $f_{bp} = 1$ and $f_{dp} = 1$.

Use of eqns. 17 and 28 in eqn. 16 leads to, after much algebra

$$\ln[R_{(a/b)(c)}/R_{(a/b)(d)}] = \ln Q_{xy} \approx (\tilde{\rho}_d)(r_a f_{ax} f_{cy})(z/k_B T)(\varepsilon_{xy} - \varepsilon_{py} - \varepsilon_{px} + \varepsilon_{pp}) \quad (19)$$

Since $r_a f_{ax} = r_{ax}$ and $f_{cy} = r_{cy}/r_c \approx r_{cy}/r_d$ (eqn. 18), then eqn. 19 may be written as

$$\ln Q_{xy} \approx (\tilde{\rho}_d)(r_x r_y / r_d)(z/k_B T)(\Delta w_{xy} - \Delta w_{px} - \Delta w_{py}) \quad (20)$$

where the first subscript on r_{ax} and r_{cy} has become unnecessary and been deleted, and

$$\Delta w_{kl} = \varepsilon_{kl} - (\varepsilon_{kk} + \varepsilon_{ll})/2 \quad (21)$$

where Δw_{kl} is the interchange energy for the formation of a k - l pair interaction¹. Inspection of eqn. 20 reveals that, provided $r_a \approx r_b$, $r_c \approx r_d$ and $\tilde{\rho}_c \approx \tilde{\rho}_d$, Q should have the same value whether type- x groups are located on solute a and type- y groups on solvent c , or *vice versa*; that is, Q should exhibit solute-solvent invariance ($Q_{xy} \approx Q_{yx}$). Therefore, writing eqn. 22 in terms of interaction parameters¹, χ_{kl} , one obtains

$$\ln Q_{xy} \approx \ln Q_{yx} \approx (\tilde{\rho}_d)(r_x r_y / r_d)(\chi_{px} + \chi_{py} - \chi_{xy}) \quad (22)$$

where

$$\chi_{kl} = -(z/k_B T)\Delta w_{kl} \quad (23)$$

To continue, if the "active" solute (a) and solvent (c) molecules have common functionality ($y = x$ or $x = y$), then $\chi_{px} = \chi_{py}$ and $\chi_{xy} = 0$ (ref. 3) and from eqn. 24

$$\ln Q_{xx} \approx (\tilde{\rho}_d)(r_x^2 / r_d)(2\chi_{px}) \quad (24)$$

$$\ln Q_{yy} \approx (\tilde{\rho}_d)(r_y^2 / r_d)(2\chi_{py}) \quad (25)$$

Eqns. 24 and 25 thus permit the characterization of px and py interactions. Substituting these equations into eqn. 22 gives

$$\ln Q_{xy} \approx \ln Q_{yx} \approx (r_y / 2r_x) \ln Q_{xx} + (r_x / 2r_y) \ln Q_{yy} - (\tilde{\rho}_d)(r_x r_y / r_d) \chi_{xy} \quad (26)$$

which permits the characterization of xy interactions and the testing of solute-solvent invariance.

Eqns. 24-26 will be applied in the next section to isolate and quantify functional group contributions to solute retention. It is important to note that products such as $(r_x r_y / r_d) \chi_{xy}$ regularly appear in theoretical (lattice-model) expressions for solute activity coefficients, absolute and relative partition coefficients in gas and liquid chromatography, as well as hydrocarbon-water bulk partition coefficients^{3,4}. Also, an additional novel feature of the theory presented above is the emergence of the factor $\tilde{\rho}_d$ in the various equations (*e.g.*, eqns. 11 and 13, and eqns. 24-26). This factor, which does not appear in earlier (incompressible) lattice-model results, explicitly accounts for the effect of the degree of expansion (or free volume) of the stationary liquid on solute retention.

APPLICATIONS

We start by considering the application of eqn. 6 (or eqns. 7-9) to the interpretation and prediction of absolute retention [$K_{b(d)}$] for relatively simple alkane solute (b) + n -alkane solvent (d) systems. As will become evident, the first term in this equation (retention-enhancing contribution from solute-solvent interactions) is comparable in magnitude to, but greater than, the sum of the second and third terms (retention-diminishing contributions from solvent-solvent interactions and configurational entropy, respectively) for the systems in question.

The initial test systems are six alkane solutes in n -C₂₄H₅₀ at 80.0°C. Listed in Table I are the r_b and \tilde{T}_b values of the solutes (from the Sanchez-Lacombe tabulation²)

TABLE I

ANALYSIS OF PARTITION COEFFICIENTS, $K_{b(d)}$, OF ALKANE SOLUTES (b) IN $n\text{-C}_{24}\text{H}_{50}$ (d) AT 80.0°C

Solute	r_b^a	\tilde{T}_b^a	$K_{b(d)}$ (experimental) ^b	$K_{b(d)}$ (calculated) ^c
<i>n</i> -Hexane	8.37	0.7416	61.9	61.5
<i>n</i> -Heptane	9.57	0.7248	146.6	148.2
<i>n</i> -Octane	10.34	0.7032	339.1	336.2
<i>n</i> -Nonane	11.06	0.6828	783.0	783.2
2,2-Dimethylbutane	8.10	0.7759	35.9	35.7
2,3-Dimethylbutane	8.29	0.7624	46.5	46.8

^a From ref. 2.^b From ref. 5.^c Calculated from eqn. 30, with $\eta_{bd} = -0.020$ for the normal alkane solutes and $\eta_{bd} = -0.017$ for the branched alkane solutes.

and the GLC partition coefficients⁵. The scale parameters (ρ_d^* and T_d^*) needed to evaluate $\tilde{\rho}_d/\tilde{T}_d^{1/2}$ (hence, $\tilde{\rho}_d^2/\tilde{T}_d$) are not directly available for $n\text{-C}_{24}\text{H}_{50}$. However, since T^* and ρ^* values have been tabulated for $n\text{-C}_6\text{H}_{14}$ through $n\text{-C}_{14}\text{H}_{30}$ (ref. 2), $\tilde{\rho}_d/\tilde{T}_d^{1/2}$ was determined as a function of n -alkane molecular weight, M_d , by fitting this available data to the form

$$\tilde{\rho}_d/\tilde{T}_d^{1/2} = C - [D/(M_d + E)] \quad (27)$$

The optimum correlation coefficient (0.9990) is obtained with the assignment $E = 121.4$, giving $C = 1.3477$ and $D = 91.628$:

$$\tilde{\rho}_d/\tilde{T}_d^{1/2} = 1.3477 - [91.628/(M_d + 121.4)] \quad (28)$$

By extrapolation to $M_d = 338.6$, eqn. 28 gives $\tilde{\rho}_d/\tilde{T}_d^{1/2} = 1.1485$ and $\tilde{\rho}_d^2/\tilde{T}_d = 1.3191$ for $n\text{-C}_{24}\text{H}_{50}$ at 80°C. Similarly, the value of $(1 - r_d^{-1})\tilde{\rho}_d$ is obtained by fitting available data² for the n -alkanes as a function of M_d^{-1} and then extrapolating to $M_d = 338.6$:

$$(1 - r_d^{-1})\tilde{\rho}_d = 0.8422 - (13.290/M_d) \quad (29)$$

with a correlation coefficient of 0.9997, giving $(1 - r_d^{-1})\tilde{\rho}_d = 0.8030$ for $n\text{-C}_{24}\text{H}_{50}$ at 80°C.

Accordingly, from eqns. 7-9 we have $A = 2.2970$, $B = 2.1221$ and

$$\ln K_{b(d)} = r_b\{[2.2970(1 + \eta_{bd})/\tilde{T}_b^{1/2}] - 2.1221\} \quad (30)$$

Using eqn. 30, the best fit to the experimental $K_{b(d)}$ values is found by letting $\eta_{bd} = -0.020$ for the normal alkane solutes and $\eta_{bd} = -0.017$ for the branched alkane solutes, indicating slight negative deviations from the geometric-mean

TABLE II

PREDICTION OF PARTITION COEFFICIENTS, $K_{b(d)}$, OF ALKANE SOLUTES IN $n\text{-C}_{30}\text{H}_{62}$ AND $n\text{-C}_{36}\text{H}_{74}$ AT 80.0°C

Solute	$n\text{-C}_{30}\text{H}_{62}$		$n\text{-C}_{36}\text{H}_{74}$	
	Experimental ^a	Predicted ^b	Experimental ^a	Predicted ^b
<i>n</i> -Hexane	57.0	56.7	52.8	53.2
<i>n</i> -Heptane	134.7	136.2	125.3	127.3
<i>n</i> -Octane	317.5	310.2	289.6	290.8
<i>n</i> -Nonane	728.2	727.2	684.8	684.5
2,2-Dimethylbutane	32.9	32.7	30.6	30.5
2,3-Dimethylbutane	43.2	43.1	39.9	40.2

^a From ref. 5.^b Calculated from eqns. 31 and 32, respectively, with $\eta_{bd} = -0.020$ for the normal alkane solutes and $\eta_{bd} = -0.017$ for the branched alkane solutes, and using the r_b and \tilde{T}_b values from Table I.

approximation for ε_{bd} . The goodness of this fit is seen in Table I, where the average difference between the experimental and calculated $K_{b(d)}$ values is only 0.6%.

As a preliminary test of the predictive ability of this approach, the same procedure as that leading to eqn. 30 is applied to $n\text{-C}_{30}\text{H}_{62}$ and $n\text{-C}_{36}\text{H}_{74}$ at 80°C . From eqns. 7–9, 28 and 29, one obtains for the two respective solvents

$$\ln K_{b(d)} = r_b \{ [2.3587(1 + \eta_{bd}) / \tilde{T}_b^{1/2}] - 2.2016 \} \quad (31)$$

$$\ln K_{b(d)} = r_b \{ [2.4038(1 + \eta_{bd}) / \tilde{T}_b^{1/2}] - 2.2606 \} \quad (32)$$

Shown in Table II is a comparison of the experimental and predicted $K_{b(d)}$ values for the same set of solutes. The average difference between the two is less than 0.8%.

Let us now apply eqn. 13 to the analysis of the partition coefficient of chlorobenzene (a) relative to *n*-hexane (b) in the three *n*-alkane solvents. Listed in Table III are the $R_{(a/b)(d)}$ values of the solute pair⁵ and the M_d values of the solvents.

TABLE III

ANALYSIS OF PARTITION COEFFICIENTS OF CHLOROBENZENE (a) RELATIVE TO NORMAL HEXANE (b), $R_{(a/b)(d)}$, IN NORMAL ALKANE SOLVENTS AT 80.0°C

Solvent	$R_{(a/b)(d)}$ ^a	$R_{(a/b)(d)}$ (calculated) ^b	M_d ^c	M_d (calculated) ^d
$n\text{-C}_{24}\text{H}_{50}$	6.531	6.526	338.6	339.7
$n\text{-C}_{30}\text{H}_{62}$	6.850	6.863	422.8	419.1
$n\text{-C}_{36}\text{H}_{74}$	7.128	7.120	507.0	509.8

^a Experimental data from ref. 5.^b Calculated using actual M_d values and eqns. 33 and 34, with $\eta_{ad} = -0.040$.^c Molecular weight (g/mol).^d Calculated from experimental $R_{(a/b)(d)}$ values and eqns. 33 and 34, with $\eta_{ad} = -0.040$.

For the solutes, $r_a = 8.38$ (ref. 2) and $r_b = 8.37$, thus clearly satisfying the condition $r_a \approx r_b$. Also, $\tilde{T}_a = 0.6034$ (ref. 2), $\tilde{T}_b = 0.7416$, $\eta_{bd} = -0.020$ and $\tilde{\rho}_d/\tilde{T}_d^{1/2}$ is given by eqn. 28, leaving η_{ad} as the only unknown. (Here, both η_{ad} and η_{bd} are assumed to be independent of M_d .)

It follows from eqns. 13 and 28 that $R_{(a/b)(d)}$ must have the form

$$\ln R_{(a/b)(d)} = F\{1.3477 - [91.628/(M_d + 121.3)]\} \quad (33)$$

where

$$F = 2.4998 + 21.5494\eta_{ad} \quad (34)$$

The determination of η_{ad} is therefore accomplished by finding the F value that best satisfies eqn. 33. (The goodness of the fit is evident from comparison of the second and third columns in Table III). From the result ($F = 1.6332$) and eqn. 34 one calculates $\eta_{ad} = -0.040$, indicating a small, but more negative (compared to η_{bd}), deviation from the geometric-mean approximation for ε_{ad} . Additional physical insight is obtained by noting that the dependence of $R_{(a/b)(d)}$ on M_d stems solely from $\tilde{\rho}_d/\tilde{T}_d^{1/2}$, *i.e.*, the increase in $R_{(a/b)(d)}$ with increasing M_d at fixed T (Table III) is primarily due to the increase in $\tilde{\rho}_d$ (decrease in the molar free volume and the average distance between molecular segments) with increasing M_d .

In addition to its predictive and interpretive aspects, the utility of this approach is that once the solute pair and solvent series have been characterized, eqns. 33 and 34 can then be employed to determine M_d for any solvent in the series by measuring $R_{(a/b)(d)}$ in that solvent⁶. The precision of such a determination of M_d for high-molecular-weight *n*-alkanes (and, presumably, the number average M_d for linear polyethylenes) may be estimated by subjecting eqn. 33 to a propagation-of-errors analysis⁶, yielding

$$(\sigma_{M_d}/M_d) = [(M_d + 121.4)^2/91.628M_d](\sigma_R/R) \quad (35)$$

where σ_{M_d}/M_d and σ_R/R are the fractional errors in M_d and $R_{(a/b)(d)}$, respectively. With an estimate of $\sigma_R/R = 0.001$ (ref. 6), eqn. 35 gives the following per cent errors in M_d : $M_d = 500$ (0.5%; see Table III), $M_d = 5000$ (3.5%), $M_d = 10\,000$ (6.8%) and $M_d = 20\,000$ (13.5%). Therefore, the per cent error increases with increasing M_d , but remains tolerable (<10%) for M_d values up to *ca.* $1.5 \cdot 10^4$. Based on the form of eqn. 13, it is anticipated that an equation having the same general form as eqn. 33 should apply to other solvent series, including polymeric ones.

Finally, we give an example of the application of Eqns. 24–26 to isolate and quantify functional-group energetics, as measured by $\tilde{\rho}_d(r_k r_l / r_d) \chi_{ml}$, where $k, l = x, y$ and $m = p$ ($k = l$) or $m = k$ ($k \neq l$). Listed in Table IV are the *n*-alkyl chloride (a or c) and di-*n*-alkyl thioether (a or c) systems under consideration and the experimental values of $\ln Q_{kl}$ at 40.0°C (ref. 7). The reference solute (b) and solvent (d) are *n*-C₇H₁₆ and *n*-C₁₇H₃₆, respectively. From Bondi's tabulation of group van der Waals volumes⁸ it is seen that $r_S \approx r_{Cl} \approx r_{CH_2}$. Therefore, $r_k \approx r_l$, $r_a \approx r_b$ and $r_c \approx r_d$, as required. Also, from density measurements on the active and reference solvents it is found that $\tilde{\rho}_c \approx \tilde{\rho}_d$ (ref. 7). Accordingly, the conditions leading to the derivation of eqns. 24–26 are satisfied.

TABLE IV
ANALYSIS OF FUNCTIONAL GROUP ENERGETICS AT 40.0°C

Solute (a)–solvent (c) ^a	<i>k</i>	<i>l</i>	<i>m</i>	$\ln Q_{kl}$ ^b	$\tilde{\rho}_d(r_x r_l / r_d) \chi_{ml}$
Di- <i>n</i> -propyl thioether–di- <i>n</i> -octyl thioether	x	x	p	0.350	0.175 ^c
<i>n</i> -Hexyl chloride– <i>n</i> -hexadecyl chloride	y	y	p	0.386	0.193 ^d
Di- <i>n</i> -propyl thioether– <i>n</i> -hexadecyl chloride	x	y	x	0.384	–0.016 ^e
<i>n</i> -Hexyl chloride–di- <i>n</i> -octyl thioether	y	x	y	0.386	–0.018 ^e

^a Reference solute (b): *n*-C₇H₁₆; reference solvent (d): *n*-C₁₇H₃₆.

^b Experimental data from ref. 7.

^c Calculated from eqn. 24.

^d Calculated from eqn. 25.

^e Calculated from eqn. 26, with $r_x \approx r_y$.

As is evident from the results in the last column of Table IV, paraffin–sulfur (px), paraffin–chloride (py), sulfur–chloride (xy) and chloride–sulfur (yx) energetics can be readily characterized, and solute–solvent invariance is confirmed ($\chi_{xy} \approx \chi_{yx}$). The unfavourable energetics associated with the paraffin segment–“active” segment interchange process (eqn. 23, with $k = p$ and $l = x$ or y) leads to the expected positive values of χ_{px} and χ_{py} . However, the energetics of the S + Cl pairing is nearly ideal [$\tilde{\rho}_d(r_x r_y / r_d) \chi_{xy} \approx -0.017$]. An estimate of the absolute value of χ_{xy} may be obtained by using Bondi’s data⁸ (from which, $r_x r_y / r_d \approx 0.693$) and the Sanchez–Lacombe tabulation² (from which, $\tilde{\rho}_d \approx 0.868$), giving $\chi_{xy} \approx -0.028$. Similar estimates yield $\chi_{px} \approx 0.313$ ($x = S$) and $\chi_{py} \approx 0.299$ ($y = Cl$). In the same manner the energetics of other functional groups can be quantified.

CONCLUSIONS

As mentioned at the outset, the derivations and analyses presented above were meant to be representative rather than exhaustive. Certainly, additional and more complex chemical systems need to be evaluated, and the dependence of retention on the reduced temperature and reduced density of the stationary liquid phase needs to be more thoroughly studied. Nevertheless, the utility, efficacy and promise of this new theoretical approach have been demonstrated.

ACKNOWLEDGEMENTS

This research is based upon work supported by the National Science Foundation. The author is also grateful to Dr. R. P. W. Scott for his friendship and advice, the many stimulating discussions, and reminders that “the truth is at the laboratory bench”. He wishes Dr. Scott continued health and happiness on the occasion of his 65th birthday and this well-deserved recognition.

REFERENCES

- 1 D. E. Martire and R. E. Boehm, *J. Phys. Chem.*, 91 (1987) 2433; and references cited therein.
- 2 I. C. Sanchez and R. H. Lacombe, *J. Phys. Chem.*, 80 (1976) 2352.

- 3 D. E. Martire and R. E. Boehm, *J. Phys. Chem.*, 87 (1983) 1045; and references cited therein.
- 4 M. M. Schantz and D. E. Martire, *J. Chromatogr.*, 391 (1987) 35.
- 5 Y. B. Tewari, D. E. Martire and J. P. Sheridan, *J. Phys. Chem.*, 74 (1970) 2345.
- 6 D. E. Martire, *Anal. Chem.*, 46 (1974) 626.
- 7 M. A. Hamzavi-Abedi, *Doctoral Dissertation*, Georgetown University, Washington, DC, 1984.
- 8 A. Bondi, *J. Phys. Chem.*, 68 (1964) 441.

CHROM. 21 397

COMPARISON BETWEEN THE CONDITIONS FOR SOLUTE FOCUSING BY THE STATIC AND DYNAMIC SOLVENT EFFECTS UNDER IDEAL CONDITIONS

PETER J. APPS* and VICTOR PRETORIUS

Institute for Chromatography, University of Pretoria, Pretoria 0002 (South Africa)

SUMMARY

In capillary gas chromatography static and dynamic solvent effect inlets provide quantitatively precise methods of sample introduction of solutes which fulfill the conditions for solute focussing. Equations are derived for the conditions for focussing on static and dynamic films. In the case of a static film a solute will be focussed if the sum of its partition coefficient between the gas phase and the film and the phase ratio are greater than the partition coefficient of the solvent. On dynamic solvent films solutes whose partition coefficients are larger than those of the solvent are focussed.

INTRODUCTION

The static and dynamic solvent effects are manifestations of the peculiar chromatographic properties of mechanically stable, evaporating solvent films¹⁻⁴. Inlets which employ the static or dynamic solvent effects offer uniquely precise methods of sample introduction for capillary gas chromatographic analysis^{5,6}. Dynamic solvent effect sampling has been successfully applied to a variety of problems in semiochemistry⁷⁻¹¹.

Here we present comparative models of the behaviour of static and dynamic sample films under ideal conditions, that is, in the absence of band spreading. In the interest of a clearer comparison between the two systems the treatment of the static solvent effect differs somewhat from that presented by Deans¹ and Pretorius *et al.*².

THE STATIC SOLVENT EFFECT

Consider a tube with a porous layer on its inside wall, in which a pure liquid is held by capillary attraction as a mechanically stable film. Along the axis of the tube is an open channel down which flows a stream of gas at a velocity sufficiently low that the shape of the liquid film is not altered by shear forces. The liquid will evaporate into, and be carried away by, the stream of gas at a rate governed by the liquid's vapour pressure and the volume flow-rate of the gas. Under conditions of ideal gas behaviour

the mass rate of removal of the solvent vapour is given by (symbols are defined at the end of the text)

$$E_{om} = \frac{P_v V_g m_o}{RT} \quad (1)$$

The mass rate at which liquid evaporates from the film must, obviously, be the same as the mass rate of removal of the vapour. The evaporation rate in terms of liquid volume is then

$$E_{ov} = \frac{E_{om}}{\rho_o} \quad (2)$$

$$= \frac{P_v V_g m_o}{RT \rho_o} \quad (3)$$

Provided that equilibrium between the gas and liquid phases is quickly established the gas will become saturated with vapour after passing over only a short length of the film. Evaporation will then effectively be confined to the upstream edge of the film. Because the film is held in place by the capillarity of the porous layer in which it lies, evaporation at the upstream edge removes liquid from that area alone. As a result of this removal the position of the film's edge moves downstream. The film therefore becomes shorter, but does not move as a whole with respect to the tube wall.

The rate at which the upstream edge moves at a given evaporation rate is determined by the volume of liquid held in unit length of the film, which is given by

$$A_o = \frac{Q_o}{l_f} \quad (4)$$

A_o is simply the cross sectional area of the liquid annulus, and the rate of downstream movement of the position of the upstream edge of the film is the volume evaporation rate divided by this area:

$$U_o = \frac{E_{ov}}{A_o} \quad (5)$$

$$= \frac{P_v V_g m_o}{RT \rho_o A_o} \quad (6)$$

Now consider the behaviour of a volatile solute dissolved in the liquid film. Being volatile it will partition between the gas and the liquid and will consequently be carried chromatographically downstream at a velocity determined, in the absence of lagging¹², by its partition ratio and the gas linear velocity:

$$v_x = \frac{U_g}{k_x + 1} \quad (7)$$

If, at the upstream edge of the film the solute is moving downstream faster than the position of the film's upstream edge *i.e.* if

$$v_x > U_o \quad (8)$$

the solute concentration at the upstream edge of the film will fall as the solute is moved forward and ultimately stripped from the film by the gas. If, on the other hand, the solute moves downstream more slowly than the film's edge *i.e.* if

$$v_x < U_o \quad (9)$$

at the upstream edge of the film the solvent is being removed from the solution by evaporation faster than the solute is being removed by chromatographic migration. The solute's concentration consequently rises. These solutes are focussed by the static solvent effect.

If the gas contains volatiles before it encounters the liquid film the vapours will impinge on, and dissolve in, the upstream edge of the film. They will then behave in the same way as solutes originally in the film.

Inequality 9 can be rewritten from eqn. 6 as

$$v_x < \frac{P_v V_g m_o}{RT \rho_o A_o} \quad (10)$$

The linear flow-rate of the gas phase is its volume flow-rate per unit area of the gas channel's cross section:

$$U_g = \frac{V_g}{A_g} \quad (11)$$

Eqn. 10 then becomes

$$v_x < \frac{P_v U_g A_g m_o}{RT \rho_o A_o} \quad (12)$$

The area of the gas channel and that of the liquid annulus determine the phase ratio:

$$\beta = \frac{A_g}{A_o} \quad (13)$$

Substituting in eqn. 12 then gives

$$v_x < \frac{P_v U_g m_o \beta}{RT \rho_o} \quad (14)$$

Substituting from eqn. 7 in eqn. 14, and rearranging:

$$(k_x + 1) > \frac{RT\rho_o}{P_v m_o \beta} \quad (15)$$

Consider now the partitioning of the solvent between the liquid and gas phases. For dilute solutions the concentration of solvent in the liquid phase is the solvent density. The concentration in the gas phase is the mass rate of solvent evaporation into the volume of gas sweeping the film in unit time (eqn. 1):

$$k_o = \frac{RT\rho_o}{P_v m_o \beta} \quad (16)$$

Eqn. 15 can now be rewritten:

$$(k_x + 1) > k_o \quad (17)$$

$$k_x = \frac{K_x}{\beta} \quad (18)$$

$$k_o = \frac{K_o}{\beta} \quad (19)$$

The condition for solute focussing by the static solvent effect then becomes

$$(K_x + \beta) > K_o \quad (20)$$

CONSEQUENCES OF SOLUTE FOCUSING BY THE STATIC SOLVENT EFFECT

As the upstream edge of the liquid film moves downstream solutes for which the condition for solvent effect focussing is met accumulate in a short band at the upstream edge of the film. In the ideal case the length of the band of concentrated solutes is small compared to the length of the film, and the solute focussing mechanism continues to operate until nearly all the film has evaporated. At this stage the length of the film has become the same as that of the concentrated band so that the solutes are no longer chromatographically retarded by a film of liquid lying downstream of them. The last traces of the liquid film therefore consist of a concentrated solution of the solutes occupying a short region of the porous layer at the position previously occupied by the downstream end of the liquid film. It is the high concentration and small volume of the solution which makes possible its efficient transfer to a capillary column, and it is in this respect that static solvent effect focussing is useful as a sampling technique for large, dilute, liquid specimens.

THE DYNAMIC SOLVENT EFFECT

In the case of the dynamic solvent effect the downstream end of the film is in

contact with a source of the liquid it consists of. Now when gas is passed over the film, liquid removed by evaporation from its upstream edge is replaced by liquid drawn by capillary attraction from the liquid source. Thus there is a continuous bulk movement of liquid towards the evaporation zone, which retains its position until the source of liquid is removed. Solutes are carried towards the evaporation zone by this bulk movement of liquid, and in the opposite direction by the gas. Solutes whose net upstream velocity is higher than their net downstream velocity accumulate in the evaporation zone⁴.

Consider a tube with a porous layer on its inside wall and an open channel along its axis. If the tube is dipped into a liquid which wets the porous layer the liquid will rise into it (passage of liquid into the axial channel is ignored for present purposes).

The height to which the liquid will rise against gravity is given by¹³

$$h = \frac{2\gamma}{\rho_{\text{o}}gr_{\text{h}}} \quad (21)$$

If the porous layer can be approximated by a random packing of solid, spherical particles¹⁴:

$$r_{\text{h}} = \frac{\varepsilon}{S_{\text{p}}(1 - \varepsilon)} \quad (22)$$

$$S_{\text{p}} = \frac{6(1 - \varepsilon)}{d_{\text{p}}} \quad (23)$$

and from eqns. 21, 22 and 23:

$$h = \frac{12\gamma(1 - \varepsilon)^2}{\rho_{\text{o}}g\varepsilon d_{\text{p}}} \quad (24)$$

For *n*-hexane, the most commonly used solvent, $\gamma = 20 \text{ dynes cm}^{-1}$, $\rho = 0.7 \text{ g cm}^{-3}$ and for randomly packed spheres $\varepsilon = 0.35$, and if the mean size of the particles is 0.1 mm: $h = 376 \text{ mm}$. This is six to seven times as high as the liquid film rises when the dynamic solvent effect is used for sampling. Consequently the effects of hydrostatic pressure on the behaviour of the film can be neglected in the following model.

When there is no pressure gradient, as here, the velocity with which a liquid enters a pore due to capillarity is given by¹³

$$U_{\text{pp}} = \frac{r_{\text{h}}\gamma}{4\eta L} \quad (25)$$

The speed with which a liquid front is drawn into a porous bed is reduced by the tortuosity of the channels in which it flows:

$$U_{\text{pb}} = \frac{U_{\text{pp}}}{\tau} = \frac{r_{\text{h}}\gamma}{4\eta L\tau} \quad (26)$$

The volume rate at which the liquid flows into the porous layer depends on the cross sectional area of the liquid annulus:

$$V_{pb} = \frac{r_h \gamma A_o}{4\eta L \tau} \quad (27)$$

The volume of liquid held in the porous layer depends on the length of wetted bed and the liquid annulus cross sectional area:

$$Q_o = l_f A_o \quad (28)$$

When gas is passed down the axial channel the liquid which has risen into the bed will evaporate into the gas. As in the case of the static film (eqn. 3) evaporation will be confined to the upstream edge of the film and its rate will be given by

$$E_{ov} = \frac{m_o V_g P_v}{RT \rho_o} \quad (29)$$

If the rate of evaporation is greater than the rate at which liquid flows into the porous layer there will be a decrease with time in the volume of liquid in the layer and from eqn. 28 the length of the film will decrease (A_o is fixed by the geometry of the porous layer).

Since

$$l_f = \frac{L}{\tau} \quad (30)$$

and from eqn. 27 the volume of liquid entering the bed is inversely dependent on the length of the pores through which the liquid has to permeate, the shortening of the film allows a faster flow-rate into the porous layer. As the film shortens a point is reached at which

$$V_{pb} = E_{ov} \quad (31)$$

and no further change in film volume, film length or liquid flow-rate occurs. The upstream edge of the liquid film will now hold a fixed position within the porous layer, and liquid is supplied to it by capillarity at a rate given by eqn. 27, and removed from it by evaporation at a rate given by eqn. 29.

In this equilibrium condition

$$V_{pb} = \frac{m_o V_g P_v}{RT \rho_o} \quad (32)$$

The average linear velocity of the upward movement of the liquid is related to the volume flow of liquid by eqns. 26 and 27:

$$U_{pb} = \frac{m_o V_g P_v}{RT \rho_o A_o} \quad (33)$$

so that, as is intuitively obvious, the liquid in a dynamic solvent film flows upstream with the same linear velocity as that with which the upstream edge of the equivalent static film moves downstream.

Under equilibrium conditions solutes are moved chromatographically away from the evaporation zone by the gas, and towards it by the liquid flow.

The rate of downstream movement is given by

$$v_{xd} = \frac{U_g}{(k_x + 1)} \quad (34)$$

and the rate of upstream movement by

$$v_{xu} = \frac{U_{pb}}{\frac{1}{k_x} + 1} \quad (35)$$

Solutes for which

$$v_{xd} > v_{xu} \quad (36)$$

experience a net downstream movement and are stripped from the liquid film (compare eqn. 8).

Solutes for which

$$v_{xd} < v_{xu} \quad (37)$$

experience a net upstream movement towards the evaporation zone, where they accumulate. This is the condition for solute focussing by the dynamic solvent effect (compare eqn. 9).

From eqns. 34 and 35 inequality 37 can be rewritten as

$$\frac{U_g}{k_x + 1} < \frac{U_{pb}}{\frac{1}{k_x} + 1} \quad (38)$$

$$\frac{U_{pb}}{\frac{1}{k_x} + 1} = \frac{U_{pb} \cdot k_x}{k_x + 1} \quad (39)$$

Inequality eqn. 38 then becomes

$$U_g < (U_{pb} \cdot k_x) \quad (40)$$

$$k_x > \frac{U_g}{U_{pb}} \quad (41)$$

now:

$$U_g = \frac{V_g}{A_g} \quad (42)$$

and so from eqn. 33:

$$k_x > \frac{V_g}{(m_o V_g P_v A_g)/(RT \rho_o A_o)} \quad (43)$$

$$k_x > \frac{1}{(m_o P_v \beta)/(RT \rho_o)} \quad (44)$$

$$k_x > \frac{RT \rho_o}{m_o P_v \beta} \quad (45)$$

As in the case of the static film (eqn. 16),

$$k_o = \frac{\rho_o RT}{P_v m_o \beta} \quad (46)$$

so that eqn. 45 can be rewritten:

$$k_x > k_o \quad (47)$$

from which it follows that solutes for which

$$K_x > K_o \quad (48)$$

will be focussed by the dynamic solvent effect. Thus the condition for solute focussing by the dynamic solvent effect is somewhat more stringent than that for focussing by the static solvent effect.

SYMBOLS

A_g	cross sectional area of gas channel
A_o	cross sectional area of liquid annulus
d_p	mean particle diameter in a porous material
E_{om}	mass rate of solvent evaporation
E_{ov}	volume rate of solvent evaporation
g	acceleration due to gravity
h	height of a liquid column

k_o	partition ratio of solvent between itself and the gas
k_x	partition ratio of solute between liquid and gas
K_o	partition coefficient of solvent between itself and the gas
K_x	partition coefficient of solute between liquid and gas
l_f	length of liquid film
L	length of a pore
m_o	molecular weight of solvent
M_o	mass of solvent
P_v	partial pressure of a vapour
Q_o	volume of liquid
r_h	hydraulic radius
R	universal gas constant
S_p	specific surface area of a porous solid
T	temperature
U_f	velocity of upstream edge of film
U_g	linear velocity of gas
U_{pb}	linear velocity with which a liquid permeates a porous solid
U_{pp}	linear velocity with which a liquid permeates a pore
v_x	chromatographic velocity of solute plug (static film)
v_{xd}	chromatographic downstream velocity of a solute plug (dynamic film)
v_{xu}	chromatographic upstream velocity of a solute plug (dynamic film)
V_g	volumw flow-rate of gas
V_{pb}	volume rate at which liquid flows into a porous solid
β	phase ratio
η	viscosity
ϵ	porosity of a porous solid
τ	tortuosity of the pores in a porous solid
γ	surface tension of a liquid
ρ_o	density of solvent

REFERENCES

- 1 D. R. Deans, *Anal. Chem.*, 43 (1971) 2026.
- 2 V. Pretorius, C. S. G. Phillips and W. Bertsch, *J. High Resolut. Chromatogr. Chromatogr. Commun.*, 6 (1983) 273.
- 3 P. J. Apps, V. Pretorius, E. R. Rohwer and K. Lawson, *J. High Resolut. Chromatogr. Chromatogr. Commun.*, 7 (1984) 212.
- 4 P. J. Apps, V. Pretorius, K. Lawson, E. R. Rohwer, M. R. Centner, H. W. Viljoen and G. Hulse, *J. High Resolut. Chromatogr. Chromatogr. Commun.*, 10 (1987) 122.
- 5 K. H. Lawson, V. Pretorius and P. J. Apps, *J. High Resolut. Chromatogr. Chromatogr. Commun.*, 10 (1987) 235.
- 6 P. J. Apps, *The Quantitative Analysis of Semiochemicals. Ph. D. Thesis*, University of Pretoria, 1988, pp. 109-142.
- 7 P. J. Apps, H. W. Viljoen, V. Pretorius and E. R. Rohwer, *S. Afr. J. Zool.*, 23 (1988) 136.
- 8 P. J. Apps, H. W. Viljoen and V. Pretorius, *Onderstepoort J. Vet. Res.*, 55 (1988) 135.
- 9 D. Jacobs, P. J. Apps and H. W. Viljoen, *J. Comp. Biochem. Physiol.*, in press.
- 10 P. J. Apps, H. W. Viljoen, P. R. K. Richardson and V. Pretorius, *J. Chem. Ecol.*, in press.
- 11 P. J. Apps, H. W. Viljoen and A. Rasa, *Aggressive Behav.*, 14 (1988) 451.
- 12 V. Pretorius, C. S. G. Phillips and W. Bertsch, *J. High Resolut. Chromatogr. Chromatogr. Commun.*, 6 (1983) 321.
- 13 V. G. Levich, *Physicochemical Hydrodynamics*, Prentice Hall, Englewood Cliffs, p. 383.
- 14 H. Purnell, *Gas Chromatography*, Wiley, New York, 1962, p. 63.

CHROM. 21 293

COMPARISON OF SOLVENT MODELS FOR CHARACTERIZING STATIONARY PHASE SELECTIVITY IN GAS CHROMATOGRAPHY

SALWA K. POOLE, BRIAN R. KERSTEN and COLIN F. POOLE*
Department of Chemistry, Wayne State University, Detroit, MI 48202 (U.S.A.)

SUMMARY

Two experimental approaches to the measurement of stationary phase selectivity using the thermodynamic models proposed by Rohrschneider–McReynolds and Golovnya–Poole are tested theoretically and experimentally to establish their reliability. The retention index difference of Rohrschneider–McReynolds is demonstrated to incorrectly determine selectivity since this difference is largely determined by the difference in solubility of the *n*-alkane retention index markers in the polar and non-polar phases. Also, the assumption that the contribution of dispersion to the index value is equivalent to the retention of a hypothetical *n*-alkane on squalane with the same retention time as the test solute on the polar phase fails to take account of the differences in the free energy of solution per index unit on the compared phases. These inconsistencies are not found when differences in the partial molar Gibbs free energy of solution for a series of test solutes are used to determine stationary phase selectivity. A general equation relating the free energy differences to retention index differences is derived and indicates that there is no simple relationship between the two models which, therefore, predict very different selectivity changes for the same test solutes for a group of compared phases. It is concluded that the ordering of stationary phases with respect to their ability to interact selectively with a particular test solute should be determined from free energies of solution (determined from gas–liquid partition coefficients corrected for interfacial adsorption) and that the use of the McReynolds phase constants be abandoned for this purpose.

INTRODUCTION

The selectivity of the chromatographic system and thus the ease of obtaining a particular separation in gas–liquid chromatography (GLC) is determined primarily by differences in solute vapor pressures and the strength of solute–solvent interactions in the liquid phase^{1,2}. To a first approximation at normal column operating pressures and sample sizes it can be assumed that samples behave ideally in the gas phase with the inert gases commonly used as carriers. A theoretical understanding of selectivity differences between individual solvents is unavailable and must await the development of exact descriptions of the intermolecular forces that exist between complex molecules as are encountered in gas chromatography (GC). A pragmatic solution to this problem

has been found by adopting several largely empirical experimental approaches to characterize the solvent properties of stationary phases used in GC. The most widely used approach is that of Rohrschneider as later modified by McReynolds (see refs. 3–11). In this instance solvent selectivity was quantitatively determined by the differences in the retention index values of a series of test solutes chosen to express particular solute–solvent interactions for the stationary phase to be characterized with respect to the properties (retention index values) for the same solutes measured on squalane as a non-polar reference phase. Rohrschneider–McReynolds phase constants are commonly used by vendors of chromatographic supplies to define the application areas for new phases and by users to identify phases having identical (or similar) properties. In spite of the more or less universal adoption of the Rohrschneider–McReynolds phase constants it has been suggested that these values may be unreliable due to a combination of theoretical and practical deficiencies in the protocol used for their calculation^{10–17}. Briefly summarized these problems can be stated to be: (1) a failure to account for the contribution of interfacial adsorption, particularly for the retention index standards, as a significant retention mechanism; (2) the phase constants are composite terms embodying both the contribution of selective solute–solvent interactions and solubility differences of the *n*-alkane retention index markers on the compared phases (the latter contribution tending to dominate); and (3) there is insufficient retention of some test solutes on certain phases to permit the determination of the phase constants with the required degree of accuracy.

An alternative approach to that of Rohrschneider–McReynolds has been adopted by Golovnya–Poole (see refs. 10, 11, 13, 16 and 18). These workers defined differences in stationary phase selectivity as equivalent to the differences in the partial molar Gibbs free energy of solution for a series of test solutes on the phases to be characterized and on a reference phase exhibiting minimal selectivity. In most cases the same test solutes as used by McReynolds have been used in these studies as well as the adoption of squalane as the reference phase exhibiting minimal selectivity. In general there are substantial differences between the ranking of individual phases by their ability to interact with a particular test solute using phase constants derived by the two different approaches. The purpose of this paper is to demonstrate why this difference arises based on fundamental and experimental considerations, to show how the two selectivity scales can be interrelated, and to provide a corrected set of experimental data to be used to test new hypotheses that may be developed in the future.

EXPERIMENTAL

General experimental conditions and sources of phases and standards, etc. are identical with those reported elsewhere^{12,13}. Common abbreviations and trade names for stationary phases are identified in Table I. All GC measurements were made by headspace injection of test solutes under infinite dilution conditions conforming to the linear portion of the sorption isotherms. All peak shapes were symmetrical and there was no dependence of retention on sample size in the measurement region. On-column silanization of packings prepared from non-polar phases was used as required to control peak tailing¹³. The column temperature was 80.8°C ($\pm 0.2^\circ\text{C}$) and the column pressure drop less than 1 atm (determined to ± 1 mmHg) in all cases. Nitrogen was used as carrier gas. Retention volumes are uncorrected for gas phase non-ideality since

TABLE I

GAS-LIQUID PARTITION COEFFICIENTS FOR McREYNOLDS TEST SOLUTES ON SOME REPRESENTATIVE STATIONARY PHASES AT 80.8°C

The uncertainty in the measurements is given by the standard deviation in parenthesis. X' = benzene, Y' = butanol, Z' = 2-pentanone, U' = nitropropane, S' = pyridine, H' = 2-methy-2-pentanol, J' = iodobutane, K' = 2-octyne, L' = dioxane and M' = *cis*-hydrindane.

Stationary phase ^a	Gas-liquid partition coefficient									
	X'	Y'	Z'	U'	S'	H'	J'	K'	L'	M'
Squalane	80.8 (0.5)	47.8 (1.2)	67.2 (0.8)	80.9 (1.0)	114.7 (2.2)	111.9 (1.1)	310.8 (2.9)	420.1 (4.4)	81.4 (0.7)	1394.1 (15.0)
OV-17	77.6 (1.0)	69.6 (1.0)	94.8 (0.8)	198.4 (10.6)	196.9 (1.2)	104.9 (2.5)	258.2 (3.7)	312.4 (5.3)	129.2 (3.2)	688.8 (14.1)
OV-105	61.5 (3.0)	87.0 (8.2)	78.9 (2.5)	126.3 (3.1)	118.9 (3.5)	110.1 (3.7)	186.2 (5.2)	256.9 (7.4)	84.7 (2.3)	575.0 (14.5)
OV-330	88.9 (0.7)	199.5 (3.7)	111.9 (0.9)	350.4 (2.6)	291.2 (3.0)	197.2 (1.3)	247.3 (4.9)	247.2 (4.7)	161.0 (5.7)	432.9 (2.9)
OV-225	69.1 (0.1)	133.7 (2.4)	129.6 (1.4)	378.6 (3.8)	256.7 (4.5)	152.2 (1.2)	197.4 (1.6)	167.2 (2.7)	148.1 (9.6)	320.4 (3.9)
QF-1	45.6 (1.1)	53.4 (4.2)	136.8 (4.0)	274.1 (7.9)	146.9 (5.0)	85.9 (3.2)	118.4 (4.0)	100.2 (3.5)	102.2 (1.7)	228.0 (7.0)
Carbowax 20M	97.6 (0.4)	292.1 (4.8)	114.2 (0.5)	483.6 (1.9)	401.2 (4.6)	212.9 (1.5)	204.3 (2.0)	180.3 (3.9)	199.6 (0.7)	264.1 (3.3)
DPAT	80.2 (12.9)	583.3 (14.1)	177.0 (5.3)	479.2 (12.0)	—	425.0 (11.1)	143.4 (2.9)	74.8 (2.5)	229.8 (6.0)	130.8 (1.7)
DEGS	59.4 (2.7)	240.2 (6.2)	97.9 (1.8)	372.8 (12.2)	—	186.9 (4.8)	89.9 (3.6)	68.7 (2.7)	236.1 (4.5)	86.1 (2.3)
BAT	37.6 (0.8)	658.4 (25.0)	203.6 (9.5)	304.7 (12.6)	—	476.7 (17.9)	74.2 (2.5)	38.2 (1.0)	406.3 (9.6)	79.0 (4.1)
sBAT	38.3 (2.7)	795.8 (15.0)	249.1 (3.1)	355.8 (9.0)	—	553.9 (11.2)	74.4 (2.3)	38.7 (2.8)	505.2 (11.7)	65.2 (3.6)
TCEP	63.4 (2.4)	205.0 (1.3)	133.7 (2.4)	543.1 (3.4)	424.9 (3.0)	139.7 (1.0)	92.3 (2.3)	62.6 (2.4)	245.9 (3.3)	68.1 (0.5)
OV-275	40.9 (1.2)	110.6 (4.4)	67.7 (3.0)	313.1 (13.1)	225.5 (7.8)	65.2 (3.1)	49.6 (2.4)	25.5 (1.2)	126.4 (4.7)	37.6 (3.1)

^a Squalane = 2,6,10,15,19,23-hexamethyltetracosane, OV-17 = poly(phenylmethylsiloxane), OV-105 = poly(cyanopropylmethylphenylmethylsiloxane), OV-330 = dimethylsilicone/Carbowax copolymer), QF-1 = poly(trifluoropropylmethylsiloxane), Carbowax 20M = poly(ethylene glycol), DPAT = di-*n*-propylammonium thiocyanate, DEGS = poly(diethyleneglycol succinate), BAT = *n*-butylammonium thiocyanate, sBAT = *sec*-butylammonium thiocyanate, TCEP = 1,2,3-tris(2-cyanoethoxypropane) and OV-275 = poly(dicyanoallylsiloxane).

these corrections were found to be small for the experimental conditions employed using the few accurately determined virial coefficients available¹⁹.

Gas-liquid partition coefficients were calculated by linear extrapolation of plots of V_N^*/V_L vs. $1/V_L$ based on eqn. 1:

$$\frac{V_N^*}{V_L} = K_L + (A_{GL}K_{GL} + A_{LS}K_{GLS}) \frac{1}{V_L} \quad (1)$$

where V_N^* is the net retention volume per gram of packing; V_L the volume of liquid phase per gram of packing; K_L the gas-liquid partition coefficient; A_{GL} the gas-liquid interfacial area; K_{GL} the coefficient for adsorption at the gas-liquid interface; A_{LS} the gas-liquid interfacial area; and K_{GLS} the coefficient for adsorption at the support surface.

Values for the gas-liquid partition coefficients of test solutes are given in Table I together with the uncertainty in their determination. These values supercede those given in ref. 13 which have been corrected for an error in the extrapolation procedure which affected the accuracy of some K_L values. The partition coefficients for the *n*-alkane and 2-alkanone retention index markers were fitted to eqn. 2:

$$\log K_L = A + Bn \quad (2)$$

where B is the slope of the plot of $\log K_L$ vs. carbon number n and A is a constant for any particular phase. A gives the intercept for $n = 0$ on the same plot and n the number of carbon atoms for the *n*-alkanes and the number of carbon atoms minus 2 for the 2-alkanones. The coefficients obtained by linear regression are summarized in Table II.

The retention index for each test solute was determined from the adjusted retention time using the standard procedure¹. Retention index values corrected for interfacial adsorption were calculated using eqn. 3:

$$I_p^c(X) = 100Z + 100 \frac{\log K_L^X - \log K_L^Z}{\log K_L^{Z+1} - \log K_L^Z} \quad (3)$$

where $I_p^c(X)$ is the retention index for solute X corrected for interfacial adsorption on

TABLE II

COEFFICIENTS FOR CALCULATING PARTITION COEFFICIENTS FOR *n*-ALKANES AND 2-ALKANONES (EQN. 2)

Stationary phase	<i>n</i> -Alkanes		Correlation coefficient (r^2)	2-Alkanones		Correlation coefficient (r^2)	$\Delta G_R^0(CH_2)^P$	
	<i>B</i>	<i>A</i>		<i>B</i>	<i>A</i>		<i>n</i> -Alkanes	2-Alkanones (cal/mol)
Squalane	0.361	-0.4180	1.000	0.358	0.7673	1.000	-585	-579
OV-17	0.325	-0.5596	0.999	0.317	1.0517	0.999	-525	-513
OV-105	0.314	-0.3339	1.000	0.311	0.9841	0.999	-508	-503
OV-330	0.302	-0.6023	1.000	0.298	1.1844	0.999	-488	-482
OV-225	0.293	-0.6556	1.000	0.284	1.2894	0.999	-469	-459
QF-1	0.262	-0.3152	1.000	0.270	1.3499	0.999	-424	-437
Carbowax 20M	0.264	-0.5754	0.999	0.265	1.2939	0.999	-427	-428
DPAT	0.228	-0.6058	1.000	0.239	1.5658	0.999	-369	-386
DEGS	-	-	-	0.218	1.3653	0.999	-	-352
BAT	0.223	-0.8211	0.999	0.215	1.6994	0.997	-361	-347
sBAT	0.188	-0.5733	0.998	0.204	1.8350	0.998	-304	-330
TCEP	-	-	-	0.199	1.5552	0.999	-	-322
OV-275	-	-	-	0.180	1.3233	0.998	-	-330

phase P; K_L^X the gas-liquid partition coefficient for solute X; K_L^Z the gas-liquid partition coefficient for an n -alkane with Z carbon atoms eluting immediately before solute X; and K_L^{Z+1} the gas-liquid partition coefficient for an n -alkane with $Z + 1$ carbon atoms eluting after solute X.

When the 2-alkanones were used as the fixed points on the retention index scale, eqn. 3 was used with Z equal to the number of carbon atoms minus 2. Phase constants according to McReynolds were calculated from retention index differences using eqn. 4:

$$\text{Phase constant} = \Delta I^X = I_P^X - I_{SQ}^X \quad (4)$$

where I_P^X is the retention index for test solute X on stationary phase P; and I_{SQ}^X the retention index for test solute X on squalane.

Phase constants corrected for interfacial adsorption or based on the 2-alkanone retention index scale were calculated by substituting the appropriate values of the retention index into eqn. 4.

The partial molar Gibbs free energy of solution, ΔG_k° , for the test solutes was calculated from the gas-liquid partition coefficient, K_L^X , according to eqn. 5:

$$(\Delta G_k^\circ X)^P = -2.3RT_C \log K_L^X \quad (5)$$

where $(\Delta G_k^\circ X)^P$ is the partial molar Gibbs free energy of solution of solute X on phase P; R the universal gas constant ($1.987 \text{ cal mol}^{-1} \text{ K}^{-1}$); and T_C the column temperature (K).

The difference in free energies for solute X on two compared phases is given by eqn. 6

$$\partial(\Delta G_k^\circ X)_{SQ}^P = (\Delta G_k^\circ X)^P - (G_k^\circ X)^{SQ} \quad (6)$$

where $\partial(\Delta G_k^\circ X)_{SQ}^P$ is the difference in partial molar Gibbs free energy of solution for solute X on stationary phase P and squalane. The partial molar Gibbs free energy of solution for a methylene group, $\Delta G_k^\circ(\text{CH}_2)^P$ was calculated according to eqn. 7:

$$\Delta G_k^\circ(\text{CH}_2)^P = -2.3RT_C B_P \quad (7)$$

where $\Delta G_k^\circ(\text{CH}_2)^P$ is the partial molar Gibbs free energy of solution for a methylene group on phase P; and B_P the slope of $\log K_L$ vs. carbon number for the n -alkane or 2-alkanones on phase P. Values for the variable B_P together with $\Delta G_k^\circ(\text{CH}_2)^P$ are given in Table II.

RESULTS AND DISCUSSION

A good starting point is the thermodynamic definition of the phase constant as proposed by Rohrschneider^{3,4}. With respect to Fig. 1, which shows a plot of $\log K_L$ against carbon number for a homologous series of n -alkanes on squalane and Carbowax 20M, used to determine the phase constant for solute X (experimental data for dioxane are used in the figure shown). The retention index value for solute X, by definition, is equal to 100 times the carbon number of the hypothetical n -alkane that

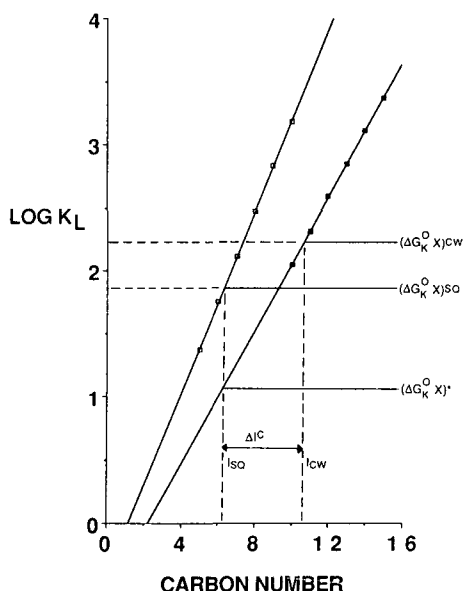


Fig. 1. Plot of the logarithm of the gas-liquid partition coefficients for n -alkanes as a function of carbon number on Carbowax 20M (3%) and squalane (□). The test solute, X, was dioxane. The free energy scale is plotted on the right without units and is related to K_L through eqn. 5.

co-elutes with solute X on both phases and the stationary phase selectivity constant to the difference in retention index values as defined by eqn. 4. In thermodynamic terms Rohrschneider identified the difference in retention index values, ΔI , with the difference in the partial molar Gibbs free energy of solution for solute X on the polar phase and squalane as a non-polar reference phase according to eqn. 8:

$$\Delta I^R = 100 \frac{(\Delta G_R^0 X)^P - (\Delta G_R^0 X)^*}{\Delta G_R^0(\text{CH}_2)^P} \quad (8)$$

where ΔI^R is the calculated value of ΔI^C according to Rohrschneider and $(\Delta G_R^0 X)^*$ is the partial molar Gibbs free energy of solution for a hypothetical n -alkane co-eluting with solute X on squalane and having the same carbon number as the n -alkane used to calculate $(\Delta G_R^0 X)^*$ on the polar phase using eqns. 2 and 5. The correctness of eqn. 8 is easily tested by inserting experimental values into eqn. 8 and comparing the calculated phase constants with those determined experimentally, Table III. As can be seen there is excellent agreement between the calculated, ΔI^R , and experimental values of ΔI corrected for contributions to retention arising from interfacial adsorption, ΔI^C . Uncorrected values of ΔI , calculated directly from adjusted retention times as is normally done, show substantial variation from the calculated values for the polar phases. For the most polar phases investigated, DEGS, TCEP and OV-275 the n -alkane retention index markers are retained predominantly by interfacial adsorption and appropriate values for ΔI^C cannot be calculated. This problem is generally associated with the properties of the n -alkanes as can be seen by contrasting the plots of Figs. 2 and 3 which represent data for n -decane and 1-nitropropane on a number of

TABLE III

CALCULATION OF McREYNOLDS PHASE CONSTANTS AT 80.83C ACCORDING TO THE PROCEDURE OF ROHRSCHEIDER

Stationary phase	Index difference	Test solute				
		Benzene	Butanol	2-Pentanone	Nitropropane	Dioxane
OV-17	ΔI	111	156	160	239	179
	ΔI^C	110	158	158	235	177
	ΔI^R	110	158	158	236	177
OV-105	ΔI	34	145	91	134	77
	ΔI^C	32	143	89	132	75
	ΔI^R	32	143	89	132	75
OV-330	ΔI	206	381	261	404	290
	ΔI^C	201	380	256	398	285
	ΔI^R	201	380	256	399	285
OV-225	ΔI	213	370	326	469	325
	ΔI^C	207	368	323	460	320
	ΔI^R	210	372	326	465	323
Carbowax 20M	ΔI	308	541	357	559	420
	ΔI^C	327	571	375	591	444
	ΔI^R	327	571	375	591	444
QF-1	ΔI	116	203	320	413	250
	ΔI^C	109	195	314	407	241
	ΔI^R	109	195	314	407	241
DPAT	ΔI	430	859	606	761	632
	ΔI^C	457	898	630	797	656
	ΔI^R	457	897	629	797	656
BAT	ΔI	404	1019	751	808	856
	ΔI^C	430	1051	781	838	893
	ΔI^R	430	1050	781	838	892

phases of different polarity. 1-Nitropropane, which can be considered representative of the properties of the first five McReynolds test solutes, is retained by gas-liquid partitioning on all phases while *n*-decane is retained by a mixed retention mechanism on many phases. The model proposed by Rohrschneider, expressed by eqn. 8, is fundamentally sound for predicting values of ΔI when retention of the *n*-alkanes and test solutes occurs solely by gas-liquid partitioning. It is not applicable to those situations where either the test solute, or more likely, the *n*-alkane retention index standards are retained predominantly by interfacial adsorption. Experimental values of ΔI on polar phases are unreliable with respect to the thermodynamic model of eqn. 8.

Eqn. 8 can be derived directly from the equations for a straight line from Fig. 1 and consequently any homologous series of retention index standards that obeys eqn. 2 could be substituted for the *n*-alkanes. Using the 2-alkanones, which are retained largely by partitioning on non-polar and polar phases, the limitation that eqn. 8 can be applied only to non-polar and moderately polar phases using the *n*-alkane retention index standards is removed, Table IV. There is excellent agreement between the values of ΔI^C and ΔI^R for all phases but on the other hand, if the phases are ranked in order of their ΔI^C values for their ability to interact with a given test solute there is

only poor agreement in order between the phases ranked on the scale determined with the 2-alkanone and *n*-alkane retention index standards. Whereas it might be reasonable to assume that a hypothetical *n*-alkane experiences the same magnitude of interactions in squalane and on the polar phase (as is implied in the derivation of eqn. 8) this would seem to be unrealistic for the 2-alkanones which have modest dipole moments (*ca.* 2–3 D) and a reasonable potential for significant induction, orientation, and solvent proton–donor interactions in the compared phases. In terms of eqn. 8 this difference is reflected in the different values of $(\Delta G_K^{\circ}X)^*$ since the values of $(\Delta G_K^{\circ}X)^P$ and $\Delta G_K^{\circ}(\text{CH}_2)^P$ are not affected by the choice of homologous retention index standards provided that eqn. 2 is obeyed. The 2-alkanones are more sensible retention index standards than the *n*-alkanes for the accurate prediction of retention but should not be used for the specific application of determining selectivity phase constants.

Golovnya–Poole have equated the quantitative differences in stationary phase selectivity with the difference in the partial molar Gibbs free energy of solution of the test solute on a polar phase and on a reference phase exhibiting minimum selectivity as described by eqn. 6. As can be seen from Fig. 1 this approach differs significantly in the manner that the non-polar contribution to retention is estimated (it is reasonable to assume that the non-polar retention contribution includes contributions from induction as well as dispersion for the retention of polar test solutes). It has the further practical advantage that this approach is not limited by the problems associated with the use of the retention index system discussed above.

Golovnya and co-workers^{16,18,20,21} have derived several relationships between the retention index of a solute and solution thermodynamic parameters that can be used as the basis to derive a general equation relating Rohrschneider's ΔI parameter to

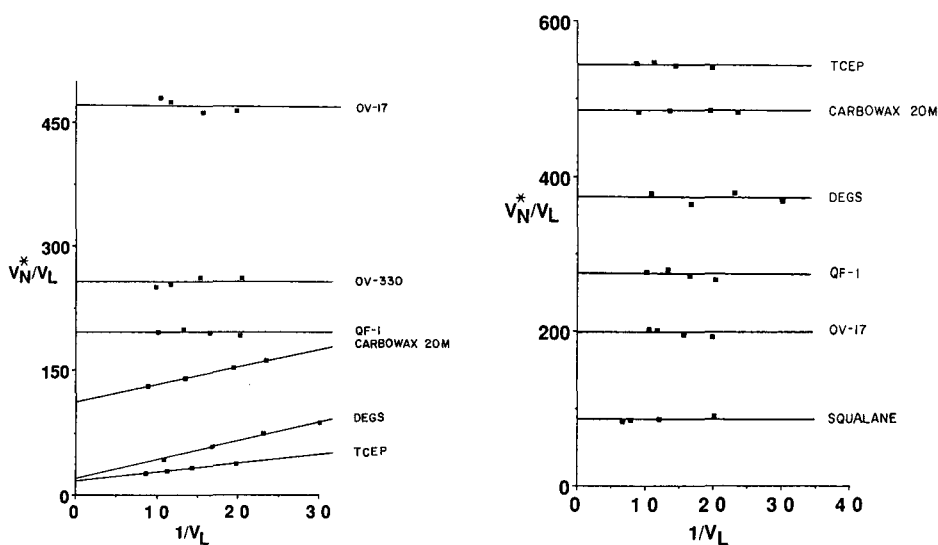


Fig. 2. Plot of V_N^*/V_L vs. $1/V_L$ for *n*-decane on a series of stationary phases of different polarity. The stationary phases are identified in Table I.

Fig. 3. Plot of V_N^*/V_L vs. $1/V_L$ for 1-nitropropane on a series of stationary phases of different polarity. The stationary phases are identified in Table I.

TABLE IV

CALCULATION OF McREYNOLDS PHASE CONSTANTS AT 80.8°C USING 2-ALKANONES AS RETENTION INDEX STANDARDS

Stationary phase	Index difference	Test solute			
		Benzene	Butanol	Nitropropane	Dioxane
OV-17	ΔI	-53	-8	76	19
	ΔI^C	-54	-5	75	15
	ΔI^R	-54	-5	75	15
OV-105	ΔI	-56	57	41	-14
	ΔI^C	-60	52	41	-16
	ΔI^R	-60	52	41	-15
OV-330	ΔI	-60	121	139	28
	ΔI^C	-62	120	138	24
	ΔI^R	-62	120	138	24
OV-225	ΔI	-128	46	138	-2
	ΔI^C	-125	40	136	-9
	ΔI^R	-125	40	136	-9
Carbowax 20M	ΔI	-56	187	204	63
	ΔI^C	-56	188	207	60
	ΔI^R	-56	188	207	60
QF-1	ΔI	-206	-117	84	-73
	ΔI^C	-204	-118	85	-76
	ΔI^R	-204	-118	85	-76
DPAT	ΔI	-191	243	143	21
	ΔI^C	-177	247	148	14
	ΔI^R	-177	247	149	14
DEGS	ΔI	-142	202	222	135
	ΔI^C	-131	211	-31	143
	ΔI^R	-131	211	-31	143
TCEP	ΔI	-194	124	262	99
	ΔI^C	-194	125	-31	101
	ΔI^R	-194	125	-31	101
OV-275	ΔI	-175	135	277	84
	ΔI^C	-158	146	-36	113
	ΔI^R	-159	146	-36	114

$\partial(\Delta G_k^o X)_{SQ}^p$ defined by eqn. 6. The retention index of a solute can be defined in terms of the gas-liquid partition coefficient of solute X and the retention index standards by eqn. 3. Substituting eqn. 2 into eqn. 3 and rearranging gives eqn. 9:

$$I^X = 100n + \frac{100}{B} (\log K_L^X - A - Bn) \quad (9)$$

which after simplification gives

$$\log K_L^X = \frac{I^X B}{100} + A \quad (10)$$

where A and B are the coefficients obtained by linear regression for the retention index standards defined by eqn. 2. The partial molar Gibbs free energy of solution for solute X is defined by eqn. 5, which after substituting for K_L^X from eqn. 10, gives

$$(\Delta G_K^{\circ} X)^P = -2.3RT \frac{I_P^X B_P}{100} + A_P \quad (11)$$

and by similar reasoning for squalane

$$(\Delta G_K^{\circ} X)^{SQ} = -2.3RT \frac{I_{SQ}^X B_{SQ}}{100} + A_{SQ} \quad (12)$$

Substituting eqns. 11 and 12 into eqn. 6 and rearranging gives

$$\partial(\Delta G_K^{\circ} X)_{SQ}^P = \frac{2.3RT}{100} (I_{SQ}^X B_{SQ} - I_P^X B_P) + 2.3RT(A_{SQ} - A_P) \quad (13)$$

Substituting for I_P^X from eqn. 4 into eqn. 13 gives

$$\partial(\Delta G_K^{\circ} X)_{SQ}^P = \frac{2.3RT}{100} [I_{SQ}^X (B_{SQ} - B_P) - \Delta I^X B_P] + 2.3RT(A_{SQ} - A_P) \quad (14)$$

The correctness of eqns. 13 or 14 can be tested using the values of I , ΔI , A and B given in Tables II-IV to calculate $\partial(\Delta G_K^{\circ} X)_{SQ}^P$ which can be compared to the experimental values of $\partial(\Delta G_K^{\circ} X)_{SQ}^P$. Table V, obtained from the gas-liquid partition coefficients. The

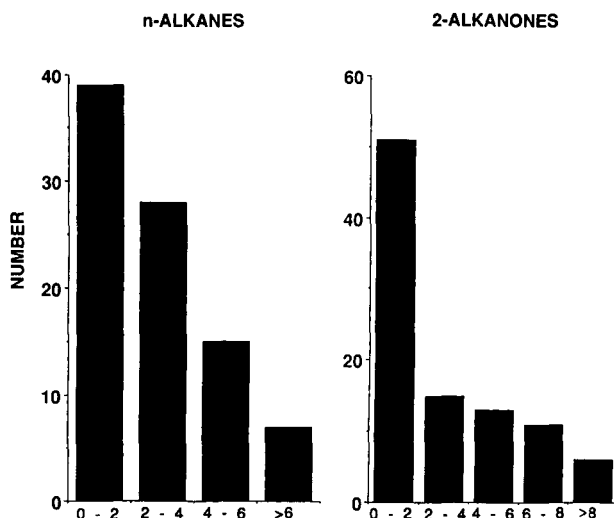


Fig. 4. Frequency distribution of the relative error in $\partial(\Delta G_K^{\circ} X)_{SQ}^P$ determined by eqn. 13 using n -alkanes and 2-alkanones as retention index standards and the experimental value determined from K_L^X for the McReynolds test solutes.

agreement is very good as can be seen from the error frequency distribution in Fig. 4. For the *n*-alkane retention index standards of 89 measurements only seven show a relative error greater than 6% and most of these are associated with benzene and other poorly retained solutes that have a greater uncertainty associated with their determination (Table I). Eqns. 13 and 14 are correct for any homologous series that obeys eqn. 2 and substituting the appropriate values for the 2-alkanones gives a similar goodness of fit to the *n*-alkanes.

Eqn. 14 reveals that there is no simple dependence of $\partial(\Delta G_k^o X)_{SQ}^P$ on ΔI^X and the magnitude of $\partial(\Delta G_k^o X)_{SQ}^P$ changes with the phase specific properties represented by the coefficients *A* and *B* as well as ΔI^X . Thus, one can expect no general correlation in the ranking of stationary phases to interact with a particular test solute and the two selectivity scales should be considered as independent and different from each other.

In earlier studies a strong correlation between ΔI^C for the McReynolds test solutes and the partial molar Gibbs free energy of solution for a methylene group on a wide range of conventional and liquid organic salt phases has been reported^{10,14,15,17,22}. The selectivity index values for ΔI^C and $\partial(\Delta G_k^o X)_{SQ}^P$ for nitropropane are plotted against *B_p* in Fig. 5 (*B_p* is a measure of the solubility of the *n*-alkanes in the polar stationary phase, see eqn. 7). The value of the retention index difference corrected for interfacial adsorption is seen to vary linearly with *B_p* (except for OV-105 and QF-1) indicating that ΔI^C is determined largely by the interactions of the *n*-alkanes with the stationary phase and to a lesser extent by selective interactions of the test solute with the phase. This is probably the reason why the magnitude of the McReynolds phase constants tend to increase monotonously with increasing phase polarity for all test solutes. The $\partial(\Delta G_k^o X)_{SQ}^P$ scale shows no similar correlation with *B_p* which is in agreement with chemical intuition.

TABLE V

THERMODYNAMICALLY CALCULATED PHASE CONSTANTS DERIVED FROM THE PARTIAL MOLAR GIBBS FREE ENERGY OF SOLUTION AT 80.8°C

Test solutes are identified in Table I. $\partial(\Delta G_k^o X)_{SQ}^P = (\Delta G_k^o X)_P - (\Delta G_k^o X)_{SQ}$. Absolute values for squalane (kcal/mol); X' = -3.085; Y' = -2.717; Z' = -2.956; U' = -3.084; S' = -3.332; H' = -3.315; J' = -4.032; K' = -4.244; L' = -3.091; M' = -5.087.

Stationary phase	$\partial(\Delta G_k^o X)_{SQ}^P$ (cal/mol)									
	X2'	Y2'	Z2'	U2'	S2'	H2'	J2'	K2'	L2'	M2'
OV-17	28	&264	&242	-633	-380	45	130	208	-325	516
OV-105	191	-421	-113	-316	-25	11	360	346	-28	622
OV-330	-67	-1004	-358	-1033	-655	-398	161	378	-479	821
OV-225	110	-723	-461	-1087	-566	-216	319	647	-421	1033
Carbowax 20M	-133	-1272	-373	-1259	-880	-452	295	594	-630	1169
QF-1	402	-65	-499	-860	-173	191	678	1007	-156	1272
DPAT	5	-1758	-683	-1252	-	-938	543	1212	-729	1663
DEGS	216	-1134	-264	-1076	-	-360	871	1272	-748	1956
BAT	537	-1843	-779	-934	-	-1018	1006	1684	-1129	2017
sBAT	524	-1976	-921	-1043	-	-1124	1004	1675	-1283	2152
TCEP	170	-1023	-483	-1340	-920	-156	853	1338	-777	2121
OV-275	478	-589	-50	-953	-475	380	1289	1969	-309	2539

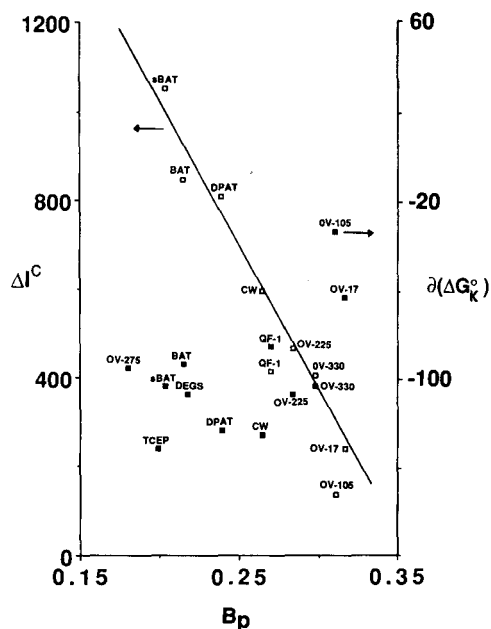


Fig. 5. Plot of $\partial(\Delta G_K^\circ X)_{SQ}^P$ (○) and ΔI^C (□) against the slope of the plot of eqn. 2 for nitropropane. There is a linear correlation for ΔI^C and no correlation for $\partial(\Delta G_K^\circ X)_{SQ}^P$.

The data presented in this paper supports the view that the Rohrschneider–McReynolds system for phase constants should be abandoned as it suffers from experimental and theoretical deficiencies. Mixed retention mechanisms make data for polar phases spurious. The phase constants are determined largely by the character of the retention index standards than by specific interactions with the test solute. Since the Gibbs free energy per index unit varies from one phase to another (typically from 1 to 6 cal/mol) it cannot be assumed that a hypothetical hydrocarbon co-eluting with the test solute on squalane should have the same free energy on a polar phase. These inconsistencies are absent from the $\partial(\Delta G_K^\circ X)_{SQ}^P$ scale which is to be preferred on theoretical and practical grounds. A much larger data set for 35 common stationary phases is in preparation to make the $\partial(\Delta G_K^\circ X)_{SQ}^P$ scale more useful and to permit studies of the correlation of this parameter with the phase structure.

ACKNOWLEDGEMENT

Acknowledgement is made to the donors of the Petroleum Research Fund administered by the American Chemical Society for support of this research.

REFERENCES

- 1 C. F. Poole and S. A. Schuette, *Contemporary Practice of Chromatography*, Elsevier, Amsterdam, 1984, p. 31.
- 2 C. F. Poole and S. K. Poole, *Anal. Chim. Acta*, 216 (1989) 109.
- 3 L. Rohrschneider, *Adv. Chromatogr.*, 4 (1967) 333.

- 4 L. Rohrschneider, *J. Chromatogr. Sci.*, 11 (1973) 160.
- 5 W. O. McReynolds, *J. Chromatogr. Sci.*, 8 (1970) 685.
- 6 W. R. Supina and L. P. Rose, *J. Chromatogr. Sci.*, 8 (1970) 214.
- 7 A. Hartkopf, *J. Chromatogr. Sci.*, 12 (1974) 113.
- 8 L. S. Ettre, *Chromatographia*, 7 (1974) 261.
- 9 J. K. Haken, *Adv. Chromatogr.*, 14 (1976) 366.
- 10 S. K. Poole, B. R. Kersten, R. M. Pomaville and C. F. Poole, *LC · GC, Mag. Liq. Gas Chromatogr.*, 6 (1988) 400.
- 11 C. F. Poole and S. K. Poole, *Chem. Rev.*, 89 (1989) in press.
- 12 B. R. Kersten and C. F. Poole, *J. Chromatogr.*, 399 (1987) 1.
- 13 B. R. Kersten, C. F. Poole and K. G. Furton, *J. Chromatogr.*, 411 (1987) 43.
- 14 C. F. Poole, S. K. Poole, R. M. Pomaville and B. R. Kersten, *J. High Resolut. Chromatogr. Chromatogr. Commun.*, 10 (1987) 670.
- 15 R. M. Pomaville and C. F. Poole, *Anal. Chem.*, 60 (1988) 1103.
- 16 R. V. Golovnya and T. A. Misharina, *J. High Resolut. Chromatogr. Chromatogr. Commun.*, 3 (1980) 51.
- 17 W. A. Aue and V. Paramasigamani, *J. Chromatogr.*, 166 (1978) 253.
- 18 R. V. Golovnya and T. A. Misharina, *Chromatographia*, 10 (1977) 658.
- 19 B. R. Kersten and C. F. Poole, *J. Chromatogr.*, 452 (1988) 191.
- 20 R. V. Golovnya and Yu. N. Arsenyev, *Chromatographia*, 4 (1971) 250.
- 21 R. V. Golovnya, *Chromatographia*, 12 (1979) 533.
- 22 M. Roth and J. Novák, *J. Chromatogr.*, 234 (1982) 337.

CHROM. 21 317

DETERMINATION OF THE GAS CHROMATOGRAPHIC PERFORMANCE CHARACTERISTICS OF SEVERAL GRAPHITIZED CARBON BLACKS

W. R. BETZ* and W. R. SUPINA

Supelco, Inc., Supelco Park, Bellefonte, PA 16823-0048 (U.S.A.)

SUMMARY

Two graphitized carbon blacks have been evaluated as solid supports (adsorbents) for the chromatographic determination of adsorbate-adsorbent interactions.

Adsorption isotherms were chromatographically derived to provide insight into the behavior of several *n*-alkanes, aromatic hydrocarbons, and aliphatic alcohols, with four adsorbents functioning as chromatographic packings. These four adsorbents, Carbopack B, Carbopack C, Carbopack B modified with 5% (w/w) Carbowax 20M, and Carbopack C modified with 0.5% (w/w) Carbowax 20M, subsequently were utilized for the chromatographic analyses of the adsorbate groups, in the low coverage (Henry's Law) region.

INTRODUCTION

Utilization of adsorbents as solid supports for both gas-solid and gas-liquid-solid chromatography has become increasingly effective over the past two decades. The availability of adsorbents which possess homogeneous, non-porous, non-specific surfaces has allowed for linearity in the adsorption isotherms throughout a wide temperature range¹. Graphitized carbon blacks, which possess homogeneous, non-porous, non-specific surfaces², provide effective chromatographic analyses of a wide range of adsorbates. For this study, choices of the surface area and/or liquid phase coated on the non-specific surface have allowed for chromatographic analyses of several *n*-alkanes (group A molecules), aromatic hydrocarbons (group B molecules), and aliphatic alcohols (group D molecules) in the equilibrium region³. Chromatographic determination of the BET adsorption isotherms for the adsorbates, using the peak maxima method^{4,5}, has provided information about the adsorbates' behavior in the chromatographic columns.

EXPERIMENTAL

Gas-solid and gas-liquid-solid chromatographic columns were utilized to obtain the adsorption isotherms and chromatographic separations for the chosen adsorbates. Carbopack B (60–80 mesh; surface area, 100 m²/g) and Carbopack

C (60–80 mesh; surface area, 10 m²/g), which are commercially available graphitized carbon black adsorbents (Supelco), were utilized for the gas–solid chromatographic profiles. Two gas–liquid–solid packings, 5% Carbowax-20M on 60–80 mesh Carbopack B and 0.5% Carbowax 20M on 60–80 mesh Carbopack C (also available from Supelco), were utilized to generate comparative chromatographic profiles and to improve the behavior of the alcohols. Each adsorbent and coated adsorbent was packed in a 2 ft. × 2 mm I.D. silanized glass column. High-purity nitrogen (scrubbed to remove traces of oxygen and water) was used at a pressure-corrected⁶ flow-rate of 20 ml/min. Each column was thermally conditioned at 220°C for at least 8 h prior to use.

The adsorbates were obtained from Polysciences and were not purified further. The adsorbates chosen were *n*-pentane, *n*-hexane, *n*-octane, *n*-decane, benzene, toluene, ethylbenzene, ethanol, *n*-butanol, *n*-hexanol and *n*-octanol. The injection volume ranged from 0.2 to 20.0 μl (30.0 μl for aliphatic alcohols and 40.0 μl for *n*-alkanes and aromatic hydrocarbons on Carbopack B adsorbent). Adsorbate response was determined by using a flame ionization detector with a Spectra-Physics Model 4270 integrator to obtain peak height and peak area data.

Chromatographic pictures were obtained by using a Houston Instruments strip chart recorder, and adsorption isotherm plots were generated with a Macintosh II personal computer.

Procedure

Adsorption isotherms for the eleven adsorbates were obtained at temperatures which provided similar retention volume windows for each of the adsorbent packings. The peak maxima elution method was utilized, with the adsorbate vapor pressure determined as a function of the recorder pen displacement. To obtain the isotherm plots, this pressure value was plotted against the adsorbate concentration divided by the adsorbent packing weight. The equations utilized for the *X* and *Y* axis values are:

$$\begin{array}{ll} \text{X-Axis (pressure axis)} & \text{Y-Axis (uptake axis)} \\ P = \frac{mxRT}{Sf} \cdot h & q = \frac{m \cdot 10^5}{W} \end{array}$$

where *m* = moles of adsorbate injected, *x* = chart speed, *R* = universal gas constant, *T* = temperature, *S* = adsorbate peak area, *f* = corrected flow rate, *h* = adsorbate peak height, *q* = moles of sample adsorbed, *W* = adsorbent packing weight.

The chromatographic analyses were performed in a defined temperature programmed range: 40°C (2 min) to 220°C at 16°C per min (250°C final temperature for the Carbopack B column).

RESULTS AND DISCUSSION

Adsorption isotherm data

Fig. 1 illustrates the adsorption isotherms obtained from the interactions between the *n*-alkanes and the surface of Carbopack B. They are representative of Type II isotherms as classified by Brunauer *et al.* and discussed by Gregg and Sing⁷. The choice of different temperatures for the adsorbates appears to minimize the trend of adsorption for a greater number of carbon atoms³. Fig. 2 illustrates the behavior of

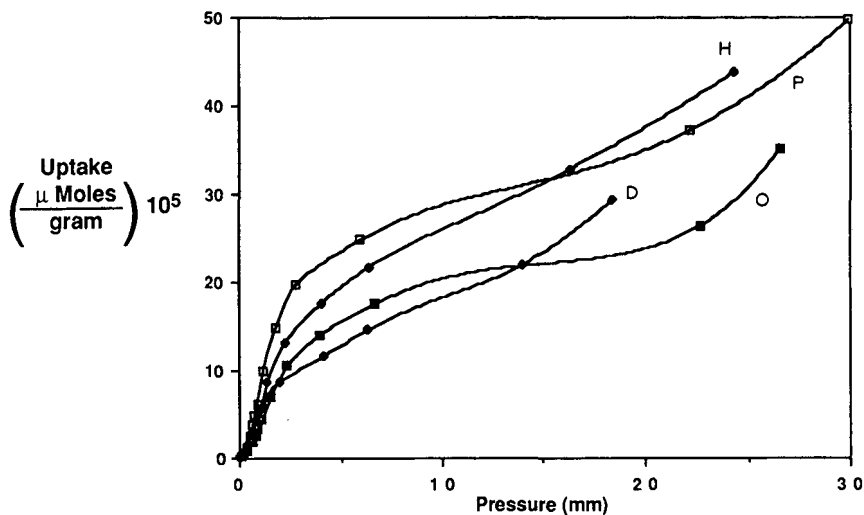


Fig. 1. Adsorption isotherms of *n*-alkanes on Carbpac B. (P) Pentane (50°C); (H) hexane (90°C); (O) octane (160°C); (D) decane (210°C).

toluene with the Carbpac B surface, and confirms the use of this elution method for isotherm determination. Fig. 3 illustrates the behavior of the aromatic hydrocarbons with the Carbpac B surface. Again, Type II isotherms appear to be well defined¹.

Fig. 4 illustrates the behavior of two aliphatic alcohols with the Carbpac B surface. The behavior is indicative of weak surface-surface interactions at low coverage (isotherms are convex to the pressure axis). Uptake becomes more significant as multiple layer coverage occurs; hence second points on inflection are present with the plots, as noted in previous documents¹.

Behavior similar to that of the *n*-alkanes and aromatic hydrocarbons and the Carbpac B surface was noted with the Carbpac C surface as well. As with the surface to surface interactions occurring with Carbpac B, Type II isotherms were

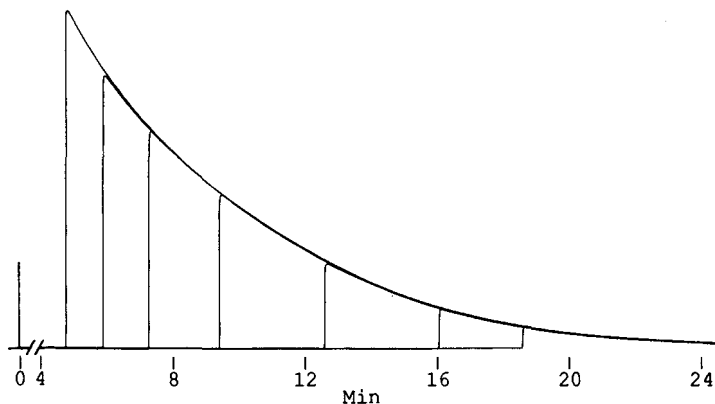


Fig. 2. Chromatographic profile of toluene using 60-80 Carbpac B, injection volumes: 0.2-5.0 μl at 110°C.

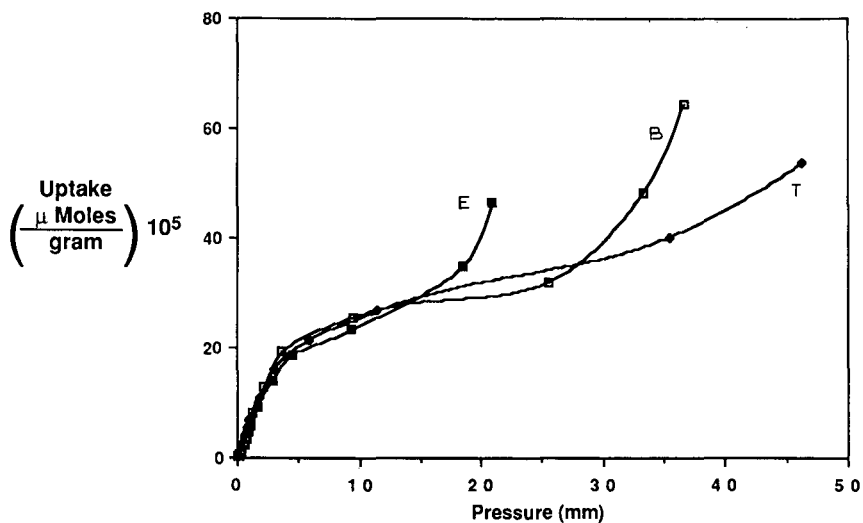


Fig. 3. Adsorption isotherms of aromatic hydrocarbons on Carbpac B. (B) Benzene (70°C); (T) toluene (110°C); (E) ethylbenzene (140°C).

represented. The homogeneous, non-porous surfaces of both of these graphitized carbon blacks allow for these similarities.

Behavior of the aliphatic alcohols with the surface of Carbpac C also was similar to that seen with the Carbpac B surface. Again, as with the Carbpac B, two points of inflection were observed.

Fig. 5 illustrates the behavior of the aromatic hydrocarbons with the modified Carbpac B surface. The isotherms for both the group A and group B molecules begin to approach those obtained for the alcohols and the unmodified graphitized

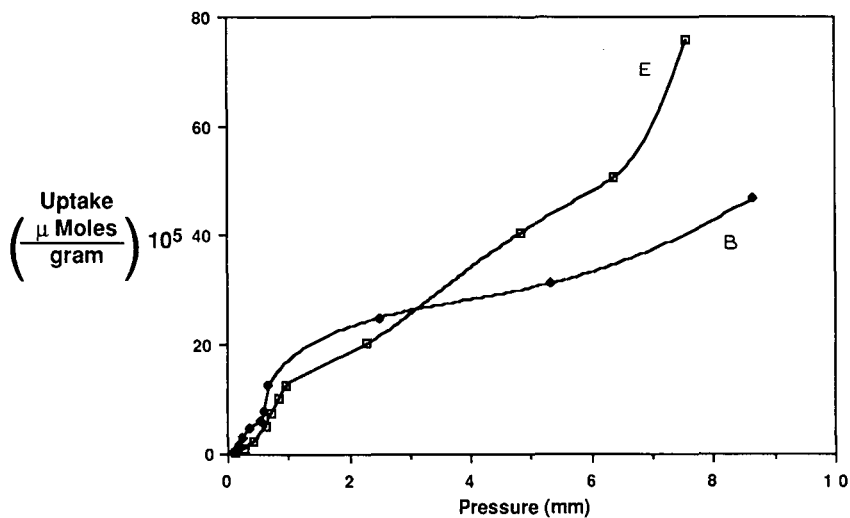


Fig. 4. Adsorption isotherms of alcohols on Carbpac B. (E) Ethanol (35°C); (B) butanol (70°C).

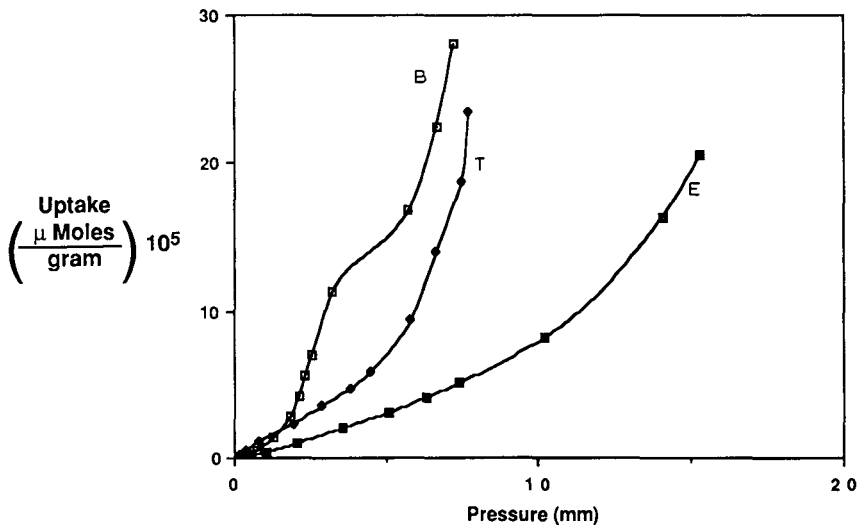


Fig. 5. Adsorption isotherms of aromatic hydrocarbons on 5% CW-20M on Carbopack B. (B) Benzene (35°C); (T) toluene (60°C); (E) ethylbenzene (100°C).

carbon black surfaces; however the inflection points are less severe and begin to approach linearity. This trend in the isotherms relates to the chromatographic analyses of the adsorbates, at low coverage, as a spreading of the hydrocarbon peaks (which retain a Gaussian shape). Similar behavior was noted with the *n*-alkanes as well. Figs. 6 and 7 illustrate this chromatographic behavioral difference between the hydrocarbons and the unmodified Carbopack B and the modified Carbopack B surface.

Fig. 8a and b illustrate the behavior of ethanol with the unmodified and modified Carbopack B surfaces. In the low coverage region, ethanol interacts weakly with the

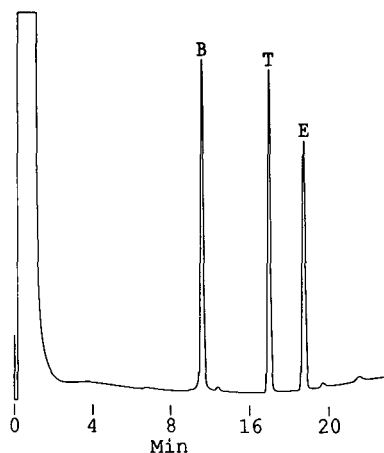


Fig. 6. Chromatographic analysis of aromatic hydrocarbons using 60–80 mesh Carbopack B. Column temperature: 40°C (2 min) to 240°C at 16°C per min; concentration: 150–200 ng on column. B = Benzene, T = toluene, E = ethylbenzene.

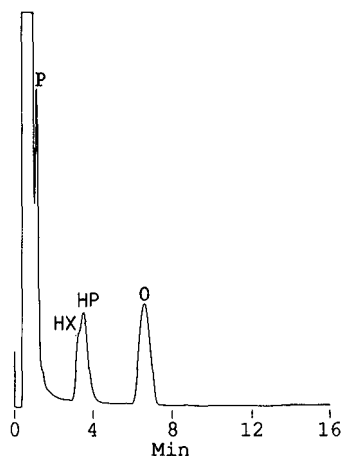


Fig. 7. Chromatographic analysis of C_5 - C_8 alkanes using 5% CW-20M on 60-80 mesh Carbopack B. Column temperature: 40°C (2 min) to 210°C at 16°C per min; concentration: 250-300 ng on column. P = pentane, HX = hexane, HP = heptane; O = octane.

unmodified Carbopack B surface and chromatographically behaves poorly, while the modified Carbopack B surface allows for effective chromatographic analyses of ethanol. The utilization of a solid support (for liquid phase addition), with a large homogeneous surface, such as Carbopack B, allows for improvement of these surface-surface interactions, since adsorbate interactions are not solely dependent on the gas-liquid or gas-solid partitions and the electronic activity of the support surface is adequately modified.

Fig. 9a and b illustrates the chromatographic profiles for ethanol with the modified and unmodified Carbopack B surfaces, obtained to generate the isotherm plots. In the isotherm plots of the aliphatic alcohols with the modified Carbopack B surface, one inflection point was noted.

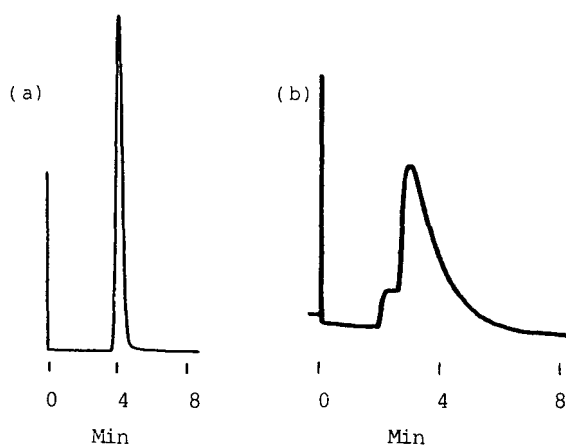


Fig. 8. Chromatographic analyses of ethanol (low coverage) using (a) 5% CW-20M on 60-80 Carbopack B, 35°C ; (b) 60-80 Carbopack B, 35°C .

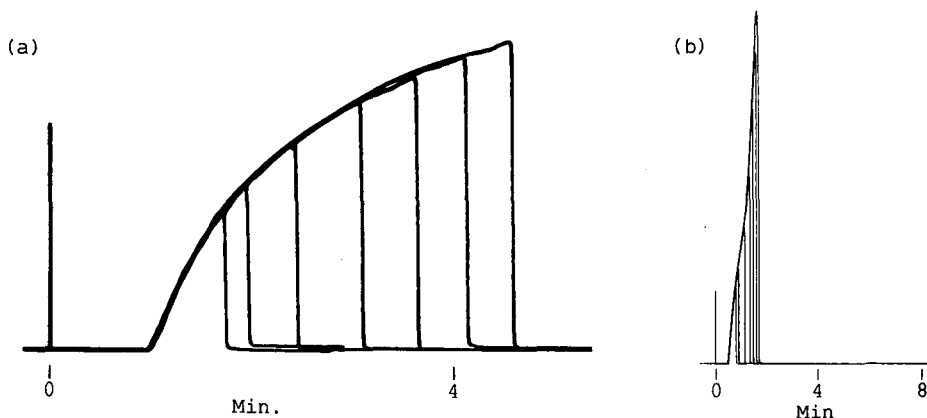


Fig. 9. Chromatographic profile of ethanol. (a) 60–80 Carbpac B (60°C); (b) 5% CW-20M on 60–80 Carbpac B (60°C). 0.2–5.0 μ l.

The behavior of the *n*-alkanes, aromatic hydrocarbons, and aliphatic alcohols with the modified Carbpac C surface is similar to that seen with the modified Carbpac B. Fig. 10 illustrates the chromatographic behavior of the alcohols (low coverage) with the unmodified Carbpac C surface throughout a temperature programmed profile. Fig. 11 illustrates the improved adsorbate–adsorbent surface behavior for these alcohols with the modified Carbpac C surface. Behavior for the modified Carbpac B surface is similarly improved.

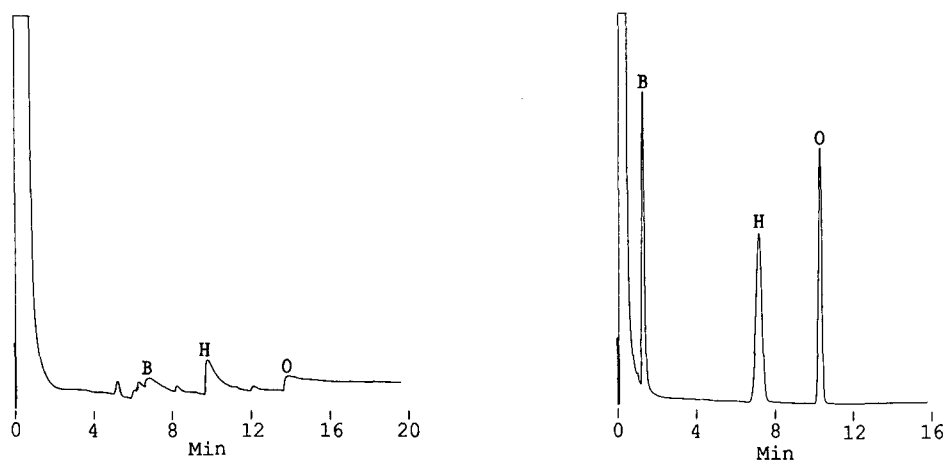


Fig. 10. Chromatographic analysis of C_4 – C_8 alcohols using 60–80 Carbpac C. Column temperature: 40°C (2 min) to 210°C at 16°C per min; concentration: 250–300 ng on column. B = *n*-butanol, H = *n*-hexanol, O = *n*-octanol.

Fig. 11. Chromatographic analysis of C_4 – C_8 alcohols using 0.5% CW-20M on 60–80 Carbpac C. Column temperature: 40°C (2 min) to 210°C at 16°C per min; concentration: 250–300 ng on column. B = *n*-butanol, H = *n*-hexanol, O = *n*-octanol.

CONCLUSION

Utilization of non-specific, non-porous, homogeneous graphitized carbon black adsorbents as gas-solid chromatographic packings allows for excellent chromatographic behavior of *n*-alkanes and aromatic hydrocarbons (group A and group B adsorbates). Use of appropriate surface modifiers for these adsorbents also ensures effective chromatographic behavior of aliphatic alcohols (group D adsorbates). The chromatographic behavior of these three groups of adsorbates is well represented by the defined adsorption isotherms and chromatographic analyses (in the low coverage region) presented herein. Further investigations will be conducted to evaluate the use of other surface modifiers for other group D adsorbates.

REFERENCES

- 1 A. V. Kiselev and Y. I. Yashin, *Gas Adsorption Chromatography*, Plenum Press, New York, 1969.
- 2 F. Bruner, P. Ciccioli, G. Crescentini and M. T. Pistolesi, *Anal. Chem.*, 45 (1973) 1851.
- 3 W. R. Supina, *The Packed Column in Gas Chromatography*, Supelco, Bellefonte, PA, 1974.
- 4 J. F. K. Huber and R. G. Gerritse, *J. Chromatogr.*, 58 (1971) 137.
- 5 M. Domingo-Garcia, F. J. López-Garzón, R. López-Garzón and C. Moreno-Castilla, *J. Chromatogr.*, 324 (1985) 19.
- 6 J. R. Conder, *Chromatographia*, 7 (1974) 387.
- 7 S. J. Gregg and K. S. W. Sing, *Adsorption, Surface Area and Porosity*, Academic Press, New York, 1982.

CHROM. 21 284

CHARACTERISTICS OF GLASS BASED PACKINGS AS A SUPPORT IN CHROMATOGRAPHY

L. SHAYNE GREEN and WOLFGANG BERTSCH*

The University of Alabama, Department of Chemistry, P.O. Box 870336, Tuscaloosa, AL 35487-0336 (U.S.A.)

SUMMARY

The preparation and properties of glass beads as a support for gas–liquid chromatography was studied. A comparison between diatomaceous earth type supports and glass beads was made in terms of activity to polar components. The procedure originally suggested by Grob was used to determine specific solute–surface interactions. We unexpectedly found it difficult to deactivate glass beads by conventional means. This is possibly due to the large number of silanol groups remaining on the surface of the support after deactivation. Several methods of deactivation were evaluated.

INTRODUCTION

Glass has been used widely as a support in gas–liquid chromatography (GLC), mainly as a support for open tubular columns (OTC). Numerous publications have dealt with the topic of glass surface modification for gas chromatography and much is known about deactivation and coating of glass^{1,2}. One such support for packed column GLC is glass beads. Since much is known about surface modification of glass, glass beads should serve as an excellent support. Glass composition can be well controlled and this material should be superior to diatomaceous type supports since the latter have batch-to-batch variations and contain many metal impurities. Even with these drawbacks, diatomaceous earth type supports remain the overwhelming choice as a support for packed column GLC.

Diatomaceous type supports in packed column GC have a checkered history in terms of deactivation. It has been found to be quite difficult to prepare well deactivated packed columns. Trace analysis of polar components often requires columns with near to perfect deactivation. The inability to prepare sufficiently inert supports is one of the factors that has brought about a decrease in the use of packed columns.

Glass beads have several advantages over other supports. One is that columns packed with glass beads have higher permeabilities than diatomaceous earth type supports³. Another is that glass beads of narrow size distribution and spherical shape should also decrease the eddy diffusion term of the van Deemter equation when compared to irregular shaped particles of similar dimensions and thus decrease plate

height. However, glass beads as a chromatographic support is not without limitation. Early work with glass beads demonstrated poor efficiency due to phase pooling at the contact points of the beads^{4,5}. Efforts were made in the early sixties to stabilize stationary-phase coatings by surface roughening techniques but development was discontinued after having achieved only modest success^{6,7}. A new concept to overcome the most serious limitations of glass beads, lack of adequate phase loading and film instability, has recently been introduced⁸. From a practical point of view, columns packed with stationary phase stabilized glass beads should occupy a niche between OTC and classical packed columns. This paper deals with the preparation of spherical glass packings and compares their performance to other chromatographic supports, in particular, diatomaceous earth.

EXPERIMENTAL

Materials

Glass beads (Alltech Assoc., Applied Science Labs., Deerfield, IL, U.S.A.; Ferro, Cataphot Division, Jackson, MS, U.S.A.; Phase Separations, Norwalk, CT, U.S.A.), Chromosorb (Johns-Manville, Denver, CO, U.S.A.), and Ultrabond® (Supelco, Bellefonte, PA, U.S.A.) were the supports used in this evaluation. Activity testing of uncoated supports was performed by a coupled column technique, as described previously⁹. The precolumn was a 5 m × 0.53 mm I.D. OV-1 fused-silica OTC (2.65 μm film thickness, Hewlett-Packard, Palo Alto, CA, U.S.A.). Packed columns were prepared from 0.33 m × 1.1 mm I.D. deactivated Pyrex tubing using the procedure suggested by Rijks¹⁰. The columns were tested (Grob test mix II, Fluka, Ronkoukoma, NY, U.S.A.) following standard procedures¹¹. The chromatograph used for the evaluation was a Hewlett-Packard 5890.

Sample capacity was determined by injecting variable amounts of *n*-hexadecane in hexane at a column temperature of 120°C. Overloading was reached when the leading edge of the peak at 10% peak height divided by the tailing edge approached a value of 1.1. *H* versus *u* curves were obtained on a 1.7 m × 1.1 mm column packed with 3% OV-1 on 80–100 mesh Chromosorb W HP and a 1.0 m × 1.1 mm column packed with 1.5% (three coatings of 0.5%) OV-1 on 80–100 mesh glass beads. The standard used was *n*-hexadecane in hexane with a 1:20 split at a column temperature of 160°C.

Elemental analysis

The glass beads and Chromosorb were digested in a PTFE beaker using 48% HF on low heat overnight. The remaining solution was evaporated to near dryness and diluted with 3 M HNO₃ (distilled in-house) and heated to dissolve the residue. The solution was then diluted to 50 ml in a volumetric flask and immediately transferred to a polyethylene bottle. Appropriate standards were prepared and elemental analysis was performed on a Perkin-Elmer 5500 ICP following standard procedures¹².

Etching

Glass beads were washed at room temperature with a 3 M NaOH solution that was prepared from a mixture of distilled water and ethanol. Glass beads were etched

with either KHF_2 (Alfa Products, Danvers, MA, U.S.A.), HF, or NH_4HF_2 (BDH Chemicals, U.K.). Solutions in the range 0.1–20% were prepared with distilled water. Etching was performed in a PTFE beaker at temperatures ranging from room temperature to 100°C . The solutions were constantly stirred using a PTFE coated magnetic stirring bar. Etching times ranged from 10 min to 1 h. After etching, the beads were rinsed with distilled water and dried. When etching was performed with KHF_2 the glass beads were washed with a 50% H_2SO_4 solution.

Leaching and dehydration

Glass beads were leached with HCl of varying concentrations ranging from 0.1 to 20%. The temperature range varied from room temperature to 160°C and exposure times varied from a few minutes to overnight. During leaching, the glass beads were placed in 6 in. \times 3 in. Pyrex glass vessels and sealed under a vacuum. After leaching, the beads were washed with 50-ml aliquots of 20, 10, 5, 1 and 0.1% HCl. In some situations the glass beads were rinsed with a 0.3% solution of H_3PO_4 after leaching. The beads were then dried and subjected to immediate dehydration under vacuum at 200°C for 2 or 3 h.

Deactivation

Glass beads were deactivated with either hexamethyldisilazane (HMDS, Aldrich, Milwaukee, WI, U.S.A.), octamethylcyclotetrasiloxane (D_4), or polymethylhydrosiloxane (PMHS, Petrarch Systems, Bristol, PA, U.S.A.) following standard procedures^{2,13–15}. The glass beads and appropriate amounts of deactivating agent were sealed under vacuum in a Pyrex vessel. A range of temperatures were examined. The H_3PO_4 washed beads were deactivated with HMDS and PMHS. After deactivation, the beads were washed and dried. Glass beads were also deactivated with a non-extractable layer of Carbowax 20M (Supelco, Bellefonte, PA, U.S.A.), following the method suggested by Daniewski and Aue¹⁶.

Cab-O-Sil[®] HS-5 (Cabot, Tuscola, IL, U.S.A.) was deactivated according to Rutten *et al.*^{17,18} and Silanox Grade 101[®] (Cabot Corporation, Tuscola, IL, U.S.A., now marketed as Tullanox, Tulco, North Billerica, MA, U.S.A.) also gas phase deactivated with Carbowax 20M¹⁹. In this procedure a glass injector sleeve was packed with 15% Carbowax 20M on 80–100 mesh Chromosorb W AW DMCS and placed in the injector of a GC. The Silanox[®] was loosely packed in a short length of Pyrex tubing and connected to the injector. The injector and oven were heated at 280°C overnight with helium flowing through the column. After deactivation, the Silanox was washed with methanol.

Coating

Glass beads were coated with either OV-1, OV-101-OH, (Ohio Valley Specialty Chemical, Marietta, OH, U.S.A.), or OV-1-OH (prepared according to Blum²⁰) using the layering technique previously described⁸. After coating with OV-101-OH, the glass beads were heated from 100 to 380°C and kept at the final temperature for 12 h. The OV-1-OH gum was treated in a similar fashion except that the upper temperature was 330°C .

RESULTS AND DISCUSSION

Chromosorb supports show a large range in batch-to-batch elemental composition. This is particularly prevalent among the two different types of chromosorb, pink and white. These supports contain a significant amount of metal impurities even after extensive acid treatment²¹. Elemental determination of bulk composition of two types of Chromosorb supports is presented in Table I. Fig. 1 presents chromatograms of the test mixture on various Chromosorb supports that were obtained from commercial sources. All supports show activity, except for the Ultrabond variety, which is a Carbowax 20M deactivated material²². Large differences in terms of chemical composition and shape have also been found among different manufacturers of glass beads. This is not surprising since some of the materials tested were intended for industrial use. The differences in bulk composition of three different glass beads sources is presented in Table I. Glass beads for chromatography should be made from high quality glass of well defined composition and should contain few irregular shaped beads.

Etching and leaching of glass surfaces is relatively well understood^{1,2}. Etching has traditionally been carried out on glass to induce surface roughening so that polar stationary phases could be coated efficiently. We adapted this technology to glass beads to increase surface area and allow for higher initial phase loading. The use of high concentrations of HF resulted in the dissolution of the glass. When the concentration was lowered, etching could not be observed. Little or no roughening occurred at intermediate concentrations. In contrast to gaseous HF, which is very effective²³, aqueous HF can obviously not be used to induce roughening. NH_4HF_2 produced no surface roughening at any concentration or temperature but KHF_2 was found to produce coarsely roughened surfaces. It was found that the surface was not etched by removal of glass but was roughened by deposition of a layer of K_2SiF_6 ²⁴. The layer was easily disrupted with strong stirring of the solution. Treatment with dilute H_2SO_4 readily removed the layer. The resulting surface was very active.

Leaching provides a surface composed of a xerogel which constitutes an ideal, metal-free, silanol rich surface that can be adapted to chromatography. Even though the bulk composition of glass beads contains a significant number of metals, leaching should remove these metals from the surface of the glass. Studies have shown that leaching forms a surface depleted of most metals^{25,26} and that the bulk metals do not migrate to the surface under ordinary chromatographic conditions²⁵. Standard pro-

TABLE I
ELEMENTAL COMPOSITION OF SUPPORTS

<i>Support</i>	<i>Na</i>	<i>K</i>	<i>Mg</i>	<i>Ca</i>	<i>B</i>	<i>Al</i>	<i>Fe</i>
Glass beads A	6.5	— ^a	2.9	6.9	—	0.2	0.2
Glass beads B	6.9	—	2.7	7.9	—	0.3	0.2
Glass beads C	3.8	8.0	0.1	0.2	0.3	0.4	—
Chromosorb P NAW	—	—	0.4	—	—	2.2	1.1
Chromosorb W AW	13.5	3.0	0.6	—	—	2.1	0.8

^a Could not be detected.

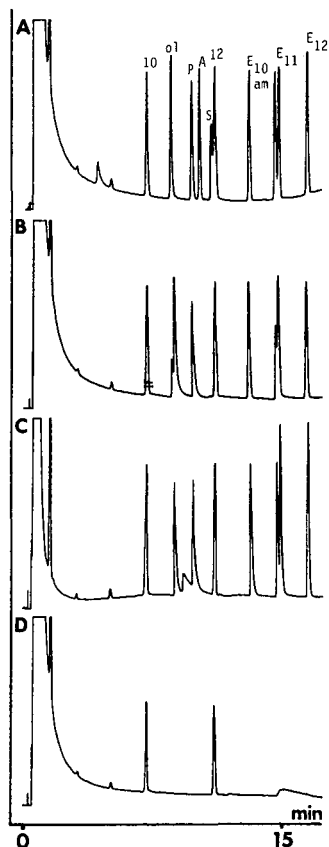


Fig. 1. Chromatograms of test mixture on: (A) Ultrabond; (B) Chromosorb G AW DMCS; (C) Chromosorb W AW DMCS; (D) Chromosorb W AW. Peaks: 10 = decane, ol = 1-octanol, P = 2,6-dimethylphenol, A = 2,6-dimethylaniline, S = 2-ethylhexanoic acid, 12 = dodecane, am = dicyclohexylamine, E₁₀-E₁₂ = methyl esters of C₁₀-C₁₂ fatty esters.

cedures for leaching capillary columns involve overnight heat treatment at 110–150°C with a 20% metal-free HCl solution^{2,25}. The glass beads did not withstand these conditions. The surfaces changed drastically in appearance, showing extensive attack. These conditions are believed to remove most of the metal impurities but leave a very thick hydrated layer that collapses during dehydration. Beads were found to contain small fractures even under less severe conditions. Leaching under very mild conditions, *e.g.* with 5% HCl for 1 h at 110°C, produced smooth surfaces. Excessive leaching, as indicated by surface distortion, was not only related to time and temperature, but also to concentration. Beads treated at temperatures lower than 90°C were insufficiently leached and could not be deactivated.

The deactivation of glass beads with commonly used agents such as HMDS, D₄, or PMHS would appear to be quite routine. The gas phase deactivation with HMDS should yield a surface where most silanol groups have been converted to the corresponding trimethylsilyl moieties. The deactivation of the glass tubing used for

the preparation of test column material was straightforward and yielded perfectly inert surfaces. To our surprise, the use of these agents did not render the surface of the glass beads nearly as inert, in spite of careful optimization of the individual steps. Some residual activity, which most likely is due to remaining silanol groups, always remained. Fig. 2 presents chromatograms of the test mixture with HMDS deactivated glass beads as a function of column length. As the column length was increased overall, activity also increased. The glass beads were also subjected to multiple HMDS treatments. One batch was found to exhibit increased deactivation for the second treatment and an overall decrease in deactivation for the third treatment. D_4 , a cyclic octamethyltetrasiloxane, was applied in an inert atmosphere and also in an oxygen atmosphere as suggested by Xu *et al.*¹⁵. No decrease in activity was observed.

Deactivation with PMHS was also somewhat disappointing. An attempt was made to wash the beads with a 0.3% H_3PO_4 solution after leaching². The beads proved to be extremely sticky after washing with H_3PO_4 . After washing with H_3PO_4 and dehydrating, the beads were deactivated with either HMDS or PMHS. Deactivation of these beads with HMDS failed, but deactivation with PMHS provided almost perfect deactivation. This is believed to be due to H_3PO_4 serving as an acid catalyst. Fig. 3 presents a chromatogram of the test mixture with PMHS deactivated

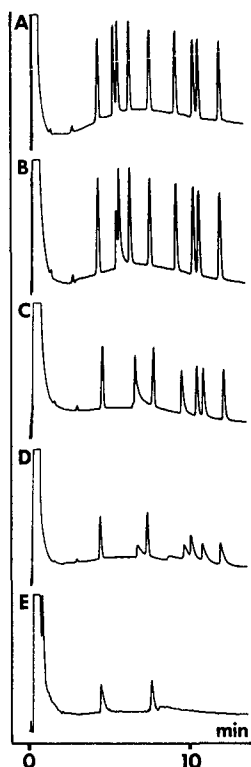


Fig. 2. Chromatograms of test mixture on HMDS deactivated glass beads of various lengths: (A) 4 cm; (B) 8 cm; (C) 14 cm; (D) 28 cm; (E) 50 cm. Preparation conditions: 80–100 mesh glass beads cleaned with NaOH–ethanol and washed with 50-ml aliquots of 20, 10, 5, 1 and 0.1% HCl; dehydrated at 200°C for 2 h.

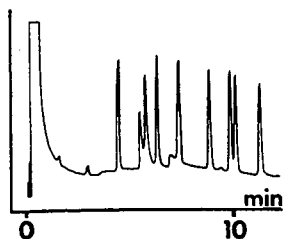


Fig. 3. Chromatogram of test mixture on glass beads washed with 0.3% H_3PO_4 and deactivated with PMHS.

glass beads. After PMHS deactivation the beads were still extremely tacky. H_3PO_4 has been found to be undesirable because it attacks the glass surface²⁵.

Another deactivation procedure which consists of deactivation with Carbowax 20M proved to be very effective in reducing the surface activity. These beads exhibited excellent deactivation as shown in Fig. 4A. Unfortunately, the stability of the Carbowax 20M layer is questionable. It is known that Carbowax 20M deactivated supports are not stable above 300°C and are very susceptible to degradation by traces of oxygen¹⁶. We decided to test the Carbowax 20M deactivation for different time periods and temperatures. Stability testing revealed that deactivation deteriorated slightly after heating for 2 h at 280°C. Raising the temperature to 300°C for short periods of time did not cause noticeable deterioration. Prolonged heating at 320°C caused serious disruption of the protective layer as evidenced by severe tailing of all components, as shown in Fig. 5. It is possible to use Carbowax 20M deactivated beads at temperatures up to 300°C for only short periods of time.

The coating procedure previously advocated⁸ was found to be very effective in providing an even layer of phase. Silanox proved to be an excellent means for removing the stickiness of individual particles and producing free-flowing glass beads. Attempts were also made to directly deactivate the surface of the glass with OV-101-OH. It was observed that a new substance had actually been formed, which appears to be a

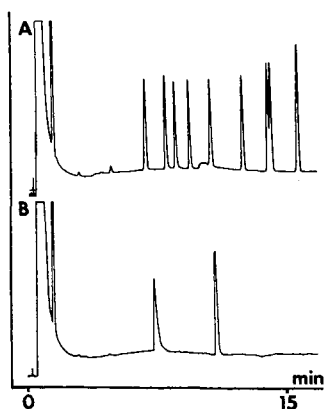


Fig. 4. Chromatogram of test mixture on: (A) Carbowax 20M deactivated glass beads; (B) after dusting with 4.3 mg of Silanox.

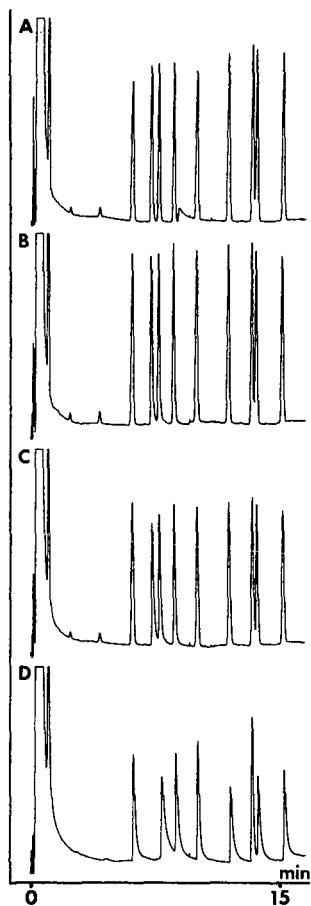


Fig. 5. Chromatogram of test mixture on Carbowax 20M deactivated glass beads after heating for 2 h at: (A) 220°C; (B) 280°C; (C) 300°C; (D) 320°C.

cyclosiloxane²⁷. When the gumified OV-101-OH phase was used, the glass beads were not deactivated as well and no cyclosiloxanes were observed.

Silanox, which is produced by gas phase deactivation of Cab-O-Sil HS-5 with HMDS, was found to be very active. This activity was demonstrated in an experiment where Carbowax 20M deactivated beads were dusted with only 4.3 mg of the Silanox. Fig. 4B shows a chromatogram. The observed activity is surprising in view of the extensive literature that appeared in the early seventies for Silanox-modified glass capillary columns²⁸⁻³². These columns were mainly used for the analysis of steroid mixtures and critical activity testing was obviously not performed. Attempts to deactivate fully hydroxylated Cab-O-Sil with HMDS failed. The Cab-O-Sil clumped together during the drying-dehydration process. It was not possible to control the particle size. An attempt was made to use a gas phase Carbowax 20M procedure to deactivate Silanox. The Silanox still exhibited some activity after this treatment and the activity reappeared after washing with methanol.

TABLE II

SAMPLE CAPACITY OF 80-100 MESH GLASS BEADS WITH 1-5 COATINGS OF OV-1

No. of coatings	Sample capacity (ng)
1	130
2	300
3	400
4	600
5	900

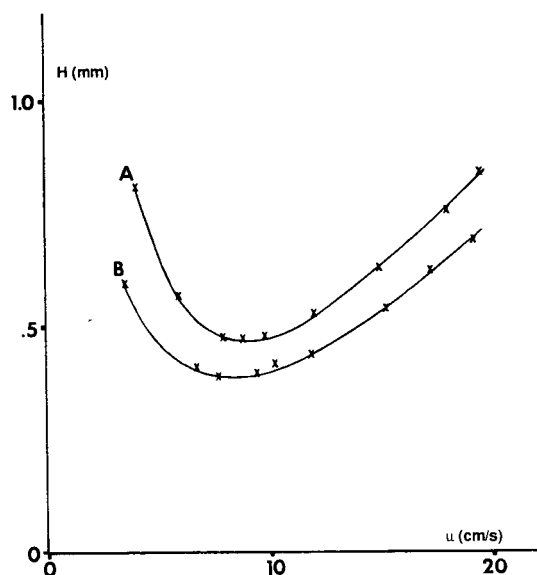


Fig. 6. H vs. u curve for: (a) 3% OV-1 on 80-100 Chromosorb W HP; (B) 1.5% (three Coatings) OV-1 on 80-100 mesh glass beads.

The major advantage of packed columns over OTC is their large sampling capacity. Table II presents the sample capacities for glass beads at different phase loadings. As expected, sample capacity increases significantly as the phase loading is increased. In terms of efficiency, glass beads should be superior to diatomaceous earth type supports of comparable size. H versus u values of glass beads were found to be smaller than those of Chromosorb, as seen in Fig. 6.

CONCLUSION

The deactivation of capillary tubing produced a well deactivated surface, but the deactivation of glass beads has unexpectedly proved to be very difficult. Common deactivation agents cannot render a surface perfectly inert³³. The introduction of new deactivation techniques that could produce more inert surfaces should make this support more popular, especially for preparative column GLC.

ACKNOWLEDGEMENT

We would like to thank J. Rijks and K. Markides for helpful discussions.

REFERENCES

- 1 V. Pretorius and J. C. Davidtz, *High Resolut. Chromatogr. Chromatogr. Commun.*, 2 (1979) 703.
- 2 K. Grob, *Making and Manipulating Capillary Columns for Gas Chromatography*, Huethig, New York (1986), pp. 124-135.
- 3 G. Guiochon, *Chromatogr. Rev.*, 8 (1966) 1.
- 4 J. C. Giddings, *Anal. Chem.*, 34 (1962) 458.
- 5 J. C. Giddings, *Anal. Chem.*, 35 (1963) 439.
- 6 R. A. Dewar and V. E. Maier, *J. Chromatogr.*, 11 (1963) 295.
- 7 R. W. Ohline and R. Jojola, *Anal. Chem.*, 36 (1964) 1681.
- 8 S. Green and W. Bertsch, *High Resolut. Chromatogr. Chromatogr. Commun.*, 10 (1987) 517.
- 9 W. Bertsch, V. Pretorius and K. Lawson, *High Resolut. Chromatogr. Chromatogr. Commun.*, 5 (1982) 568.
- 10 J. A. Rijks, *Ph.D. Dissertation*, Eindhoven University of Technology, Eindhoven, 1973.
- 11 K. Grob, Jr., G. Grob and K. Grob, *J. Chromatogr.*, 156 (1978) 1.
- 12 V. Anigbogu, *Ph.D. Dissertation*, University of Alabama, Tuscaloosa, AL, 1986
- 13 B. W. Wright, P. A. Peaden, M. L. Lee and T. J. Starks, *J. Chromatogr.*, 248 (1982) 17.
- 14 C. L. Woolley, R. C. Kong, B. E. Ritcher and M. L. Lee, *High Resolut. Chromatogr. Chromatogr. Commun.*, 7 (1984) 329.
- 15 B. Xu and N. P. E. Vermeulen, *Proceedings of the 7th International Symposium on Capillary Chromatography, May 11-14, 1986, Gifu, Japan*, Nagoya Press, Gifu, 1986, p. 228.
- 16 M. M. Damiewski and W. A. Aue, *J. Chromatogr.*, 147 (1978) 119.
- 17 G. Rutten, A. van de Ven, J. de Haan, L. van de Ven and J. Rijks, *High Resolut. Chromatogr. Chromatogr. Commun.*, 7 (1984) 607.
- 18 G. Rutten, J. de Haan, L. van de Ven, A. van de Ven, H. Van Cruchten and J. Rijks, *High Resolut. Chromatogr. Chromatogr. Commun.*, 8 (1985) 664.
- 19 N. F. Ives and L. Giuffrida, *J. Assoc. Off. Anal. Chem.*, 53 (1970) 973.
- 20 W. Blum, *High Resolut. Chromatogr. Chromatogr. Commun.*, 8 (1985) 718.
- 21 D. M. Ottestein, *J. Chromatogr. Sci.*, 25 (1987) 536.
- 22 W. A. Aue, C. R. Hastings and S. Kapila, *J. Chromatogr.*, 77 (1973) 299.
- 23 F. I. Onuska and M. E. Comba, *J. Chromatogr.*, 126 (1976) 133.
- 24 R. A. Heckman, C. R. Green and F. W. Best, *Anal. Chem.*, 50 (1978) 2157.
- 25 B. W. Wright, M. L. Lee, S. W. Graham, L. V. Philips and D. M. Hercules, *J. Chromatogr.*, 199 (1980) 355.
- 26 G. A. F. M. Rutten, C. C. E. van Tilburg, C. P. M. Schutjes and J. A. Rijks, *Proceedings of the 4th International Symposium on Capillary Chromatography, May 3-7, 1981, Hindelang, F.R.G.*, Hüthig, New York, 1981, p. 779.
- 27 A. Bengard, L. Blomberg, M. Lymann, S. Claude and R. Tabacchi, *High Resolut. Chromatogr. Chromatogr. Commun.*, 10 (1987) 302.
- 28 A. L. German, D. C. Pfaffenberger, J.-P. Thenot, M. G. Horning and E. C. Horning, *Anal. Chem.*, 45 (1973) 930.
- 29 A. L. German and E. C. Horning, *J. Chromatogr. Sci.*, 11 (1973) 76.
- 30 P. van Hout, J. Szafrank, C. D. Pfaffenberger and E. C. Horning, *J. Chromatogr.*, 99 (1974) 103.
- 31 R. S. Deelder, J. J. M. Ramaekers, J. H. M. van den Berg and M. L. Wetzels, *J. Chromatogr.*, 119 (1976) 99.
- 32 P. G. McKeag and F. W. Hougen, *J. Chromatogr.*, 136 (1977) 308.
- 33 B. J. Tarbet, J. S. Bradshaw, K. E. Markides, M. L. Lee and B. A. Jones, *LC · GC, Mag. Liq. Gas Chromatogr.*, 6 (1988) 232.

CHROM. 21 306

NEW METHOD FOR MEASURING OBSTRUCTIVE FACTORS AND POROSITY USING GAS CHROMATOGRAPHIC INSTRUMENTATION

N. A. KATSANOS* and Ch. VASSILAKOS

Physical Chemistry Laboratory, University of Patras, 26110 Patras (Greece)

SUMMARY

A method for measuring obstructive factors γ and the external porosity ε in solid beds by using the reversed-flow gas chromatographic technique is described. The method does not have any of the disadvantages connected with the carrier gas flow and the instrumental spreading of the chromatographic bands, because the phenomena being studied are taking place inside a diffusion column through which no carrier gas flows. Measurements of elution velocities, height equivalent to a theoretical plate and theoretical diffusion coefficients are not needed, the calculations being based simply on the slopes of three linear plots obtained experimentally. The necessary mathematical equations are derived in detail and applied to determine the γ and ε values with six packing materials, using four different glass cells.

INTRODUCTION

A flow perturbation technique, reversed-flow gas chromatography (RF-GC), was introduced in 1980¹ and used to study the kinetics of various surface-catalysed reactions^{2–12} and for other physico-chemical measurements. The latter include gas diffusion coefficients^{13–15}, relative molar responses, collision diameters and critical volumes of gases¹⁶, Lennard–Jones parameters¹⁷, adsorption equilibrium constants¹⁸, the kinetics of drying of catalysts¹⁹, rate coefficients for evaporation of pure liquids²⁰, activity coefficients in liquid mixtures²¹, kinetic studies of reactivity of marble with sulphur dioxide²², interaction between the components of salt-modified adsorbents²³ and mass transfer and partition coefficients across phase boundaries^{24–27}. Two general reviews on the method have been published^{28,29}, a review on the analytical applications of the method³⁰ and recently a book³¹.

The new technique is based on reversing the direction of flow of the carrier gas from time to time. It uses a conventional gas chromatograph with any kind of detector, accommodating in its oven a so-called sampling cell. This consists of a sampling column and a diffusion column and is connected to the carrier gas inlet and the detector via a four- or six-port valve, as shown schematically in Fig. 1. By switching the valve from one position to the other, the carrier gas is made to flow through the sampling column either from D_2 to D_1 or in the reverse direction. It also fills the

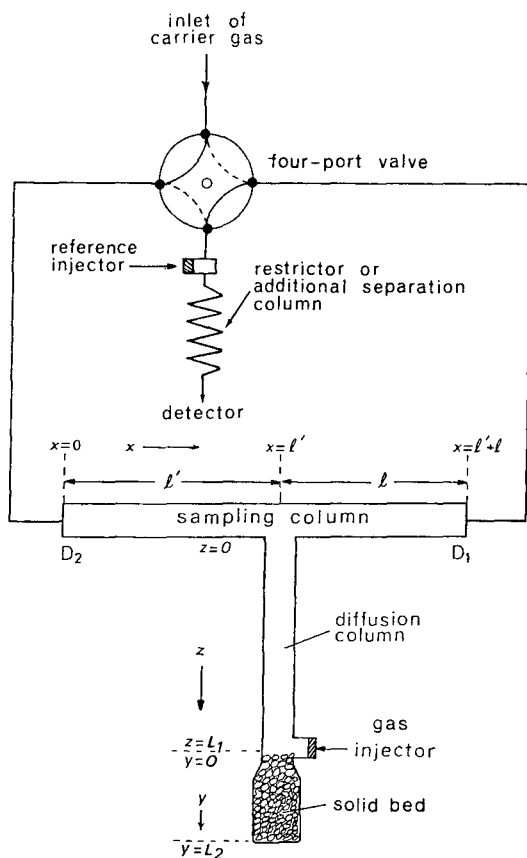


Fig. 1. Gas connections and columns in the RF-GC technique (from ref. 30).

diffusion column L_1 and the vessel L_2 . More details of the experimental set-up used with the RF-GC technique can be found elsewhere^{29,31}.

The flow reversal for a time period t' shorter than the gas hold-up time of a solute in the sections l and l' of the sampling column records the concentration of the solute in the junction $x = l'$, if this solute comes out of column L_1 as the result of its diffusion into the carrier gas. This concentration recording has the form of extra chromatographic peaks (sample peaks) superimposed on the otherwise continuous detector signal. An example is given in Fig. 2. The area under the curve or the height h from the continuous concentration-time curve of these sample peaks, measured as a function of time t_0 (when the flow reversal was made) is the basic mathematical tool giving the physico-chemical quantities mentioned above.

In most instances this is done in a simple, although accurate way, using cheap conventional GC instrumentation, without the need to perform any of the usual gas chromatographic operations and measurements. An example is provided by the accurate measurement of gaseous diffusion coefficients¹³⁻¹⁵, without concern for the main difficulties associated with the traditional GC methods, *e.g.*, the disadvantages

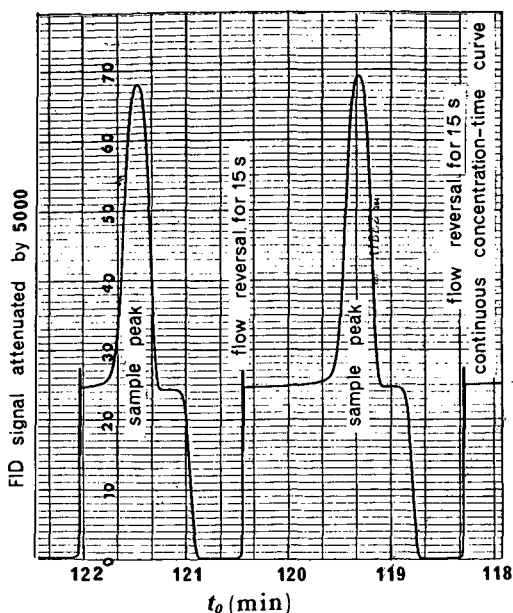


Fig. 2. A reversed-flow chromatogram with two sample peaks recording the concentration of propene in nitrogen at $x = l'$ ($\dot{V} = 0.36 \text{ cm}^3\text{s}^{-1}$, $T = 324.7 \text{ K}$, $p = 1 \text{ atm}$) (from ref. 26).

inherent in operation at low flow-rates and the difficulty of correctly allowing for the instrumental spreading of the chromatographic band outside the column. The same and other problems are met in the determination of the obstructive factor γ , as it is the product γD which is usually determined from HETP measurements in packed columns, employing a range of carrier gas velocities around the optimum value. Then, γ is usually found by assuming a theoretical value for the diffusion coefficient D . An additional disadvantage of this method is that the experimental data are fitted to an height equivalent to a theoretical plate (HETP) equation, assumed to be correct.

The arrested elution method of Knox and McLaren³² bypasses some of the experimental and theoretical difficulties of the standard continuous elution method, but it still relies heavily on the time of passage along the column and the accurate measurement of the outlet elution velocity.

The RF-GC technique does not have any of the disadvantages connected with the carrier gas flow and the instrumental spreading of the chromatographic bands, because the phenomena being studied are taking place inside the diffusion column L_1 and the vessel L_2 , and no carrier gas flows through those vessels. The gas flows only through the column $l' + l$, and is merely used as a means for repeated sampling of the concentrations at the point $x = l'$, *i.e.*, at the exit of the column L_1 . This is done with the help of the narrow and symmetrical sample peaks, mentioned above (*cf.*, Fig. 2), without measuring their elution velocity and without even knowing the carrier gas flow-rate. The experimental data recorded are the height h of the sample peaks in arbitrary units (say cm), and the time t_0 elapsing between the solute injection and the respective flow reversal, the duration of the latter being always the same (say 30 s). If

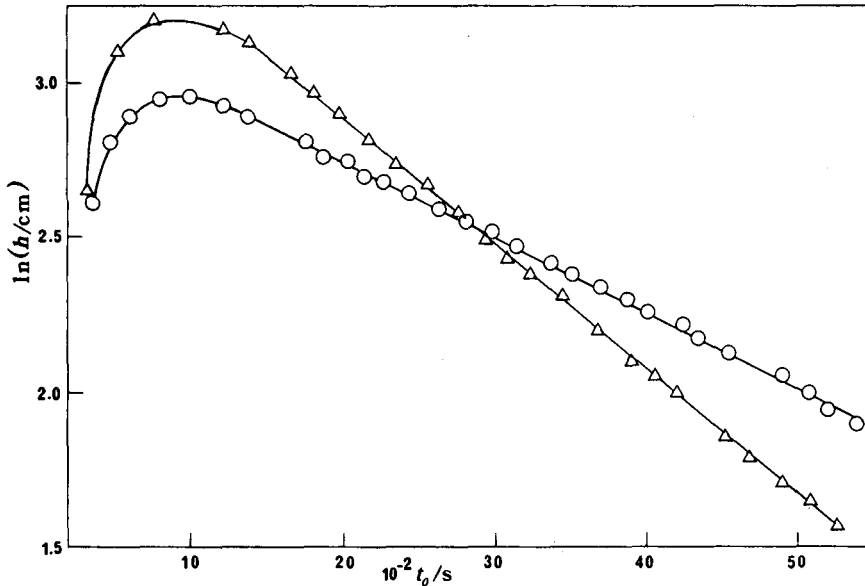


Fig. 3. Diffusion bands obtained at 313.2 K with a thermal conductivity detector, using helium as carrier gas and nitrogen as solute. @, Vessel L_2 empty; Δ , vessel L_2 filled with glass beads of diameter 3 mm.

one plots $\ln h$ against t_0 , a so-called diffusion band is obtained, like those shown in Fig. 3.

An obvious difference between the old elution GC and RF-GC is that in the former longitudinal gaseous diffusion currents are parallel to the chromatographic current and the diffusion coefficients D or γD are extracted from this mixed current by mathematical analysis. In the second method, the diffusion current is from the outset physically separated from the chromatographic current, and this is done by placing the diffusion process perpendicular to the chromatographic process. A diffusion band, rather than an elution band, is now mathematically analysed to yield diffusion coefficients, or other physico-chemical parameters from its distortion, in the same way that a distorted elution chromatographic band permits similar calculations. It must be pointed out that instrumental or other spreading of the sample peaks does not influence the results, as it is the same in all peaks of the same run. If the duration of the flow reversals is changed, the above spreading changes, but the physico-chemical quantity extracted from the diffusion band comes out the same, provided that the same duration is maintained in all flow reversals in the same experiment.

A general chromatographic sampling equation, describing the concentration-time curve of the sample peaks created by the flow reversals, has been derived^{14,28,31} using mass balances, rates of change, etc., and integrating the resulting partial differential equations under given initial and boundary conditions. It was proved^{28,31}, however, that the height h of each sample peak above the ending baseline is proportional to the concentration of the solute at the junction $x = l'$ of the sampling cell and at time t_0 of the flow reversal. This peak height for a linear detector, like the flame ionization detector, is given by the relation

$$h \approx 2c(l', t_0) \quad (1)$$

MATHEMATICAL ANALYSIS

The function for the diffusion band

The mathematical function describing the diffusion band has been derived for some specific cases, namely, (a) when no vessel L_2 exists³¹ and the diffusion column is empty and closed at $z = L_1$ (*cf.*, Fig. 1); (b) when L_2 is absent and column L_1 is filled with a reactive solid²²; (c) when vessel L_2 contains an agitated liquid²⁶; (d) when vessel L_2 is filled with a reactive solid^{27,30}. In all these derivations, various degrees of approximations were adopted in solving the differential equations, according to the precision required and the complexity of the problem. In the present case the function for the diffusion band is sought independently of the gas injected into the cell, with a better precision than before, and for the following arrangements: (1) when both column L_1 and vessel L_2 are empty of any solid or liquid material; (2) when both column L_1 and vessel L_2 are packed with a solid material that does not interact in any way with the injected solute; and (3) when L_1 is empty and only L_2 is packed with the above solid. Case 3 gives a general solution with 1 and 2 as special cases. Therefore, it is treated first.

Following the same mathematical practice as before^{22,26,27,29,31}, the diffusion equation (Fick's second law) is written for the regions z and y (*cf.*, Fig. 1):

$$\partial c_z / \partial t_0 = D_1 \partial^2 c_z / \partial z^2 \quad (2)$$

$$\partial c_y / \partial t_0 = D_2 \partial^2 c_y / \partial y^2 \quad (3)$$

where $c_z = c_z(z, t_0)$ and $c_y = c_y(y, t_0)$ are the gaseous concentrations of the injected solute in the region z (diffusion column) and y (vessel L_2), respectively, D_1 and D_2 being the gaseous diffusion coefficients of the solute in the carrier gas in regions z and y , respectively.

The initial conditions are

$$c_z(z, 0) = \frac{m}{a_G} \delta(z - L_1) \quad (4)$$

$$c_y(y, 0) = 0 \quad (5)$$

where m is the amount of solute injected at $z = L_1$, a_G the cross-sectional area in column z (and also in column $l + l$) and $\delta(z - L_1)$ the Dirac delta function.

There are boundary conditions at three regions: at $z = 0$, at $z = L_1$ or $y = 0$, and at $y = L_2$:

$$c_z(0, t_0) = c(l', t_0) \quad (6)$$

$$D_1(\partial c_z / \partial z)_{z=0} = v c(l', t_0) \quad (7)$$

$$c_z(L_1, t_0) = c_y(0, t_0) \quad (8)$$

$$a_G D_1(\partial c_z / \partial z)_{z=L_1} = a'_G D_2(\partial c_y / \partial y)_{y=0} \quad (9)$$

$$(\partial c_y / \partial y)_{y=L_2} = 0 \quad (10)$$

where $c(l, t_0)$ is the solute concentration at $x = l$ given in eqn. 1, v is the linear velocity of the carrier gas and a'_G the cross-sectional area of vessel L_2 .

The system of partial differential equations 2 and 3 can be solved by using Laplace transformation with respect to t_0 (transform parameter p_0), under the initial conditions 4 and 5, and subject to the boundary conditions 6–10. The first results are two ordinary linear second-order differential equations in $C_z(z, p_0)$ and $C_y(y, p_0)$, the capital letters C_z , C_y denoting the t_0 Laplace transformed functions c_z and c_y , respectively:

$$\frac{d^2 C_z}{dz^2} - q_1^2 C_z = -\frac{m}{a_G D_1} \delta(z - L_1) \quad (11)$$

$$\frac{d^2 C_y}{dy^2} - q_2^2 C_y = 0 \quad (12)$$

where

$$q_1^2 = p_0/D_1 \quad \text{and} \quad q_2^2 = p_0/D_2 \quad (13)$$

Both eqns. 11 and 12 can be integrated either classically or by using z and y Laplace transformation, respectively, with the following results:

$$C_z = C_z(0) \cosh q_1 z + \frac{C'_z(0)}{q_1} \sinh q_1 z - \frac{m}{a_G D_1 q_1} \sinh q_1 (z - L_1) \cdot u(z - L_1) \quad (14)$$

$$C_y = C_y(0) \cosh q_2 y + \frac{C'_y(0)}{q_2} \sinh q_2 y \quad (15)$$

where $C_z(0)$ and $C_y(0)$ are the t_0 transforms of c_z and c_y at $z = 0$ and $y = 0$, respectively, $C'_z(0) = (dC_z/dz)_{z=0}$, $C'_y(0) = (dC_y/dy)_{y=0}$ and $u(z - L_1)$ is the Heaviside unit step function, with values 0 for $z < L_1$ and 1 for $z \geq L_1$.

The values or the relations of $C_z(0)$, $C'_z(0)$, $C_y(0)$ and $C'_y(0)$, which would be constants of integration had eqns. 11 and 12 been solved classically, can be found with the help of the boundary conditions 6–10, all transformed with respect to t_0 , thereby changing c_z , c_y and c to C_z , C_y and C , respectively. Therefore, $C_z(0)$ is replaced by $C(l, p_0)$ according to eqn. 6, and $C'_z(0)$ is substituted by $vC(l, p_0)/D_1$ from eqn. 7, giving

$$C_z = C(l, p_0) \left(\cosh q_1 z + \frac{v}{D_1 q_1} \sinh q_1 z \right) - \frac{m}{a_G D_1 q_1} \sinh q_1 (z - L_1) \cdot u(z - L_1) \quad (16)$$

whereas, by using eqn. 10, eqn. 15 is simplified to

$$C'_y(0) = -C_y(0) q_2 \tanh q_2 L_2 \quad (17)$$

Finally, eqns. 16 and 17 are linked together using the boundary conditions 8 and 9, with the result

$$C(l', p_0) = \frac{m}{a_G D_1 q_1} \left[\sinh q_1 L_1 + \frac{v}{D_1 q_1} \cosh q_1 L_1 + \frac{a'_G D_2 q_2}{a_G D_1 q_1} \tanh q_2 L_2 (\cosh q_1 L_1 + \frac{v}{D_1 q_1} \sinh q_1 L_1) \right]^{-1} \tag{18}$$

This relationship is similar to eqn. 21 in ref. 27, but some of the approximations used to effect its inverse Laplace transformation with respect to p_0 are now different, leading to a more precise result. First, it is assumed as before that $v/D_1 q_1 \gg 1$ for high enough flow velocities and $\sinh q_1 L_1$ is omitted compared with $(v/D_1 q_1) \cosh q_1 L_1$, and also $\cosh q_1 L_1$ compared with $(v/D_1 q_1) \sinh q_1 L_1$. After this approximation, and some rearrangement, eqn. 18 becomes

$$C(l', p_0) = \frac{m}{\dot{V}} \left[D_1 q_1 \sinh q_1 L_1 \left(\frac{\coth q_1 L_1}{D_1 q_1} + \frac{a'_G D_2^2 q_2^2}{a_G D_1^2 q_1^2} \cdot \frac{\tanh q_2 L_2}{D_2 q_2} \right) \right]^{-1} \tag{19}$$

where $\dot{V} = a_G v$ is the volume flow-rate of the carrier gas.

The following approximations are new and adopted for the first time. These refer to the hyperbolic functions $\sinh q_1 L_1$, $\coth q_1 L_1$ and $\tanh q_2 L_2$. The first is simply set equal to the argument $q_1 L_1$, but the latter two functions are subject to the following procedure. First, the inverse Laplace transforms of $\coth q_1 L_1 / D_1 q_1$ and $\tanh q_2 L_2 / D_2 q_2$ are taken³³ in the form of an elliptic function θ_3 or θ_2 , respectively, and then the series representing each θ function is transformed back, term by term, to obtain

$$\frac{\coth q_1 L_1}{D_1 q_1} = \frac{1}{L_1} \left(\frac{1}{p_0} + \frac{2}{p_0 + \beta} + \frac{2}{p_0 + 4\beta} + \frac{2}{p_0 + 9\beta} + \dots \right) \tag{20}$$

$$\frac{\tanh q_2 L_2}{D_2 q_2} = \frac{2}{L_2} \left(\frac{1}{p_0 + \alpha} + \frac{1}{p_0 + 9\alpha} + \frac{1}{p_0 + 25\alpha} + \dots \right) \tag{21}$$

where

$$\beta = \pi^2 D_1 / L_1^2 \tag{22}$$

$$\alpha = \pi^2 D_2 / 4L_2^2 \tag{23}$$

The approximation starts from this point by omitting the time parameter p_0 from a particular term onwards as compared with the diffusion parameters $n\beta$ or $n\alpha$. In series 20, p_0 is omitted compared with $4\beta, 9\beta, \dots$, etc., while in series 21, p_0 is omitted in comparison with $9\alpha, 25\alpha, \dots$, etc.:

$$\frac{\coth q_1 L_1}{D_1 q_1} \approx \frac{1}{L_1} \left[\frac{1}{p_0} + \frac{2}{p_0 + \beta} + \frac{2}{\beta} \left(\frac{1}{4} + \frac{1}{9} + \frac{1}{16} + \dots \right) \right]$$

$$\begin{aligned}
&= \frac{1}{L_1} \left(\frac{1}{p_0} + \frac{2}{p_0 + \beta} + \frac{2}{\beta} \sum_{n=1}^{\infty} \frac{1}{n^2} - \frac{2}{\beta} \right) \\
&= \frac{1}{L_1} \left(\frac{1}{p_0} + \frac{2}{p_0 + \beta} + \frac{2}{\beta} \cdot \frac{\pi^2}{6} - \frac{2}{\beta} \right) \\
&= \frac{1}{L_1} \left(\frac{1}{p_0} + \frac{2}{p_0 + \beta} + \frac{1.29}{\beta} \right) \tag{24}
\end{aligned}$$

$$\begin{aligned}
\frac{\tanh q_2 L_2}{D_2 q_2} &\approx \frac{2}{L_2} \left[\frac{1}{p_0 + \alpha} + \frac{1}{\alpha} \left(\frac{1}{9} + \frac{1}{25} + \dots \right) \right] \\
&= \frac{2}{L_2} \left[\frac{1}{p_0 + \alpha} + \frac{1}{\alpha} \sum_{n=0}^{\infty} \frac{1}{(2n+1)^2} - \frac{1}{\alpha} \right] \\
&= \frac{2}{L_2} \left(\frac{1}{p_0 + \alpha} + \frac{1}{\alpha} \cdot \frac{\pi^2}{8} - \frac{1}{\alpha} \right) \tag{25}
\end{aligned}$$

The sums $\sum_{n=1}^{\infty} n^{-2}$ and $\sum_{n=0}^{\infty} (2n+1)^{-2}$ are evaluated as equal to $\pi^2/6$ and $\pi^2/8$, respectively, by means of the Riemann zeta function.

Approximating in eqn. 19 the function $\sinh q_1 L_1$ by $q_1 L_1$, $(\coth q_1 L_1)/D_1 q_1$ by the far right-hand side of eqn. 24 and $(\tanh q_2 L_2)/D_2 q_2$ by the far right-hand side of eqn. 25, one obtains, after rearrangement, an equation containing only numerical constants and three dimensionless parameters λ , A and R :

$$\begin{aligned}
C(l, p_0) &= \frac{m}{V} (A\lambda + 1)(\lambda + 1) [A(1.29 + 1.87R)\lambda^3 + \\
&\quad + (1.29 + 4.29A + \pi^2 R + 1.87AR)\lambda^2 + (4.29 + A + \pi^2 R)\lambda + 1]^{-1} \tag{26}
\end{aligned}$$

where

$$\lambda = p_0/\beta \tag{27}$$

$$A = \frac{\beta}{\alpha} = \frac{4L_2^2}{L_1^2} \cdot \frac{D_1}{D_2} \tag{28}$$

$$R = \frac{a'_G L_2}{a_G L_1} = \frac{V'_G}{V_G} \tag{29}$$

$V_G = a_G L_1$ and $V'_G = a'_G L_2$ being the gaseous volumes of column L_1 and vessel L_2 , respectively. If the roots of the denominator in eqn. 26 are $-r_1$, $-r_2$ and $-r_3$, this equation is simply written as

$$C(l', p_0) = \frac{m}{\bar{V}A(1.29 + 1.87R)} \cdot \frac{(A\lambda + 1)(\lambda + 1)}{(\lambda + r_1)(\lambda + r_2)(\lambda + r_3)} \quad (30)$$

and its inverse Laplace transformation with respect to p_0 is easily taken after breaking it into three partial fractions. The result is the desired function $c(l', t_0)$ given as sum of three exponential functions of time:

$$c(l', t_0) = N_1 \left[\frac{(Ar_1 - 1)(r_1 - 1)}{(r_1 - r_2)(r_1 - r_3)} \exp(-r_1\beta t_0) + \frac{(Ar_2 - 1)(r_2 - 1)}{(r_2 - r_1)(r_2 - r_3)} \exp(-r_2\beta t_0) + \frac{(Ar_3 - 1)(r_3 - 1)}{(r_3 - r_1)(r_3 - r_2)} \exp(-r_3\beta t_0) \right] \quad (31)$$

where

$$N_1 = \frac{m\beta}{\bar{V}A(1.29 + 1.87R)} \quad (32)$$

If the right-hand side of eqn. 31 is substituted for $c(l', t_0)$ in eqn. 1, the height h of the sample peaks as a function of time is obtained, *i.e.*, the function describing the diffusion band (*cf.*, Fig. 3), when the column L_1 is empty and the vessel L_2 is packed with a solid not interacting with the injected solute. The ratio D_1/D_2 in this case is equal to $D_1/\gamma D_1 = 1/\gamma$, where γ is the obstructive factor in the packed vessel L_2 as defined by Giddings³⁴, and also stressed by Knox and McLaren³² as arising from two effects, namely, the tortuosity of the paths through the medium and the alternating constriction and widening of the paths. Hence the parameter A is given, according to eqn. 28, by

$$(33) \quad A = 4L_2^2/L_1^2\gamma$$

Eqn. 31 also describes the diffusion band when column L_1 and vessel L_2 are both empty of any solid material or both packed with non-sorbing material. In these two cases, however, $D_1/D_2 = 1$ and

$$A = 4L_2^2/L_1^2 \quad (34)$$

Moreover, the parameter R will have the same value irrespective whether L_1 and L_2 are both empty or packed with solid. Therefore, the values of A and R in these cases are characteristic of the cell dimensions, and with their help the roots $-r_1$, $-r_2$ and $-r_3$ of the denominator in eqn. 26 can be found with any desired precision. These roots differ considerably from one another, making the exponential coefficients $-r_1\beta$, $-r_2\beta$ and $-r_3\beta$ of the three functions in eqn. 31 very different, and therefore easily determinable from the experimental diffusion band. For example, the absolutely smallest root, say $-r_3$, describes the diffusion band at long enough times, *i.e.*, after its maximum (*cf.*, Fig. 3), when the other two exponential functions have already decayed to negligibly low values. It corresponds to the last linear part of the band, as the latter is

a semilogarithmic plot. The slope of this part gives $-r_3\beta$ and, using eqn. 22, the diffusion coefficient D_1 of the solute in the carrier gas is easily calculated.

Two limiting cases of eqn. 31 are worth mentioning. The first arises when $L_2 = 0$ and $V'_G = 0$, *i.e.*, when vessel L_2 is absent. Then, $A = 0$ and $R = 0$, the denominator of eqn. 26 reduces to $1.29\lambda^2 + 4.29\lambda + 1$, with roots $-r_1 = -3.073$ and $-r_2 = -0.2522$, and eqn. 30 becomes

$$C(l', p_0) = \frac{m}{\dot{V} \cdot 1.29} \cdot \frac{\lambda + 1}{(\lambda + 3.073)(\lambda + 0.2522)}$$

giving on inversion the first limiting case of eqn. 31:

$$c(l', t_0) = \frac{m\beta}{\dot{V}} [0.2055 \exp(-0.2522\beta t_0) + 0.5697 \exp(-3.073\beta t_0)] \quad (35)$$

Therefore, the slope of the last linear part is $-0.2522\beta = -0.2522\pi^2 D_1/L_1^2 = -\pi^2 D_1/3.97L_1^2$, which coincides with that predicted by eqn. 4-39 in ref. 31. The second limiting case of eqn. 31 is obtained when $L_2 \ll L_1$ and thus A can be set equal to zero. In that case only the volume ratio $R = V'_G/V_G$ determines the roots of the denominator of eqn. 26, which reduces to

$$C(l', p_0) = \frac{m}{\dot{V}} \cdot \frac{\lambda + 1}{(1.29 + \pi^2 R)\lambda^2 + (4.29 + \pi^2 R)\lambda + 1} \quad (36)$$

If these roots are $-r_1$ and $-r_2$, the inverse transform gives, instead of eqn. 31, the expression

$$c(l', t_0) = N'_1 \left[\frac{r_1 - 1}{r_1 - r_2} \cdot \exp(-r_1\beta t_0) + \frac{r_2 - 1}{r_2 - r_1} \cdot \exp(-r_2\beta t_0) \right] \quad (37)$$

where

$$N'_1 = \frac{m\beta}{\dot{V}(1.29 + \pi^2 R)} \quad (38)$$

Determination of the obstructive factor, γ

Two experimental plots at the same temperature, using the same cell, are required for this determination: (1) a diffusion band (*cf.*, Fig. 3) with both the diffusion column L_1 and the vessel L_2 empty of any solid material; and (2) a diffusion band with both L_1 and L_2 packed with the solid material under study, provided that a gaseous solute, that is not sorbed by the solid or does not interact with it in any way, is used in the diffusion experiment. If the slopes of the last linear parts after the maximum of the above bands are $b(\text{empty})$ and $b(\text{packed})$, their ratio gives directly the value of the obstructive factor, without any other measurement or correction:

$$\frac{b(\text{packed})}{b(\text{empty})} = \frac{-r_3\beta(\text{packed})}{-r_3\beta(\text{empty})} = \frac{\pi^2\gamma D_1/L_1^2}{\pi^2 D_1/L_1^2} = \gamma \quad (39)$$

This relationship is based on the fact that the parameters A and R have the same value, given by eqns. 34 and 29, respectively, in both experiments (1) and (2) described above. Therefore, all roots $-r_1$, $-r_2$ and $-r_3$ of eqn. 31 are the same whether the cell is empty or packed. The root $-r_3$ is taken as having the smallest value, thus describing the last linear part of the diffusion band. The value of the diffusion parameter β is given by eqn. 22, with the diffusion coefficient being D_1 when the cell is empty and γD_1 when it is packed with solid.

It must be noted that the simpler functions described by eqns. 37 and 35 lead to exactly the same eqn. 39 with $-r_2$ or -0.2522 , respectively, substituted for $-r_3$. This means that the experiments could be conducted with column L_1 alone, without the presence of vessel L_2 , although in this instance only the obstructive factor, and not the porosity of the solid bed, could be determined, as is shown below.

Determination of the external porosity, ϵ

One more diffusion band, in addition to those described under (1) and (2) above, is required for this determination: (3) a band obtained with the diffusion column L_1 empty and vessel L_2 packed with the solid under study. This is case 3 mentioned at the beginning of the Mathematical Analysis section, as leading to the most general solution, *i.e.*, eqn. 31 with A given by eqn. 33. Experimentally, the slope of the last linear part of the band, b (semi-packed), is again required, together with the lengths L_1 and L_2 , and the gaseous volumes V_G and V'_G of the empty cell. From these lengths and volumes, the values of A (empty) and R (empty) for the empty cell are calculated using eqn. 34 and 29, respectively. The roots of the denominator (in brackets) of eqn. 26 are then found by using the above values of A (empty) and R (empty), as all the others are known numerical constants. The absolutely smallest root, $-r_3$, multiplied by $\beta = \pi^2 D_1 / L_1^2$, gives the slope of the last linear part of the band obtained in experiment 1:

$$b(\text{empty}) = -r_3 \pi^2 D_1 / L_1^2 \tag{40}$$

From this relation, D_1 is accurately calculated, although its value is not required for the present purposes.

The root $-r_{3s}$ for case 3, *i.e.*, for the semi-packed cell cannot be found in the same way as described above, as now the value of A is calculated using eqn. 33, but the value of R (semi-packed) is not known because V'_G (packed) for the packed vessel L_2 is unknown and equal to $\epsilon V'_G$ (empty), where ϵ is the external porosity of the packed solid bed, *i.e.*, its void fraction. Conversely, R (semi-packed) is found using the root $-r_{3s}$, and from that the porosity ϵ . This is accomplished by calculating the unknown root from the experimental slopes and the known $-r_3$:

$$\frac{b(\text{semi-packed})}{b(\text{empty})} = \frac{-r_{3s} \beta}{-r_3 \beta} = \frac{-r_{3s}}{-r_3} \tag{41}$$

where β cancels out, because it has the same value for the empty and the semi-packed cell, pertaining only to L_1 but not to L_2 (*cf.*, eqn. 22). The value of $-r_{3s}$ found by means of eqn. 41 is now substituted for λ in the denominator of eqn. 26, together with A (semi-packed) found by eqn. 33, thus yielding an equation in R (semi-packed), from which its value is calculated:

$$R(\text{semi-packed}) = \frac{1.29Ar_{3s}^3 - (1.29 + 4.29A)r_{3s}^2 + (4.29 + A)r_{3s} - 1}{-1.87Ar_{3s}^3 + (\pi^2 + 1.87A)r_{3s}^2 - \pi^2 r_{3s}} \quad (42)$$

Finally, the porosity ε is calculated from the ratio

$$\varepsilon = \frac{R(\text{semi-packed})}{R(\text{empty})} = \frac{V'_G(\text{packed})}{V'_G(\text{empty})} \quad (43)$$

Instead of using the denominator of eqn. 26 for the above calculations, the less precise but simpler eqn. 36 can be employed. Using the known value of $R(\text{empty})$, the two roots of the denominator can be found, and the absolutely smaller of them, $-r_2$, can be used in eqn. 40 to find D_1 (if required) or in eqn. 41 in place of $-r_3$ to find $-r_{3s}$. This is substituted back for λ in the denominator of eqn. 36 to find

$$R(\text{semi-packed}) = \frac{1.29r_{3s}^2 - 4.29r_{3s} + 1}{\pi^2(r_{3s} - r_{3s}^2)} \quad (44)$$

a relation which could also be obtained directly from eqn. 42 by setting $A = 0$.

To summarize the steps taken for calculating the porosity, the experimental quantities required are the slopes $b(\text{empty})$ and $b(\text{semi-packed})$, the lengths L_1 and L_2 , the volumes $V'_G(\text{empty})$ and V'_G and the value of γ from the previous determination. Using the values of $A(\text{empty}) = 4L_2^2/L_1^2$ and $R(\text{empty}) = V'_G(\text{empty})/V'_G$ in the denominator of eqn. 26 or 36, its roots are found, the absolutely smallest one, $-r_3$ or $-r_2$, respectively, being retained. Then, using eqn. 41, $-r_{3s}$ is calculated. This is used, together with the new value of $A(\text{semi-packed}) = 4L_2^2/L_1^2\gamma$, in eqn. 42 or 44 to find $R(\text{semi-packed})$, and finally the latter and $R(\text{empty})$ are put in eqn. 43 to give ε .

In a previous paper²⁹ a much simpler relation (eqn. 4) was written for calculating ε , but that was only a first approximation, and a limiting case easily obtained from the more sophisticated equations derived here.

EXPERIMENTAL

Two chromatographs were used, equipped with devices for either flame ionization detection (FID) or thermal conductivity detection (TCD). In the first instance the lengths l' and l of the sampling cell (*cf.*, Fig. 1) were each 103 cm and L_1 was 55 cm. In the second instance (with TCD), l' and l were each 72 cm and L_1 was 43.8–55.5 cm. The material of the above columns was either stainless steel or glass of I.D. 3.9–7.6 mm. The I.D. of vessel L_2 was 17.5 mm in all instances. The gas volumes V'_G of columns L_1 ranged from 6.02 to 21.47 cm³, whereas V'_G of empty vessels L_2 was 7.90–14.95 cm³.

The carrier gas was nitrogen (FID) or helium (TCD) at flow-rates ranging from 0.333 to 0.500 cm³s⁻¹. The duration of the carrier gas flow reversal was 15 s.

The pressure drop along $l' + l$ was negligible, and the pressure inside the whole cell was 1 atm.

Six solid beds were used, two with glass beads of diameter 3 and 4 mm, one with pieces of marble of mesh size 120–150, one with γ -alumina of 10–22 mesh, a bed with

Chromosorb P of 60–80 mesh, and a bed with silica gel of 60–80 mesh. The solute gases were methane (FID) or nitrogen (TCD).

Before experiments were carried out with packed or semi-packed cells, the solid materials were conditioned *in situ* by heating them at 503 K for 20 h under a continuous flow of carrier gas. After conditioning, the oven gas was brought to the desired working temperature and kept there for 1 h. Then, 20 cm³ of solute gas were injected, and after 24 h the actual experiments were performed by injecting 2 cm³ of solute (methane or nitrogen), and repeatedly making 15-s flow reversals. The temperature of the thermal conductivity detector was always 373 K. Each experiment lasted about 2 h.

Plots and calculations were made with an RT-Unitron desk-top computer connected to a Star SG10 printer.

RESULTS AND DISCUSSION

Both the obstructive factors γ and the external porosities ε in the various solid beds were determined using four glass cells with different geometric characteristics, and therefore different $A(\text{empty})$ and $R(\text{empty})$ values. Table I gives all particulars of these cells, together with their $A(\text{empty})$ calculated according to eqn. 34, $R(\text{empty})$ found from eqn. 29 and the absolutely smallest root $-r_3$ of the denominator of eqn. 26.

In Table II obstructive factors and porosities measured with TCD are collected, and Table III gives the results of porosity measurements based on experiments with FID.

The calculations of γ values were made using eqn. 39, whereas for ε the procedure summarized in the paragraph following eqn. 44 was followed. The more precise eqns. 26 and 42 were employed in all ε calculations.

The obstructive factor for glass beads of diameter 3 mm was not very different when measured with a single tube L_1 of diameter 7.6 mm (cell No. 1) and with cell No. 2 having two vessels L_1 and L_2 of very different diameters (3.9 and 17.5 mm, respectively). The γ value found by Knox and McLaren³² for glass beads of diameters 0.28 and 0.50 mm was 0.58–0.62, under very different experimental conditions and by a different method. With materials other than glass beads (alumina, Chromosorb P and silica gel) the γ values differed considerably from those of glass beads using identical experimental conditions. This is probably due to the irregularities in the shape of the particles.

As regards the porosity of the glass beads, when it was determined with nitrogen

TABLE I

CHARACTERISTICS OF THE FOUR CELLS USED TO DETERMINE THE OBSTRUCTIVE FACTOR AND THE POROSITY

Cell No.	L_1 (cm)	L_2 (cm)	V_G (cm ³)	V'_G (cm ³)	$10^2 A(\text{empty})$	$R(\text{empty})$	$-r_3$
1 ^a	43.8	—	21.47	—	0	0	-0.2522
2	50.4	4.2	6.02	7.90	2.78	1.312	$-6.102 \cdot 10^{-2}$
3	55.0	6.0	9.59	14.95	4.76	1.559	$-5.313 \cdot 10^{-2}$
4	55.5	4.2	6.63	8.90	2.29	1.342	$-5.996 \cdot 10^{-2}$

^a The I.D. of column L_1 in this cell was 7.6 mm, whereas in cells 2, 3 and 4 it was 3.9 mm.

TABLE II

OBSTRUCTIVE FACTORS γ AND EXTERNAL POROSITY ϵ OF SOLID BEDS, MEASURED WITH A THERMAL CONDUCTIVITY DETECTOR, HELIUM CARRIER GAS AND NITROGEN SOLUTE GAS

Cell No.	Packing material	Particle size	T (K)	γ	ϵ
1	Glass beads	Diameter 3 mm	323.2	0.757	—
2	Glass beads	Diameter 3 mm	323.2	0.862	0.498
4	Glass beads	Diameter 3 mm	313.2	—	0.495
2	γ -Alumina	10–22 mesh	323.2	0.331	0.997
2	Chromosorb P	60–80 mesh	323.2	0.643	0.858
2	Silica gel	60–80 mesh	323.2	0.195	0.863

as solute gas (Table II), it was found 0.498 and 0.495 at two temperatures. These values differ by only 4% from the calculated value of 0.478, cited for beds of spherical particles. The porosity with glass beds of smaller diameter (0.28 and 0.50 mm), found by Knox and McLaren³² by the use of a different chromatographic method, was 0.38. However, with methane as solute gas (Table III), the glass beads of 4 mm diameter show a porosity that decreases with increasing temperature, which may be due to reversible adsorption of methane on the glass surface, the adsorption decreasing as the temperature rises. This is confirmed by the results obtained with γ -alumina (*cf.*, Table III), where ϵ is greater than unity and decreases again with temperature rise. The apparent porosity in this instance is $\epsilon(1 + k)$, k being the partition ratio of methane between the carrier gas and the solid surface. Dividing the apparent porosity in Table III by the calculated value of 0.478 for spherical particles, the value of $1 + k$ is obtained, and from this the k values in the last column in Table III are found. As expected, these values decrease with increasing temperature. This is not the first time that adsorption of methane on alumina has been detected. Non-zero partition ratios for methane have been determined previously¹⁸. These, together with the present results, stress the need to use a gaseous solute that is not sorbed by the solid material or does not interact with it in anyway. The porosity value of 0.997 for alumina, found

TABLE III

EXTERNAL POROSITY ϵ OF SOLID BEDS AND PARTITION RATIO k OF METHANE MEASURED WITH CELL NO. 3, USING A FLAME IONIZATION DETECTOR, NITROGEN CARRIER GAS AND METHANE SOLUTE GAS, AT VARIOUS TEMPERATURES

Packing material	Particle size	T (K)	ϵ	k
Glass beads	Diameter 4 mm	353.2	0.525	—
Glass beads	Diameter 4 mm	383.2	0.466	—
Glass beads	Diameter 4 mm	413.2	0.386	—
Marble pieces	120–150 mesh	322.2–423.2	0.455	—
γ -Alumina	10–22 mesh	353.2	1.321	1.764
γ -Alumina	10–22 mesh	383.2	1.156	1.418
γ -Alumina	10–22 mesh	413.2	0.875	0.831

with nitrogen as solute gas (Table II), is probably due to the contribution of the internal porosity of this material, which is highly porous.

The values of ε found for pieces of marble, Chromosorb P and silica gel appear to be normal.

REFERENCES

- 1 N. A. Katsanos and I. Georgiadou, *J. Chem. Soc., Chem. Commun.*, (1980) 242.
- 2 N. A. Katsanos, *J. Chem. Soc., Faraday Trans. I*, 78 (1982) 1051.
- 3 G. Karaiskakis, N. A. Katsanos, I. Georgiadou and A. Lycourghiotis, *J. Chem. Soc., Faraday Trans. I*, 78 (1982) 2017.
- 4 M. Kotinopoulos, G. Karaiskakis and N. A. Katsanos, *J. Chem. Soc., Faraday Trans. I*, 78 (1982) 3379.
- 5 G. Karaiskakis, N. A. Katsanos and A. Lycourghiotis, *Can. J. Chem.*, 61 (1983) 1853.
- 6 N. A. Katsanos, G. Karaiskakis and A. Niotis, in *Proceedings of the 8th International Congress on Catalysis, West Berlin, 1984, Dechema*, Vol. III, Verlag Chemie, Weinheim, p. 143.
- 7 G. Karaiskakis and N. A. Katsanos, in *Proceedings of the 3rd Mediterranean Congress on Chemical Engineering, Barcelona, Spain, 1984*, p. 68.
- 8 N. A. Katsanos and M. Kotinopoulos, *J. Chem. Soc., Faraday Trans. I*, 81 (1985) 951.
- 9 N. A. Katsanos, G. Karaiskakis and A. Niotis, *J. Catal.*, 94 (1985) 376.
- 10 E. Dalas, N. A. Katsanos and G. Karaiskakis, *J. Chem. Soc., Faraday Trans. I*, 82 (1986) 2897.
- 11 B. V. Ioffe, N. A. Katsanos, L. A. Kokovina, A. N. Marinitsev and B. V. Stolyarov, *Kinet. Katal.*, 28 (1987) 805.
- 12 N. A. Katsanos, *Catal. Today*, 2 (1988) 605.
- 13 N. A. Katsanos and G. Karaiskakis, *J. Chromatogr.*, 237 (1982) 1.
- 14 N. A. Katsanos and G. Karaiskakis, *J. Chromatogr.*, 254 (1983) 15.
- 15 G. Karaiskakis, N. A. Katsanos and A. Niotis, *Chromatographia*, 17 (1983) 310.
- 16 G. Karaiskakis, A. Niotis and N. A. Katsanos, *J. Chromatogr. Sci.*, 22 (1984) 554.
- 17 G. Karaiskakis, *J. Chromatogr. Sci.*, 23 (1985) 360.
- 18 G. Karaiskakis, N. A. Katsanos and A. Niotis, *J. Chromatogr.*, 245 (1982) 21.
- 19 G. Karaiskakis, A. Lycourghiotis and N. A. Katsanos, *Chromatographia*, 15 (1982) 351.
- 20 G. Karaiskakis and N. A. Katsanos, *J. Phys. Chem.*, 88 (1984) 3674.
- 21 N. A. Katsanos, G. Karaiskakis and P. Agathonos, *J. Chromatogr.*, 349 (1986) 369.
- 22 N. A. Katsanos and G. Karaiskakis, *J. Chromatogr.*, 395 (1987) 423.
- 23 A. Niotis, N. A. Katsanos, G. Karaiskakis and M. Kotinopoulos, *Chromatographia*, 23 (1987) 447.
- 24 E. Dalas, G. Karaiskakis, N. A. Katsanos and A. Gounaris, *J. Chromatogr.*, 348 (1985) 339.
- 25 G. Karaiskakis, P. Agathonos, A. Niotis and N. A. Katsanos, *J. Chromatogr.*, 364 (1986) 79.
- 26 N. A. Katsanos and E. Dalas, *J. Phys. Chem.*, 91 (1987) 3103.
- 27 N. A. Katsanos, P. Agathonos and A. Niotis, *J. Phys. Chem.*, 92 (1988) 1645.
- 28 N. A. Katsanos and G. Karaiskakis, *Adv. Chromatogr.*, 24 (1984) 125.
- 29 N. A. Katsanos, *J. Chromatogr.*, 446 (1988) 39.
- 30 N. A. Katsanos and G. Karaiskakis, *Analyst (London)*, 112 (1987) 809.
- 31 N. A. Katsanos, *Flow Perturbation Gas Chromatography*, Marcel Dekker, New York, 1988.
- 32 J. H. Knox and L. McLaren, *Anal. Chem.*, 36 (1964) 1477.
- 33 F. Obberhettinger and L. Badii, *Tables of Laplace Transforms*, Springer, Berlin, 1973.
- 34 J. C. Giddings, *Anal. Chem.*, 35 (1963) 439.

CHROM. 21 297

USE OF GAS CHROMATOGRAPHY FOR A STUDY OF CROWN ETHERS

ALENA KOHOUTOVÁ, EVA SMOLKOVÁ-KEULEMANSOVÁ* and LADISLAV FELTL
Department of Analytical Chemistry, Charles University, Albertov 2030, 128 40 Prague 2 (Czechoslovakia)

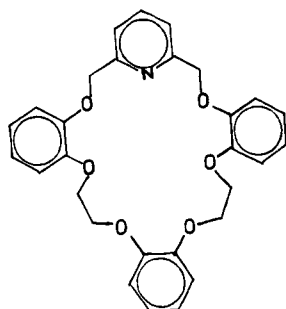
SUMMARY

The inclusion properties of dibenzo-18-crown-6 and the recently described tribenzopyridine-21-crown-7 were studied gas chromatographically. Substances potentially capable of interacting with the cavities of the above crown ethers (alkanes, alcohols, amines) were used as the sorbates. It was found that inclusion compounds are formed with lower members of the homologous series of *n*-alcohols, whereas amines interact through hydrogen bonding.

INTRODUCTION

Studies of various crown ethers have indicated that substitution on the basic skeleton affects their physical properties and inclusion selectivity^{1–6}. Peripheral substituents influence the shape of the space within the crown ether and the overall lipophilicity of the system, which is manifested in an increased selectivity toward guest molecules. The inclusion selectivity is also affected by the basicity of the heteroatoms.

Whereas crown ethers have often been employed in liquid chromatography for selective separations, as components of either the stationary or the mobile phase, their use in gas chromatography has so far been rare. Graphitized carbon black and Carbochrome have been modified by dibenzo-18-crown-6 and dinitrobenzo-18-crown-6 and used as stationary phases for the separation of *n*-alkanes, aromatic hydrocarbons and chlorinated compounds⁷. This modification leads to a lowering in the number of non-specific interaction sites and in the energy of interaction and thus to a shortening of the retention times with preservation of the original elution order. Crown ethers deposited on Firebrick have been used for separation of dichloro-



Tribenzopyridine-21-crown-7

phenols⁸. Capillary columns with crown ethers chemically bonded to polymers have also been employed⁹.

The present paper is concerned with dibenzo-18-crown-6 [DB(18)C-6], whose inclusion properties have been studied and whose selectivity has been utilized in various liquid chromatographic separations¹⁰⁻¹⁶, and with the recently described tribenzopyridine-21-crown-7 [TBP(21)C-7] which has not yet been used in chromatography¹⁷.

EXPERIMENTAL

The measurements were carried out on a Chrom 5 gas chromatograph (Laboratorní přístroje, Prague, Czechoslovakia). The stationary phases were prepared by dissolving the crown ethers in dimethylformamide, depositing them on Gas Chrom Q (60-80 mesh) and evaporating the solvent at 50°C and a decreased pressure (10-20

TABLE I

RETENTION DATA FOR ALKANES, ALCOHOLS AND AMINES ON DB(18)C-6, TBP(21)C-7 AND SOLID SUPPORT

$t_{\text{column}} = 70^\circ\text{C}$, flow-rate 6.7 ml N₂/min.

Compound	B.p. (°C)	Solid support		DB(18)C-6		TBP(21)C-7	
		t'_R (s)	log r_{12}	t'_R (s)	log r_{12}	t'_R (s)	log r_{12}
Pentane	36.1	1.2	0	1.3	0	1.2	0
Hexane	69.0	2.2	0.263	2.2	0.228	2.3	0.283
Heptane	98.0	4.1	0.534	4.2	0.509	4.9	0.611
Octane	125.7	7.4	0.790	8.6	0.821	7.9	0.818
Nonane	150.8	13.2	1.041	12.3	0.976	15.9	1.122
Decane	174.1	19.7	1.215	20.8	1.204	24.0	1.301
Undecane	195.0	36.3	1.481	35.3	1.434	40.8	1.531
Dodecane	216.0	50.1	1.621	51.8	1.600	65.6	1.738
Cyclohexane	81.0	2.9	0.383	2.9	0.348	3.0	0.398
Isoheptane	90.0	3.4	0.452	3.2	0.391	3.6	0.477
Isooctane	99.3	4.3	0.554	4.2	0.509	4.5	0.574
Methanol	64.7	64.3	1.729	378.4	2.464	344.2	2.458
Ethanol	78.5	72.5	1.781	308.9	2.376	527.5	2.643
<i>n</i> -Propanol	97.2	85.1	1.851	237.6	2.262	375.8	2.496
<i>n</i> -Butanol	117.3	109.4	1.960	162.9	2.098	326.7	2.435
<i>n</i> -Pentanol	138.0	120.2	2.001	136.2	2.020	229.8	2.282
<i>n</i> -Hexanol	158.0	139.4	2.065	175.0	2.129	267.2	2.348
<i>n</i> -Heptanol	177.0	175.1	2.164	232.8	2.253	372.8	2.492
<i>n</i> -Octanol	194.0	204.2	2.231	301.5	2.365	420.6	2.545
2-Propanol	82.4	62.3	1.715	65.2	1.700	80.5	1.827
2-Butanol	108.0	83.8	1.844	88.4	1.835	90.6	1.878
2-Pentanol	132.0	102.6	1.932	105.5	1.909	110.4	1.964
Butylamine	77.8	308.5	2.410	841.3	2.811	892.8	2.871
Cyclohexylamine	134.5	384.8	2.506	983.9	2.879	1074.4	2.952
Diethylamine	56.3	299.4	2.397	633.8	2.688	645.9	2.731
Dipropylamine	110.0	345.3	2.459	649.0	2.698	680.6	2.754
Triethylamine	90.0	314.2	2.418	256.9	2.296	289.8	2.383

Tribenzopyridine-21-crown-7

Pa). This material, containing 10% (w/w) of a given crown ether, was packed in glass columns 1.2 m \times 1 mm I.D.

The crown ether DB(18)C-6 was obtained from the Laboratory of Adsorption and Chromatography, Moscow State University, and TBP(21)C-7 was provided by the Institute of Organic Chemistry and Biochemistry, University of Bonn.

The sorbate's involved molecules of various structural types with various inclusion abilities (alkanes, alcohols, amines).

RESULTS AND DISCUSSION

The retention data for the test substances, obtained at 70°C on the stationary phases with DB(18)C-6, TBP(21)C-7 and on the pure support, are summarized in Table I. From the table and Figs. 1 and 2 in which the data are plotted for DB(18)C-6 and the pure support, respectively, non-polar alkanes are very weakly retained on DB(18)C-6 and are eluted in the order of their boiling temperatures irrespective of their structures.

Alcohols are bound much more firmly than alkanes on this phase because of hydrogen bonding. Methanol to butanol exhibit an anomalous behaviour. The significant increase in the retention of methanol can be explained by inclusion of the whole molecule in the DB(18)C-6 cavity. The retention decreases with increasing length of the *n*-alcohol chain, in agreement with decreasing stability of the complexes

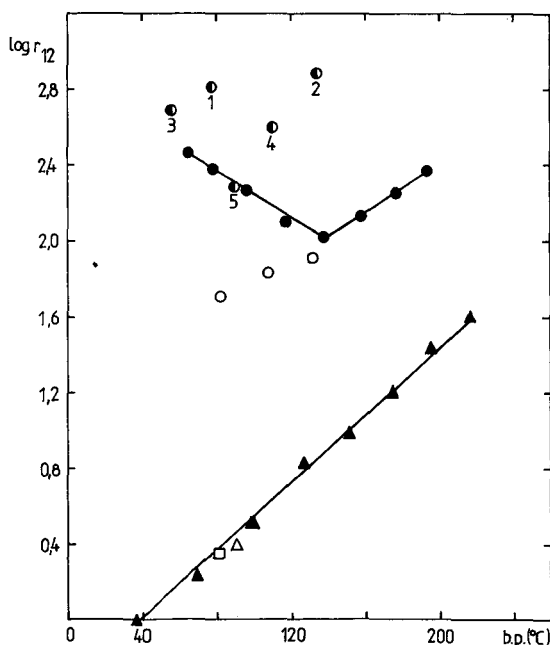


Fig. 1. Relationship between the relative retention and the boiling point on the solid support; $t_c = 70^\circ\text{C}$. \blacktriangle , *n*-alkanes (pentane to dodecane); \square , cyclohexane; \triangle , isoheptane and isooctane; \bullet , *n*-alcohols (methanol to octanol); \circ , 2-propanol, 2-butanol and 2-pentanol; \odot , amines (1 = butylamine, 2 = cyclohexylamine, 3 = diethylamine, 4 = dipropylamine, 5 = triethylamine).

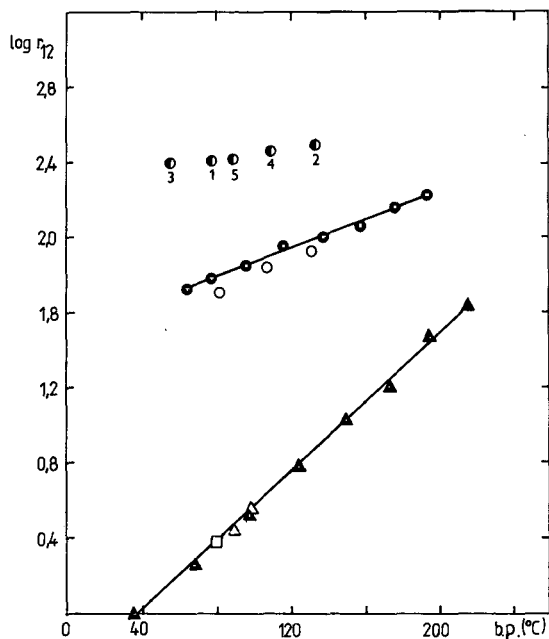


Fig. 2. Relationship between the relative retention and the boiling point on DB(18)C-6. Details as in Fig. 1.

between DB(18)C-6 and *n*-alcohols. The retention times of higher alcohols (*n*-pentanol to *n*-octanol) increase with increasing boiling temperatures. These alcohols form no inclusion compounds with DB(18)C-6, apparently due to the increasing non-polar character of the molecule. The selectivity of the crown ether for the lower members of the *n*-alcohol homologous series is also connected with the fact that DB(18)C-6 is capable of forming cage-shaped inclusion structures but cannot form channel structures as do some other host molecules. Branching of the alcohol chain is a steric hindrance for the formation of inclusion compounds and thus branched alcohols are eluted in the order of the boiling temperatures.

The amines studied in this paper (butyl-, cyclohexyl-, diethyl-, dipropyl- and triethylamine) are apparently not included and their retention is caused by hydrogen bonding. Primary amines, forming hydrogen bonds between the NH₂ group and the oxygen atoms of the crown ether, are retained most strongly. Complexes are probably formed, in which a single amine molecule is hydrogen bonded at each side of the crown ether ring. Secondary amines that can form only a weak hydrogen bond between the NH group and the crown ether oxygen atoms are eluted more rapidly. Triethylamine, incapable of hydrogen bonding, is eluted most rapidly and its retention time is identical with that observed on the pure support.

The experimental results obtained for TBP(21)C-7 (see Table I and Fig 3) are analogous to those for DB(18)C-6. Alkanes and branched alcohols are eluted in the order of the boiling temperatures.

The retention times of *n*-alcohols are, on the whole, higher than those obtained on DB(18)C-6, owing to hydrogen bonding between the pyridine nitrogen and the

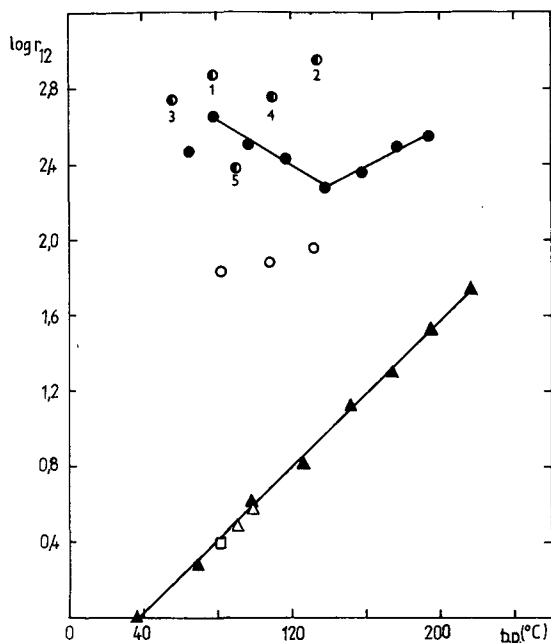


Fig. 3. Relationship between the relative retention and the boiling point on TBP(21)C-7. Details as in Fig. 1.

hydrogen of the hydroxyl group. Compared to the measurement with DB(18)C-6, ethanol is retained most strongly, as the TBP(21)C-7 cavity is larger. This finding is in agreement with the results for the formation of inclusion complexes in solution, when during crystallization from a methanol + ethanol mixture, ethanol is preferentially bound¹⁸. Methanol, propanol and butanol also exhibit significantly higher retention times than those corresponding to their boiling temperatures. The retention times of higher members of the homologous series again increase as a function of their boiling temperatures.

The elution order of the amines is again the same as on the phase with DB(18)C-6. Triethylamine is retained least, followed by secondary amines and the longest retention times are exhibited by primary amines. The retention times on the two phases are not very different. This confirms the assumption that the amines are not included in the crown ether cavities, as the increase in the cavity diameter does not lead to pronounced changes in the retention times.

The results obtained indicate that gas chromatographic measurements can significantly contribute to the evaluation of the properties of newly prepared crown ethers and to characterization of their interaction with various organic substances.

REFERENCES

- 1 C. J. Pedersen, *J. Am. Chem. Soc.*, 89 (1967) 2495.
- 2 C. J. Pedersen, *J. Am. Chem. Soc.*, 89 (1967) 7017.
- 3 C. J. Pedersen, *J. Am. Chem. Soc.*, 92 (1970) 391.
- 4 C. J. Pedersen, *Fed. Proc., Fed. Am. Soc. Exp. Biol.*, 27 (1968) 1305.

- 5 C. J. Pedersen, *J. Am. Chem. Soc.*, 92 (1970) 386.
- 6 C. J. Pedersen and H. K. Frensdorf, *Angew. Chem.*, 84 (1972) 16.
- 7 E. V. Zagorevskaya and N. V. Kovaleva, *J. Chromatogr.*, 365 (1986) 7.
- 8 A. Ono, *Analyst (London)*, 108 (1983) 1265.
- 9 D. D. Fine, H. L. Gerhart and H. A. Mottola, *Talanta*, 32 (1985) 751.
- 10 R. B. King and P. R. Heckley, *J. Am. Chem. Soc.*, 96 (1974) 3118.
- 11 W. Smulek and W. Lada, *Radiochem. Radioanal. Lett.*, 30 (1977) 199.
- 12 W. Smulek and W. Lada, *Radiochem. Radioanal. Lett.*, 34 (1978) 41.
- 13 L. A. Fernando, M. L. Miles and L. H. Bowen, *Anal. Chem.*, 52 (1980) 1115.
- 14 E. Blasius, K.-P. Janzen, W. Klein, H. Klotz, T. Nguyen-Tien, R. Pfeiffer, G. Scholten, H. Simon, J. Stockemer and A. Toussaint, *J. Chromatogr.*, 201 (198) 147.
- 15 E. Blasius, W. Adrian, K.-P. Janzen and G. Klautke, *J. Chromatogr.*, 96 (1974) 89.
- 16 M. Lauth and P. Gramain, *J. Liq. Chromatogr.*, 8 (1985) 2403.
- 17 E. Weber, F. Vögtle, H. P. Josel, G. R. Newkome and W. E. Puckett, *Chem. Ber.*, 116 (1983) 1906.
- 18 E. Weber and F. Vögtle, *Angew. Chem.*, 92 (1980) 1067.

CHROM. 21 291

ISOMERISATION OF PROPYNE TO PROPADIENE STUDIES BY GAS CHROMATOGRAPHY

P. M. LYNE*^a and C. S. G. PHILLIPS

Inorganic Chemistry Laboratory, Oxford University, Oxford (U.K.)

SUMMARY

The use of displacement chromatography with a moving heater has enabled propadiene to be formed from the more thermodynamically favoured propyne in quantities beyond the equilibrium proportions. The heater acts as both a displacement device and moving reactor zone, while the stationary phase acts as both a separation medium and catalyst. Elution and microcatalytic reactor studies have demonstrated that carefully activated alumina provided the required properties. A conversion of 70% has been achieved in total product.

A combination of vacancy and pseudo sample vacancy gas chromatography has been shown to provide an effective means of following the kinetics of the above isomerisation. The route to propyne from its constituent elements via the high-temperature phase of magnesium carbide has also been investigated.

INTRODUCTION

The use of displacement chromatography for preparative scale separations and reactions with a moving heater has been described^{1,2} and referred to as heater displacement chromatography. Its use to force a reaction beyond the point of thermodynamic equilibrium has been demonstrated in the case of alkane isomerisation¹. This paper describes a similar use of the technique to cause isomerisation of propyne to propadiene in proportions substantially beyond those at equilibrium. The principle of the method involves the use of a gas chromatographic (GC) column containing an adsorbent which at lower temperatures (in this case around room temperature) separates the two isomers with the desired isomer (propadiene) moving ahead. The two isomers are then driven through the column by means of a moving heater (external to the column) in the region of which the column temperature is sufficiently high (in this case around 275°C) for the column packing to act as a catalyst for the isomerisation process. The desired isomer then moves ahead of the undesired (propyne) isomer, which comes thus continuously into contact with the hotter catalytic zone of the

^a Present address: B.P. Research International, Sunbury Research Centre, Chertsey Road, Sunbury-on-Thames, Middlesex TW16 7 LN, U.K.

column and is reisolated. In this way conversion to the less strongly adsorbed isomer (propadiene) is driven beyond the equilibrium point of the isomerisation reaction.

Success in our particular case required, therefore, a column material which allowed the propadiene to move ahead (especially at lower temperatures) while producing a clean and rapid isomerisation at the higher temperatures generated in the heater zone. Alumina, activated in a particular manner, has been found to satisfy both these requirements, although the temperature of the heater had to be kept below certain limits to prevent more complex reactions becoming significant, or propyne being eluted out of the reaction zone.

ISOMERISATION

The retention properties of activated alumina were first studied using it as a column material in a straightforward elution GC system, where it was found that over the temperature range of interest (20–200°C) propadiene was always eluted well ahead of propyne. At room temperature (20°C) the ratio of retention times was 10.1 while at 200° this fell to 2.5 corresponding to heats of adsorption of 31.5 and 40.2 kJ mol⁻¹ for propadiene and propyne respectively. Furthermore the retention of propyne was such that it would not elute away from the heater zone under the expected conditions of the heater displacement experiment unless the column temperature ahead of the heater was grossly high. However there was a risk that it would elute out of the heater itself and for this reason (see below) the nitrogen flow-rate in the heater displacement experiments was kept very low.

The catalytic properties were studied at higher temperatures by means of a microreactor combination. This consisted of a 10 cm × 3 mm I.D. reactor containing 0.745 g of activated alumina, the temperature of which could be varied, followed by a 5-m analytical column of 10% β,β' -oxydipropionitrile on Chromosorb P at 22.5°C. Dry, oxygen-free³, nitrogen at a flow-rate of 30 ml min⁻¹ was used as carrier gas with flame ionisation detection. It was found that the same (equilibrium) mixture (20% propadiene) was obtained by either injection of propyne or propadiene at a reactor temperature of 280°C. Moreover there was no measurable loss of material to the column. At lower temperatures the reaction was incomplete, but still sufficiently rapid to expect heater displacement to be effective at 250°C. Above 325°C a number of lower-molecular-weight products began to appear in small quantities, presumably as a result of cracking reactions, so that column temperatures in excess of 325°C were clearly to be avoided in the heater displacement experiments.

Evidence of an irreversible effect of high temperatures on the alumina suggested that further investigation was required. For example, alumina, which had been heated to 386°C, held there for 90 min and then cooled to 312°C, showed markedly different properties with respect to the isomerisation. Only 0.24% propyne was recovered from samples of either propyne or propadiene, while unidentified and highly asymmetric peaks representing 12–41% recovery were also obtained. Treatment of this alumina with water (100 μ l of liquid, then removed) caused a regeneration of the catalyst with a resulting propyne–propadiene recovery in excess of 90% and in a ratio of 80:20 (the equilibrium proportions). At 367°C, under a carrier gas which had been bubbled through water at room temperature, equilibrium proportions of propyne

and propadiene were detected, but the total was only 72% of that injected for propyne, and 77% for propadiene. It thus appeared that preconditioning with water vapour was essential, and that even so above say 320°C significant quantities of material began to be lost to the column at the same time as the isomerisation was taking place.

The kinetics of the isomerisation reaction were studied between 167 and 200°C using the same microreactor column as had been used in the above studies, and following in particular the isomerisation of propadiene to propyne. However syringe injection was not felt to be sufficiently reliable here. A system was devised which made use of a continuous feed of propadiene with a loop in the system for regular monitoring of the feed level by vacancy chromatography (injection of pure carrier gas into the feed prior to detection), and for the reaction measurements used a modification of sample vacancy chromatography (in which the same loop volume of reaction product could be injected into the feed sample prior to detection)⁴. The feed of propadiene was obtained by passing the nitrogen carrier gas through a 1-l flask containing 1 ml of propadiene thoroughly diluted in nitrogen. Fig. 1 provides a schematic of the experimental set-up: the six-port valve marked as valve 1 selects either vacancy or sample vacancy mode, and valve 2 allows injection of either a nitrogen vacancy or reaction product into the continuous propadiene feed stream. Fig. 2 indicates the relevant valve positions for these operations. The results from the vacancy chromatography

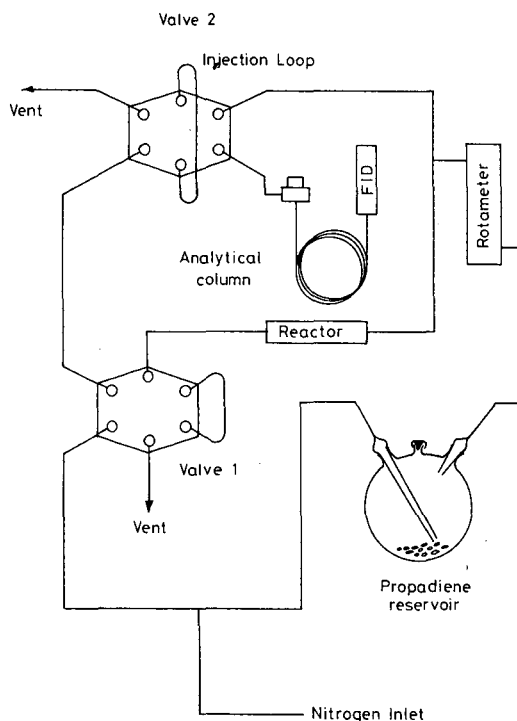


Fig. 1. Apparatus for the determination of the kinetics of the propyne-propadiene isomerisation. FID = Flame ionization detector.

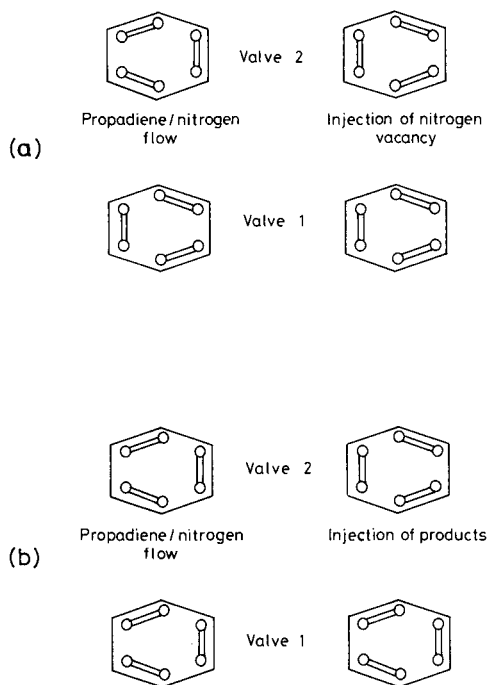


Fig. 2. Valve sequences for (a) vacancy chromatography and (b) sample vacancy chromatography.

showed the expected exponential decay of propadiene concentration in the feed vessel. This decay profile was interpolated to provide the propadiene concentrations at the point of sample vacancy injection. Use of the same loop for both obviated any need for cross-calibration of the two techniques. The isomerisation was found to follow first order kinetics, the velocity constants for propyne to propadiene being 2.05, 2.93 and 3.72 and for propadiene to propyne 7.70, 11.0 and $14.0 \cdot 10^{-2} \text{ s}^{-1}$ at 167.0, 184.5 and 200.0°C respectively.

EXPERIMENTAL

The heater displacement gas chromatograph has been described elsewhere^{1,2}. The column was packed with 67.5 g of alumina (80–100 mesh chromatographic grade, Phase Separations, Queensferry, U.K.). The column dimensions were 1 m \times 1 cm I.D. The alumina was conditioned at 300°C (using a heater temperature of 350°C, see Fig. 3, a heater speed of 1.67 cm min⁻¹, a nitrogen flow-rate of 15 ml min⁻¹ and three descents of the heater).

HEATER DISPLACEMENT

It was clearly necessary to know the actual column temperatures within the heater and this was done by inserting a NiCr–NiAl thermocouple in the column under normal operating conditions. The results obtained are given in Fig. 3, from

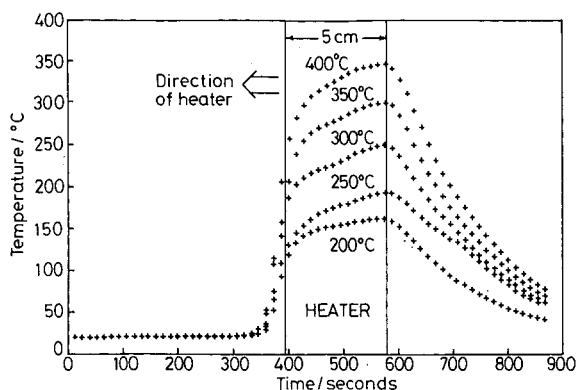


Fig. 3. Temperature profiles experienced by the stationary phase as the heater descends at 1.67 cm min^{-1} at various temperatures.

which it will be seen that in order, for example, to achieve a catalyst temperature around 300°C a heater temperature of *ca.* 350°C is required. The temperature of the column ahead of the moving heater varied between 20 and 25°C depending on the ambient room temperature. For the isomerisation process a low flow-rate (2.1 ml min^{-1}) was used in order to keep as much propyne in the catalytic zone as was reasonably possible, and the heater descent rate was kept at 1.67 cm min^{-1} . Samples of propyne (10 ml) were first injected into the column with the heater poised some 10 cm above the adsorbent but preheated to its operating temperature. The run was then started and the heater moved down the column causing both isomerisation and displacement. The total effluent was trapped at liquid nitrogen temperature in a stainless-steel vessel equipped with isolating taps, and analysed off-line by means of a 10% β,β' -oxydipropionitrile on a $5 \text{ m} \times 3 \text{ mm}$ I.D. Chromosorb P column at 22.5°C . The results for different heater temperatures are given in Table I.

It will be seen that satisfactory conversions are obtained with heater temperatures of 280 or 300°C . At lower temperatures, lower conversions are achieved presumably because the isomerisation reaction is then too slow. At higher temperatures propyne is presumably insufficiently well retained in the catalytic zone. Repeated use of the column at the higher temperatures can also lead to a deterioration of performance (as described above) and loss of material to the column, some of which could be

TABLE I

HEATER DISPLACEMENT RESULTS

Temperature of moving heater ($^\circ\text{C}$)	Propadiene (%)	Propyne (%)
350	3.5	96.5
300	69.2	30.8
280	71.0	29.0
260	56.3	43.7

displaced with water and shown to consist of material of high molecular weight. However this water-treated column could no longer be made to function efficiently as an isomerising medium. If the column was packed with fresh activated alumina which had been treated with water, little isomerisation could be achieved until the bulk of this had been removed by conditioning. This was due to displacement of the propyne out of the hot reaction zone by water. Clearly the quantity of water present on the alumina surface is very critical.

PROPYNE SYNTHESIS VIA MAGNESIUM CARBIDE

A synthetic route from carbon to propyne, and subsequently to propadiene using the above isomerisation reaction, was investigated to enable isotopic doping of the hydrocarbons. This was achieved by the formation of calcium carbide (CaC_2) from calcium and carbon by high temperature fusion⁵. Reactants were maintained at 1250°C in a stainless-steel boat under 825 Torr dry oxygen-free argon for 10–30 min, followed by 1150°C under 3–6 Torr argon for 15 min to vaporize residual calcium. The CaC_2 was subsequently reacted with anhydrous MgCl_2 (in the presence of a suitable fluxing agent, such as NaCl) to yield a high-temperature phase of magnesium carbide (Mg_2C_3)⁶, which incorporates C_3 chains and releases primarily propyne on hydrolysis. Experiments showed that the optimum reaction conditions were 625°C under a flow of dry oxygen-free argon for about 100 min. In both of the above preparations extreme care was needed to avoid any atmospheric hydrolysis of either reactants or products. The Mg_2C_3 was then hydrolysed (or deuterolysed) under a flow of nitrogen to introduce the hydrolysate on to the head of a preconditioned alumina-packed heater displacement gas chromatography column for isomerisation. In addition to propyne, some propadiene is formed as a side product of hydrolysis of Mg_2C_3 , and some acetylene from hydrolysis of residual CaC_2 and the low temperature phase of magnesium carbide (MgC_2), formed as an impurity.

REFERENCES

- 2 C. M. A. Badger, J. A. Harris, K. F. Scott, M. J. Walker and C. S. G. Phillips, *J. Chromatogr.*, 126 (1976) 11.
- 2 J. P. Horrocks, J. A. Harris, C. S. G. Phillips and K. F. Scott, *J. Chromatogr.*, 197 (1980) 109.
- 3 C. R. McIlwrick and C. S. G. Phillips, *J. Phys. E*, 6 (1973) 1208.
- 4 P. M. Lyne, *D. Phil. Thesis*, Oxford University, Oxford, 1986.
- 5 *Gmelin, Handbuch der Anorganischen Chemie, Ca(B)*, 1950, p. 824.
- 6 V. A. Schneider and F. F. Cordes, *Z. Anorg. Chem.*, 278 (1955) 94.

CHROM. 21 290

SAMPLE PREPARATION BY MEANS OF A SUPPORTED LIQUID MEMBRANE FOR THE DETERMINATION OF CHLOROPHENOXYALKANOIC ACIDS

GÖRAN NILVÉ*, GUDJON AUDUNSSON^a and JAN ÅKE JÖNSSON

Department of Analytical Chemistry, University of Lund, P.O. Box 124, S-221 00 Lund (Sweden)

SUMMARY

A sample preparation system for the determination of chlorophenoxyalkanoic acids by liquid chromatography was investigated. The technique permits enrichment and sample clean-up in a flow system, and is used on-line with the liquid chromatograph. The acidified sample comes in contact with a liquid membrane into which the analytes are extracted. On the other side of the membrane, acidic constituents may be trapped by dissociation in an appropriate buffer solution. The accumulated fraction is transported to the injection loop of the liquid chromatograph. The technique has been used for determinations of chlorophenoxyalkanoic acids in solutions containing humic substances.

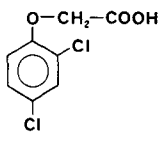
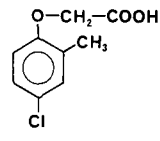
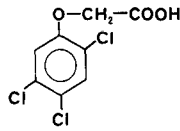
INTRODUCTION

Chlorophenoxyalkanoic acids (CPAs) are widely used for weed control in crops. These acids show auxin-like activity¹, as they produce uncontrolled proliferation of portions of the plant, resulting in death because it can no longer feed itself. In Table I some common CPAs are listed. In Sweden, MCPA is the most commonly used of these acids; its consumption in Sweden in 1987 was 1540 tons/year and that of 2,4-D was 60 tons/year. The use of 2,4,5-T has been prohibited in Sweden since 1977, as it is often contaminated with traces of 2,3,7,8-tetrachlorodibenzo-*p*-dioxin. Because of the extensive use of CPAs, contamination of rivers and lakes can be expected and has actually been confirmed².

CPAs are commonly determined by gas chromatography (GC) after derivatization to more volatile compounds^{3–5}. Diazomethane, in spite of its toxicity and safety hazards, is often used as a derivatization agent^{2,6–9}. Pentafluorobenzyl bromide has been used as a reagent to obtain increased sensitivity in GC with electron-capture detection^{10–13}. 2-Chloroethanol^{14,15} and (2-cyanoethyl)dimethyl(diethylamino)silane¹⁶ are other reagents that have been applied. The need for derivatization, which is time consuming and may introduce errors in the analytical method, has made liquid chromatography (LC) an attractive alternative for the determination of these compounds^{17–20}.

^a Present address: Icelandic Fisheries Laboratories R.F., P.O. Box 1390, Skulagata 4, 121 Reykjavik, Iceland.

TABLE I
CHLOROPHENOXYALKANOIC ACIDS (CPAs) USED IN THIS WORK

<i>Compound</i>	<i>Abbreviation</i>	<i>Structure</i>
2,4-Dichlorophenoxyacetic acid	2,4-D	
2-Methyl-4-chlorophenoxyacetic acid	MCPA	
2,4,5-Trichlorophenoxyacetic acid	2,4,5-T	

LC detection is usually carried out by means of UV-absorbance measurements^{19,21-23}, but LC-mass spectrometry has been used in some instances to increase the selectivity of detection²⁴⁻²⁶. In the analysis of environmental samples for pollutants, sample enrichment and clean-up are almost always necessary. With CPAs, the most frequently used sample preparation technique is liquid-liquid extraction^{3,4,6,8,9,12-14}. After a first extraction, back-extraction followed by another extraction and/or clean-up of the derivatized acids on columns are often performed to obtain low background signals²⁷. Solid-phase extraction has also been used for sample preparation^{2,7,16,19,22,28,29}. Liquid-liquid extraction and column techniques have been compared for the analysis of soil³⁰ and water³¹.

The liquid membrane technique developed by Audunsson³² has been shown to have excellent properties for the concentration and clean-up of amines in urine³³. The application to acidic compounds is a matter of choosing the appropriate pH in the donor and acceptor phases. The membrane system was originally coupled directly to a gas chromatograph, but the replacement of the gas chromatograph by a liquid chromatograph is straightforward, as shown in this work. The system performs extraction and back-extraction in a single step, with simultaneous sample clean-up of the concentrated analytes. The sample preparation is performed in a closed system, which minimizes the risk of losses and contamination due to sample handling. For the analysis of natural waters there is also a possibility of on-site enrichment, which makes transportation of large volumes of water unnecessary. The process can also be easily automated, which is valuable if a large number of samples are to be analysed and, additionally, increases the quantitative precision.

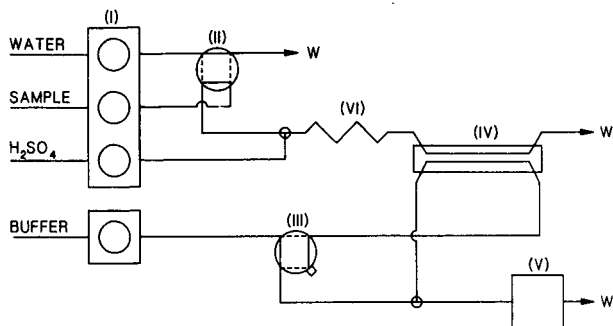


Fig. 1. Schematic diagram of the experimental set-up.

EXPERIMENTAL

Equipment

A schematic diagram of the experimental setup is shown in Fig. 1. Two peristaltic pumps (I) (Minipuls 2; Gilson Medical Electronics, Villiers-le-Bel, France) with standard PVC manifold pump tubing (Elkay Products, Shrewsbury, MA, U.S.A.) were used to control the donor and acceptor flow-rates independently. The various parts of the flow manifold were connected with 0.5 and 0.3 mm. I.D. Teflon tubing and Altex screw fittings. The confluences, where the channels meet at an angle of 60°, were made of PTFE. Both the sample inlet valve (II) and the switching valve (III) were pneumatically actuated four-way Kel-F slider valves [Cheminert; Laboratory Data Control (U.K.)]. The membrane separator (IV) was machined from blocks of PTFE by cutting two U-shaped grooves on the opposite faces of the blocks. The grooves were 0.25 mm deep, 1.5 mm wide and 150 mm long, giving a geometric volume of each groove of *ca.* 56 μl . The membrane was clamped tightly and evenly between the surfaces of the blocks by ten screws. To make the membrane separator more rigid, the PTFE blocks were backed up with aluminium blocks (6 mm thick) in which the threads for clamping screws were machined. The liquid membrane support was Fluoropore FG (average pore size 0.2 μm , total thickness 175 μm , of which 115 μm is polyethylene backing, porosity 0.70; Millipore, Bedford, MA, U.S.A.). The liquid membrane was prepared by immersing the membrane in the chosen solvent for about 15 min. After installation in the separator, excess solvent on the membrane surface was removed by pressing water through both channels.

Operation of the system

The sample is introduced by valve II. The sample volume is determined by time and flow-rate. The sample is acidified by mixing with acid in the mixing coil (VI) (100 cm \times 0.5 mm I.D.). Non-ionized species in the donor phase will be extracted into the liquid membrane. After traversing the membrane, acidic constituents may be trapped in the acceptor by dissociation. During sample introduction, valve III is in its bypass position, *i.e.*, the acceptor phase in the membrane separator is stagnant. After the sample has passed the separator on the donor side, valve III is switched and the accumulated analyte is transferred to the detector (V). The CPA peaks were mon-

itored at 285 nm by a Spectra-Physics Model 770 spectrophotometer (Schoeffel Instrument U.S.A.) equipped with a Servogor 210 recorder (Goerz Electro, Austria).

The chromatographic separations were performed with a Spectra-Physics SP 8000 liquid chromatograph equipped with a Valco loop injector (100 μ l), and a 150 \times 4.6 mm I.D. ODS-2 C₁₈ reversed-phase column (Phase Separations, Queensferry, U.K.). Spectrophotometric detection was carried out with an LDC Spectromonitor III variable-wavelength UV detector (LDC, Riviera Beach, FL, U.S.A.).

Chemicals

The organic solvents used were undecane (Merck) (pro analysi), 1-decanol (Riedel-de Haën) (pro analysi), 1-dodecanol (Fluka) (puriss), 1-tetradecanol (Merck) (purum), and di-*n*-hexyl ether (Sigma). The analytes were 2,4-D (Janssen Chimica) (pract.), MCPA (Fluka) (purum) and 2,4,5-T (Janssen Chimica) (purum) (see Table I). Humic acid (Fluka) (pract.) was used as an interferent. All other chemicals were purchased from Merck and were of analytical-reagent grade. Water was purified with a Milli-Q/RO-4 unit (Millipore, Bedford, MA, U.S.A.).

RESULTS AND DISCUSSION

The aim of this work was to apply the liquid membrane configuration for the sample preparation of CPAs in water containing humic substances with subsequent analysis by LC. The parameters studied were the choice of solvent in the liquid membrane, interferences from humic substances and the direct coupling of the sample preparation system with the LC system.

Unless stated otherwise, the sample flow-rate was 0.25 ml/min and the acid flow-rate was 0.25 ml/min, resulting in a total donor flow-rate of 0.50 ml/min, 0.1 *M* in sulphuric acid. Further, the acceptor flow-rate was 0.25 ml/min, 0.1 *M* in phosphate buffer (pH \approx 7), and the analyte used as a model substance was 2,4-D in water.

Choice of membrane liquid

To evaluate the membrane performance, the enrichment factor is plotted as a function of sample volume introduced. The enrichment factor is expressed as $C_p^{\max}/C_{o,s}$, where C_p^{\max} is the maximum concentration in the peak measured by the detector and $C_{o,s}$ is the concentration of analyte in the introduced sample. The enrichment factor per unit sample volume, $C_p^{\max}/(C_{o,s}V_s)$, is the slope of the resulting regression line.

The desired properties of the solvent in the liquid membrane have been discussed elsewhere^{32,34}. *n*-Undecane was shown to be suitable for the extraction and sample clean-up of amines in urine samples³³. However, *n*-undecane could not be used for the CPAs as the distribution ratio between the donor phase and the *n*-undecane in the liquid membrane was too small to give a sufficient transport rate of the analytes, leading to an enrichment factor per unit sample volume of only 0.4 ml⁻¹. A marked improvement was obtained with a more polar liquid in the membrane. For 1-decanol, the enrichment factor per unit sample volume was 3.6 ml⁻¹. It should be noted that the enrichment factors are strongly dependent on the donor flow-rates^{32,33}.

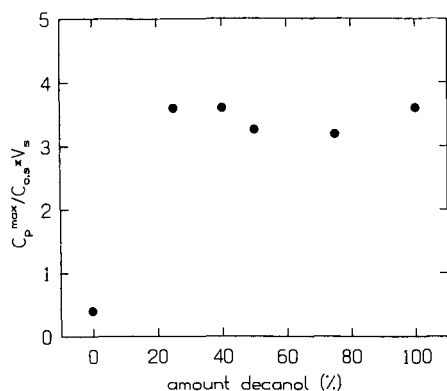


Fig. 2. Enrichment per unit sample volume as a function of the amount of 1-decanol in the liquid membrane.

The use of 1-decanol as the immobilized liquid decreases the selectivity of the technique as polar interferents will be coextracted with the analytes. In order to increase the selectivity of the membrane, mixtures of 1-decanol and *n*-undecane were used. In Fig. 2 the enrichment factor per unit sample volume as a function of the amount of 1-decanol in the membrane is illustrated.

The initial increase in enrichment with 1-decanol is due to an enhanced transfer rate from the donor interfacial layer into the membrane, which is proportional to the distribution ratio between the phases. At the same time, the transfer rate from the membrane phase into the acceptor interfacial layer decreases as it is inversely proportional to the distribution ratio between these phases. The difference in the distribution ratio of the analyte on each side of the membrane is due solely to the different ionic strengths in the donor and acceptor phases. Thus the total permeability in the membrane increases with an increased distribution, reaching a plateau for large distribution ratios. The mechanism for this behaviour has been studied theoretically and experimentally elsewhere³⁴. As can be seen in Fig. 2, this plateau of mass transfer is reached for an immobilized liquid containing 25% 1-decanol in *n*-undecane and further increases in the amount of 1-decanol do not change the enrichment factor. This independence of mass transfer rate on the distribution ratio at the plateau makes the sample workup much less sensitive to the matrix interferences which usually affect the distribution ratio.

Increasing the polarity of the membrane solvent will not only decrease the selectivity towards polar interferents, but will also decrease the physical stability of the liquid membrane, owing to an increased solubility of the solvent in water. As a thin film of large area of the solvent comes into contact with a large volume of water, the solubility in water must be very low and will determine the lifetime of the membrane.

In Fig. 3, the enrichment factor per unit sample volume as a function of operation time of the membrane is shown for three different liquid membranes. Curve a represents a membrane with a liquid consisting of 25% 1-decanol in *n*-undecane. After 20 h the enrichment factor per unit sample volume has decreased to about 75% of the value at 10 h. This is primarily due to losses of 1-decanol from the liquid

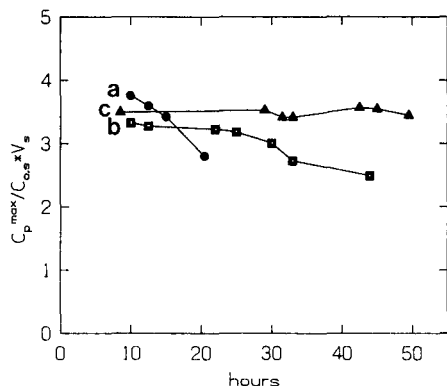


Fig. 3. Comparison of the stability of the membranes expressed as the enrichment factor per unit sample volume for different operation times. (a) 25% 1-decanol in *n*-undecane; (b) 5% 1-dodecanol in *n*-undecane; (c) 5% 1-tetradecanol in *n*-undecane.

membrane. Curve b illustrates the behaviour of a membrane consisting of 5% 1-dodecanol in *n*-undecane. This membrane is stable for 20–25 h, after which the enrichment factor decreases markedly. These curves confirm the fact that the enrichment factor per unit sample volume is virtually independent of the distribution ratio once the mass transfer limit has been reached. As the amount of alcohol in the membrane is lowered, a critical value is reached after which a further decrease in the amount of alcohol, and hence the distribution ratio, will result in a decreased enrichment factor. Curve c represents a membrane with a liquid consisting of 5% 1-tetradecanol in *n*-undecane. This membrane was stable for at least 50 h with an enrichment factor per unit sample volume of 3.5 ml^{-1} and a variation of 2% relative standard deviation (R.S.D.) during this time, which is slightly higher than the R.S.D. for the measurement at each point (1.3%). Each point represents the slope of a line where the concentration in the acceptor is measured as a function of sample volume for five different volumes between 0.5 and 3.5 ml.

The 5% 1-tetradecanol membrane was used for the enrichment of large sample volumes of low concentrations. On injecting volumes greater than 4 ml a negative deviation from linearity appeared, as can be seen in Fig. 4. This deviation is probably due to ester formation in the membrane, but this has not been confirmed. This deviation from linearity with injection volume is not satisfactory, as enrichment factors for large sample volumes are not easily predictable. However, if a constant injection volume is used, the acceptor concentration will vary linearly with the concentration of the injected sample.

To circumvent the problem of deviation from linearity, a membrane with 50% dihexyl ether in *n*-undecane as the immobilized liquid was examined. This membrane did not cause deviation from linearity for injection volumes up to 7 ml and gave an enrichment factor per unit sample volume of 3.8 ml^{-1} for 2,4-D. In order to increase the selectivity towards polar interferences, a solvent consisting of 25% dihexyl ether in *n*-undecane was chosen, which resulted in a decrease in the enrichment factor to 2.6 ml^{-1} . The amount of dihexyl ether needed to reach the plateau of mass transfer is therefore larger than that for the alcohols. This is probably due to the greater ability

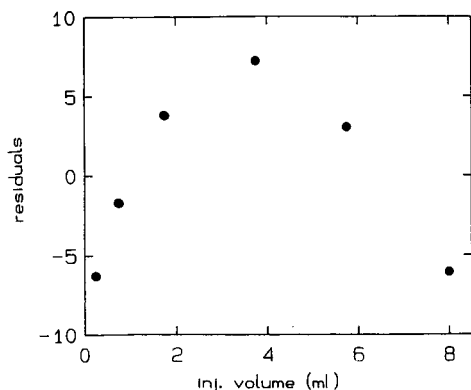


Fig. 4. Differences between the regression line and the experimental points for different injection volumes. Liquid membrane consisting of 5% 1-tetradecanol.

of the alcohols to dissolve by hydrogen bonding, which makes them more efficient as solvents for extraction of CPAs.

Using the membrane of 50% dihexyl ether in *n*-undecane, the enrichment factors per unit sample volume for MCPA and 2,4,5-T were 4.2 and 3.6 ml⁻¹ respectively. This membrane was stable for several weeks and was used in the subsequent experiments.

Interferents

In the analysis of natural waters, problems arising from humic substances are almost always encountered. Humic substances consist of species with molecular weights ranging from a few hundred to several millions. The chemical structure is undefined and includes an unusually large number of functional groups³⁵.

Humic substances are detrimental to both GC and LC columns and must be removed prior to injection. The processing of 1.5 ml of a 350 ppm humic acid solution, in the same way as for CPAs, results in a 99% reduction in the absorbance at 285 nm. Using an *n*-undecane membrane instead of the 50% dihexyl ether membrane is considerably more effective.

However, as can be seen in Fig. 5, there is a fraction of humic acid absorbing at 285 nm that is enriched. This enriched fraction could not be washed back into the donor side by means of a sample-free donor stream as described previously³³. Hence the fraction is ionized at pH 7 but partially ionized or non-ionized at pH 1. In the experiments discussed below, no adverse effects related to this fraction were observed.

On-line coupling of the flow system to liquid chromatography

The coupling of the sample preparation system discussed above to reversed-phase LC is straightforward. The enriched sample plug in the acceptor is transported to the injection loop of the liquid chromatograph. The pneumatically controlled injector automatically injects a major part of the plug into the chromatographic set-up.

The chromatographic column and eluent system chosen in this work were used previously for the separation of CPAs^{22,23}. Throughout, the chromatographic sep-

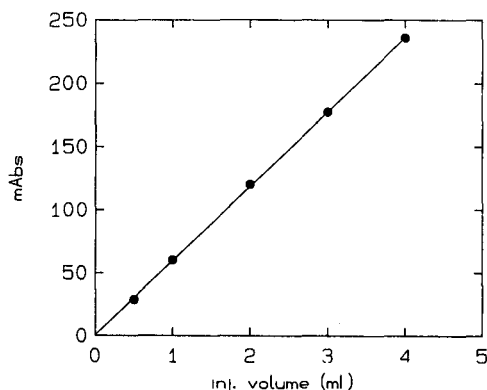


Fig. 5. Detector signals obtained for injections of a 350 mg/l humic acid solution with a membrane of 50% dihexyl ether.

ations were performed with a reversed-phase C_{18} column and methanol–1% acetic acid (3:2) as the mobile phase.

The concentration profile of the enriched sample reaching the injector of the liquid chromatograph is not rectangular, leading to an inhomogeneous concentration in the injector loop. Therefore, comparison of the chromatographic signals on injecting enriched samples and on injecting standard solutions into the chromatograph gives an observed practical enrichment factor which is smaller (about 50%) than the concentration-based enrichment factor described above [$C_p^{\max}/(C_{o,s}V_s)$].

By using a lower flow-rate of a more concentrated sulphuric acid solution on the donor side of the membrane, the total flow-rate passing the membrane could be lowered. This resulted in a larger practical enrichment factor owing to the longer contact time of the sample with the membrane, which means that the recovery is increased. By using a 1.3 M sulphuric acid solution at a flow-rate of 0.04 ml/min instead of a 0.2 M solution at a flow-rate of 0.25 ml/min, the practical enrichment factor of 2,4-D was increased from about 2 to 3.5 ml⁻¹.

Determination of CPAs in water samples

The detection limit in the chromatographic step, taken as the concentration that gives a signal-to-noise ratio of 2, is about 0.1 ppm. The enrichment factor needed for the determination of a given concentration can be calculated and thence the sample volume or alternatively the time required for the sample preparation.

As an example, if a 1 ppb sample is to be analysed, this will demand an enrichment factor of 100, which will require a 30 ml or take 120 min with the following typical flow-rates: sample, 0.25 ml/min; sulphuric acid stream, 0.04 ml/min; and acceptor, 0.15 ml/min.

Standard solutions of CPAs in water were analysed and the signal was plotted as a function of concentration. The enrichment time was 10 min and the second sample preparation is performed while the first one is being chromatographed. The time required for each analysis is 11–15 min with continuous use of the system.

Solutions containing the same amount of CPAs in 350 mg/l humic acid were also analysed in the same manner. As shown in Table II, no differences at a 95% level

TABLE II

REGRESSION PARAMETERS OF CALIBRATION GRAPHS (PEAK HEIGHT VS. CONCENTRATION IN ppm) FOR THREE DIFFERENT CPAs

Experimental conditions as in Fig. 6A. Four concentrations were measured ranging from 0.05 to 1 ppm.

Compound	Slope ^a	Intercept ^a
2,4-D	56.4 ± 3.0	0.4 ± 1.7
MCPA	42.8 ± 2.4	0.4 ± 1.4
2,4,5-T	38.4 ± 2.7	0.3 ± 1.5
2,4-D ^b	58.1 ± 1.8	0.0 ± 1.0
MCPA ^b	44.0 ± 1.4	0.1 ± 0.8
2,4,5-T ^b	39.4 ± 1.0	-0.2 ± 0.6

^a Limits for 95% confidence intervals.^b In a solution of 350 mg/l humic substances.

of significance were found between the slopes of the calibration graphs for the determination of the CPAs, whether they are in pure water or in solutions containing humic acid. Fig. 6 shows separations of 10 and 50 ppb CPAs in 350 mg/l humic acid solution.

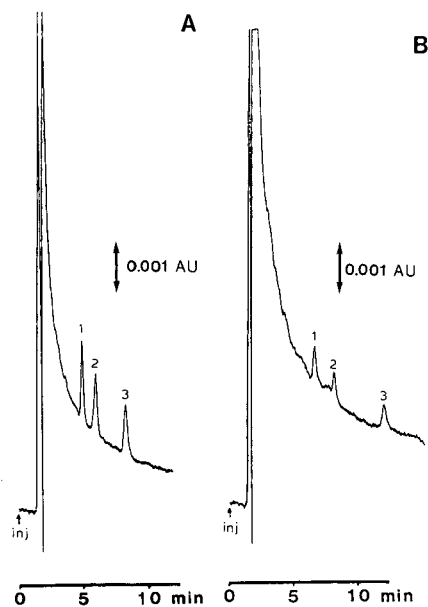


Fig. 6. Chromatograms showing the separations of (1) 2,4-D, (2) MCPA and (3) 2,4,5-T. (A) Concentration, 50 ppb of each CPA; injection volume, 2.5 ml; chromatographic system as described in the text. (B) Concentration, 10 ppb; injection volume, 7.5 ml; eluent, methanol-acetic acid (58:42); other parameters as described in the text.

ACKNOWLEDGEMENTS

The authors thank Lennart Mathiasson, Analytical Chemistry, University of Lund, Sweden, for valuable discussions during the course of this investigation. The financial support of the Swedish Council for Forestry and Agricultural Research is gratefully acknowledged.

REFERENCES

- 1 *Kirk-Othmer Encyclopedia of Chemical Technology*, Wiley-Interscience, New York and London, Vol. 12, 3rd ed., 1980, pp. 297–351.
- 2 J. J. Richards, C. D. Chriswell and J. S. Fritz, *J. Chromatogr.*, 199 (1980) 143–148.
- 3 H. Agemian and A. S. Y. Chau, *J. Assoc. Off. Anal. Chem.*, 60 (1977) 1070–1075.
- 4 N. P. Hill, A. E. MacIntyre, R. Perry and J. N. Lester, *Intern. J. Environ. Anal. Chem.*, 15 (1983) 107–130.
- 5 M. L. Hopper, *J. Agric. Food Chem.*, 35 (1982) 265–269.
- 6 R. Purkayastha, *J. Agric. Food Chem.*, 22 (1974) 453–458.
- 7 J. J. Richards and J. S. Fritz, *J. Chromatogr. Sci.*, 18 (1980) 35–38.
- 8 W. Draper, *J. Agric. Food Chem.*, 30 (1982) 227–231.
- 9 A. J. Cessna, R. Grover, L. A. Kerr and M. L. Aldred, *J. Agric. Food Chem.*, 33 (1985) 504–507.
- 10 A. S. Y. Chau and K. Terry, *J. Assoc. Off. Anal. Chem.*, 59 (1976) 633–636.
- 11 H. Roseboom, H. A. Herbold and C. J. Berkhoff, *J. Chromatogr.*, 249 (1982) 323–331.
- 12 S. M. Walizewski and G. A. Szymczyński, *Fresenius Z. Anal. Chem.*, 322 (1985) 510–511.
- 13 V. Lopez-Avila, P. Hirata, S. Kraska and J. H. Taylor, Jr., *J. Agric. Food Chem.*, 34 (1986) 530–535.
- 14 D. W. Woodham, W. G. Mitchell, C. D. Loftis and C. W. Collier, *J. Agric. Food Chem.*, 19 (1971) 186–188.
- 15 A. S. Y. Chau and K. Terry, *J. Assoc. Off. Anal. Chem.*, 58 (1975) 1294–1301.
- 16 M. J. Bertrand, A. W. Ahmed, B. Sarrasin and V. N. Mallet, *Anal. Chem.*, 59 (1987) 1302–1306.
- 17 J. F. Lawrence and D. Turton, *J. Chromatogr.*, 159 (1978) 207–226.
- 18 F. Eisenbeiss and H. Sieper, *J. Chromatogr.*, 83 (1973) 439–446.
- 19 P. Jandera, L. Svoboda, J. Kubát, J. Schvantner and J. Churáček, *J. Chromatogr.*, 292 (1984) 71–84.
- 20 H. Ruckendorfer and W. Lindner, *Int. J. Environ. Anal. Chem.*, 18 (1984) 87–99.
- 21 P. Cabras, P. Diana, M. Meloni and F. M. Pirisi, *J. Chromatogr.*, 234 (1982) 249–254.
- 22 M. Åkerblom, *J. Chromatogr.*, 319 (1985) 427–431.
- 23 S. H. Hoke, E. E. Brueggeman, L. J. Baxter and T. Trybus, *J. Chromatogr.*, 357 (1986) 429–432.
- 24 D. E. Games, M. S. Lant, S. A. Westwood, M. J. Cocksedge, N. Evans, J. Williamson and B. J. Woodhall, *Biomed. Mass Spectrom.*, 9 (1982) 215–224.
- 25 R. D. Voyksner, J. T. Bursey and E. D. Pellizari, *J. Chromatogr.*, 312 (1984) 221–235.
- 26 J. A. Apfel, U. A. Th. Brinkman and R. W. Frei, *J. Chromatogr.*, 312 (1984) 153–164.
- 27 N. Vural and S. Burgaz, *Bull. Environ. Contam. Toxicol.*, 33 (1984) 518–524.
- 28 S. Mierzwa and S. Witek, *J. Chromatogr.*, 136 (1977) 105–111.
- 29 R. L. Smith and D. J. Pietrzyk, *J. Chromatogr. Sci.*, 21 (1983) 282–287.
- 30 E. G. Cotterill, *Analyst (London)*, 107 (1982) 76–81.
- 31 J. E. Woodrow, M. S. Majewski and J. N. Seiber, *J. Environ. Sci. Health*, B21 (1986) 143–164.
- 32 G. Audunsson, *Anal. Chem.*, 58 (1986) 2714–2723.
- 33 G. Audunsson, *Anal. Chem.*, 60 (1988) 1340–1347.
- 34 G. Audunsson, *Thesis*, University of Lund, 1988.
- 35 G. G. Choudhry, *Humic Substances*, Gordon and Breach, New York, 1984.

CHROM. 21 301

QUANTITATIVE HIGH-RESOLUTION GAS CHROMATOGRAPHY AND MASS SPECTROMETRY OF TOXAPHENE RESIDUES IN FISH SAMPLES

F. I. ONUSKA* and K.A. TERRY

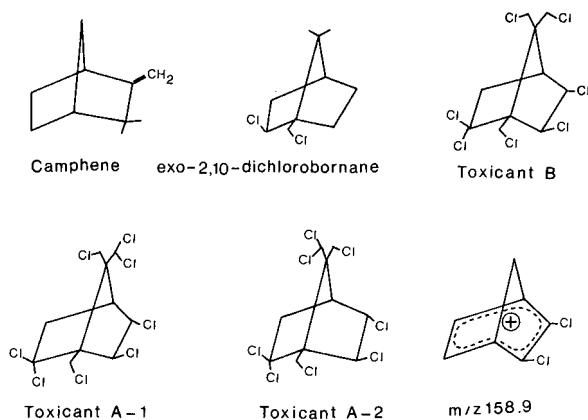
Research and Applications Branch, National Water Research Institute, Canada Centre for Inland Waters, 867 Lakeshore Road, Burlington, Ontario, L7R 4A6 (Canada)

SUMMARY

This report describes an analytical method which permits the determination of ppb (1 $\mu\text{g}/\text{kg}$) level of toxaphene in fish tissues. Interferences both from biogenic and from xenobiotic substances are reduced even with low-resolution mass spectrometry. The methodology has a low susceptibility to false positive determinations, which could result from the presence of a wide variety of co-contaminants. The method is based on the measurement of a signal representative of the toxaphene residue (m/z 158.9) relative to a known amount of an internal standard ^{37}Cl -labelled compound. A modular approach to toxaphene enrichment has permitted a moderately simple procedure, significantly reducing analytical time requirements and the number of sample manipulations, and making the procedure amenable to automation. The reliability and accuracy of the procedure are demonstrated by the results of intra- and interlaboratory studies. The methodology has been validated and the presented data indicate that the detection limit is 1 $\mu\text{g}/\text{kg}$ of total toxaphene. Toxaphene recovery from fish at concentration levels between 0.1 and 10 $\mu\text{g}/\text{g}$ is $84 \pm 12\%$.

INTRODUCTION

Problems in multiresidue trace analysis represent a major proportion of research activities in environmental applications of mass spectrometry (MS) and gas chromatography–mass spectrometry (GC–MS). The quality of such analyses may be evaluated by an assessment of selectivity, sensitivity and precision. In general, the quantitative MS of environmental contaminants is performed on the basis of a real-time measurement in the selected-ion monitoring (SIM) mode. SIM permits the quantitation of picogram quantities of an analyte. Such low detection limits may not be achievable in analyses of samples containing many congeners where sensitivity may be limited by the simultaneous detection of individual congeners or their characteristic moieties formed during analysis. Improvements in selectivity during the analysis of environmental samples in addition to increasing confidence in the characterization of trace components will affect the accuracy of quantitation. One of the techniques for improving selectivity includes the use of enhanced resolution but it involves a reduction in the absolute signal intensity in MS¹.



Scheme 1. Some structural moieties assumed to be present in toxaphene mixtures.

Several recent reports indicate that toxaphene is a widespread pollutant^{2,3}. Many compounds of environmental interest cannot be determined by GC-MS, since they are either thermally unstable and suffer thermal decomposition at the injector or on the GC column, or else they are too involatile to pass through the system into the ion source. Toxaphene represents a complex mixture of at least 300 separated components by high-resolution gas chromatography (HRGC)⁴. It is known to be toxic to various species of fish. Toxic effects in fish include decreased viability of ova and decreased bone collagen synthesis⁵. The acute toxicity of toxaphene residues to fish is similar to that of endrin and endosulfane⁶. Quantitative determination of toxaphene has presented problems and validated methodology in environmental samples does not exist today⁷.

The validity of a technique or a methodology for any environmental samples containing toxaphene depends on it having adequate sensitivity to determine the components and sufficient specificity to ensure the absence of possible interferences. Sensitivity is limited by the number of separated components when HRGC is employed.

Our laboratory has been engaged in investigations related to the development of analytical methodology for toxaphene in environmental samples for the last three years⁸.

This paper reports our methodology which has been applied to fish tissue analyses and is based on the direct inlet probe (DIP) MS-SIM analysis. The DIP offers a means of quantifying toxaphene down to low levels. The simple treatment for a multicomponent mixture cannot be applied since the number of isomeric compounds is unknown. However, it is possible to choose a m/z value (158.9) to which the majority of toxaphene constituents contribute and in the SIM mode of operation, the background and possible impurities from biological extracts do not contribute significantly to cleaned-up extracts. It is the aim of this paper to show the general applicability and advantages of the proposed method by presenting an analysis of the data collected from a series of toxaphene determinations and to discuss some of the experimental aspects of the methodology.

EXPERIMENTAL

Fish samples

The collection of fish samples was performed by the Department of Fisheries and Oceans personnel in Burlington (Ontario, Canada) and homogenate fish samples (samples 3 and 4; Serial Nos. 0009, 0033, 1161 and 1154) were obtained from the United States Environmental Protection Agency-Environmental Monitoring Systems Laboratory (Cincinnati, OH, U.S.A.). Our samples were wrapped in hexane-rinsed aluminum foil, frozen, and homogenates were supplied in wide-mouthed dark glass bottles. Whole fish from a single site were then frozen into a composite sample and kept frozen at -12°C until used.

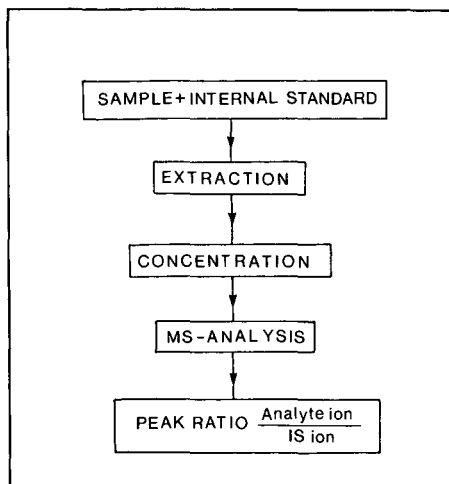
At the laboratory 10 g of fish tissue was mixed with 40 g of anhydrous sodium sulfate. The dried mixture was ground to a fine powder and packed in a chromatographic column (30 cm \times 2 cm I.D.). Several basic principles are common to most quantitative MS assays, as summarized in Scheme 2.

Sample extraction

The column was equipped with a coarse-fritted plate on the bottom and a PTFE stopcock, and a 250-ml reservoir bulb at the top which flared out into a funnel shape. The samples were extracted with 200 ml of methylene chloride at a flow-rate of 3.5 ml/min⁷. The lipid extracts were collected in a 250 ml round-bottom flask and the solvent volume was reduced to 5 ml by rotary evaporation.

Cleanup and fractionation

Automated gel permeation chromatography (GPC) was employed to separate the polychlorinated biphenyls (PCBs), toxaphene and other chlorinated hydrocarbon pesticides from lipids⁹. An automated GPC system Autoprep 1001 (Analytical Biochemistry Lab., Columbia, MO, U.S.A.) was used. The solvent mixture, cyclohexane and methylene chloride was pumped through the GPC column (BioBeads SX-3) at 5 ml/min with the FMI laboratory pump, Model RRP-S4.



Scheme 2. Extraction and quantification scheme.

A volume of 5 ml or no more than 0.8 g of lipid should be placed on the GPC column. The first portion (150 ml) of the eluate was discarded and the next 120 ml were collected in a 250-ml round-bottom flask. The eluate was concentrated to 3 ml using the Rotavap.

Florisil column adsorption chromatography

A Florisil column was prepared by placing a charge of activated Florisil in a chromatographic column (30 × 1 cm I.D.) over a 1-cm layer of anhydrous Na₂SO₄. An amount of 5 g of 60–80 mesh Florisil previously activated at 130°C for 16 h was added and topped with a 1.5-cm layer of anhydrous Na₂SO₄. Each column was prewashed with 20 ml of *n*-hexane. When the solvent reached the top of the Na₂SO₄ layer, the concentrate from the GPC was quantitatively transferred to the column and allowed to drain onto the bed of Florisil. The column walls were washed with a 10-ml portion of 50 ml *n*-hexane–diethyl ether (94:6). When the solvent reached the top of the Florisil the remaining part of the eluent (40 ml) was added. The eluate was collected for further analyses. It usually contained aldrin, BHC, chlordanes, 1,1-dichloro-2,2-bis(*p*-chlorophenyl)ethane (DDD), DDE, and 1,1,1-trichloro-2,2-bis(*p*-chlorophenyl)ethane (DDT) isomers, heptachlor, lindane, methoxychlor, mirex, PCBs and toxaphene. More polar compounds, such as endosulfane, endrin, dieldrin and phthalates were removed from the column with 50 ml of diethyl ether–hexane (20:80) solution. PCBs can be removed from most of the pesticides by silica gel column chromatography¹⁰. About 20 g of silica gel (*e.g.*, silicagel 60 from E. Merck), was placed in a 100-ml beaker and activated at 130°C for 16 h. It was then transferred to a 100-ml glass-stoppered bottle. The silica gel columns was prepared by plugging a chromatographic column (30 × 1 cm I.D.) with glass wool, filling it with a 1-cm layer of anhydrous Na₂SO₄, and 5 g of activated silica gel and topping it with a second 1-cm layer of anhydrous Na₂SO₄. The column was prewashed with 20 ml *n*-hexane. The sample was added to the column and rinsed with 5 ml of the first eluent and allowed to percolate into the bed. The rest of the first eluent was added and the effluent collected in a 125-ml round-bottom flask. The first eluate (40 ml of diethyl ether–*n*-hexane, 6:94) contained the PCBs, HCB, aldrin, heptachlor, mirex and the *p,p'*-DDE. The second fraction eluate (40 ml of diethyl ether–*n*-hexane, 25:75) contained a small amount of *p,p'*-DDE, BHC isomers, toxaphene, DDT and its homologues, chlordanes, nonachlor, heptachlor epoxide and methoxychlor. The eluate volumes were reduced in volume on the Rotavap and the resulting residues adjusted to 1 ml with isooctane prior to their quantitation using HRGC or MS–SIM.

Preparation of ³⁷Cl-labelled toxaphene

³⁷Cl-labelled toxaphene was synthesized from a solution of camphene (142 mg) in CCl₄ (60 ml) in a chlorination flask. A mixture of Na³⁷Cl (2 g), MnO₂ (3 g) and concentrated H₂SO₄ (3 g) diluted with about an equal volume of distilled water was placed in the chlorine generating flask and heated in an oil bath to 190°C. The chlorine generating flask was equipped with a water-cooled condenser and connected to a nitrogen gas cylinder. The camphene in CCl₄ solution was placed in the chlorination flask containing a submerged UV-lamp (254 nm, PCQ UV-Product, San Gabriel, CA, U.S.A.). The chlorination flask was connected with Tygon tubing to a water trap, which in turn was connected to an open oil-bubbler. Irradiation of the solution

began as soon as the characteristic chlorine color appeared. The heating continued until gas production ceased (*ca.* 2.5 h), at that time a barely noticeable nitrogen flow was introduced. The flow was maintained throughout the entire irradiation procedure (15 h). The chlorination mixture was then washed with saturated sodium bicarbonate solution, dried (anhydrous Na_2SO_4) and gently evaporated to dryness. The yield was 400 mg of toxaphene. The chlorine content was 66.1%. A high-resolution gas chromatogram is shown in Fig. 1. This product was used as an internal standard for the MS solid-probe quantitation and was spiked prior to this analysis.

Electron impact fragmentation of toxaphene

The electron impact ionization mass spectra of toxaphene are dominated by characteristic chlorinated clusters¹¹. It has been noted that primary fragmentation characterizing the mass spectra of toxaphene congeners involved elimination of the chlorine or HCl of the toxaphene moiety. The structure and origin of the fragments of chlorinated bornenes have also been discussed in detail^{11,12}. The mass spectrum of ³⁷Cl-labelled toxaphene is shown in Fig. 2.

Instrumentation

High-resolution gas chromatography with electron-capture detection (ECD). Standards and samples were analyzed on a Varian Vista 6000 gas chromatograph equipped with a 25×0.1 mm ($d_f = 0.25$ μm) bonded-phase SE-52 fused-silica column with hydrogen as the carrier gas. The chromatographic time-temperature

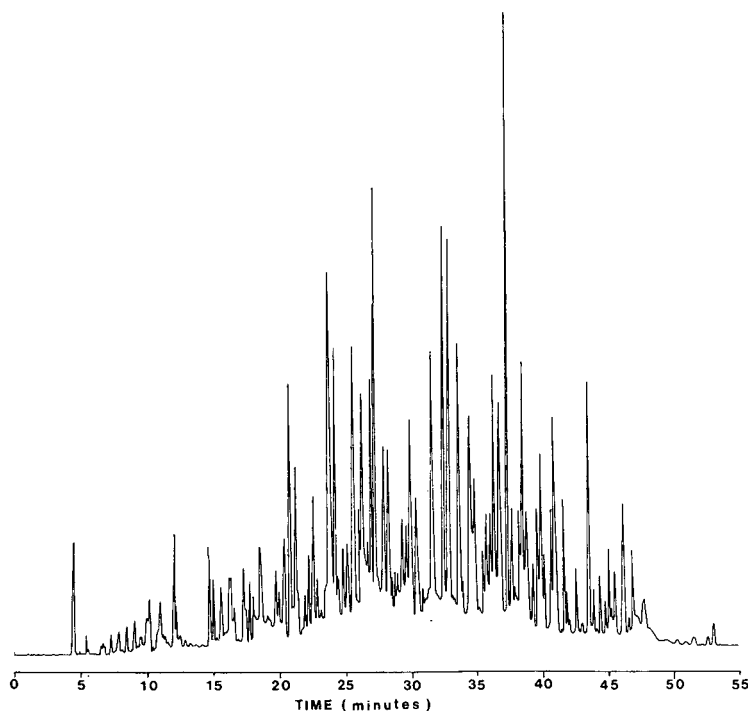


Fig. 1. Gas chromatogram of toxaphene labelled with ³⁷Cl.

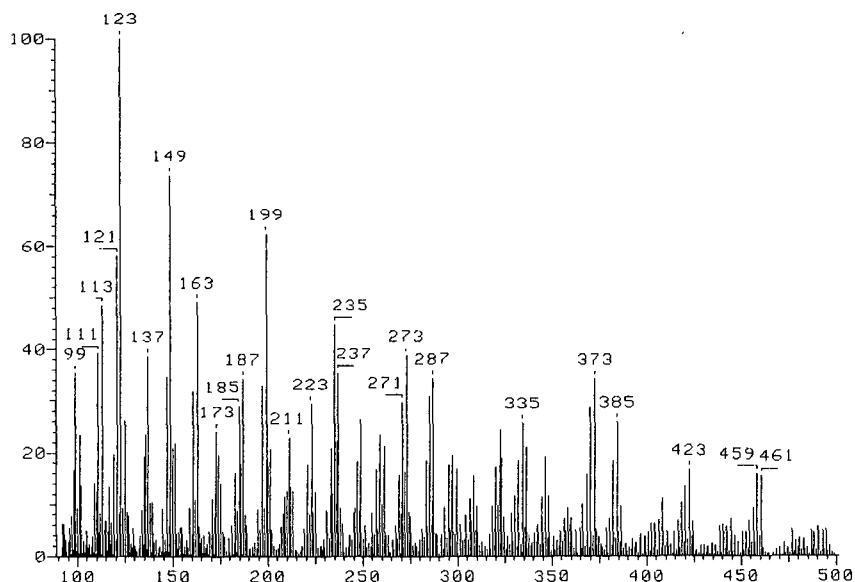


Fig. 2. The mass spectrum of ^{37}Cl -labelled toxaphene obtained under electron impact conditions.

conditions were as follows: splitless injection, 0.6 min; initial temperature 80°C , hold for 1 min; to 160°C at $20^\circ\text{C}/\text{min}$, hold for 5 min; to 230°C at $2^\circ\text{C}/\text{min}$ and to 260°C at $10^\circ\text{C}/\text{min}$. The injector port was maintained at 230°C .

Mass-spectrometry. A Varian MAT 311 A Model high-resolution sector instrument, equipped with both electron impact (EI) and chemical ionization (CI) sources was used. The EI-EI detector source temperature was maintained at 170°C with an ionization voltage of 70 eV, and the combined EI-CI source at 150°C . The resolution was set at 1200 (10% valley). The mass spectrometer was equipped with a water cooled solid probe insert, which could be heated from 20 to 200°C in 5 s. The SIM recording was achieved by Varian MAT hardware kit and traces were recorded on a Spectra Physics 4100 printer-plotter. In the SIM mode m/z 158.9 and 162.9 traces were recorded.

Gas chromatography-mass spectrometry-selected ion monitoring. The GC-MS system (Finnigan MAT 311A with a Carlo Erba 4160 GC) equipped with a $30\text{ m} \times 0.25\text{ mm}$ I.D. bonded-phase SE-54 fused-silica open tubular column was directly interfaced to a Finnigan MAT 311 A mass spectrometer ion source. Cool on-column injection was employed. The initial column temperature of 75°C was programmed to 160°C at $30^\circ\text{C}/\text{min}$ and was held for 10 min and then increased to 225°C at $2^\circ\text{C}/\text{min}$. A transfer line temperature of 230°C and an ion source temperature of 150°C were maintained. Helium was used as carrier gas. The instrument was sequentially set to monitor m/z 130.9 (perfluorokerosene, PFK) and 158.9. Ion dwell times of 0.01 s for 130.9 and 0.1 s for the late ion were employed.

General description of the inlet system of a mass spectrometer

The majority of organic compounds may be introduced into the ion source of a

mass spectrometer by means of a direct insertion device. This device allows the introduction of samples which have insufficient thermal stability to be heated quickly up to 350°C, or have very low vapor pressures even at this temperature. The sample is introduced directly into the ion source on the cooled end of the probe. The end of the probe can be heated fast by means of a heater in the probe. An increased vapor pressure of about 5 Torr permits a mass spectrum to be obtained using this technique. Samples of toxaphene down to 200 pg were analyzed in the SIM-EI mode. Direct probe sample vials (aluminium) with tops were obtained from Finnigan MAT.

Procedure

Reference solutions for calibration purposes were prepared by mixing a ^{37}Cl -labelled toxaphene solution (2 ng/ μl) in isooctane with the native toxaphene at different concentration levels (0.2–5.0 ng/ μl). Fish extracts were also analyzed with an addition of the internal standard. A 1- μl volume was brought into a crucible (10 mm \times 2 mm I.D.). After the solvent was evaporated, the lid was tapped and the crucible was properly inserted to the probe tip. The probe tip was placed in an isolation chamber for 10 s. Afterwards, the probe was inserted for measurement into the ion source. When the probe was fully inserted a stop-watch was started to run. Filament, probe insertion, a probe heater and SIM hardware switching were turned on. Two masses (m/z 158.9 and 162.9) were recorded during a fast temperature programming of the probe tip (40°C/min). During the subsequent evaporation of a sample, the preselected ions were monitored at 45 s and the corresponding accelerating voltage

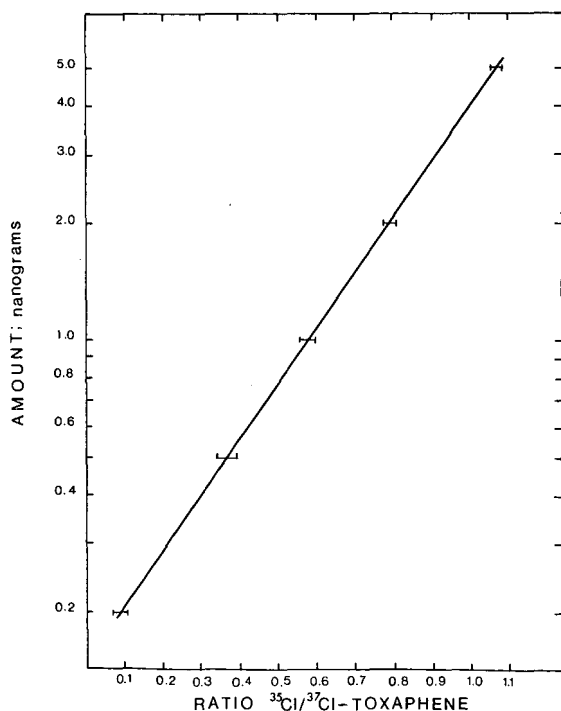


Fig. 3. Calibration curve for toxaphene using a direct insertion probe technique.

traces were recorded by two SP-4100 printer-plotter integrators. The peak profile width at half maximum current was typically smaller than 25 s. The calibration curve was designed as shown in Fig. 3. However, for high accuracy and precision measurements, calibration mixtures of accurately weighed toxaphene and its ^{37}Cl -labelled analogue were used to bracket the sample and checked with standard curves¹³.

Solid probe-SIM conditions

- (1) Spike 1 μl sample with 1 μl of 2 ng/ μl [^{37}Cl]toxaphene in isoctane.
- (2) Evaporate for 30 min at room temperature.
- (3) Place in probe, evacuate in isolation chamber for 10 s, then insert probe into source.
- (4) Start the timer when the probe is fully inserted, turn-on filament, probe heater and MIS hardware switching.
- (5) At 30 s, start both recorders (m/z 158.9 and 162.9) monitoring baseline.
- (6) At 45 s, start solid-probe temperature programming.

Conditions: electron multiplier, 1.5 kV; filament current, 0.6 mA; $m/\Delta m$, 1200; source temperature, 150°C. SIM: attenuation, 0.1; filter, 0.1 Hz; dwell time, 100 ms. Attenuation, 256 \times (both recorders). Solid-probe programming: 25°C to 175°C in 10 s. PFK reference peak: m/z 130.9.

RESULTS AND DISCUSSION

Fig. 4 shows the recorder output of a low-resolution ($R=1000$) dual SIM analysis of a native and a ^{37}Cl -labelled toxaphene sample of a fish extract. The mass spectrometer was focused to achieve a Gaussian peak shape. Following each sample introduction, the accelerating voltage, filament current and probe programmer were turned on. A reference ion of m/z 130.9 (derived from PFK) which was independently introduced into the ion source via a reference inlet, was used for setting individual masses to be monitored and to assure a proper focusing. Any required correction for drift (generally less than 10 ppm) was made by adjustment of the magnet current before analysis began. PFK was removed prior to running samples. The solvent blank showed no significant background contribution.

The precision for the determination of response ratios, analyte-internal standard, is influenced by fluctuations in the intensities of the selected ion currents and by

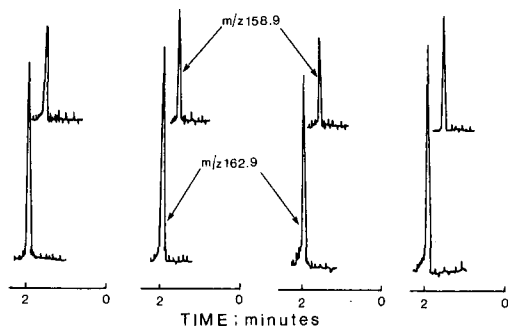


Fig. 4. The recorder-output traces of m/z 158.9 and 162.9 and its replicate analyses.

TABLE I
REPLICATE ANALYSES OF TOXAPHENE IN FISH SAMPLES

Sample	Amount found (ng)	Response ratio	Total conc. (µg/g)	Sample	Amount found (ng)	Response ratio	Total conc. (µg/g)
E-3	2.0	0.79	48.8	E-4	1.0	0.59	6.0
	2.0	0.79	48.8		1.0	0.59	6.0
	2.1	0.80	51.2		1.0	0.60	6.0
	2.3	0.84	56.1		1.0	0.60	6.0
	2.4	0.85	58.6		1.1	0.63	6.6
	2.4	0.85	58.6		1.2	0.65	7.2
\bar{x}	2.2	0.82	53.7		1.05	0.61	6.3
S.D.	0.1897	0.029	3.929		0.0763	0.0224	0.458
C.V.(%)	8.62	3.62	7.31		7.27	3.66	7.27

drift or noise from the peak centroid. The effect of drift is minimal at lower MS resolution. The results of replicate analyses ($n = 16$) of a single fish extract with DIP-SIM for two ions at low resolution ($R = 1200$) gave a peak area ratio of 0.84 and a coefficient of variation of 2.6%.

Fig. 4 shows the recorder output of approximately 7.0 and 60 µg/g of toxaphene and ^{37}Cl -labelled toxaphene, respectively.

Table I records the precision of the determination of response ratios for replicate analyses of toxaphene in fish samples.

Results reflecting recoveries and accuracy for the given procedure are evaluated in Table II. These data of toxaphene for fish samples provided by the supplier were

TABLE II
RECOVERIES FOR THE U.S.-EPA FISH HOMOGENATE CONTAINING TOXAPHENE BY THE TWO DIFFERENT TECHNIQUES

U.S.-EPA value^a: fish 3, 90.8 µg/g; S.D. = 6.9; 95% confidence interval, 77–105 µg/g; fish 4, 7.2 µg/g; S.D. = 2.6; 95% confidence interval, 2–12.4 µg/g.

Batch	HRGC-ECD		(%) Recovery		DIP-MS-SIM		(%) Recovery	
	Fish 3	Fish 4	Fish 3	Fish 4	Fish 3	Fish 4	Fish 3	Fish 4
2	—	7.87	—	109.3	—	6.02	—	83.6
3	59.3	7.18	65.3	99.7	62.2	7.83	68.5	108.8
4	56.9	8.21	62.7	114.0	53.7	6.28	59.1	87.2
5	67.2	5.85	74.0	81.3	52.5	7.83	57.8	108.8
6	58.6	6.94	64.5	96.4	53.7	6.32	59.1	87.8
7	67.7	8.91	74.6	123.8	76.4	7.54	84.1	104.7
\bar{x}	62.0	7.49	68.2	104.0	59.7	6.97	65.7	96.8
S.D.	5.09	1.07	—	—	10.1	0.85	—	—
R.S.D.(%)	8.2	14.3	—	—	16.9	12.18	—	—

^a True value is unknown; results obtained from the referee laboratories by packed-column gas chromatography.

TABLE III

TOXAPHENE RESULTS ($\mu\text{g/g}$) FOR SAMPLE EXTRACTS ANALYZED BY THE DIFFERENT TECHNIQUES AT TWO LABORATORIES

Sample	HRGC-ECD		GC-MS-SIM	DIP-MS-SIM
	Lab 1	Lab 2	Lab 2	Lab 2
1	0.17	0.17	^a	0.15
2	7.87	8.54	8.84	11.40
3	1.21	1.36	1.14	1.70
4	0.47	0.52	0.72	0.67
5	1.00	1.15	1.34	1.12
6	3.09	3.01	3.36	4.10
7	15.50	16.80	17.10	17.00

^a Below detection limit of 500 pg/ μl ; equivalent to 0.5 $\mu\text{g/g}$.

obtained by packed column GC. As can be seen from the results obtained by two different techniques, the data are in good agreement. Comparing the effectiveness of DIP-MS-SIM *versus* HRGC-ECD, it is evident that the former would allow up to 35 analyses per day. This is a significant improvement over the 5-6 samples per day when HRGC-ECD is used. Another advantage of this technique is that a large amount of sample can be introduced into the ion source and thus increased response and higher sensitivity.

The limit of detection in 10-g fish samples varied depending both on the toxaphene degradation and the fat content in the fish. In general, using a signal-to-noise ratio (S/N) of 3 for toxaphene as detection limit, it required at least 100 pg of toxaphene to be introduced into the ion source under the given instrumental conditions.

Using the same extraction techniques, seven fish samples were analyzed at two different laboratories. These samples were analyzed by HRGC-ECD, HRGC-MS-SIM and DIP-MS-SIM. Results of the interlaboratory quantitation are given in Table III.

It is evident that estimated values differ slightly not only between HRGC-ECD data but also between the different techniques. The HRGC-ECD results are usually lower than those of DIP-MS-SIM due to the omission of many peaks. Significant alteration of GC peaks including some interferences from other components in the fish extracts could lower these values. Considering the low toxaphene levels in the samples, it is premature to draw conclusions as to the origin of the differences.

CONCLUSIONS

The results in this paper demonstrate the feasibility of the rapid direct probe determination of toxaphene residues in fish tissue, without the attendant problems of extraction and exhaustive purification steps. Where comparisons are drawn with published data, the correlation is satisfactory. The use of sample-dependent standards has proven to be an alternative means of MS quantitation complementary to techniques based on sample-independent standards used in HRGC and GC-MS.

ACKNOWLEDGEMENTS

This work has been performed at the National Water Research Institute, Analytical Methods Division, as a part of a project requested by the Great Lakes Toxic Contaminants Committee of the Great Lakes Water Quality Program, whose financial support is gratefully acknowledged. We are grateful to Dr. J. Zajicek and Dr. D. L. Stalling from the U.S.-Fish and Wildlife Laboratory, Columbia, MO and U.S.-EPA, Quality Assurance Branch, Cincinnati, OH for providing some of the fish samples. This is National Water Research Institute contribution No. 85-113.

REFERENCES

- 1 B. J. Millard, *Quantitative Mass Spectrometry*, Heyden, New York, 1978.
- 2 C. J. Musial and J. F. Uthe, *Int. J. Environ. Anal. Chem.*, 14 (1983) 116-126.
- 3 M. Zell and K. Ballschmiter, *Fresenius Z. Anal. Chem.*, 300 (1980) 387-402.
- 4 F. I. Onuska, *J. Chromatogr.*, 289 (1984) 207-221.
- 5 F. L. Mayer, Jr., P. M. Mehrle, Jr., and W. P. Dwyer, *U.S. Nat. Technol. Information Service*, PB-249303, Washington, DC, 1975.
- 6 G. A. Pollock and W. W. Kilgore, *Res. Rev.*, 69 (1978) 87.
- 7 T. Cairns, E. G. Siegmund and J. E. Froberg, *Biomed. Mass Spectrom.*, 8 (1981) 569-574.
- 8 F. I. Onuska and K. A. Terry, *Toxaphene: Analytical Techniques for Determining Low Concentrations of Toxaphene Residues, NWRI Report, Analytical Methods Division*, Burlington, 1984.
- 9 M. A. Ribick, G. R. Dubay, D. L. Stalling, J. D. Petty and C. J. Schmitt, *Environ. Sci. Technol.*, 16 (1982) 310-318.
- 10 S. Jensen, L. Reutergardh and B. Jansson, *Manual of Methods in Aquatic Environmental Research, Part 9. FAO Fisheries Technical Paper No. 212*, Rome (1983) p. 21.
- 11 R. L. Holmstead, S. Khalifa and J. E. Casida, *J. Agric. Food Chem.*, (1974) 939-944.
- 12 R. Vaz and G. Blomkvist, *Chemosphere*, 14 (1985) 223-231.
- 13 F. C. Falkner, *Biomed. Mass Spectrom.*, 8 (1980) 43-46.

CHROM. 21 295

DETERMINATION OF SENSORIAL ACTIVE TRACE COMPOUNDS BY MULTI-DIMENSIONAL GAS CHROMATOGRAPHY COMBINED WITH DIFFERENT ENRICHMENT TECHNIQUES

S. NITZ*, H. KOLLMANNBERGER and F. DRAWERT

Institut für Lebensmitteltechnologie und Analytische Chemie, Technische Universität München, D-8050 Freising-Weihenstephan (F.R.G.)

SUMMARY

Gas chromatographic equipment and appropriate procedures are described for the identification and determination of sensorial active compounds in complex mixtures. Different sampling systems (liquid injection, thermal desorption, dynamic headspace) were integrated in a single double-oven gas chromatograph, additionally allowing multi-dimensional separation, detection by simultaneous sniffing–mass spectrometric monitoring or micro-preparative enrichment of capillary effluents. The modular construction easily adapts to the diverse requirements of sample analysis without great modifications. The versatility and flexibility of such a combination are illustrated with different applications.

INTRODUCTION

The identification of trace components in complex mixtures is a fundamental problem in chromatography. In the field of aroma and pheromone research, for example, samples are frequently characterized only because of the presence of minor components with physiological activity¹. As these substances are often masked by co-eluting major components, one-dimensional high-resolution gas chromatographic (GC) analysis is insufficient to resolve them. Therefore, when dealing with trace components in complex mixtures, the use of multi-dimensional techniques (*e.g.*, abbreviated to GC²) is necessary to increase the information derived from a chromatographic analysis. The capability to produce on-line in a single run two independent sets of retention data is a second major benefit².

In combination with mass spectrometry (MS), an efficient system for structure elucidation is obtained. Simultaneous “sniffing” of the column effluent with the sensitive human nose is a powerful extension for the localization of sensorial active trace compounds^{3,4}. Although MS provides, in addition to molecular weight and chemical composition data, structural information which is sometimes sufficient for the characterization of a substance, additional spectroscopic data (IR, NMR, UV) are required for chemical structure assignment, especially when dealing with unknown substances. Therefore, the isolation and enrichment of individual components at trace levels is

also necessary (micro-scale preparative GC)⁵. A modular-type construction that can easily be adapted for different instrumentation (single column, GC² with packed-capillary or capillary-capillary columns) is preferable⁶. Depending on the analytical problem to be solved and the amounts of substance available, facilities for both thermal desorption and solvent elution analysis of enriched column effluent are desirable.

Finally, the kind of sample material for analysis remains to be considered. The interesting and significant components occur in different homogeneous or heterogeneous gas, solid or liquid matrices, from which they have to be isolated, as most matrices are not compatible with GC. Therefore, different sampling techniques have been developed. Examples of the types of sample introduction include split-splitless and on-column liquid injection, equilibrium headspace, dynamic headspace and direct thermal desorption analysis. Such sampling procedures, combined with multi-dimensional GC, micro-scale preparative enrichment and "sniffing"-MS monitoring, substantially improve the identification and determination of sensorial active trace components in complex mixtures. Examples of applications to demonstrate the potential of such combinations are described in this paper.

SYSTEM DESCRIPTION AND OPERATION

A simplified schematic diagram of the combinations available with a single double-oven gas chromatograph is shown in Fig. 1. Solvent extracts can be introduced by liquid injection (split-splitless, on-column) with a programmable temperature vaporizer (PTV). Volatiles from solid or liquid samples are enriched by means of gas extraction on a cold-trap and thermally desorbed into the chromatographic column (dynamic headspace). For samples obtained by the concentration of large volumes of gases or the enrichment of selected cuts of column effluents on adsorbing traps, the introduction of the sample is achieved with a modified PTV (for focussing purposes) and a device for thermal desorption.

The separation stage consists of two columns of different polarities, coupled directly with a Live-T switching device or a total transfer system (cold trapping of a

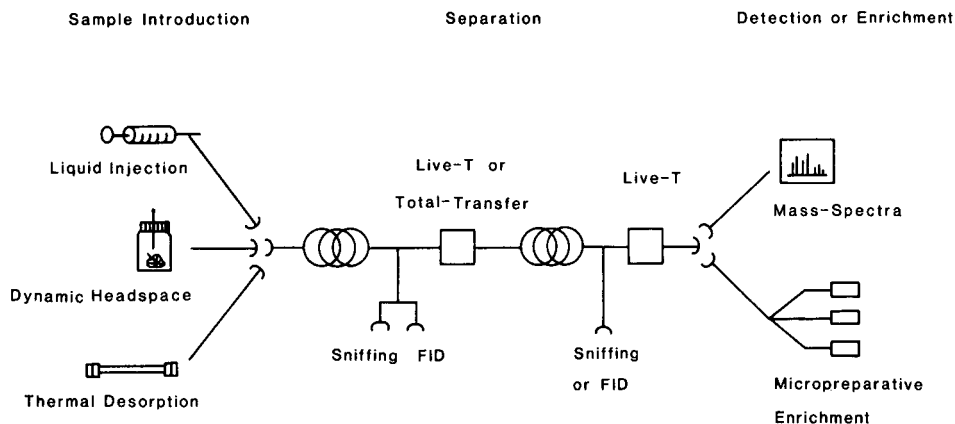


Fig. 1. Schematic diagram of the analytical system.

selected cut or cuts from the first column before transfer into the second column). Each column effluent is connected to a "sniffing mask" and a flame-ionization detector; the end of the second column is coupled to the mass spectrometer or a micro-preparative system by means of a second Live-T switching device.

Liquid injection

The system description and operation need no explanation within the scope of this contribution.

Dynamic headspace

A schematic diagram of the system used for enrichment of headspace volatiles and multi-dimensional analysis is shown in Fig. 2. Extraction of volatile components is achieved by stripping the headspace vial (8-ml capacity) with a constant flow of helium (30 ml/min) followed by cryogenic concentration in a cooled trap packed with Tenax TA (-20°C) or 5% OV-101 on Chromosorb W (-130°C). The total purging volume can be adjusted by time programming solenoid valve SV_3 . During this sampling period breakthrough of substances into the first column is avoided by actuating SV_1 , thus maintaining the preselected column pressure (adjustment with pressure regulator PM_4) and establishing a minor gas flow through a restriction capillary into the aforementioned trap (Fig. 3). The sampling period is interrupted by closing SV_1 and SV_3 . The gas flow in the trap is reversed by actuating SV_1 and enriched volatiles are introduced into column 1 by thermal desorption (Fig. 4). After admittance into the column, the original column pressure is re-established by operating SV_1 again.

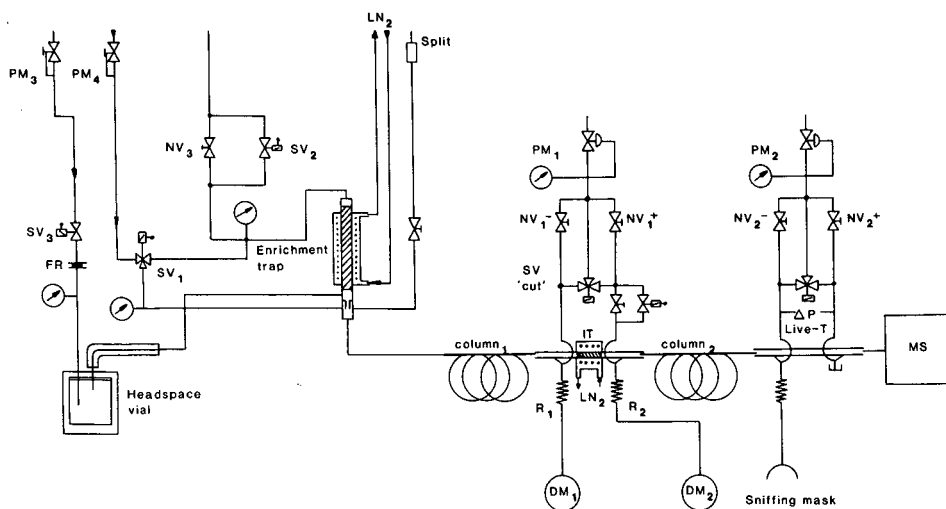


Fig. 2. Schematic diagram of dynamic headspace combined with multi-dimensional GC. PM_1 - PM_4 = pressure regulators; R_1 - R_3 = restriction capillaries; SV_1 - SV_3 = solenoid valves; FR = flow regulator; NV_1 - NV_3 = needle valves; DM_1 , DM_2 = flame ionization detectors; LN_2 = liquid nitrogen; IT = intermediate trap.

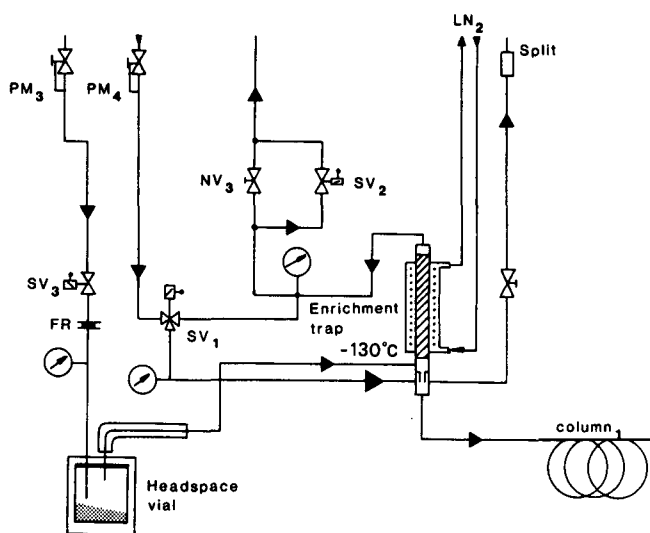


Fig. 3. Gas and substance flows during sampling.

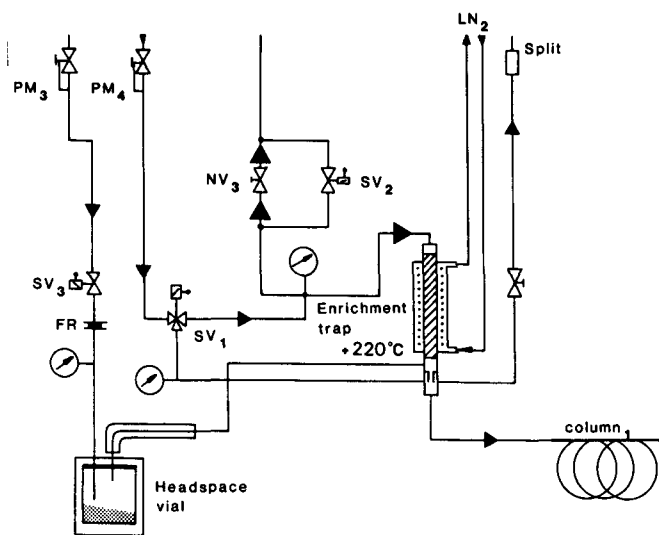


Fig. 4. Gas and substance flows during thermal desorption.

Thermal desorption system

Intermediate trap. For intermediate trapping of the desorbed volatiles, a modified programmable temperature vaporizer (Siemens PTV) was used. The following modifications were necessary. The original septum connector was replaced with a trap connector which accommodates the desorption oven and the desorption trap (Fig. 5). The capillary glass insert (4 cm longer than the original) was filled with 5% OV-101 on Chromosorb W and plugged at both ends with silanized glass-wool.

Before heating the desorption oven, the intermediate trap is cooled with liquid nitrogen to -150°C . For desorption, the carrier gas is closed and the desorption gas

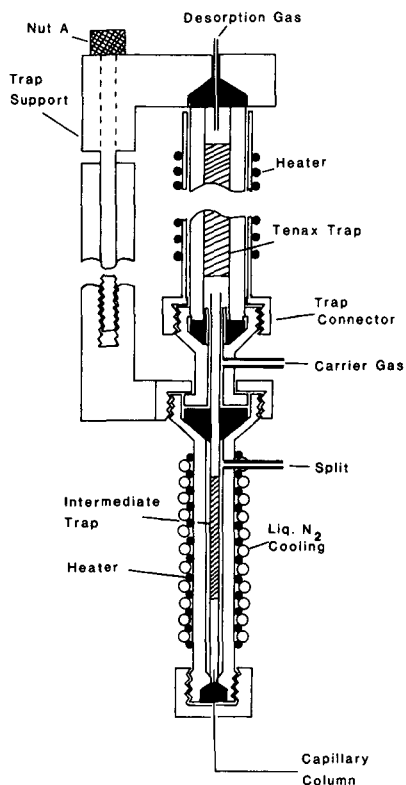


Fig. 5. Construction of thermal desorption system coupled to PTV injector for intermediate trapping.

is opened. During this step, the open split vent allows the components to desorb at high flow-rates, thus reducing the desorption time. When the condensation in the intermediate trap is complete, the split vent is closed and the trap is heated to the preset temperature within a few seconds. At the same time the desorption gas is closed and carrier gas is opened. The gas chromatograph has built-in facilities for timing the split valve open–close functions and for the carrier and desorption gas on–off functions.

Desorption device. A cross-sectional view of the desorption device is shown in Fig. 5. The traps (glass tubes, 100 mm × 5 mm O.D. × 3 mm I.D.) are held in place and sealed by pressing them against the PTFE ferrules integrated in the trap support and the trap connector. This is accomplished by tightening the nut A. An insulated cylindrical heating device with integrated thermocouple allows the temperature to be regulated up to 300°C.

Micro-preparative system

The chromatographic and pneumatic configuration for multi-dimensional operation is shown in Fig. 6. The gas chromatograph, equipped with an automatic injection device, is operated by the integrated microprocessor. The sample is injected into the first column where a pre-separation is achieved. By means of the valveless

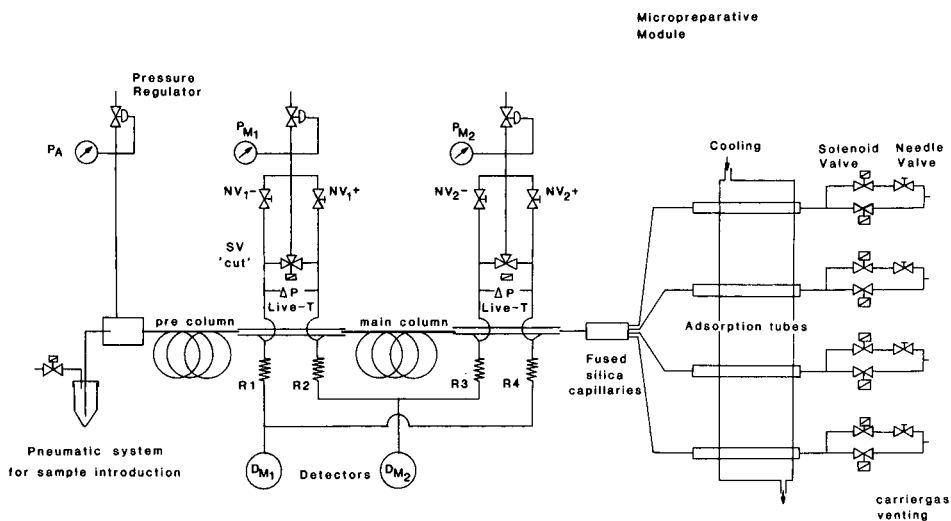


Fig. 6. Schematic diagram of multi-dimensional GC system coupled to micro-preparative system.

Live-T column-switching system, only the peak group of interest is entirely transferred to the main column without any sample loss. After final separation on the main column, the substances to be isolated are directed to the cooled traps by means of a second Live-T switching device. As can be seen in Fig. 6, the column effluent can be switched between the detector and a multiple channel manifold. Each channel of the manifold is connected to the trap, their exits being connected to solenoid valves. Manual operation of the aforementioned device is also possible. Three different flow conditions through the traps are encountered during operation:

Cut mode: (1) high flow, 10 ml/min (through the activated trap); (2) no flow, 0 ml/min (through the non-activated traps).

Stand-by mode: (3) low flow, 0.3 ml/min (through all traps to avoid back-diffusion).

In the cut mode, substances are transferred to the corresponding activated trap; in the stand-by mode, substances are diverted to the monitoring detector. The solenoid valves are controlled by means of the gas chromatograph's microprocessor, which provides high flexibility in term of sequencing. The temperature of the traps can be preset from room temperature to -80°C .

Apparatus

A Siemens Sichromat II double-oven gas chromatograph with autoinjector for liquid injection was used. The micropreparative module was of our own construction, as described⁶. The modified Siemens PTV⁷ and the modified Siemens headspace module⁸ have been described. The mass spectrometer was a Finnigan 4021 quadrupole instrument.

APPLICATIONS

The following applications were selected to demonstrate the advantages and possibilities of the described system for the determination of sensorial active trace compounds.

Analysis of a "musty-earthy" off-flavour in wheat grains

The development of microflora on cereal grains results in the appearance of various volatiles and different odours^{9,10}. We investigated wheat grains exhibiting a "musty-earthy" odour, which showed a higher bacterial and mould infection compared with sound grains¹¹. A pre-chromatogram with simultaneous "sniffing" registration obtained by liquid injection of a pentane-diethyl ether (1:1) extract is shown in Fig. 7. The compounds responsible for the off-flavour are masked by major components of the sample. For identification of both substances, GC² with a megabore pre-column (SE-54, 5- μ l injection volume) and cold trapping of selected cuts (at the retention times of the sniffing impressions marked in Fig. 7) was necessary, before separation on the analytical column (Carbowax 20M). The reconstructed ion chromatogram of the aforementioned cuts is shown in Fig. 8. Sniffing-MS monitoring and comparison with authentic reference substances showed that 2-methylisoborneol (1 ppb) and geosmine (17 ppb) are the trace compounds responsible for the off-flavour.

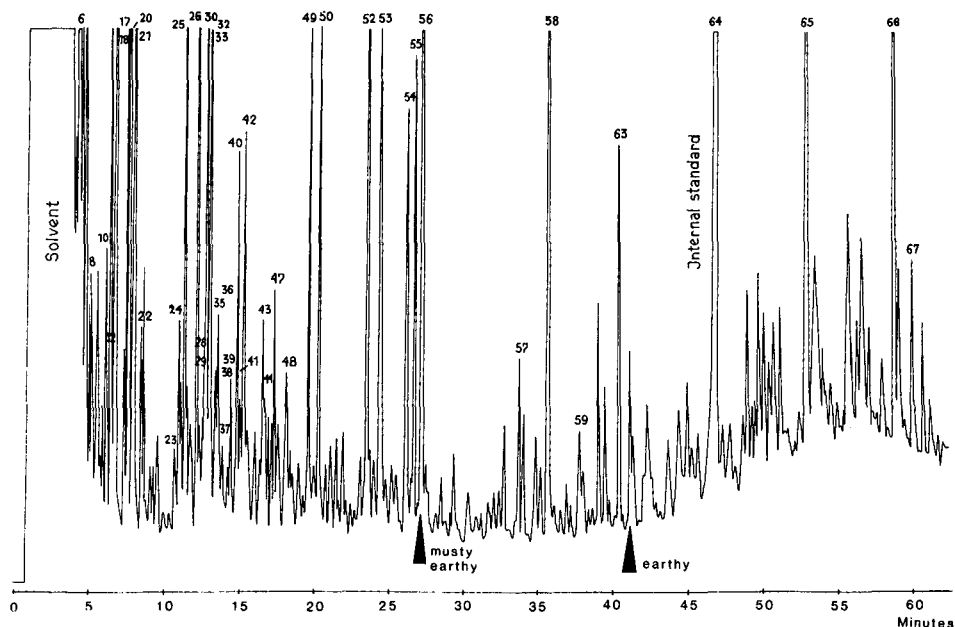


Fig. 7. Gas chromatogram of volatiles from wheat grain with "musty-earthy" odour (arrows show the retention ranges of sensorial interest).

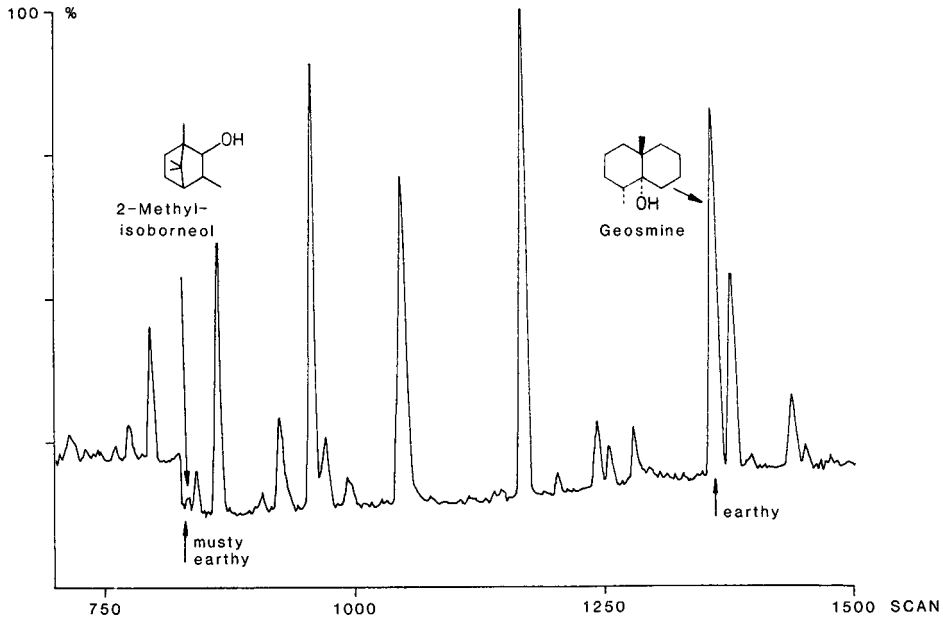


Fig. 8. Sniffing-MS trace of selected cuts of volatiles of wheat grain with "musty-earthy" odour from pre-column 1 (SE-54, two cuts) separated on the main column 2 (Carbowax 20M).

Analysis of a "peasy" off-flavour in coffee beans

Coffee defects derived from moulds, overfermentation, insects or other factors often considerably impair the flavour of the roasted end product. Certain African coffee beans with an off-flavour, known among experts as "peasy", were investigated¹².

In this instance the major advantages of the system are exploited to a large extent: determination of trace volatiles in a complex matrix without clean-up procedures, small sample amounts (only three coffee beans), adjustable enrichment effect due to continuous gas extraction conditions and cryofocusing, heart-cutting of off-flavour-related peaks by means of GC² and identification of the responsible compounds by simultaneous sniffing-MS.

The aforementioned analytical steps are summarized in Fig. 9. The enriched coffee headspace and the heart-cuts at the retention times corresponding to the elution of the "peasy" compounds are shown in Fig. 9A. The chromatograms of the cuts from column 1 (Carbowax 20M) on column 2 (SE-54) for three normal and three defective coffee beans are shown in Fig. 9B and C, respectively. Whereas 2-methoxy-3-isobutylpyrazine is present in nearly equal amounts in both samples, 2-methoxy-3-isopropylpyrazine is markedly increased (10-fold) in the defective beans, and has to be considered as responsible for the off-flavour. Overloading of the first column in this instance is of secondary importance, as the main separation is performed on column 2 with a preselected cut.

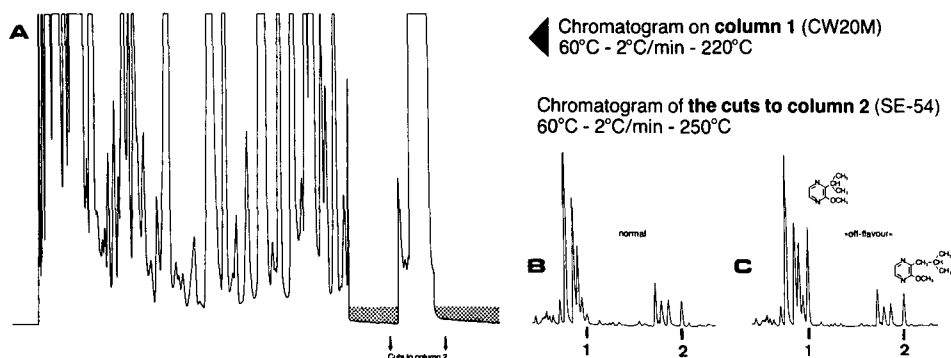


Fig. 9. (A) Headspace of defective coffee beans on column 1; (B) selected cut of a normal coffee bean on column 2; (C) selected cut of a defective coffee bean on column 2. Odorous compounds identified (simultaneous sniffing-MS): 1 = 2-methoxy-3-isopropylpyrazine ("peasy" odour); 2 = 2-methoxy-3-isobutylpyrazine ("bellpepper" odour). Compound 1 was identified as responsible for the "peasy" off-flavour. Sample, 3 coffee beans (≈ 300 mg); sampling, 5 min at 80°C.

Analysis of an "obnoxious rotten" odour of a car mat

The automobile industry is often confronted with customer claims concerning offensive and pungent odours in new cars. The source of the substances responsible for the odour is plastics and synthetic materials. These compounds are present in very low concentrations and their release is markedly increased in summer owing to sun irradiation. The identification of the substances is also of interest in the fields of toxicology and environmental chemistry, as they constitute an additional source of human exposure to abiotic and possibly noxious chemicals.

In the present instance we investigated a felt-coated rubber mat principally to identify the odorous trace components. The chromatogram obtained after direct thermal desorption of 500 ml of enriched headspace (from 10 g of mat at 80°C) on Tenax TA is shown in Fig. 10. The usefulness of smell analysis is illustrated by the

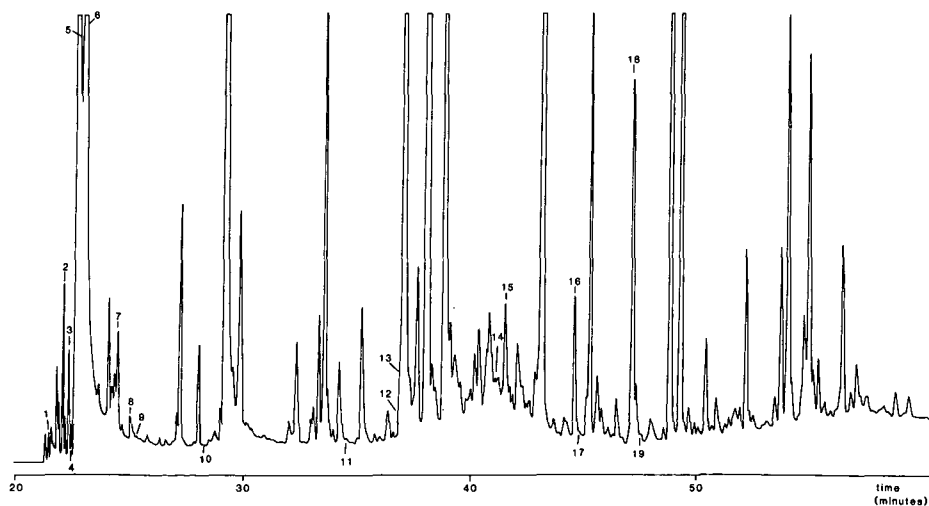


Fig. 10. Gas chromatogram of volatiles from a car mat on column 1 (SE-54).

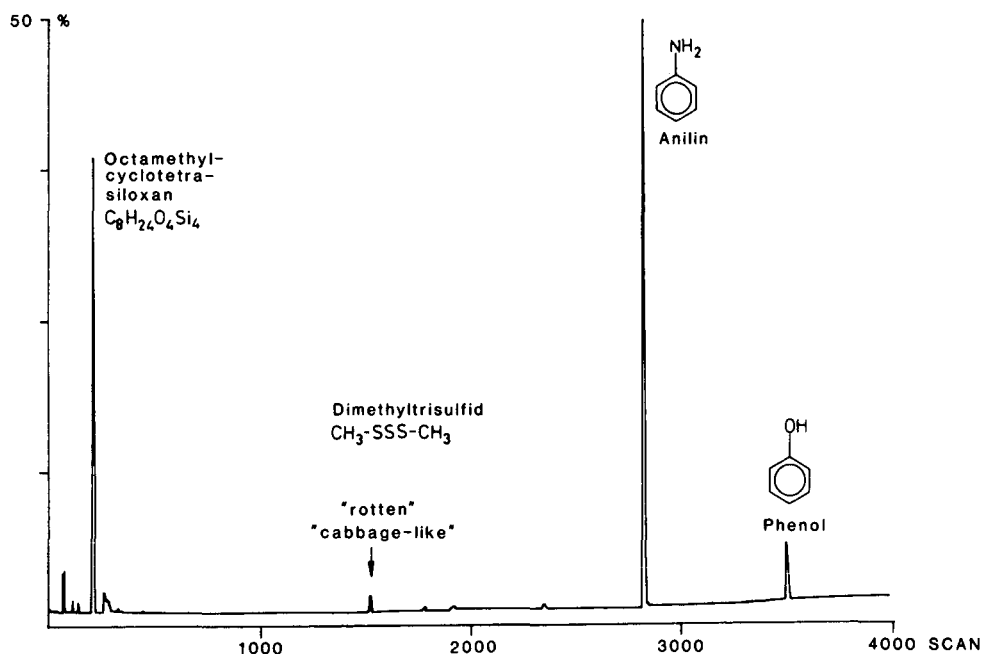


Fig. 11. Sniffing-MS trace of a selected cut (peak 13) of volatiles from a car mat on column 2 (Carbowax 20M).

fact that compounds present in small amounts, totally or partially masked by major components, can be characterized by this technique. It can be seen from Fig. 10 also that reliable identification without additional separation is impossible. Therefore, dynamic headspace (which allows on-line repetitive sampling) combined with GC² and sniffing-MS monitoring was applied for identification purposes. The analysis of a composite peak consisting of several components is discussed as an example.

A smell resembling the general odour impression of the car mat was observed at peak 13 (see Fig. 10). The MS analysis revealed that at least four components were present in that peak, the major one being aniline. It was clear that the rotten cabbage-like odour could not be attributed to this substance. The chromatogram of a selected cut of this peak from column 1 on column 2 is shown in Fig. 11. Smell analysis and MS monitoring revealed that the minor component (dimethyl trisulphide) was responsible for the perceived odour; the siloxane, aniline and phenol were odourless at these concentrations. The results obtained by performing selected heart-cuts at the corresponding retention times of elution of sensorial active compounds, separation on a second analytical column and subsequent smell assessment and MS registration are summarized in Table I.

The results indicate that the composite smell of the car mat can be principally attributed to sulphur compounds and alkyl isocyanides. Especially methanethiol and dimethyl trisulphide have low odour threshold values and have been reported to possess a pheromone character for polecat, mink and skunk¹³.

TABLE I
ODOROUS COMPONENTS IN A CAR-MAT

Peak No. ^a	Compound ^b	Odour description
1	Methanethiol	Putrid
2	Dimethyl sulphide	Cabbage, cooked vegetable
3	Carbon disulphide	Putrid, pungent, vegetable
4	2-Methylpropanal	Milky, chocolate
5	2,3-Butanedione	Butter-like
6	Diethylamine	Fish-like
7	n.i.	Chocolate
8	Propyl? isocyanide	Repulsive, obnoxious
9	Ethyl acrylate	Like plastic
10	n.i.	Like plastic
11	n.i.	Sweet, nutty
12	1-Octen-3-one?	Fungal
13	Dimethyl trisulphide	Typical mat, cabbage-like
14	n.i.	Burnt, nutty
15	n.i.	Soap-like
16	n.i.	Plastic
17	Tetralin	Burnt vegetable
18	Benzothiazole	Typical mat, plastic
19	n.i.	Herbaceous

^a Peak Nos. according to Fig. 10.

^b n.i. = Not identified.

Isolation of components from parsley oil

1,3,8-*p*-Menthatriene and the corresponding aromatized terpene (α ,*p*-dimethylstyrene) were isolated from parsley oil (Fig. 12), applying GC² combined with automated liquid injection and micro-preparative enrichment of the capillary GC effluents⁶. The first component was required for photochemical studies¹⁴ and the second for unequivocal identification by NMR. Although the Kováts retention index of 1092 (100°C) on SE-54 is consistent with that (1080 on OV-101) of α -*p*-dimethylstyrene reported by Jennings and Shibamoto¹⁵, the retention index was different to the value of 1277 (100°C) on OV-101 found by Swigar and Silverstein¹⁶. The same was observed for the Kováts retention index on Carbowax 20M of 1491 (100°C) when compared with the value given by Jennings and Shibamoto (1278 on Carbowax 20M). The mass and ¹H NMR spectra obtained from the enriched substance confirmed the postulated structure; the retention data reported in the literature have to be corrected.

The chromatographic parameters, column load and amount and purity of the isolated components are given in Table II as an example.

As can be seen from Table I, the purity of the isolated compounds is fairly good, although the column load selected was near the overloading limit of wide-bore capillaries. These operating conditions were deliberately chosen in order to achieve maximum efficiency (maximum throughput per unit time) and to demonstrate that in this extreme situation, the resolution losses can be overcompensated by means of multi-dimensional operation (in this instance the combination of two columns with different polarities).

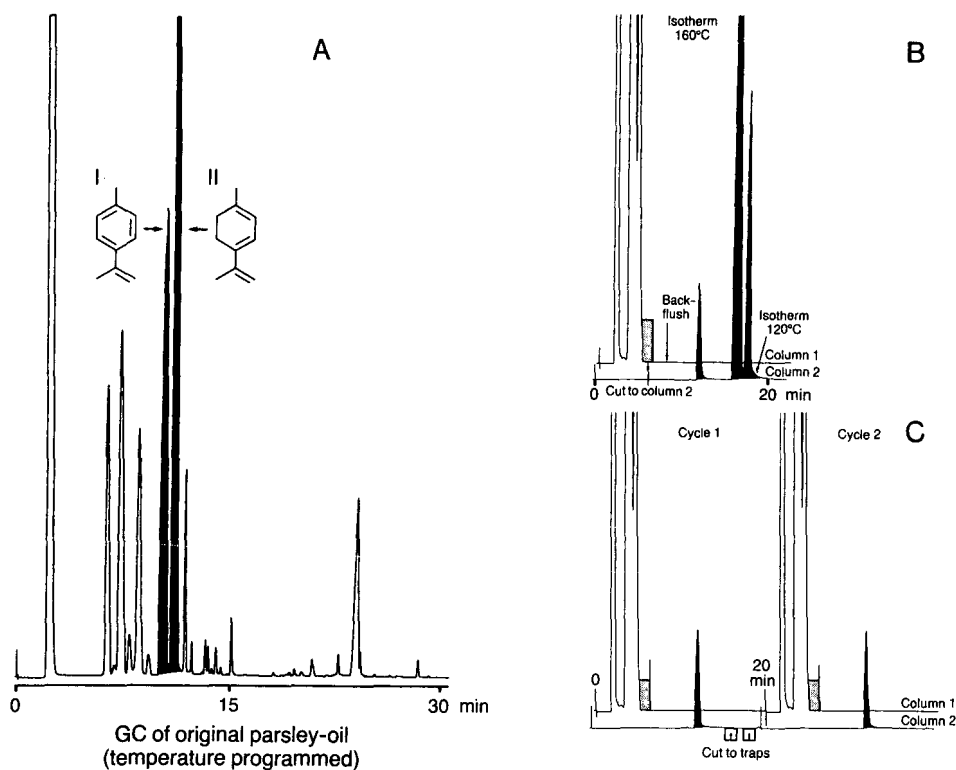


Fig. 12. (A) Chromatogram of parsley oil, temperature programmed. (B) Chromatogram of parsley oil on column 1 (isothermal) and cut chromatogram on column 2 (isothermal). (C) Same as (B), but with cut of eluents from column 2 into traps. Peak 1 = α -*p*-dimethylstyrene; peak 2 = 1,3,8-*p*-menthatriene.

TABLE II

ANALYTICAL PARAMETERS AND YIELDS OF COMPOUNDS ISOLATED FROM PARSLEY OIL

GC parameters:

Column 1: 30 m \times 0.4 mm I.D., SE-54, film thickness 2 μ m. Carrier gas: helium at 25 cm/s. Temperature: 160°C.

Column 2: 30 m \times 0.53 mm I.D., Carbowax 20M, film thickness 2 μ m. Carrier gas: helium at 23 cm/s. Temperature: 120°C.

Concentration of components in undiluted sample to be isolated: I, 18,2%; II, 32,8%.

Sample volume per cycle: 1 μ l [25% parsley oil in pentane-diethyl ether (1:1)].

No. of cycles: 40.

Separation time per cycle: 20 min.

Total analysis time: 13.3 h.

Trap material: Tenax TA.

Trap temperature: -28°C.

Yields of isolated compounds:

I: 1.6 mg (purity 98.5%)

II: 3 mg (purity 99.2%)

Recovery:

>90% for both substances

REFERENCES

- 1 G. Ohloff, *Helv. Chim. Acta*, 65 (1982) 1785.
- 2 G. Schomburg, H. Husmann, L. Podmaniczky and F. Weeke, in P. Schreier (Editor), *Proceedings of International Workshop, Analysis of Volatiles, Würzburg, 1983*, Walter de Gruyter, Berlin, New York, 1984, pp. 121–150.
- 3 S. Nitz and F. Drawert, *Chromatographia*, 22 (1986) 51.
- 4 M. Verzele, P. Sandra, T. Saced, G. Redant, M. Godefroot and M. Verstappe in W. Bertsch, W. G. Jennings and R. E. Kaiser (Editors), *Recent Advances in Capillary Gas Chromatography*, Vol. 3, Hüthig, Heidelberg, Basle, New York, 1982, pp. 523–541.
- 5 J. Roeraade, S. Blomberg and H. D. J. Pietersma, *J. Chromatogr.*, 356 (1986) 271.
- 6 S. Nitz, F. Drawert, M. Albrecht and U. Gellert, *J. High Resolut. Chromatogr. Chromatogr. Commun.*, 11 (1988) 322.
- 7 S. Nitz, F. Drawert and O. Schlarp, in preparation.
- 8 S. Nitz, H. Kollmannsberger and F. Drawert, in P. Schreier (Editor), *Proceedings of Bioflavour 87*, Walter de Gruyter, Berlin, New York, 1988, pp. 123–135.
- 9 S. Stawicki, E. Kaminski, A. Niewiarowicz, M. Trojan and E. Wasowicz, in J. L. Multon and A. Guilboud (Editors), *Preservation of Wet Harvest Grain*, Institut National de la Recherche Agronomique, Paris, 1973, pp. 309–336.
- 10 E. Kaminski, E. Wasowicz, R. Zawirska-Wojtasiak and L. Gruchala, in I. D. Morton (Editor), *Cereals in a European Context*, Ellis Horwood, Chichester, 1987, pp. 446–461.
- 11 E. Wasowicz, E. Kaminski, H. Kollmannsberger, S. Nitz, R. G. Berger and F. Drawert, *Chem. Mikrobiol. Technol. Lebensm.*, 11 (1988) 161.
- 12 R. Becker, B. Döhla, S. Nitz and O. G. Vitzthum, in *Proceedings of the XII International Conference on Coffee Science, Montreux, 1987*, pp. 203–215.
- 13 *Ullmanns Encyclopedie der technischen Chemie*, Vol. 23, Verlag Chemie, Weinheim, 4th ed., 1983, p. 185.
- 14 S. Nitz and F. Drawert, in preparation.
- 15 W. Jennings and T. Shibamoto, *Qualitative Analysis of Flavor and Fragrance Volatiles by Glass Capillary GC*, Academic Press, New York, 1980.
- 16 A. A. Swigar and R. M. Silverstein, *Monoterpenes*, Aldrich, Milwaukee, WI, 1981, p. 30.

CHROM. 21 278

RELATIVE GAS-LIQUID CHROMATOGRAPHIC RETENTION FACTORS OF TRIMETHYLSILYL ETHERS OF DIRADYLGLYCEROLS ON POLAR CAPILLARY COLUMNS

J. J. MYHER and A. KUKSIS*

Banting and Best Department of Medical Research, University of Toronto, 112 College Street, Toronto M5G 1L6 (Canada)

SUMMARY

Gas-liquid chromatography (GLC) on polar capillary columns provides a highly reproducible resolution and quantitation of molecular species of diradylglycerols when analyzed as the trimethylsilyl (TMS) ethers. In the absence of peak collection and determination of fatty acids or mass spectrometry, peak identification is obtained on the basis of relative retention times of reference standards or of relative retention times calculated from the additive contributions of component fatty chains. Unlike simple esters, complex mixtures of diradylglycerols present special problems in GLC peak identification, which must be attended to by auxiliary separations prior to GLC analysis. In the present study the positional *sn*-1,2(2,3)- and X-1,3-isomers were resolved by borate thin-layer chromatography (TLC) while the alkenylacyl-, alkylacyl- and diacylglycerols were separated as their TMS ethers by normal-phase high-performance liquid chromatography. The diradylglycerol nature of the sample was further verified by GLC determination of the carbon number distribution, which must be consistent with the composition of the fatty chains of the sample. Under these conditions the identification and quantitation of the molecular species on the polar capillary columns was always consistent with the total fatty acid composition of the sample, as well as with the fatty acid composition of any argentation TLC fractions isolated from some of the samples prior to the polar capillary GLC. Due to the great complexity of the natural diradylglycerol mixtures some peak overlaps occurred, which were reflected in their relative retention times. Nevertheless, a determination of diradylglycerol peak identity from relative retention times proved very satisfactory provided the above described procedures were employed.

INTRODUCTION

The availability of polar capillary columns of high temperature stability now permits the resolution of molecular species of diradylglycerols with the ease of fatty acids¹⁻⁴. In comparison to the packed columns containing polyester^{5,6} and cyanoalkylpolysiloxane⁷ liquid phases, the polar capillary columns give shorter retention times at comparable oven temperatures and higher recoveries, while retaining the same overall order of elution of molecular species. The polar capillary columns have been

further improved by cross-bonding of the liquid phase, which has reduced the column bleed and improved overall performance. The polar capillary columns described by Geeraert and Sandra⁸ for the resolution of natural triacylglycerols on the basis of degree of unsaturation, and which have proved adequate for gas chromatography-mass spectrometry (GC-MS)⁹, however, are not suitable for the separation of polyunsaturated diacylglycerols in the form of trimethylsilyl (TMS) or *tert.*-butyldimethylsilyl (TBDMS) ethers, because of the adverse effects of the high temperature needed to maintain column polarity.

The high-resolution capillary columns yield a large number of major and minor peaks, which in the case of natural diacylglycerols require knowledge of fatty acid composition and in the case of the alkylacyl and alkenylacylglycerols also the knowledge of the alkylglycerol and dimethylacetal composition. Since peak collection is impractical in capillary gas-liquid chromatography (GLC) and MS not available in most laboratories, the peak identities must be established by comparison of the relative retention times of the unknowns to those of the reference compounds, which are difficult to prepare and impossible to purchase. The present report describes a variety of retention factors, which we have determined by reference to the few standard diacylglycerols, that are commercially available, or to secondary reference standards easily prepared in the laboratory. We have found them useful for the identification of the TMS ethers of natural diacyl, alkylacyl and alkenylacylglycerols.

EXPERIMENTAL

The structures of the compounds to be resolved are shown in Fig. 1. Compound 1 represents an *sn*-1,2-diacylglycerol, which is the major diacylglycerol moiety of

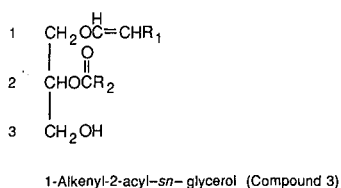
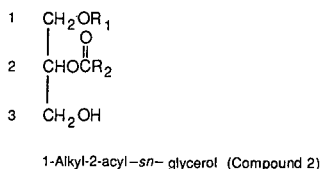
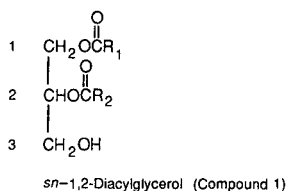


Fig. 1. General structures of diacyl-, alkylacyl- and alkenylacylglycerols.

natural glycerophospholipids. It usually contains a saturated fatty acid in the *sn*-1-position, while the 2-position is occupied by an unsaturated fatty acid. However, isomers, where the positional placement of the fatty acids is reversed, are also known. Compound **2** represents an *sn*-1-alkyl 2-acylglycerol, which is a minor diradylglycerol moiety in natural glycerophospholipids. The alkyl group is usually saturated, while the fatty acyl group is unsaturated. Compound **3** represents an *sn*-1-alkenyl 2-acylglycerol, which may also be a minor diradylglycerol moiety of natural glycerophospholipids, although in special instances it can represent the bulk of a natural glycerophospholipid class (*e.g.* ethanolamine phosphatide). The alkenyl groups may be saturated or oligo-unsaturated, while the fatty acid chains are oligo- and polyunsaturated. The alkyl and alkenyl groups are not known to occur in the 2-position of the diradylglycerol moieties of natural glycerophospholipids.

Sources of diradylglycerols

The natural diradylglycerols used in the compilation of the retention data were obtained as described in recent studies on the glycerophospholipids in human erythrocytes¹⁰ and plasma¹¹, rat intestinal mucosa¹² and soybean phosphatidylinositols⁴. Reference *sn*-1,2-diacylglycerols, *rac*-1,2-diacylglycerols and X-1,3-diacylglycerols containing the more common fatty acids were purchased from Serdary Research Labs. (London, Canada; Supelco, Bellefonte, PA, U.S.A.; and Sigma, St. Louis, MO, U.S.A.). Other *sn*-1,2- and *sn*-2,3-diacylglycerols of known composition were synthesized in the laboratory¹³. Secondary reference *sn*-1,2(2,3)-diacylglycerol standards were obtained by Grignard degradation of randomized mixtures of synthetic and natural triacylglycerols¹.

Preparation of derivatives

It is important to avoid even a minimal conversion of the *sn*-1,2-diradylglycerols to 1,3-isomers during trimethylsilylation because these compounds may overlap and interdigitate during GLC separation of the TMS ethers. We have found that the formation of 1,3-isomers is avoided if the *sn*-1,2-diradylglycerols are silylated with trimethylchlorosilane in the presence of hexamethyldisilazane and pyridine as described². Alkylglycerol diacetates are prepared with acetic anhydride-pyridine (1:1, v/v) after transmethylation of the alkylacylglycerol TMS ether with 1 *M* sodium methoxide in methanol-toluene (3:2, v/v) for 15 min at 20°C¹⁰. The identity of the reference compounds and of the major diradylglycerols in the natural mixtures was confirmed by MS^{2,13,14}.

Resolution of diradylglycerol subclasses

It is important to avoid even a minimal cross-contamination of the *sn*-1,2-diacylglycerols with the *sn*-1,2-alkylacyl- and *sn*-1,2-alkenylacylglycerols because some of the members of these classes of compounds tend to overlap and interdigitate during the GLC separation of the TMS ethers. It was found that the natural diradylglycerols are readily resolved into the alkenylacyl-, alkylacyl- and diacylglycerols, when run as the TMS ethers using high-performance liquid chromatography (HPLC) on a Supelco sil LC-Si-15 (5 μ m) column (250 mm \times 4.6 mm I.D.) with 0.3% isopropanol in hexane (1 ml/min)¹⁰⁻¹². Total running time was 10 to 15 min at 30°C. The peaks were detected at 214 nm.

GLC analyses

Diradylglycerol TMS ethers and alkylglycerol diacetates were resolved principally on the basis of carbon number using a fused-silica capillary column (8 m × 0.32 mm I.D.) coated with bonded SE-54 liquid phase. Samples were injected on-column and temperature was programmed in four ramps from 40 to 350°C as described¹⁴. The molecular species were separated according to carbon number and degree of unsaturation on a fused-silica capillary column (15 m × 0.32 mm I.D.) coated with cross-bonded RTx 2330 (Restek, Port Matilda, PA, U.S.A.). Diradylglycerol TMS ethers were separated isothermally at 250 or 260°C using a split injector (split ratio, 7:1). Some analyses were made using a 15 m × 0.32 mm I.D. fused-silica column coated with stabilized SP 2380 (Supelco). All the samples were analyzed on a Hewlett-Packard Model 5880 gas chromatograph equipped with a hydrogen flame ionization detector and a Level IV microprocessor. The carrier gas was hydrogen at 2 p.s.i. or 3 p.s.i. head pressure.

Calculation of relative retention times

The calculated relative retention times for any combination of fatty chains in a diradylglycerol molecule were obtained by computing retention factors, as described under Results and discussion. These could be used as multiplication factors for the estimation of theoretical retention times for any diradylglycerol containing the corresponding fatty chains.

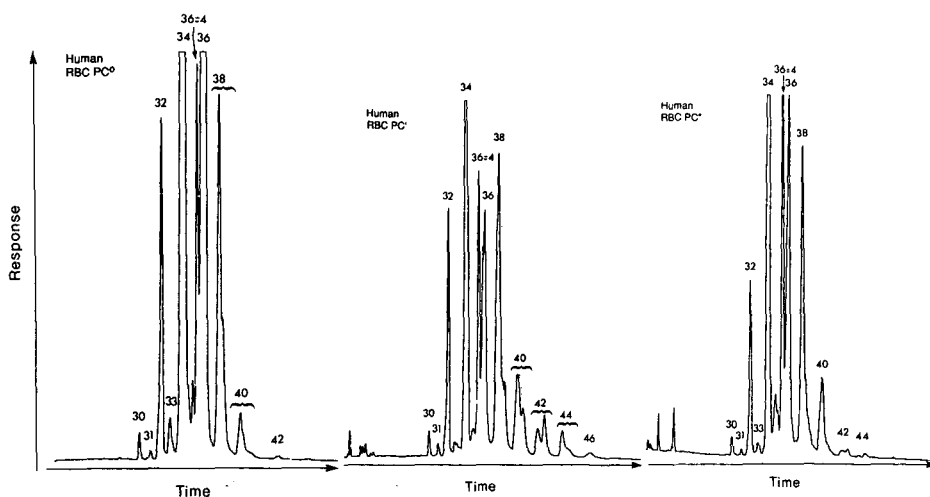


Fig. 2. Carbon number resolution of diacyl (PC^0), alkylacyl (PC^1) and alkenylacyl (PC^2) glycerol moieties of human red cell diradylglycerophosphocholine. GLC conditions: column, 8 m × 0.32 mm I.D. fused-silica capillary coated with cross-linked 5% phenylmethylsilicone (HP-5), 0.17 μ m film thickness; carrier gas, hydrogen, 6 p.s.i.; instrument and other operating conditions as given in text. Sample: diradylglycerol TMS ethers. Peaks are identified by the number of carbons in the two radyl moieties. The peak containing the species 16:0–20:4 ω 6 is indicated as 36:4.

RESULTS AND DISCUSSION

Retention on non-polar columns

Fig. 2 shows the separation obtained on a non-polar capillary column for the TMS ethers of the diacyl-, alkylacyl- and alkenylacylglycerol moieties of the choline phosphatides of human red cells. Although each of the subclasses of diradylglycerols yields excellent peak resolution with full baseline separation, there is considerable overlapping and shouldering when the diradylglycerols are run as a mixture. Extensive peak overlapping occurs also between the *sn*-1,2- and X-1,3-diradylglycerols in a mixture. Table I gives the absolute retention times (in minutes) for the *sn*-1,2-diradylglycerols in the 30–46 carbon range. The presence of polyunsaturated species within a carbon number resulted in a doublet with the unsaturated species being eluted ahead of the saturated ones. It is seen that the diacylglycerol species are retained longer than the alkylacylglycerol species, which are retained longer than the alkenylacylglycerol species of the same carbon number. Although the principle of elution is different, the order is similar to that noted on normal-phase HPLC, where the alkenylacylglycerol species also are eluted first and diacylglycerol species last.

Retention on polar columns

Fig. 3 compares the elution patterns obtained on two polar capillary columns for the TMS ethers of the diacylglycerol moieties of total phosphatidylcholine of rat liver. Both columns, which are presently commercially available, give about the same resolution and elution order of the components, indicating closely similar polarities. Similar polarities were also evident from the elution order of standard and natural (menhaden oil) mixtures of fatty acid methyl esters, although the absolute retention times were slightly different on the two columns. Table II gives the mean relative retention times and standard deviations (S.D.) as determined for the *sn*-1,2-diacylglycerol species from a variety of sources along with the calculated relative retention

TABLE I
ABSOLUTE RETENTION TIMES OF SELECTED *sn*-1,2-DIRADYLGLYCEROLS ON A NON-POLAR CAPILLARY COLUMN (SE-54)

Carbon number	Diradylglycerols		
	Diacyl	Alkylacyl	Alkenylacyl
30	9.57	9.30	9.1
32	10.34	10.1	9.82
33	10.72		
34	11.16	10.82	10.60
36:4	11.78	11.41	11.21
36:(1-3)	11.94	11.60	11.41
38	12.56	12.19	12.04
40	13.36	13.00	12.84
42 ^a		13.9	13.61
44 ^a		14.95	14.57
46 ^a		16.0	15.65

^a Unsaturated part of doublet.

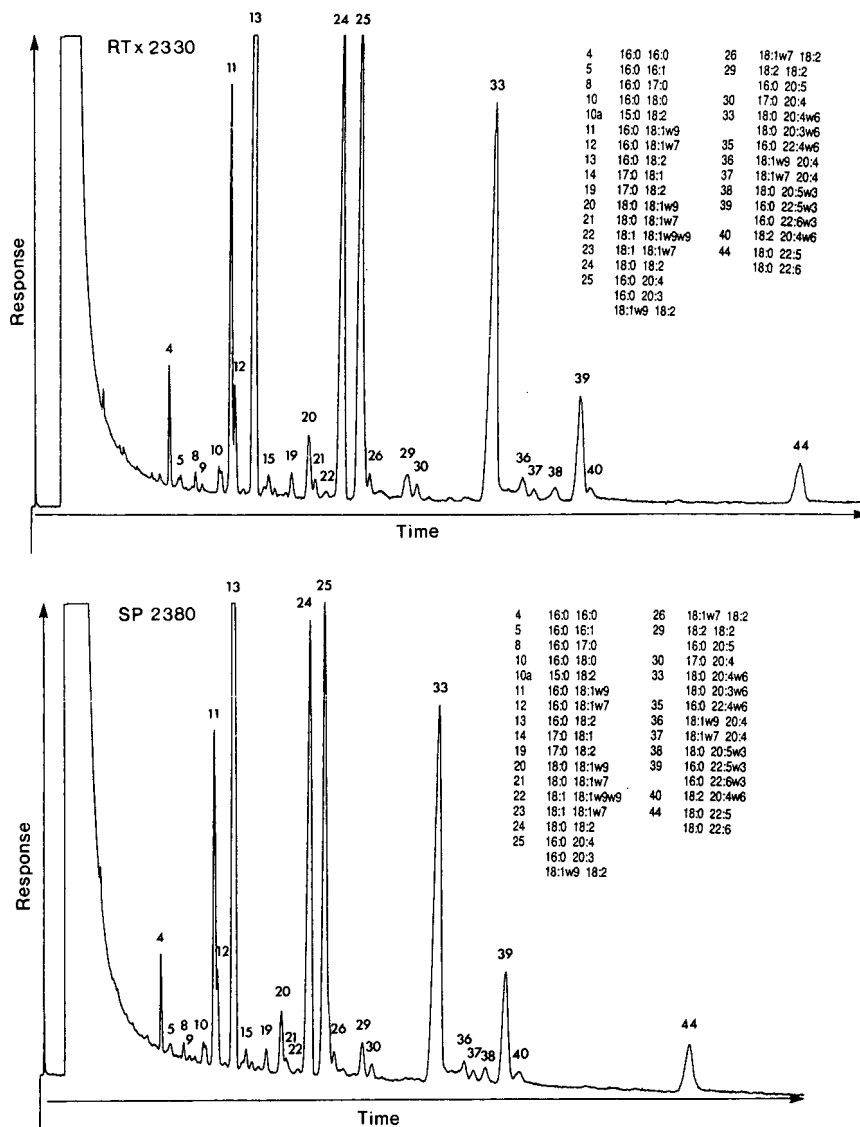


Fig. 3. Polar capillary GLC profiles of the diacylglycerol moieties of rat liver phosphatidylcholine on RTx-2330 and SP 2380 columns. GLC conditions: first column, 15 m \times 0.32 mm I.D. fused-silica capillary coated with cross-bonded RTx-2330 (Restek); second column, 15 m \times 0.32 mm I.D. fused-silica capillary coated with cross-bonded SP 2380 (Supelco); carrier gas, hydrogen, 3 p.s.i.; temperature, 250°C, isothermal; instrument and other operating conditions as given in text. Sample: 1 μ l of 0.1% diacylglycerol TMS ethers in hexane. Split ratio: 7:1.

times for the RTx-2330 column. The standard deviations are very small and range from 0.001 to 0.005, attesting to a high reproducibility of the runs at least over short periods of time. There is a close agreement between the determined and the calculated

TABLE II
RELATIVE RETENTION TIMES OF SELECTED MOLECULAR SPECIES OF *sn*-1,2-DIACYL-
GLYCEROLS ON A POLAR CAPILLARY COLUMN (RTx-2330)

Peak No.	Molecular species	Relative retention time		
		Mean	S.D.	Calculated ^a
1	14:0-16:0	0.445	0.01	0.445
	15:0-16:0			
4	16:0-16:0	0.636	0.01	0.635
5	16:0-16:1 ω 7	0.710	0.01	0.710
8	14:0-18:2 ω 6	0.781	0.01	0.768
9	15:0-18:1	0.825	0.01	0.789
10	16:0-18:0	0.931	0.003	0.928
10a	15:0-18:2	0.948	0.003	0.943
11	16:0-18:1 ω 9	1.000	0.000	0.997
12	16:0-18:1 ω 7	1.025	0.002	1.021
13	16:0-18:2 ω 6	1.135	0.003	1.126
14	17:0-18:1	1.204	0.005	1.205
15	16:1-18:2	1.234	0.004	1.259
18	16:0-18:3	1.338	0.004	1.328
	18:0-18:0	1.332	0.006	1.357
19	17:0-18:2	1.358	0.004	1.362
20	18:0-18:1 ω 9	1.452	0.003	1.457
21	18:0-18:1 ω 7	1.490	0.005	1.492
22	18:1 ω 9-18:1 ω 9	1.557	0.005	1.564
24	18:0-18:2	1.633	0.006	1.646
25	16:0-20:4	1.748	0.008	1.723
	18:1 ω 9-18:2	1.763	0.009	1.767
26	18:1 ω 7-18:2	1.807	0.007	1.810
	18:0-18:3	1.889	0.007	1.941
28		1.89	0.008	
29	16:0-20:5	2.018	0.008	1.963
	18:2-18:2	2.018	0.008	1.997
30	17:0-20:4	2.074	0.009	2.083
32		2.37	0.008	
	18:2-18:3	2.398	0.009	2.355
33	18:0-20:4 ω 6	2.487	0.012	2.519
34		2.540	0.007	
35	16:0-22:4 ω 6	2.604	0.013	2.570
36	18:1 ω 9-20:4 ω 6	2.698	0.010	2.704
37	18:1 ω 7-20:4 ω 6	2.761	0.012	2.770
38	18:0-20:5 ω 3	2.878	0.012	2.869
39	16:0-22:5 ω 3	3.017	0.016	2.967
	16:0-22:6 ω 3	3.017	0.016	
40	18:2-20:4 ω 6	3.093	0.015	3.080
	18:1 ω 9-20:5 ω 3	3.131	0.017	3.080
41a		3.578	0.014	
41	18:0-22:4 ω 6	3.726	0.016	3.757
	18:0-22:5 ω 6	3.825	0.019	
	18:1 ω 9-22:4 ω 6	4.017	0.018	4.033
	18:0-22:5 ω 3	4.273	0.020	4.337
	18:0-22:6 ω 3	4.273	0.020	4.337
	18:1 ω 9-22:5	4.646	0.020	4.656
	18:1 ω 9-22:6	4.646	0.020	4.656
	20:4 ω 6-20:4 ω 6			4.674
	18:2 ω 6-22:6 ω 3			5.262
	20:5 ω 3-20:5 ω 3			6.066

^a Calculated relative retention, $R_{AB} = F_A \cdot F_B$, where F_A and F_B are retention factors characteristic of fatty chains in *sn*-1- and *sn*-2-positions of the diradylglycerol molecule, respectively.

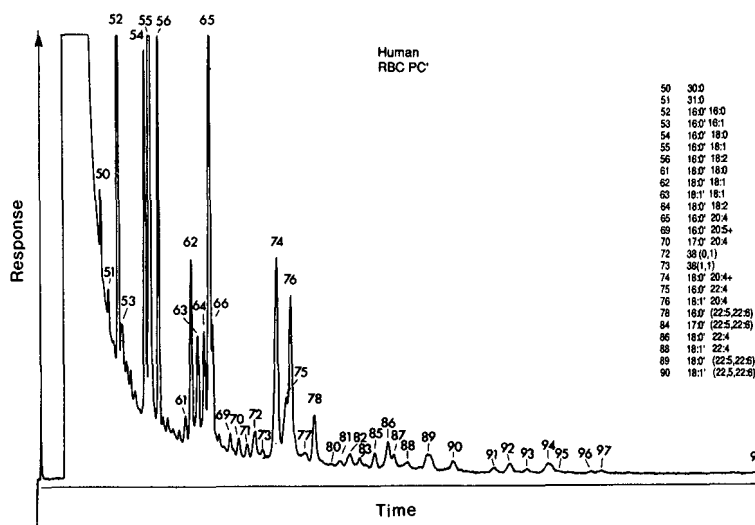


Fig. 4. Polar capillary GLC profile of the alkylacylglycerol moieties of human red cell alkylacylglycerophosphocholine. GLC conditions as given in Fig. 3 first column. Sample: 1 μ l of 0.1% diradylglycerol TMS ethers in hexane.

values, which indicates that the contributions to the free energy of interaction of the various acyl groups are independent and additive.

Fig. 4 shows the elution pattern obtained for the alkylacylglycerol moieties of the choline phosphatide of human erythrocytes. Table III gives the means and standard deviations determined for the RRT of the alkylacylglycerols from a variety of sources, along with the calculated relative retention times for the RTx-2330 column. Again the runs are readily reproduced as indicated by the small standard deviations (0.001–0.005). The agreement between the determined and calculated values was also close, which suggests that the alkyl groups contribute independently and additively to the total retention time of an alkylacylglycerol molecule.

Fig. 5 shows the elution pattern obtained for the alkenylacylglycerol moieties of the ethanolamine phosphatides from human erythrocytes. Table IV gives the means and standard deviations for the RRT of the alkenylacylglycerols from a variety of sources, along with the calculated values. There is good reproducibility of the retention times with the standard deviation ranging from 0.003 to 0.009, as well as a good agreement between the determined and calculated relative retention time values. Obviously, the alkenyl group also makes an independent and additive contribution to the total retention time of the alkenylacylglycerol molecule.

Fig. 6 shows the GLC separation on a polar capillary column of an isomerized sample of diacylglycerols containing approximately equal amounts of *sn*-1,2(2,3)- and X-1,3-isomers. We have calculated that the X-1,3-isomers are eluted later than the corresponding *sn*-1,2(2,3)-isomers by a factor ranging from 1.070 for the monoenes and dienes to 1.085 for the tetraenes and hexaenes.

The performance of the 15-m RTx-2330 columns was determined by calculating the Trennzahl from the measured retention times and peak widths of various homologous pairs of fatty acid methyl esters and diacylglycerols. The average

TABLE III
RELATIVE RETENTION TIMES OF SELECTED MOLECULAR SPECIES OF *sn*-1-ALKYL-2-ACYLGLYCEROLS ON A POLAR CAPILLARY COLUMN (RT_x-2330)

Peak No.	Molecular species	Relative retention time		
		Mean	S.D.	Calculated ^a
50	30:0	0.245	0.001	0.254
51	31:0	0.300	0.001	0.304
52	32:0	0.366	0.002	0.363
53				
54	34:0	0.542	0.002	0.531
55	16:0-18:1 ω 9	0.576	0.001	0.570
56	16:0-18:2 ω 6	0.634	0.002	0.644
57		0.665	0.002	
58	35:1	0.697	0.002	0.689
59		0.728	0.003	
60	35:2	0.769	0.003	0.779
61	36:0	0.813	0.004	0.776
62	18:0-18:1 ω 9	0.849	0.004	0.833
63	18:1 ω 9-18:1 ω 9	0.894	0.003	0.888
64	18:0-18:2 ω 6	0.938	0.004	0.941
65	16:0-20:4 ω 6	0.976	0.005	0.986
66		0.996	0.005	
69	16:0-20:5 ω 3	1.116	0.005	1.123
70	17:0-20:4 ω 6	1.174	0.005	1.191
71		1.228	0.004	
72	20:0-18:1	1.278	0.003	1.210
73	20:1-18:1	1.329	0.002	1.277
74	18:0-20:4 ω 6	1.429	0.003	1.440
75	16:0-22:4 ω 6	1.500	0.003	1.471
76	18:1 ω 9-20:4 ω 6	1.525	0.002	1.535
		1.551		
77	18:0-20:5 ω 3	1.619	0.003	1.640
78	16:0-22:5 ω 3	1.695	0.005	1.698
78	16:0-22:6 ω 3	1.695	0.005	1.698
79		1.732	0.004	
80		1.818		
81		1.863	0.004	
82		1.932	0.004	
83		1.992	0.003	
84		2.022	0.004	
85	20:0-20:4 ω 6	2.088	0.004	2.093
86	18:0-22:4 ω 6	2.176	0.005	2.148
87	20:1-20:4 ω 6	2.217	0.004	2.207
88	18:1-22:4 ω 6	2.307	0.005	2.290
89	18:0-22:5 ω 3	2.444	0.005	2.480
89	18:0-22:6 ω 3	2.444	0.005	2.480
		2.461	0.006	
90		2.614	0.004	
91		2.901	0.005	
92		2.990	0.006	
93	22:0-20:4 ω 6	3.109	0.006	3.092
94	22:1-20:4 ω 6	3.266	0.006	3.249
95	22:1-20:4 ω 6	3.327	0.005	
96	22:2-20:4 ω 6	3.547	0.007	3.528

(Continued on p. 196)

TABLE III (continued)

Peak No.	Molecular species	Relative retention time		
		Mean	S.D.	Calculated ^a
97	20:0-22:5 ω 3	3.607	0.008	3.604
97	20:0-22:6 ω 3	3.607	0.008	3.604
97a	20:1-22:5 ω 3	3.787	0.006	3.801
97a	20:1-22:6 ω 3	3.787	0.006	3.801
98	24:0-20:4 ω 6	4.618	0.008	4.627
99	24:1-20:4 ω 6	4.865	0.008	4.839
100	24:1-20:4 ω 6	4.960	0.009	
100a	24:2-20:4 ω 6	5.321	0.008	5.293
100b	22:1-22:5 ω 3	5.564	0.009	5.596
100b	22:1-22:6 ω 3	5.564	0.009	5.596

^a See footnote to Table II.

Trenzahl value (number of peaks resolved between homologues differing by one methylene unit) of 5.9 found for the diacylglycerols was significantly lower than the average value of 8.2 obtained for the fatty acid methyl esters. In spite of this slight loss in column efficiency the achieved separations are very good.

Columns may vary slightly in properties from batch to batch even if supplied by the same manufacturer, and it is important to test them with a few known mixtures. Columns also age. In the short term, columns may initially show some effective increase in polarity following use at 250–260°C. In long term, effective column polarity gradually decreases due to loss of liquid phase.

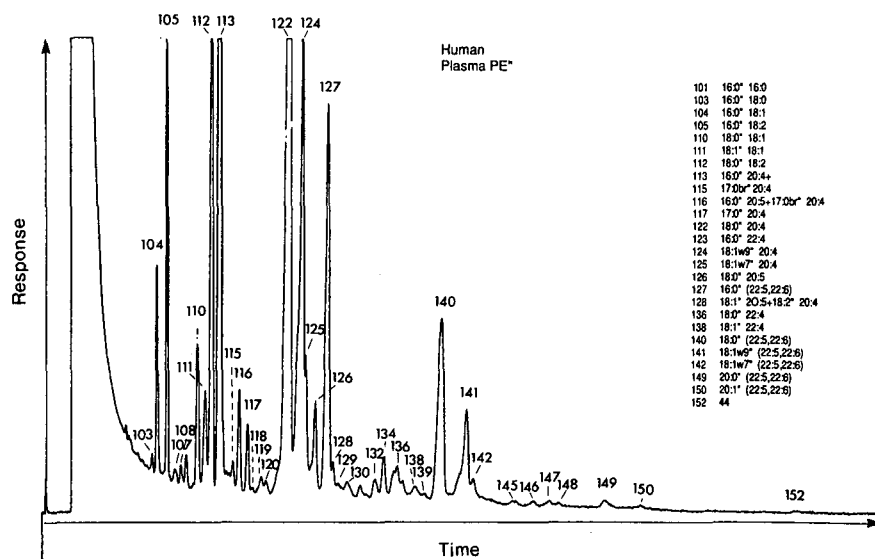


Fig. 5. Polar capillary GLC profile of the alkenylacylglycerol moieties of human red cell diradylglycerophosphoethanolamine. GLC conditions as in Fig. 4. Sample: 1 μ l of 0.1% diradylglycerol TMS ethers in hexane.

TABLE IV
RELATIVE RETENTION TIMES OF SELECTED MOLECULAR SPECIES OF *sn*-1-ALKENYL-2-ACYLGLYCEROLS ON A POLAR CAPILLARY COLUMN

Peak No.	Molecular species	Relative retention time		
		Mean	S.D.	Calculated ^a
	30:0	0.225	0.003	
101	16:0-16:0	0.335	0.002	0.340
102a	16:0-17:0	0.412	0.003	0.410
103	16:0-18:0	0.501	0.004	0.496
104	16:0-18:1 ω 9	0.534	0.003	0.538
105	16:0-18:2 ω 6	0.598	0.002	0.602
107		0.648	0.003	
108		0.683	0.004	
109		0.716	0.003	
110	18:0-18:1 ω 9	0.787	0.003	0.777
111	18:1 ω 9-18:1 ω 9	0.833	0.004	0.833
112	18:0-18:2 ω 6	0.874	0.003	0.878
113	16:0-20:4 ω 6	0.922	0.004	0.921
115		1.013	0.003	
116	16:0-20:5 ω 3	1.055	0.003	1.049
116	17:0br-20:4 ω 6	1.055	0.003	1.049
117	17:0-20:4 ω 6	1.105	0.004	1.109
118		1.130	0.003	
119		1.191	0.005	
120		1.218	0.004	
121				
122	18:0-20:4 ω 6	1.340	0.004	1.343
123	16:0-22:4 ω 6	1.411	0.006	1.374
124	18:1 ω 9-20:4 ω 6	1.437	0.005	1.440
125	18:1 ω 7-20:4 ω 6	1.464	0.006	1.457
126	18:0-20:5 ω 3	1.521	0.005	1.530
127	16:0-22:5 ω 3	1.597	0.005	1.586
127	16:0-22:6 ω 3	1.597	0.005	1.586
128		1.636	0.005	
129		1.675	0.006	
130		1.725	0.004	
131		1.814	0.006	
132		1.882	0.005	
133	17:0-22:5 ω 3	1.927	0.004	1.910
133	17:0-22:6 ω 3	1.927	0.004	1.910
134	20:0-20:4 ω 6	1.956	0.006	1.939
136	18:0-22:4 ω 6	2.037	0.006	2.003
137				
138	18:1-22:4 ω 6	2.157	0.005	2.148
139		2.203	0.007	
140	18:0-22:5 ω 3	2.295	0.007	2.312
140	18:0-22:6 ω 3	2.295	0.007	2.312
141	18:1 ω 9-22:5 ω 3	2.455	0.008	2.480
141	18:1 ω 9-22:6 ω 3	2.455	0.008	2.480
142	18:1 ω 7-22:5 ω 3	2.508	0.008	2.509
142	18:1 ω 7-22:6 ω 3	2.508	0.008	2.509
145		2.759	0.007	
146		2.883	0.009	
147		2.979	0.007	

(Continued on p. 198)

TABLE IV (continued)

Peak No.	Molecular species	Relative retention time		
		Mean	S.D.	Calculated ^a
148		3.036	0.008	
149	20:0-22:5 ω 3	3.328	0.009	3.339
149	20:0-22:6 ω 3	3.328	0.009	
150	20:1-22:5 ω 3	3.544	0.011	3.555
150	20:1-22:6 ω 3	3.544	0.011	

^a See footnote to Table II.

Calculation of retention factors

The relative retention time, R_{AB} , of any species AB, where A and B are alkyl, alkenyl or acyl moieties, is given by the expression

$$R_{AB} = F_A \cdot F_B$$

or

$$\log R_{AB} = \log F_A + \log F_B$$

where F_A and F_B are appropriate retention factors for the A and B portions of the molecular species. This relationship is in accordance with Martin's equation¹⁶ and assumes that each ester or ether moiety contributes independently to the retention time of the whole molecule. This assumption has been shown previously to apply to the GLC retention factors of diacylglycerols^{1,7} and HPLC retention factors of triacylglycerols¹⁷. In the present case contributions from the rest of the molecule are assumed

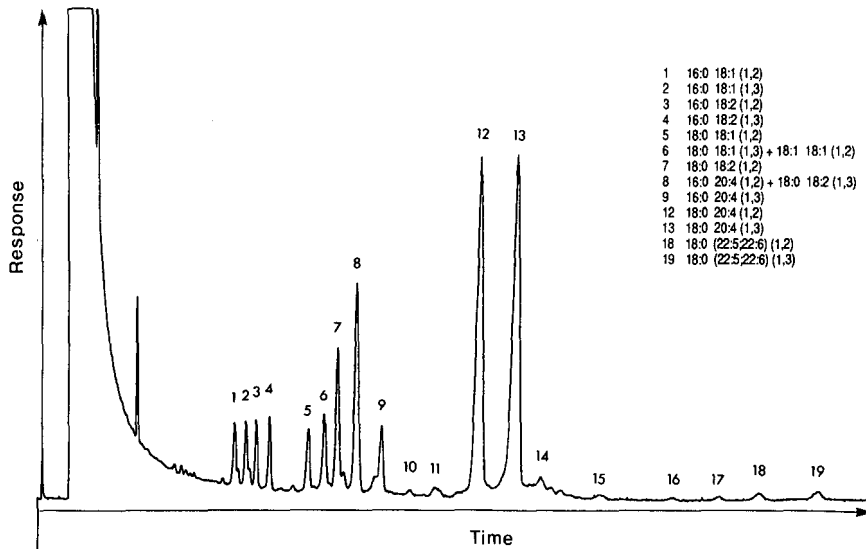


Fig. 6. Polar capillary GLC profile of isomerized diacylglycerol moieties of human plasma phosphatidylinositol. GLC conditions as given in Fig. 4. Sample: 1 μ l of 0.1% diacylglycerol TMS ethers.

to be constant and are incorporated into the individual factors. Each factor has been determined in several ways by an iterative procedure and then averaged. The retention time of a single acid species, such as 16:0–16:0 and 18:1–18:1, are used to initiate the process. Thus,

$$\bar{F}_{16:0} = \sqrt{R_{16:0-16:0}} \text{ and } F_{18:1} = \sqrt{R_{18:1-18:1}}$$

Other determinations of $F_{18:1}$ can be made from the retention data of other species, such as 16:0–18:1 and 18:0–18:1, using the factors for 16:0 and 18:0. In the end the factors represent averages from as many combinations of fatty chains as the experimental data permit.

It is assumed that the factors are independent of the positional placement of the fatty chains in the diradylglycerol molecules. This is consistent with the observation that reverse isomers, such as 16:0–18:1 and 18:1–16:0, are not resolved. GLC runs of random mixtures containing equal proportions of reverse isomers show no resolution or peak broadening due to the presence of both isomers in a peak.

TABLE V
RETENTION FACTORS USED TO CALCULATE THEORETICAL RETENTION TIMES

Fatty chain	Retention factors (F_x)		
	Acyl ^a	Alkyl ^b	Alkenyl ^c
14:0	0.558		
15:0	0.667		
16:0	0.797	0.456	0.426
16:1 ω 7	0.891		
17:0	0.964	0.551	0.513
18:0	1.165	0.666	0.621
18:1 ω 9	1.251	0.710	0.666
18:1 ω 7	1.281		0.674
18:2 ω 6	1.413		
18:3 ω 3	1.666		
20:0	1.70	0.968	0.897
20:1		1.021	0.955
20:4 ω 6	2.162		
20:5 ω 3	2.463		
22:0		1.430	
22:1		1.503	
22:2		1.632	
22:4 ω 6	3.225		
22:5 ω 6	3.284		
22:5 ω 3	3.723		
22:6 ω 3	3.723		
24:0		2.140	
24:1		2.238	
24:2		2.448	

$$^a F_{\text{acyl}} = R_{\text{diacyl}}/F_{\text{acyl}}$$

$$^b F_{\text{alkyl}} = R_{\text{alkylacyl}}/F_{\text{acyl}}$$

$$^c F_{\text{alkenyl}} = R_{\text{alkenylacyl}}/F_{\text{acyl}}$$

In the case of the alkylacyl- and alkenylacylglycerol species, the acyl factors were set equal to those found for the diacyl species. The factors for the alkyl and alkenyl moieties were found by dividing the retention times of the molecular species by the appropriate acyl factors. For example,

$$F_{16:0} = R_{16:0-18:1}/F_{18:1}$$

Again, the final factors are averages.

Table V gives the retention factors calculated for the acyl, alkyl and alkenyl groups of the diradylglycerols. There are marked differences in the retention factors among these different radyl moieties. For corresponding carbon numbers, the acyl retention factor is larger than the alkyl retention factor, which is larger than the alkenyl retention factor. Since each diradylglycerol class has the secondary acyl group in common, these factors represent the elution order of equivalent diradylglycerol species from the polar capillary column.

If one plots the carbon number, C , versus $\log Fx$ for the saturated acyl, alkyl and alkenyl factor (Fx) three parallel lines corresponding to the equation

$$C = m \log Fx + b$$

are obtained. The (m, b) values obtained by linear regression are (12.16, 17.20), (12.24, 20.17) and (12.36, 20.58) for the acyl, alkyl and alkenyl factors, respectively. By substitution of the Fx values for the three types of 16:0, 18:0, 18:1 and 20:0 moieties into the regression line for the acyl moieties, it is possible to show that equivalent alkylacyl and alkenylacyl species elute 2.97 and 3.34 carbon number units earlier than the corresponding diacyl species. In terms of relative retention times equivalent alkylacyl- and alkenylacylglycerol species elute earlier than diacylglycerol species by factors of 0.570 and 0.532, respectively. On a glass capillary column coated with SP-2330 we found² a value of 0.525 for the ratio of the relative retention times of the TMS ethers of corresponding alkenylacyl/diacylglycerol species.

Identification of diradylglycerols containing isomeric fatty chains

The identification of diradylglycerol species containing isomeric fatty acids, such as 16:0-18:1 ω 9 and 16:0-18:1 ω 7 is based on a number of different experimental lines of evidence. Thus, the observed splitting for species containing ω 9 and ω 7 monoenoic fatty acids is consistent with the known behavior of these acids on this and similar liquid phases^{1,18}. Although other octadecenoic acids can be present especially in samples from subjects consuming partly hydrogenated fats, the principal isomers present in mammalian tissues are the ω 9 and ω 7 isomers¹⁹. Therefore, peaks coeluting with reference samples of 18:1 ω 9 and 18:1 ω 7 can be justifiably assumed to be identical with the standards. In some cases, monoenoic fractions isolated by argentation thin-layer chromatography (TLC) have been characterized by GC-MS¹³. The GC-MS data shows that no unknown species are present that can be responsible for the observed splitting.

Effect of temperature and flow-rate

As expected, a change in flow-rate changes all the retention times by the same factor. In contrast a temperature shift affects the various molecular species differently

TABLE VI
EFFECT OF TEMPERATURE AND FLOW-RATE ON THE RELATIVE RETENTION TIME (RRT)
OF SELECTED DIACYLGLYCEROLS ON POLAR CAPILLARY GLC COLUMNS

Molecular species	260 °C		RRT ^a	250 °C	
	Adjusted retention time			Adjusted retention time (3 p.s.i.)	RRT
	2 p.s.i.	3 p.s.i.			
16:0-16:0	3.30	2.09	0.653	3.37	0.639
16:0-18:0	4.72	3.00	0.936	4.91	0.932
16:0-18:1	5.04	3.205	1.000	5.27	1.000
16:0-18:2	5.61	3.59	1.117	5.88	1.116
18:0-18:1	7.19	4.56	1.425	7.69	1.459
18:0-18:2	8.00	5.08	1.585	8.52	1.617
16:0-20:4	8.59	5.39	1.693	8.99	1.706
16:0-20:5	9.66	6.14	1.916	10.20	1.935
17:0-20:4	9.99	6.34	1.980	10.67	2.025
18:0-20:4	11.92	7.61	2.370	12.92	2.452
16:0-22:6	14.08	8.98	2.798	15.21	2.886
18:0-22:6	19.70	12.54	3.911	21.77	4.131

^a Average of retention times at 2 and 3 p.s.i.

due to an increase in column polarity at higher temperatures²⁰. In general increasing the oven temperature decreases the separation between homologous species and increases the separation between species differing in unsaturation. A relatively sensitive indicator of the temperature effect due to differing degrees of unsaturation is provided by the 16:0-20:4/18:0-18:2 diacylglycerol retention time ratio, which increases with increasing temperature. Tables VI and VII gives the shifts in the retention times obtained for various diacylglycerol species by increasing the column temperature from 250 to 260°C or by increasing the head pressure of the hydrogen carrier gas from 2 to 3 p.s.i. In general, the diradylglycerol species containing 20:4 elute earlier than anticipated from the retention time of the fatty acid methyl esters on the same polar phase. This is due to two opposing effects. It is known that on non-polar phases the 16:0-20:4 elutes earlier than either 18:0-18:2, 18:1-18:2 or 16:0-20:3

TABLE VII
EFFECT OF TEMPERATURE ON THE SEPARATION FACTORS OF SELECTED PAIRS OF
DIACYLGLYCEROLS

Ratio of Molecular species	Oven temperature		Ratio ^a
	260 °C	250 °C	
18:0-18:1/16:0-18:1	1.425	1.459	0.977
18:0-18:2/18:0-18:1	1.113	1.108	1.005
16:0-20:4/18:0-18:2	1.067	1.1055	1.011
16:0-20:4/18:0-18:1	1.188	1.169	1.016
16:0-22:6/18:0-20:4	1.181	1.177	1.003
17:0-20:4/16:0-20:5	1.033	1.047	0.987

^a Ratio of relative retention times at 260 and 250°C.

TABLE VIII
RELATIVE RETENTION TIMES (RRT) AND EQUIVALENT CHAIN LENGTH (ECL) VALUES
OF ALKYLGLYCEROL DIACETATES

<i>Alkyl glycerol</i>	<i>Retention time (min)</i>	<i>RRT^a</i>	<i>ECL₁^a</i>	<i>ECL₂^b</i>
14:0	8.66	0.748	14.00	
15:0	9.35	0.808	15.00	
16:0 (iso)	9.66	0.835	15.42	
16:0	10.08	0.871	16.00	16.00
17:0 (iso)	10.39	0.898	16.42	16.46
17:0 (ai)	10.58	0.914	16.67	16.69
17:0	10.81	0.934	17.00	17.00
18:0	11.57	1.000	18.00	18.00
18:1t ^c	11.97	1.035	18.53	18.52
18:1c (ω 9)	12.10	1.046	18.70	18.71
18:1c (ω 7)	12.21	1.055	18.84	18.83
18:2	12.92	1.117	19.78	19.75
20:0	13.09	1.131	20.00	20.00
20:1t ^c	13.48	1.165	20.51	20.47
20:1c ^c	13.64	1.179	20.72	20.67
20:1c ^c	13.75	1.188	20.87	
20:2	14.45	1.249	21.79	21.61
22:0	14.62	1.264	22.00	22.00
22:1t ^c	15.02	1.298	22.52	22.41
22:1c ^c	15.18	1.312	22.72	22.59
22:1c ^c	15.27	1.320	22.84	22.70
22:2	15.97	1.380	23.74	23.48
24:0	16.17	1.398	24.00	24.00
24:1	16.68	1.442		24.53
24:2	17.52	1.514		25.35

^a Temperature programmed, from 100°C to 180°C at 20°C/min, then to 240°C at 5°C/min.

^b Isothermal, 210°C.

^c Unidentified positional isomers.

species. As the polarity of the liquid phase increases, 16:0–20:4 tends to elute later. For SP-2380 or RTx-2330, 16:0–20:4 elutes later than 18:0–18:2, but slightly earlier than 18:1–18:2. Similarly, the species pairs, such as 16:0–22:5 ω 3 and 16:0–22:6 ω 3 elute either together or with 16:0–22:5 ω 3 slightly delayed.

Effect of column age

As the column ages, the effective polarity of the liquid phase decreases. This is apparently due to loss of liquid phase, although changes in the properties of the phase also could have taken place. Again a good indication of the gradual loss of polarity is the ratio of the retention times of the species 16:0–20:4/18:0–18:2, which decreases with increasing column usage. Eventually these species begin to overlap and it is time to replace the column. It is not possible to reverse the loss in separation sufficiently by increasing the column temperature.

Resolution of enantiomers and reverse isomers

The enantiomeric *sn*-1,2- and *sn*-2,3-diradylglycerols are not resolved on either the non-polar or polar capillary columns. It is possible that such resolution could be

obtained following preparation of diastereoisomeric derivatives, which can be resolved on non-chiral liquid phases. A chiral HPLC column has been reported to effect a complete resolution of the enantiomeric diradylglycerols in the form of dinitrophenylurethane derivatives²¹.

There was no resolution between reverse isomers, such as 16:0–18:2 and 18:2–16:0. The interaction with the liquid phase is probably different for primary and secondary functions, but any positional effect must be largely independent of the exact identity of the acyl chains. Thus, interchanging the two acyl chains makes no net difference in the interaction. However, it is possible that reverse isomers differing significantly in two fatty chains could be resolved on longer capillary columns containing either a non-polar or polar liquid phase.

Resolution of alkylglycerol diacetates

The alkylglycerol diacetates elute much later than the corresponding fatty acid methyl esters. Whereas methyl stearate elutes at 4.77 min, the corresponding stearyl glycerol diacetate elutes at 11.57 min. In fact, palmityl glycerol diacetate elutes after methyl docosaheptaenoate. Only myristyl glycerol diacetate emerges in the elution range of the common mammalian fatty acid methyl esters. The alkylglycerols recovered from mammalian diradylglycerophospholipids are predominantly of 16 and 18 carbons, but 20–26 carbon species are also known to occur^{10,11}. Table VIII gives the retention times of the alkylglycerol diacetates, prepared from the glycerophospholipids of human plasma and erythrocytes, as obtained on the RTx-2330 column. The equivalent chain length (ECL) values are based on isothermal runs made at 210°C. Retention times and relative retention times are also given for temperature programmed runs, which are better from an analytical standpoint. As expected, there is good resolution between the saturated and unsaturated glyceryl ethers. There is also some resolution of isomeric monoenes. Although these isomers have not been completely characterized, each monoenoic species from human blood has at least three components. An early component tentatively identified as *trans*-isomers and two *cis*-isomers. This identification of these components is consistent with their behavior on argentation TLC. The peak identified as *cis*-18:1 ω 9 coelutes with authentic *cis*-18:1 ω 9 from dogfish²². The peak identified as *cis*-18:1 ω 7 coelutes with the minor 18:1 satellite of the salachyl alcohol from dogfish. These assignments are also consistent with the major isomers of 18:1 fatty acids found in human body fats, which are known to be precursors of the alkylglycerol moieties²³. The longer chain length homologues, C_{20–24}, may be chain elongation products. Similarly, the alkenyl chains from mammalian lipids are predominantly ω 9 and ω 7 isomers²⁴.

Comparison with other methods

Molecular species of glycerophospholipids have been resolved using reversed-phase HPLC²⁵. This method has the advantage of eliminating the need for chemical derivatization and possible distortion of species profile. It permits metabolic studies with radiolabeled bases, which are lost using other methods. The direct method, however, has the major disadvantage of not being able to resolve the three diradylglycerophospholipid classes occurring in natural mixtures. There is no convenient method of resolving intact glycerophospholipids into the diacyl, alkylacyl and alkenylacyl subclasses, although the plasmalogens can be selectively destroyed²⁶.

Furthermore, the direct method is difficult to reproduce and the resolution of species is not as good as that after dephosphorylation and derivatization.

After dephosphorylation with phospholipase C, the diradylglycerols can be converted into UV absorbing²⁷ or fluorescent²⁸ derivatives, and the molecular species resolved by reversed-phase HPLC. This method has the advantage that peaks can be collected for further analysis. The principles of analysis by retention data are the same for isothermal GLC and isocratic HPLC. Reversed-phase HPLC also permits the resolution of diradylglycerols. The main disadvantages of this method are lower sensitivity and poorer resolution, when compared to capillary GLC. The HPLC peaks can be admitted to a mass spectrometer only via special interfaces, while the effluent of capillary GLC columns can be admitted directly to the mass spectrometer for peak identification. Thus, polar capillary GLC holds a clear advantage over other methods of analysis of the molecular species of glycerophospholipids.

ACKNOWLEDGEMENTS

These studies were supported by funds from the Medical Research Council of Canada, Ottawa, Ontario and the Heart and Stroke Foundation of Ontario, Toronto, Ontario, Canada.

REFERENCES

- 1 J. J. Myher and A. Kuksis, *Can. J. Biochem.*, 60 (1982) 638–650.
- 2 J. J. Myher and A. Kuksis, *Can. J. Biochem.*, 62 (1984) 352–362.
- 3 J. J. Myher, A. Kuksis, S. Pind and E. R. M. Kay, *Lipids*, 23 (1988) 398–404.
- 4 J. J. Myher and A. Kuksis, *J. Biochem. Biophys. Methods*, 10 (1984) 13–23.
- 5 A. Kuksis, *Can. J. Biochem.*, 49 (1971) 1245–1250.
- 6 A. Kuksis, *J. Chromatogr. Sci.*, 10 (1972) 53–56.
- 7 J. J. Myher and A. Kuksis, *J. Chromatogr. Sci.*, 13 (1975) 138–145.
- 8 E. Geeraert and P. Sandra, *J. Am. Oil Chem. Soc.*, 64 (1987) 100–105.
- 9 J. J. Myher, A. Kuksis, L. Marai and P. Sandra, *J. Chromatogr.*, 452 (1988) 93–118.
- 10 J. J. Myher, A. Kuksis and S. Pind, *Lipids*, (1989) in press.
- 11 J. J. Myher, A. Kuksis and S. Pind, *Lipids*, (1989) in press.
- 12 A. Kuksis and J. J. Myher, in A. Kuksis (Editor), *Fat Absorption*, Vol. 1, CRC Press, Boca Raton, FL, 1986, pp. 1–41.
- 13 N. H. Morley, A. Kuksis, J. J. Myher and D. Buchnea, *J. Biol. Chem.*, 250 (1975) 3414–3418.
- 14 J. J. Myher, A. Kuksis, L. Marai and S. K. F. Yeung, *Anal. Chem.*, 50 (1978) 557–561.
- 15 J. J. Myher and A. Kuksis, *Biochim. Biophys. Acta*, 795 (1984) 85–90.
- 16 A. J. P. Martin, *Biochem. Soc. Symp.*, 3 (1950) 4.
- 17 K. Takahashi, T. Hirano, M. Egi and K. Zama, *J. Am. Oil Chem. Soc.*, 62 (1985) 1489–1492.
- 18 R. G. Ackman, in H. K. Mangold (Editor), *Handbook of Chromatography, Vol. 1, Lipids*, CRC Press, Boca Raton, FL, 1984, pp. 95–240.
- 19 R. Wood, F. Chumblor and R. Wiegand, *J. Biol. Chem.*, 255 (1977) 1965.
- 20 J. R. Haken, *J. Chromatogr. Sci.*, 13 (1975) 430.
- 21 T. Takagi and Y. Itabashi, *Lipids*, 22 (1987) 596–600.
- 22 D. J. Hanahan, J. Ekholm and C. M. Jackson, *Biochemistry*, 2 (1963) 630–641.
- 23 A. K. Hajra, in H. K. Mangold and F. Paltauf (Editors), *Ether Lipids*, Academic Press, New York, 1983, pp. 85–106.
- 24 R. V. Panganomala, L. A. Horrocks, J. C. Geer and D. G. Cornwell, *Chem. Phys. Lipids*, 6 (1971) 97–102.
- 25 G. M. Patton, J. M. Fasulo and S. J. Robbins, *J. Lipid Res.*, 23 (1982) 190–196.
- 26 L. A. Horrocks and M. Sharma, in J. N. Hathorne and G. B. Ansell (Editors), *Phospholipids*, Elsevier, Amsterdam, 1982, pp. 51–93.
- 27 M. L. Blank, M. Robinson, V. Fitzgerald and F. Snyder, *J. Chromatogr.*, 298 (1984) 473–482.
- 28 J. H. Krüger, H. Rabe, H. Reichmann and B. Rustow, *J. Chromatogr.*, 307 (1984) 387–392.

CHROM. 21 282

GAS CHROMATOGRAPHIC RETENTION OF CARBOHYDRATE TRIMETHYLSILYL ETHERS

III^a. KETOHEXOSES

A. GARCÍA-RASO

Departament de Química Orgànica, Facultat de Ciències, Universitat de les Illes Balears, 07071 Palma de Mallorca (Spain)

and

M. FERNÁNDEZ-DÍAZ, M.I. PÁEZ, J. SANZ* and I. MARTÍNEZ-CASTRO

Instituto de Química Orgánica General (CSIC), Juan de la Cierva 3, 28006 Madrid (Spain)

SUMMARY

Five tautomeric forms, four cyclic and one acyclic, of the four ketohexoses (fructose, sorbose, tagatose and psicose) were separated as their O-trimethylsilyl (TMS) ethers by gas chromatography on several capillary columns, and identified by gas chromatography - mass spectrometry. The retention indices changed slightly with temperature. As with aldoses, their chromatographic behaviour was different from that of other ethers. Principal component analysis showed the specific behaviour of some phases towards some compound groups. A mathematical approach developed for aldoses was applied to ketohexose retention indices in order to relate them to their structural characteristics. The results were similar to those found for aldoses, except for pyranose forms, where equatorial OTMS groups seemed to have a negative effect on the retention.

INTRODUCTION

Ketohexoses are carbohydrates of great interest in many fields of chemistry. Although the physical and chemical properties of fructose have been extensively described and its five equilibrium tautomeric forms have been quantified by NMR spectroscopy¹⁻⁴ and gas chromatography (GC)⁵⁻⁷, data on the tautomers of the other three ketoses are scarce. The retention times of their O-isopropylidene derivatives⁸ and O-*n*-butoxime pertrifluoroacetates⁹ on OV-225 have been reported. Nevertheless, these methods do not afford peaks corresponding to the present tautomeric forms. Hence, although complete NMR data exist for psicose⁴, sorbose^{3,10} and tagatose^{4,10}, only a few GC peaks have been identified for the trimethylsilyl derivatives of sorbose^{11,12}; eight unidentified peaks have been reported for those of tagatose¹³ and no data exist for psicose.

^a For Part II, see ref. 15.

TABLE I
CAPILLARY COLUMNS USED FOR GC ANALYSIS OF TMS ETHERS OF CARBOHYDRATES

<i>Stationary phase</i>	<i>Origin</i>	<i>Material</i>	<i>Dimensions (m × mm I.D.)</i>	<i>Temperature (°C)</i>
OV-1	Laboratory-made	Pyrex glass	25 × 0.22	170,180,190
OV-17	Chrompack	Fused silica	25 × 0.22	150,160,180
OV-215	Laboratory-made	Pyrex glass	25 × 0.18	180,190
OV-225	Laboratory-made	Pyrex glass	25 × 0.18	170,180,190
FFAP	Perkin-Elmer	Fused silica	24 × 0.22	150,160,170

In previous papers^{14,15}, chromatographic retention data for aldopentose and aldohexose O-trimethylsilyl ethers were presented. Some general features were found: an unusual chromatographic behaviour when these compounds and other ethers are compared; a decrease in their retention indices with increasing temperature; and a relationship between retention and structure, in which descriptors related to a planar conformation contribute positively to the retention.

In this work, GC retention data have been obtained for the TMS ethers of the five tautomeric forms of each ketohexose. Some aspects of their chromatographic behaviour are outlined, and their retention indices on several stationary phases are correlated with different structural parameters as was done with aldoses.

EXPERIMENTAL

Samples

D-Fructose and L-sorbose were obtained from Fluka (Buchs, Switzerland) and D-tagatose and D-psicose from Sigma (Eisenhofen, F.R.G.). Pure samples of sugars were dissolved in water, pyridine or dimethyl sulphoxide and left to stand until equilibrated. Aliquots containing about 1 mg of carbohydrate were silylated^{7,14,16}. Aqueous samples were first lyophilized.

GC analysis

Chromatographic analysis was carried out as described previously^{14,15}. The columns and conditions are summarized in Table I. Four of the stationary phases were silicones with different substituent groups (methyl, phenyl, trifluoropropyl, cyanopropyl) and the most polar was FFAP (polyethylene glycol 20M esterified with nitroterephthalic acid).

Kováts retention indices were calculated from the retention times of TMS ethers and suitable *n*-alkanes. The dead time was determined by linear regression¹⁷

Calculations

Calculations of retention indices and normal and stepwise linear regressions were carried out on an Olivetti M-20 microcomputer.

RESULTS AND DISCUSSION

Identification

Silylated equilibrium mixtures of each of the four ketohexoses were analysed by GC-mass spectrometry (GC-MS). Chromatographic patterns on OV-17 are presented in Fig. 1. The five peaks of each sugar were well resolved under these conditions. The proportion of acyclic forms in fructose, tagatose and psicose is clearly excessive, and depends on the silylation method used¹⁸; however, it was useful in order to obtain good mass spectra.

The ring size of cyclic forms could be clearly assigned from the mass spectra. Furanoses were characterized by a very intense fragment at m/z 217 and pyranoses by a high value of the ratio m/z 204/217. The fragment at m/z 437, typical of ketoses¹⁹ was also an intense peak in both furanoses and pyranoses. Open forms were detected by the very intense fragment at m/z 306 (ref. 6).

Some traces of sorbose were detected in tagatose, as previously found by Angyal²⁰ in the NMR spectrum. Sorbose and tagatose also contained a component which was characterized from its mass spectrum as a 2,5-hexodiulose, with the base peak at m/z 305, as described by Novina¹¹. This can explain the eight peaks found by Tesařik¹³ for tagatose samples.

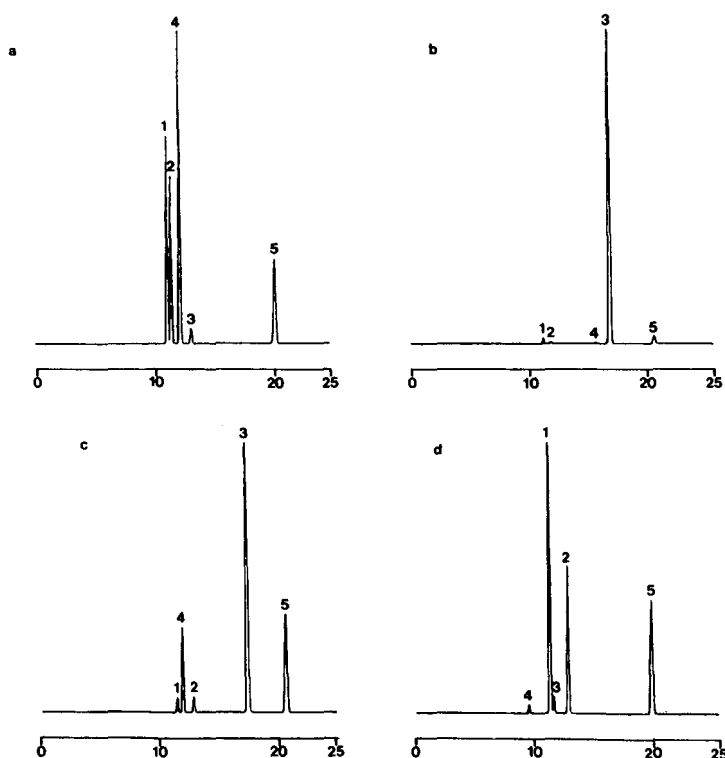


Fig. 1. Chromatographic patterns of ketohexose TMS ethers on OV-17 at 150°C. (a) Fructose; (b) sorbose; (c) tagatose; (d) psicose. Peaks: 1 = α -furanose; 2 = β -furanose; 3 = α -pyranose; 4 = β -pyranose; 5 = acyclic form.

TABLE II
RETENTION INDICES OF KETOHEXOSE TMS ETHERS (*I_x*)

No.	Component	Stationary phase, McReynolds polarity, temperature (°C)				
		OV-1, 217, 180	OV-17, 884, 180	OV-215, 1545, 180	OV-225, 1813, 180	FFAP, 2546, 170
1	α -Psicofuranose	1875	1755	1752	1883	1709
2	β -Psicofuranose	1911	1783	1804	1938	1762
3	α -Psicopyranose	1897	1763	1781	1900	1709
4	β -Psicopyranose	1869	1719	1734	1868	1673
5	Acyclic form	1956	1896	1952	2124	1869
6	α -Fructofuranose	1849	1763	1730	1877	1693
7	β -Fructofuranose	1857	1763	1757	1877	1712
8	α -Fructopyranose	1873	1804	1800	1928	1731
9	β -Fructopyranose	1867	1775	1745	1877	1685
10	Acyclic form	1932	1887	1942	2099	1859
11	α -Sorbofuranose	1835	1746	1717	1858	1682
12	β -Sorbofuranose	1846	1762	1731	1858	1696
13	α -Sorbopyranose	1908	1844	1813	1949	1757
14	β -Sorbopyranose	1908	1833	1813	1949	1757
15	Acyclic form	1922	1885	1939	2092	1847
16	α -Tagatofuranose	1861	1764	1740	1896	1721
17	β -Tagatofuranose	1871	1788	1767	1926	1753
18	α -Tagatopyranose	1935	1860	1832	1983	1776
19	β -Tagatopyranose	1879	1780	1751	1913	1698
20	Acyclic form	1929	1891	1945	2119	1853

The α - and β -forms were assigned by comparison with NMR equilibrium data in water or pyridine, as in previous work²¹. For psicose, assignment of α - and β -pyranoses was made according to the equilibrium values in dimethyl sulphoxide²².

The retention indices of the different tautomeric forms are presented in Table II.

Effect of temperature

The retention indices of ketohexoses changed slightly with temperature, except in the FFAP column, where the change was more evident (see Table III).

Effect of stationary phase

As with other monosaccharides^{14,15}, no correlation was found between the polarity of the stationary phase and retention indices. The overall retention was higher on OV-225 and OV-1, decreased on OV-215 and OV-17 and attained a minimum on FFAP (it was not possible to obtain data at 180°C because the retention times became too short to be measured reliably). Comparative data for other monosaccharides are shown in Table IV.

A data matrix including the retention indices in Table II (180°C for the silicone

TABLE III
TEMPERATURE DEPENDENCE OF THE RETENTION INDICES OF KETOHEXOSE TMS ETHERS ON SEVERAL STATIONARY PHASES ($\Delta I/10^\circ\text{C}$ VALUES)

Component	Stationary phase and temperature range ($^\circ\text{C}$)				
	OV-1, 170-190	OV-17, 150-180	OV-215, 180-190	OV-225, 170-190	FFAP, 150-170
α -Fructofuranose	-4	-5	-13	-13	-28
β -Fructofuranose	-5	-8	-7	-13	-28
α -Fructopyranose	-14	-5	-5	-8	-24
β -Fructopyranose	-2	-9	-12	-13	-24
Acyclic form	-4.5	-9	2	-2	-23
α -Sorbofuranose	-2.5	-9	-12	-16	-30
β -Sorbofuranose	-2.5	-8	-12	-16	-30
α -Sorbopyranose	-0.5	-7	-5	-11	-23
β -Sorbopyranose	-0.5	-6	-5	-11	-23
Acyclic form	-2	-9	1	-4.5	-25
α -Tagatofuranose	-9	-7	-2	-11	-28
β -Tagatofuranose	-8	-8	-3	-9	-23
α -Tagatopyranose	-1.5	-7	-1	-5	-22
β -Tagatopyranose	-2	-5	0	-11	-24
Acyclic form	-5	-9	2	1	-23
α -Psicofuranose	-	-7	-14	-6	-27.5
β -Psicofuranose	-	-8	-16	-4	-30
α -Psicopyranose	-	-6	-12	-8	-27.5
β -Psicopyranose	-	-6	-12	-10	-27
Acyclic form	-	-3	-3	4	-26

phases, 170°C for FFAP) was submitted to principal component analysis²³. The first component values can be used as an estimate of the relative polarity of the stationary phases towards the selected compounds, and they are usually positively correlated with the McReynolds polarity values. The other components are related to the selectivity of the stationary phases towards some compounds in the data set; however, the physical significance of the lower components is less reliable, as they are more affected by experimental errors²³. Fig. 2 shows a plot of the first (a) and second (b) component loadings against the stationary phase polarity according to McReynolds. No correlation is found for the first component, and the second-component plot shows a correlation only for the silicone-based stationary phases. The third and fourth components are related to OV-17 and FFAP, respectively.

Open forms can be clearly distinguished from the others from their high second-component scores, as their retention is relatively higher for the polar silicone stationary phases. The negative third-component scores for psicose forms are related to the low retention of these compounds on OV-17. Furanose and pyranose forms can be distinguished from their fourth-components scores, as FFAP retains the furanoses selectively.

A plot of second- and fourth-component scores (Fig. 3) shows that open forms, furanoses and pyranoses can be clearly distinguished.

TABLE IV

ELUTION RANGE (i.u.) OF MONOSACCHARIDES ON DIFFERENT STATIONARY PHASES

Temperatures (°C) are given in parentheses.

Stationary phase	Polarity	Aldopentoses	Aldohexoses	Ketohexoses
OV-1	217	—	—	1830–1955 (170–190)
SE-54	334	1610–1780 (180–200)	1810–2020 (180–200)	—
OV-17	884	1585–1760 (160–190)	1730–2000 (160–190)	1720–1920 (150–180)
OV-215	1545	1610–1845 (150–160)	1740–2175 (170)	1705–1950 (180–190)
OV-225	1813	1600–1720 (150–160)	1700–1985 (170)	1840–2110 (170–190)
Carbowax 20M	2308	1545–1860 (160)	1695–1972 (160)	—
FFAP	2546	—	—	1670–1920 (150–170)

Effect of the carbohydrate structure

The most retained peaks were usually the acyclic forms (see Table II). The elution order was sorbose, fructose, tagatose and psicose (except on FFAP, where tagatose eluted before fructose) (Scheme 1). The I_x values on each phase were very close, covering a maximum of 35 i.u. A similar behaviour has been reported for isomeric alditols²⁴.

The elution orders of pyranose forms were similar on the five stationary phases used. The β -anomers eluted before the α -anomers. When conformation 5C_2 is as-

TABLE V

STRUCTURAL DESCRIPTORS AND CODES

Code	Value	Structural significance
P/F	0–1	Pyranose/furanose ring
Σ Eq	0–4	Total number of equatorial OTMS groups
Σ 2c	0–3	Total number of OTMS pairs in a <i>cis</i> configuration
Σ 3c	0–2	Total number of OTMS triplets in a <i>cis</i> configuration
Eq2	0–1	OTMS equatorial at C-2 (α/β)
Eq3	0–1	OTMS equatorial at C-3
Eq4	0–1	OTMS equatorial at C-4
23c	0–1	OTMS/OTMS <i>cis</i> at C-2–3
23C	0–1	OTMS/CH ₂ OTMS <i>cis</i> at C-2–3
34c	0–1	OTMS/OTMS <i>cis</i> at C-3–4
45c	0–1	OTMS/OTMS <i>cis</i> at C-4–5
13c	0–2	OTMS/OTMS/OTMS <i>cis</i>
13C	0–2	OTMS/OTMS/CH ₂ OTMS <i>cis</i>
13a	0–1	OTMS axial at C-2 and C-4
13A	0–1	CH ₂ OTMS axial in C-2 and OTMS axial at C-4

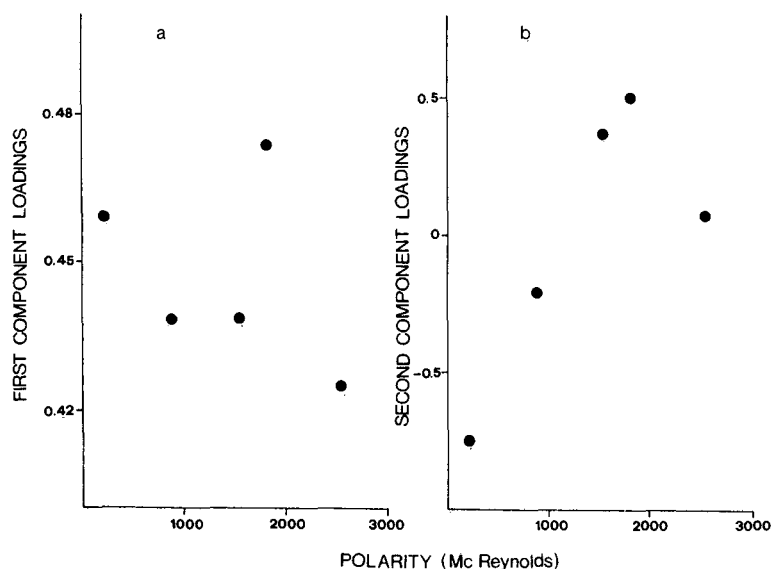


Fig. 2. (a) First- and (b) second- component loadings, calculated from data in Table II, versus McReynolds polarity.

sumed, the bulky CH_2OTMS group is axial in β -anomers (Scheme 2) and equatorial in α -anomers. Hence these are more planar molecules and their retention would be greater, as was found for similar compounds¹⁴⁻¹⁶.

The most retained compound on the five stationary phases was the TMS deriv-

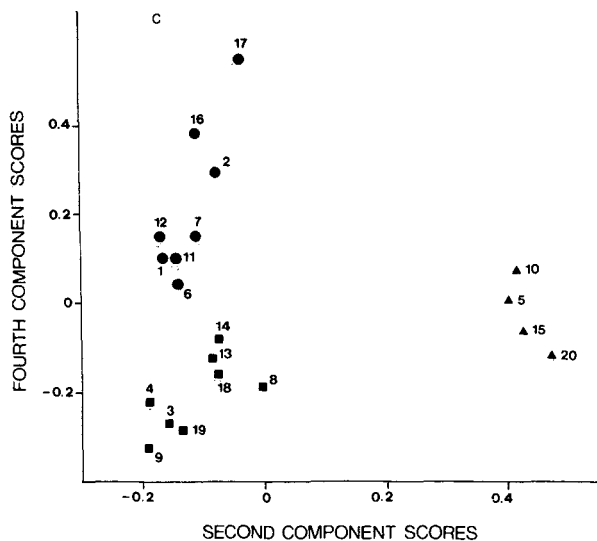
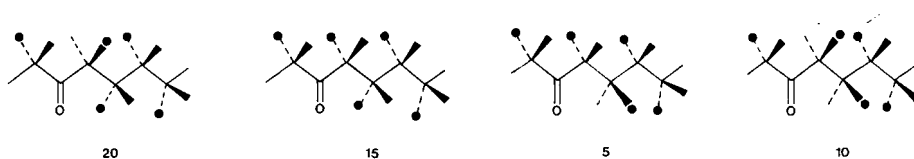


Fig. 3. Plot of second- and fourth-component scores calculated from data in Table II: (●) furanoses; (■) pyranoses; (▲) acyclic forms.



Scheme 1.

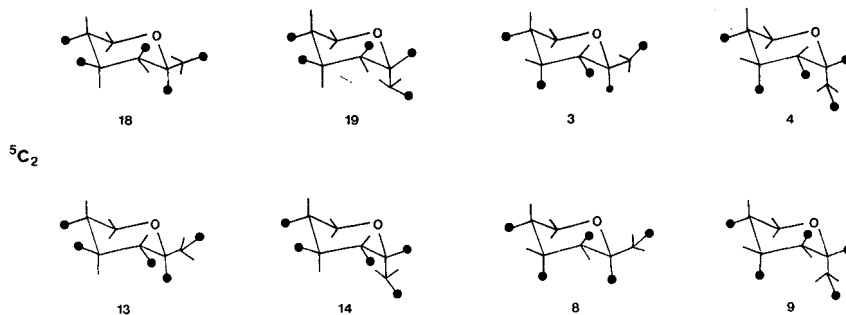
ative of α -tagatopyranose, followed by those of α - and β -sorbose. β -Psicopyranose and β -fructopyranose were the least retained compounds. The better resolved anomeric pair corresponded to tagatose (covering a range from 56 i.u. on OV-1 to 82 i.u. on OV-17) and the least resolved corresponded to sorbose, whose α - and β -anomers coeluted on most phases.

Aldopyranoses and ketopyranoses show a different chromatographic behaviour: the aldopyranoses having an all-equatorial substitution (β -xylose among pentoses¹⁴ and β -glucose among hexoses¹⁵) were the most retained, whereas the most retained ketopyranose (α -tagatose) has an axial substituent at C-3.

The elution order of ketofuranose TMS ethers on the five columns was also regular. The α -anomers eluted before the β -anomers. The least retained compound was always α -sorbofuranose and the most retained was β -psicopyranose. The least separated anomeric pairs were those corresponding to sorbose and fructose, and the best resolved corresponded to psicose (which ranged from 40 i.u. on OV-1 to 55 i.u. on OV-255).

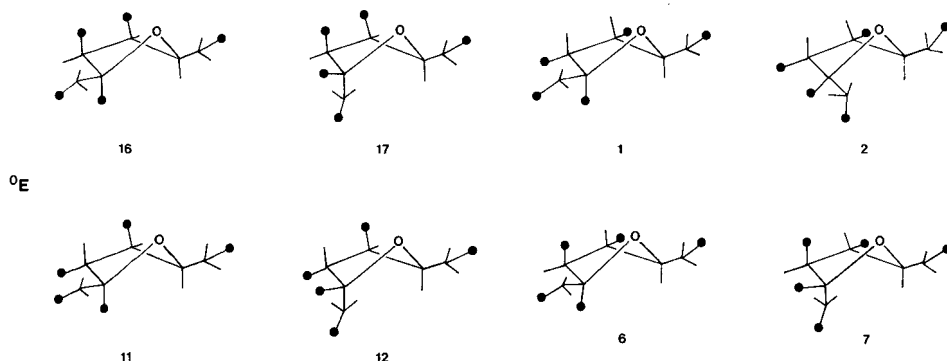
Correlation between structure and retention

The preferred conformations of ketohexose TMS ethers have not been reported. For ketopyranoses we used a 5C_2 conformation (see Scheme 2) in which the OTMS group at C-5 is always equatorial. The ketofuranose substituents were considered as pseudo-axial or pseudo-equatorial in order to determine their descriptor values, from the envelope 0E conformations shown in Scheme 3.



Scheme 2.

Table V lists the structural descriptors used in this work and their identification codes. The number of descriptors is too high, and many of them are redundant as they are related to others in the set; for instance, the total number of equatorial TMS groups is equal to the sum of equatorial TMS groups at C-2, -3, -4 and -5. When the



Scheme 3.

ketoses are divided into furanose and pyranose groups, more descriptors become redundant. Only six descriptors are really independent in the furanose and pyranose sets.

As in previous papers^{14,15}, we used two different approaches in order to relate the retention indices and structures of cyclic ketoses. The small number of acyclic forms precludes their use in the calculation of these models.

Prediction of retention data from structural descriptors. We assume that the retention index I_{xp} of a compound x on a stationary phase p can be expressed as a sum of contributions c_{jp} from its descriptors d_{xj} :

$$I_{xp} = \sum d_{xj} c_{jp}$$

I_{xp} values are listed in Table II, descriptor values (d_{xj}) were obtained from Schemes 2 and 3 and c_{jp} values can be calculated by multiple linear regression.

When ketofuranoses and ketopyranoses were considered as a single data set, the quality of fit was not good ($r = 0.45-0.70$ using seven variables). Only a few descriptor values (the positive contribution of pyranose rings P/F and the negative contribution of 1,3-diaxial substituents, 13a and 13A) seem to have significance. In order to improve the fit, it seemed to be necessary to distinguish furanose and pyranose descriptors.

The descriptor values for ketopyranoses are highly related. Only ΣEq , $\Sigma 2c$, $\Sigma 3c$, $Eq2$, $23c$ and $13c$ were chosen for the regression, as the other descriptors can be calculated from these values (Table VI). The quality of fit was fair ($r = 0.90-0.98$ and mean error = 6-12 i.u. when using six descriptors). Although the ratio between variables in the fit and experimental data is too high and the high degree of redundancy avoids the assignment of an absolute significance to the descriptor values, some conclusions can be drawn from them. The highest positive contribution corresponded to $\Sigma 3c$ (number of triplets in a *cis* configuration, including both OTMS and CH_2OTMS groups), while $\Sigma 2c$ (number of OTMS pairs in a *cis* configuration) had the highest negative value. This difference must be related to the interaction between the bulky CH_2OTMS group and the *cis* OTMS groups in C-3 and C-4. Also it is worth noting that, in contrast to aldopyranoses¹⁴⁻¹⁶, the total number of equatorial substituents (ΣEq) had a low negative contribution.

TABLE VI

MULTIPLE LINEAR REGRESSION LEAST-SQUARES FIT FOR KETOPYRANOSSES ON FIVE STATIONARY PHASES

Contributions of the six ketopyranose descriptors (I_x units) and correlation coefficients.

Descriptor ^a	Stationary phase				
	OV-1	OV-17	OV-215	OV-225	FFAP
Σ Eq	-17.5	-56.0	-17.7	-66.2	-27.0
Σ 2c	-73.0	-161.0	-76.0	-179.0	-103.0
Σ 3c	60.0	91.0	31.5	108.5	55.0
Eq2	-5.0	15.0	-28.0	28.0	-13.0
23c	-3.0	-9.0	-27.5	-25.5	-23.0
13c	-11.0	-9.0	10.5	6.5	2.0
Ring	2046.2	2192.5	1978.9	2358.6	1972.5
Correlation coefficient	0.902	0.971	0.963	0.985	0.970
α -Fructopyranose Exp.	1873	1804	1800	1928	1731
Calc.	1882.7	1814.5	1809.1	1934.4	1739.5
β -Fructopyranose Exp.	1867	1775	1745	1877	1685
Calc.	1857.2	1764.5	1735.8	1870.6	1676.5

^a See Table V.

The same six descriptors (Σ Eq, Σ 2c, Σ 3c, Eq2, 23c and 13c) were chosen for ketofuranoses (Table VII). The quality of fit was better than for pyranoses; when using six descriptors the r values were higher than 0.97 and the mean error was lower

TABLE VII

MULTIPLE LINEAR REGRESSION LEAST-SQUARES FIT FOR KETOFURANOSSES ON FIVE STATIONARY PHASES

Contributions of the six ketofuranose descriptors (I_x units) and correlation coefficients.

Descriptor ^a	Stationary phase				
	OV-1	OV-17	OV-215	OV-225	FFAP
Σ Eq	24.6	2.7	22.8	18.1	14.8
Σ 2c	-12.5	-9.0	-19.5	-19.0	-13.5
Σ 3c	34.7	21.3	40.7	55.7	44.7
Eq2	-15.1	5.3	-2.3	-18.1	1.7
23c	-7.3	-5.0	-3.0	-6.3	-4.0
13c	-13.5	-18.0	-19.0	-42.5	-26.0
Ring	1815.2	1765.2	1708.6	1863.0	1680.2
Correlation coefficient	0.991	0.993	0.983	0.984	0.993
α -Fructofuranose Exp.	1849	1763	1730	1877	1693
Calc.	1851.9	1761.5	1734.8	1880.1	1696.3
β -Fructofuranose Exp.	1857	1763	1757	1877	1712
Calc.	1854.1	1764.6	1752.3	1873.9	1708.8

^a See Table V.

than 5 i.u. The descriptor values seemed also to be more significant. Σ Eq and Σ 3c showed positive contributions, whereas Σ 2c, Eq2, 23c and 13c had negative values. The main difference between furanose and pyranose descriptor values corresponded to Σ Eq, which is clearly related to the overall structure of the molecule; some conformations in Scheme 2 are probably not the preferred ones. The 13c descriptor (OTMS groups *cis* in C-1,C-3) also has a negative value in aldoses¹⁴⁻¹⁵. The presence of a CH₂OTMS substituent on the anomeric carbon could be the reason, as for some ketopyranose descriptor values, for the negative contribution of Eq2 in ketofuranoses on OV-1 and OV-225.

When the number of descriptors used in the regression was reduced, the quality of fit decreased, but the remaining descriptor contributions were roughly similar to those shown in Tables VI and VII. The most important descriptors for furanoses are Σ Eq and Σ 3c, whereas for pyranoses they are Σ 3c, Eq2 and 23c.

Tables VI and VII also show the calculated and experimental retention indices of cyclic forms of fructose on OV-17, using five descriptors that take different values for ketofuranoses and ketopyranoses.

Prediction of structural descriptor values from retention data. In this approach, we assume that the value of the descriptor y in a compound x (d_{xy}) can be calculated from the retention indices I_{xp} of compound x on the five stationary phases p , using the expression:

$$d_{xy} = \sum I_{xp} q_{py}$$

The coefficients q for each descriptor y and stationary phase p can be obtained by multiple linear regression. A good fit between real and calculated d_{xy} descriptor

TABLE VIII
TRUE AND CALCULATED VALUES OF FRUCTOSE DESCRIPTORS

Descriptor ^a	α -Fructofuranose		β -Fructofuranose		α -Fructopyranose		β -Fructopyranose	
	True	Calc. ^b	True	Calc.	True	Calc.	True	Calc.
Σ Eq	2	2.2(2)	3	3.3(3)	1	1.2(1)	2	2.2(2)
Σ 2c	1	1.1(1)	1	1.2(1)	2	1.9(2)	2	1.9(2)
Σ 3c	0	-0.1(0)	0	-0.2(0)	0	0.0(0)	0	0.0(0)
13a	0	-	0	-	1	1.0(1)	0	0.1(0)
13A	0	-	0	-	0	-0.1(0)	1	0.8(1)
Eq2	0	0.1(0)	1	1.1(1)	0	0.0(0)	1	0.9(1)
Eq3	0	0.2(0)	0	0.4(0)	0	0.1(0)	0	0.2(0)
Eq4	1	0.9(1)	1	0.8(1)	0	0.1(0)	0	0.1(0)
23c	0	0.1(0)	1	1.1(1)	0	0.1(0)	1	1.3(1)
23C	1	0.9(1)	0	-0.1(0)	1	0.9(1)	0	-0.3(0)
34c	0	0.0(0)	0	-0.1(0)	0	0.0(0)	0	0.0(0)
45c	0	0.1(0)	0	0.2(0)	1	0.9(1)	1	0.9(1)
13c	0	-0.1(0)	0	-0.3(0)	0	0.1(0)	0	0.3(0)
13C	0	0.0(0)	0	0.1(0)	0	-0.1(0)	0	-0.2(0)

^a See Table V

^b Numbers in parentheses are the calculated values rounded of.

values indicates that the descriptor y could be related to the differences in retention between stationary phases.

When using the full data matrix, the best results were found for acyclic/cyclic forms ($r=0.984$) and for pyranose/furanose rings (P/F, $r=0.903$). In order to find a better correlation for the other descriptors, it was necessary to study furanoses and pyranoses separately. The furanose retention indices were related to twelve different descriptors; the multiple correlation coefficients ranged from 0.68 to 0.99, eight being higher than 0.90. After rounding up (descriptor values are always integral numbers), nine descriptors were correctly predicted for the eight compounds. A similar fit was found for pyranoses, with $r = 0.66-0.99$; twelve of fourteen descriptors were correctly predicted. As an example, Table VIII shows real and calculated descriptor values for α - and β -fructopyranose.

ACKNOWLEDGEMENTS

This work was supported by the Comisión Interministerial de Ciencia y Tecnología (CICYT), project no. 237/84. The authors thank M.I. Jiménez for technical assistance. M. Fernández-Díaz also thanks CICYT for a grant.

REFERENCES

- 1 D. J. Nicole, B. Gillet, E. N. Eppiger and J. J. Delpuch, *Tetrahedron Lett.*, 23 (1982) 1669.
- 2 D. Horton and Z. Walaszeck, *Carbohydr. Res.*, 105 (1982) 145.
- 3 W. Funcke, C. von Sonntag and C. Triantaphylides, *Carbohydr. Res.*, 75 (1979) 305.
- 4 S. T. Angyal and G. S. Bethell, *Aust. J. Chem.*, 29 (1976) 1249.
- 5 E. Bayer, *Anal. Chem.*, 36 (1964) 1453.
- 6 H.-Ch. Curtius, M. Müller and J. A. Völlmin, *J. Chromatogr.*, 37 (1968) 216.
- 7 M. Cockman, D. G. Kubler, A. S. Oswald and L. Wilson, *J. Carbohydr. Chem.*, 6 (1987) 181.
- 8 S. Morgenlie, *Carbohydr. Res.*, 80 (1980) 215.
- 9 P. Decker and H. Schweer, *J. Chromatogr.*, 243 (1982) 372.
- 10 G. J. Wolff and E. Breitwaier, *Chem. Ztg.*, 103 (1979) 232.
- 11 R. Novina, *Chromatographia*, 17 (1983) 441.
- 12 H. Ch. Curtius, J. A. Völlmin and M. Müller, *Fresenius Z. Anal. Chem.*, 243 (1968) 341.
- 13 K. Tesařík, *J. Chromatogr.*, 65 (1972) 295.
- 14 A. García-Raso, I. Martínez-Castro, M. I. Páez, J. Sanz, J. García-Raso and F. Saura-Calixto, *J. Chromatogr.*, 398 (1987) 9.
- 15 I. Martínez-Castro, M. I. Páez, J. Sanz and A. García-Raso, *J. Chromatogr.*, 462 (1989) 49.
- 16 C. C. Sweeley, R. Bentley, M. Makita and W. W. Wells, *J. Am. Chem. Soc.*, 85 (1968) 2497.
- 17 R. J. Smith, J. K. Haken and M. S. Wainwright, *J. Chromatogr.*, 334 (1985) 95.
- 18 T. Okuda and K. Konishi, *Chem. Commun.*, (1969) 1117.
- 19 S. Karady and S. H. Pines, *Tetrahedron*, 26 (1970) 4527.
- 20 S. J. Angyal, *Adv. Carbohydr. Chem. Biochem.*, 42 (1984) 15.
- 21 M. I. Páez, I. Martínez-Castro, J. Sanz, A. García-Raso, F. Saura-Calixto and A. Olano, *Chromatographia*, 23 (1987) 43.
- 22 P. C. M. Hervé du Penhoat and A. S. Perlin, *Carbohydr. Res.*, 36 (1974) 111.
- 23 E. R. Malinowski and D. G. Howery, *Factor Analysis in Chemistry*, Wiley, New York, 1980.
- 24 P. De Smedt, P. A. P. Liddle, B. Cresto and A. Bossard, *Ann. Falsif. Expert. Chim.*, 72 (1979) 633.

CHROM. 21 303

DISPERSION AND SELECTIVITY INDICES IN GAS CHROMATOGRAPHY

PART II^a. STUDIES OF HOMOLOGOUS CARBONYL AND CARBOXYL COMPOUNDS

M. B. EVANS

Division of Chemical Sciences, Hatfield Polytechnic, College Lane, Hatfield, Hertfordshire (U.K.)

and

J. K. HAKEN

Department of Polymer Science, University of New South Wales, P.O. Box 1, Kensington, NSW 2033 (Australia)

SUMMARY

The division of the retention indices of simple carbonyl-containing compounds into components indicative of apolar and polar interactions is reported. About 200 compounds in 40 homologous series were studied, including simple esters with branching and unsaturation in both the alkyl or alcohol and acyl chains, simple and difunctional ketones and simple and branched-chain pyruvate esters. The effects of the various structural parameters are compared with those observed in earlier studies which considered the relationship between retention behaviour and structural parameters.

INTRODUCTION

An extension of the retention index scheme has recently been reported¹ in which the retention index of a solute was divided to show the contributions of apolar forces and polar interactions moderated by steric effects. The apolar forces, described as dispersion indices (I_M), are assumed to be related to the molecular weight of the solute and the polar interactions, described as selectivity indices (I^*), are influenced by structure and the stationary phase used. The relationship is

$$I = I_M + I^* \quad (1)$$

where I_M is defined as the retention index of a hypothetical *n*-alkane having the same molecular weight as the solute and determined by eqn. 2 and I^* is determined by subtraction.

^a For Part I, see ref. 1.

$$I_M = \frac{MW - 2.016}{0.14026} \quad (2)$$

It has been shown generally that solutes possessing polar functional groups tend towards positive I^* values whereas solutes with screened electrons yield negative I^* values. The selectivity parameter has also been shown to be influenced by structural considerations and the effects were examined using a wide range of carbonyl compounds in which the functional groups are of varying but modest polar character using stationary phases that are generally regarded as being of low polarity and to possess donor and acceptor characteristics.

EXPERIMENTAL

The retention indices were determined isothermally at 150°C using 12 ft. \times $1/4$ in. O.D. aluminium columns packed with 10% stationary phase on 62–72-mesh acid-washed, silanized Celatom as reported previously^{2–5}.

RESULTS AND DISCUSSION

Dispersion and selectivity indices for the various homologous compounds considered are shown in Table I. It is apparent that the values of I^* for the *n*-alkyl alkanoates with a constituent carboxyl group of modest polarity decrease both as the

TABLE I

DISPERSION (I_M) AND SELECTIVITY (I^*) INDICES FOR CARBOXYL AND CARBOXYL COMPOUNDS AT 150°C ON SE-30, OV-25 AND SILAR 5CP

Series	Compound	I_M	I^*		
			SE-30	OV-25	SILAR 5CP
Formates	<i>n</i> -C ₁	413.8	-27.8	157.2	348.2
	<i>n</i> -C ₂	513.8	-18.8	141.2	346.2
	<i>n</i> -C ₃	613.8	-11.8	142.2	341.2
	<i>n</i> -C ₄	713.8	-6.8	138.2	345.2
	<i>n</i> -C ₅	813.8	-3.8	138.2	342.2
	<i>n</i> -C ₆	913.8	-6.8	133.2	340.2
	Isopropyl	613.8	-61.8	72.2	255.2
	Isobutyl	713.8	-43.8	89.2	301.2
	Isopentyl	813.8	-36.8	101.2	299.2
Acetates	<i>n</i> -C ₁	513.8	-4.8	179.2	336.2
	<i>n</i> -C ₂	613.8	-21.8	146.2	309.2
	<i>n</i> -C ₃	713.8	-18.8	139.2	299.2
	<i>n</i> -C ₄	813.8	-19.8	135.2	302.2
	<i>n</i> -C ₅	913.8	-22.8	130.2	298.2
	<i>n</i> -C ₆	1013.8	-25.8	119.2	389.2
	Isopropyl	713.8	-70.8	68.2	200.2
	Isobutyl	813.8	-63.8	84.2	249.2
	Isopentyl	913.8	-54.8	87.2	258.2

TABLE I (continued)

Series	Compound	I_M	I^*		
			SE-30	OV-25	SILAR 5CP
Propionates	<i>n</i> -C ₁	613.8	3.2	161.2	333.2
	<i>n</i> -C ₂	713.8	-21.8	131.2	284.2
	<i>n</i> -C ₃	813.8	-24.8	120.2	284.2
	<i>n</i> -C ₄	913.8	-27.8	118.2	281.2
	<i>n</i> -C ₅	1013.8	-33.8	111.2	275.2
	<i>n</i> -C ₆	1113.8	-39.8	101.2	274.2
	Isopropyl	813.8	-80.8	57.2	187.2
	Isobutyl	913.8	-65.8	71.2	227.2
	Isopentyl	1013.8	-65.8	72.2	229.2
Butanoates	<i>n</i> -C ₁	713.8	-11.8	154.2	318.2
	<i>n</i> -C ₂	813.8	-35.8	117.2	271.2
	<i>n</i> -C ₃	913.8	-38.8	108.2	265.2
	<i>n</i> -C ₄	1013.8	-44.8	100.2	258.2
	<i>n</i> -C ₅	1113.8	-51.8	97.2	248.2
	<i>n</i> -C ₆	1213.8	-57.8	78.2	237.2
	Isopropyl	913.8	-93.8	41.2	177.2
	Isobutyl	1013.8	-80.8	51.2	203.2
	Isopentyl	1113.8	-74.8	49.2	202.2
Pentanoates	<i>n</i> -C ₁	813.8	-6.8	147.2	317.2
	<i>n</i> -C ₂	913.8	-37.8	100.2	265.2
	<i>n</i> -C ₃	1013.8	-42.8	97.2	207.2
	<i>n</i> -C ₄	1113.8	-50.8	91.2	242.2
	<i>n</i> -C ₅	1213.8	-58.8	91.2	200.2
	<i>n</i> -C ₆	1313.8	-66.8	68.2	225.2
	Isopropyl	1013.8	-98.8	32.2	166.2
	Isobutyl	1113.8	-85.8	42.2	193.2
	Isopentyl	1213.8	-81.8	39.2	191.2
Hexanoates	<i>n</i> -C ₁	913.8	-11.8	142.2	311.2
	<i>n</i> -C ₂	1013.8	-37.8	104.2	261.2
	<i>n</i> -C ₃	1113.8	-49.8	93.2	249.2
	<i>n</i> -C ₄	1213.8	-57.8	81.2	200.2
	<i>n</i> -C ₅	1313.8	-67.8	70.2	225.2
	<i>n</i> -C ₆	1413.8	-76.8	56.2	212.2
	Isopropyl	1113.8	-95.8	17.2	161.2
	Isobutyl	1213.8	-94.8	32.2	183.2
	Isopentyl	1313.8	-101.8	28.2	180.2
Isobutanoates	<i>n</i> -C ₁	713.8	-48.8	98.2	243.2
	<i>n</i> -C ₂	813.8	-81.8	61.2	202.2
	<i>n</i> -C ₃	913.8	-77.8	54.2	193.2
	<i>n</i> -C ₄	1013.8	-82.8	45.2	187.2
	<i>n</i> -C ₅	1113.8	-89.8	41.2	180.2
	<i>n</i> -C ₆	1213.8	-96.8	24.2	169.2
	<i>iso</i> -C ₃	913.8	-133.8	-25.8	200.2
	<i>iso</i> -C ₄	1013.8	-114.8	-6.8	135.2
	<i>iso</i> -C ₅	1113.8	-119.8	-5.8	135.2

(Continued on p. 220)

TABLE 1 (continued)

Series	Compound	I_M	I^*		
			SE-30	OV-25	SILAR 5CP
Isopentanoates	<i>n</i> -C ₁	813.8	-50.8	88.2	249.2
	<i>n</i> -C ₂	913.8	-74.8	53.2	200.2
	<i>n</i> -C ₃	1013.8	-84.8	45.2	192.2
	<i>n</i> -C ₄	1113.8	-92.8	35.2	182.2
	<i>n</i> -C ₅	1213.8	-101.8	24.2	176.2
	<i>n</i> -C ₆	1313.8	-109.8	22.2	160.2
	<i>iso</i> -C ₃	1013.8	-139.8	-24.8	113.2
	<i>iso</i> -C ₄	1113.8	-128.8	-17.8	132.2
	<i>iso</i> -C ₅	1213.8	-132.8	-18.8	129.2
Isohexanoates	<i>n</i> -C ₁	913.8	-38.8	105.2	263.2
	<i>n</i> -C ₂	1013.8	-70.8	64.2	205.2
	<i>n</i> -C ₃	1113.8	-78.8	51.2	199.2
	<i>n</i> -C ₄	1213.8	-90.8	38.2	188.2
	<i>n</i> -C ₅	1313.8	-98.8	26.2	176.2
	<i>n</i> -C ₆	1413.8	-107.8	13.2	160.2
	<i>iso</i> -C ₃	1113.8	-134.8	-18.8	115.2
	<i>iso</i> -C ₄	1213.8	-124.8	-11.8	126.2
	<i>iso</i> -C ₅	1313.8	-132.8	-15.8	128.2
2-Methylpentanoates	<i>n</i> -C ₁	913.8	-60.8	75.2	217.2
	<i>n</i> -C ₂	1013.8	-96.8	39.2	159.2
	<i>n</i> -C ₃	1113.8	-104.8	22.2	152.2
	<i>n</i> -C ₄	1213.8	-116.8	9.2	138.2
	<i>n</i> -C ₅	1313.8	-126.8	-3.8	126.2
	<i>n</i> -C ₆	1413.8	-136.8	-15.8	113.2
	<i>iso</i> -C ₃	1113.8	-161.8	-53.8	62.2
	<i>iso</i> -C ₄	1213.8	-149.8	-34.8	88.2
	<i>iso</i> -C ₅	1313.8	-159.8	-64.8	80.2
2-Ethylbutanoates	<i>n</i> -C ₁	913.8	-68.8	65.2	202.2
	<i>n</i> -C ₂	1013.8	-99.8	23.2	157.2
	<i>n</i> -C ₃	1113.8	-111.8	16.2	146.2
	<i>n</i> -C ₄	1213.8	-120.8	3.2	129.2
	<i>n</i> -C ₅	1313.8	-130.8	-10.8	120.2
	<i>n</i> -C ₆	1413.8	-140.8	-20.8	106.2
	<i>iso</i> -C ₃	1113.8	-159.8	-56.8	-39.8
	<i>iso</i> -C ₄	1213.8	-153.8	-46.8	-19.8
	<i>iso</i> -C ₅	1313.8	-164.8	-50.8	-26.8
Pivalates	<i>n</i> -C ₁	713.5	-107.8	-30.8	137.2
	<i>n</i> -C ₂	813.5	-142.8	-71.8	86.2
	<i>n</i> -C ₃	913.5	-143.8	-74.8	83.2
	<i>n</i> -C ₄	1013.5	-148.8	-82.8	87.2
	<i>n</i> -C ₅	1113.5	-152.8	-89.8	80.2
	<i>n</i> -C ₆	1213.5	-	-	77.2
	<i>iso</i> -C ₃	913.5	-206.8	-150.8	-19.7
	<i>iso</i> -C ₄	1013.5	-177.8	-120.8	28.2
	<i>iso</i> -C ₅	1113.5	-183.8	-126.8	34.2

TABLE I (continued)

Series	Compound	I_M	I^*		
			SE-30	OV-25	SILAR 5CP
2-Propenoates	<i>n</i> -C ₁	599.7	3.3	177.3	352.3
	<i>n</i> -C ₂	699.7	-13.7	136.3	314.3
	<i>n</i> -C ₃	799.7	-14.7	144.3	312.3
	<i>n</i> -C ₄	899.7	-19.7	137.3	309.3
	<i>n</i> -C ₅	999.7	-24.7	131.3	302.3
	<i>n</i> -C ₆	1099.7	-31.7	121.3	292.3
	<i>iso</i> -C ₃	799.7	-70.7	57.3	227.3
	<i>iso</i> -C ₄	899.7	-57.7	87.3	250.3
	<i>iso</i> -C ₅	999.7	-57.7	89.3	256.3
2-Methyl-2-propenoates	<i>n</i> -C ₁	699.7	-0.7	160.3	326.3
	<i>n</i> -C ₂	799.7	-27.7	121.3	272.3
	<i>n</i> -C ₃	899.7	-34.7	115.3	273.3
	<i>n</i> -C ₄	999.7	-37.7	108.3	264.3
	<i>n</i> -C ₅	1099.7	-45.7	99.3	256.3
	<i>n</i> -C ₆	1199.7	-53.7	88.3	245.3
	<i>iso</i> -C ₃	899.7	-90.7	32.3	182.3
	<i>iso</i> -C ₄	999.7	-74.7	56.3	110.3
	<i>iso</i> -C ₅	1099.7	-77.7	57.3	113.3
2-Butenoates	<i>n</i> -C ₁	699.7	53.3	240.3	443.3
	<i>n</i> -C ₂	799.7	26.3	209.3	399.3
	<i>n</i> -C ₃	899.7	22.3	205.3	392.3
	<i>n</i> -C ₄	999.7	17.3	198.3	386.3
	<i>n</i> -C ₅	1099.7	10.3	190.3	379.3
	<i>n</i> -C ₆	1199.7	2.3	180.3	367.3
	<i>iso</i> -C ₃	899.7	-35.6	211.3	304.3
	<i>iso</i> -C ₄	999.7	-24.6	248.3	337.3
	<i>iso</i> -C ₅	1099.7	-27.6	250.3	333.3
3-Butanoates	<i>n</i> -C ₁	699.7	-7.6	173.3	368.3
	<i>n</i> -C ₂	799.7	-29.6	137.3	323.3
	<i>n</i> -C ₃	899.7	-37.3	129.3	310.3
	<i>n</i> -C ₄	999.7	-42.3	120.3	302.3
	<i>n</i> -C ₅	1099.7	-51.3	111.3	295.3
	<i>n</i> -C ₆	1199.7	-58.3	100.3	282.3
	<i>iso</i> -C ₃	899.7	-93.8	56.3	226.3
	<i>iso</i> -C ₄	999.7	-79.8	80.3	248.3
	<i>iso</i> -C ₅	1099.7	-83.8	79.3	249.3
3-Methyl-2-butenoates	<i>n</i> -C ₁	799.7	31.3	218.3	396.3
	<i>n</i> -C ₂	899.7	2.3	188.3	354.3
	<i>n</i> -C ₃	999.7	-4.7	177.3	344.3
	<i>n</i> -C ₄	1099.7	-11.7	170.3	335.3
	<i>n</i> -C ₅	1199.7	-20.7	162.3	322.3
	<i>n</i> -C ₆	1299.7	-28.7	152.3	313.3
	<i>iso</i> -C ₃	999.7	-59.7	111.3	259.3
	<i>iso</i> -C ₄	1099.7	-49.7	120.3	279.3
	<i>iso</i> -C ₅	1199.7	-53.7	119.3	279.3

(Continued on p. 222)

TABLE I (continued)

Series	Compound	I_M	I^*		
			SE-30	OV-25	SILAR 5CP
<i>trans</i> -2-Hexenyl esters	Formate	899.7	4.3	157.3	373.3
	Acetate	999.7	-16.7	148.3	331.3
	Propionate	1099.7	-29.7	132.3	305.3
	Butyrate	1199.7	-46.0	111.3	277.3
	Pentanoate	1299.7	-56.0	102.3	265.3
	Hexanoate	1399.7	-62.0	91.3	235.3
<i>cis</i> -2-Hexenyl esters	Formate	899.7	3.3	168.3	378.3
	Acetate	999.7	-17.7	156.3	330.3
	Propionate	1099.7	-30.7	142.3	303.3
	Butyrate	1199.7	-47.7	119.3	275.3
	Pentanoate	1299.7	-56.7	110.3	264.3
	Hexanoate	1399.7	-66.7	99.3	250.3
Alk-1-ene-3-yl acetates	Pentyl	876.7	-58.7	76.4	264.4
	Hexyl	976.7	-79.7	65.4	249.4
	Heptyl	1076.7	-87.7	55.4	232.4
	Octyl	1176.7	-93.7	42.4	213.4
	Nonyl	1276.7	-101.7	29.4	201.4
	Decyl	1376.7	-109.7	15.4	184.4
2-Alkanones	Propanone	399.7	59.3	174.3 ^a	507.3
	Butanone	499.7	69.3	190.3	394.3
	Pentanone	599.7	73.3	186.3	378.3
	Hexanone	699.7	78.3	192.3	387.3
	Heptanone	799.7	75.3	198.3	388.3
	Octanone	899.7	77.3	206.3	388.3
Diketones	2,3-Butanedione	599.2	-44.2	90.8 ^a	405.8
	2,3-Pentanedione	699.2	-32.2	98.8	418.8
	2,4-Pentanedione	699.2	79.2	231.8	740.8
	2,3-Hexanedione	799.2	-35.2	85.8	394.8
	2,5-Hexanedione	799.2	106.8	310.8	800.8
	3,5-Heptanedione	899.2	77.8	213.8	689.8
	2,3-Octanedione	999.2	-31.2	85.8	395.8
	4,6-Nonanedione	1099.2	52.8	168.8	547.8
Pyruvates	<i>n</i> -C ₁	713.5	-12.5	159.5 ^a	574.5
	<i>n</i> -C ₂	813.5	-39.5	127.5	527.5
	<i>n</i> -C ₃	913.5	-43.5	114.5	511.5
	<i>n</i> -C ₄	1013.5	-45.5	106.5	507.5
	<i>n</i> -C ₅	1113.5	-46.5	98.5	503.5
	<i>n</i> -C ₆	1213.5	-49.5	90.5	497.5

^a Stationary phase DC-710.

alkyl or alcohol chain (R^1) length increases and as the acyl or acid chain (R) length increases. Both effects are due to increasing methylene content of the compounds, the reduced polar character tending towards the behaviour of hydrocarbons.

All of the values are higher than those obtained on low polarity SE-30, on OV-25 with accepted donor character and on Silar 5CP with acceptor characteristics. The

increased values of I^* with the alkyl esters are largely due, however, to the increased general polarity of the phases rather than the effects of particular interactions.

Table II shows representative esters of the same molecular weight, *i.e.*, $C_7H_{14}O_2$, where it is apparent that I^* decreases as R^1 decreases and R increases, and also as R^1 increases and R decreases. The effect is common with other series as shown previously² and demonstrates that the addition of a methylene group has a greater effect on retention when introduced into the alcohol (R^1) than the acyl (R) chain. The effect is due to the lone pair of electrons on the ethereal oxygen atom.

TABLE II
SELECTIVITY INDICES OF ESTERS OF EMPIRICAL FORMULA $C_7H_{14}O_2$

Ester	Chain length		Selectivity index		
	R	R^1	SE-30	OV-25	Silar 5CP
Hexyl formate	0	6	-6.8	133.2	340.2
Pentyl acetate	1	5	-22.8	130.2	298.2
Butyl propanoate	2	4	-27.8	118.2	281.2
Propyl butanoate	3	3	-38.8	108.2	265.2
Ethyl pentanoate	4	2	-37.8	100.2	265.2
Methyl hexanoate	5	1	-11.8	142.2	311.2
Isopentyl acetate	1	5	-54.8	78.2	258.2
Isobutyl propanoate	2	4	-65.8	71.2	229.2
Isopropyl butanoate	3	3	-93.8	41.2	177.2

It is evident from Table II that the value for methyl hexanoate is atypical and from Table I it is observed that the I^* values for the methyl esters are much higher than those for the other homologues owing to their higher retention. This methyl effect is well known, with the methyl group having a greater effect on the carbonyl group.

With branched-chain alkyl groups, I^* is decreased relative to the *n*-alkyl group, with the effect being most apparent with the isopropyl group and being progressively reduced with the isobutyl and isopentyl groups. The effect of branching on the carbonyl group, which is essentially responsible for I^* , is reduced as the pendant group becomes more distant from the carbonyl group.

When branching is introduced into the acyl chain similar effects are observed. By examination of the series of alkyl isobutanoates and isobutylalkanoates and of the alkyl isopentanoates and isopentylalkanoates, shown in Table III, it is evident that the presence of the branched-chain group in the alkyl chain has a greater effect on retention than when it is in the acid chain.

The effect of branching in other than the terminal position is shown by the homologous 2-methyl pentanoates and 2-ethyl butanoate esters. The first series show I^* values which are much lower than those of both the normal and the isoesters, the effect of a methyl substituent at the 2- rather than the 4-position having a profound effect on the carbonyl group. The ester of the same molecular weight having an ethyl group at the 2-position has a slightly greater effect with reduced retention and reduced I^* .

TABLE III
INFLUENCE OF BRANCHING OF ALKYL AND ACYL CHAINS

<i>Isoalkanoate esters</i>	<i>I*</i>		<i>Isoalkyl esters</i>	<i>I*</i>	
	<i>OV-25</i>	<i>Silar 5CP</i>		<i>OV-25</i>	<i>Silar 5CP</i>
<i>Isobutanoates</i>			<i>Isobutyl esters</i>		
Ethyl	61	202	Acetate	84	249
Propyl	54	193	Propanoate	71	227
Butyl	45	187	Butanoate	51	203
Pentyl	41	180	Pentanoate	42	193
Hexyl	24	169	Hexanoate	32	183
<i>Isopentanoates</i>			<i>Isopentyl esters</i>		
Ethyl	53	200	Acetate	87	258
Propyl	45	192	Propanoate	72	229
Butyl	35	182	Butanoate	49	202
Pentyl	24	172	Pentanoate	39	191
Hexyl	22	100	Hexanoate	28	180

The effect of chain branching is further evident with the pivalate esters, where on all stationary phases substantially lower I^* values are evident than with the *n*-acyl esters and with branched alkyl chain esters. With the pivalate esters further shielding of the carbonyl occurs with branching in the alcohol chain, and further reductions in I^* occur.

The effect of introducing unsaturation into the esters is considered at several positions along the acyl chain. The homologous series of 2-propenoates show only slightly greater values of I^* than the corresponding propanoates. A greater enhancement of I^* might have been expected owing to the conjugated type of structure. The values of I^* are only slightly reduced by the presence of a methyl group adjacent to the carbonyl, but the enhancement of I^* is considerable relative to the saturated counterparts, *i.e.* alkyl isobutanoates, as shown in Table IV.

TABLE IV
EFFECT OF UNSATURATION IN PROPANOIC AND ISOBUTANOIC ACIDS

<i>Alkyl group</i>	<i>I*</i>							
	<i>Propanoates</i>		<i>2-Propenoates</i>		<i>Isobutanoates</i>		<i>2-Methyl-2-propenoates</i>	
	<i>SE-30</i>	<i>Silar 5CP</i>	<i>SE-30</i>	<i>Silar 5CP</i>	<i>SE-30</i>	<i>Silar 5CP</i>	<i>SE-30</i>	<i>Silar 5CP</i>
Methyl	161	333	177	352	98	243	160	326
Ethyl	130	284	136	314	61	202	121	272
Propyl	120	284	144	312	54	193	115	273
Butyl	118	281	137	309	45	187	108	264
Pentyl	111	275	131	302	41	180	99	256
Hexyl	101	274	121	292	24	169	88	245
Isopropyl	57	187	57	227	-25	200	32	182
Isobutyl	71	227	87	250	-7	135	56	110
Isopentyl	72	229	89	256	-6	135	57	113

The 2-butenates show much higher values of I^* (50%) than the corresponding saturated esters, the only difference from the 2-propenoates being the terminal methyl group. The influence of the conjugated type of structure is evident particularly as the 3-butenates show only slightly greater values of I^* than the saturated homologues.

The alkyl-1-enyl-3-yl acetates show reduced values of I^* in the isolated examples where comparison with normal esters is possible and with the branched-chain structure, and this is to be expected.

Pyruvate esters with a double carbonyl group show the same effect as esters with a single carbonyl group in that decreased values of I^* are observed as the methylene content is increased. The absolute values of I^* on the non-polar and phenyl phases are slightly lower than for the corresponding acetate, but a considerable enhancement is experienced on the Silar 5CP phase.

The simple ketones, *i.e.*, 2-alkanones, show higher values of I^* than the almost comparable acetate esters on both the low-polarity and the phenyl phase; the values for the ketones increase slightly with increasing methylene content whereas the esters show a much more pronounced decrease. The values of I^* for the ketones on the highly polar phase are increased considerably and the values tend to be relatively stable with increasing number of methylene groups. Here the effects are due principally to polar interactions of the carbonyl group and the polar groups of the stationary phase. The overall increases in the I^* values of the ketones are not unexpected as the dipole moments of the ketones are substantially higher than those of the esters.

The 2,3-diketones on SE-30 and the phenyl phase surprisingly show lower I^* values than for the simple ketones and slightly higher values on Silar 5CP. Variation of the position of the carbonyl group, however, has a profound effect on the I^* values. On Silar 5CP the carbonyl groups at the 2,4- rather than the 2,3-position cause a 75%

TABLE V
SELECTIVITY INDICES OF ALIPHATIC DIKETONES

Structure	Selectivity index	
	SE-30	Silar 5CP
$\begin{array}{c} \text{O} \quad \text{O} \\ \quad \\ \text{C}-\text{C}-\text{C}-\text{C}-\text{C} \end{array}$	98.8	418.8
$\begin{array}{c} \text{O} \quad \text{O} \\ \quad \\ \text{C}-\text{C}-\text{C}-\text{C}-\text{C} \end{array}$	231.8	740.8
$\begin{array}{c} \text{O} \quad \quad \text{O} \\ \quad \quad \\ \text{C}-\text{C}-\text{C}-\text{C}-\text{C}-\text{C} \end{array}$	310.8	800.8
$\begin{array}{c} \text{O} \quad \text{O} \\ \quad \\ \text{C}-\text{C}-\text{C}-\text{C}-\text{C}-\text{C} \end{array}$	213.8	689.8
$\begin{array}{c} \text{O} \quad \text{O} \\ \quad \\ \text{C}-\text{C}-\text{C}-\text{C}-\text{C}-\text{C}-\text{C}-\text{C} \end{array}$	168.8	547.8

increase, whereas on increasing the chain length to maintain the CH_3CO - end groups and to increase the distance between the carbonyl groups to two methylene groups a further increase in I^* occurs. Similarly, maintaining a single methylene group between the carbonyl groups and with $\text{CH}_3\text{CH}_2\text{CO}$ - and $\text{CH}_3\text{CH}_2\text{CH}_2\text{CO}$ - end groups progressive decreases in I^* occur, as shown in Table V.

The values of I^* may in part be explained by enolization and the inductive effect of the methyl groups, where dipole moment studies show an increased polarity of the carbonyl bond adjacent to a methyl group. However, such inductive effects are not transmitted greatly along an alkyl chain.

The propyl effect, *i.e.* the intramolecular interaction between a propyl group and a π -electron system of the solute, has been shown to have a pronounced effect on retention⁶. The low values for 2-pentanone (Table I) and the diketones (Table V) may be due to steric hindrance. Steric hindrance has previously been shown to affect the reactivity of various ketones in studies involving on-column chemical reactions⁷.

As the selectivity and dispersion indices are determined from the retention indices, no contribution or allowance is made for adsorption effects, which in certain circumstances are significant. The same limitation applies in the Rohrschneider and McReynolds systems. If allowances are to be made for adsorption effects it is likely that a primary reference series other than the *n*-alkanes is necessary. Despite many reports over several decades, it is apparent that no alternative standards have been universally acceptable.

ACKNOWLEDGEMENT

The authors acknowledge the care taken by Jane Fordham in the preparation of the manuscript.

REFERENCES

- 1 M. B. Evans, J. K. Haken and T. Toth, *J. Chromatogr.*, 351 (1986) 155.
- 2 J. R. Ashes and J. K. Haken, *J. Chromatogr.*, 101 (1974) 103.
- 3 J. K. Haken, D. K. M. Ho and C. E. Vaughan, *J. Chromatogr.*, 106 (1975) 317.
- 4 J. K. Haken, D. K. M. Ho and M. S. Wainwright, *J. Chromatogr.*, 106 (1975) 327.
- 5 J. R. Ashes and J. K. Haken, *J. Chromatogr.*, 111 (1975) 171.
- 6 L. Soják, I. Ostrovský and J. Janák, *J. Chromatogr.*, 406 (1987) 43.
- 7 J. R. Ashes and J. K. Haken, *Anal. Chem.*, 45 (1973) 1131.

CHROM. 21 281

QUANTITATIVE RELATIONSHIPS BETWEEN THE STRUCTURE OF ALKYL BENZENES AND THEIR GAS CHROMATOGRAPHIC RETENTION ON STATIONARY PHASES WITH DIFFERENT POLARITY

N. DIMOV*

Chemical Pharmaceutical Institute, Kl. Okhridsky str. 3, 1156 Sofia (Bulgaria)

and

Ov. MEKENYAN

Higher School of Chemical Technology (VHTI), 8010 Burgas (Bulgaria)

SUMMARY

The retention indices of 28 C₆-C₁₀ and *n*-C₁₁ alkylbenzenes were determined on silicone oil OV-101, UCON LB-550-X, Carbowax 20M and TCEP. Additionally, retention indices of the same compounds on squalane, PEG-4000 and Carbowax 1540 were taken from the literature for quantitative structure-retention investigations. A general mode for deriving adequate precalculation equations was used. Two different kinds of regressors were studied.

The best results, presented as the maximum discrepancy between the experimental and calculated retention indices, are 1.5 for squalane, 2.5 for OV-101, 2.9 for UCON, 2.4 for Carbowax 20M, 5.6 for Carbowax 1540, 11.3 for PEG-4000 and 7 for TCEP. A very high correlation between the polarity of the studied phases and some of the regressors has been found.

INTRODUCTION

Recently, an adequate equation for the precalculation of the retention indices of alkylbenzenes on squalane has been proposed¹. This stationary phase is widely applied in petroleum analysis but, especially for alkylbenzenes, stationary phases such as silicone oil OV-101^{2,3} or equivalents, more polar phases such as Carbowax 20M^{4,5} and even strongly polar phases such as TCEP (triscyanoethoxypropane)⁶ are preferred.

The derivation of equations for the precalculation of the retention indices of alkylbenzenes on phases more polar than squalane is of practical interest. There have been many investigations to find a satisfactory correlation between the retention and physico-chemical properties or topological and/or electronic indices of the alkylbenzenes (*e.g.*, refs. 7-11), but the discrepancies between the calculated values (I_{calc}) and the experimentally obtained retention indices (I) are too great.

A new model has now been used for deriving an adequate equation for the precalculation of the retention indices of alkylbenzene. The model is based on the assumption that the retention is an additive property depending on some basic and

several tuning contributors¹². The value of I_{calc} obtained from the basic contributor(s) is 90–110% of the I_{exp} value. The deviations are then compensated by addition of suitable tuning contributors. As the basic and tuning contributors in this study, all of the indices given previously¹ were considered. The retention indices of 28 C₆–C₁₀ and *n*-C₁₁ alkylbenzenes were obtained experimentally on OV-101, UCON LB-550-X, Carbowax 20M and TCEP. Unified retention indices on squalane¹³ and literature data for the retention indices of alkylbenzenes on Carbowax 1540¹⁴ and Carbowax 4000¹¹ were also included.

EXPERIMENTAL

The retention indices of the alkylbenzenes studied were determined on fused-silica capillary columns with flame ionization detection under the following conditions (stationary phase, column dimensions, column temperature, splitting ratio): OV-101, 50 m × 0.25 mm I.D., 100°C, 1:80; UCON LB-550-X, 50 m × 0.32 mm I.D., 100°C, 1:80; Carbowax 20M, 30 m × 0.32 mm I.D., 100°C, 1:100; and TCEP, 30 m × 0.32 mm I.D., 80°C, 1:100.

The retention times of *n*-alkanes on the column with TCEP showed poor repeatability. To obtain more reliable results, their retention time was calculated from the regression equation of their retention at different temperatures.

DATA HANDLING AND RESULTS

The general model given previously¹² was rearranged to the equation

$$I_{\text{calc.}} = b_0 + b_1 I_p + \sum b_j T_j$$

where I_p is the vapour pressure index, proposed by Bonastre and Grenier¹⁵, T_j are selected tuning structural indices and b_0 , b_1 and b_j are constants (estimates of the parameter contributions).

The indices selected are explained after the corresponding equations. The criteria used for selection are the values of the variance and the maximum discrepancy between I_{exp} and I_{calc} . (Δ_{max}). The best equations are presented in Table I.

The upper limit of the number of parameters is taken as eight in order to avoid chance correlations¹⁶. A decrease in the number of parameters depends on the accuracy required. It is seen from Table I that equations with different numbers of parameters have the same value of Δ_{max} . Hence several equations might be derived, depending on the availability of values for the tuning indices. These equations might be used not only for the exact precalculation of the retention indices in the interpolation region, but also for predictive calculations. From a statistical point of view, the equations with the least number of independent regressors have the best extrapolation possibilities. These requirements are fulfilled only for eqns. 7, 8, 9 and 19, because the intercorrelation between I_p , X_1 , E_{LUMO} , qA and qB and qT is insignificant. This is why the predictive ability was checked for a large number of equations. Two compounds, namely 1,2,3-trimethylbenzene (123TMB) and *n*-pentylbenzene (*n*PeB) were removed from the initial set of retention data. 123TMB has a unique structure with its three neighbouring substituents and differs substantially from all other alkylarenes with

nine carbon atoms. nPeB is a homologue of *n*-alkylbenzenes, but with its eleven carbon atom lies in the extrapolation n_C region. New constants for the corresponding predictive equations were calculated:

$$I_{SQ} = 155.9 + 0.97994 I_p - 13.34 X1 - 26.12 E_{LUMO} + 28.48 qA \quad (1)$$

$$I_{OV-101} = 21.3 + 0.9808 I_p + 6.172 X1 + 118.67 qA - 60.42 qB + 1.115 qT \quad (2)$$

$$I_{UCON} = 104.8 + 1.14009 I_p - 3.62 L_{max} - 0.4536 \varepsilon + 98.87 qA - 155.6 qB + 35.1 qT \quad (3)$$

$$I_{C-20M} = 148.4 + 1.37267 I_p - 6.265 L_{max} + 20.59 E_{LUMO} - 1.1868 \varepsilon + 233.7 qA - 177.79 qB \quad (4)$$

$$I_{TCEP} = 404.4 + 1.60548 I_p - 13.5 L_{max} - 2.0216 \varepsilon + 331.86 qA - 335.48 qB + 56.47 qT \quad (5)$$

where

$X1$ is the first eigenvector in the graph spectrum of the solute molecule;

L_{max} is the maximum geometric distance between the atoms of the solute molecule;

ε is I'Haya's electropy index¹⁷;

E_{LUMO} is the energy of the LUMO orbitals of the solute molecule; all quantum chemical calculations were done at VHTI, Burgas, by the standard CNDO method;

qA is the sum of the absolute charges of the carbon atoms in the functional group;

qB accounts for the charges of carbon atoms at α -positions to the aromatic ring; and

qT is the sum of the absolute charges of all carbon atoms in the solute molecule¹⁸.

The value of the predicted retention index, I_{pred} , of *n*-PeB and 123TMB and also the values of I_{calc} are compared with the experimental values in Table II.

To establish the significance of the parameters in equation 1-5 for the quantitative relationships between the retention and the structure of the alkylbenzenes, the same indices were applied to retention data for alkylbenzenes obtained by other workers on the same or different stationary phases. The new equations obtained (eqns. 6-8) are similar to eqns. 3-5 in the magnitudes of the parametric estimates and have the same sign, accuracy and predictive possibilities.

$$I_{UCON} = 99.7 + 1.15484 I_p - 2.93 L_{max} - 0.52 \varepsilon + 169.1 qA - 197.4 qB + 56.6 qT \quad (6)$$

TABLE I
PARAMETRIC ESTIMATIONS (b_1 - b_j) OF THE REGRESSORS USED AND VALUES OF THE MAXIMUM DISCREPANCY (Δ_{\max}) BETWEEN I_{calc} AND I_{exp} .

Stationary phase	Eqn. No.	No. of regressors	b_1 (I_p)	b_2 ($X1$)	b_3 (E_{lumo})	b_4 (qA)	b_5 (qB)	b_6 (L_{\max})	b_7 (ϵ)	b_8 (qT)	Δ_{\max} (i.u.)
Squalane	1	8	0.99685	-21.68	-24.623	32.07	4.47	-0.55	-0.020	-8.148	1.4
	2	7	0.9987	-22.25	-26.42	40.70	-12.37	-0.60	-0.021		1.5
	3	7	0.99731	-21.61	-25.083	34.52		-0.55	-0.020	-6.23	1.5
	4	7	0.99486	-14.55	-22.783	36.06	5.45		-0.039	-9.05	1.7
	5	6	0.98282	-15.29	-25.68	26.85	11.56			-11.91	1.7
	6	6	0.9954	-14.4	-23.33	39.10			-0.040	-6.72	1.7
	7	5	0.98326	-15.01	-27.06	32.97				-6.94	1.7
	8	5	0.98358	-15.03	-28.53	39.28	-13.06				1.7
	9	4	0.98235	-16.71	-26.66	30.22					1.8
	10	3	0.97619		-23.08	25.52					2.5
OV-101	11	8	0.96272	-1.88	-2.00	89.89	-36.84	-0.89	0.069	-8.13	2.7
	12	7	0.95895	-2.39	1.79	69.71		-0.85	0.076	-23.90	2.5
	13	7	0.96447	-2.11	-3.72	98.65	-53.70	-0.93	0.067		2.5
	14	7	0.97377	7.98	3.60	105.36	-42.60	-0.19		-6.05	2.5
	15	6	0.97094	10.35	3.73	105.13	-41.16			-6.87	2.5

	16	5	0.97245	9.12	115.07	- 59.48				0.73	2.5
	17	5	0.97566	6.23	113.86	- 58	-0.22				2.5
	18	5	0.954		68.13		-0.74	0.086		-24.54	2.5
	19	4	0.9725	8.98	114.5	- 58.21					2.5
	20	4	0.98036		112.76	- 56.15	-0.49				2.5
UCON-LB-550X	21	8	1.12489	- 0.22	144.46	- 189.83	-3.06	-0.41		46.31	2.4
	22	7	1.11592	- 1.78	93.59	- 93.28	-2.99	-0.40			3.0
	23	7	1.1248		144.54	- 189.92	-3.05	-0.41		46.33	2.9
	24	6	1.11513	5.08	94.08	- 93.72	-2.91	-0.40			3.0
	25	6	1.14247		104.8	- 162.37	-3.39	-0.46		37.54	2.8
	26	5	1.10758		92.49	- 98.34	-2.93	-0.37			3.6
Carbowax 20M	27	8	1.4189	-24.6	243.75	- 281.94	-8.1	-1.23		0.05	4.7
	28	7	1.3853	-22.25	230.48	- 175.91	-7.3	-1.17			6.3
	29	7	1.4179	-28.88	241.85	- 289.49	-8.37	-1.21		58.78	4.8
	30	6	1.4064		254.37	- 309.36	-7.03	-1.246		64	6.3
	31	6	1.3802	22.39	240.4	- 179.84	-6.16	-1.21			5.8
	32	5	1.3469		233.4	- 200.21	-6.24	-1.09			6.1
TCEP	33	8	1.5998	0.035	347.36	- 346.9	-12.07	-2.087		0.06	6.8
	34	7	1.5663	0.038	333.97	- 239.41	-11.22	-2.024			7
	35	7	1.6085	- 3.94	331.72	- 341.99	-13.84	-2.018		0.06	7.2
	36	6	1.6100		331.78	- 332.27	-13.78	-2.03		53.72	7
	37	5	1.5613		314.22	- 241.12	-13.12	-1.9			8.0

TABLE II
COMPARISON OF $I_{\text{calc.}}$ OF 26 C_6-C_{10} ALKYL BENZENES AND $I_{\text{pred.}}$ OF *n*-PeB AND 123TMB WITH $I_{\text{exp.}}$ ON SIX STATIONARY PHASES WITH DIFFERENT POLARITY

No.	Alkylbenzene	Squalane		OV-101		UCON LB		Carbowax 20M		TCEP	
		$I_{\text{exp.}}$	$I_{\text{calc.}}$	$I_{\text{exp.}}$	$I_{\text{calc.}}$	$I_{\text{exp.}}$	$I_{\text{calc.}}$	$I_{\text{exp.}}$	$I_{\text{calc.}}$	$I_{\text{exp.}}$	$I_{\text{calc.}}$
1	Benzene (B)	650.4	649.6	663	660.7	760	760.9	935	931.2	1127	1122.4
2	Toluene (MB)	757.6	757.7	766	765	864	863	1032	1030.6	1219	1217.0
3	EthylB (EtB)	847.5	847.3	857	856	952	954.5	1117	1119.3	1289	1290.2
4	<i>n</i> -PropylB (nPrB)	936.3	936.4	947.5	947.4	1038.5	1037.6	1197	1198.1	1350	1351.4
5	<i>n</i> -ButylB	1036.2	1037.0	1046	1048.6	1136	1134.9	1291	1290.6	1431	1429
6	iPrB	907.5	909.2	919	920.4	1009	1010.4	1164	1167.7	1320	1324.1
7	iBuB	989.9	990.0	1002	1002.6	1083	1083.1	1228	1233.8	1365	1372.2
8	<i>sec</i> -BuB	990.0	991.4	1004	1003.1	1089	1088.5	1235	1237.3	1372	1378.9
9	<i>tert</i> -BuB	973.3	973.7	986	988	1075	1072.1	1223	1224.4	1373	1373.1
10	<i>p</i> -Xylene	861.9	862.6	866	865.5	963	961.3	1126	1127.6	1304	1307.9
11	<i>m</i> -Xylene	864.4	863.9	866	866.4	966	964.8	1130	1130	1308	1308.5
12	<i>o</i> -Xylene	884.0	883.6	888	889.4	995	995	1171	1171.5	1359	1360.9
13	1-M-4-iPrB	1010.5	1010.1	1016.5	1017.5	1100	1101.7	1254.5	1254.7	1402	1402.4
14	1-M-3-iPrB	1002.8	1002.0	1010	1008.6	1094	1093.8	1248	1242.6	1395	1389.1
15	1-M-2-iPrB	1016.9	1015.8	1031	1028.9	1114	1115	1280	1277	1439	1432.8
16	1-M-4-nPrB	1039.8	1039.3	1046.5	1047.4	1131	1131.3	1287.5	1288	1429	1432.3
17	1-M-3-nPrB	1034	1034.6	1042	1041.2	1126	1127.1	1284	1280.2	1425	1424.5
18	1-M-2-nPrB	1046.1	1046.1	1057.5	1055.9	1146	1145.9	1313	1309.1	1467	1462.1
19	1-M-4-EtB	951.5	951.7	957	957.7	1049	1049.3	1208.5	1210.8	1371	1370.6
20	1-M-3-EtB	948.7	949.4	955	953.8	1049	1048.7	1209	1207.4	1371	1369.3
21	1-M-2-EtB	965.3	964.2	973	971.9	1071	1070.6	1242.5	1239.8	1414	1410.5
22	1,4-DiEtB	1040.7	1039.4	1047	1048.6	1136	1136.9	1291.5	1293.7	1439	1438.2
23	1,3-DiEtB	1028.8	1029.3	1038.5	1036.5	1127	1126.3	1282	1277	1427	1420
24	1,2-DiEtB	1039.3	1037.5	1051	1049.3	1144	1144.7	1308.5	1308.9	1465	1465.3
25	1,3,5-TriMB	967.7	968.8	969	970.2	1064	1065	1228	1232.9	1398	1401
26	1,2,4-TriMB	986.3	986.7	988	988.9	1088	1087.1	1260	1261.7	1436	1441
27	<i>n</i> -PentylB	1135.5	1133.9	1144.9	1146.5	1228	1223.8	1381	1379.3	1505	1507.9
28	1,2,3-TriMB	1012.4	1011	1016	1017.6	1121	1121.5	1308	1307.1	1493	1495.4

$$I_{C-1540} = 122.6 + 1.4605 I_p - 7.67 L_{\max} + 27.58 E_{LUMO} - 1.3815 \varepsilon + 271 qA - 190.3 qB \quad (7)$$

$$I_{TCEP} = 352.8 + 1.5484 I_p + 33.9 X1 - 10.92 L_{\max} - 1.9284 \varepsilon + 352.8 qA - 300.8 qB \quad (8)$$

The values of $I_{\text{calc.}}$ calculated according to eqns. 6–8 are compared with the literature values of $I_{\text{exp.}}$ in Table III. Coincidence of the $I_{\text{calc.}}$ and $I_{\text{exp.}}$ values is evident even for the data on PEG-4000, which are greater than those on TCEP and seemed to be unreliable.

Obviously, any data obtained on a particular column might be used to calculate the parametric estimates valid for this column. Once available, the equation might be used for predictive calculations, to search for the best analysis temperature (the

TABLE III

COMPARISON OF $I_{\text{calc.}}$ WITH $I_{\text{exp.}}$ OF DIFFERENT ALKYL BENZENES OBTAINED ON UCON-LB-550-X BY DÖRING *ET AL.*⁴, ON CARBOWAX 1540 BY KUMAR *ET AL.*¹⁴, ON PEG-4000 BY HÉBERGER¹¹ AND ON TCEP BY SOJÁK AND RIJKS⁶

No.	Alkylbenzene	UCON LB		Carbowax 1540		PEG-4000		TCEP	
		$I_{\text{calc.}}$	$I_{\text{exp.}}$	$I_{\text{calc.}}$	$I_{\text{exp.}}$	$I_{\text{calc.}}$	$I_{\text{exp.}}$	$I_{\text{calc.}}$	$I_{\text{exp.}}$
1	Benzene (B)	759.7	760.5	965.3	958.8	1270	1266	1128.2	1122.7
2	Toluene (MB)	864.3	863	1060.8	1060	1549	1548.1	1219.1	1216.2
3	EthylB (EtB)	951.5	954.5	1145.2	1150.2	1802	1802.8	1289.8	1290.4
4	<i>n</i> -PropylB	1039.3	1039.2	1227.3	1229.5	2050	2051.5	1349.9	1352.5
5	<i>n</i> -ButylB	1135.1	1136.2	1325	1323			1431.3	1431.2
6	<i>n</i> -PentylB	1233.4	1229.5	—	—			1506.4	1505.5
7	iPrB	1008.3	1010.9	1193.3	1198.2			1319.5	1325.4
8	iBuB	1083.2	1084.2	1258.2	1264.2			1363.1	1372.8
9	<i>sec.</i> -BuB	1088.8	1087.8	1266.7	1267.5			1371.7	1379.6
10	<i>tert.</i> -BuB	1075	1073.2	1254	1255.5			1372.7	1372.7
11	<i>p</i> -Xylene	962.9	961.7	1154	1158.4	1830	1832.8	1302.1	1307
12	<i>m</i> -Xylene	966.6	965.4	1161.1	1161.6	1844	1832.7	1306.1	1305.9
13	<i>o</i> -Xylene	999.6	994.3	1204.5	1206.5	1975	1977.8	1357.5	1360.7
14	1-M-4-iPrB	1099.7	1101.8	1284.4	1285.6			1403.2	1402.3
15	1-M-3-iPrB	1095.3	1094.3	1281.1	1273.5			1396.4	1386.9
16	1-M-2-iPrB	1114.5	1114.9	1315.5	1312.4			1439.4	1431.8
17	1-M-4-nPrB	1130.5	1132.4	1318.9	1319.9			1430.3	1433.4
18	1-M-3-nPrB	1128.2	1128.7	1315.5	1312.4			1425	1423.5
19	1-M-2-nPrB	1145.9	1146.5	1346.6	1343.6			1467.5	1463.5
20	1-M-4-EtB	1050.1	1049.2	1242	1242.1	2080	2075.5	1372.1	1371
21	1-M-3-EtB	1050.1	1048.9	1243.9	1239.4	2072	2080.6	1370.4	1367.5
22	1-M-2-EtB	1071.6	1073.9	1278.6	1274.2	2193	2188.2	1415	1411.3
23	1,4-DiEtB	1135.9	1136.2	1322.8	1326			1439.4	1439.6
24	1,3-DiEtB	1127.2	1125.9	1313.8	1308.7			1428.4	1419.1
25	1,2-DiEtB	1142.3	1142.7	1342	1344.4			1465.4	1466.5
26	1,3,5-TriMB	1066.5	1067.9	1261.6	1268			1387.9	1396.1
27	1,2,4-TriMB	1089.6	1090	1297.5	1297.7			1435.5	1439.9
28	1,2,3-TriMB	1123.6	1125.2	1348.8	1347.1			1493.1	1491

regressor I_p is temperature dependent), to identify or to predict the retentions of additional compounds of the same type, without additional analysis of standard compounds, etc.

If we reconsider the data in Table I, some interesting peculiarities can be observed: (i) the less polar the stationary phase, the greater is the number of equations with equal accuracy (Δ_{\max}); (ii) the less polar the stationary phase, the lower is the number of necessary tuning indices for the same Δ_{\max} ; and (iii) some of the indices increased in importance with increasing polarity of the stationary phase, while others became insignificant.

To evaluate the real significance of the regressors used, the parametric estimates of eqns. 2, 13, 22, 29 and 34 in Table I (equal number of the same parameters) were made equal to the mean value of I_p (taken as 1). The reduced parametric estimations are given in Table IV.

It is seen that I_p is the most significant contributor to the I_{exp} value and in all instances it is higher by at least one order of magnitude. The index qA is also an important contributor and occurs in all parameter combinations (see Table I). The indices qB and qT might be used interchangeably on stationary phases with low polarity. On polar stationary phases the simultaneous presence of qA , qB and L_{\max} becomes necessary. It is interesting that the parametric estimates of L_{\max} , E_{LUMO} and ε change almost linearly with the polarity of the stationary phase with respect to benzene, according to McReynolds¹⁹. For example, $(\text{polarity})_{\text{st.ph.}} = -39.47 - 53.6273 b_6$, with correlation coefficient 0.996; and $(\text{polarity})_{\text{st.ph.}} = 10.08 - 282.92 b_7$, with correlation coefficient 0.982.

The negative sign of the regression with L_{\max} is assumed to be due to the thicker packing of the stationary phase molecules^{20,21}. The stronger the intermolecular forces between the stationary phase molecules, the more difficult is the penetration of longer solute molecules. The correlation with ε also has a negative sign. We assume that the greater the space of electron distribution, the weaker are the actions between the solute and stationary phase molecules.

The approach given above gives stable results when applied to data obtained on stationary phases with different polarity and also to data obtained by different workers. It might be used for a preliminary orientation with regard to a suitable stationary phase, for the precalculation of a suitable analysis temperature, for identification without the additional analysis of standard compounds, for the prediction of the retention of new alkylbenzenes, not routinely present in the samples, and for studying retention as a function of the structure of alkylbenzenes.

TABLE IV
REDUCED PARAMETRIC ESTIMATES FOR THE INDICES IN EQNS. 1-5

Stationary phase	I_p	$X1$	E_{LUMO}	qA	qB	L_{\max}	ε
Squalane	0.9987	-0.049	-0.106	0.0041	-0.0012	-0.004	-0.0042
OV-101	0.96447	-0.005	-0.015	0.0099	-0.0054	-0.006	0.0134
UCON LB	1.11592	-0.004	0.019	0.0093	-0.0093	-0.020	-0.0080
Carbowax 20M	1.3853	-0.390	0.069	0.0230	-0.0023	-0.049	-0.2320
TCEP	1.5663	0.079	0.068	0.0333	-0.0239	-0.075	-0.3820

TABLE V
REDUCED PARAMETRIC ESTIMATES (b_1 - b_6) OF THE STRUCTURAL FRAGMENTS USED AND THE VALUES OF THE MAXIMUM DISCREPANCY (Δ_{max}) BETWEEN $I_{exp.}$ AND $I_{calc.}$

Stationary phase	b_1 (I_p)	b_2 (n_0)	b_3 (HO)	b_4 ($H1$)	b_5 (n_{CH_3} , n_L)	b_6 (n_i)	b_0	Δ_{max} (i.u.)
Squalane	1.06718	-0.08	-0.003	-0.0005	0.0028	0.0014	19.4	3.6
OV-101	0.86095	0.1071	0.002	0.0053	-0.0038	-0.0003	49.5	4.7
UCON-LB	0.9379	-0.0012	0.003	0.0077	0.0011	-0.0033	163.5	4.2
Carbowax 20M	1.02265	-0.116	-0.0045	0.0179	0.0036	-0.0061	353.5	3.1
Carbowax 1540	1.08141	-0.1603	-0.009	0.021	0.005	-0.0053	372.9	4.2
TCEP	1.09585	-0.303	-0.009	0.0027	0.0187	-0.0101	610.3	5.9

If no data on the structural indices (topological, geometric and electronic) are available and there is no corresponding software, the structural fragments²² might alternatively be used as tuning regressors. We selected for study the same structural fragments as given previously¹, to which were added the following: n_i = the number of C-C bonds between the aromatic ring and the branched C atom in the substituent (e.g., in iPrB $n_i = 1$, in iBuB $n_i = 2$); n_{CH_3} = the number of CH₃ groups in the compound; and n_L = the number of C-C bonds in the straight chain of the substituent. The results are presented in Table V. With fewer regressors, better results were obtained than previously²³. Again, for the less polar stationary phases fewer regressors are necessary. Comparison of the variances and the maximum discrepancies shows that they are of the same magnitude, as if structural indices had been used.

The simplicity of the determination of such regressors makes this approach a promising tool for use in routine chromatographic practice.

The data in Table V confirm the stated²⁰ correlation between the constants b_0 and the polarity ($r = 0.9982$). In addition, high correlation coefficients exist between the polarity and the parametric estimates of the fragments $H1$ (number of *o*-substituents) and n_i . A two parametric equation:

$$(\text{polarity})_{st.ph.} = -31.42 + 1.0914 b_0 - 1723.5 b_6$$

TABLE VI
COMPARISON OF CALCULATED ($P_{calc.}$) AND EXPERIMENTAL [$P(C_6H_6)$] POLARITIES WITH RESPECT TO BENZENE ACCORDING TO McREYNOLDS

Stationary phase	Polarity	
	$P_{calc.}$	$P(C_6H_6)$ ¹⁹
Squalane	-9.6	0
OV-101	13.5	17
UCON LB-550-X	118	133
Carbowax 20M	322	323
Carbowax 1540	371	372
TCEP	593	588

with $r = 0.9993$ describes the stationary phases studied very well, as shown in Table VI. The results obtained on stationary phases with very different polarities, the wide range of alkylbenzenes studied, the different types of tuning parameters used for the derivation of the predictive equations illustrate the potential of the general model for quantitative structure investigations.

REFERENCES

- 1 N. Dimov and Ov. Mekenyan, *Anal. Chim. Acta*, 212 (1988) 317.
- 2 V. Gerasimenko, A. Kirilenko and V. Nabivach, *J. Chromatogr.*, 208 (1981) 9.
- 3 V. Gerasimenko and V. Nabivach, *Zh. Anal. Khim.*, 37 (1982) 110.
- 4 C. Döring, P. Estel and R. Fisher, *J. Prakt. Chem.*, 316 (1971) 15.
- 5 W. Engewald and L. Wennrich, *Chromatographia*, 9 (1976) 540.
- 6 L. Soják and J. Rijks, *J. Chromatogr.*, 119 (1976) 505.
- 7 J. Bermejo and M. Guillén, *Chromatographia*, 17 (1983) 664.
- 8 J. Bermejo, J. Canga, O. Gayol and M. Guillén, *J. Chromatogr. Sci.*, 22 (1984) 252.
- 9 J. Bermejo and M. Guillén, *J. Environ. Anal. Chem.*, 43 (1985) 88.
- 10 D. Bonchev, Ov. Mekenjan, G. Protić and N. Trinajstić, *J. Chromatogr.*, 176 (1979) 149.
- 11 K. Héberger, *Chromatographia*, 25 (1988) 725.
- 12 N. Dimov, *Anal. Chim. Acta*, 201 (1987) 217.
- 13 D. Papazova and N. Dimov, *J. Chromatogr.*, 356 (1986) 320.
- 14 B. Kumar, R. Kuchhal, P. Kumar and P. Gupta, *J. Chromatogr. Sci.*, 24 (1986) 99.
- 15 J. Bonastre and P. Grenier, *Bull. Soc. Chim. Fr.*, (1967) 1395.
- 16 J. Topliss and R. Edwards, *J. Med. Chem.*, 22 (1979) 1238.
- 17 W. Yee, K. Sakamoto and Y. l'Haya, *Rep. Univ. Electro-Commun. Tokyo*, 27 (1976) 53; 28 (1977) 227.
- 18 D. Bonchev, *Information Theoretic Indices for Characterization of Chemical Structures*. Research Studies Press, Chichester, 1983.
- 19 W. McReynolds, *J. Chromatogr. Sci.*, 8 (1970) 685.
- 20 N. Dimov and D. Papazova, *Chromatographia*, 12 (1979) 443.
- 21 N. Dimov and S. Boneva, *Zh. Anal. Khim.*, 44 (1988) 96.
- 22 N. Dimov and D. Papazova, *J. Chromatogr.*, 137 (1977) 265.
- 23 D. Papazova and N. Dimov, *J. Chromatogr.*, 216 (1981) 321.

CHROM 21 304

EFFECT OF REPEATED CROSS-LINKING OF SE-54 STATIONARY PHASE FILM ON THE CHROMATOGRAPHIC PROPERTIES OF CAPILLARY COLUMNS

KAREL JANÁK*, MARIE HORKÁ and KAREL TESAŘÍK

Institute of Analytical Chemistry, Czechoslovak Academy of Sciences, Leninova 82, 611 42 Brno (Czechoslovakia)

SUMMARY

The effects of repeated cross-linking of SE-54 stationary phase with *azo-tert.*-butane on the degree of stationary phase film immobilization and on the chromatographic properties were studied. The optimum numbers of repeated immobilizations in the columns for gas and liquid chromatography were determined. Excessive repetition of immobilization adversely affected the chromatographic properties. The contribution of chemical bonding to the degree of stationary phase immobilization was studied with capillaries silylated with octamethylcyclotetrasiloxane.

INTRODUCTION

The quality of capillary columns in gas chromatography has been increased markedly by stationary phase film immobilization¹. Perfect immobilization is obtained by the cross-linking of stationary phase chains and their chemical bonding to the capillary surface [2]. One well established method of silicone stationary phase immobilization consists in cross-linking the polysiloxane chains by reactions of free radicals. These originate from methyl and vinyl groups in the stationary phase by the action of radical reaction initiators¹. In the same way, bonds between the stationary phase and the silylated capillary surface are also formed, as Grob and Grob³ have shown for silylation with divinyltetramethyldisilazane. For a silylated surface carrying only methyl groups, however, they supposed a substantially lower occurrence of bonding with the stationary phase².

As radical reaction initiators, most often organic peroxides are used, and also dialkylazo compounds, especially *azo-tert.*-butane. The application of *azo-tert.*-butane has certain advantages over organic peroxides; its main decomposition products are nitrogen, isobutane and isobutene, which do not react with the polysiloxane chain, do not oxidize oxidizable phases⁴, do not change the stationary phase polarity and do not increase the column activity⁵. Optimum conditions for cross-linking non-polar and medium-polarity silicone phases by means of *azo-tert.*-butane have been established^{5,6}. Owing to its volatility, *azo-tert.*-butane can be diffused to the stationary phase film in the form of vapour. This procedure permits multiple repetition of cross-linking with the same column.

After the first application of azo-*tert.*-butane the SE-54 stationary phase extractability is only about 5%, nevertheless some workers have recommended carrying out cross-linking several times^{7,8}. According to the literature^{7,8}, however, the stationary phase extractability after three or five cross-linkings does not change from that of the same phase cross-linked only once (5%). Apart from stating that the phase remains gummy, the separation properties of the columns were not described.¹

It is still unclear if further cross-bonds are formed during the repeated cross-linking or whether the possibilities of cross-linking are exhausted after the first cross-linking of the stationary phase film.

The aim of this work was to establish the effect of repeated cross-linking of SE-54 stationary phase film on its extractability and on the efficiency and capacity of columns coated with this material. The effect of silylation of the capillary surface with octamethylcyclotetrasiloxane on the stationary phase immobilization was also studied.

EXPERIMENTAL

Materials and chemicals

Glass tubes from Simax Glas (Kavalier Sázava, Czechoslovakia), octamethylcyclotetrasiloxane (VCHZ Synthesia, Kolín, Czechoslovakia), SE-54 silicone stationary phase (W. Günter, Düsseldorf, F.R.G.), azo-*tert.*-butane (Ventron, Karlsruhe, F.R.G.), *n*-butane (Kaučuk Kralupy nad Vltavou, Czechoslovakia) were used. Other chemicals of analytical-reagent grade were supplied by Lachema (Brno, Czechoslovakia).

Apparatus

The device for drawing the glass capillaries and the device for filling and coating the capillaries with a solution of the stationary phase in a liquefied gas were designed in the Institute of Analytical Chemistry (Czechoslovak Academy of Sciences, Brno, Czechoslovakia). The capillaries and capillary columns were tested and thermostated in a Fractovap Model 2300 AC gas chromatograph with a flame ionization detector (Carlo Erba, Milan, Italy).

Procedures

Capillary surface treatment. Prior to coating, some capillaries were leached with 20% hydrochloric acid at 170°C⁹ and silylated with octamethylcyclotetrasiloxane¹⁰ (D₄) for 2 h at 420°C.

Capillary coating and column testing. Capillaries ca. 15 m × 0.25 mm I.D. were filled with a 0.4% (w/v) solution of the SE-54 stationary phase in liquefied butane¹¹. The capillaries were coated statically without using a vacuum¹¹. Immediately after coating, they were blown with nitrogen and conditioned at a low nitrogen flow-rate by heating from 40 to 230°C at 1°C/min. The columns were tested for their separation efficiency and the capacity ratio of the solutes with a mixture of C₇-C₁₁ *n*-alkanes at 80°C and a mixture naphthalene and methyl nonanoate at 110°C. For reasons of economy of time, the average linear velocity of the carrier gas was adjusted to 25 cm/s.

Immobilization. The column was blown with a stream of nitrogen saturated at 25°C with azo-*tert.*-butane vapour for 1 h per 10 m of column length at a flow-rate of

2 $\mu\text{l/s}$. A sealed column was heated in a thermostat from 40 to 220°C at 10°C/min and then left at 220°C for 1 h. After immobilization, the column was always conditioned under a flow of nitrogen by heating from 60 to 240°C at 1°C/min and then for 1 h at 240°C. After testing, the column was subjected to another cycle of immobilization, conditioning and testing. After a certain number of cycles, it was washed with chloroform of volume 1 ml per 1 m of column length at a flow-rate of 1.4 $\mu\text{l/s}$ and tested again.

Resistance of stationary phase film to solvents. The column was washed with 10 ml of the chosen solvent, filled with this solvent and left for 48 h. The solvent was then ejected and the column was washed with 4 ml of dichloromethane. Conditioning was carried out under a flow of nitrogen with heating from 60 to 240°C at 3°C/min and then for 15 min at 240°C. After testing with the mixture of *n*-alkanes, the column was subjected to the action of another solvent.

The extent of extractability of the stationary phase by a solvent (z) is most often interpreted as the degree of stationary phase film cross-linking. This term, however, does not relate specifically to stationary phase extractability because the immobilization includes not only cross-linking but also bonding of the stationary phase chains to the capillary surface. A more suitable term for characterizing the extent of immobilization seems to be the degree of non-extractability or the degree of immobilization, designated z' , which is used in this work. The degree of stationary phase film immobilization in the treated columns was calculated as the ratio of the capacity ratio of undecane after washing the column to that of the same solute determined after the last immobilization, expressed as a percentage. The changes in the column efficiency (number of theoretical plates per metre of column) and the capacity ratio of the selected solutes during immobilization were expressed as the relative efficiency (N_{rel}) and the relative capacity ratio of the solute (k_{rel}). These represent the percentage of the column efficiency and the capacity ratio of the solute prior to first immobilization.

Unless stated otherwise, all the results given are mean values from at least three columns under the same experimental conditions.

RESULTS AND DISCUSSION

Dependence of the degree of immobilization on its repetition

The repeated immobilization of SE-54 stationary phase film initiated by azo-*tert*.-butane was studied on silylated columns and on the columns with the capillary surface untreated.

As can be seen from Fig. 1, the degree of immobilization increases with increasing number of immobilizations. The possibilities of cross-linking (the existence and steric accessibility of methyl and vinyl groups, their compatible configuration in adjacent chains) are therefore not exhausted after the first immobilization. It is evident from comparison of the two curves in Fig. 1 that the cross-linking continues even with multiple repetition of immobilization (up to 10 times), even though the stationary phase film in the silylated columns is fully immobilized. Wright *et al.*⁵ observed a slight decrease in the polarity of polar silicone stationary phases after their immobilization with azo-*tert*.-butane and connected this effect with fixation of the non-polar azo-*tert*.-butane decomposition products on the stationary phase film. It can be

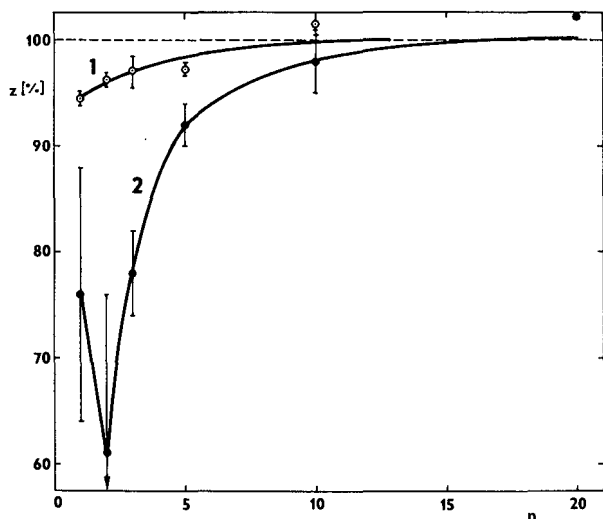


Fig. 1. Dependence of the degree of immobilization, z' (%), of SE-54 stationary phase film ($d_f = 0.25 \mu\text{m}$) on repeated immobilization with *azo-tert.*-butane (n = number of repeated immobilizations). 1, Columns with the surface modified by leaching and silylation; 2, columns with the surface untreated.

assumed that on repeated immobilization, this fixation effect may become a source of other cross-links.

For the practical application of the capillary columns, it is necessary to use the optimum cross-linking to prevent any marked decrease in mass transfer through the stationary phase film. The optimum degree of immobilization of the stationary phase film is 95% for the columns used in gas chromatography. Denser cross-linking together with chemical bonding is more advisable for the columns used in liquid and supercritical fluid chromatography. It follows from Fig. 1 that one immobilization is sufficient to immobilize the stationary phase film with *azo-tert.*-butane when preparing the capillary columns for gas chromatography. Resistance of the immobi-

TABLE I

EFFECT OF STATIC ACTION OF THE SOLVENTS ON THE CHROMATOGRAPHIC PROPERTIES OF COLUMNS ($0.25 \times 15 \text{ mm I.D.}$) WITH REPEATEDLY IMMOBILIZED STATIONARY PHASE SE-54 ($d_f = 0.25 \mu\text{m}$)

The degree of immobilization (z') and the number of theoretical plates per metre of column length were calculated from the characteristics of the *n*-undecane peak.

No. of immobilizations	Initial state		Water		Methanol		Acetonitrile	
	z' (%)	n/m	z' (%)	n/m	z' (%)	n/m	z' (%)	n/m
1	93.8	3400	92.5	3200	82.3	2800	80.9	3000
2	95.9	3450	95.9	3350	86.5	3050	87.8	3200
3	95.5	3000	95.5	3200	91.0	3050	92.5	2800
5	97.1	3000	96.3	2600	91.1	2800	86.8	2600

lized film to the long-term action of solvents was verified statically with water, methanol and acetonitrile as components suitable for the preparation of mobile phases for reversed-phase liquid chromatography. The results are given in Table I. Of the solvents used, water hardly affects the chromatographic properties of the columns and methanol and acetonitrile cause further extraction of the stationary phase. For the column immobilized three times, the decrease in the degree of stationary phase immobilization is negligible. The column immobilized five times showed tailing after extraction with acetonitrile and its capacity decreased.

The course of curve 2 in Fig. 1 is interesting from the theoretical point of view. The dispersions in the degree of immobilizations assessed after the first, as well as after the second immobilization are fairly large, and show a considerable effect of the conditions during saturation of the stationary phase film with azo-*tert.*-butane (*e.g.*, variation of temperature and nitrogen flow-rate, and also the effect of the film homogeneity) and an effect of the time sequence of heating and further conditioning of the columns. Still, it can be observed systematically that the degree of stationary phase film immobilization is lower after the second than after the first immobilization. The number of columns tested was increased to six (immobilized once) or seven (immobilized twice). To verify the effect, one of the columns was broken into two halves after the first immobilization and both halves were tested. Then, one was washed with a solvent and the other was immobilized a second time. The degree of immobilization was lower again ($z'_1 = 65\%$, $z'_2 = 53\%$).

It is assumed that the decrease in the degree of immobilization in this instance is illusory and is only a consequence of the decrease in the capacity ratio of the solutes after washing the column with the solvent. The decrease in capacity ratio, however, cannot be caused by the loss of the stationary phase in the column, but is probably due to the decreased interaction of the solutes with the stationary phase after its washing. This interpretation is also confirmed by the result of a test in which the column, after its first immobilization, was washed with the solvent and, after testing, immobilized again. The result was very close to that in the preceding test ($z'_1 = 65\%$, $z'_2 = 50\%$). A third immobilization forms a system so rigid that washing with the solvent hardly affects the stationary phase film. For the silylated columns, the dependence of the degree of immobilization on its repetition has a monotonous course; the chemical bonding of the stationary phase film to the surface limits the changes in its arrangement.

Silylation of the capillary surface with D_4 increased the stationary phase immobilization markedly (see Fig. 1). The degree of the stationary phase film immobilization after the first immobilization was 18% higher with the silylated columns. Comparison with data in the literature³ shows that the immobilization is affected in the same way by chemical binding of the stationary phase to the surface silylated with an agent containing vinyl groups (divinyltetramethyldisilazane) as with an agent containing methyl groups (D_4). From the point of view of surface wettability and suitable acid-base properties, the latter agent is preferred for silylation of the capillary before its coating with the SE-54 stationary phase.

Effect of repeated immobilization on chromatographic properties of the columns

A large number of cross-links in the stationary phase film may be the cause of the lower diffusive permeability of the stationary phase film and, consequently, of the

decrease in interactions of the solute with the functional groups of the stationary phase. This is manifested, on the one hand, by a decrease in the column efficiency and, on the other, by a change in its capacity. It can be also affected by the decomposition products of the initiator fixed on the stationary phase film.

The dependence of the relative efficiency of the capillary columns determined for undecane on the number of immobilizations is shown in Fig. 2. Whereas the first immobilization does not affect the efficiency of the capillary columns, further immobilizations decrease it. The decrease in efficiency is less marked with the columns with a silylated surface (see curves 1 and 3). When comparing these efficiencies with the efficiency of a column prepared in the same way but with the stationary phase film non-saturated with *azo-tert.*-butane, the reason for the decrease in efficiency can be attributed to the stationary phase film cross-linking. The dependences of the relative efficiencies of the columns determined after washing the columns with the solvent on repeated immobilization show similar courses (curves 2 and 4). The efficiency of most of the silylated columns increased slightly after washing, whereas the efficiency of the columns with an untreated surface decreased. The dependences of the column efficiency on repeated immobilization expressed for naphthalene and methyl nonanoate acid had similar courses, as shown in Table II. After multiple repetition of immobilization, the efficiency of the columns with a silylated surface decreased to *ca.* 80% of the original value. To retain the original column efficiency, however, only one or a maximum of two immobilizations are permissible.

The effect of repeated stationary phase film immobilization on the capacity ratio of undecane is shown in Fig. 3. Whereas the relative capacity ratio on the

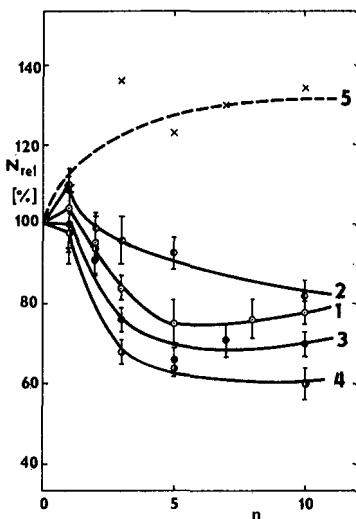


Fig. 2. Effect of repeated immobilization of SE-54 stationary phase film on the relative efficiency of the capillary columns (n = number of repeated immobilizations). 1, 2, Columns with the surface modified by leaching and silylation; 3, 4 columns with the surface untreated; 1, 3, columns tested for efficiency prior to their washing with the solvent; 2, 4, column efficiency after washing the columns with the solvent; 5, column with the untreated surface heated and conditioned in the same way as for immobilization but without *azo-tert.*-butane vapour in the column.

TABLE II
EFFECT OF REPEATED IMMOBILIZATION ON THE COLUMN EFFICIENCY (NUMBER OF PLATES PER METRE)

Column 1: 13 m × 0.25 mm I.D., silylated, immobilized with *azo-tert.*-butane. Column 2: 12 m × 0.25 mm I.D., surface untreated, immobilization only simulated without *azo-tert.*-butane.

Column No.	Solute	Initial state	No. of immobilizations				After washing
			1	5	8	10	
1	Decane	3450	3500	3050	2450	3000	2950
	Naphthalene	3450	3400	3150	2750	2650	2800
	Methyl nonanoate	3650	3550	3150	3000	3200	3200
2	Decane	2500	2650	2750	3150	3050	—
	Naphthalene	3200	3450	3050	3350	3400	—
	Methyl nonanoate	2850	3100	3350	3300	3350	—

non-immobilized comparative column practically does not change (curve 1), a marked decrease occurs on the columns with silylated surfaces after the third immobilization and on the columns with untreated surfaces even after the first immobilization. After 5–7 immobilizations the capacity ratio of undecane on both types of the columns stabilized at 86–88% of the original capacity ratio, which correlates well with levelling of the degree of immobilization on both types of columns. The decrease in the capacity ratio cannot be caused by the presence of *azo-tert.*-butane decomposition products in the stationary phase film because, owing to their non-polar character, they should slightly increase the capacity ratio of undecane. The decrease in the capacity ratio of naphthalene and methyl nonanoate acid was of a similar character but less marked. It

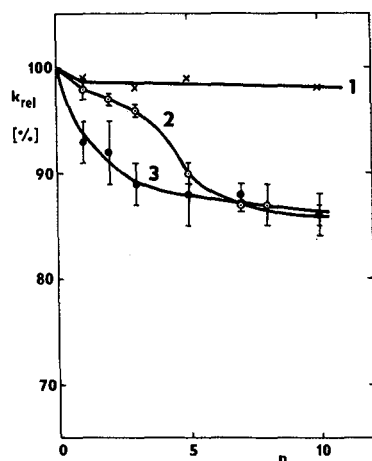


Fig. 3. Change in the capacity ratio of undecane during repeated immobilization of SE-54 stationary phase film (k_{rel} = relative capacity factor of undecane; n = number of repeated immobilizations). 1, Column with the untreated surface subjected to simulated immobilization (see 5 in Fig. 2); 2, columns with the surface modified by leaching and silylation; 3, columns with the surface untreated.

can therefore be assumed that similarly to the decrease in the column efficiency, the decrease in the capacity ratios is also caused by a decrease in interactions of the solutes with the stationary phase.

CONCLUSION

The repeated immobilization of an SE-54 stationary phase film can increase the degree of immobilization up to 100%. Multiple immobilization of the stationary phase film, however, is not desirable from the point of view of the chromatographic properties of the columns. The columns show the optimal separation properties after the first immobilization, and after further immobilizations their efficiency and capacity decrease. It is sufficient to immobilize the capillary columns in the described way once for gas chromatography and twice or at most three times for liquid chromatography.

Silylation of the surface with D₄ increased the degree of immobilization of the stationary phase film markedly, which shows that the stationary phase film immobilization is due to both cross-linking and chemical bonding to the capillary surface.

REFERENCES

- 1 V. Borek, J. Hubáček and V. Řeháková, *Chem. Listy*, 79 (1985) 364.
- 2 K. Grob and G. Grob, *J. High Resolut. Chromatogr. Chromatogr. Commun.*, 6 (1983) 153.
- 3 K. Grob and G. Grob, *J. High Resolut. Chromatogr. Chromatogr. Commun.*, 4 (1981) 491.
- 4 B. E. Richter, J. C. Kuei, J. I. Shelton, L. W. Castle, J. S. Bradshaw and M. L. Lee, *J. Chromatogr.*, 279 (1983) 21.
- 5 B. W. Wright, P. A. Peaden, M. L. Lee and T. J. Stark, *J. Chromatogr.*, 248 (1982) 17.
- 6 B. E. Richter, J. C. Kuei, N. J. Park, S. J. Crowley, J. S. Bradshaw and M. L. Lee, *J. High Resolut. Chromatogr. Chromatogr. Commun.*, 6 (1983) 371.
- 7 M. Novotný and P. David, *J. High Resolut. Chromatogr. Chromatogr. Commun.*, 9 (1986) 647.
- 8 R. C. Kong, S. M. Fields, W. P. Jackson and M. L. Lee, *J. Chromatogr.*, 289 (1984) 105.
- 9 K. Grob, *Making and Manipulating Capillary Columns for Gas Chromatography*, Hüthig, Heidelberg, 1986, p. 113.
- 10 L. Blomberg, K. Markides and T. Wännman, in R. E. Kaiser (Editor), *Proceedings of the Fourth International Symposium on Capillary Chromatography —Hindelang IV*, Hüthig, Heidelberg, 1981, p. 73.
- 11 K. Janák, V. Kahle, K. Tesařík and M. Horká, *J. High Resolut. Chromatogr. Chromatogr. Commun.*, 8 (1985) 843.

NON-LINEARITY OF THE PLOT OF LOG (ADJUSTED RETENTION TIME) VERSUS CARBON NUMBER FOR *n*-ALKANES IN SERIES-COUPLED GAS CHROMATOGRAPHIC COLUMNS

T. MAURER, Th. WELSCH and W. ENGEWALD *

Department of Chemistry, Karl-Marx-University Leipzig, Talstrasse 35, 7010 Leipzig (G.D.R.)

SUMMARY

The validity of the fundamental relationship of the Kováts retention index concept, namely the linear dependence of $\log t'_R$ on the carbon number of *n*-alkanes, was studied for a system of two series-coupled columns without intermediate trapping. Non-linearity of the $\log t'_R$ versus carbon number plot for the system was deduced from basic equations and confirmed experimentally. It was shown that the discrepancy from the Kováts concept in such a system will be especially large if the slopes of the *n*-alkane plots for the two individual columns differ significantly.

INTRODUCTION AND THEORY

Multi-dimensional gas chromatography (GC) is increasingly used for the separation of very complex mixtures (for reviews, see refs. 1–6; for the theoretical background, see refs. 7 and 8). The use of Kováts retention indices in series-coupled systems for the characterization of the separated compounds has been described^{9–15}. It is based on different concepts: (i) determination of two independent sets of retention index data by intermediate trapping⁹ in order to create a defined starting point for the separation on the second column or determination of the indices on the second column after separating the compounds of interest on the first column in a temperature-programmed mode and with intermediate trapping^{10,11}; (ii) determination of the retention index data on each column without intermediate trapping by calculating retention time differences¹²; (iii) determination of retention indices with the coupled system without intermediate trapping^{13–15}.

Retention indices determined according to concepts (i) and (ii) are valid for a particular column. In contrast, the retention indices determined according to concept (iii) are not related on a single column. They are “system indices” which reflect the interplay of two retention characteristics (different retention systems or different separation conditions). A feature of series-coupled columns run without intermediate trapping is the opportunity to adjust the polarity and selectivity by changing the temperatures and/or the flow-rates¹⁶.

In this work the validity of the fundamental relationship of the Kováts retention index concept, namely the linear dependence of $\log t'_R$ on the carbon number of *n*-alkanes¹⁷, was studied for such a series-coupled column system. The flow dependence¹⁵ of the "system indices" will be not discussed here.

The linearity between $\log t'_R$ and the carbon number, *Z*, is expressed by

$$\log t'_R(Z) = A + BZ \quad (1)$$

The slope *B* equals the logarithm of the ratio of the adjusted retention times of two neighbouring *n*-alkanes:

$$B = \log \left[\frac{t'_R(Z+1)}{t'_R(Z)} \right] \quad (2)$$

The retention times in the series-coupled column system are additive:

$$t_{R(S)} = t_{R(1)} + t_{R(2)} \quad (3)$$

$$t'_{R(S)} = t'_{R(1)} + t'_{R(2)} \quad (4)$$

$$t_{M(S)} = t_{M(1)} + t_{M(2)} \quad (5)$$

where t_R is the total retention time, t'_R the adjusted retention time, t_m the dead time and the subscripts 1 and 2 refer to columns 1 and 2 and S represents the system.

Substituting $t'_{R(S)}$ for t'_R in eqn. 1 gives

$$t'_{R(S)}(Z) = \exp [A_{(1)} + B_{(1)}Z] + \exp [A_{(2)} + B_{(2)}Z] \quad (6)$$

Using this expression for $t'_{R(S)}$, the slope $B_{(S)}$ can be written as

$$B_{(S)} = \log \left\{ \frac{\exp [A_{(1)} + B_{(1)}(Z+1)] + \exp [A_{(2)} + B_{(2)}(Z+1)]}{\exp [A_{(1)} + B_{(1)}Z] + \exp [A_{(2)} + B_{(2)}Z]} \right\} \quad (7)$$

This expression implies that the slope $B_{(S)}$ (valid for the system) varies with the carbon number of the *n*-alkanes used for the measurement. This means that one has to take into account a more or less curved plot of $\log t'_{R(S)}$ versus carbon number.

A schematic plot for both the single columns and the column system (Fig. 1) illustrates the non-linearity of this dependence for the system. The plot reveals further that the discrepancy from the Kováts concept will be especially large if the slope on the first column differs very much from that on the second column.

EXPERIMENTAL

A Siemens Sichromat 2 gas chromatograph, equipped with a split injector and 2 flame ionization detectors was used. Column 1 (50 m × 0.32 mm I.D.) contained FS-WG-PB-1 (OV-1) (WGA) and column 2 (1.5 m × 1 mm I.D.) contained Carboxack C particles (0.16–0.2 mm). The column temperatures were $T_1 = 100^\circ\text{C}$ and

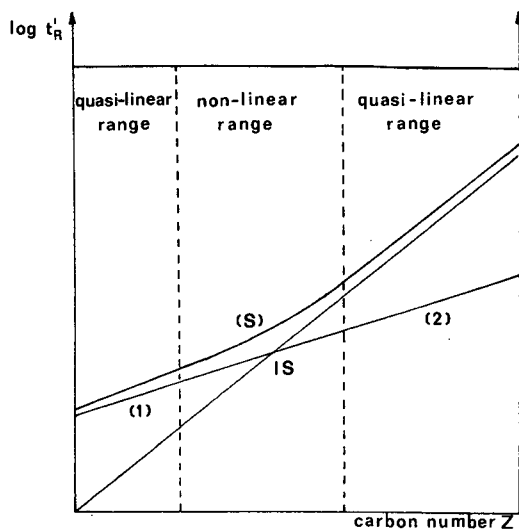


Fig. 1. Schematic graph of the $\log t'_R$ versus carbon number plots for the system (S) and the single columns (1) and (2); IS = intersection.

$T_2 = 220^\circ\text{C}$ and the pressures (hydrogen) were $P_I = 4.4$ bar and $P_M = 4.0$ bar (I = inlet; M = mid-point).

The Live-T-Piece of the Sichromat 2 was used in a monitoring mode; thus the first detector shows which part of the sample is entering the second column. The percentage of sample going to the first detector was adjusted by changing the positive pressure difference.

RESULTS AND DISCUSSION

In order to illustrate the phenomenon of non-linearity, two columns with very different retention characteristics have to be applied. Using two capillary columns coated with liquid stationary phases of different polarity, we could not measure such non-linearities. To meet the requirements mentioned above, an OV-1 capillary column was coupled with a graphitized carbon black micropacked column, because the slopes of the *n*-alkane plots are very different on these columns¹⁸. The slopes *B* were calculated according to eqn. 2.

The dead times $t_{M(1)}$ and $t_{M(2)}$ were evaluated from *n*-alkane retention times with a computer program described by Ebel and Kaiser¹⁹. The calculated dead times were compared with those determined by injection of methane. The dead time for the system was calculated using eqn. 5 and also compared with the retention time of methane. Eqn. 3 was applied for calculating the net retention times for the second column.

Table I shows the non-linearity of the *n*-alkane plot for the coupled system. Whereas the slopes $B_{(1)}$ and $B_{(2)}$ for the single columns remain constant, the slope $B_{(S)}$ for the system increases. The slopes $B_{(S)}$ agree well with those calculated according to eqn. 7.

In this example the intersection, IS, of the *n*-alkane plots of the single columns is in the range of the *n*-alkanes used. The non-linearity is especially large in this range,

TABLE I

SLOPES OF THE *n*-ALKANE PLOT FOR THE INDIVIDUAL COLUMNS [$B_{(1)}$ AND $B_{(2)}$] AND THE COUPLED SYSTEM [$B_{(S)}$]

Results of linear regression: $t_{M(1)} = 2.54$, $A_{(1)} = -4.462$, $B_{(1)} = 0.648$; $t_{M(2)} = 0.15$, $A_{(2)} = -6.742$, $B_{(2)} = 0.917$.

Compound	Carbon number (Z)	$t_{R(1)}$ (meas.) min	$t_{R(2)}$ (eqn. 3) min	$t_{R(S)}$ (meas.) min	$B_{(1)}$ (eqn. 2)	$B_{(2)}$ (eqn. 2)	$B_{(S)}$ (eqn. 2)	$B_{(S)}$ (eqn. 7)
Methane	1	2.540	0.150	2.695				
Hexane	6	3.103	0.439	3.542	0.65	0.92	0.75	0.75
Heptane	7	3.617	0.873	4.490	0.65	0.92	0.77	0.76
Octane	8	4.603	1.960	6.563	0.65	0.92	0.78	0.78
Nonane	9	6.481	4.675	11.156	0.65	0.92	0.80	0.80
Decane	10	10.059	11.461	21.520				

as can also be seen from Fig. 1. The carbon number of the intersection can be calculated according to

$$IS = \frac{A_{(2)} - A_{(1)}}{B_{(1)} - B_{(2)}} \quad (8)$$

The correct values of the constants A and B for the single columns can be calculated by linear regression. This means that dead-time determinations based on linear regression may be not applicable or may give erroneous results. Similar effects can possibly be expected when applying mixed stationary phases in one column. On the other hand, on coupling columns with similar retention characteristics this effect is small.

The extraordinary features of a coupled system consisting of a gas-liquid and a gas-adsorption column will be described elsewhere²⁰ (utilization of both vapour pressure and geometry for separation).

ACKNOWLEDGEMENTS

The authors acknowledge the invaluable help of Siemens, Berlin, F.R.G., for the loan of a Sichromat 2 gas chromatograph. Thanks are due to WGA (Pfungstadt, F.R.G.) for supporting the work with the FS capillary column.

REFERENCES

- 1 W. Bertsch, *J. High Resolut. Chromatogr. Chromatogr. Commun.*, 1 (1978) 85.
- 2 W. Bertsch, *J. High Resolut. Chromatogr. Chromatogr. Commun.*, 1 (1978) 187.
- 3 W. Bertsch, *J. High Resolut. Chromatogr. Chromatogr. Commun.*, 1 (1978) 289.
- 4 J. C. Giddings, *J. High Resolut. Chromatogr. Chromatogr. Commun.*, 10 (1987) 319.
- 5 B. M. Gordon, C. E. Rix and M. F. Borgerding, *J. Chromatogr. Sci.*, 23 (1985) 1.
- 6 G. Schomburg, *LC · GC Mag. Liq. Gas Chromatogr.*, 5 (1987) 304.
- 7 J. V. Hinshaw and L. S. Ettre, *Chromatographia*, 21 (1986) 661.
- 8 J. V. Hinshaw and L. S. Ettre, *Chromatographia*, 21 (1986) 669.
- 9 G. Schomburg, H. Husmann and F. Weeke, *J. Chromatogr.*, 112 (1975) 205.
- 10 G. Schomburg, H. Husmann and E. Hübinger, *J. High Resolut. Chromatogr. Chromatogr. Commun.*, 8 (1985) 395.

- 11 R. W. Slack and A. C. Heim, *Int. Lab.*, 16 (1986) 88.
- 12 J. A. Rijks, J. M. M. van den Berg and J. P. Diependaal, *J. Chromatogr.*, 91 (1974) 603.
- 13 J. Krupčík, G. Guiochon and J. M. Schmitter, *J. Chromatogr.*, 213 (1981) 189.
- 14 T. Tóth and F. Garay, in P. Sandra (Editor), *Proceedings of the 8th International Symposium on Capillary Chromatography, Riva del Garda, May 19–21, 1987*, Hüthig Verlag, Heidelberg, 1987, pp. 585–595.
- 15 R. E. Kaiser and R. I. Rieder, *Labor-Praxis*, 9 (1985) 1465.
- 16 P. Sandra, F. David, M. Proot, G. Dirricks, M. Verstappe and M. Verzele, *J. High Resolut. Chromatogr. Chromatogr. Commun.*, 8 (1985) 782.
- 17 M. V. Budahegyi, E. R. Lombosi, T. S. Lombosi, S. Y. Mészáros, S. Nyiredy, G. Tarján, I. Timár and J. M. Takács, *J. Chromatogr.*, 271 (1983) 213.
- 18 W. Engewald, U. Billing, T. Welsch and G. Haufe, *Chromatographia*, 23 (1987) 590.
- 19 S. Ebel and R. E. Kaiser, *Chromatographia*, 7 (1974) 696.
- 20 W. Engewald, T. Maurer and A. Schiefke, *Pure Appl. Chem.*, (1989) in press.

CHROM. 21 309

INTERFACE ADSORPTION AND REPRODUCIBILITY OF RETENTION INDICES IN GLASS CAPILLARY COLUMNS WITH DIMETHYLPOLY-SILOXANE STATIONARY PHASES CROSS-LINKED BY γ -IRRADIATION

PAVEL FARKAŠ

Food Research Institute, Bratislava 825 09 (Czechoslovakia)

LADISLAV SOJÁK

Chemical Institute, Comenius University, Bratislava 842 15 (Czechoslovakia)

MILAN KOVÁČ

Food Research Institute, Bratislava 825 09 (Czechoslovakia)

and

JAROSLAV JANÁK*

Institute of Analytical Chemistry, Czechoslovak Academy of Sciences, Brno 611 42 (Czechoslovakia)

SUMMARY

The influence of the interphase adsorption on the retention of polar and non-polar analytes analyzed in glass capillary columns with the non-cross-linked and γ -irradiated cross-linked OV-1 stationary phase has been studied. The separation systems are characterized by a low contribution of adsorption to the retention of polar analytes, which is for film thicknesses above 0.3 μm less than 0.3% and upon cross-linking the stationary phase decrease further by 10–90% of this value. This enables high reproducibility of retention indices of the substances analyzed. The invariant retention indices of polar analytes in systems with both types of OV-1 stationary phases correspond to 0.4 i.u.

INTRODUCTION

Adsorption of chromatographed substances at the surface of phase boundaries, liquid–gas and liquid–solid support (capillary column wall), can have a decisive influence on retention characteristics as well as their reproducibility and on the possibility to identify the substances analyzed on the basis of retention data. This is connected with the fact that classical methods for expressing the analyte retention in qualitative analysis, the retention index and the retention ratio do not take into account their dependence on the properties of the support and the amount of stationary phase in the column.

In an earlier paper Berezkin and Korolev¹ reported the rôle of adsorption at the phase boundaries in fused-silica capillary columns coated with non-polar non-cross-linked and cross-linked polysiloxane stationary phases using benzoyl peroxide as a cross-linking initiator. They found that by cross-linking the non-polar dimethylpolysiloxane stationary phase SE-30 the contribution of adsorption to the retention of polar substances increased and their retention indices were higher on the cross-linked

stationary phase than on the non-cross-linked one. The changes in retention have been explained by changes in the interactions of chromatographed substances with the stationary phase resulting from certain changes in the character and composition of the stationary phase due to its cross-linking.

The influence of cross-linking the polysiloxane stationary phases OV-1, OV-1_{vin} and SE-54 while using dicumyl peroxide on the retention indices of polyaromatics and other polar substances in fused-silica capillary columns has been studied by Juutilainen and Enqvist². They found that the polarity and selectivity of the stationary phases studied changed upon cross-linking due to reaction of cumyloxy radicals with the stationary phase, resulting in certain changes in its properties.

Cross-linking of the stationary phases by γ -irradiation seems to be more advantageous since when compared to cross-linking with peroxides there is no change in the stationary phase polarity or in the column resolution power and the column preparation is more simple³⁻⁵.

In this work the influence of interphase adsorption and stationary phase cross-linking on the reproducibility of retention indices of polar and non-polar substances analyzed in glass capillary columns with the non-polar dimethylpolysiloxane phase OV-1 non-cross-linked and cross-linked by γ -irradiation was investigated.

EXPERIMENTAL

The columns (14–19 m \times 0.325 \pm 0.13 mm I.D.) were prepared from glass capillaries made of sodium–calcium Unihost glass (Kavalier, Teplice, Czechoslovakia) drawn on a laboratory-made drawing device. Their inside surfaces were treated with a slight modification of a procedure according to Grob *et al.*⁶

Capillaries packed to 95% of their volume with 20% analytical grade HCl (Merck, Darmstadt, F.R.G.) and fused under vacuum were leached at 130°C for 16 h. Then they were washed with two capillary volumes of 1% HCl at a linear velocity of approximately 1.5 cm s⁻¹. Immediately afterwards the capillaries were dehydrated at 295°C (temperature programme: 40 to 295°C at 20°C min⁻¹) and in a flow of dry nitrogen of 4–6 cm³ min⁻¹ for 1.5–2.5 h according to the capillary length. After cooling, the capillaries were packed to about 20% of their volume with hexamethyldisilazane (HMDS) (Fluka Chemie, Buchs, Switzerland) and then the HMDS was forced through the column with nitrogen at a linear velocity of approximately 1 cm s⁻¹. The fused capillaries were silanized at 380°C for 2 h in an oven (temperature programme 30 min at 150°C, then increased by 50°C every 15 min up to 380°C). The silanized capillaries were carefully cooled and washed immediately with about 25% of their volume with toluene, methanol and diethyl ether at a linear velocity of about 1.5 cm s⁻¹. On the toluene front usually tiny white crystals or a white precipitate was observed (see ref. 7). After brief passage of nitrogen through the capillaries at the laboratory temperature, they were placed in a gas chromatograph equipped with flame ionization detection (FID) and conditioned for 30–60 min at 250°C until the baseline signal of the detector was stabilized. Some of the capillaries were tested at 110°C by injection of pure 1-octanol and methane. The capacity factor of 1-octanol was 0.04. The stationary phase OV-1 (Supelco, Bonaduz, Switzerland) was coated on the capillary walls statically by means of a 0.06–1.64% (v/v), solution in *n*-pentane. The OV-1 film thickness was calculated from the concentration of its solution and the capillary I.D.⁸

The coated columns were conditioned at 250°C for 2 h and then tested. The tested columns were fused under vacuum and irradiated with the ^{60}Co γ -radiation in doses of 4–10 Mrad at a radiation intensity of *ca.* 0.16 Mrad h⁻¹. The irradiated columns were washed with 10 ml of dichloromethane at a flow-rate of about 4 ml h⁻¹, dried under a flow of nitrogen, conditioned at 250°C for 15 h and tested. The film thickness of cross-linked OV-1 was calculated from that of non-cross-linked OV-1 and the cross-linking percentage determined from the difference in capacity factors of *n*-decane in non-irradiated and irradiated columns. At the given doses of γ -radiation an average 97% cross-linking of OV-1 was obtained. The efficiency of the columns with film thickness 0.3–0.6 μm reached an average of 3200 theoretical plates per metre for the capacity factor, $k > 5$ (*ca.* 90% of the theoretical efficiency).

All the chromatographic measurements were carried out with a 4200 Fractovap gas chromatograph (Carlo Erba, Milan, Italy) with FID. The column thermostat temperature was calibrated by a platinum resistance thermometer with an accuracy of $\pm 0.1^\circ\text{C}$. The carrier gas, pure hydrogen, was applied at a linear flow-rate of 35 cm s⁻¹. The test mixture comprised *n*-decane, *n*-undecane, *n*-dodecane, 1-octanol, 2,6-dimethylaniline, 2,6-dimethylphenol and naphthalene in benzene, concentration 0.5–1.0 mg cm⁻³. Methane was injected on the column simultaneously with 0.05 μl of the test mixture using a 1- μl syringe (Hamilton, Bonaduz, Switzerland) at the splitting ratio of 1:50. No asymmetry of the peaks of the tested analytes was observed on any of the columns studied (Fig. 1). Retention times were measured with an accuracy of 0.1 s on a SP 4100 programmable integrator (Spectra Physics). Columns with non-cross-linked and cross-linked OV-1 were tested at 110°C by measuring the capacity factors and retention indices of the analytes. The capacity factors were measured with an accuracy of $\pm 0.5\%$ and retention indices on the columns with film thickness up to 0.1 μm with an accuracy characterized by a standard deviation of up to 0.8 i.u. and of 0.1 i.u. for the columns with higher OV-1 film thickness. All the calculations were carried out with a TI-59 programmable calculator (Texas Instruments).

RESULTS AND DISCUSSION

For separation systems in which polar substances are analyzed on non-polar stationary phases using gas-liquid chromatography, adsorption interactions of the analytes at the liquid phase-capillary surface boundary are characteristic^{1,9}. The value of the analyte retention index is a linear function of the reciprocal of the amount of liquid phase in the column or the reciprocal of the thickness of the stationary phase film or of the capacity factor of the analyte with negligible adsorption at the system interphase⁹

$$I_i = I_{0i} + a_i \frac{1}{k_{st}} \quad (1)$$

$$I_{0i} = 100 \left[z + \frac{\log(K_i/K_z)}{\log(K_{z+1}/K_z)} \right] \quad (2)$$

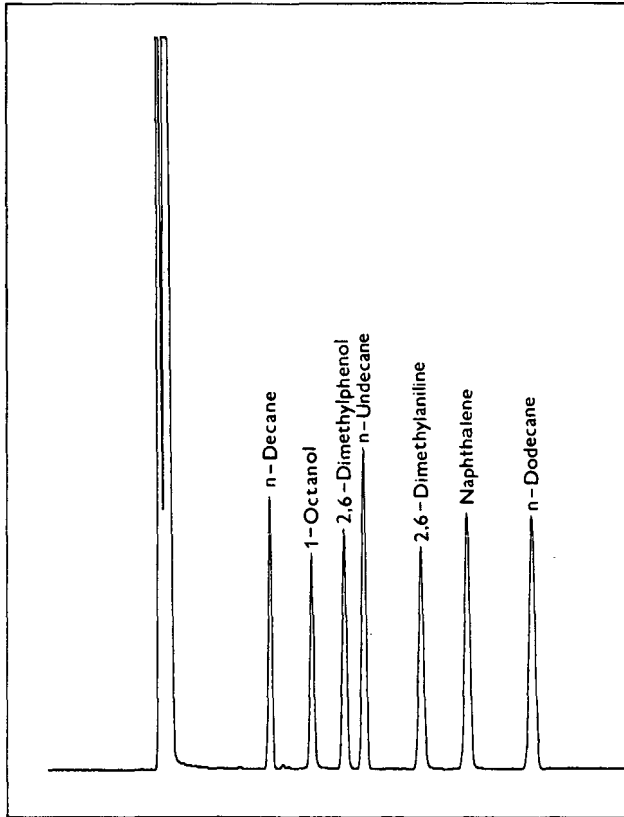


Fig. 1. Chromatogram of the tested substances on a column with cross-linked OV-1, film thickness, $d_f = 0.310 \mu\text{m}$.

where I_i is the retention index of the substance analyzed, I_{0i} the invariant retention index of the substance analyzed independent of adsorption in the chromatographic system, K_i the absorption coefficient of the substance analyzed, k_{st} the capacity factor of the standard substance whose adsorption in the system is negligible, and z is the number of carbon atoms of the n -alkane used as a comparison standard.

The contribution of adsorption to the retention of the substances studied in the systems with the non-cross-linked OV-1 stationary phase was calculated from

$$k_i = A_{i_t} + r_{0i}k_{st} \quad (3)$$

where k_i is the capacity factor of the substance analyzed, A_{i_t} the contribution of adsorption to its retention and $r_{0i} = t'_{Ri}/t'_{Rst}$ is the invariant retention ratio of the substance analyzed independent of adsorption.

In accord with previous studies^{1,9}, n -decane was selected as the analyte with negligible adsorption in the given system. Fig. 2 presents the dependence of the measured capacity factors of n -decane at 110°C in ten capillary columns with $0.325 \pm$

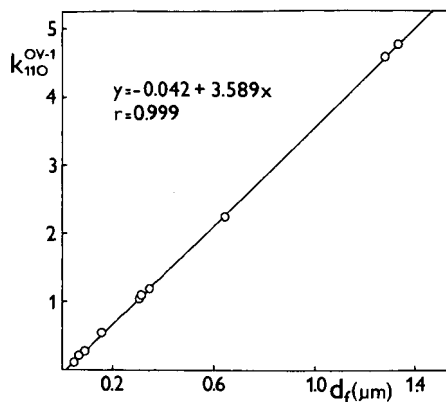


Fig. 2. Dependence of the capacity factor for *n*-decane on non-cross-linked OV-1 with different film thicknesses.

0.13-mm I.D. and different contents of the non-cross-linked phase OV-1 on the stationary phase film thickness; a very good correlation is seen. The capacity factor as an expression of the liquid phase content can be measured more easily and with higher accuracy; the film thickness is one of the basic parameters of the column.

The contribution of adsorption to the retention was calculated from the measured capacity factors of the analytes studied (1-octanol, 2,6-dimethylphenol, 2,6-dimethylaniline, naphthalene), k_i , and *n*-decane as the standard with negligible adsorption in the system, k_{st} , at 110°C by linear regression from eqn. 3 (Tables I and II).

In the columns with the non-cross-linked stationary phase OV-1 the adsorption contribution changes from 0.0006 to 1.04% in the film thickness range 0.092–0.647 μm . It increases with decreasing thickness of the phase film and with increasing polarity of the analytes studied. In the columns with the cross-linked phase the contribution of adsorption is 10–90% lower than that of the non-cross-linked phase. In the film thickness range 0.081–0.642 μm the contribution of adsorption reaches a maximum at 0.85% and decreases with increasing film thickness. Low values of the adsorption contribution to the retention of polar analytes in glass capillary columns coated with the non-polar phase OV-1 show that the method of surface deactivation of glass capillaries used leads to suppression of the adsorption and the method of cross-linking the stationary phase by γ -irradiation also suppresses the adsorption.

Even if the interphase adsorption in the systems studied is relatively small, it is reflected characteristically in the values of the retention indices of the analytes. Table III presents the measured retention indices of the analytes studied and the capacity factors of *n*-decane in ten capillary columns with different film thicknesses (0.047–1.336 μm) of the non-cross-linked phase OV-1. The graphic representation of the dependences $I_i = f(d_f)$, $I_i = f(k_{st})$ or $I_i = f(1/k_{st})$ (Fig. 3) shows the characteristic asymptotic decrease in retention indices of the analytes with increasing film thickness of the stationary phase as the result of suppression of the adsorption of polar analytes on the surface of the non-polar stationary phase–capillary column wall boundary. The character of this dependence is related to the polarity of the substances analyzed, the retention index of 2,6-dimethylphenol decreasing by 6.3 i.u. and of naphthalene by 0.5

TABLE I
CONTRIBUTION OF ADSORPTION TO THE RETENTION OF THE ANALYTES STUDIED AND THE VALUES OF THE COEFFICIENTS OF EQN. 3 FOR NON-CROSS-LINKED OV-1

DMP = Dimethylphenol; DMA = dimethylaniline.

Analyte	$d_t = 0.092 \mu\text{m}$		$d_t = 0.305 \mu\text{m}$		$d_t = 0.648 \mu\text{m}$		$d_t = 0.500 \mu\text{m}^a$				
	k_i	A_i (%)	k_i	A_i (%)	k_i	A_i (%)	k_i	A_i (%)			
1-Octanol	0.393	1.04	1.426	0.29	3.090	0.11	0.0041	1.361	0.999	2.387	0.17
2,6-DMP	0.474	0.44	1.727	0.12	3.746	0.06	0.0021	1.651	0.999	2.893	0.07
2,6-DMA	0.669	0.61	2.440	0.17	5.287	0.08	0.0041	2.330	0.999	4.084	0.10
Naphthalene	0.784	0.005	2.860	0.001	6.212	0.0006	0.00004	2.739	0.999	4.796	0.0008
<i>n</i> -Decane k_{st}	0.285	—	1.046	—	2.267	—	—	—	—	1.751	—

^a Hypothetical column with film thickness of 0.500 μm .

TABLE II
CONTRIBUTION OF ADSORPTION TO THE RETENTION OF THE ANALYTES STUDIED AND THE VALUES OF THE COEFFICIENTS OF EQN. 3 FOR CROSS-LINKED OV-1

Analyte	$d_t = 0.081 \mu\text{m}$		$d_t = 0.309 \mu\text{m}$		$d_t = 0.642 \mu\text{m}$		$d_t = 0.500 \mu\text{m}^a$				
	k_i	A_i (%)	k_i	A_i (%)	k_i	A_i (%)	k_i	A_i (%)			
1-Octanol	0.351	0.85	1.390	0.22	2.073	0.10	0.0030	1.364	0.999	2.392	0.13
2,6-DMP	0.422	0.09	1.681	0.02	3.721	0.01	0.0004	1.654	0.999	2.896	0.01
2,6-DMA	0.595	0.12	2.372	0.03	5.249	0.01	0.0007	2.333	0.999	4.086	0.02
Naphthalene	0.693	—	2.786	—	6.163	—	-0.0037	2.742	0.999	4.797	—
<i>n</i> -Decane k_{st}	0.252	—	1.021	—	2.248	—	—	—	—	1.751	—

^a Hypothetical column with film thickness of 0.500 μm .

i.u. At film thicknesses higher than $0.3 \mu\text{m}$ the retention indices of the analytes are practically independent of the stationary phase film thickness (standard deviation of retention indices, $s = 0.1$ i.u.).

Table IV presents the measured retention indices of the analytes in ten capillary columns with different film thicknesses of OV-1 cross-linked by γ -irradiation at doses of 4.0–10.0 Mrad. Irradiation doses in the range 4–8 Mrad practically do not influence the value of the retention index. However, at a dose of 10 Mrad an increase in retention by 0.5–1.0 i.u. was observed with increasing polarity of the analytes. Therefore, only the data obtained on the columns irradiated with doses of 4–8 Mrad were evaluated.

During conditioning of the columns with OV-1 cross-linked by γ -irradiation at 250°C , the retention indices of the analytes decrease slightly with time, by 0.1–0.3 i.u. After 15 h of conditioning the retention practically did not change and, therefore, the data obtained after 15 h of conditioning at 250°C were selected for evaluation.

The dependence of the retention indices of the analytes studied on the film thickness of the cross-linked OV-1 phase is illustrated in Fig. 4. For film thicknesses above $0.08 \mu\text{m}$ the dependences are similar to those for non-cross-linked OV-1. For film thicknesses less than $0.08 \mu\text{m}$ a remarkable decrease in the retention indices of the analytes is observed with decreasing film thickness. This shows that the thin films of cross-linked and non-cross-linked OV-1 have different characters.

From the measured retention indices of the analytes and their capacity factors on the given columns with film thicknesses above $0.08 \mu\text{m}$, the values of the invariant retention indices, I_{0i} , and adsorption coefficients, a_i , were calculated by linear regression from eqn. 1. The data for the calculation were tested for irrelevant values according to Grubbs¹⁰ and these values were excluded from the set (one value for 1-octanol, two values for 2,6-dimethylphenol and one value for naphthalene, all on non-cross-linked OV-1). The invariant retention indices were calculated with an accuracy (Table V) characterized by a standard deviation, $s = 0.1$ – 0.2 i.u. within the interval, $L_{1,2}(I_{0i}) \pm 0.2$ – 0.5 i.u. at a significance level of 95% ($\alpha = 0.05$). The correlation coefficients, r , show that the correlation of the dependence $I_i = f(1/k_{si})$ is high. For naphthalene analyzed on non-cross-linked OV-1, the low value of the

TABLE III

RETENTION INDICES AND CAPACITY FACTORS OF THE ANALYTES STUDIED ON COLUMNS WITH DIFFERENT FILM THICKNESSES OF NON-CROSS-LINKED OV-1

Column	I_{110}				k_{st110} <i>n-Decane</i>	d_f (μm)
	<i>1-Octanol</i>	<i>2,6-DMP</i>	<i>2,6-DMA</i>	<i>Naphthalene</i>		
1	1052.2	1089.4	1141.8	1167.2	0.127	0.047
2	1052.1	1084.5	1141.0	1167.5	0.215	0.070
3	1053.3	1084.1	1141.2	1167.5	0.285	0.092
4	1051.7	1084.1	1140.7	1167.4	0.551	0.156
5	1051.3	1083.2	1140.3	1167.1	1.046	0.305
6	1051.1	1083.2	1140.5	1167.4	1.092	0.314
7	1051.0	1083.1	1140.4	1167.2	1.183	0.351
8	1051.2	1083.1	1140.3	1167.1	2.267	0.647
9	1051.1	1083.0	1140.1	1166.9	4.570	1.283
10	1051.1	1083.2	1140.2	1167.1	4.758	1.336

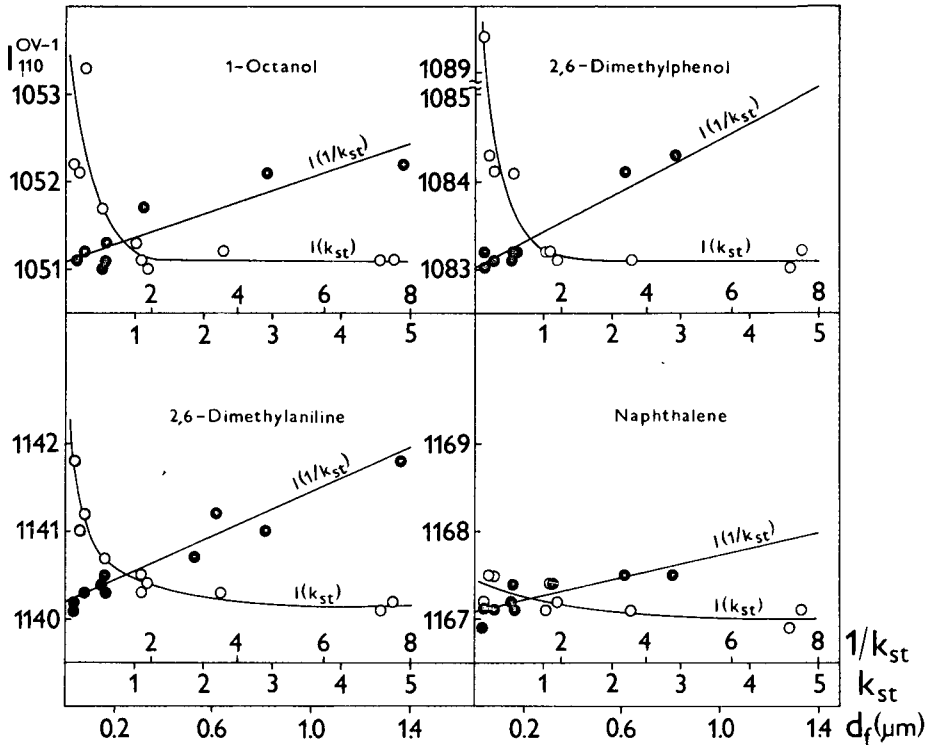


Fig. 3. Dependences of retention indices of the analytes studied on non-cross-linked OV-1 with different film thicknesses.

correlation coefficient is connected with a small dependence of the retention index on the stationary phase film thickness. In the case of cross-linked OV-1, the low value of the correlation coefficient, $r = -0.505$, is connected with the fact that the dependence $I = f(k_{st})$ for naphthalene on thin OV-1 films is not described by eqn. 3 so precisely as in the cases of the other analytes studied.

The calculated invariant retention indices of polar analytes, I_{0i} , on non-cross-linked and cross-linked OV-1 differ on average by $\Delta I_{0i} = 0.4$ i.u. and they are systematically higher on cross-linked OV-1. The value of $\Delta I_{0i} = 0.6$ i.u. for naphthalene is slightly higher than expected, which is connected with the above-mentioned character of the dependence $I = f(k_{st})$ for this analyte on non-cross-linked OV-1.

The results obtained show that upon cross-linking OV-1 with γ -irradiation the stationary phase polarity increases only slightly. For comparison, the published invariant retention indices of the same substances measured in fused-silica capillary columns coated with the phase SE-30 cross-linked with benzoyl peroxide¹ were higher by 6.4–14.5 i.u., and the similar retention indices in the fused-silica capillary columns with OV-1 cross-linked with dicumyl peroxide² were higher by 6.1–18.1 i.u. as on the non-cross-linked stationary phase.

TABLE IV
RETENTION INDICES AND CAPACITY FACTORS OF THE ANALYTES STUDIED ON COLUMNS WITH DIFFERENT FILM THICKNESSES OF
CROSS-LINKED OV-1

Column	I_{110}				k_{st110} <i>n-Decane</i>	d_f (μm)	Radiation dose (Mrad)	Cross-linking (%)
	<i>l-Octanol</i>	2,6-DMP	2,6-DMA	<i>Naphthalene</i>				
1	1053.4	1082.1	1137.5	1160.4	0.126	0.047	4.0	99.2
2	1055.9	1084.0	1141.4	1166.7	0.212	0.069	4.0	98.6
3	1054.8	1085.5	1142.0	1167.3	0.252	0.081	4.0	98.4
4	1052.2	1084.4	1141.3	1167.5	0.534	0.151	6.5	96.9
5	1051.9	1083.7	1141.0	1167.8	1.021	0.309	4.0	97.6
6	1052.0	1083.8	1141.1	1167.8	1.107	0.310	8.0	101.4
7	1052.5	1083.9	1141.1	1167.5	1.167	0.343	6.0	98.6
8	1051.9	1083.6	1140.9	1167.6	2.248	0.642	6.5	99.2
9	1051.6	1083.6	1140.6	1167.4	4.437	1.246	6.5	97.1
10	1052.8	1084.7	1141.8	1168.1	4.558	1.280	10.0	95.8

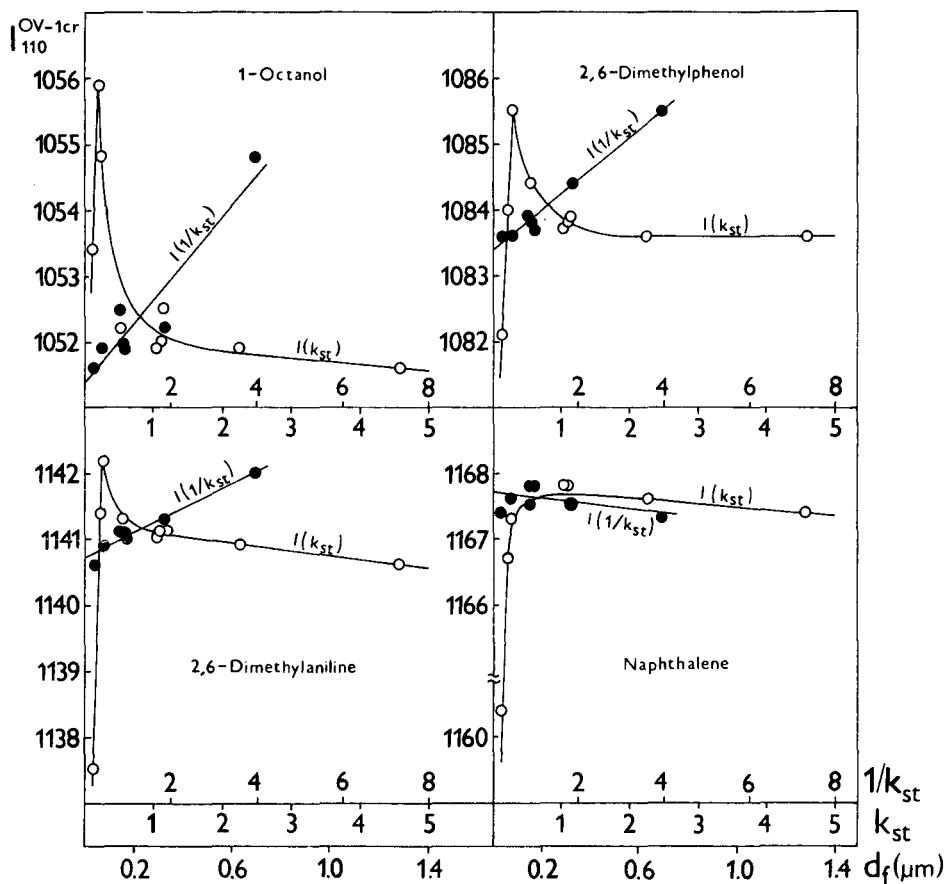


Fig. 4. Dependences of retention indices of the analytes studied on cross-linked OV-1 with different film thicknesses.

TABLE V

INVARIANT RETENTION INDICES OF THE ANALYTES STUDIED ON NON-CROSS-LINKED AND CROSS-LINKED OV-1

Analyte	St. phase ^a	I_{0i}	$S_{(10i)}$	$L_{1,2(10i)}$	a_i	r	ΔI_{0i}	$I_{0.5} - I_{0i}$
1-Octanol	OV-1	1051.1	0.1	0.2	0.163	0.917	0.3	0.1
	OV-1 cr.	1051.4	0.2	0.5	0.802	0.941		
2,6-DMP	OV-1	1083.0	0.1	0.2	0.295	0.999	0.4	0.1
	OV-1 cr.	1083.4	0.1	0.3	0.533	0.990		
2,6-DMA	OV-1	1140.2	0.1	0.2	0.208	0.968	0.5	0.1
	OV-1 cr.	1140.7	0.1	0.3	0.332	0.974		
Naphthalene	OV-1	1167.1	0.1	0.2	0.110	0.813	0.6	0.0
	OV-1 cr.	1167.7	0.1	0.3	-0.075	-0.505		

^a cr. = Cross-linked.

ACKNOWLEDGEMENT

The authors thank Professor V. G. Berezkin from the Institute of Petrochemical Syntheses, Academy of Sciences of the USSR, Moscow, for his suggestions.

REFERENCES

- 1 V. G. Berezkin and A. A. Korolev, *Chromatographia*, 8 (1985) 482.
- 2 T. Juutilainen and J. Enqvist, *J. Chromatogr.*, 279 (1983) 91.
- 3 G. Schomburg, H. Husmann, S. Ruthe and M. Herraiz, *Chromatographia*, 15 (1982) 63.
- 4 W. Bertsch, V. Pretorius, M. Pearce, J. C. Thompson and G. Schnautz, *J. High Resolut. Chromatogr. Chromatogr. Commun.*, 5 (1982) 432.
- 5 J. A. Hubbal, P. DiMauro, E. E. Barry and G. E. Chabot, *J. High Resolut. Chromatogr. Chromatogr. Commun.*, 6 (1983) 241.
- 6 K. Grob, G. Grob, W. Blum and W. Walter, *J. Chromatogr.*, 244 (1982) 197.
- 7 M. Godefroot, M. Van Roelenbosch, M. Verstappe, P. Sandra and M. Verzele, *J. High Resolut. Chromatogr. Chromatogr. Commun.*, 3 (1980) 337.
- 8 J. Bouche and M. Verzele, *J. Gas Chromatogr.*, 6 (1968) 501.
- 9 V. G. Berezkin, *J. Chromatogr.*, 159 (1978) 359.

CHROM. 21 275

DETERMINATION OF THE ENANTIOMERS OF α -H- α -AMINO ACIDS, α -ALKYL- α -AMINO ACIDS AND THE CORRESPONDING ACID AMIDES BY HIGH-PERFORMANCE LIQUID CHROMATOGRAPHY^a

A. DUCHATEAU*, M. CROMBACH, J. KAMPHUIS, W. H. J. BOESTEN, H. E. SCHOEMAKER and E. M. MEIJER

DSM Research, P.O. Box 18, 6160 MD Geleen (The Netherlands)

SUMMARY

o-Phthalaldehyde in combination with N-acetyl-L-cysteine is a useful derivatization reagent for the optical resolution of enantiomeric α -H- α -amino acids, α -alkyl- α -amino acids and the corresponding acid amides. By using reversed-phase high-performance liquid chromatography with a mobile phase containing copper(II) acetate and L-proline, the diastereomeric derivatives of the α -amino compounds can be separated under isocratic conditions. The rate of reaction of α -alkyl- α -amino compounds with *o*-phthalaldehyde–N-acetyl-L-cysteine can be increased by selectively increasing the amount of *o*-phthalaldehyde in the reaction mixture. When the derivatization parameters were controlled automatically, the derivatization process showed good reproducibility and the method was found to be suitable for quantitative measurements. The method was applied to monitor the enantiomeric purity of α -H- α -amino acids and α -alkyl- α -amino acids obtained by enantioselective hydrolysis of the corresponding acid amides using an aminopeptidase.

INTRODUCTION

Optically pure α -amino acids (α -AA) are of great interest to the biochemist and pharmaceutical chemist. One of the routes to obtain these compounds is through organic synthesis of racemic α -amino acid amides (α -AA-NH₂) followed by the use of a broad-specificity aminopeptidase to achieve resolution on a large scale^{1,2}. In conjunction with this synthesis, analytical methods are required to monitor the enantiomeric purity of both α -AA and α -AA-NH₂. Several high-performance liquid chromatographic (HPLC) methods have been developed for the optical resolution of α -H- α -AA^{3–8}. Resolution of α -alkyl- α -AA enantiomers has been achieved by ligand-exchange chromatography (LEC) on both reversed-phase columns⁹ and chiral columns¹⁰.

The aim of this work was to develop an HPLC method for the enantiomeric resolution of α -H- α -AA and α -alkyl- α -AA together with the corresponding acid amides. With the aid of LEC, enantiomeric mixtures of α -H- α -AA and α -H- α -AA-NH₂

^a Parts of this paper were presented at the *International Symposium on Chiral Separations*, September 3–4, 1987, Guildford, U.K.

could be separated¹¹. However, the same approach was unsuccessful with the α -alkyl substituted analogues.

In this paper, we report on the use of *o*-phthalaldehyde (OPA) in combination with N-acetyl-L-cysteine (NAC) for the derivatization of α -H- α -AA, α -alkyl- α -AA and the corresponding acid amides. For the amino compounds studied, we optimized the derivatization reaction. By using a copper complex of L-proline (L-Pro) as an additive to the mobile phase, separation of the amino acid and amide enantiomers could be achieved in an isocratic HPLC run. When the derivatization process was automated, the method was found to be suitable for quantitative measurements.

EXPERIMENTAL

Materials

α -H- α -AA-NH₂, α -alkyl- α -AA and α -alkyl- α -AA-NH₂ were synthesized in our laboratory^{1,2}. α -H- α -AA were procured from Sigma (St. Louis, MO, U.S.A.). For each compound, both the racemic form and at least one optically pure enantiomer were available. NAC was obtained from Janssen (Beerse, Belgium). OPA, HPLC-grade methanol (CH₃OH) and acetonitrile (CH₃CN) were supplied by Merck (Darmstadt, F.R.G.). Water was purified with a Milli-Q system. All other chemicals were of analytical-reagent grade.

Instrumentation

The chromatographic system consisted of a Hewlett-Packard (Palo Alto, CA, U.S.A.) Model 1081B liquid chromatograph and a Gilson Model 231-401 auto-sampling injector for derivatization and injection. The injection loop had a 20- μ l capacity. The columns used were Nucleosil-120-C₁₈ (250 \times 4.0 mm I.D., 5 μ m, and 125 \times 4.0 mm I.D., 3 μ m) from Marcherey, Nagel & Co. (Düren, F.R.G.). The flow-rate was 1 ml/min and the column temperature was kept at 40°C. The derivatives were monitored with a Waters Assoc. (Milford, MA, U.S.A.) Model 420 fluorescence detector. For excitation a 338-nm band-pass filter was used, and for emission a 415-nm long-pass filter was chosen. Quantitation was performed with a Hewlett-Packard 3350 Laboratory Automation System.

Eluent, reagent and derivatization procedure

The mobile phase consisted of 2.5 mM copper(II) acetate buffer, titrated to pH 6.0 with ammonium acetate, and 5 mM L-Pro. The concentrations of CH₃OH and CH₃CN varied, depending on the compounds studied, and are indicated in the tables. The OPA reagent was prepared by dissolving 3.3 mg of OPA per ml of water-CH₃OH (1:1, v/v). For the NAC reagent, 4 mg of NAC were dissolved per ml of water-CH₃OH (1:1, v/v). Amino acids and amino acid amides were dissolved in water.

Derivatization was performed automatically with a Gilson Model 231-401 system. Into an empty vial the following were successively dispensed: 35 μ l of sample solution, 35 μ l of OPA reagent, 35 μ l of NAC reagent and 175 μ l of 0.4 M potassium borate buffer (pH 9.4). The largest volume, i.e., the borate solution, was added at a high speed in order to ensure good mixing of the reaction medium. The vial was allowed to stand for at least 2 min at room temperature, after which 140 μ l of 1 M sodium phosphate buffer (pH 3.5) were added to neutralize the mixture. An

aliquot of the reaction mixture was then injected directly into the chromatographic system.

RESULTS AND DISCUSSION

Choice of the mobile phase

For the optical separation of OPA-NAC derivatives of α -H- α -AA, reversed-phase systems have been described^{5,6,12}, in which the usual buffer salts (sodium acetate or sodium phosphate) in combination with an organic solvent were used as mobile phases. A different approach was taken by Lam¹³, who used mixed chelation to resolve the OPA-NAC derivatives of α -H- α -AA. We compared both approaches for the optical resolution of α -CH₃-Val, Val and the corresponding α -AA-NH₂. The results are given in Table I. The separation factors (α) of the enantiomers of the α -AA and α -AA-NH₂ studied are comparable in both chromatographic systems. In contrast to Lam and Malikin¹⁴, we found that the use of reversed-phase ligand-exchange chromatography (RP-LEC) did not improve the enantioselectivity as compared with RP-HPLC. However, mixed chelation changes the selectivity of the system with respect to the α -AA and the corresponding α -AA-NH₂. The α -value of the last-eluting α -AA enantiomer and the first-eluting α -AA-NH₂ enantiomer (Table I) is much smaller in the RP-LEC system than in the RP-HPLC system. The decrease in the α -value in the RP-LEC system results from a decrease of the k' value of the α -AA-NH₂.

The difference in retention characteristics of α -AA-NH₂ in an RP-LEC system and an RP-HPLC system may be explained as follows. The polar amide function of α -AA-NH₂ may interact with free silanol sites on the RP column and this interaction will result in an additional increase in retention time. In the presence of Cu^{II} and L-Pro mixed-ligand complexes of α -AA-NH₂ with Cu^{II}-L-Pro will be formed. In the resulting complex the polar acid amide group will be coordinated with Cu^{II} and will thus be unavailable to interact with the free silanol sites in the matrix. The absence of the latter interaction may explain the observed decrease in retention time when the RP-LEC system is used. The relative retention time of α -AA and α -AA-NH₂ was also dependent

TABLE I
SELECTIVITY (α) OF THE OPA-NAC DERIVATIVES OF Val, Val-NH₂, α -CH₃-Val AND α -CH₃-Val-NH₂ ENANTIOMERS IN RP-HPLC AND RP-LEC SYSTEMS

Mobile phases: RP-LEC, 5 mM L-Pro-2.5 mM copper(II) acetate adjusted to pH 6.0 with ammonium acetate-40%CH₃OH; RP-HPLC, 2.5 mM sodium acetate adjusted to pH 6.0 with acetic acid-15% CH₃OH.

Enantiomer	α^a		Enantiomer	α^a	
	RP-HPLC	RP-LEC		RP-HPLC	RP-LEC
L-Val I	1.35	1.33	D- α -CH ₃ -Val I	1.22	1.23
D-Val II			L- α -CH ₃ -Val II		
L-Val-NH ₂ I	1.22	1.17	D- α -CH ₃ -Val-NH ₂ I	1.22	1.27
D-Val-NH ₂ II			L- α -CH ₃ -Val-NH ₂ II		
D-Val I	10.03	1.96	L- α -CH ₃ -Val I	8.67	1.16
L-Val-NH ₂ II			D- α -CH ₃ -Val-NH ₂ II		

$$^a \alpha = t_{R(II)}/t_{R(I)}$$

on the organic modifier used in the RP-LEC system. By using CH₃CN instead of CH₃OH, the α -value of L- α -H- α -AA and D- α -H- α -AA-NH₂ increased by a factor of 2 on average.

Employment of the RP-HPLC system for enantioselective analysis will necessitate the use of gradient elution to obtain the enantiomers of an α -AA and α -AA-NH₂ within a reasonable time. However, this will be at the expense of the resolution of the α -AA-NH₂ enantiomers. Use of the RP-LEC system gives the possibility of analysing the enantiomers of both α -AA and α -AA-NH₂ under isocratic conditions. In our further study, we therefore chose to use the RP-LEC system, employing CH₃OH as organic modifier.

Enantioselective analysis

The enantioselectivity of the RP-LEC system was tested with several α -H- α -AA, α -alkyl- α -AA and the corresponding acid amides. By varying the concentration of CH₃OH in the mobile phase, each tested α -AA and the corresponding α -AA-NH₂ could be baseline separated into their enantiomers in one analysis. Table II shows the chromatographic data for various α -H- α -AA and the corresponding α -AA-NH₂. The data for the α -alkyl- α -AA and α -alkyl- α -AA-NH₂ are given in Table III. Representative chromatograms are given of an α -H- α -AA and the α -H- α -AA-NH₂ (Fig. 1) and of an α -alkyl- α -AA and the α -alkyl- α -AA-NH₂ (Fig. 2). As far as the order of elution of the enantiomers is concerned, all the tested α -AA-NH₂ show the same order as the corresponding α -AA. The order of elution of the tested α -H- α -AA was L- before D-. For the aliphatic α -H- α -AA, the same order of elution was reported by Lam and Malikin¹⁴. The order of elution of the α -alkyl- α -AA studied was the reverse of that of

TABLE II
CAPACITY FACTOR (k'), SELECTIVITY (α) AND RESOLUTION (R_s) OF OPA-NAC DERIVATIVES OF α -H- α -AA AND THE CORRESPONDING α -H- α -AA-NH₂

For chromatographic conditions, see Experimental.

Methanol concentration (%)	α -H- α -AA α -H- α -AA-NH ₂	k'_L	k'_D	α	R_s^b
20	Ala	5.3	5.9	1.11	2.4
	Ala-NH ₂	10.7	13.4	1.25	5.9
25	But	7.3	8.9	1.22	5.0
	But-NH ₂	15.1	19.3	1.28	7.0
40	Val	1.8	2.4	1.33	4.7
	Val-NH ₂	4.7	5.5	1.17	3.3
	Leu	2.8	3.2	1.14	1.4
	Leu-NH ₂	9.5	11	1.16	3.3
35	α -Ph-Gly	6.7	7	1.05	1.2
	α -Ph-Gly-NH ₂	14.4	16.1	1.12	2.4
	Phe	9.0	9.7	1.08	1.8
	Phe-NH ₂	25.4	26	1.02	-
	β -Bz-Ala	27.7	30.5	1.10	2.2
	β -Bz-Ala-NH ₂	50	58	1.16	2.7

$$^a \alpha = k'_D/k'_L$$

$$^b R_s = 1.177 (t_{RD} - t_{RL}/W_{1/2L} + W_{1/2D})$$

TABLE III

CAPACITY FACTOR (k'), SELECTIVITY (α) AND RESOLUTION (R_s) OF OPA-NAC DERIVATIVES OF α -ALKYL- α -AA AND THE CORRESPONDING α -ALKYL- α -AA-NH₂

For chromatographic conditions, see Experimental.

Methanol concentration (%)	α -Alkyl- α -AA α -Alkyl- α -AA-NH ₂	k'_D	k'_L	α^a	R_s^b
30	α -CH ₃ -But	5.1	5.7	1.12	2.2
	α -CH ₃ -But-NH ₂	8.6	9.8	1.14	2.9
40	α -CH ₃ -Val	3.1	3.8	1.23	3.7
	α -CH ₃ -Val-NH ₂	4.4	5.6	1.27	4.8
37.5	α -CH ₃ -Leu	9.1	10.1	1.11	2.4
	α -CH ₃ -Leu-NH ₂	14	15.5	1.11	2.8
35	α -CH ₃ - α -Ph-Gly	7.9	8.7	1.10	2
	α -CH ₃ - α -Ph-Gly-NH ₂	13.5	14.6	1.08	1.8
37.5	α -CH ₃ -Phe	8.2	9.8	1.20	2.7
	α -CH ₃ -Phe-NH ₂	14.0	16.7	1.19	4.3
	α -CH ₃ - β -Bz-Ala	18.9	20.3	1.07	1.5
	α -CH ₃ - β -Bz-Ala-NH ₂	28	30.8	1.10	2.2
	α -C ₂ H ₅ -Phe	40	44	1.10	1.9
	α -C ₂ H ₅ -Phe-NH ₂	67.8	83.9	1.24	4.3

$$^a \alpha = k'_L/k'_D.$$

$$^b R_s = 1.177 (t_{R_L} - t_{R_D})/W_{0.5L} + W_{0.5D}.$$

the α -H- α -AA analogues in all instances. This phenomenon may be explained by the fact that replacement of the hydrogen on the α -carbon by a methyl or ethyl group leads to a change in intramolecular binding in the diastereomers, through which the order of elution reverses.

For Ala, using the chromatographic conditions listed in Table I, we found in both the RP-HPLC and RP-LEC system that the order of elution of the enantiomers was L- before D-, which is the reverse of that reported previously^{8,12}.

Depending on the nature of the substituent on the α -carbon of α -AA and α -AA-NH₂, different concentrations of CH₃OH were used to regulate the retention times. Comparison of the retention behaviours of the α -H- α -AA studied showed that the retention times of the aliphatic compounds increased with increasing carbon content of the substituent (Leu > Val > But > Ala). With the aromatic compounds,

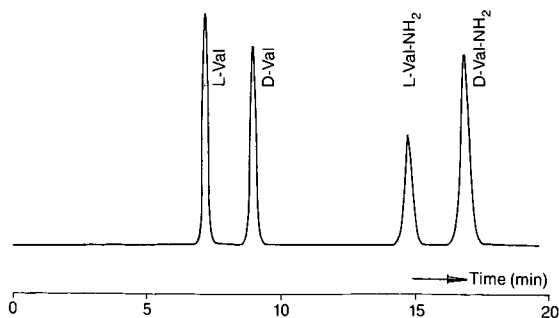


Fig. 1. Chromatogram of OPA-NAC derivatives of L,D-Val and L,D-Val-NH₂. For chromatographic conditions, see Experimental.

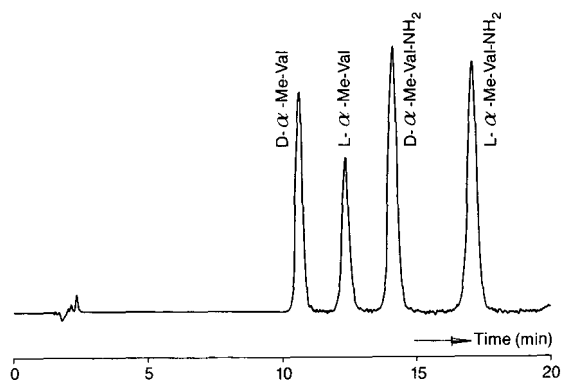


Fig. 2. Chromatogram of OPA–NAC derivatives of L,D- α -CH₃-Val and L,D- α -CH₃-Val-NH₂. For chromatographic conditions, see Experimental. Me = methyl.

the k' values increased with increasing number of methylene units between the phenyl group and the α -carbon (β -Bz-Ala > Phe > α -Ph-Gly). Because of the higher carbon content, α -alkylated compounds were retained more than the corresponding α -H analogues.

For all the aliphatic and aromatic enantiometric pairs studied, the α -values ranged from 1.1 to 1.3, except for Phe-NH₂ (1.02). Val and α -CH₃-Val showed the highest enantioselectivity. Among the α -H- α -AA studied by Lam and Malikin¹⁴, the Val enantiomers also showed the highest α -value.

Rate of the OPA–NAC derivatization reaction

In accordance with others^{9,15,16}, we found that α -alkyl- α -AA react more slowly than the α -H analogues with the OPA reagent, under the same reaction conditions. The rates of derivative formation of some α -AA and α -AA-NH₂ are shown in Fig. 3 as a function of the reaction time. For Val and α -Ph-Gly, both α -H- α -AA, the maximum fluorescence occurs after about 2 min, whereas for α -CH₃-Val and α -CH₃-Val-NH₂, maximum fluorescence has still not been reached after 25 min. In order to improve the rate of reaction of α -alkylated compounds with the OPA–NAC reagent, we studied the influence of both OPA and NAC concentrations in the reaction mixture. Fig. 4 shows the fluorescence response of the OPA–NAC derivative of α -CH₃-Val as a function of the reaction time at different reagent concentrations. Compared with an equimolar excess of OPA–NAC, a 10-fold molar increase in OPA leads to an increase in the reaction rate, whereas a 10-fold molar increase in NAC decreases the reaction rate. These results indicate that the thiol competes with the amine for the OPA. By using an excess of OPA with respect to NAC, nucleophilic attack of the sterically hindered α -alkyl- α -AA on the carbonyl function of OPA is thus facilitated. By choosing a 100-fold molar excess of OPA and a 10-fold molar excess of NAC with respect to the α -alkyl-AA, maximum fluorescence is obtained within 10 min.

Depending on the structure of the α -AA and α -AA-NH₂ studied, different fluorescence intensities were obtained. Some examples are given in Fig. 3. The maximum fluorescence intensities for the α -AA-NH₂ were about one order of magnitude lower than those for the corresponding α -AA, while the α -alkylated

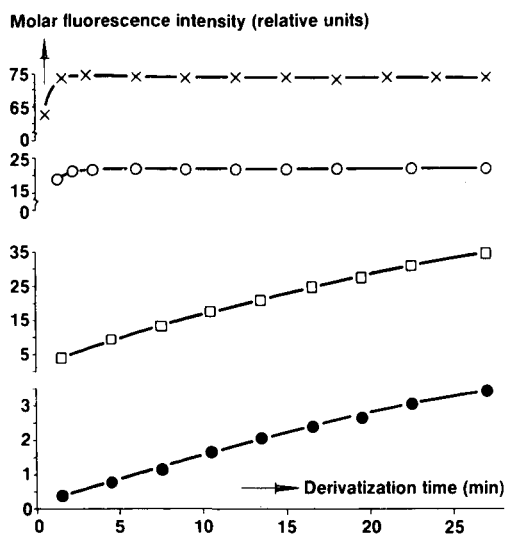


Fig. 3. Molar fluorescence response of the OPA-NAC derivatization as a function of reaction time for (x) Val, (○) α -Ph-Gly, (□) α -CH₃-Val and (●) α -CH₃-Val-NH₂. The molar excess of both OPA and NAC was 10-fold with respect to the compounds studied.

compounds showed lower intensities than the α -H-analogues. Differences in fluorescence intensity were also seen for the enantiomeric forms of the compounds studied. For the α -AA and α -alkyl- α -AA-NH₂ enantiomers, differences in specific fluorescence between 0 and 30% were observed. In some instances the D-isomer showed a higher fluorescence than the L-isomer, whereas in other instances the reverse was seen; however, no relationship could be established with structural aspects of the compounds. For the α -H- α -AA-NH₂ consistency was found, viz., all D-isomers studied

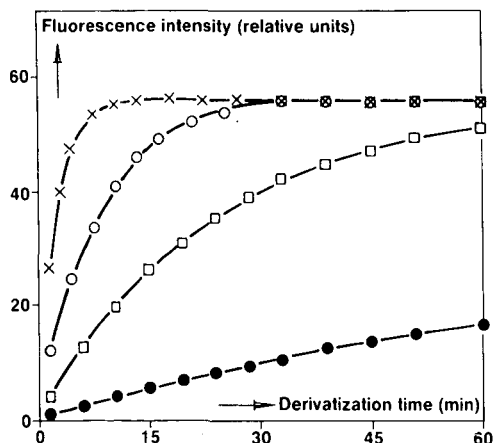


Fig. 4. Fluorescence response of the OPA-NAC derivatization as a function of reaction time for α -CH₃-Val. Molar excess of reagent: (x) OPA 100, NAC 10; (○) OPA 100, NAC 100; (□) OPA 10, NAC 10; and (●) OPA 10, NAC 100.

had a higher fluorescence intensity (by a maximum factor of about 2) than the L-isomers.

The difference in the fluorescence intensities of the OPA–NAC derivatives could be attributed to differences in intramolecular bonding in the isoindole reaction product. According to Lindner¹⁷, intramolecular binding can occur between the carboxyl function of NAC and the isoindole nitrogen. These interactions, which will be dipolar or hydrogen bonding, may change by replacing an α -H by an α -alkyl group, by replacing a carboxyl function by an acid amide function or by replacing the entire L-enantiomer by the D-configuration.

Quantitative determinations were carried out by comparing the peak areas of samples with those of standard solutions, employing the external standard method. As an example of the linearity, precision and detection limit of the method, data are given for α -CH₃-Val. The linearity of the amount–response relationship was established over the range 2–20 nmol for each of the enantiomers. Linear regression analysis from calibration graphs indicated that the correlation coefficient for both enantiomers was 0.9999. The within-run precision of the assay gave a coefficient of variation of <2% ($n = 5$) over the range 2–20 nmol. The detection limit for L- α -CH₃-Val, based on a signal-to-noise ratio of 2, was 10 pmol.

REFERENCES

- 1 E. M. Meijer, W. H. J. Boesten, H. E. Schoemaker and J. A. M. van Balken, in J. Tramper, H. C. van der Plas and P. Linko (Editors), *Biocatalysis in Organic Synthesis*, Elsevier, Amsterdam, 1985, p. 135.
- 2 W. H. Kruizinga, J. Bolster, R. M. Kellogg, J. Kamphuis, W. H. J. Boesten, E. M. Meijer and H. E. Schoemaker, *J. Org. Chem.*, 53 (1988) 1826.
- 3 C. Gilon, R. Leshem, Y. Taphui and E. Grushka, *J. Am. Chem. Soc.*, 101 (1979) 7612.
- 4 J. N. LePage, W. Lindner, G. Davies, D. E. Seitz and B. L. Karger, *Anal. Chem.*, 51 (1979) 433.
- 5 D. W. Aswad, *Anal. Biochem.*, 137 (1984) 405.
- 6 R. H. Buck and K. Krummen, *J. Chromatogr.*, 315 (1984) 279.
- 7 S. Einarsson, S. Folestad and B. Josefsson, *J. Liq. Chromatogr.*, 10 (1987) 1589.
- 8 R. H. Buck and K. Krummen, *J. Chromatogr.*, 387 (1987) 255.
- 9 S. Weinstein and N. Grinberg, *J. Chromatogr.*, 318 (1985) 117.
- 10 H. Brückner, *Chromatographia*, 24 (1987) 725.
- 11 A. Duchateau, M. Crombach, M. Aussems and J. Bongers, *J. Chromatogr.*, 461 (1989) 419.
- 12 N. Nimura and T. Kinoshita, *J. Chromatogr.*, 352 (1986) 169.
- 13 S. Lam, *J. Chromatogr.*, 355 (1986) 157.
- 14 S. Lam and G. Malikin, *J. Chromatogr.*, 368 (1986) 413.
- 15 H. Brückner, I. Bosch, T. Graser and P. Fürst, *J. Chromatogr.*, 386 (1987) 251.
- 16 J. R. Cronin, S. Pizzarello and W. E. Gandy, *Anal. Biochem.*, 93 (1979) 174.
- 17 W. Lindner, in M. Zief and L. J. Crane (Editors), *Chromatographic Chiral Separations (Chromatographic Science Series, Vol. 40)*, Marcel Dekker, New York, 1988, Ch. 4, p. 116.

CHROM. 21 277

IMPROVED CHIRAL STATIONARY PHASE FOR THE SEPARATION OF THE ENANTIOMERS OF CHIRAL ACIDS AS THEIR ANILIDE DERIVATIVES

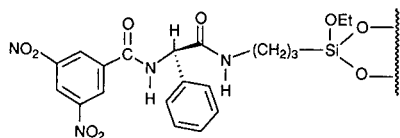
WILLIAM H. PIRKLE* and JOHN E. McCUNE
School of Chemical Sciences, University of Illinois, Urbana, IL 61801 (U.S.A.)

SUMMARY

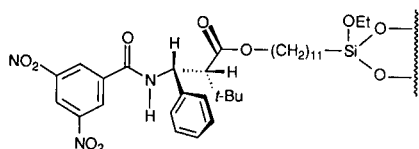
Liquid chromatographic separation of the enantiomers of anilide derivatives of chiral carboxylic acids is facile on a chiral stationary phase derived from a conformationally restricted β -amino acid. This new chiral stationary phase, a variant of the (*R*)-N-(3,5-dinitrobenzoyl)phenylglycine-derived chiral stationary phase, is markedly superior to its predecessor for separation of the enantiomers of a wide variety of anilides derived from carboxylic acids.

INTRODUCTION

A variant of the widely used and commercially available phenylglycine-derived chiral stationary phase (CSP), **1**, was recently described¹. This stationary phase, CSP **2**, differs structurally from CSP **1** in two ways. First, a second center is, in effect, interposed between the single stereogenic center of CSP **1** and the carbonyl moiety which links it to the solid support. Secondly, CSP **2** is ester-linked to an eleven carbon connecting arm rather than amide-linked to a three carbon connecting arm. The enantiomers of many analytes show larger separation factors on CSP **2** than on CSP **1**. This is perhaps surprising since the distance between the primary interaction sites, the 3,5-dinitrobenzoyl group and the C-terminal carbonyl, is greater in CSP **2** than in CSP **1**. The second stereogenic center is not believed to be a "primary" source of enantiodifferentiation, but, in those cases where separation is greater on CSP **2**, is thought to complement the phenylglycine-like stereogenic center. Normally, increasing the distance between the interaction sites of either a CSP or an analyte will engender increased conformational freedom and a reduced level of chiral recognition. However, the bulky substituents on the vicinal stereogenic centers of CSP **2** confer considerable conformational rigidity, apparently holding the interaction sites in such spatial positions as to frequently enhance the chiral recognition properties of CSP **2**. Even so, the mode of enantiodifferentiation by CSP **2** is expected to be analogous to that of CSP **1**².



CSP 1



CSP 2

As part of the on-going evaluation of CSP 2, a number of anilides of chiral carboxylic acids were prepared and chromatographed, the data being presented herein. From an analysis of the relationships between analyte structure and chromatographic behavior, a chiral recognition model is advanced to rationalize the experimental observations.

EXPERIMENTAL

Apparatus

Chromatography was performed using a Bischoff Model 2200 isocratic high-performance liquid chromatography pump, a Rheodyne Model 7125 injector with a 20- μ l sample loop, a 250 \times 4.6 mm stainless-steel column packed with CSP 2 as described previously¹, two Milton Roy UV Monitor® D fixed-wavelength detectors (254 and 280 nm) connected in series, and a Kipp & Zonen Model BD 41 dual-pen chart recorder.

Reagents

Racemic ibuprofen was isolated from a Motrin® tablet. Ibuprofen was partially resolved according to the procedure of Nicoll-Griffith³. Fenoprofen was a gift of Eli Lilly and Company. The racemate and the (S)-(+ enantiomer of 2-phenylbuteric acid was obtained from Aldrich as were 2-ethoxy-1-ethoxycarbonyl-1,2-dihydroquinoline (EEDQ) and the various anilines and amines used herein. The remaining acids were available from prior studies.

Derivatization

The anilides were made either via the acid chloride or through the agency of EEDQ. Acids 1 and 5 were converted to the acid chlorides using thionyl chloride. The remaining acids were converted to the mixed anhydrides with EEDQ. The former derivatization sequence has been described³.

General anilide synthesis using EEDQ

Equal quantities (ca. 10 mg) of the acid and EEDQ were added to a 5-ml screw-capped test tube followed by two drops of the aniline and 0.5 ml of

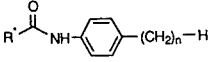
dichloromethane. After 30 min, 1.5 ml additional dichloromethane and 1 ml of 1 M sodium hydroxide was added, the mixture was shaken vigorously, and the upper layer was removed with a pipet. The lower layer was similarly washed several times with water, than 1 ml of 1 M hydrochloric acid was added. The mixture was shaken vigorously, centrifuged if necessary to separate layers (the higher-molecular-weight *p*-alkylanilines form emulsions when acidified; excesses of these reagents were avoided) and the upper layer was withdrawn. The lower layer was repeatedly washed with water, especially in the case of the higher-molecular-weight alkylanilines. The resulting solution was dried over anhydrous magnesium sulfate and analyzed directly. Early eluting impurities were noted in some instances but did not interfere with the analyses³.

Conversion of otherwise non-functionalized acids to anilide derivatives is quite straightforward. To verify that the reported procedure does afford the intended derivatives, *p*-ethylanilides of acids 2–5 were prepared on a larger scale and characterized by NMR and IR spectroscopy and by elemental analysis. These characterization data are in accord with the assigned structures.

RESULTS AND DISCUSSION

The enantiomers of a variety of anilides of chiral carboxylic acids are separable on CSP 2. Table I provides chromatographic data for the normal-phase separation of the enantiomers of a homologous series of *p*-alkyl anilide derivatives of 2-(α -naphthyl)propionic acid (1), ibuprofen (2), fenopropfen (3), α -isopropoxyphenylacetic acid (4) and 2-phenylbuteric acid (5) on CSP 2. All analytes show considerably larger

TABLE I
NORMAL-PHASE SEPARATION ON (2*R*,3*R*)-CSP 2 OF CHIRAL ACIDS 1-5 AS THEIR *p*-ALKYLANILIDES



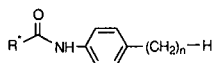
<i>n</i>	1		2		3		4		5	
	α^a	$k'_1{}^b$	α^a	$k'_1{}^b$	α^a	$k'_1{}^b$	α^a	$k'_1{}^b$	α^a	$k'_1{}^b$
0	1.94	8.37	1.54	3.71	1.49	5.87	1.71	2.76	1.64	4.20
1	1.91	11.4	1.57	5.01	1.47	8.08	1.71	3.60	1.68	6.00
2	1.91	9.40	1.56	4.13	1.47	6.73	1.70	3.07	1.69	4.80
4	1.98	8.00	1.55	3.57	1.47	5.73	1.74	2.51	1.69	4.20
6	1.96	6.93	1.51	3.33	1.46	5.13	1.71	2.33	1.68	3.73
8	1.96	6.27	1.53	2.96	1.46	4.67	1.73	2.09	1.66	3.44
10	1.96	5.71	1.51	2.77	1.44	4.40	1.71	1.87	1.65	3.13
12	1.99	5.20	1.52	2.56	1.44	3.97	1.73	1.73	1.67	2.80
14	1.98	4.83	1.52	1.37	1.43	3.73	1.75	1.60	1.65	2.67

^a Chromatographic separation factor.

^b Capacity factor for the first eluted enantiomer using 10% (v/v) 2-propanol in hexane as the mobile phase; flow-rate 2 ml/min.

TABLE II

REVERSED-PHASE SEPARATION ON (2*R*,3*R*)-CSP 2 OF CHIRAL ACIDS 1-5 AS THEIR *p*-ALKYLANILIDES

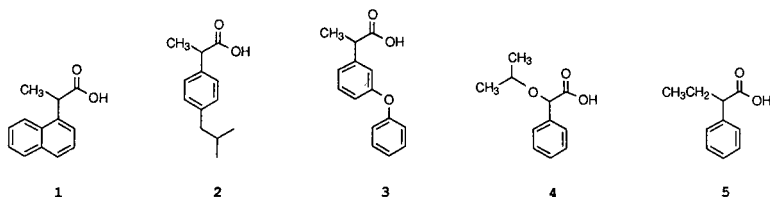


<i>n</i>	1		2		3		4		5	
	α^a	$k'_1{}^b$	α^a	$k'_1{}^b$	α^a	$k'_1{}^b$	α^a	$k'_1{}^b$	α^a	$k'_1{}^b$
0	1.68	0.87	1.32	0.49	1.21	0.66	1.31	0.42	1.34	0.22
1	1.68	1.22	1.32	0.75	1.25	0.90	1.30	0.64	1.38	0.39
2	1.64	1.39	1.35	0.77	1.25	0.97	1.27	0.71	1.38	0.42
4	1.65	1.74	1.34	1.08	1.25	1.26	1.27	0.92	1.33	0.58
6	1.62	2.32	1.34	1.42	1.23	1.73	1.28	1.26	1.31	0.84
8	1.61	3.16	1.32	1.92	1.23	2.26	1.27	1.71	1.32	1.16
10	1.61	4.24	1.32	2.58	1.36	2.74	1.24	2.39	1.28	1.58
12	1.60	5.68	1.30	3.45	1.22	4.13	1.24	3.11	1.30	2.10
14	1.61	7.61	1.30	4.64	1.21	5.54	1.23	4.21	1.27	2.93

^a Chromatographic separation factor.

^b Capacity factor for the first eluted enantiomer using methanol-water (9:1, v/v) as the mobile phase; flow-rate 1 ml/min.

chromatographic separation factors on CSP 2 than on CSP 1². Additionally, excellent reversed-phase separations are obtained for these analytes on CSP 2 (Table II).



In order for enantiodifferentiation to occur, a minimum of three simultaneous interactions, at least one of which is enantiodependent, must occur between the analyte and the CSP⁴. From prior investigation of these anilide analytes on CSP 1, there is reason to expect two competing chiral recognition mechanisms, having different modes of dipole stacking as important associative interactions^{2,3,5,6}. These are shown in Figs. 1 and 2. The three interactions which lead to enantiodifferentiation in Fig. 1 are

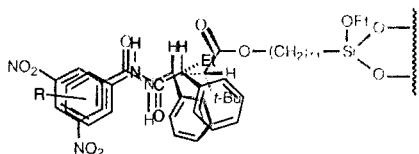


Fig. 1. A head-to-tail dipole stacking chiral recognition model.

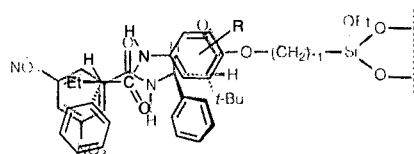


Fig. 2. A head-to-head dipole stacking chiral recognition model.

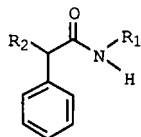
a "head-to-tail" dipole stack, a π - π association between the 3,5-dinitrobenzoyl moiety of the CSP and the anilide functionality of the analyte and a stereochemically dependent steric interaction between the analyte and the CSP. The alternate chiral recognition model (Fig. 2) is one in which the dipole stacking is of a "head-to-head" nature. In Fig. 2, a π - π interaction can occur between the aryl portion of the acid and the 3,5-dinitrobenzoyl group of the CSP, the enantiodifferentiating interaction again being a steric interaction between the alkyl group on the stereogenic center of the analyte and the CSP.

For analytes in which the π -basic aryl group is either the aniline system or is an aryl substituent on the stereogenic center of the acid portion of the molecule, the mechanism deemed most important for the retention of the more strongly retained enantiomer is clear; it is the dipole-stacking mode which permits simultaneous π - π bonding with the 3,5-dinitrobenzoyl group. For analytes having π -basic groups in both locations, the two processes are in competition. Since both stacking modes give rise to the same elution order, this datum is of no particular aid in distinguishing between the two competing stacking modes.

Note that in the head-to-tail mode, a substituent of the anilide in the *para*-position is directed away from the solid support and into the mobile phase, the converse being true for the head-to-head arrangement. Consequently, analysis of the chromatographic data for analytes derived from a homologous series of *p*-alkyl-anilides was expected to yield considerable mechanistic information. For example, if the head-to-tail arrangement is the dominant contributor to chiral recognition, the length of the *p*-alkyl substituent should have little effect on the chromatographic separation factor of the enantiomers. However, if the head-to-head arrangement is dominant, then the *p*-alkyl substituent should interact sterically with the neighboring strands of bonded phase and with the underlying solid support. This effect increases as the length of the *p*-substituent increases, causing a decrease in the stability of the diastereomeric adsorbate in which this is occurring. This results in reduced retention of this enantiomer relative to its antipode and hence a change in the magnitude of the chromatographic separation factor. This effect is expected to be the most pronounced for CSPs having short connecting arms (such as CSP 1) and somewhat attenuated for CSPs having long connecting arms, such as CSP 2. Examination of the data in Table I for the separation of the enantiomers of homologous series of the *p*-alkylanilides of chiral acids reveals that no definite diminution of α is observed. This observation, though suggestive, does not necessarily rule out head-to-head stacking, owing to the aforementioned attenuation expected from the long connecting arm of CSP 2.

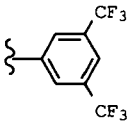

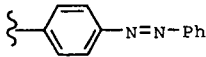
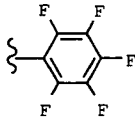
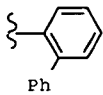
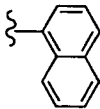
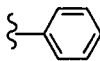
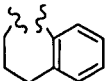
If the head-to-tail stacking process is indeed operative, then increasing the π -basicity of the N-aryl substituent should increase the separation factors for the enantiomers. That this is the case is shown by the data for the N-1-naphthyl-, N-2-naphthyl- (Table III) and N-phenylamide (Table I) derivatives of **5**. Similarly, introduction of substituents on to the anilide ring, by altering π -basicity, should affect α . This is observed for anilides of **5**. The unsubstituted anilide has an α of 1.64 while the *p*-methylanilide gives an α of 1.68. The *p*-CF₃-, *p*-CN- and *p*-NO₂-anilides show α values of 1.52, 1.32 and 1.26, respectively. Similar trends are noted for 3,5-disubstituted anilides of **5**. The observation that α is directly affected by the π -basicity of the anilide moiety provides strong evidence for head-to-tail stacking being the dominant process involved in chiral recognition. Similar observations for ibuprofen

TABLE III

SEPARATION ON (2*R*,3*R*)-CSP 2 OF VARIOUS ANILIDES OF α -PHENYLBUTANOIC ACID AND 2-ISOPROPOXYPHENYLACETIC ACID

R_1	R_2	Normal phase		Reversed-phase	
		α^a	$k'_1{}^b$	α^a	$k'_1{}^c$
	C_2H_5	1.39	4.13	1.07	0.94
	C_2H_5	3.03	31.9	2.26	1.13 ^d
	C_2H_5	2.28	27.7	1.81	2.00
	C_2H_5	2.01	10.5 ^d	1.48	0.68 ^d
	C_2H_5	1.26	3.24 ^d	1.13	0.39 ^d
	C_2H_5	1.29	3.04 ^d	1.10	0.44
	C_2H_5	1.15	2.73 ^d	1.06	0.52 ^d
	C_2H_5	1.52	1.40 ^d	1.20	0.26 ^d

TABLE III (continued)

R_1	R_2	Normal phase		Reversed-phase	
		α^a	k_1^b	α^a	k_1^c
	C_2H_5	1.00	0.51	1.00	0.40
	C_2H_5	1.32	4.71	~1.00	0.32
	C_2H_5	1.58	4.37	1.20	129
	C_2H_5	1.43	1.27	1.00	≈1.00
	C_2H_5	1.31	2.13	1.15	0.56
	$(CH_3)_2CH-O-$	2.55	17.4	1.74	1.74
	$(CH_3)_2CH-O-$	1.76	2.87	1.28	0.45
		1.28	1.40 ^d	1.10	0.68 ^d

^a Chromatographic separation factor.

^b Capacity factor for the first eluted enantiomer using 10% (v/v) 2-propanol in hexane as the mobile phase; flow-rate 2 ml/min.

^c Capacity factor for the first eluted enantiomer using methanol-water (9:1, v/v) as the mobile phase; flow-rate 1 ml/min.

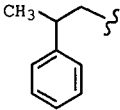
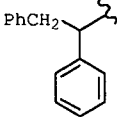
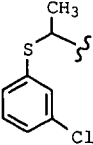
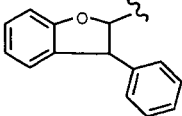
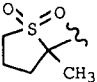
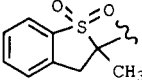
^d The (S)-(+)-enantiomer was most strongly retained.

TABLE IV

SEPARATION ON (2*R*,3*R*)-CSP 2 OF THE 3,5-DIMETHYLANILIDES OF VARIOUS CARBOXYLIC ACIDS

<i>R</i>	<i>Normal phase</i>		<i>Reversed-phase</i>	
	α^a	$k'_1{}^b$	α^a	$k'_1{}^c$
	2.90	16.3 ^d	2.13	2.35 ^d
	2.09	8.27 ^d	1.70	1.48
	1.77	12.80	1.41	1.81
	2.21	4.16	2.02	0.76
	2.20	9.20 ^d	1.77	0.77 ^d
	2.25	9.40	1.65	0.77

TABLE IV

R	Normal phase		Reversed-phase	
	α^a	$k'_1{}^b$	α^a	$k'_1{}^c$
	1.33	11.3	1.22	0.84
	1.51	9.73	1.77	0.84
	1.74	8.71	1.48	1.14
	1.24	4.73	1.12	2.55
	1.46	9.20	1.22	0.57
	1.70	14.1	1.30	0.97

^a Chromatographic separation factor.

^b Capacity factor for the first eluted enantiomer using 10% (v/v) 2-propanol in hexane as the mobile phase; flow-rate 2 ml/min.

^c Capacity factor for the first eluted enantiomer using methanol-water (9:1, v/v) as the mobile phase; flow-rate 1 ml/min.

^d The (S)-(+)-enantiomer was most strongly retained.

anilides have been reported by Nicoll-Griffith³ and were used to support a similar mechanistic conclusion for the separation of these enantiomers on CSP **1**.

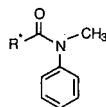
Table IV contains chromatographic data for the separation of a variety of chiral acids as their 3,5-dimethylanilides on CSP **2**. Note that the 3,5-dimethylanilide derivatives show enantioselectivity which, using both normal and reversed-phase conditions, surpasses that shown by the enantiomers of the *p*-alkylanilide derivatives of acids **1–5** (Tables I and II). This observation is also consistent with the dominance of a head-to-tail process.

Tertiary amide derivatives of acids **1–5** were prepared to determine the effects of hydrogen bonding interactions between the anilide proton of the analyte and a basic site on the CSP. If the anilide N–H participates in some essential hydrogen bonding interaction, its replacement by an alkyl substituent would be expected to seriously erode chiral recognition, consequently reducing α significantly. Chromatographic data for the separation of the N-methylanilides of acids **1–5** on CSP **2** are provided in Table V. The chromatographic separation factors for the enantiomers of the N-methyl anilides of acids **2**, **3** and **5** are slightly reduced, but still comparable in magnitude to those noted for the corresponding anilides (Table I). However, the capacity ratios of the former are significantly reduced relative to the latter. These results indicate that hydrogen bonding of the anilide N–H proton is not essential to chiral recognition of these analytes, although its presence may lead to achiral retention. Indeed, the N-methyl anilide of **1** exhibits a considerably larger α than does the anilide itself.

The chromatographic separation factor for separation of the enantiomers of the N-methylanilide of acid **4** is reduced and the capacity ratio for the first eluted enantiomer is much larger than that noted for the corresponding anilide. Apparently, hydrogen bonding of the anilide N–H proton of this analyte contributes significantly to the overall chiral recognition process. However, the hydrogen bond may be to the oxygen of the neighboring isopropoxyl group rather than to the CSP. This could explain the reduced retention and might entail a change in conformational preference. Since elution orders are not yet established for the derivatives of acid **4**, a chiral recognition model is not presently suggested for these analytes.

TABLE V

CHROMATOGRAPHIC BEHAVIOR ON (*R,R*)-CSP **2** OF CHIRAL ACIDS **1–5** AS THEIR N-METHYLANILIDES



	1	2	3	4	5
α^a	2.46	1.47	1.32	1.34	1.45
$k'_1{}^b$	2.44	1.48	2.69	4.94	1.27

^a Chromatographic separation factor.

^b Capacity factor for the first eluted enantiomer using 10% (v/v) 2-propanol in hexane as the mobile phase; flow-rate 2 ml/min.

CONCLUSION

Chiral carboxylic acids are readily resolved as their anilide derivatives by high-performance liquid chromatography (HPLC) on the β -amino acid-derived CSP **2**. The enantiomeric purity of chiral carboxylic acids can be determined and, in many cases, enantioselectivity is sufficient for facile preparative resolution.

ACKNOWLEDGEMENTS

This work was partially supported by grants from the National Science Foundation and the Eli Lilly Company.

REFERENCES

- 1 W. H. Pirkle and J. E. McCune, *J. Chromatogr.*, 441 (1988) 311–322.
- 2 W. H. Pirkle and J. E. McCune, *J. Chromatogr.*, 469 (1989) 67–75.
- 3 D. A. Nicoll-Griffith, *J. Chromatogr.*, 402 (1987) 179–187.
- 4 W. H. Pirkle and T. C. Pochapsky, *Adv. Chromatogr.*, 27 (1987) 73–127.
- 5 I. W. Wainer and T. D. Doyle, *J. Chromatogr.*, 284 (1984) 117–124.
- 6 D. M. McDaniel and B. G. Snider, *J. Chromatogr.*, 404 (1987) 123–132.

CHROM. 21 298

CHROMATOGRAPHIC EVALUATION OF OLIGOMERIC C₈ REVERSED PHASES FOR USE IN HIGH-PERFORMANCE LIQUID CHROMATOGRAPHY

S. O. AKAPO*, ALEXANDRA FURST, T. M. KHONG and C. F. SIMPSON

Analytical Science Group, Chemistry Department, Birkbeck College, University of London, 20 Gordon Street, London WC1H 0AJ (U.K.)

SUMMARY

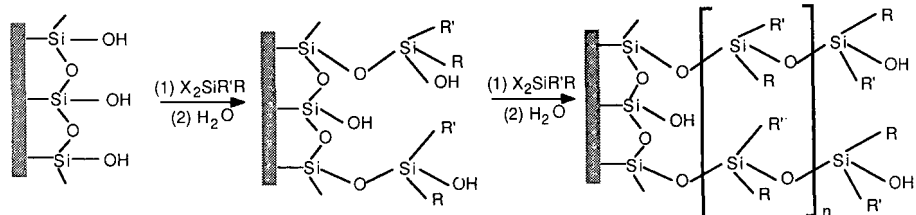
Stepwise silanisation of porous silica gel with *n*-octyldichlorosilane and subsequent hydrolysis of the unreacted chlorine atoms have been shown to produce a dense-layered C₈ chemically bonded stationary phase. Increase in carbon load results in decrease in specific surface area and pore volume of the starting silica material. Chromatographic properties obtained for aromatic hydrocarbons and alkyl benzoates under isocratic conditions were correlated with carbon content of the stationary phases. It was found that at high carbon content (> 11%) both capacity factor and separation factor are independent of carbon load.

INTRODUCTION

Over the past decade, reversed-phase high-performance liquid chromatography (RP-HPLC) has become a popular analytical technique. The use of the technique has led to intensive studies both on column design and synthesis of the stationary phases employed. These non-polar stationary phases are produced by the reaction of organochlorosilanes (or alkoxy-silanes) with the silanol groups on the surface of the porous silica. Generally, organochlorosilanes are preferred as the silanising agent, and depending on the functional group of the reactive moiety (mono-, di- or trihalides), monomeric or polymeric phases are produced.

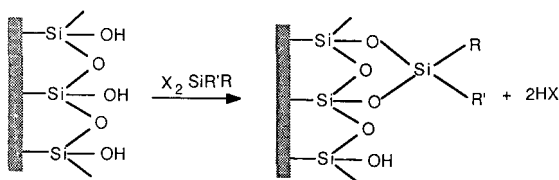
Treatment of the porous silica with di- or trichlorosilanes, for example, octylmethyl-dichlorosilane, results in the formation of polymeric phases in which the alkyl groups are attached to the silica surface via siloxane bonds. Unreacted halogen atoms are hydrolysed by traces of water present in the reaction medium and the newly formed silanols can either undergo condensation reaction with surface hydroxyl groups and/or react with more halogenated silane molecules to produce cross-linked polymeric phase.

Apart from the above reaction mechanism, a new, dense, polymer layer can be built up on the silica surface by exhaustive silanisation under controlled conditions resulting in a multilayer of the desired thickness. In this case, after the initial silanisation and subsequent hydrolysis of the unreacted functional group of the



Scheme 1.

organic moiety, the modified silica is again silanised with another portion of the starting silanising agent to form a second layer and so on. The structure of the final product is that of an oligomer made up of repeating units of the silanising agent as shown in Scheme 1, where $R' = \text{CH}_3$, $R = \text{CH}_3(\text{CH}_2)_7$ and $n = 0, 1, 2$, etc., depending on the number of reaction steps. Another possible reaction mechanism between silica and bifunctional silanes under anhydrous conditions is that of a silane molecule with two adjacent surface silanol groups to form a closed ring of siloxane bonds as shown in Scheme 2.



Scheme 2.

Whilst both reaction mechanisms are possible, the reaction shown in Scheme 2 is sterically unlikely to occur and if it actually takes place, it can be viewed as a terminating step since all the reactive functional groups of the silanising agent are covalently bonded during the first reaction. Consequently, subsequent treatment of the bonded silica with more silane molecules will result in little or no change in the carbon loading.

This paper describes the preparation of *n*-octylsilyl reversed phases by repeated silanisation of the silica support with *n*-octylmethyldichlorosilane and hydrolysing the unreacted chloro group of the silane as shown in Scheme 1. The effect of such exhaustive silanisation on the physical characteristics of the oligomeric bonded phases produced are discussed. Data on the chromatographic properties of each oligomeric phase for aromatic hydrocarbons, alkyl benzoates and strongly polar solutes are reported and correlated with carbon load.

EXPERIMENTAL

Materials

The spherical silica gel [average particle diameter = $20 \mu\text{m}$, specific surface area (S_{BET}) = $250 \text{ m}^2 \text{ g}^{-1}$, specific pore volume (V_p) = 1.08 ml g^{-1}] used in this work was

a research sample from Professor K. K. Unger's laboratory (Johannes Gutenberg Universität, Mainz, F.R.G.).

Octylmethyldichlorosilane was prepared by a hydrosilation reaction¹ of distilled octene (Aldrich) with methyldichlorosilane (Fluka). The reaction was catalysed by chloroplatinic acid (Johnson Mathey Chemicals, London, U.K.). The chemical composition of the compound was confirmed by elemental analysis [Anal. calc. for C₉H₂₀SiCl₂ (227.25): C (47.56%), H (8.81%), Cl (31.26%); found: C (47.50%), H (8.78%), Cl (31.20%)].

HPLC-grade solvents were used for all the chromatographic measurements. Mobile phases were prepared on a volume basis and degassed before use. Solutes were analytical grade and were made up in the mobile phase.

Elemental analyses were performed on the phases at the Microanalysis Laboratory (University College, London, U.K.).

The S_{BET} [molecular cross-sectional area of nitrogen ($a_{\text{m}(\text{N}_2)}$) = 16.2 Å² molecule⁻¹] and $V_{\text{p}(\text{N}_2)}$ values of the untreated and treated silica supports were determined according to the BET nitrogen adsorption isotherm using a Micromeritics Model 2100E physical adsorption analyzer (Micromeritics, Norcross, GA, U.S.A.).

Column packing

The bonded phases were packed into 250 × 4.6 mm I.D. stainless-steel columns fitted with stainless-steel frits of 2 μm porosity (Thames Chromatography). The columns were slurry packed using a high-pressure Haskel pump, Model DSTV-122. The slurry mixture consisted of isopropyl alcohol–cyclohexanol–chloroform (2:1:1, v/v). Methanol was used as the displacement solvent and columns were packed at a pressure of about 8000 p.s.i.

Chromatography

The chromatographic equipment used consisted of a Shimadzu LC-5A pump and an SPD 2AM variable-wavelength UV detector operated at 254 nm. Solutes were injected into the column using a Rheodyne 7143 valve fitted with a 5-μl internal loop. The void volume, t_0 , was obtained by including potassium nitrate in the test mixtures and was used to calculate the capacity ratio, k' , defined as $k' = (t_{\text{R}} - t_0)/t_0$, where t_{R} is retention time of the test solute.

Preparation of bonded phases

The bonded phases were prepared using the fluidised bed technique in the apparatus previously described^{2,3}. About 50.0 g of silica gel was placed in the fluidising tower and hydrothermally treated at 200°C for 6 h using nitrogen as the fluidising gas. This was undertaken to remove any physically adsorbed water and to ensure a reproducible level of surface silanols. The treated silica was silanised under anhydrous conditions with octylmethyldichlorosilane at 200°C for 4 h using dry nitrogen as the fluidising gas. The bonded material was again hydrolysed with steam as in the hydrothermal treatment and the above silanisation reaction was repeated. This procedure was repeated nine times. Samples were taken at the end of each reaction step and packed for evaluation.

TABLE I
CHARACTERISTICS OF THE BONDED PHASES

Reaction step number	%Carbon (g/g)	Surface area S_{BET} ($m^2 g^{-1}$)	Pore volume V_p ($ml g^{-1}$)
0	0.00	250.00	1.00
1	7.58	153.04	0.82
2	9.69	144.99	0.71
3	11.14	132.69	0.60
4	12.18	126.59	0.63
5	12.69	118.64	0.59
6	14.43	115.97	0.59
7	14.90	107.11	0.54
8	15.80	106.50	0.49
9	16.79	105.21	0.48
10	17.45	105.14	0.45

RESULTS AND DISCUSSION

Characteristics of the bonded phases

The surface of the silica is only reacted once since subsequent silanisation occurred on the newly formed silanols produced by hydrolysis of the residual halogen atoms. Hence the stationary phases are characterised only by the percentage carbon load as shown in Table I. Included in Table I are values of the specific surface area and specific pore volume of the bonded phases.

Fig. 1 shows the effect of the exhaustive silanisation on carbon loading of the bonded phases. It can be seen that there is a rapid increase in the percentage carbon between step 1 and 3 after which further silanisation steps result in a linear increase in carbon load over the range of steps investigated. This observation suggests that the reaction according to Scheme 1 dominates at all stages of the process and more newly formed hydroxyls are available for bonding on hydrolysing the unreacted chlorine

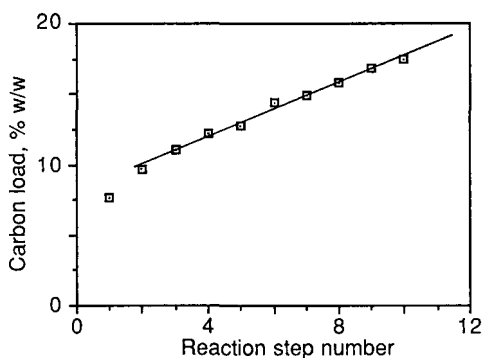


Fig. 1. Plot of percentage carbon load against reaction step number.

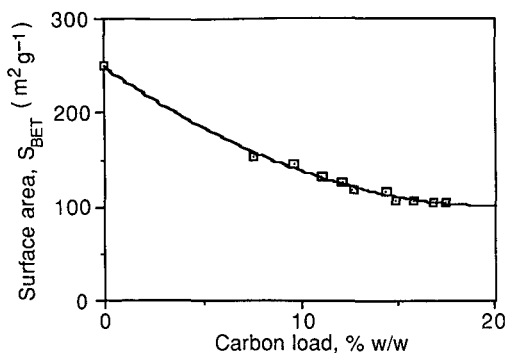


Fig. 2. Effect of carbon load on specific surface area of the silica support.

atoms. However the extent of further reaction may reach a limiting value due to steric hindrance and/or non-availability of sufficient hydroxyl groups for further bonding. A similar investigation⁴ of such a silanisation process with octadecyltrichlorosilane showed a minimal increase in carbon loading after the first three steps. While this might be true considering the molecular cross-sectional area of C₁₈ as compared to that of C₈, Verzele and Mussche⁵ have shown that their bonding procedure depends on the amount of water added to the reaction mixture and this directly affects the carbon load. However, their procedures were carried out in solvents; thus the procedure is different to the present one.

The effect of surface modification on surface area and pore volume of the phases produced is shown in Figs. 2 and 3 respectively. Generally, the surface area and pore volume decreases with increase in carbon load as measured by BET nitrogen adsorption isotherm up to step 7 after which a limiting value is reached for the surface area but pore volume continues to decrease in a linear manner. As shown in Table I both the surface area and the pore volume have decreased by about 60%. This is thought to be due to the increase in hydrocarbonaceous layer of the alkyl ligand on the porous silica matrix. The effect becomes minimal when further reactions with the silanols are sterically hindered indicating a dense surface coverage. As noted by Erdel

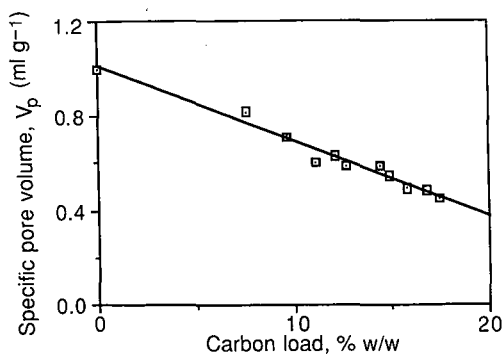


Fig. 3. Effect of carbon load on specific pore volume of the silica support.

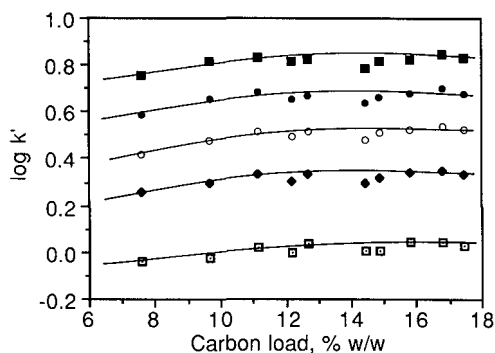


Fig. 4. Plot of $\log k'$ for aromatic hydrocarbons against carbon load. Symbol representation: (□) benzene, (◆) naphthalene, (○) biphenyl, (●) anthracene, (■) pyrene.

and Unger⁶ surface modification of porous silica leads to: (i) a specific increase in weight of the starting material, (ii) a decrease in the adsorption potential of the bonded phase since the pore structures are determined from adsorption and desorption measurements, and (iii) an increase in the thickness of the surface layer which in turn decreases the mean pore diameter of the support. The above effects becomes more significant with purely microporous materials and can lead to total blockage of the pores when exhaustively silanised thus resulting in effectively a non-porous packing.

Chromatographic properties

Retention times and capacity ratio. The retention properties of the stationary phases were determined at 20°C using methanol–water (70:30, v/v) as mobile phase. The dependence of the logarithm of capacity factor on carbon content of the bonded phases are shown in Figs. 4 and 5 for the test solutes. As shown in Figs. 4 and 5, the capacity factor increased slightly up to about 11% carbon after which it remains almost constant with further increase in carbon load. Statistical analysis of the results at carbon load greater than 11% gave no significant difference in $\ln k'$ with increasing

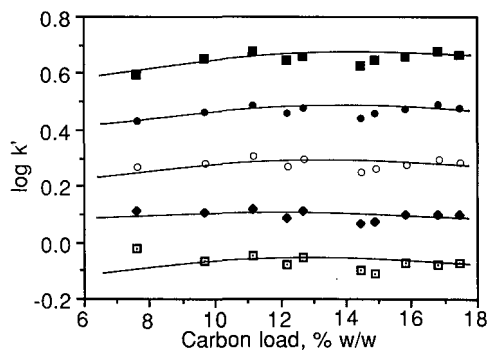


Fig. 5. Plot of $\log k'$ for *n*-alkyl benzoates against carbon load. Symbol representation: (□) methyl benzoate, (◆) ethyl benzoate, (○) propyl benzoate, (●) butyl benzoate, (■) pentyl benzoate.

carbon load. Evidence for the absence of significant differences in the means and variances of the results was obtained when the calculated t and F values are less than the true or statistics table values ($P = 0.05$). Thus while the carbon load increased with the reaction step, the retention properties of the solutes are independent of the carbon content of more than 11%. However there is a slight difference in the shape of the graph when compared to that obtained with increasing carbon content or alkyl chain length⁷⁻⁹ of the bonded ligand. This observation confirms the importance of bonded ligand structure and conformation on solute retention in reversed-phase chromatography.

While several mechanisms¹⁰⁻¹² have been proposed for solute retention in reversed-phase chromatography, the experimental results given in this paper indicate that the logarithm of the capacity factor depends on the molecular contact area between the test solutes and the hydrocarbonaceous layer of the stationary phase. Therefore, for an oligomeric phase solute molecules are unable to interact completely with the ligands and further increase in the extent of the bonded alkyl layer reduces the effective interactive surface between the solute molecules and the stationary phase.

Fig. 6 clearly illustrates the effect of non-polar interaction on retention times for two types of solute with increasing carbon content (columns 1, 3, 5 and 10).

It was observed that the retention of aromatic hydrocarbons slightly increased with increasing carbon content. A possible explanation for this is that the aromatic molecules are capable of penetrating into the hydrocarbon layer as compared to polar compounds where the retention generally decreases with carbon load simply because the molecules either interact with the surface layer or a small proportion of the ligands. Also the decrease in solute retention times can be attributed to the decrease in the specific pore volume of the silica matrix resulting in some solutes being partially excluded from the pores of the silica support.

Selectivity. Selectivity of two solutes, 1 and 2 is defined as

$$\alpha = \frac{k'_2}{k'_1} \quad (k'_2 > k'_1) \quad (1)$$

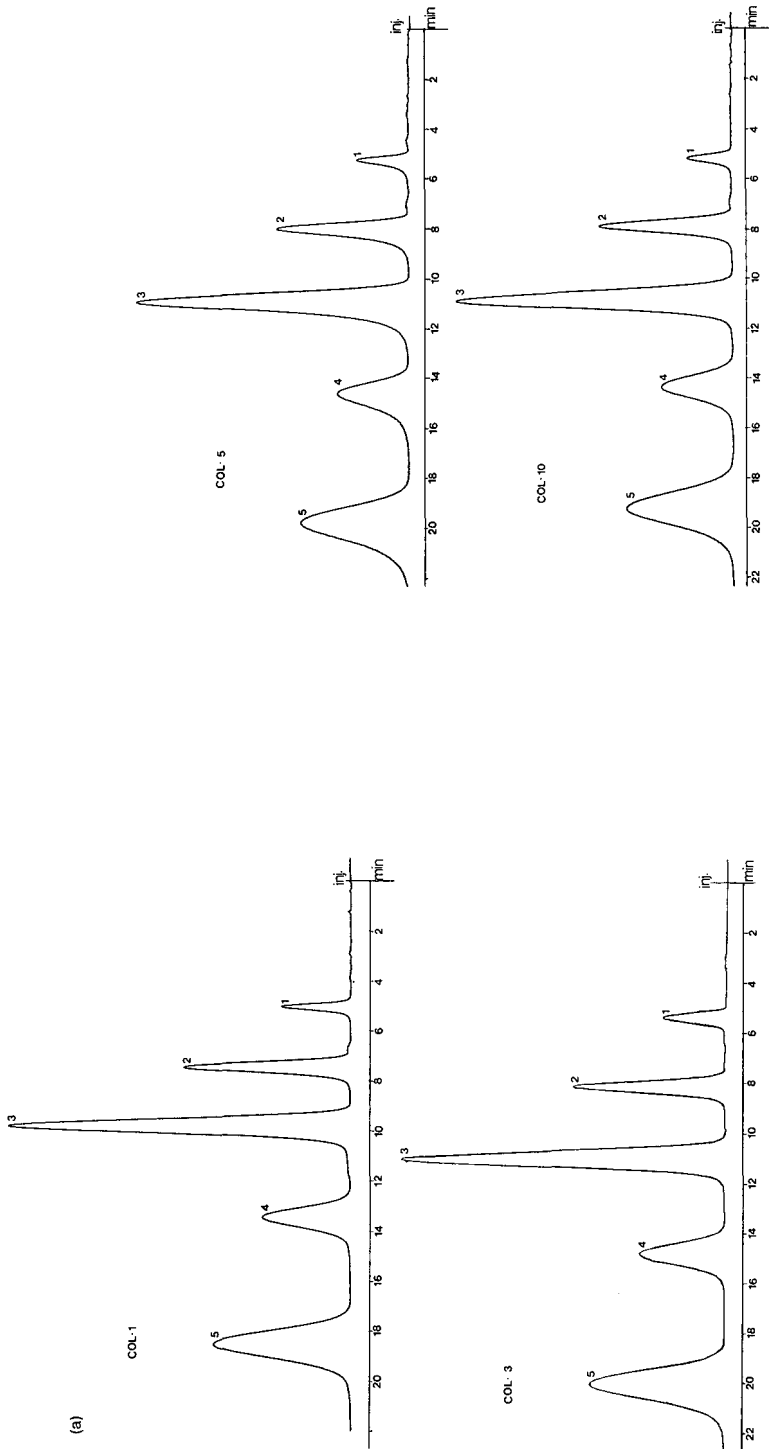
As shown in Figs. 7 and 8 the selectivity for various solute pairs generally increases up to about 10% carbon load after which it remains substantially constant with increasing carbon content. This stresses the importance of retention time being independent of carbon content at high carbon load

Resolution. Resolution, R_s , for a given pair of solutes is expressed as

$$R_s = \frac{t_{R_2} - t_{R_1}}{0.5(w_1 + w_2)} \quad (2)$$

where t_{R_i} and w_i are the retention time and baseline peak width for solute i . As shown in Fig. 6, the solutes are completely resolved ($R_s > 1$) except on columns 5 and 10 where acetone and 2-acetylpyridine peaks overlapped which will partly be due to slightly different column efficiencies.

Peak asymmetry. In order to qualitatively determine the presence of residual silanols on the bonded phases, peak asymmetry, A_s , was calculated for a variety of solutes. This parameter is defined as



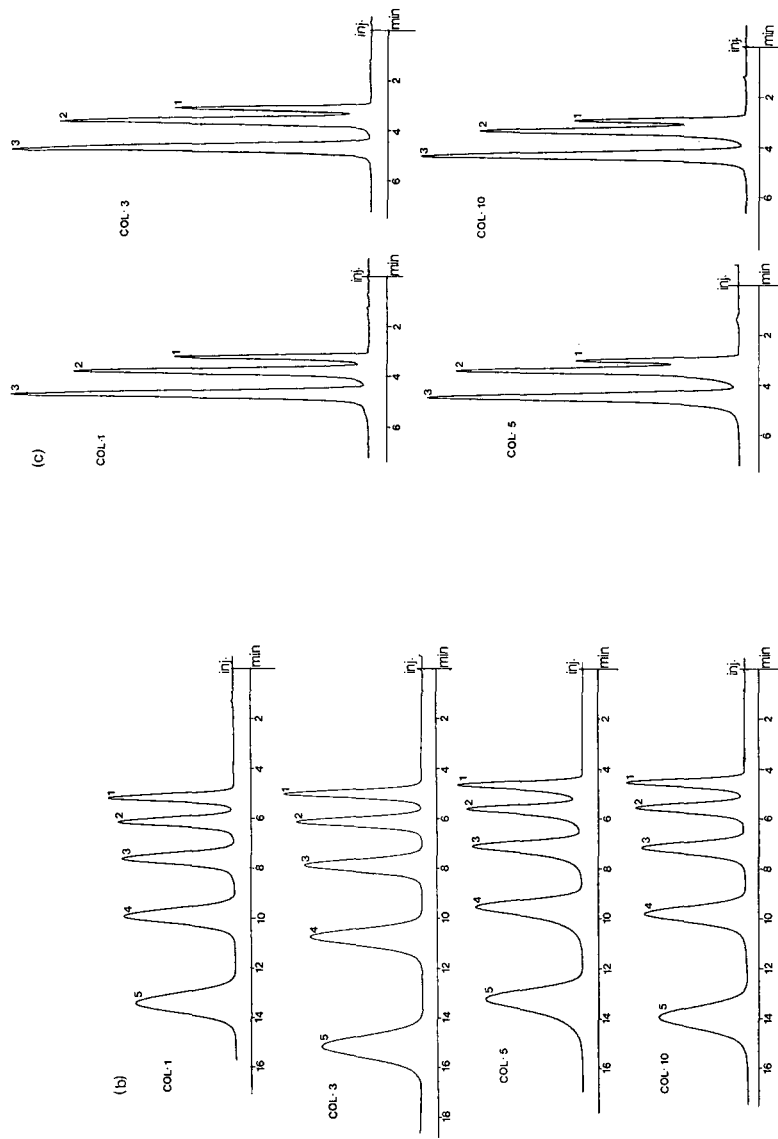


Fig. 6. Chromatograms of the test solutes. Column: 250 × 4.6 mm I.D. Mobile phase: methanol-water (70:30, v/v). Flow-rate: 1 ml/min. Temperature: 20°C. Detector: UV photometer, wavelength 254 nm. Solutes: (a) 1 = benzene; 2 = biphenyl; 3 = naphthalene; 4 = anthracene; 5 = pyrene. (b) 1 = Methyl benzoate; 2 = ethyl benzoate; 3 = propyl benzoate; 4 = butyl benzoate; 5 = pentyl benzoate. (c) 1 = Acetone; 2 = 2-acetyl pyridine; 3 = nitrobenzene.

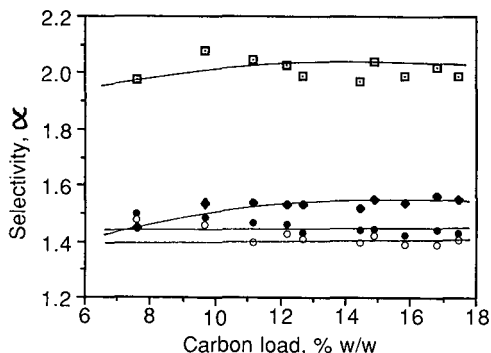


Fig. 7. Dependence of selectivity for aromatic hydrocarbons on carbon load. Symbol representation: (□) naphthalene-benzene, (◆) biphenyl-naphthalene, (●) anthracene-biphenyl, (○) pyrene-anthracene.

$$A_s = \frac{w_t}{w_l} \quad (3)$$

where w_t and w_l are the trailing and the leading half widths at 10% peak height respectively. An examination of Fig. 6 shows that the peaks both for polar and non-polar solutes were symmetrical and values of A_s as obtained from similar chromatograms under identical conditions are shown in Table II for columns 1, 3, 5, 7, 9 and 10. Surprisingly, A_s is about unity for all solutes indicating the absence of an appreciable number of residual silanols considering the fact that the phases were not endcapped. Alternatively, the acidic surface silanols, held to be the cause of peak tailing, are shielded by the oligomeric surface layer and hence are unable to interact. Amongst the six representative columns, column 3 produced the best symmetrical peaks with $A_s \approx 1.00$.

Retention behaviour of homologous series. Earlier work¹³⁻¹⁵ on the retention behaviour of homologous series in reversed-phase chromatography has shown that the

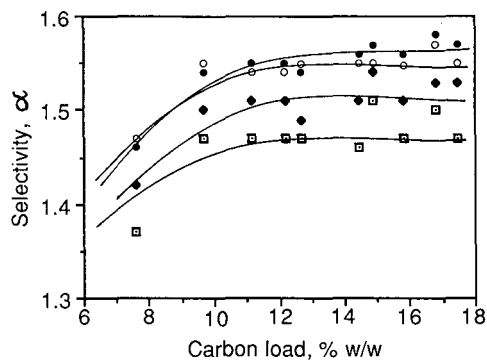


Fig. 8. Dependence of selectivity for *n*-alkyl benzoates on carbon load. Symbol representation: (□) ethyl-methyl benzoate, (◆) propyl-ethyl benzoate, (○) butyl-propyl benzoate, (●) pentyl-butyl benzoate.

TABLE II
PEAK ASYMMETRY

Step or column number	Coverage (weight%)	Peak asymmetry		
		Pyrene	Pentyl benzoate	Nitrobenzene
1	7.58	1.01	1.06	1.00
3	11.14	1.02	1.01	1.04
5	12.69	1.13	1.15	1.03
7	14.90	1.04	1.04	1.04
9	16.79	1.05	1.05	1.04
10	17.45	1.08	1.05	1.03

logarithm of capacity factor depends linearly on the carbon number or number of methylene groups in a homologous series of bonded ligands. A similar trend was observed in this work as shown in Figs. 9 and 10 for aromatic hydrocarbons and *n*-alkyl benzoates, respectively. Each plot shows an increase in retention time with increasing molecular surface area of the eluite. This set of lines can be expressed as

$$\log k' = an_c + b \quad (4)$$

where n_c is the number of carbon atoms or CH₂ groups and a and b are constants determined by the mobile phase, stationary phase and the nature of the eluite. The slopes and intercepts for each series obtained on each column are given in Table III. From the plots and the correlation coefficient values which are near unity in all cases it can be concluded that the experimental data gave excellent fit. The slopes are represented by $a = 0.18 \pm 0.0095$ and 0.081 ± 0.018 and the intercepts by $b = -0.077 \pm 0.022$ and -0.48 ± 0.034 for alkyl benzoates and aromatic hydrocarbons, respectively. Substituting the mean values of a and b into eqn. 4 for each series gives two linear equations, that is, for alkyl benzoates, eqn. 4 becomes

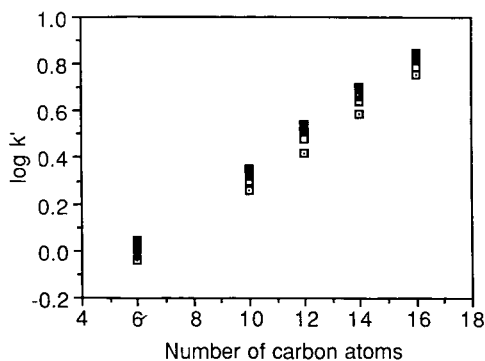


Fig. 9. Plot of $\log k'$ for aromatic hydrocarbons versus carbon number. Symbol representation: (\square) column 1, (\blacklozenge) column 2, (\bullet) column 3, (\circ) column 4, (\blacksquare) column 5, (\square) column 6, (\blacktriangle) column 7, (\blacktriangledown) column 8, (\triangle) column 9, (∇) column 10.

TABLE III

PARAMETERS OF $\log k' = an_c + b$ RELATIONSHIPS FOR HOMOLOGOUS *n*-ALKYL BENZOATES AND AROMATIC HYDROCARBONSCorrelation coefficient, $r \approx 1$ for all the plots.

Column number	<i>n</i> -Alkyl benzoates		Aromatic hydrocarbons	
	Slope <i>a</i>	Intercept <i>b</i>	Slope <i>a</i>	Intercept <i>b</i>
1	0.1559	-0.0340	0.0796	-0.5254
2	0.1803	-0.0738	0.0846	-0.5357
3	0.1835	-0.0614	0.0821	-0.4739
4	0.1827	-0.0900	0.0822	-0.4987
5	0.1794	-0.0626	0.0795	-0.4436
6	0.1822	-0.0974	0.0789	-0.4745
7	0.1891	-0.1074	0.0819	-0.4867
8	0.1832	-0.0810	0.0793	-0.4365
9	0.1900	-0.0842	0.0814	-0.4454
10	0.1849	-0.0810	0.0807	-0.4565
Mean	0.1811	-0.0773	0.0810	-0.4777
S.D.	0.0095	-0.0218	0.0177	-0.0342

$$\log k' = 0.18n_c - 0.077 \quad (5a)$$

and for aromatic hydrocarbons

$$\log k' = 0.081n_c - 0.48 \quad (5b)$$

Therefore eqns. 5a and 5b can be used to estimate the retention for any member of the series under the same chromatographic conditions. Furthermore, an examination of Table III shows that *b* values for benzoates are generally less than that of aromatic hydrocarbons which may be due to the increase in polarity of the test solutes.

Column efficiency. As shown in Table IV, column performance in terms of reduced plate height, *h* ($h = H/d_p$) and reduced velocity, *v* ($v = ud_p/D_m$) where *H* is

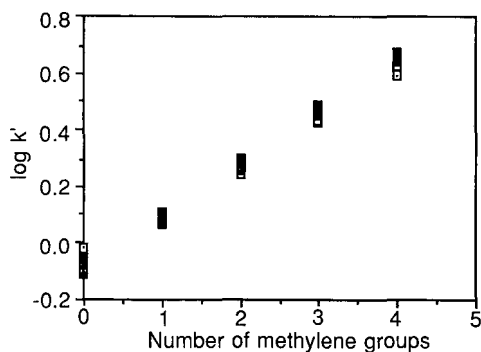


Fig. 10. Plot of $\log k'$ for *n*-alkyl benzoates versus number of methylene groups. Symbol representation as for Fig. 9.

TABLE IV
EFFECT OF CARBON LOAD ON REDUCED PARAMETERS FOR ANTHRACENE ($k' = 4$)

Column number	Carbon load (% w/w)	h	v
1	7.58	9.19	5.43
3	11.14	8.34	5.39
5	12.59	10.91	5.67
7	14.90	10.57	5.49
9	16.79	9.84	5.41
10	17.45	10.15	5.64

plate height and D_m the diffusion coefficient of the solute, were obtained for columns 1, 3, 5, 7, 9 and 10 using the elution peak of anthracene ($k' = 4$) and mobile phase flow-rate of 1 ml min⁻¹. While there is no clear correlation between carbon load and reduced plate height, h , column 3 has the minimum h value and hence appears to be the best packing material. Little appears to be gained on increasing the number of the reactions steps above $n = 3$ on the performance of the stationary phases produced.

CONCLUSION

This work has demonstrated that both the pore volume and surface area of the silica support decreases with increasing carbon load for an oligomeric series of reversed phases. Furthermore while the surface area approached a limiting value with increasing carbon load, the pore volume continued to decrease in a linear manner over the range of bonding reactions investigated.

The results have shown that after the third reaction all the columns exhibit very similar chromatographic properties, indicating that the type of interaction between the solutes and the bonded phases are the same for all the columns. Linear correlations were obtained between $\log k'$ and carbon number for members of a homologous series and the slope of the plots increases up to 11% carbon load after which it remained almost constant. Amongst the two classes of test solutes, the slope of $\log k'$ versus carbon number for alkyl benzoates is greater than that of aromatic hydrocarbons indicating that the benzoates are more retained than aromatic hydrocarbons.

While selectivity for all the columns appeared to be affected by the carbon load up to 10%, all the columns produced symmetrical peaks. Hence with fluidised bed method good oligomeric packings can be produced.

Based on these results, further investigation on stability and the influence of temperature and mobile phase composition on the chromatographic properties of the phases are in progress in the authors laboratory and the results will be the subject of a subsequent paper.

ACKNOWLEDGEMENTS

The authors would like to thank Prof. K. K. Unger and his research students for the supply of the silica and their assistance during the study visit of one of us (S.O.A.) to the F.R.G. We would also like to thank Prof. R. P. W. Scott for his helpful comments.

REFERENCES

- 1 J. L. Speier, *Adv. Organomet. Chem.*, 17 (1979) 407.
- 2 T. M. Khong and C. F. Simpson, *Chromatographia*, 24 (1987) 385.
- 3 T. M. Khong and C. F. Simpson, *U.K. Pat.*, 86 18322 (1986).
- 4 L. C. Sander and S. A. Wise, *Anal. Chem.*, 56 (1984) 504.
- 5 M. Verzele and P. Mussche, *J. Chromatogr.*, 254 (1983) 117.
- 6 G. Erdel and K. K. Unger, in S. Modry and M. Srata (Editors), *IUPAC Symposium on Pore Structure*, Vol. III, Academia, Prague, 1973, p. B-127.
- 7 H. Hemetsberger, W. Maasfeld and H. Richen, *Chromatographia*, 9 (1976) 303.
- 8 M. C. Hennion, C. Picard and M. Caude, *J. Chromatogr.*, 166 (1978) 21.
- 9 G. E. Berendsen and L. de Galan, *J. Chromatogr.*, 196 (1980) 21.
- 10 J. H. Knox and A. Pryde, *J. Chromatogr.*, 112 (1975) 171.
- 11 R. P. W. Scott and K. Kucera, *J. Chromatogr.*, 142 (1977) 213.
- 12 Cs. Horváth, W. Melander and I. Molnár, *J. Chromatogr.*, 125 (1976) 129.
- 13 R. B. Sleight, *J. Chromatogr.*, 83 (1973) 31.
- 14 N. Tanaka and R. Thornton, *J. Am. Chem. Soc.*, 99 (1977) 7300.
- 15 H. Colin and G. Guiochon, *J. Chromatogr.*, 141 (1977) 289.

CHROM. 21 302

MASS DETECTION LIMITS ACHIEVED WITH A COMMERCIALY AVAILABLE FLUORIMETER IN MICRO HIGH-PERFORMANCE LIQUID CHROMATOGRAPHY

TOYOHIDE TAKEUCHI*, TAKAAKI ASANO and DAIDO ISHII

Department of Applied Chemistry, Faculty of Engineering, Nagoya University, Chikusa-ku, Nagoya 464 (Japan)

SUMMARY

The effects of the cell structure on the mass detection limits in fluorimetric detection in micro high-performance liquid chromatography were examined. Scatter of the light by reflection or refraction from the cylindrical quartz cell wall increased the noise level. This type of scattered light could effectively be prevented from entering the photomultiplier by either tilting the flow cell or using appropriate cut-off filters. In fluorimetric detection in the presence of a packing material, scattered light from the surface of the packing material could be shut out by the latter method.

INTRODUCTION

Mass detection limits as low as the sub-femtogram level have been demonstrated by laser-induced fluorimetric detection in high-performance liquid chromatography (HPLC)¹⁻³. This is due to the high intensity of the laser, its better focusing properties and miniaturization of the column dimensions. In order to achieve such low mass detection limits, various types of flow cell structures have been proposed¹⁻³, most effort having been devoted to the elimination of the scattering of light from the cell wall. For example, the photomultiplier was tilted 30° from the plane of scattered laser light in order to reduce the collection of excitation light¹. Another approach to eliminating scattering involved a free-falling jet⁴. In spite of the excellent detectability of laser-induced fluorimetric detection, it is not popular in routine analysis because of its inconvenience in operation and the limited choice of excitation wavelengths in the ultraviolet region. There are many commercially available fluorimeters for HPLC that already achieve respectable detectability levels.

This paper reports the mass detection limits of a commercially available fluorimeter with a laboratory-made flow cell for micro HPLC.

EXPERIMENTAL

The liquid chromatograph was assembled from a Microfeeder pump (Azumadenki Kogyo, Tokyo, Japan) equipped with an MS-GAN 050 gas-tight syringe (0.5

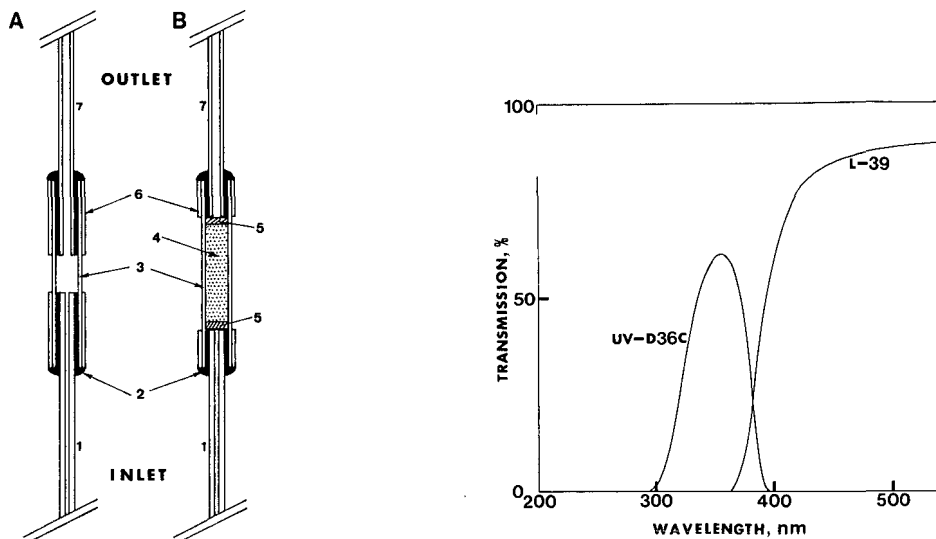


Fig. 1. Schematic diagram of the flow cell. (A) Empty cell; (B) packed cell. 1 = Stainless-steel tubing (0.05 mm I.D. \times 0.30 mm O.D.); 2 = adhesive; 3 = fused-silica tubing (0.32 mm I.D.); 4 = packing material; 5 = quartz-wool; 6 = polyimide resin; 7 = stainless-steel tubing (0.13 mm I.D. \times 0.31 mm O.D.).

Fig. 2. Optical data for the cut-off filters employed.

ml) (Ito, Fuji, Japan), an ML-422 micro valve injector with an injection volume of 20 μ l (JASCO, Tokyo, Japan), a laboratory-made micropacked separation column, an 820-FP spectrofluorimeter with a xenon lamp (JASCO) and a chart recorder. The separation column was composed of fused-silica tubing of 0.35 mm I.D. (Gasukuro Kogyo, Tokyo, Japan) packed with Develosil ODS-3K (3- μ m particle diameter) (Nomura Chemical, Seto, Japan).

Flow cells for the fluorimeter were prepared in the laboratory by using fused-silica tubing of 0.32 mm I.D. (SGE, Ringwood, Victoria, Australia) and stainless-steel tubing of 0.13 mm I.D. \times 0.31 mm O.D. (Hakkoshoji, Tokyo, Japan) and 0.05 mm I.D. \times 0.30 mm O.D. (Nomura Chemical). These capillary tubes were glued with and epoxy-resin adhesive. The structures of the flow cells are illustrated in Fig. 1. For the packed flow cell, the same stationary phase as used for the separation column was packed in the fused-silica tubing, and the packing was prevented from leakage by quartz-wool (1–6 μ m) (Wako, Osaka, Japan). The time constant of the detector was kept at 1.5 s in this investigation. The outlet of the flow cell was attached to an MS-GAN 100 gas-tight syringe (1 ml) (Ito) to apply a back-pressure to the flow cell so that the formation of air bubbles in it could be repressed.

UV-D36C and L-39 (JASCO) cut-off filters were employed to reduce the scattering of light or to prevent the scattered light from reaching the photomultiplier of the detector. The former cut-off filter was used for the excitation side and the latter for the emission side. The optical data of these filters are shown in Fig. 2. The transmission is plotted against the wavelength.

All the reagents employed, except for HPLC-grade distilled water (Wako), were of analytical-reagent grade from Wako or Tokyo Chemical Industry (Tokyo, Japan) and were used as received.

RESULTS AND DISCUSSION

Cylindrical quartz tubing is commonly employed as the flow cell in micro HPLC because it is convenient for minimizing the dead volume. However, such cylindrical tubing strongly scatters the incident light by reflection or refraction, which leads to an increase in the noise level. Collection of such scattered light is simply reduced by tilting the photomultiplier from the plane of the scattered light¹. In laser-induced fluorimetric detection, various types of flow cell such as a sheath flow cell, an optical fibre capillary tube cell and a free-falling jet have been evaluated for eliminating the scatter of light². When a fluorimeter with a common lamp as a light source was employed as the detector, problems caused by the scattering of light were still encountered. The detector employed in this work allowed the measurement of emission spectra by the stopped flow method. In order to compare the mass detection limits achieved by the fluorimeter with those of a medium-pressure mercury lamp⁵, the excitation wavelength of the present fluorimeter was kept at 365 nm, that is, the strongest line of the former detector. The flow cell was fixed on the cell block either in the normal position or a tilted position, as illustrated in Fig. 3.

Fig. 4A shows a spectrum of the scattered light emitted from the empty fused-silica capillary cell fixed in the normal position. Three peaks are observed, at 425, 505 and 665 nm. The wavelengths of the emission spectra were independent of the flow cell material, which indicates that they originated from the incident light. The pattern of the spectrum varied with the excitation wavelength.

Fig. 5 shows noise levels observed at various wavelengths under the same operating conditions as in Fig. 4A. It is found that the stronger the scattered light, the higher is the noise level.

Collection of this scattered light is simply reduced by tilting the flow cell by *ca.* 30°, as illustrated in Fig. 3B. Fig. 4B shows the emission spectrum for this tilted empty flow cell. The intensity of the scattered light is considerably reduced in Fig. 4B compared with that in Fig. 4A. In addition, the noise level of the baseline did not vary with the emission wavelength and it was extremely reduced, which is different from the results in Fig. 5. These results indicate that the noise observed in Fig. 5 is mostly caused by the scattered light.

The scattered light from the cell wall can also be eliminated by using appropriate cut-off filters. UV-D36C and L-39 cut-off filters were selected, considering their optical properties and the wavelengths of both the excitation and scattered light. Fig. 4C shows the intensity of the scattered light for the flow cell with these cut-off filters

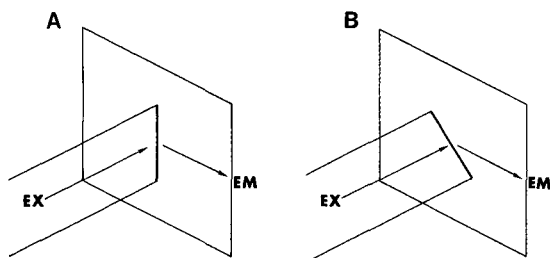


Fig. 3. Schematic diagram of the flow cell positions. (A) Normal position; (B) tilted position.

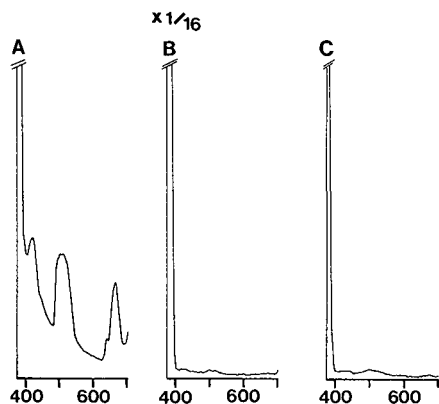


Fig. 4. Emission spectra of scattered light for the empty flow cells. (A) Normal position without cut-off filters; (B) tilted position without cut-off filters; (C) normal position with cut-off filters.

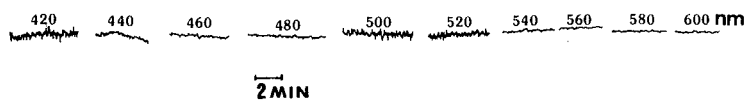


Fig. 5. Noise levels at various emission wavelengths for the empty flow cell set in the normal position without cut-off filters. Excitation wavelength, 365 nm.

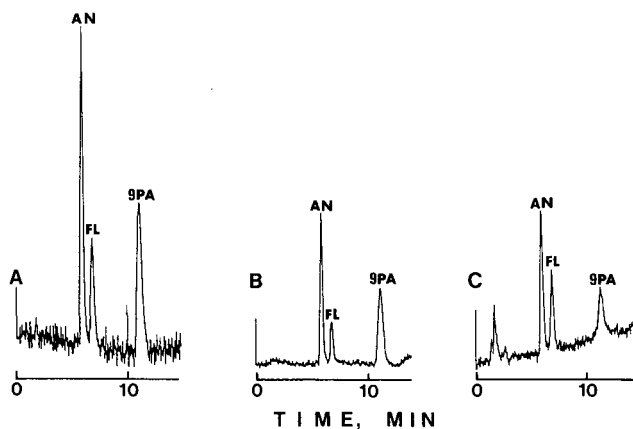


Fig. 6. Chromatograms of aromatic hydrocarbons obtained with the empty flow cells. Column, Develosil ODS-3K (100 × 0.35 mm I.D.); mobile phase, acetonitrile-water (80:20); flow-rate, 4.2 μ l/min; excitation wavelength, 365 nm; emission wavelength, 430 nm. Flow cells: (A) normal position without cut-off filters; (B) tilted position without cut-off filters; (C) normal position with cut-off filters. Samples: AN = anthracene; FL = fluoranthene; 9PA = 9-phenylanthracene. Sample amounts: (A) AN = 110 pg, FL = 130 pg, 9PA = 22 pg; (B) and (C) AN = 28 pg, FL = 32 pg, 9PA = 5.5 pg.

set in the normal position. When the excitation wavelength is changed, the cut-off filters must be re-optimized. This is not a convenient situation.

Chromatograms obtained by using the above three types of flow cells are compared in Fig. 6. The amounts of sample injected in Fig. 6A are four times larger than those in Fig. 6B and C. The mass detection limits at a signal-to-noise ratio (S/N) of 2 are given in Table I. With the empty flow cell, the mass detection limits achieved by the tilted flow cell were improved by a factor of *ca.* 10 for the analytes examined, whereas those achieved with the cut-off filters were improved by a factor of *ca.* 5 for anthracene and 9-phenylanthracene and *ca.* 10 for fluoranthene. It is uncertain why the improvement factors differ.

On-column detection, which relates to the detection of analytes on a separation column, improves the mass detection limits owing to the focussing effect of the stationary phase⁵⁻⁸. This advantage is also realized by the use of a packed flow cell⁹. When the flow cell packed with the same stationary phase as for the separation column is used, the effect of the stationary phase is essentially same as in on-column detection.

Fig. 7A shows the spectrum of the scattered light for the tilted packed flow cell. Although the flow cell tubing was tilted, the scattered light still reached the photomultiplier and the same profile of the emission spectrum was observed as in Fig. 4A. This is because the scattered light from the surface of the packing material was propagated in all directions. Collection of this scattered light could also be reduced by using the same cut-off filters as in Fig. 4C. The spectrum of the scattered light for the tilted packed flow cell with the cut-off filters is shown in Fig. 7B. It is observed that the cut-off filters effectively reduced the collection of the scattered light.

The chromatogram obtained with the packed flow cell with the cut-off filters is shown in Fig. 8. A difference in the profile of the chromatograms is observed between the empty and the packed flow cells, which is due to the focussing effect of the stationary phase for the latter flow cell. Detection in the presence of the stationary phase has the potential to improve the mass detection limits of analytes.

Table I also gives the mass detection limits for the tilted packed flow cell. The use of the cut-off filters improved the mass detection limits for the tilted packed flow cell by a factor of *ca.* 5 for anthracene and 9-phenylanthracene and 8 for fluoran-

TABLE I

MASS DETECTION LIMITS AT S/N=2

Column, Develosil ODS-3K, 100 × 0.35 mm I.D.; mobile phase, acetonitrile-water (80:20); flow-rate, 4.2 μl/min; excitation wavelength, 365 nm; emission wavelength, 430 nm.

Flow cell			Mass detection limit (pg)		
Stationary phase	Position	Filters ^a	Anthracene	Fluoranthene	9-Phenylanthracene
Empty	Normal	-	13	45	5.3
Empty	Tilted	-	1.3	4.5	0.48
Empty	Normal	+	2.1	4.1	1.0
Packed	Tilted	-	6.8	20	1.4
Packed	Tilted	+	1.5	2.4	0.25

^a -, detection without filters; +, detection with filters.

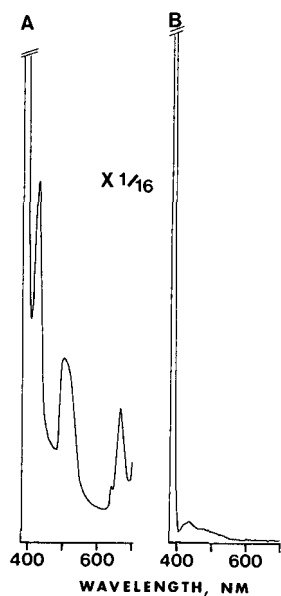


Fig. 7. Emission spectra of scattered light for the packed flow cells. (A) Tilted position without cut-off filters; (B) tilted position with cut-off filters.

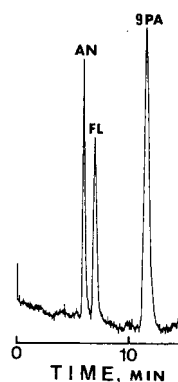


Fig. 8. Chromatograms of aromatic hydrocarbons obtained with the tilted packed flow cell with the cut-off filters. Sample amounts: AN=28 pg, FL=32 pg, 9PA=5.5 pg. Other conditions as in Fig. 6.

there. The lowest mass detection limits were achieved with the tilted packed flow cell with the cut-off filters. In addition, the mass detection limits achieved with a medium-pressure mercury lamp⁵ were comparable to those achieved with the tilted packed flow cell with the cut-off filters.

REFERENCES

- 1 E. J. Guthrie, J. W. Jorgenson and P. W. Dluzneski, *J. Chromatogr. Sci.*, 22 (1984) 171.
- 2 S. Folestad, B. Galle and B. Josefsson, *J. Chromatogr. Sci.* 23 (1985) 273.
- 3 H. P. M. van Vliet and H. Poppe, *J. Chromatogr.*, 346 (1985) 149.
- 4 S. Folestad, L. Johnson, B. Josefsson and B. Galle, *Anal. Chem.*, 54 (1982) 925.
- 5 T. Takeuchi and D. Ishii, *J. Chromatogr.*, 435 (1988) 319.
- 6 E. J. Guthrie and J. W. Jorgenson, *Anal. Chem.*, 56 (1984) 483.
- 7 T. Takeuchi and E. S. Yeung, *J. Chromatogr.*, 389 (1987) 3.
- 8 M. Verzele and C. Dewaele, *J. High Resolut. Chromatogr. Chromatogr. Commun.*, 10 (1987) 280.
- 9 T. Takeuchi and D. Ishii, *Chromatographia*, 25 (1988) 697.

CHROM. 21 279

SIMULTANEOUS PHOTOMETRIC AND CONDUCTIVITY DETECTION FOR MICROCOLUMN LIQUID CHROMATOGRAPHY

M. JANEČEK and K. ŠLAIS

Institute of Analytical Chemistry, Czechoslovak Academy of Sciences, Leninova 82, 611 42 Brno (Czechoslovakia)

SUMMARY

A miniature detector for microcolumn liquid chromatography is described that provides simultaneous conductivity and UV photometric signals. The total volume of the detection space is less than 100 nl and the optical path length is 1 mm. Light is guided by optical fibres. The function of simultaneous detection was verified in the ion chromatography of inorganic and organic anions.

INTRODUCTION

Two recent trends can be noticed in the development of detection techniques for liquid chromatography (LC): miniaturization of detection cells compatible with microcolumns and efforts to increase the versatility of detection. It would be useful to solve both problems simultaneously. A simple and effective solution consists in detectors that provide more independent signals from one detection cell. Compared with the connection of several detectors in series, the advantages of the above-mentioned approach are the smaller contribution to extra-column zone spreading and the fact that there is no time shift of the signals. Simultaneous detectors have been described in which the effluent is monitored on the basis of different detection modes such as conductivity and permittivity detectors¹, UV photometric, fluorimetric and conductivity detectors² and amperometric and UV photometric detectors³. These detectors, however, are not compatible with microcolumn LC with respect to the volume of the measuring cells. An electrochemical detector⁴ has been described recently with a measuring cell of volume 20 nl, providing at the same time independent conductivity and amperometric signals separated electronically.

For UV photometric detection, which is the most widely used detection technique in LC, a miniature flow cell with optical fibres⁵ has been developed and tested successfully. Its improved version⁶ was used as a basis for the detector described below.

This paper presents a description of the design and verification of the properties of a combined detector with the measuring cell with a volume of less than 100 nl providing the UV photometric and conductivity signals. As the combination of these two detection modes is suitable especially for monitoring ionized substances, the detector was used in ion-pair chromatography for simultaneous conductivity and indirect photometric detection.

Conductivity detection is a frequently used technique in ion chromatography⁷⁻¹⁰. This method is universal for monitoring the ions, but solutes having a similar conductivity to the ion of the elution agent are detected with lower sensitivity.

Photometry has found wide application in ion chromatography in connection with indirect photometric detection¹¹. In contrast to direct photometric detection¹²⁻¹⁴ when the ions of the solutes absorb radiation more than the eluent, the indirect method needs an elution agent that absorbs at a suitable wavelength (usually 254 nm). In this region the absorption of inorganic ions is negligible and the detector provides negative peaks. The sensitivity of this method depends on several factors. The molar absorptivity of the eluent and its concentration should be selected in such a way that the absorbance is in the range 0.2-0.8¹¹. If the background absorbance is not in this range, the signal-to-noise ratio deteriorates. From the practical point of view, however, the apparatus used also seems to play an important role because it has been found experimentally that a significant increase in noise arises even if the values of the background absorbance are, e.g., 0.5¹⁵ or 1.0¹⁶.

EXPERIMENTAL

Measuring cell design

The design of the combined microcell is based on the design of the UV photometric cell⁶. It is made of stainless steel (Fig. 1a). Optical fibres (4), the inlet capillary from the column (1) and the outlet metal capillary (5) serving as an electrode for conductivity detection are connected to the cell by plastic screws (3). The metal cell

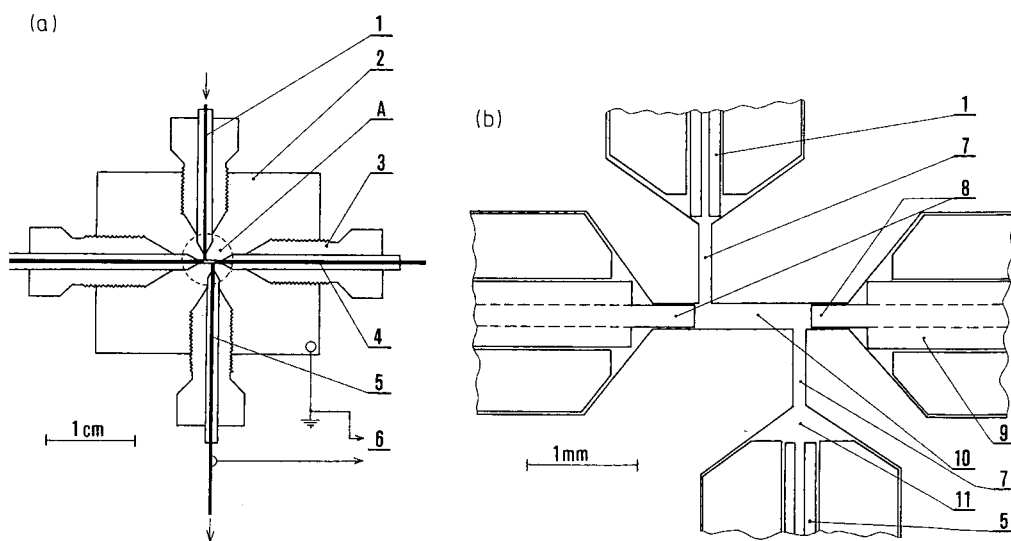


Fig. 1. Measuring flow-through microcell. (a) Schematic representation: 1 = fused-silica inlet capillary (0.1 mm I.D.); 2 = detector body; 3 = plastic sealing screw; 4 = optical fibre; 5 = metal outlet capillary; 6 = contacts of conductivity detection. (b) Detail A: 7 = outlet opening (0.12 mm I.D.); 8 = quartz core of the optical fibre; 9 = cladding of the optical fibre; 10 = detection space of the optical cell (0.25 mm I.D., length 1 mm); 11 = detection space of the conductivity cell.

body (2) is used as the other conductivity electrode. Fig. 1b shows that there are two detection spaces in the cell: one for photometric detection (10) of volume *ca.* 50 nl and optical path length 1 mm and the other for conductivity detection (11) of volume *ca.* 30 nl. The cell constant (K) was measured with a calibration solution and the value $K = 40 \text{ cm}^{-1}$ was verified by calculation. It is evident from Fig. 1b that the total space can be considered to be less than $0.1 \mu\text{l}$, including connections (7). However, the difference in volume between the centres of the two detection spaces is decisive for the volume and time shift of both of the signals obtained. Fig. 1b shows that this volume difference is about $0.05 \mu\text{l}$.

The UV light from a mercury discharge lamp is guided to the optical part of the detector by the optical fibre and then the other optical fibre guides the radiation to a photomultiplier. The advantages of using optical fibres in miniaturized detection systems have been described earlier^{5,6,17,18}. The operating alternating voltage on the electrodes of the conductivity detector was 0.6 V.

Chromatography

The described cell was tested in a chromatograph assembled from modular units. The mobile phase was supplied by an SP 8700 pump (Spectra-Physics, Santa Clara, CA, U.S.A.). The sample of volume $1 \mu\text{l}$ was injected by a laboratory-made four-port injection valve. The glass cartridge microcolumn (Tessek, Prague, Czechoslovakia) of dimensions $30 \times 0.7 \text{ mm}$ I.D. was packed with the sorbent SGX C₁₈ Separon, $5 \mu\text{m}$ (Lachema, Brno, Czechoslovakia). The cell was connected directly to the column outlet by a fused-silica capillary of 0.1 mm I.D. The optical part of the detection cell was connected by optical fibres with a FS 950 detector (Kratos, Ramsey, NJ, U.S.A.) modified to a single-beam photometer at the wavelength 254 nm. The electric outlet of the conductivity cell was connected by a coaxial cable with the electronic part of the electrochemical detector⁴. Both the signals were monitored with a TZ 4200 double-pen recorder (Laboratory Instruments, Prague, Czechoslovakia).

The chromatographic separation of anions was carried out on the sorbent dynamically coated with quaternary ammonium salt¹⁹. The tetrabutylammonium ion (TBA⁺)⁸ was used as the ion-pair agent. It was present in the mobile phase at a concentration of 0.1 mmol l^{-1} . The anions can be eluted from the column with organic acids²⁰, *e.g.*, phthalic acid, salicylic acid²¹, nitrophthalic acid²² or nicotinic acid²⁰; we used 3 mmol l^{-1} nicotinic acid ($\text{p}K_{\text{a}} = 4.8$). The mobile phase conductivity was $400 \mu\Omega^{-1} \text{ cm}^{-1}$ at pH 5.2, adjusted by with potassium hydroxide.

RESULTS AND DISCUSSION

The described combined microcell was used for the indirect UV photometric detection of anions in microcolumn ion chromatography. Its volume ($<0.1 \mu\text{l}$) is approximately 100 times smaller than that of the photometric cells (*ca.* $10 \mu\text{l}$) used in commercial LC, although the optical path length (1 mm) was only ten times shorter (10 mm for commercial cells). To maintain the sensitivity of indirect photometric detection, *i.e.*, the value of the background absorbance in the range 0.2–0.8, it is necessary to select a suitable elution agent with a higher molar absorptivity (ϵ). Therefore, nicotinic acid was selected, having $\log \epsilon = 3.4$ at 262 nm ²³. With a concentration of 3 mmol l^{-1} of nicotinic acid in the mobile phase the value of

background absorbance is 0.82 AU. From the chromatographic point of view nicotinic acid is a substance with a low elution strength, and therefore a short (30 mm) microcolumn can be used.

Fig. 2 shows calibration graphs for the photometric and conductivity channels of the detector. The calibration was carried out with Cl^- , NO_2^- and NO_3^- ions. The peak height (h) represents the magnitude of the detector response corresponding to the concentration of the substance at the peak maximum. Individual points represent the averages of 2–3 values and the regression line results from points corresponding to the NO_3^- ion. The values of twice the peak-to-peak noise ($2n$) are shown and are as follows, with the resulting minimum detectable concentrations (c_{\min}): for the optical detector, $2n = 0.002$ AU and $c_{\min} = 0.02$ mmol l $^{-1}$, corresponding to the minimum value of the fluctuation of the nicotinic acid concentration in the mobile phase; for the conductivity detector, $2n = 0.16$ $\mu\Omega^{-1}$ cm $^{-1}$ and $c_{\min} = 0.004$ mmol l $^{-1}$ for the Cl^- ion.

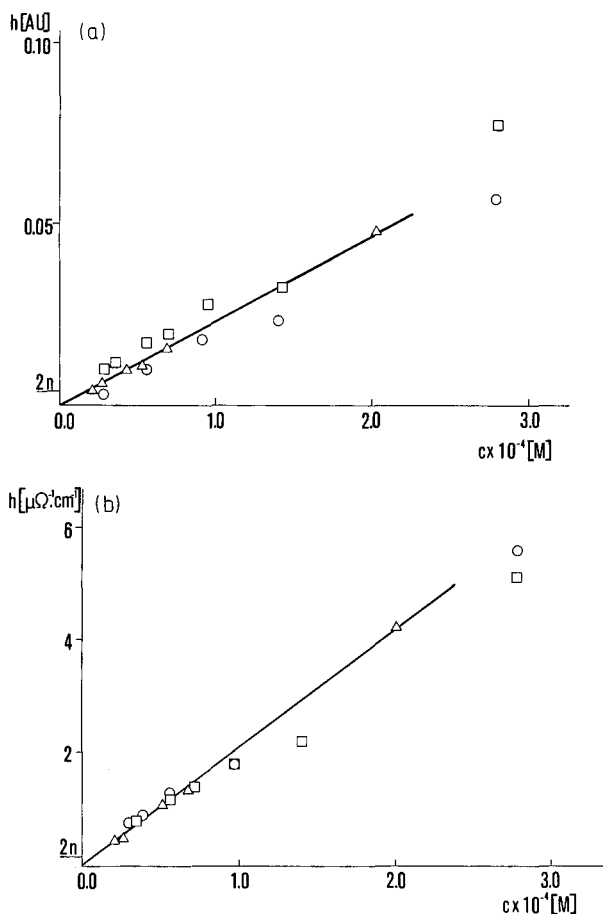


Fig. 2. Calibration graphs for (a) optical and (b) conductivity detectors. Injection volume, 1 μ l. Solutes: \square , Cl^- ; \circ , NO_2^- ; \triangle , NO_3^- . Column, CGC (30×0.7 mm I.D.), packed with SGX C_{18} Separon, 5 μ m. Mobile phase: 3 mmol l $^{-1}$ nicotinic acid–0.1 mmol l $^{-1}$ TBA $^+$; pH = 5.2 adjusted with KOH; conductivity, 400 $\mu\Omega^{-1}$ cm $^{-1}$. h = Peak height; n = noise; regression line resulting from points corresponding to NO_3^- ion.

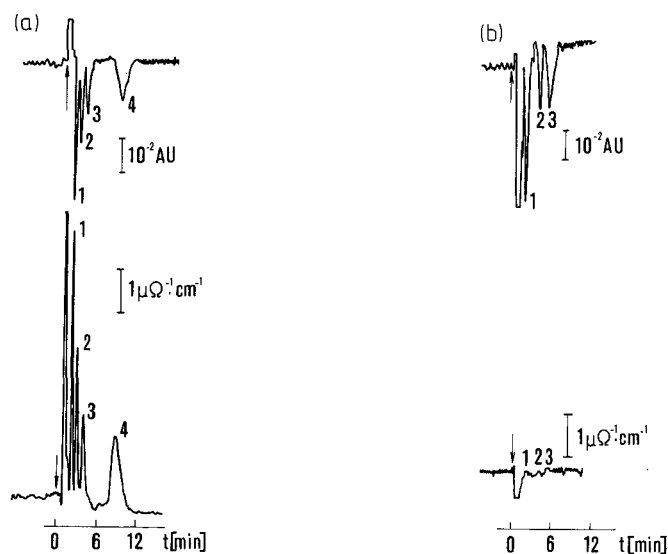


Fig. 3. Simultaneous UV photometric and conductivity detection of anions. (a) Chromatogram of inorganic anions. Mobile phase flow-rate, $26 \mu\text{l min}^{-1}$; sample volume, $1 \mu\text{l}$. Solutes: 1 = Cl^- (1 mmol l^{-1}); 2 = NO_2^- (1 mmol l^{-1}); 3 = NO_3^- (1 mmol l^{-1}); 4 = I^- (3 mmol l^{-1}). Detection: simultaneous indirect UV photometric detection at 254 nm (upper line) and conductivity detection (lower line) with the described detector. Other conditions as in Fig. 2. (b) Chromatogram of carboxylic acids. Solutes: 1 = butyric acid (0.4 mmol l^{-1}); 2 = isovaleric acid (0.8 mmol l^{-1}); 3 = valeric acid (1.2 mmol l^{-1}). Other conditions as in (a).

An example of the chromatographic separation of inorganic anions is shown in Fig. 3a. These substances are optically transparent at 254 nm and, considering the value of their equivalent ion conductivities (see Table I), the combined detector provides a simultaneous record of both chromatograms. The time shift (Δt) of individual signals obviously depends on the flow-rate (F) of the mobile phase. Taking into account the actual value of the flow-rate ($F = 26 \mu\text{l min}^{-1}$), the time delay ($\Delta t = 0.11 \text{ s}$) caused by the cell arrangement can be neglected.

TABLE I
EQUIVALENT ION CONDUCTIVITIES (λ) OF THE IONS USED AT 25°C

Ion	$\lambda \times 10^4 \text{ (m}^2 \Omega^{-1} \text{ mol}^{-1}\text{)}$			
	Ref. 24	Ref. 25	Ref. 26	Ref. 27
Nicotinate			29.5	33.4
Cl^-	76.5	76.3		
NO_2^-	71.8	71.8		
NO_3^-	71.4	71.4		
I^-	76.6	76.8		
Butyrate	32.6	32.6		32.6
Isovalerate		32.7		31.0
Valerate	28.8		30.5	

Similarly to other simultaneous detection methods, the independent conductivity and photometric signals enhance the identification possibilities of solutes. Moreover, this approach increases the versatility of the detector when one of the detection modes has a low sensitivity; see Fig. 3b, showing the chromatogram of a mixture of carboxylic acids. These compounds cannot be detected sensitively in the system used with the conductivity method, as can be seen from the chromatogram and from the equivalent ion conductivities of the ions used in Table I. Organic solutes and nicotinic acid have similar ion conductivities and, therefore, the conductivity detector response is very low. The photometric channel, on the other hand, permits sensitive detection as for inorganic ions.

CONCLUSION

The detector for liquid flow analyses was designed and tested to provide simultaneous photometric and conductivity signals. With respect to the small volume of the measuring cell ($<0.1 \mu\text{l}$) it can be connected to a microcolumn chromatograph. The detector design is simplified substantially by using optical fibres in the optical section. The design of the flow cell permits its easy dismantling. The time shift of the photometric and conductivity responses is negligible with respect to the values of the mobile phase flow-rate in microcolumn LC. In practical applications the combined detector increases the possibilities of solute identification due to selective detection and improves the detector versatility. It could also be used in chromatography with varying compositions of the mobile phase for simultaneous recording of the course of the mobile phase gradient and the chromatogram.

REFERENCES

- 1 J. F. Alder, P. R. Fielden and A. J. Clark, *Anal. Chem.*, 56 (1984) 185.
- 2 G. J. Smidt and R. P. W. Scott, *Analyst (London)*, 110 (1985) 757.
- 3 H. D. Dewald and J. Wang, *Anal. Chim. Acta*, 166 (1984) 163.
- 4 K. Šlais, *J. Chromatogr.*, 436 (1988) 413.
- 5 M. Janeček, V. Kahle and M. Krejčí, *J. Chromatogr.*, 438 (1988) 409.
- 6 V. Kahle and M. Janeček, *Chem. Listy*, in press.
- 7 D. T. Gjerde, J. S. Fritz and G. Schmuckler, *J. Chromatogr.*, 186 (1979) 509.
- 8 R. M. Cassidy and S. Elchuk, *J. Chromatogr. Sci.*, 21 (1983) 454.
- 9 J. S. Fritz, D. T. Gjerde and Ch. Pohlandt, *Ion Chromatography*, Hüthig, Heidelberg, 1982.
- 10 P. R. Haddad, *Chromatographia*, 24 (1987) 217.
- 11 H. Small and T. E. Miller, *Anal. Chem.*, 54 (1982) 462.
- 12 N. E. Skelly, *Anal. Chem.*, 54 (1982) 712.
- 13 G. Schmuckler, *J. Chromatogr.*, 313 (1984) 47.
- 14 R. G. Gerritse and J. A. Adeney, *J. Chromatogr.*, 347 (1985) 419.
- 15 L. Hackzell, T. Rydberg and G. Schill, *J. Chromatogr.*, 282 (1983) 179.
- 16 W. E. Barber and P. W. Carr, *J. Chromatogr.*, 316 (1984) 211.
- 17 F. Foret, M. Deml, V. Kahle and P. Boček, *Electrophoresis*, 7 (1986) 430.
- 18 M. Janeček, F. Foret, K. Šlais and P. Boček, *Chromatographia*, 25 (1988) 815.
- 19 R. M. Cassidy and S. Elchuk, *Anal. Chem.*, 54 (1982) 1558.
- 20 J. S. Fritz, D. L. DuVal and R. E. Barren, *Anal. Chem.*, 56 (1984) 1177.
- 21 B. A. Bidlingmeyer, C. T. Santasania and F. V. Warren, Jr., *Anal. Chem.*, 59 (1987) 1843.
- 22 D. H. Fröhlich, *J. High Resolut. Chromatogr. Chromatogr. Commun.*, 10 (1987) 12.
- 23 M. Pestemer, *Correlation Tables for the Structural Determination of Organic Compounds*, Verlag Chemie, Weinheim, 1974.

- 24 Landolt-Börnstein, *Zahlwerte und Funktionen aus Physik-Chemie-Astronomie-Geophysik und Technik*, Vol. 2, Part 7, Springer, Berlin, Göttingen, Heidelberg, 6th, ed., 1960.
- 25 R. C. Weast (Editor), *CRC Handbook of Chemistry and Physics*, CRC Press, Boca Raton, FL, 68th ed., 1987, p. D-168.
- 26 J. Pospichal, M. Deml, Z. Žemlová and P. Boček, *J. Chromatogr.*, 320 (1985) 139.
- 27 T. Hirokawa, M. Nishino, N. Aoki, Y. Kiso, Y. Sawamoto, T. Yagi and J.-I. Akiyama, *J. Chromatogr.*, 271 (1983) D1.

CHROM. 21 355

EFFECT OF THE POSITION OF THE LASER BEAM FOCAL POINT ON A CAPILLARY FLOW-THROUGH CELL ON THE SIGNAL-TO-NOISE RATIO FOR A FLUORIMETRIC DETECTOR IN CAPILLARY COLUMN LIQUID CHROMATOGRAPHY

TAKAO TSUDA*

Nagoya Institute of Technology, Gokiso-cho, Showa-ku, Nagoya 466 (Japan)
and

HIROSHI NODA

Shimadzu Corp., Nishinokyo-Kuwabaracho, Nakagyo-ku, Kyoto 604 (Japan)

SUMMARY

The use of a high-sensitivity laser-induced fluorescence detector with a capillary flow-through cell (100 μm I.D.) in capillary column liquid chromatography was studied. To reduce the background noise from scattering of the laser light from the cell walls by reflection and refraction, the geometric position of the focal point of the laser beam on the capillary cell is very important. By moving the focusing lens of the laser beam, the best position of the laser on the capillary cell was examined. The use of a video camera was also helpful in setting the laser beam on the capillary cell. With the optimum geometric arrangement, 1.3 fmol of the 4-bromomethyl-7-methoxycoumarine derivative of caproic acid ($k' = 3$) was detected at a signal-to-noise ratio of 5.

INTRODUCTION

Micro-column liquid chromatography (LC) has the advantages of a higher resolution and a smaller amount of sample than those in conventional column LC¹⁻⁶. Micro-column LC has a greater potential for the analysis of complex samples in biological and medical areas where the amount of sample available may be limited^{1,4}. As the amount of sample injected in micro-LC is very small owing to the low loading capacity of the micro-column, suitable detection techniques of high sensitivity are necessary. Several novel devices, such as laser-based⁵⁻¹² and electrochemical^{13,14} detectors, have been studied.

Fluorescence is one of the most sensitive detection techniques available in LC. The use of lasers as excitation sources^{5-12,15} is very suitable for a micro-cell, because the beam can be focused on to a very small area with high intensity. Although laser fluorescence detectors have been well studied, there have been few reports concerning the position of the focused area of the laser beam in or on the very small cell. Folestad *et al.*⁶ discussed the relationship between the relative fluorescence intensity and the distance between the lens and the cell, and Dovichi *et al.*⁷ examined the fluorescence

intensity as a function of laser-induced position in the cell. Lyons and Faulker¹⁵ examined the position of the collection lens and the effect of the shapes of cells for conventional LC.

In this work we examined the focused position of the laser beam on a capillary flow-through cell. We found that the position of the spot of the laser beam is important for obtaining a good signal-to-noise (S/N) ratio. After finding the optimum position of the laser beam spot, we applied the present system to the separation of fluorescent derivatives of carboxylic acids.

EXPERIMENTAL

Chromatographic system

A schematic diagram of the analytical system is shown in Fig. 1. A 25 cm \times 320 μ m I.D. fused-silica capillary tube (Quadrex, supplied from Tokyo Kasei Kogyo, Tokyo, Japan) was slurry packed with Shim-pack CLC-ODS, 5 μ m (Shimadzu, Kyoto, Japan). The slurry solvent was carbon tetrachloride-liquid paraffin (1:1)¹⁶. A Model LC-6A pump (Shimadzu) was used at constant pressure or constant flow-rate. A Shim-pack SBC-ODS column (15 cm \times 2.5 mm I.D.) was used as a resistance in the split-flow line. A 0.06- μ l internal loop injector (Model C-14W; Valco Europe, Schenkon, Switzerland) was used. The column head was inserted into the injector. Just after a PTFE frit (Kusano Kagaku Kogyo, Tokyo, Japan) at the end of the slurry-packed capillary column, a length of fused-silica capillary (50 or 100 μ m I.D.) was used for connection to a flow-through capillary cell.

Laser fluorescence detector

The 325 nm output of a helium-cadmium laser (Model 4240 NB, 10 mW) (Liconix, Sunnyvale, CA, U.S.A.) passed through a short-pass filter (Type UV D 36C; Toshiba, Tokyo, Japan), then the beam passed through a focussing convex lens (synthesized quartz, focus 25 mm;

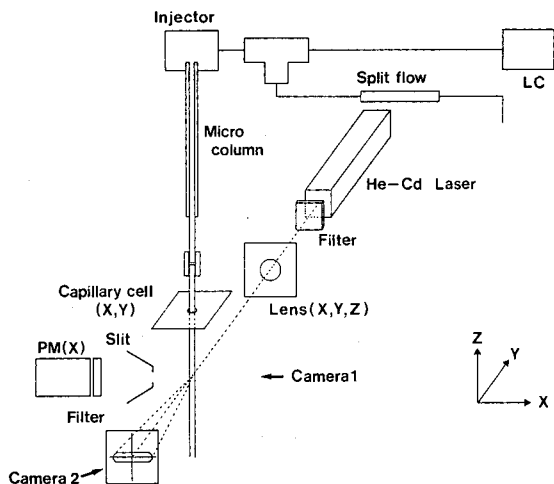


Fig. 1. Schematic diagram of laser fluorescence detector device for micro-LC.

Sigma Kohki, Irima-gun, Saitama, Japan). The focusing lens was moved in the x and z directions by a positioner with help of synchronous motors (225 s per rotation per 0.5 mm) and in the y direction manually by a positioner, as shown in Fig. 1. By adjusting the positioner on the y axis, the laser was focused on the capillary flow-through cell. The spot of the laser beam on the capillary was transferred according to the position of the focusing lens (x and z axes). Fluorescence, scattered light and refracted light from the cell were received by a photomultiplier tube (PM) (Type R374; Hamamatsu Photonix, Shizuoka, Japan) after passing through a slit of 1 mm I.D., and a long-pass filter which cut the wavelength down to 380 nm (Type SCP-38L; Shigma). A high-voltage supply (Model C665) and a pre-amplifier (Model C1556) (Hamamatsu Photonix) were used. The amplified output of the PM was recorded with a data-handling instrument (C-R5A; Shimadzu). The positions of the long-pass filter and the PM were adjustable on the x axis. The PM was arranged perpendicularly to the laser beam. A video camera-TV screen system (Model GX-N4CH; Japan-Victor, Tokyo, Japan) was used.

Detector cell

As a capillary flow-through cell, a fused-silica capillary tube (100 μm I.D. and 160–180 μm O.D.) was used. The polyimide coating of the capillary tube had been removed for a length of about 10 mm in the region on which laser beam was focused. The capillary cell was moved by positioners in the x and y directions. The capillary column and the capillary cell were connected with PTFE tubing (*ca.* 10 mm \times 0.1 mm I.D.) as described by others⁵.

Reagent

Carboxylic acids were derivatized with the fluorescence reagent 4-bromomethyl-7-methoxycoumarin (Br-Mmc) (Tokyo Kasei Kogyo) according to the procedure of Duges¹⁷. All reagents used were of guaranteed grade.

RESULTS AND DISCUSSION

Because of the coherence properties of a laser, it can deliver to a target a highly collimated beam of light with high power levels. The 325-nm (10mW) laser beam used was focused as a small, round spot of diameter 30 μm . The area of the spot was observed with the video camera and its diameter was measured by using a 10- μm slit. In capillary column LC, the capillary cell has a very small (sub-nanolitre) volume to avoid band broadening in the extra column parts. Therefore, light for excitation should be focused accurately on a very small area of the capillary cell, and this can be achieved without much difficulty with a laser beam. Although a strong excitation beam is desirable for obtaining strong fluorescence, it is also necessary to reduce the background interference and to collect as much fluorescent light from the cell as possible for high-sensitivity detection. This background interference arises from (a) scattering of the laser light from the cell walls by reflection and refraction (RR), (b) elastic (Rayleigh) scattering of the light, (c) inelastic (Raman) scattering of the laser light and (d) fluorescence from other interfering species¹⁵. Raman scattering is usually excluded by a suitable combination of excitation and detection wavelengths. The fluorescence from other interfering species comes mostly from the eluent itself, its

impurities and the LC system, especially impurities from the column. Our concern is therefore with processes (a) and (b) above.

Even though a long-pass filter is used, shown in Fig. 1, for eliminating the scattered light produced by processes (a) and (b), the detection system cannot separate light at the detection wavelength perfectly from light scattered at the excitation wavelength. To obtain a higher sensitivity of detection, it is very important to find a means of decreasing the background interference. For this purpose, we searched for the optimum geometric position of the spot of the laser beam by scanning the position of the spot on the cell in the x , y and z directions. In this experiment, fluorescence and scattered light were received by the PM just after passing a long-pass filter.

Visual arrangement of the line of the capillary cell and laser beam

Using video camera 1 and a TV screen, as shown in Fig. 1, we could see roughly the position of the laser beam on the capillary cell by magnifying the image up to 100-fold on the TV screen (1 mm equal to 10 cm on the screen). By adjusting the position of the focusing lens in the x , y and z directions, we could obtain a round spot of laser light as small as $30\ \mu\text{m}$ in diameter on the capillary cell. After the laser light had been scattered by the capillary cell, it gave several different pictures at the back of the capillary cell. We placed a sheet of paper containing fluorescence material at its back position, and observed the image on the paper with video camera 2, as shown in Fig. 1. Sketches of the images on the TV screen are shown in Fig. 2, and the assumed part of the capillary cell through which light was passed and the light loci are shown in Fig. 3a and b, respectively. For image A in Fig. 2 the laser beam was focused well at the centre of the capillary cell along the X_a line (position x_c in Fig. 3a). For C and E the laser beam was focused on the two edges of the capillary cell, that is, positions x_a and x_b , respectively, in Fig. 3a. Images B and D were obtained between x_a and x_c and between x_c and x_b , respectively. It is possible to establish the location of the focused position of the laser beam from the observation of the scattered light images, and to adjust the position of the laser at the centre of the capillary cell by using the positioners.

Adjustment of the distance between capillary cell and slit by observing the response of the PM

The slit in Fig. 3a, through which scattered light and fluorescence were passed to the PM, had a hole of 1 mm diameter. The capillary cell was set at the middle of the hole by the y positioner of the cell by observation with camera 1. Then the cell was set at different position on the X_a line with the positioner. Laser light was moved from the slit position ($x = 0$) to the cell by moving the focussing lens along the x axis with a motor. As the focus of the lens is always on the X_a line in Fig. 3a, the laser is also always focused on the X_a line. The laser mostly crosses the X_a line perpendicularly.

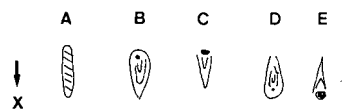


Fig. 2. Sketches of scattered patterns of the laser beam at the back of the capillary cell.

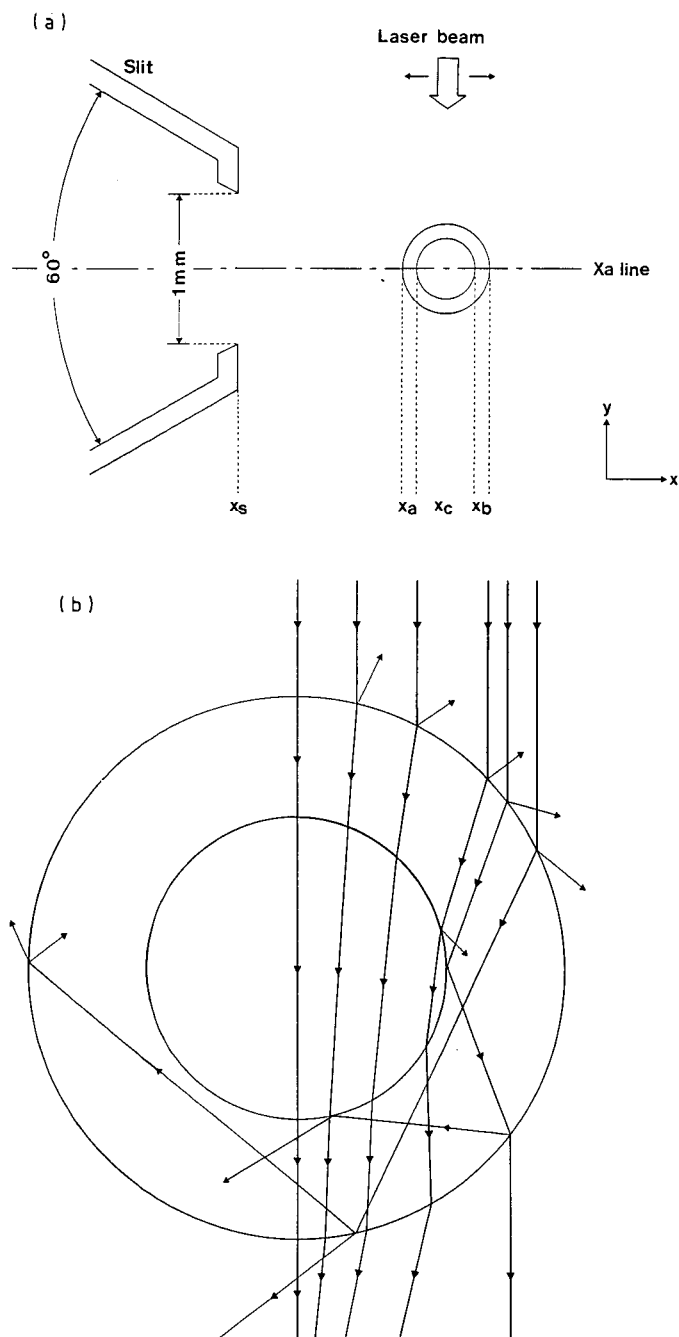


Fig. 3. (a) Sectional view of capillary cell and slit. (b) Assumed light loci at capillary cell filled with acetonitrile. Capillary cell: fused-silica tubing, $100\ \mu\text{m}$ I.D. and $180\ \mu\text{m}$ O.D. (thickness of the tube wall, $40\ \mu\text{m}$). The refractive indices of quartz and acetonitrile are assumed to be 1.458 and 1.344, respectively. The critical angles of the former and the latter are 43.3° and 67.2° , respectively.

The maximum deflection of the laser from the perpendicular to the X_a line would be 2.3° , because the focal length of the lens was 25 mm and the total transferred distance of the lens was 2 mm.

In Fig. 4, the applied voltage to the PM was set at 450 V and the response of the PM was recorded with movement of the lens. The first large peak ($x=0$) came from direct reflection of the laser beam at the edge of the slit (laser position at x_s in Fig. 3a). The second (a) and third peaks (b) correspond to the laser at positions x_a and x_b , respectively, in Fig. 3a. In these positions, the laser beam was reflected on the surface and also passed through the tube wall with complex loci, showed in Fig. 3b. However, at position x_c , the laser beam passed through the inside of the capillary cell, and minor RR might have occurred.

There are narrow regions of low noise level between peaks a and peak b in 1–3 in Fig. 4. However, there are relatively larger regions of low noise level in 4–7 in Fig. 4; here not much light due to RR would reach the PM, because the distances between the slit and the capillary cell are relatively large compared with the former. The noise levels in the region between a and b in 4–7 in Fig. 4 are also smaller than those in 1–3. It is important that the focused position of the laser beam on the capillary corresponds to the region of this lower noise level. The position of the laser spot on the z axis was also examined; this result will be discussed elsewhere.

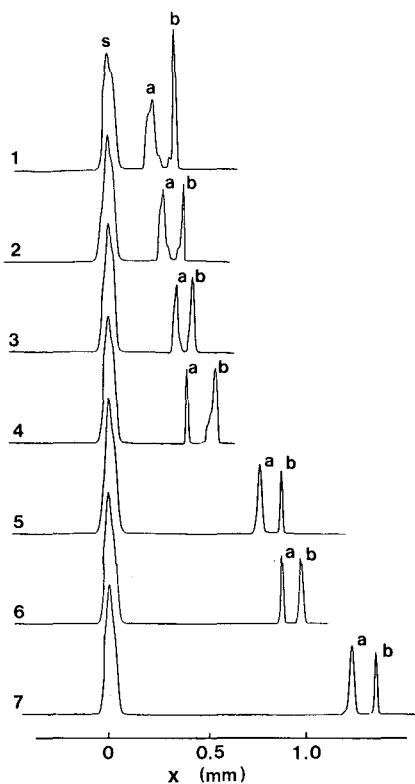


Fig. 4. Background of scattered light at different cell distances from the slit. Peaks s, a and b come from the slit, x_s and x_b in Fig. 3a, respectively.

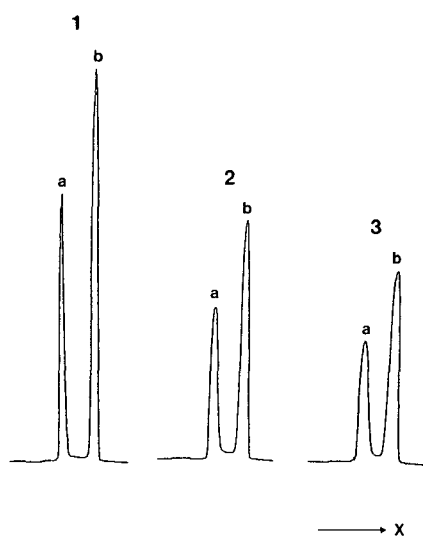


Fig. 5. Effect of focusing on the capillary cell. The optimum focusing is 1; 2 and 3 were not well focused.

Effect focusing on capillary cell

The laser beam should be focused on the capillary cell, otherwise the spot area of the laser beam becomes wider than that with optimum focusing. Three typical examples of the effect of focusing are shown in Fig. 5. We measured the noise levels; the response in Fig. 5 is equal to the noise level. In Fig. 5, the numbers 1, 2 and 3 are set at the best focused position f_a (the distance between the focusing lens and the capillary cell was assumed to be f_a mm), $f_a = 1.25$ mm and $f_a = 1.75$ mm, respectively. In the last two instances, the laser beam was not well focused on the capillary cell; as the spot areas on the capillary cell were wider here than that in case 1, larger RR was observed. Also, the background noise levels between a and b in cases of 2 and 3 were higher than that in case 1. These results indicate that focussing is very important for obtaining low background noise.

Fluorescence with continuous flow of reagent

When the fluorescent reagent (Br-Mmc derivative of caproic acid) was flowed continuously through the capillary cell, the response of the PM along the X_a line was as shown in Fig. 6 (1 and 2 represent experiments with and without a flow of Br-Mmc derivative). The capillary cell was fixed at the optimum position. The response in 1 in Fig. 6 is a combination of fluorescence and RR. Although some fluorescence was obtained even at the two edges of the capillary cell (peaks a and b), the S/N ratios at these positions were not good. From 1 in Fig. 6, the best S/N ratio is considered to be obtained near the middle between the two edges of the capillary cell.

We recommend the following procedure for adjusting the geometric position of the capillary cell to obtain low background noise: (1) place the capillary cell at the centre of the slit; (2) set the position of the capillary cell 0.5 mm from the slit along the X_a line; (3) focus the laser beam well on the capillary cell by adjusting the position of the focusing lens; and (4) adjust the position of laser spot at the centre of the capillary

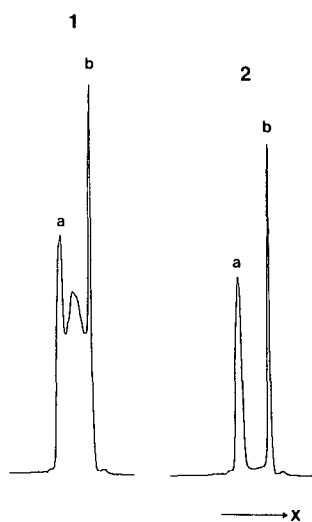


Fig. 6. Fluorescence and scattered light under conditions of continuous flow, (1) with and (2) without fluorescent reagent. Flow-rate, $4 \mu\text{l}/\text{min}$; fluorescent solution, $5 \mu\text{M}$ Br-MMc derivatives of caproic acid in acetonitrile. Eluents for 1 and 2 were fluorescent solution and pure acetonitrile, respectively.

cell in the x and z directions so as to obtain the lowest output level of background interference.

After above adjustments, we separated Br-Mmc derivatives of carboxylic acids in a test mixture. A typical example is shown in Fig. 7. The peak of 8 fmol of the Br-MMc derivative of caproic acid is eluted at 14 min with a peak height of $900 \mu\text{V}$.

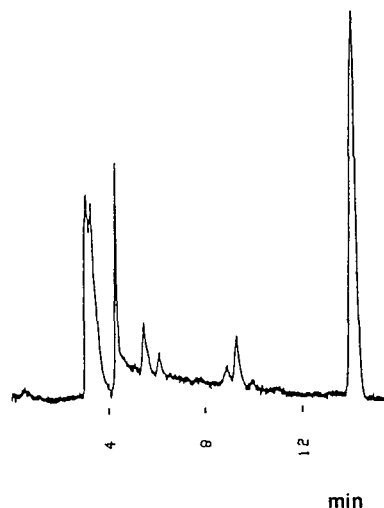


Fig. 7. Chromatogram of 8 fmol of Br-MMc derivative of caproic acid. Slurry-packed fused-silica ODS ($5 \mu\text{m}$) capillary column ($25 \text{ cm} \times 320 \mu\text{m}$ I.D.). Eluent, water-acetonitrile (1:9), $4 \mu\text{l}/\text{min}$. Br-MMc derivative of caproic acid was eluted at 14 min.

At $S/N = 5$, the minimum detectable amount of the Br-Mmc derivative of caproic acid would be *ca.* 1.3 fmol. The calibration graph for fluorescence derivatives is linear over three orders of magnitude of concentration.

REFERENCES

- 1 M. Novotny, *Anal. Chem.*, 60 (1988) 500A–510A.
- 2 R. P. W. Scott, *Small-Bore Liquid Chromatography Columns*, Wiley-Interscience, New York, 1984.
- 3 T. Tsuda, I. Tanaka and G. Nakagawa, *Anal. Chem.*, 56 (1984) 1249–1252.
- 4 T. Ishizuka, K. Ishikawa, M. Maseki, Y. Tomida and T. Tsuda, *J. Chromatogr.*, 380 (1986) 43–53.
- 5 J. Gluckman, D. Shelly and M. Novotný, *J. Chromatogr.*, 317 (1984) 443–453.
- 6 S. Folestad, L. Johnson, B. Josefsson and B. Galle, *Anal. Chem.*, 54 (1982) 925–929.
- 7 W. J. Dovichi, J. C. Martin, J. H. Jett, M. Trukula and R. A. Keller, *Anal. Chem.*, 56 (1984) 348–354.
- 8 H. Todoriki and A. Y. Hirakawa, *Chem. Pharm. Bull.*, 32 (1984) 193–197.
- 9 V. L. McGuffin and R. N. Zare, *Proc. Natl. Acad. Sci. U.S.A.*, 82 (1985) 8315–8319.
- 10 R. N. Zare, *Science*, 226 (1984) 298–303.
- 11 E. J. Gruthrie and J. W. Jorgenson, *Anal. Chem.*, 56 (1984) 483–486.
- 12 S. Einarsson, S. Folestad and B. Josefsson, *J. Liq. Chromatogr.*, 10 (1987) 1589–1601.
- 13 A. Manz and W. Simon, *Anal. Chem.*, 59 (1987) 74–79.
- 14 R. L. St.Claire, III, and J. W. Jorgenson, *J. Chromatogr. Sci.*, 23 (1985) 186–191.
- 15 J. W. Lyons and L. R. Faulkner, *Anal. Chem.*, 54 (1982) 1960–1964.
- 16 K. Unger, Johannes Gutenberg-Universitat, F.R.G., personal communication.
- 17 W. Dunges, *Anal. Chem.*, 49 (1977) 442–445.

CHROM. 21 283

TRACE ENRICHMENT OF PYRIMIDINE NUCLEOBASES, 5-FLUOROURACIL AND BROMACIL ON A SILVER-LOADED THIOL STATIONARY PHASE WITH ON-LINE REVERSED-PHASE HIGH-PERFORMANCE LIQUID CHROMATOGRAPHY

CLAUDIA LIPSCHITZ, HUBERTUS IRTH*, GERHARDUS J. DE JONG, UDO A. Th. BRINKMAN and ROLAND W. FREI^a

Department of Analytical Chemistry, Free University, De Boelelaan 1983, 1081 HV Amsterdam (The Netherlands)

SUMMARY

A silver-loaded thiol stationary phase was used for the trace enrichment of pyrimidine nucleobases (uracil, thymine and cytosine) and some related compounds (5-fluorouracil, bromacil, uridine). The critical parameters for the sorption of these compounds on Ag(I)-thiol are the pH value of the sample solution and the flow-rate with which they are flushed through the pre-column. Complete recovery for all compounds except uridine was obtained at pH 11.0 at a flow-rate of 0.6 ml/min. The desorption mechanism was based on protonation of the analytes. Efficient on-line desorption to the C₁₈ analytical column was achieved by injecting a plug of 60 μ l HNO₃ (pH 1.2) onto the Ag(I)-thiol pre-column. After separation the analytes were detected by UV detection at 269 nm. For 5-fluorouracil a detection limit of $3 \cdot 10^{-9}$ M was obtained for the preconcentration of 1.0 ml with a reproducibility of 2.3% ($n = 6, 5 \cdot 10^{-7}$ M). The column efficiency measured in terms of plate number for 5-fluorouracil was 11 000 for direct injections and 9000–10 000 for 1.0-ml preconcentrations, indicating that the desorption step causes no appreciable band broadening. Applications of the described method for the determination of 5-fluorouracil in plasma and for the herbicide bromacil in surface water are presented.

INTRODUCTION

Nucleobases are the primary building blocks of the genetic material. The five bases found in nucleic acids (Fig. 1) are heterocyclic aromatic compounds, either pyrimidines or purines, the latter containing a fused pyrimidine-imidazole ring system¹. The two nitrogen atoms in the pyrimidine ring and the carbonyl and amino substituents contribute to shifts in electronic distribution resulting in lactim-lactam and amine-imine tautomerism² which is of fundamental importance to the structure and functioning of the nucleic acids. Although at physiological pH the stable lactam and amine forms predominate, the occurrence of rare tautomeric forms has been implicated as a possible mechanism of spontaneous mutation².

^a Author deceased.

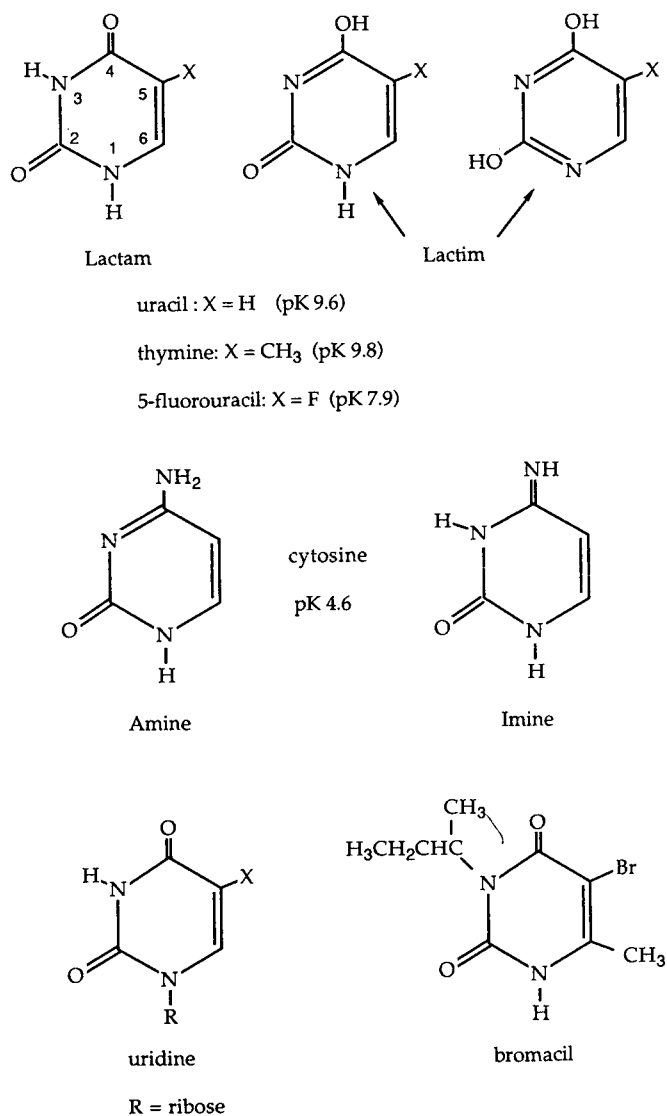


Fig. 1. Structure of pyrimidine nucleobases and derivatives.

Certain, not naturally occurring bases such as 5-fluorouracil (FU) and 6-mercaptopurine are used as chemotherapeutic and mutagenic agents, as they are readily incorporated in nucleic acids instead of the natural bases¹. FU has been used for nearly 25 years in the treatment of solid tumors, and pharmacokinetic studies on uptake, distribution and metabolism of FU have been carried out since then. Chromatographic methods such as gas chromatography (GC) and liquid chromatography (LC) make accurate and sensitive analysis of FU and its metabolites possible. However, FU is metabolized fairly rapidly after administration with an initial half life of

10–15 min, and within 3 h after bolus injection, the plasma concentration falls below $5 \cdot 10^{-8} M$, *i.e.*, below the reported detection limit for most methods, including GC–electron impact mass spectrometry³. A limit of detection of $3 \cdot 10^{-9} M$ (0.39 ng/ml) was reported for electron-capture negative-ion mass spectrometry⁴. This method, however, requires derivatization of FU with an electron-capturing sensitive reagent, in addition to other sample pretreatment steps.

Samples of biological origin usually require a multi-step clean-up sequence, including deproteination and liquid–liquid extraction, to extract the compound(s) of interest prior to chromatographic analysis. Multiple liquid–liquid extractions, apart from being time consuming, often lead to losses in analyte recovery. Sample deproteination was conventionally carried out by precipitation with perchloric or trichloroacetic acid and neutralization with alkali or an amine–freon solution⁵. More recent techniques include ultrafiltration or clean-up on a C_{18} bonded silica stationary phase⁶. The use of a C_{18} phase offers the possibility of sample clean-up and trace enrichment of apolar and weakly polar compounds. C_{18} pre-columns are often used, on-line, in automated systems as disposable cartridges⁷.

Biologically active compounds are usually weakly polar to polar and are therefore not effectively retained on a C_{18} -bonded silica phase. Frei *et al.*⁷ and Nielen *et al.*⁸ investigated the use of suitable sorbents such as ion exchangers and metal-loaded stationary phases for the on-line trace enrichment of polar organic compounds. Sorption on metal-loaded phases occurs via complexation and may therefore be applicable to the pyrimidine bases and their nucleosides and nucleotides which form complexes with a variety of metal ions^{9,10}. Metal ions have been used in LC in various ways.

(i) As complexing agents in the mobile phase: Ag(I) was used in the separation of retinyl esters¹¹ and a number of heterocyclic and unsaturated compounds¹². Mg (II) was used for the separation of nucleotides on a dithiocarbamate column¹³.

(ii) Immobilized on a chelating stationary phase: Cu(II) was loaded on a silica-polyol phase for the separation of pyrimidine bases and nucleosides¹⁴. Retention was proposed to take place via a combination of ligand-exchange, reversed-phase and adsorption mechanisms. Stationary phases developed for such systems were of the iminodiacetate silica-polyol or 8-hydroxyquinoline (oxine) silica-polyol type.

In the present study we investigated experimental parameters affecting the sorption of FU, uracil, uridine, thymine and cytosine on a Ag(I)–thiol stationary phase as well as conditions affecting on-line desorption from the stationary phase to the analytical column. This method was applied to the determination of FU in plasma, and of the herbicide bromacil, a uracil derivative, in surface and tap water.

EXPERIMENTAL

Apparatus

The LC system (Fig. 2) consisted of three laboratory-made six-port Valco-type injection valves, a 1.0-ml sample loop, a 60- μ l loop to contain HNO_3 (pH 1.2) needed for the desorption of analytes, a 10.0×4.0 mm laboratory-made stainless-steel pre-column and holder (Chrompack, Middelburg, The Netherlands) and 200×4.6 mm I.D. Hypersil ODS 5- μ m (Shandon Southern, Runcorn, U.K.) analytical column. The carrier solution for preconcentration was delivered by a Gilson (Villiers le Bel, France) Model 302 single-head reciprocating pump and the LC eluent by a Waters

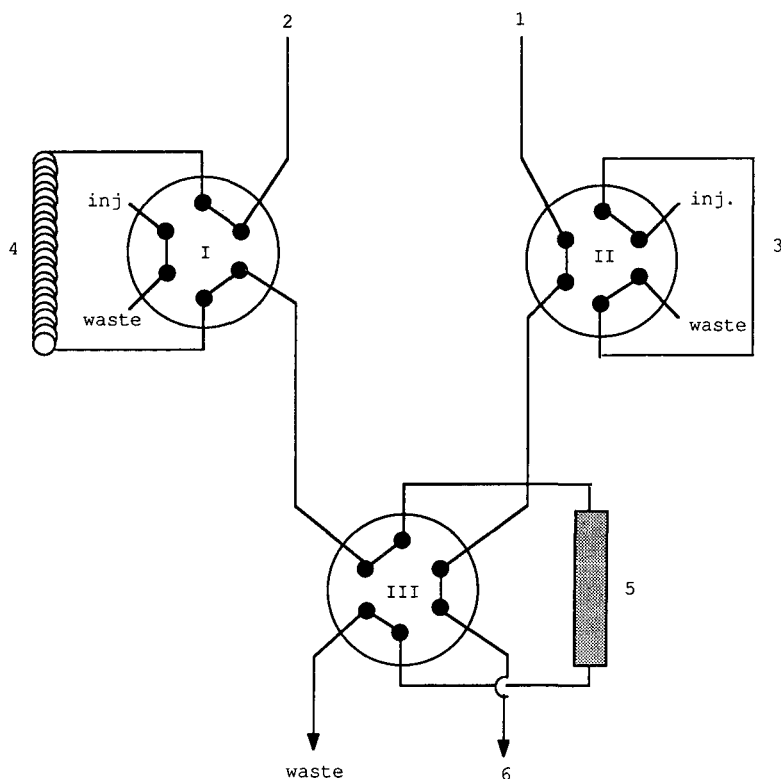


Fig. 2. Scheme of the pre-concentration system. 1, LC pump; 2, pre-concentration pump; 3, 60- μ l injection loop for HNO_3 ; 4, sample injection loop (1.0 ml); 5, Ag(I) -thiol pre-column; 6, to analytical column/detector.

(Milford, MA, U.S.A.) Model 510 dual-head reciprocating pump. Pulse dampers are incorporated into the system for each pump. The LC eluent was aqueous 2 mM acetate buffer (pH 5.8) containing 0.1 mM cetyltrimethylammonium bromide (CTAB). Two variable-wavelength UV detectors, a Pye Unicam LC-3 UV (Philips, Eindhoven, The Netherlands) and a Kratos (Ramsey, NJ, U.S.A.) Spectroflow 757, were used for detection at 269 nm.

Chemicals and reagents

Uracil, thymine, sodium *N,N*-diethyldithiocarbamate (DTC) and CTAB were obtained from Merck (Darmstadt, F.R.G.), 5-fluorouracil, 5-chlorouracil and uridine from Janssen (Beerse, Belgium), and cytosine from Sigma (St. Louis, MO, U.S.A.). Standard solutions of 10^{-3} M were prepared from these compounds in distilled, deionized water.

A standard solution of bromacil (gift of A. de Kok, Rijkskeuringsdienst van Waren, Alkmaar, The Netherlands) of 300 $\mu\text{g/ml}$ was prepared in HPLC-grade methanol (Baker, Deventer, The Netherlands). All other chemicals used were Baker analyzed reagents.

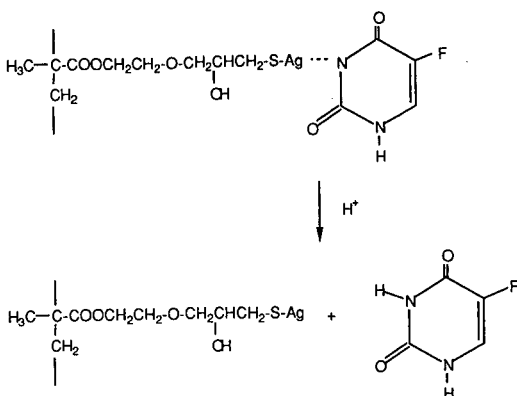


Fig. 3. Desorption of FU from the Ag(I)-thiol stationary phase.

Trace enrichment and chromatography

A 40–63 μm thiol-modified hydroxyalkyl-methacrylate gel, Spheron Thiol 1000 (Lachema, Brno, Czechoslovakia) stationary phase (Fig. 3) for trace enrichment was slurry packed via a 5 ml syringe into a stainless-steel pre-column, loaded off-line with 5 ml 10 mM AgNO_3 and flushed with 5 ml deionized, distilled water and 5 ml HPLC-grade methanol. The preconcentration carrier solution was aqueous NaOH (pH 10.5). Equilibration of the silver-loaded stationary phase was carried out on-line by flushing with the carrier solution for 10–15 min.

A 1.0 ml sample plug containing $5 \cdot 10^{-5}$ – 10^{-8} M of various combinations of model compounds was loaded onto the pre-column at a carrier flow-rate of 0.6 ml/min for 4.0–4.5 min (Fig. 2). On-line desorption to the analytical column was carried out by injecting a plug of 60 μl HNO_3 (pH 1.2) into the LC eluent stream (valve II) and switching the eluent flow (valve III) to the pre-column to desorb the preconcentrated analytes and transfer them to the analytical column. If a DTC-CTAB ion-pair was used as a displacer an additional C_{18} pre-column was inserted between the Ag(I)-thiol pre-column and the analytical column in order to remove the excess of DTC. Next, the analytes were separated under isocratic conditions at a flow-rate of 1.2 ml/min. The analytical column was allowed to equilibrate with LC eluent overnight at a flow-rate of 0.1 ml/min to ensure stable operating conditions. Pure acetonitrile was used periodically to purge the column.

Direct injections (12 μl) of $5 \cdot 10^{-5}$ M standard solutions of the five model compounds, FU, uracil, thymine, cytosine and uridine, were run daily to test the analytical column performance. Direct injections of 60 μl of the same compounds were run for recovery calculations. Direct injections were made by replacing the Ag(I)-thiol pre-column by the appropriate sample loop in order to measure peak areas under the same conditions of extra-column band broadening.

Determination of bromacil in surface water

A stock solution of bromacil was prepared in HPLC-grade methanol. The carrier solution used for preconcentration was methanol–water (50:50), adjusted to pH 10.5 with 5 M NaOH. The LC eluent was methanol–acetate buffer (10 mM, pH

6.0) (50:50) containing 0.1 mM CTAB. Surface water was collected from a nearby canal, adjusted to pH 10.5, filtered through a 0.2- μm disposable membrane filter and spiked to the desired concentration. Samples of 3–12 ml were preconcentrated according to the procedure described above.

Determination of FU in human plasma

Two different approaches were used.

(i) Non-deproteinized plasma was either filtered through a 0.2- μm disposable membrane filter or centrifuged for 15 min at 1000 *g* to remove suspended and precipitated matter. After adjusting the pH to 11.5 the supernatant was introduced into the preconcentration system. A second pre-column (60.0 \times 4.0 mm I.D.) packed with 10- μm PLRP-S (Polymer Laboratories, Church Stratton, U.K.) polymer phase was placed before the Ag(I)-thiol pre-column in order to remove macromolecular and apolar components prior to trace enrichment.

(ii) For deproteination, equal volumes of plasma and methanol were mixed and vortexed, then centrifuged for 20–25 min and the supernatant (methanol–water, 50:50) removed and adjusted to pH 10.5. Trace enrichment of deproteinized plasma proceeded without the need for an additional PLRP-S pre-column. Plasma was spiked to the desired concentrations prior to deproteination.

RESULTS AND DISCUSSION

Fundamental aspects

Tautomerism exhibited by pyrimidine nucleobases governs the acid–base and complexation behaviour of these compounds. Complexation with metal ions occurs via a Lewis-base type interaction at the electron-donating sites in the purine and pyrimidine ring. The nature of the donor atom is determined by the coordinated metal ion⁹. Uracil and its 5-halogenated derivatives form strong complexes with Ag(I)¹⁵, Pd(II)¹⁶ and a number of divalent metal ions^{17,18}. The order of stability constants for the FU complexes decreases as Ag(I) ($4.9 \cdot 10^3$) > Cu(II) ($1.23 \cdot 10^3$) > Ni(II) (28.3). A 1:1 as well as a 1:2 complex between Ag(I) and FU has been suggested^{17,18}.

Complexation with a metal ion takes place at a deprotonated site (see Fig. 1) and is therefore strongly pH dependent. Dissociation takes place at N(3) ($\text{p}K_{\text{a}1} = 7.9$)⁹ making the lone electron pair of the nitrogen available for complexation via a Lewis-base interaction. At elevated pH further deprotonation takes place at N(1) ($\text{p}K_{\text{a}2} = 13$)⁹.

Sorption of pyrimidine nucleobases on a metal-loaded pre-column on-line to the analytical system was investigated in the present study. Spheron-thiol as stationary phase and Ag(I) as the complexing ion were chosen for the following reasons. (i) The stability constant for the Ag(I)–FU complex is high enough to form stable complexes but complexation is not irreversible; (ii) Ag(I) prefers nitrogen to oxygen as electron donor⁹; (iii) Ag(I) forms π – π bonds with the thiol group, which approach covalent bond strength (*e.g.*, $\log k_1$ of Ag(I)–mercaptoethanol is 13.0¹⁹); (iv) the polymeric thiol-phase is stable over a wide pH range (1–13) and is therefore not subject to deterioration during prolonged use at high pH.

Several strategies can be employed to desorb the analyte from the stationary phase.

(a) A compound forming stronger complexes with the metal can displace the analyte. Nielen *et al.*⁸ used cysteine to displace 2-mercaptobenzimidazole from Hg (II)-loaded phases. We have initially tried diethylthiocarbamate (DTC) ions, which form strong complexes with silver, to displace FU (see Fig. 6c). Before reaching the analytical column, however, excess DTC must be trapped on another pre-column, otherwise a strong DTC signal can interfere with the detection of the analytes. Excess DTC can be trapped on a C₁₈ precolumn prior to reaching the analytical column by the addition of CTAB which forms a strongly apolar ion-pair with DTC.

(b) A metal ion can desorb the analyte by complexation with the analyte itself (I) or with the thiol group of the stationary phase (II). In both cases the analytes are eluted to the analytical column as metal complexes and must be chromatographed as such.

(c) Desorption can take place via protonation. Veuthey *et al.*²⁰ used a low pH in the LC mobile phase in order to desorb amino acids bound to a Cu(II)-loaded dithiocarbamate stationary phase.

In contrast to a and b(II), where the thiol stationary phase must be regenerated after every preconcentration, method c offers two advantages:

(i) Protonation with a strong acid such as HNO₃ converts the pre-column to the free Ag(I)-thiol form which is then immediately reusable after desorption without any further treatment. Due to the high stability of the Ag(I)-thiol bond, Ag(I) is not stripped off during analyte desorption. Therefore the use of the thiol stationary phase is favored over oxine^{8,9} which forms much weaker complexes with Ag(I) (log k_1 for Ag-8-hydroxyquinoline is 6.6)¹⁹.

(ii) Excess displacer does not interfere with the detection system, i.e., a pre-column for removal of the displacer is not necessary.

Method c was therefore chosen to desorb the uracil compounds from the stationary phase (Fig. 3).

Influence of pH and flow-rate on sorption

Breakthrough experiments have shown that the pH value of the sample solution and the flow-rate of the carrier solution with which the sample is loaded onto the stationary phase are the critical parameters which determine the sorption of the model compound, FU, on the Ag(I)-thiol column. Breakthrough of FU is mainly determined by complexation kinetics and thermodynamics and not by the capacity of the Ag(I)-thiol column. At pH 9 breakthrough occurs almost immediately, while at pH 10.8 FU is completely retained over a long time interval. At a carrier solution flow-rate of 0.4 ml/min the breakthrough volume for FU was over 15 ml.

Experiments in the preconcentration mode were carried out to determine analyte recovery as a function of the carrier solution flow-rate and of the pH value of the sample solution using a carrier solution of pH 10.5. As an example, percentage recovery as a function of carrier flow-rate at sample pH 11.0 is shown in Fig. 4 for five test compounds. Noticeable losses start to occur for flow-rates of over 0.7 ml/min. From other experiments (data not shown) it became evident that analyte recovery markedly decreased for a sample pH of 10.4, and was down to 30–40% for pH 9.9. At sample pH values of over 11, FU, uracil, cytosine and thymine consistently showed complete recovery. The relatively large losses still observed for uridine under these conditions indicate that steric hinderance prevents efficient adsorption.

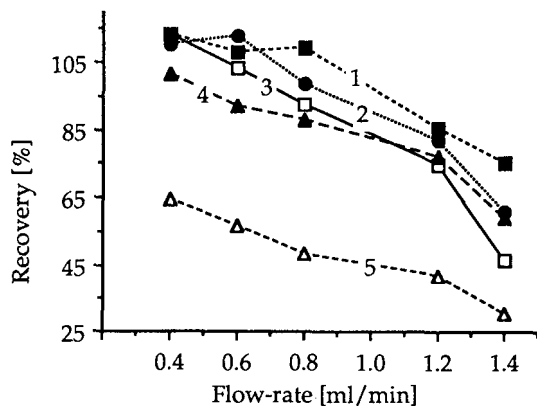


Fig. 4. Percentage recovery of FU (1), uracil (2), cytosine (3), thymine (4) and uridine (5) at pH 11.0 as a function of the carrier flow-rate.

Percentage recovery of FU *versus* carrier flow rate at four pH values is presented in Fig. 5. A flow-rate of 0.6 ml/min, a carrier solution pH of 10.5 and a sample pH of 11.0 were chosen as optimum conditions for the preconcentration of this and other uracil derivatives on the Ag(I)-thiol phase.

Trace enrichment from sample solutions containing 50% methanol also resulted in complete recovery of the analytes under the same conditions as specified above. This indicates that no hydrophobic interactions with the methylmethacrylate backbone of the Ag(I)-thiol phase were involved in the sorption process.

Influence of pH and displacer volume on desorption

At neutral pH the pyrimidine bases are protonated. Therefore it should be possible to desorb the analytes from the Ag(I)-thiol phase by flushing the pre-column

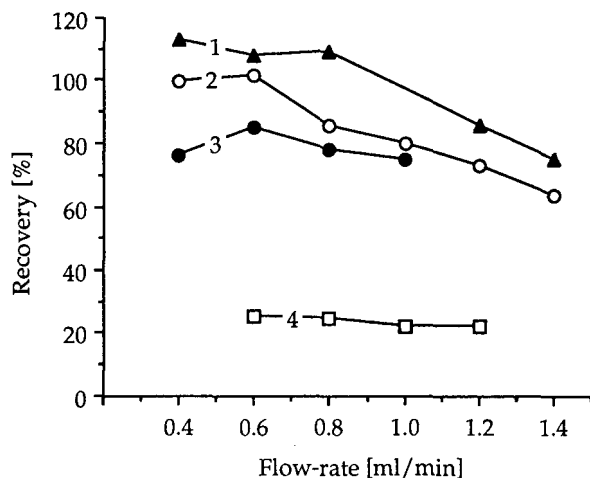


Fig. 5. Percentage recovery of FU at pH 9.9–12.2 as a function of the carrier flow-rate. 1, pH 12.1; 2, pH 11.0; 3, pH 10.4; 4, pH 9.9.

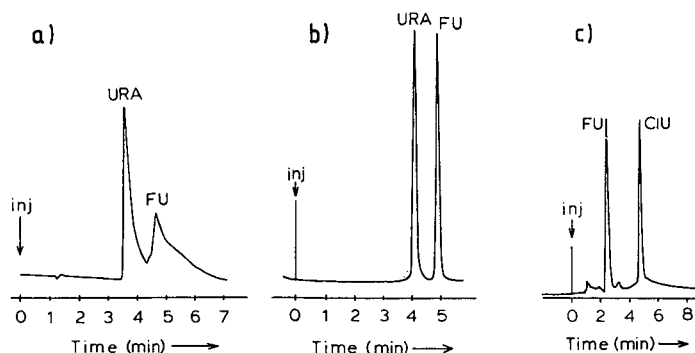


Fig. 6. On-line desorption of the analytes to the analytical column (a) by flushing the Ag(I)-thiol column with the LC mobile phase (URA=uracil), (b) by injecting 60 μl HNO_3 (pH 1.2), (c) by injecting 340 μl DTC-CTAB (1 mM, pH 6.0 adjusted with 10 mM acetate buffer) (CU=5-chlorouracil). Conditions: $5 \cdot 10^{-6}$ M of analytes (preconcentration of 1.0 ml); carrier flow-rate 0.6 ml/min; pH of the sample solution: 11.0; LC conditions: see Experimental.

with, for example, the LC eluent which has a pH of 5.8. However, slow desorption kinetics at pH 5.8 resulted in considerable peak broadening and asymmetry as shown in Fig. 6a. A lower pH value is necessary for efficient desorption and therefore plugs of HNO_3 were injected into the LC eluent (see Fig. 2). The use of 0.01 M HNO_3 resulted in improved peak shapes and optimum results were obtained at pH 1.2 (Fig. 6b).

The volume of the displacer solution is also critical in determining the desorption efficiency. The displacer volume should be large enough to efficiently desorb the analytes from the pre-column, but care should be taken not to introduce volumes too large that cause deterioration of analytical column performance. Starting with a nitric acid volume of 340 μl we could reduce this to 60 μl without loss of efficiency. Using larger volumes of higher pH resulted in poor peak shapes. This indicates that a small volume of nitric acid of low pH produces a narrow elution zone in which the sorbed analytes can be rapidly and efficiently protonated, resulting in a favorable elution profile (Fig. 6b). For means of comparison a chromatogram of FU and 5-chlorouracil obtained by the use of DTC-CTAB as a displacer (plug injection of 340 μl) is shown in Fig. 6c. While peak shapes and recoveries of the test components are similar to those obtained with protonation, the latter method has the disadvantage that an additional C_{18} pre-column is required for the removal of the excess of DTC-CTAB and that the Ag(I)-thiol pre-column must be regenerated after each preconcentration step.

In all subsequent experiments desorption of the analytes was performed by injecting a 60- μl plug of nitric acid (pH 1.2). Chromatograms of a 12- μl direct injection (concentration of the model compounds: $5 \cdot 10^{-5}$ M) and after preconcentration and desorption of a 1.0-sample of the model compounds at a concentration of $5 \cdot 10^{-7}$ M are shown in Fig. 7 (for the lower uridine recovery, see Fig. 3). Column efficiency measured in terms of plate number for FU was compared for direct injections and for 1.0 ml preconcentrations and showed only a slight decrease: 9000–10 000 for preconcentration vs. 11 000 for direct injection, indicating that the de-

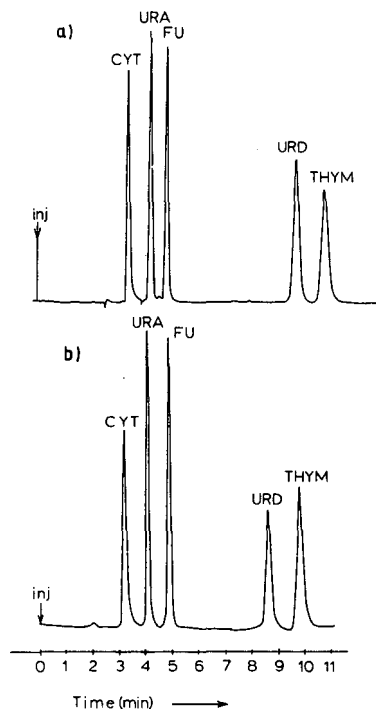


Fig. 7. Direct injection ($12 \mu\text{l}$, $5 \cdot 10^{-5} M$) and pre-concentration (1.0 ml , $5 \cdot 10^{-7} M$) of cytosine (CYT), uracil (URA), FU, uridine (URD) and thymine (THY). Conditions: carrier flow-rate, 0.6 ml/min , pH of the sample solution, 11.0 (pre-concentration), 5.8 (direct injections); attenuation, 0.02 a.u.f.s.; LC conditions, see Experimental.

sorption step causes *no* appreciable band broadening. The reproducibility for the pre-concentration of $5 \cdot 10^{-7} M$ FU was 2.3% ($n = 6$).

Regeneration of the pre-column packing

Veuthey *et al.*²⁰ eluted amino and carboxylic acids from a Cu(II) -dithiocarbamate stationary phase via protonation by flushing with the LC eluent of pH 2. Similarly, for the pyrimidine nucleobases desorption via analyte protonation leaves the silver bound to the thiol ligand and the Ag(I) -thiol phase can be continuously re-used. Each desorption step is at the same time a pre-column regeneration step. Although we found that when working with standards the Ag(I) -thiol pre-column can be used over a period of several days before noticeable deterioration of sorption occurs, it is advisable to pack a new pre-column daily, especially when complex sample matrices are introduced into the system.

Chromatography and detection

The capacity factors of the uracil derivatives are very small on a C_{18} analytical column with pure water as eluent. This system is therefore not well suited for the analysis of complex samples. We found that adding CTAB to the mobile phase, although not influencing the k' values of cytosine and uracil, produced excellent

separation and peak shapes of these compounds, whereas elution of uridine and thymine was retarded. For cytosine and uracil retention is not governed by an ion-pairing mechanism; the addition of CTAB serves mainly to cover residual silanol groups of the C_{18} phase, thereby reducing the tailing of polar compounds. In the case of FU, a small fraction of which is deprotonated at pH 5.8 ($pK_a = 7.6$), ion-pairing with CTAB may contribute to the overall retention mechanism which is indicated by higher capacity factors at increasing CTAB concentrations. Peters *et al.*²¹ used ion-pairing chromatography of the anion forms of the uracil derivatives at high pH on a hydrophobic PRP-1 polymer phase; however, such packing material will not give as high a column efficiency as a C_{18} column of the same length.

Both variable-wavelength UV detectors showed excellent linearity over three orders of magnitude in the concentration range of interest ($10^{-6} - 10^{-8} M$) with a correlation coefficient of 0.9998. Using the Kratos Spectroflow 757 a detection limit for FU of 0.4 ng ($3 \cdot 10^{-9} M$ for the preconcentration of 1.0 ml) was reached at 269 nm.

In order to increase the selectivity of the analytical system fluorescence detection was investigated. The fluorescence of FU and thymine is strongly pH-dependent and reaches maximum intensity at pH 12 (ref. 22). Achieving this pH value required post-column addition of NaOH (pH 12.1) via a mixing piece. From all compounds investigated only FU and thymine yielded a fluorescence signal. The detection limit was $2 \cdot 10^{-7} M$, or 26 ng FU which is almost two orders of magnitude higher than UV detection; therefore the latter method is favoured.

Applications

Determination of 5-fluorouracil in human plasma. The determination of FU in a biological matrix is an important application of on-line enrichment on a silver-loaded stationary phase. We therefore wanted to demonstrate that FU can be determined in, for example, human plasma. Deproteinized as well as non-deproteinized plasma samples were preconcentrated.

With non-deproteinized samples an additional PLRP pre-column was inserted between valves I and III (see Fig. 2) in the trace-enrichment scheme to trap apolar compounds. The blank plasma samples, however, gave rise to irregular interferences in the baseline as well as several large peaks eluting after approximately 13 min, indicating that the PLRP pre-column was not efficient enough in trapping interfering plasma components.

As an alternative, the plasma was deproteinized off-line prior to trace enrichment. Methanol was selected to this end, because its use is not accompanied by the drastic pH lowering which accompanies precipitation with trichloroacetic acid. Precipitation was carried out at neutral pH, the supernatant was adjusted to pH 11.0, and the sample was then introduced into the preconcentration system. Chromatograms of blank and spiked plasma samples after trace enrichment of 0.5-ml volumes are shown in Fig. 8. Even at the lowest detector attenuation setting, the plasma blank showed a rather undisturbed baseline in the region where the pyrimidine bases elute and FU concentrations of $2.5 \cdot 10^{-7} M$ could be determined in spiked plasma with an estimated detection limit of $10^{-7} M$. Several later eluting (> 25 min) non-identified peaks most likely represent other compounds containing the pyrimidine ring such as nucleotides and polar plasma constituents which are also sorbed on the Ag(I)-thiol phase.

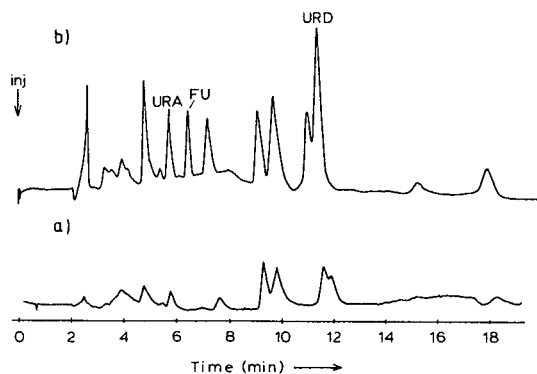


Fig. 8. Determination of FU in plasma (a) plasma blank; attenuation, 0.04 a.u.f.s. (b) Plasma spiked with $2.5 \cdot 10^{-7} M$ FU; attenuation, 0.01 a.u.f.s. Conditions: 0.5 ml plasma deproteinized with an equal volume of methanol, pH of the sample solution, 11.0; carrier flow-rate, 0.6 ml/min; LC conditions, see Experimental.

Determination of bromacil in surface water. The herbicide bromacil can be determined in surface and tap water by the above described method. Bromacil is structurally related to the parent compound uracil (see Fig. 1), but the N-3 ring position is not free for complexation to silver as it is occupied by an isobutyl group. Complexation can only occur at the N-1 position which is still subject to keto-enol tautomerism with the carbonyl oxygen. The question arose whether the minimum structure required for effective complexation with silver as a single H-N-C=O ring moiety.

Under the optimum operating conditions (described in Experimental) we were

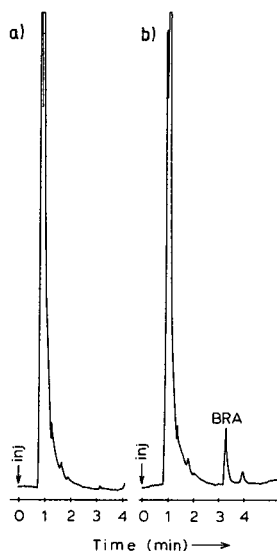


Fig. 9. Determination of bromacil in surface water. (a) Surface water blank; (b) surface water spiked with 15 ppb bromacil. Conditions: preconcentration of 3 ml; pH of the sample solution, 11.0; carrier flow-rate, 0.6 ml/min; attenuation, 0.01 a.u.f.s.; LC conditions, see Experimental.

able to preconcentrate bromacil on the Ag(I)-thiol stationary phase in the low-ppb range. Chromatograms obtained after preconcentrating 3.0 ml volumes of blank surface water spiked to 15 ppb are shown in Fig. 9. The detection limit for bromacil was 1.5 ppb (4.5 ng) for the preconcentration of 3-ml sample volumes. Sample volumes of up to 12 ml can be preconcentrated without breakthrough. With this method it is possible to determine low-ppb amounts of bromacil in water samples without the need for tedious and time-consuming sample pretreatment. Ease of automation of this method will enable large sample throughput.

CONCLUSIONS

A Ag(I)-loaded thiol stationary phase shows excellent properties as sorbent for pyrimidine nucleobases and their derivatives. The sorption is governed by complexation of the pyrimidines with the silver ion, and is strongly pH dependent. Desorption proceeds via a simple protonation mechanism. A small volume of strong acid suffices to elute the analytes to the analytical column in a narrow band and plate numbers for FU were consistently in the order of 10 000 compared to 11 000 for direct injections.

On-line trace enrichment and LC determination of pyrimidine nucleobases and their derivatives was possible with a detection limit of $3 \cdot 10^{-9}$ M for standard solutions and $1 \cdot 10^{-7}$ M for FU in plasma using UV detection. Further optimization of the clean-up process may lead to even lower detection limits. The experimental system can be easily automated, which is desirable for routine monitoring.

Metal-loaded stationary phases offer, from the applications side, a means to preconcentrate moderately polar to polar compounds and can therefore be an important tool in the routine determination of these compounds in environmental and biological matrices^{8,23}. It has thus far not been possible to successfully preconcentrate these classes of compounds on other types of sorbents. Further investigation in the use of metal-loaded stationary phases for on-line trace enrichment may extend the method to a broad spectrum of polar heterocyclic aromatic compounds that show properties similar to the pyrimidine bases. These investigations will initially have to focus on the fundamental aspects of metal-analyte interaction and the displacement of the analyte from a metal-loaded phase. The choice of metal will depend on the type of analyte(s), their acid-base behaviour, and the nature of the electron donor (N or O donor). In larger molecules, for instance the purine compounds, steric factors may play a role in the complexation process in view of the heterogeneous interaction on the solid surface of the stationary phase. The central question of whether a "minimum" structure exists, which comprises one or more functional groups and a favorable electronic distribution within the molecule, and is responsible for the desired complexation characteristics, is currently under investigation.

REFERENCES

- 1 H. R. Mahler and E. H. Cordes, *Biological Chemistry*, Harper and Row, New York, 1971.
- 2 M. J. Scanlan and I. H. Hillier, *J. Am. Chem. Soc.*, 106 (1984) 3737.
- 3 J. P. Cano, J. P. Rigault, C. Aubert, Y. Carcassonne and J. F. Seitz, *Bull. Cancer*, 66 (1979) 67.
- 4 R. M. Kok, A. P. J. M. de Jong, C. J. van Groeningen, G. J. Peters and J. Lankelma, *J. Chromatogr.*, 343 (1985) 59.
- 5 J. X. Khyrn, *Clin. Chem.*, 21 (1975) 1245.

- 6 R. A. Hartwick, D. van Haverbeke, M. McKeag and P. R. Brown, *J. Liq. Chromatogr.*, 2 (1979) 725.
- 7 R. W. Frei, M. W. F. Nielen and U. A. Th. Brinkman, *Int. J. Environ. Anal. Chem.*, 25 (1986) 3.
- 8 M. W. F. Nielen, H. E. van Ingen, A. J. Valk, R. W. Frei and U. A. Th. Brinkman, *J. Liq. Chromatogr.*, 10 (1987) 617.
- 9 R. B. Martin and Y. H. Mariam, in H. Sigel (Editor), *Metal Ions in Biological Systems*, M. Dekker, New York, 1979, Ch. 2.
- 10 D. J. Hodgson, *Progr. Inorg. Chem.*, 23 (1977) 211.
- 11 J. G. M. de Ruyter and A. P. de Leenheer, *Anal. Chem.*, 51 (1979) 43.
- 12 B. Vonach and G. Schomburg, *J. Chromatogr.*, 149 (1978) 417.
- 13 E. Grushka and F. K. Chow, *J. Chromatogr.*, 199 (1980) 283.
- 14 G. J. Krauss, *J. High Resolut. Chromatogr. Chromatogr. Commun.*, 9 (1986) 419.
- 15 M. I. Gel'fman and N. A. Kostuva, *Russian J. Inorg. Chem.*, 15 (1970) 47.
- 16 M. I. Gel'fman and N. A. Kostuva, *Russian J. Inorg. Chem.*, 14 (1970) 1113.
- 17 Y. L. Tan and A. Beck, *Biochim. Biophys. Acta*, 299 (1973) 500.
- 18 P. Ghosh, T. K. Mukhopadhyay and A. R. Sarkar, *Trans. Met. Chem.*, 9 (1984) 46.
- 19 D. D. Perrin (Editor), *Stability Constants of Metal-Ion Complexes, Part B: Organic Ligands*, Pergamon Press, Oxford, 2nd ed., 1978.
- 20 J. L. Veuthey, M. Bagnoud and W. Haerdi, *Int. J. Environ. Anal. Chem.*, 26 (1986) 157.
- 21 G. J. Peters, I. Kraal, E. Laurensse, A. Leyva and H. M. Pinedo, *J. Chromatogr.*, 307 (1984) 464.
- 22 D. Gningue and J. J. Aaron, *Talanta*, 32 (1985) 183.
- 23 M. W. F. Nielen, R. Bleeker, R. W. Frei and U. A. Th. Brinkman, *J. Chromatogr.*, 358 (1986) 393.

CHROM. 20 955

QUANTITATIVE MICROSCALE LIQUID CHROMATOGRAPHY OF PIPERINE IN PEPPER AND PEPPER EXTRACTS

M. VERZELE*, F. VAN DAMME and G. SCHUDDINCK

Laboratory of Organic Chemistry, State University of Ghent, Krijgslaan 281(S4), B-9000 Ghent (Belgium)
and

P. VYNCKE

RSL, Begoniastraat 5, B-9730 Eke (Belgium)

SUMMARY

Conventional and microscale liquid chromatographic (micro-LC) systems were compared for the determination of piperine in pepper and pepper extracts. A polyphenol-derivatized silica gel was used in normal-phase adsorption chromatography and with anthraquinone as an internal standard. Differences in capacity ratios (k') and in selectivities (α) were noted and are discussed. The standard deviation of the analysis is smaller for micro-LC, but the reasons are not obvious. Advantages claimed for micro-LC (better efficiency, permeability and quantitation) are illustrated.

INTRODUCTION

Piperine (4 in Fig. 1) occurs in concentrations of *ca.* 3–5% in ground pepper used for culinary purposes. Freshly picked pepper berries are “green pepper”, becoming “black pepper” on sun drying and “white pepper” when the dried outer shell of the berries is removed from the black variety. The geometric isomers of piperine, *i.e.*, chavicine, isopiperine and isochavicine (1, 2 and 3 in Fig. 1), also occur in pepper, but in very small amounts, together with other minor constituents of similar chemistry. We have shown that piperine is almost the only contributor to pepper pungency¹ and, therefore, that its quantitation is important. This analysis is not as easy as it may seem. For a long time, determination of the total nitrogen content was the preferred method for the quality evaluation of pepper. Hydrolysis and quantitation of the piperidine so formed has also been used. These methods do not determine piperine specifically, but rather a mixture of the stereoisomers and some other undefined compounds all together. Today it is obvious to turn to liquid chromatography (LC) for this analysis. The LC of pepper constituents and in particular the quantitation of piperine in peppers and the separation of the four possible piperine stereoisomers have been investigated by one of the laboratories involved in the present work^{2–4}.

Piperine is readily available by extraction of ground pepper with, *e.g.*, methylene chloride, and repeated crystallization of the extract residue from methanol–water until the melting point of the crystals is 131°C. The four stereoisomers are also easily

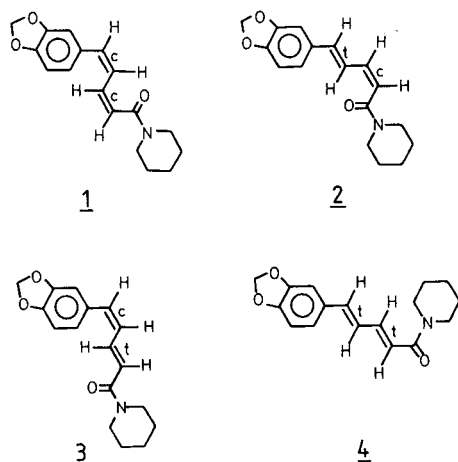


Fig. 1. Structural formulae of the four stereoisomers: 1, chavicine; 2, isopiperine; 3, isochavicine; 4, piperine.

accessible, as a mixture, since they are formed on irradiation of a methanolic piperine solution, eventually with sunlight. A 1-g amount of piperine dissolved in 100 ml of methanol and irradiated at 350 nm for 18 h affords a photostationary-state mixture containing the four stereoisomers (see Fig. 1) piperine (4, *trans-trans*), chavicine (1, *cis-cis*), isopiperine (2, *cis-trans*) and isochavicine (3, *trans-cis*). In this nomenclature for the diene system, the double bond closest to the piperidine ring is named first. These compounds are thus amides and as such can be hydrolysed. The four isomeric acids so obtained were separated by preparative chromatography and by counter-current distribution. Their structures were elucidated and assigned by NMR spectrometry⁵. Piperine or the *trans-trans* isomer has the highest UV molar absorptivity, the longest wavelength of maximum absorption and the highest melting point. The opposite is true for chavicine (the *cis-cis* isomer), as expected. The data are summarized in Table I.

The photostationary-state mixture is best suited for studying LC conditions for the quantitation of piperine. In our earlier investigations of the analytical chromatography of piperine, many stationary phases were evaluated. Although several phase systems were discovered that yielded partial or complete separation of the four stereoisomers, none was completely satisfactory. Either the phase was not characterized accurately enough and the reproducibility was therefore questionable, or the column stability was deficient or the peaks showed annoying tailing, rendering electronic integration difficult. The preparative chromatography mentioned above was carried out, for example, on alumina E (Merck, Darmstadt, F.R.G.) on a 1 m × 0.85 cm I.D. column. The resolution was good² but later we had considerable difficulty in reproducing the chromatogram or could not do so.

On nitrated-sulphonated phenyl silica gel, excellent selectivity with complete separation of the isomers has been achieved³. Later, however, we could not reproduce this phase with exactly the same selectivity characteristics. It is well known that the chromatographic separation of the stereoisomers of diene systems is difficult. Many

TABLE I
DATA FOR THE FOUR ISOMERS

Numbering as in Fig. 1.

Peak No.	Compound	M.p. ($^{\circ}$ C)	λ_{\max} (nm)	ϵ ($l\text{mol}^{-1}\text{cm}^{-1}$)	E^a	Fa^b
1	Chavicine	(75)	321	10 900	0.266	1.83
2	Isopiperine	86	335	13 200	0.207	2.00
3	Isochavicine	103	336	12 500	0.309	1.35
4	Piperine	131	343	34 100	0.418	1.00

^a E is the absorbance measured for a 1 mg per 100 ml solution at 252 nm.

^b Fa is the correction factor for quantitation of the photoisomers via peak areas versus piperine for measurements at 252 nm.

efforts were directed at finding solutions to this problem. High-surface-area silica gel chromatography can help and argentionation of silica gel is often a positive approach, but it cannot be said that these solutions are efficient, clean, reproducible, etc. Anyone with experience of argentionation chromatography knows how messy and capricious it can be.

We report here on a chromatographic system, with a polyphenol bonded to silica gel as the stationary phase, which produces acceptable peak shapes for piperine and its stereoisomers, good column efficiency and sufficient resolution of the mixture to allow quantitation, and that can be synthesized reproducibly. With the current interest in the miniaturization of LC, conventional and micro-LC were compared for the determination of piperine.

Micro-LC, or chromatography with packed fused-silica capillary columns, has several important advantages over conventional LC⁶⁻⁸. To date, micro-LC has mostly been applied to generate very large plate numbers in long columns and consequently with very long analysis times. We believe, however, that micro-LC with more usual column lengths of 10-30 cm has so many attractive features that it may well become the normal routine mode of chromatography in the near future. This paper illustrates some of the advantages of micro-LC over conventional LC.

EXPERIMENTAL

The chromatographic system for conventional LC consisted of a Model LC 5500 chromatograph, a Model 2050 UV detector and a Model CDS-401 integrator (Varian, Walnut Creek, CA, U.S.A.). The columns were 25 \times 0.46 cm I.D. Lichroma tubes provided with a 10- μ l sample loop injector (Valco, Houston, TX, U.S.A.). Polyphenol-RSiL (10 μ m) (RSL, Eke, Belgium) was packed downwards at 500 bar in a sonicated water-methanol (10:90) slurry. The columns were rinsed thoroughly with acetone, methanol-THF and hexane-methanol-THF (in that order) before equilibration with the mobile phase used for the chromatography. Alternatively, columns were packed with a 10% acetone slurry and with acetone as a follow-up solvent. All conventional LC was carried out with the columns in a thermostat.

The micro-LC system consisted of a Model LC 5020 chromatograph, a Model 2050 UV detector with a modified miniaturized cell (obtained from RSL) and a

Model CDS-401 integrator (Varian). The micro-LC columns (250×0.32 mm I.D., polyimide-coated fused silica) packed with $10\text{-}\mu\text{m}$ Polyphenol-RSiL and the split tee were obtained from RSL. The split tee was connected to a 100- μl injector (Valco C1 4W) and to an old spent column with conventional dimensions. The tee, columns and injector were placed in a water-bath thermostat.

Peppers and pepper extracts were obtained from the local market. Anthraquinone (internal standard) was purified by repeated crystallization from ethanol. Solvents were of LC grade.

RESULTS AND DISCUSSION

Chromatography of piperine and its stereoisomers

Polyphenol-RSiL is intended to be used as a strongly polar normal-phase stationary phase. It is synthesized by bonding a tannin on to silica gel. It is more polar than silica gel itself^{9,10}. A fairly large amount of modifier can therefore be used in the normal-phase solvent mixture, which is beneficial for the speed of phase equilibration and for the general reproducibility of the chromatography. Hexane mixed with various amounts of methanol, THF and dioxane was tested for the optimization of the separation of the photostationary-state mixture of the piperine stereoisomers. The best result was obtained with hexane-THF (60:40).

The elution sequence of the four stereoisomers can be established by following the changes in the composition of a pure piperine solution subjected to a photoisomerization experiment. Isochavicine appears first in the chromatogram, next to the piperine peak, then isopiperine becomes visible and finally chavicine. In the final photostationary-state mixture, chavicine is the largest peak. The elution sequence for the four stereoisomers on Polyphenol-RSiL is first chavicine, then isopiperine, isochavicine and finally piperine. On nitrated-sulphonated phenyl silica gel³ the LC elution sequence is chavicine, isochavicine, isopiperine and piperine. On acid-buffered (pH 2.5) silica gel⁴ the order of elution is chavicine, isopiperine, isochavicine and piperine. On alumina² the elution sequence is isochavicine, isopiperine, chavicine and piperine. On Polyphenol-RSiL the elution sequence is the same as on acid-buffered silica gel. The reason for these selectivity differences is unknown to us. Alumina is basic, whereas nitrated-sulphonated and polyphenol phases are fairly acidic, but this does not explain the results. Hydrogen bond formation is always important in adsorption chromatography but nothing can be deduced in this respect from the structures in Fig. 1. Rotation around the single bonds of the conjugated system is free. The conformations shown in Fig. 1. are therefore not the only important ones, although conformational equilibration is probably slow.

An increased temperature proved to have a positive effect on the chromatographic separation of the photoisomers. Fig. 2 shows the chromatograms obtained with the micro-LC system at 25, 40 and 50°C. Some data deduced from these chromatograms are given in Table II.

Similar results for the conventional LC system are shown in Fig. 3 and Table III. It is obvious that an LC determination of piperine can be based on both systems.

Efficiency (plate number) of the columns

The efficiency of the conventional LC column measured for piperine at the

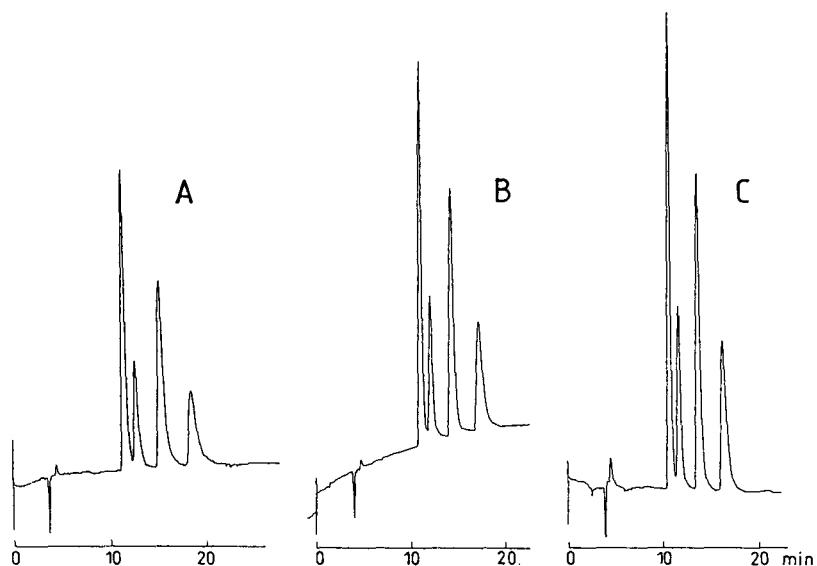


Fig. 2. Chromatograms obtained with a 250×0.32 mm I.D. fused-silica capillary column packed with $10\text{-}\mu\text{m}$ Polyphenol-RSiL. Mobile phase, hexane-THF (60:40) at $4\ \mu\text{l}/\text{min}$. UV detection at 252 nm. Peaks in order of appearance: 1, chavicine; 2, isopiperine; 3, isochavicine; 4, piperine. Temperature: (A) 25°C ; (B) 40°C ; (C) 50°C . Back-pressures at the split tee (A) 24; (B) 20; (C) 18 bar. Sample: 100 nl of the photo-stationary-state mixture obtained after irradiation for 18 h in a Rayonet photoreactor. Solution in hexane-dioxane.

TABLE II

MICRO-LC OF PIPERINE AND STEREOISOMERS AT VARIOUS TEMPERATURES (FIG. 2)

Parameter	Compound	Temperature ($^\circ\text{C}$)		
		25	40	50
Retention time (min)	Chavicine	11.22	10.92	10.53
	Isopiperine	12.48	12.03	11.53
	Isochavicine	15.03	14.20	13.48
	Piperine	18.33	17.07	16.08
k' Values	Chavicine	1.95	1.87	1.77
	Isopiperine	2.28	2.16	2.03
	Isochavicine	2.95	2.74	2.53
	Piperine	3.82	3.49	3.23
Plates/m	Chavicine	18.833	23.124	26.686
	Isopiperine	17.799	21.553	25.333
	Isochavicine	14.299	19.808	22.304
	Piperine	11.979	15.095	18.220
Peak asymmetry factor	Chavicine	2.56	2.44	2.16
	Isopiperine	2.85	2.17	2.03
	Isochavicine	3.23	2.72	2.52
	Piperine	2.98	3.22	2.83

optimum flow-rate is only 8000–12 000 plates/m, whereas micro-LC columns under comparable conditions lead to 12 000–18 000 plates/m (Tables II and III). This difference is large enough to be important. Usually 10- μm RSiL materials produce much larger plate numbers. For the very best micro-LC and conventional columns packed with high-quality reversed-phase materials (5- μm ROSiL-C₁₈-D) and with a compact rigid molecule such as pyrene as a sample, the efficiency is about the same on the two systems. It is easier, or more readily possible, with micro-LC to achieve very good results (reduced plate height below 2), but this low h value (above 100 000 plates/m) can also be achieved with conventional column dimensions. In not such ideal situations (as in the present example with complex molecules such as piperine), the higher efficiency of micro-LC is more evident. The low plate numbers for the determination of piperine with both systems is ascribed to the complexity of the piperine molecule and to slow conformational equilibration. A temperature increase is important in these instances, as shown in Tables II and III. The present results therefore illustrate that micro-LC can be more efficient (*ca.* 50%?; see below) than conventional LC. Why this is so is not clear, but it is an important aspect of micro-LC that merits further investigation.

Mostly in LC, the plate numbers increase with increasing k' value because the contribution of the extra-column dead volume decreases with longer retention. This is the case, for example, for polycyclic aromatic hydrocarbons in reversed-phase LC. The effect is even greater for micro-LC where the dead volume is relatively more important because of the small total volume of the system. The plate numbers for the four piperine stereoisomers decrease, however, with increasing retention. In comparing the efficiency of micro-LC and conventional LC for the same compound, *e.g.*,

TABLE III
CONVENTIONAL LC OF PIPERINE AND STEREOISOMERS AT VARIOUS TEMPERATURES (FIG. 3)

Parameter	Compound	Temperature ($^{\circ}\text{C}$)		
		30	40	50
Retention time (min)	Chavicine	13.75	12.88	12.27
	Isopiperine	15.26	14.23	13.48
	Isochavicine	17.33	16.08	15.14
	Piperine	21.44	19.77	18.52
k' Values	Chavicine	2.82	2.58	2.41
	Isopiperine	3.24	2.95	2.74
	Isochavicine	3.81	3.47	3.21
	Piperine	4.96	4.49	4.14
Plates/m	Chavicine	13.416	16.804	19.696
	Isopiperine	13.196	16.424	18.936
	Isochavicine	11.340	14.188	16.636
	Piperine	7.864	9.780	11.612
Peak asymmetry factor	Chavicine	2.47	2.28	2.09
	Isopiperine	—	—	—
	Isochavicine	2.77	2.47	2.28
	Piperine	3.11	2.84	2.60

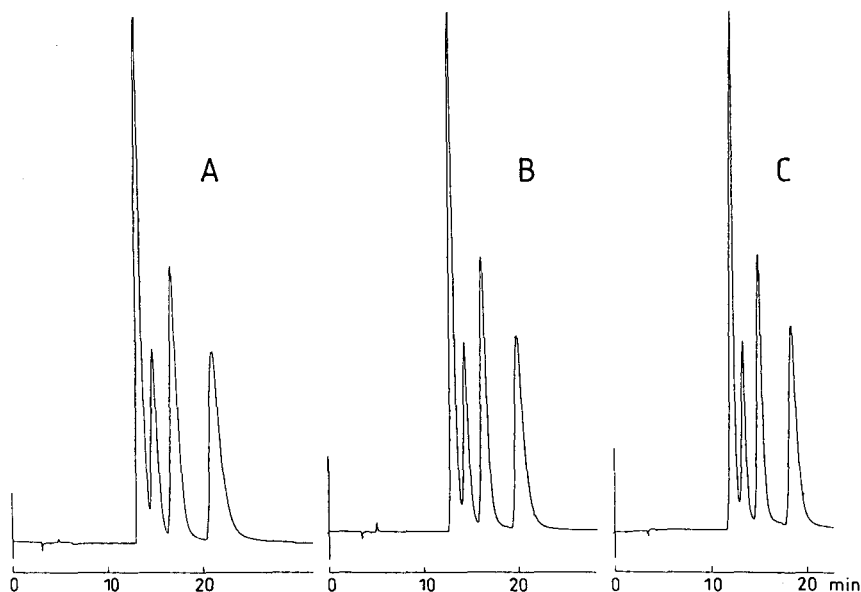


Fig. 3. Chromatograms obtained with a 25×0.46 cm I.D. column packed with $10\text{-}\mu\text{m}$ Polyphenol-RSiL. Mobile phase, hexane-THF (60:40) at 0.8 ml/min. UV detection at 252 nm.- Peaks in order of appearance: 1, chavicine; 2, isopiperine; 3, isochavicine; 4, piperine. Temperature: (A) 30°C ; (B) 40°C ; (C) 50°C . Back-pressures: (A) 34; (B) 32; (C) 30 bar. Sample injected: $10\ \mu\text{l}$ of the same solution as in Fig. 2.

piperine, this effect of the k' value should be considered. The piperine micro-LC peak at 50°C is 50% more efficient than the conventional piperine peak at 50°C , but its k' value is much lower. Even when almost identical k' values in Tables II and III are compared, micro-LC is found to be more efficient. With its lowest k' values, conventional LC does not achieve more than 20 000 plates/m in Table III. Micro-LC does better, even with k' values that are higher. Similar results were noted with a large number of columns over a long period of time. This study therefore illustrates an important advantage of micro-LC, which is clearly more efficient than conventional LC.

Retention (k' values) and relative retention (α values) in both systems

The differences in k' values, which are on average about 30% higher on the conventional system than on the micro-LC system (see Tables II and III), deserve attention. They are due to a relatively small difference in the total porosities of the columns. From the dead time (measured with hexane) and the calculated empty column volume, it can be deduced that this total porosity is 0.56 for the conventional and 0.62 for the micro-LC columns. The resulting phase ratios [the β values in gas chromatography (GC)?] are 1.27 and 1.63, respectively, or about 25% higher for the micro-LC system. The phase ratio for adsorption LC (the mobile phase is a liquid and the stationary phase an adsorbent) cannot really be compared to the phase ratio in GC, since the adsorbent surface area is not strictly related to its volume. That such a relative small difference in total porosity would have such a dramatic influence on the k' values was at first a surprise, although of course normal with hindsight. The Pol-

phenol-RSiL stationary phase was the same in both chromatographic systems. The above observation leads us to believe that differences in k' values, often ascribed to different surface chemistries of derivatized silica gels (manufacturers are blamed!), might in fact often be due to such porosity differences. Differences in total porosity can thus, inversely, be deduced from differences in k' values. The smaller k' values in micro-LC illustrate the higher permeability of this form of chromatography. Higher permeability often means lower stability, but in the present instance it does not, because the columns are made from inner wall polymer-coated fused-silica capillary tubing. The stabilizing effects of "inner wall coating and other wall effects" were discussed recently¹¹. Under these conditions, the better permeability of micro-LC must be considered an advantage.

The k' values in the two chromatographic systems do not change proportionally to the same extent and therefore the α values are also slightly different in the two systems. This is shown in Table IV.

Analysis of Table IV shows that the compounds with a double bond *trans* to the amide function are selectively more retarded on the micro-LC system. These are the more polar compounds. Piperine elutes last under normal-phase adsorption conditions and first, or is unseparated, from the other stereoisomers under reversed-phase conditions. The higher polarity of piperine and isochavicine also conforms with other physical parameters of the compounds (higher melting point and longer wavelength of maximum absorption; see Table I). This therefore means that the micro-LC column appears to be more polar than the conventional column. We have no rational explanation for this effect.

Determination of piperine in peppers and pepper extracts

For the quantitative analysis of mixtures containing piperine and its stereoisomers, the detection wavelength is of course important, not only for the compounds to be measured, but also for the internal standard. We have previously used phloracetophenone⁴ and *p*-bromoacetanilide³ as internal standards (I.S.) for this analysis. The phase system with Polyphenol-RSiL is, however, different to that in the previous procedures. Therefore, a new internal standard had to be found. Anthraquinone proved to be a possibility as it can be purified thoroughly by recrystallization from ethanol, elutes before piperine in a relatively uncomplicated part of the chromatogram and has a UV absorption maximum at 252 nm, where the photoisomers of piperine have relatively flat and similar absorption characteristics. A calibration graph was established at this wavelength with various amounts of piperine and the

TABLE IV

α VALUES ON CONVENTIONAL AND MICRO-LC SYSTEMS AT 50°C

<i>Compounds</i>	<i>Conventional LC</i>	<i>Micro-LC</i>
Isopiperine/chavicine	1.14	1.15
Isochavicine/isopiperine	1.17	1.25
Piperine/isochavicine	1.29	1.28
Piperine/isopiperine	1.51	1.59
Piperine/chavicine	1.72	1.82

same concentration of anthraquinone. Each solution was analysed several times. The equation found for the micro-LC system was

$$Y = 0.190X - 0.108$$

where Y = surface ratio of piperine/I.S. and X = concentration ratio of piperine/I.S., with a correlation coefficient $r = 0.9999$. The same solutions were used to establish the calibration graph using the conventional LC system and the equation obtained was

$$Y = 0.196X - 0.160 \quad (r = 0.9989)$$

These two equations should, of course, be the same but are in fact slightly different. Neither line (Fig. 4) passes through the origin, and this effect is slightly more pronounced for the conventional LC system. A similar observation has been made in the analysis of hop and beer bitter substances¹². This effect implies that some of the material to be analysed disappears in the system, which was ascribed to the negative influence of metals (in the columns and frits and also in the packing material). This was to be expected for hop and beer bitter acids, as these compounds are notably sensitive to metal, but it was a surprise to find that piperine was also affected.

With the above-discussed possibilities, a method for the determination of piperine was developed. The extraction time for ground pepper was evaluated by analysis after extraction for 10, 30, 60, 90 and 1440 min. No difference in result was observed. The procedure is then as follows. A standard solution (0.06356 mg/ml) of anthraquinone in hexane-THF (60:40) is prepared and 25 ml are added to about 400 mg of ground pepper and stirred for 30 min in a vessel protected from light with aluminium foil. A 100- μ l volume of the supernatant is injected on to a 250 \times 0.32 mm I.D. micro-LC column packed with 10- μ m Polyphenol-RSiL. The measuring wavelength

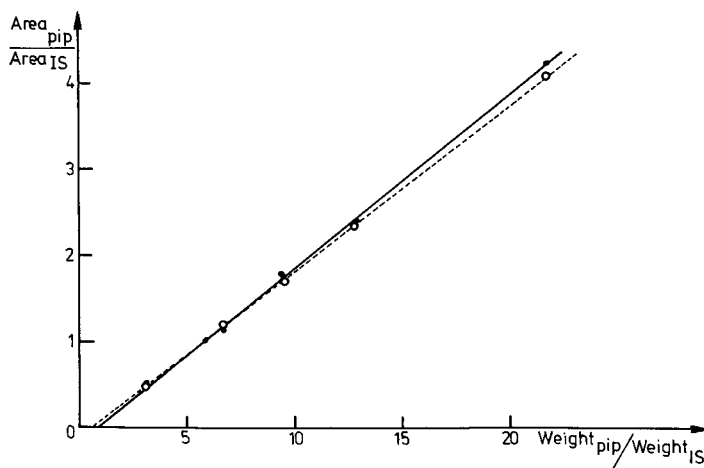


Fig. 4. Calibration graphs of peak surface area ratios *versus* weight ratios for piperine determination via micro-LC (○) and conventional LC (●). Internal standard, anthraquinone.

TABLE V
DETERMINATION OF PIPERINE BY MICRO-LC

The samples were obtained from local suppliers, except for the Zairese pepper and the extracts, which had been kept in the laboratory for more than 20 years without special precautions and apparently without much deterioration (see ref. 2). The Cayenne pepper is not supposed to contain piperine and its pungency is derived from other compounds.

Sample	Piperine (%)	Standard deviation	Relative standard deviation (%)
Black Liebig	3.95	0.5774	1.46
White Liebig	4.52	0.0306	0.68
Liebig Cayenne	0.00	—	—
Black Delhaize	4.44	0.0231	0.52
White Delhaize	4.80	0.0231	0.48
Maille 1747	4.52	0.0306	0.68
Zairese pepper (older than 1955)	1.36	0.0200	1.47
Extract (Fritzche)	26.71	0.4065	1.52
Extract (Chiris)	39.83	0.4521	1.14
Extract (Lampong)	33.26	0.2303	0.69

is 252 nm and the flow-rate of hexane-THF (60:40) is 4 μ l/min. The back-pressure (*ca.* 20 bar) is strongly dependent on temperature, but it is always lowest on the micro-LC columns (see the legends to Figs. 2 and 3). Results of the analyses were calculated with the calibration equations mentioned above. Table V shows some data for the determination of piperine in various peppers and pepper extracts following this procedure.

The standard deviations in Table V, obtained by running three analyses, are for the chromatographic run only. The mean relative standard deviation is 0.96%. The standard deviation for the total analysis (extraction and LC) was determined by running the same pepper analysis six times ($x = 4.52\%$, $s = 0.0346$, $s_{rel} = 0.77\%$).

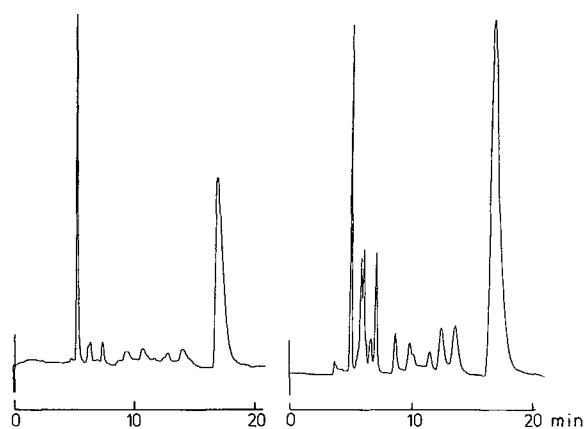


Fig. 5. Micro-LC traces for white Liebig pepper (left) and a Lampong pepper extract (right) with anthraquinone (first peak) as internal standard. Other conditions as in Fig. 2. The last peak is piperine.

TABLE VI
DETERMINATION OF PIPERINE BY CONVENTIONAL LC

Sample ^a	Piperine (%)	Standard deviation	Relative standard deviation (%)
Black Liebig	4.03	0.0608	1.51
White Liebig	4.55	0.0919	2.02
Liebig Cayenne	0.00	—	—
Black Delhaize	4.82	0.0611	1.27
White Delhaize	5.49	0.0636	1.16
Maille 1747	4.88	0.0636	1.31
Zairese pepper (older than 1955)	1.46	0.1556	10.66
Extract (Fritzche)	28.17	0.6450	2.29
Extract (Chiris)	39.92	1.3051	3.27
Extract (Lampong)	36.98	0.6689	1.81

^a As in Table V.

An example of an analytical chromatogram for white Liebig pepper and for an extract is shown in Fig. 5.

The same analyses were run on a conventional system. The amount injected was 10 μ l and the flow-rate 0.8 ml/min. The results are shown in Table VI. The mean relative standard deviation is 2.81%. Even if we exclude the outlayer of Zairese pepper, the relative standard deviation is still 1.83%, *i.e.*, considerably higher than for micro-LC. The micro-LC system was thermostated; this is more necessary with micro-LC than with conventional LC as the small micro-LC columns take up temperature fluctuations very easily. For strict comparison purposes the conventional chromatograms were also produced under thermostated conditions. Most of the results in Tables V and VI compare well, but there are differences that we cannot explain.

The above results indicate that better quantitation was achieved on micro-LC columns. A similar conclusion was drawn for the analysis of hop and beer bitter acids^{1,2}. With simpler systems and sample molecules such as phthalates or polycyclic aromatic hydrocarbons such a difference in the results given by the two chromatographic systems is not observed. Obviously, this "quantitation advantage" and the better permeability and efficiency of micro-LC deserve further attention.

ACKNOWLEDGEMENTS

We thank the Instituut tot Aanmoediging van het Wetenschappelijk Onderzoek in Nijverheid en Landbouw — IWONL, the Nationaal Fonds voor Wetenschappelijk Onderzoek — NFWO and the Ministerie voor Wetenschapsbeleid for financial support to our laboratories. We thank Varian Associates for the gift of a Model 5600 liquid chromatograph.

REFERENCES

- 1 R. De Cleyn and M. Verzele, *Bull. Soc. Chim. Belg.*, 84 (1975) 435.
- 2 R. De Cleyn and M. Verzele, *Chromatographia*, 8 (1975) 342.

- 3 M. Verzele, P. Mussche and A. Qureshi, *J. Chromatogr.*, 172 (1979) 493.
- 4 M. Verzele and A. Qureshi, *Chromatographia*, 13 (1980) 241.
- 5 M. Anteunis, R. De Cleyn and M. Verzele, *Org. Magn. Reson.*, 4 (1972) 407.
- 6 M. Verzele and C. Dewaele, *J. High Resolut. Chromatogr. Chromatogr. Commun.*, 10 (1987) 280.
- 7 M. Verzele, M. De Weerd, C. Dewaele, G. De Jong, M. Lammers and F. Spruit, *LC · GC, Liq. Chromatogr. Gas Chromatogr. Mag.*, 4 (1986) 1162.
- 8 D. Duquet, C. Dewaele and M. Verzele, *J. High Resolut. Chromatogr. Chromatogr. Commun.*, 11 (1988) 252.
- 9 F. Van Damme and M. Verzele, *J. Chromatogr.*, 351 (1986) 506.
- 10 M. Verzele, F. Van Damme, C. Dewaele and M. Ghijs, *Chromatographia*, 24 (1987) 302.
- 11 M. Verzele, C. Dewaele, M. De Weerd, S. Abbott, *J. High Resolut. Chromatogr. Chromatogr. Commun.*, (1989) in press.
- 12 G. Schuddinck and M. Verzele, *J. Chromatogr.*, 407 (1987) 159.

CHROM. 21 296

EFFECT OF PRESSURE DROP ACROSS THE COLUMN ON AVERAGE DENSITIES AND CAPACITY FACTORS IN SUPERCRITICAL FLUID CHROMATOGRAPHY

KEITH D. BARTLE, TERRY BODDINGTON, ANTHONY A. CLIFFORD* and GAVIN F. SHILSTONE

School of Chemistry, University of Leeds, Leeds LS2 9JT (U.K.)

SUMMARY

Calculations have been carried out of the average densities and capacity factors in supercritical fluid chromatographic (SFC) columns, taking into account the effect of the pressure drop along the column using, as examples, carbon dioxide as the mobile phase and phenanthrene as the solute. The values obtained were compared with those predicted for the mean pressure in the column. Differences are found which can be substantial for both the density and the capacity factor. Maximum deviations are found to move to higher pressures as the temperature rises. The effect of pressure drop needs to be taken into account by those using SFC to make quantitative measurements.

INTRODUCTION

In supercritical fluid chromatography (SFC) there will be a pressure drop across the column which will vary from around 1 bar for a short capillary column up to say 30 bar for some packed columns. Properties relevant to SFC, such as the density of the mobile phase, ρ , the dynamic viscosity, η , the capacity factor, k' , and the diffusion coefficient will vary with pressure along the column and do this more dramatically in the region of the critical point. The effect of pressure drop along a column in capillary SFC has been discussed theoretically by Peaden and Lee¹. They use a model in which the mobile phase pressure and density drop is linear with distance along the column. These approximations are less valid near the critical point, but the model does allow a comprehensive analysis of separation, efficiency and resolving power. Schoenmakers and Unk² have recently published an experimental and theoretical study of the effect of pressure drop on retention and efficiency in packed-column SFC using an alternative simple model. The present theoretical study is restricted to a discussion of average density and capacity factor, but uses a more exact treatment and experimentally based physical properties.

The capacity factor exhibited experimentally by a column and the density needed to convert retention times to retention volumes will be averages obtained by integration along the column. When quantitative measurements are made these are often referred to the mean pressure along the column, $p_{\text{mean}} = (p_{\text{in}} + p_{\text{out}})/2$, which assumes

that the pressure is dropping linearly with distance along the column, in a similar approach to those described above. The purpose of this paper is to test this model and compare the calculated true average density, $\langle \rho \rangle$, and capacity factor, $\langle k' \rangle$, with their respective values for the mean pressure for a model system: the chromatography of phenanthrene in carbon dioxide under various conditions. The work was carried out to test the validity of a quantitative study of the retention properties of polyaromatic hydrocarbons in packed-column SFC³, and data for phenanthrene obtained in this study are used as model data in the calculations given below. The results obtained are relevant whenever retention data are used to make quantitative physical property measurements, for example when supercritical fluid solubilities are obtained from chromatographic studies^{4,5}.

An asymptotic analysis of the problem of chromatography in a coated capillary column in which there is a pressure drop, and the parameters are an arbitrary function of pressure, has been carried out⁶. This shows that under typical chromatographic conditions, where the fractional change in pressure and the parameters which depend on it are small over a distance equal to the capillary radius, flow is essentially axial, and the formula given below are a very good approximation. A simpler and approximate derivation of the formulae is given here, which assumes axial flow and that the Poiseuille equation can be applied over short sections of the capillary. Although derived here for a uniform capillary column, the final results (eqns. 6 and 10) are approximately applicable to a packed column, where the pressure drop problem is more serious.

THEORY

According to Poiseuille's equation, the mean volume flow-rate, v , along a uniform cylindrical tube of radius a is given by

$$v = -(\pi a^4/8\eta)(dp/dl) \quad (1)$$

where dp/dl is the pressure gradient along the tube. The volume flow-rate varies along the tube as expansion takes place, but the mass flow rate, $m = \rho v$, is a constant. Substituting for v in eqn. 1 gives an equation for the pressure gradient,

$$dp/dl = -(8m/\pi a^4)(\eta/\rho) \quad (2)$$

The pressure falls non-uniformly along the tube determined by the dependence of the ratio η/ρ (the kinematic viscosity) on pressure. Some calculations of this ratio are presented below in Fig. 1. Rearrangement of eqn. 2 followed by integration over the column gives

$$m = (\pi a^4/8L) \int_{P_{out}}^{P_{in}} (\rho/\eta) dp \quad (3)$$

where L is the length of the column. Eqn. 3 gives a formula for the mass flow through

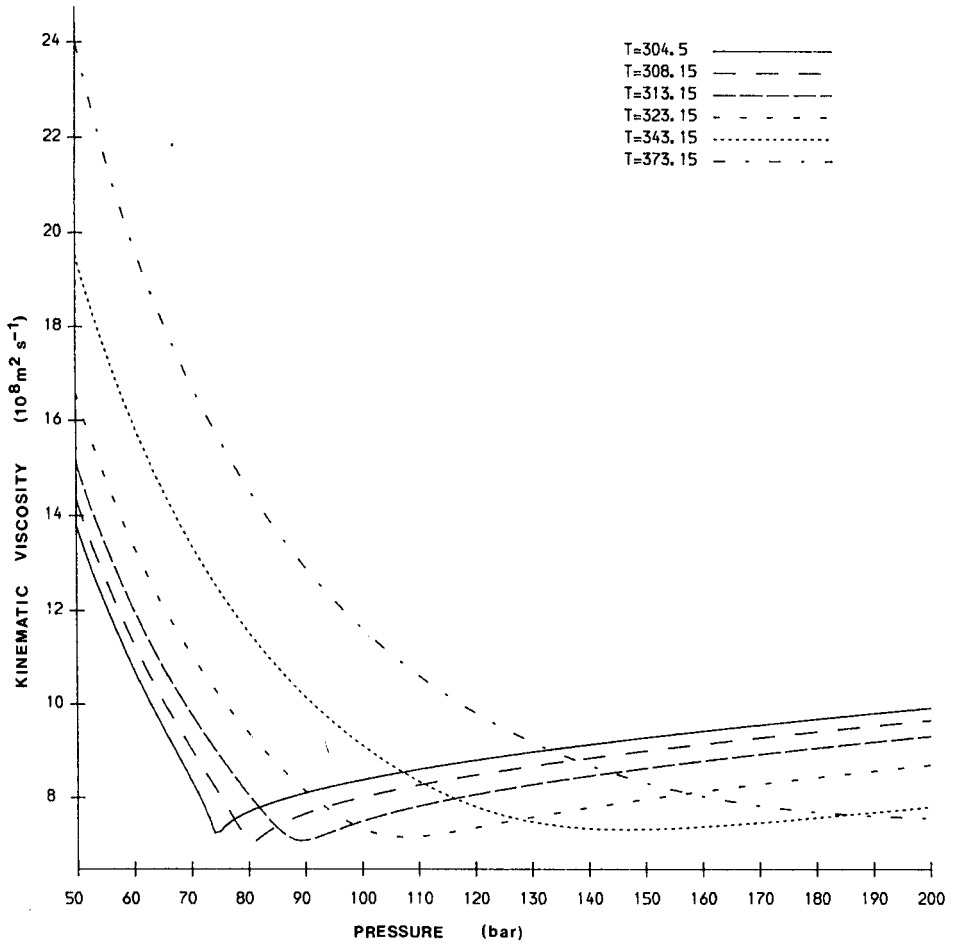


Fig. 1. Isotherms of the kinematic viscosity (η/ρ) as a function of pressure. The values are proportional to the pressure gradient (dp/dl) along a capillary. Temperatures in K.

a column in terms of its dimensions and a pressure integral of the properties of the mobile phase.

The average density in the column will be given by

$$\langle \rho \rangle = (1/L) \int_0^L \rho dl \tag{4}$$

After substituting for dl , using eqn. 2, this becomes

$$\langle \rho \rangle = (\pi a^4 / 8mL) \int_{p_{out}}^{p_{in}} (\rho^2 / \eta) dp \tag{5}$$

and on substitution for m using eqn. 3 we finally obtain

$$\langle \rho \rangle = \int_{p_{\text{out}}}^{p_{\text{in}}} (\rho^2/\eta) dp \left[\int_{p_{\text{out}}}^{p_{\text{in}}} (\rho/\eta) dp \right]^{-1} \quad (6)$$

Turning now to the calculation of $\langle k' \rangle$, the linear average velocity of a solute in the column, dl/dt , will be given by $v/\pi a^2(1+k')$, and thus

$$dt = (\pi a^2(1+k')/v) dl = -[\pi a^2 \rho(1+k')/m](dl/dp) dp \quad (7)$$

After substituting for dl/dp using eqn. 2 and integrating over the length of the column, we obtain t_R , the retention time of the solute in the column;

$$t_R = (a^2/8m^2) \int_{p_{\text{out}}}^{p_{\text{in}}} [\rho^2(1+k')/\eta] dp \quad (8)$$

For an unretained solute as k' tends to zero t_R becomes t_M , the retention time of the mobile phase, and thus

$$t_M = (a^2/8m^2) \int_{p_{\text{out}}}^{p_{\text{in}}} (\rho^2/\eta) dp \quad (9)$$

The average capacity is given by $\langle k' \rangle = (t_R - t_M)/t_M$, or

$$\langle k' \rangle = \int_{p_{\text{out}}}^{p_{\text{in}}} (\rho^2 k'/\eta) dp \left[\int_{p_{\text{out}}}^{p_{\text{in}}} (\rho^2/\eta) dp \right]^{-1} \quad (10)$$

CALCULATIONS AND RESULTS

Data for the density of carbon dioxide were obtained from the IUPAC formulation⁷, and for the viscosity from an ESDU report⁸. Calculations were first carried out to obtain the ratio η/ρ , to which the pressure gradient along the column is proportional (eqn. 2), and these are plotted as isotherms in Fig. 1. Calculations were then carried out of the percentage deviations of the average density (as given by eqn. 6) from the density at the mean pressure, *i.e.*, $100(\rho(p_{\text{mean}}) - \langle \rho \rangle)/\langle \rho \rangle$. Results at 308.15 K, close to the critical temperature, are plotted as a function of pressure in Fig. 2 for a 5-bar and a 30-bar pressure drop along the column. A diagram of the surface of these deviations as a function of pressure and temperature is also given in Fig. 3 for a 30-bar pressure drop.

For calculations of $\langle k' \rangle$ some model data for k' as a function of pressure and temperature are required and these were obtained from published data³ for

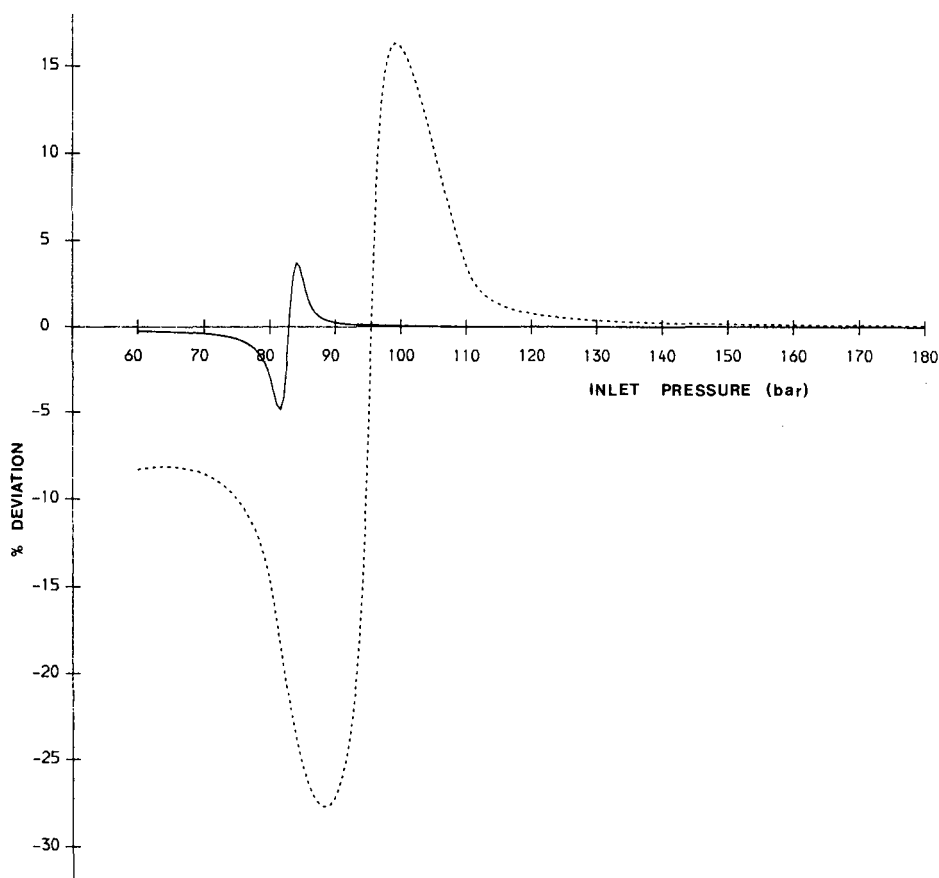


Fig. 2. Percentage deviation of the average density in a column from the density at the mean pressure, 100 ($\rho(p_{\text{mean}}) - \langle \rho \rangle$) / $\langle \rho \rangle$, as a function of inlet pressure at 308.15 K for a 5-bar (—) and 30-bar (---) pressure drop across the column.

phenanthrene in a 250 mm \times 4.6 mm I.D. ODS-2 column as follows. This study showed that the quantity $(\ln k' + \ln c - \ln \varphi)$, where c is the concentration of the supercritical fluid and φ the fugacity coefficient of the solute in the supercritical phase, is approximately a straight-line function of $1/T$. The linear relationship obtained for phenanthrene was used to back-calculate k' at any pressure and temperature, using c obtained from the density of pure carbon dioxide and φ obtained from the Peng–Robinson equation of state¹⁰ and the parameters given in the reference. An example of an isotherm of k' versus pressure at 328.15 K is given in Fig. 4. This can be compared with experimental isotherms for similar compounds¹⁰ and shows that it is reasonable model data.

Calculations were then carried out, using eqn. 10, of the percentage deviation of the average capacity factor over a column from the capacity factor at the mean pressure, *i.e.* $100(k'(p_{\text{mean}}) - \langle k' \rangle) / \langle k' \rangle$. These deviations are plotted at 308.15 K as a function of pressure in Fig. 5, for a 5-bar and a 30-bar pressure drop along the

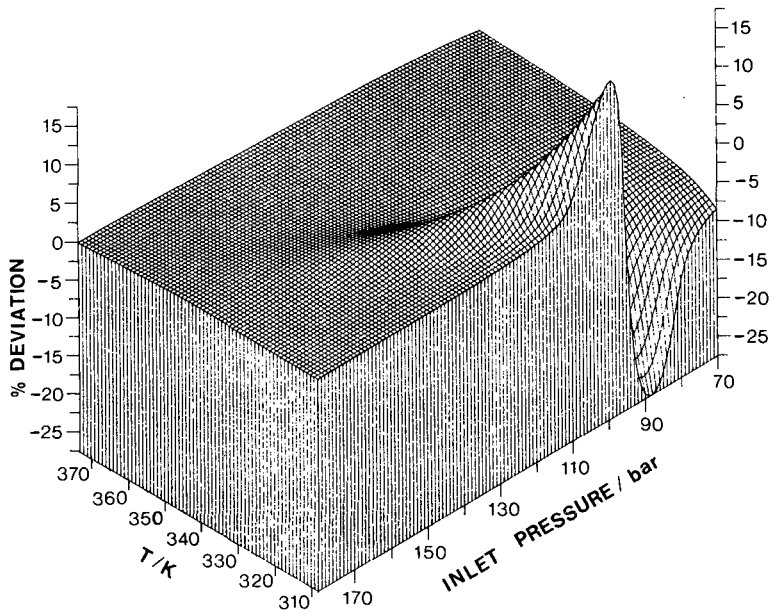


Fig. 3. Percentage deviation of the average density in a column from the density at the mean pressure, $100(\rho(p_{\text{mean}}) - \langle \rho \rangle) / \langle \rho \rangle$, as a function of inlet pressure and column temperature for a 30-bar pressure drop across the column.

column. A diagram of the surface of these deviations as a function of pressure and temperature is also given in Fig. 6 for a 30-bar pressure drop.

DISCUSSION

The pressure gradient along the column, according to eqn. 2, is proportional to the kinematic viscosity η/ρ . The curves on Fig. 1 therefore show how the pressure gradient (dp/dl) varies along a column as the pressure changes at various temperatures from 31.35°C (just above the critical temperature) to 100°C. Considering a long capillary, where the pressure fell from 100 bar to 50 bar, we can see that the pressure would fall fairly uniformly along the tube at first, but that the rate of fall would slow down to a minimum. The pressure gradient would then rise rapidly towards the end of the tube as the fluid becomes more gas-like. The minimum of dp/dl is near the critical pressure at a temperature close to the critical temperature, but rises to higher pressures (*i.e.*, towards more typical SFC pressures) as the temperature rises.

Figs. 2 and 3 show deviations of the average density from the density at the mean pressure. These are greatest at the lowest temperature, being around 25% for a 30-bar pressure drop among the column and a few percent for a 5-bar drop. The deviations fall off as the temperature rises, but move to higher pressures reflecting the behaviour of the minima in the kinematic viscosity curves.

Capacity factors change over several orders of magnitude over the range 70 bar to 170 bar as can be seen in the example for phenanthrene in Fig. 4. More dramatic

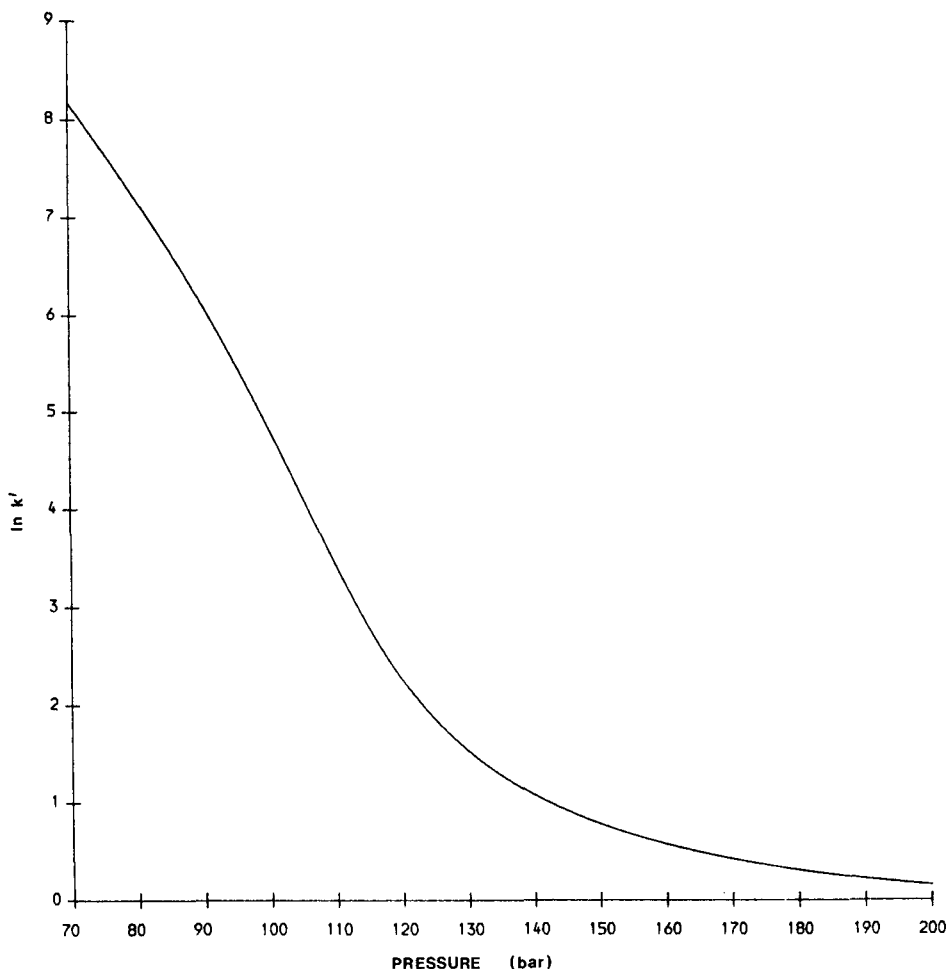


Fig. 4. An example of model data for the retention of phenanthrene by an ODS-2 column using carbon dioxide at 308.15 K: the natural logarithm of the capacity factor, $\ln k'$, is plotted as a function of pressure.

deviations are consequently obtained between the capacity factor observed over a column with pressure drop and that predicted for the mean pressure. At 35°C deviations of 90% are calculated for a 30-bar pressure drop over the column and even 40% for a 5-bar drop as shown on Fig. 5. Fig. 6, the three-dimensional diagram, shows a wide ravine again moving to higher pressures as the temperature rises.

These calculations for the system carbon dioxide and phenanthrene illustrate the extent of the effects which arise from the non-linear drop in pressure among an SFC column, which need to be considered by those attempting to make quantitative measurements using SFC. As would be expected, the very large effects are around the mobile phase critical point, but they do extend some way from it and in an unsymmetrical way, such that they are not inconsiderable for the model system at

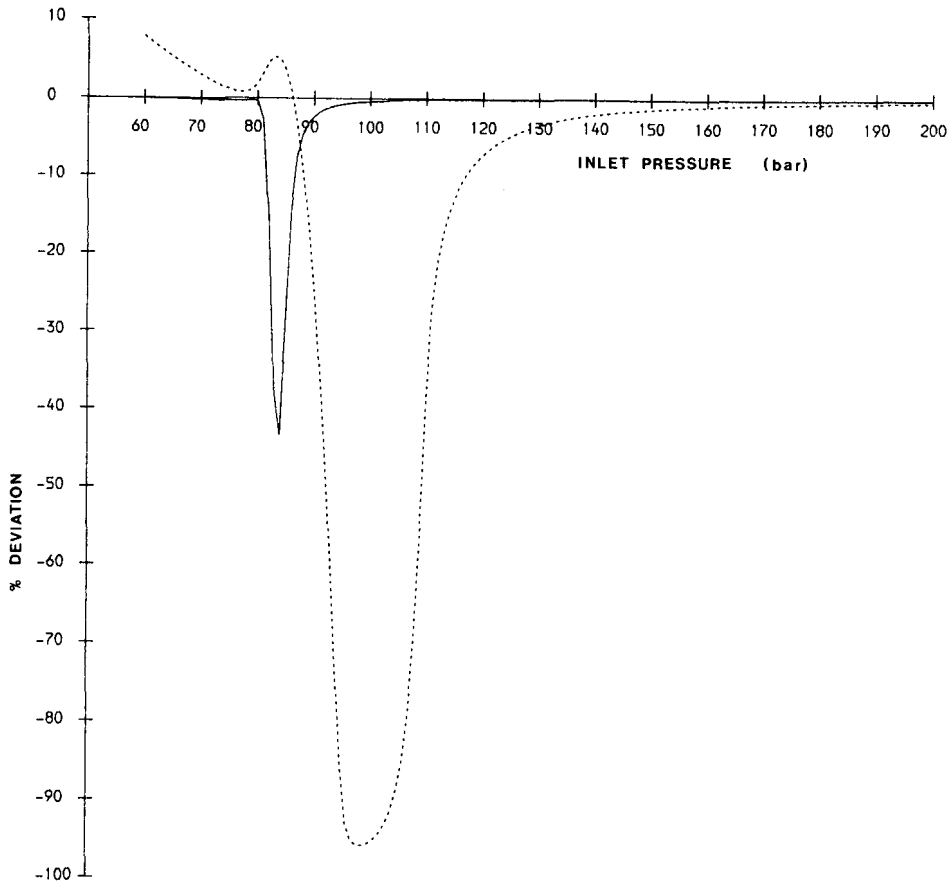


Fig. 5. Percentage deviation of the observed capacity factor, for columns with 5-bar (—) and 30-bar (---) pressure drops across the column, from the capacity factor calculated for the mean pressure, $100(k'(p_{\text{mean}}) - \langle k' \rangle) / \langle k' \rangle$, as a function of inlet pressure at 308.15 K.

a temperature of 70°C and a pressure of 150 bar, well above the critical values for carbon dioxide.

ACKNOWLEDGEMENT

The authors gratefully acknowledge financial support from the Science and Engineering Research Council (U.K.) in the form of a research grant and studentship (G.F.S.).

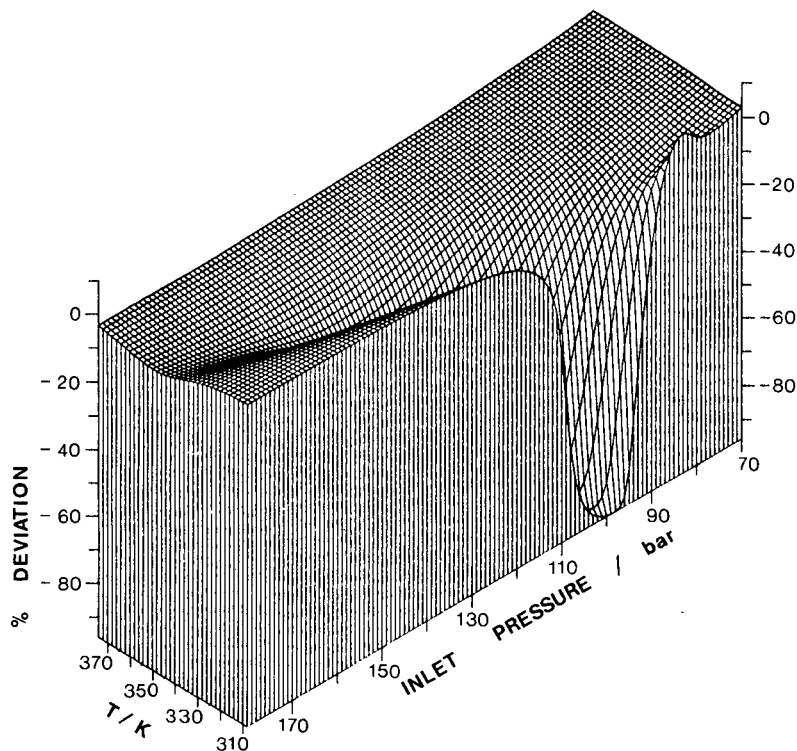


Fig. 6. Percentage deviation of the observed capacity factor for a column with a 30-bar pressure drop from the capacity factor calculated for the mean pressure, $100(k'(p_{\text{mean}}) - \langle k' \rangle) / \langle k' \rangle$, as a function of inlet pressure and temperature.

REFERENCES

- 1 P. A. Peadar and M. L. Lee, *J. Chromatogr.*, 259 (1983) 1.
- 2 P. J. Schoenmakers and L. G. M. Unk, *Chromatographia*, 24 (1987) 51.
- 3 K. D. Bartle, A. A. Clifford, J. P. Kithinji and G. F. Shilstone, *J. Chem. Soc., Faraday Trans. I*, 84 (1988) in press.
- 4 R. D. Smith, H. R. Usdeth, B. W. Wrigt and C. R. Yonker, *Sep. Sci. Technol.*, 22 (1987) 1065.
- 5 I. K. Barker, K. D. Bartle and A. A. Clifford, *Chem. Eng. Commun.*, 68 (1988) 177.
- 6 T. Boddington, personal communication.
- 7 S. Angus, B. Armstrong and K. M. de Reuck, *International Thermodynamic Tables of the Fluid State, Vol. 3, Carbon Dioxide*, Pergamon Press, Oxford, 1976.
- 8 *Dynamic Viscosity of Carbon Dioxide Gas and Liquid*, Engineering Sciences Data Unit, London, 1976.
- 9 D. Y. Peng and D. Y. Robinson, *Ind. Eng. Chem. Fundam.*, 15 (1976) 59.
- 10 C. R. Yonker, R. W. Gale and R. D. Smith, *J. Phys. Chem.*, 91 (1987) 3333.

CHROM. 21 292

ADSORPTION ISOTHERMS ON SILICA FOR METHANOL AND 1-HEXANOL MODIFIERS FROM SUPERCRITICAL CARBON DIOXIDE

C. H. LOCHMÜLLER* and L. P. MINK

Department of Chemistry, Duke University, Durham, NC 27706 (U.S.A.)

SUMMARY

Adsorption isotherms were determined for methanol and 1-hexanol on silica from supercritical carbon dioxide at four temperatures and three mobile phase densities. Maximum stationary phase concentrations were extrapolated from linear least squares fits of the data to the Langmuir equation for monolayer adsorption. From these results, maximum surface area coverages were calculated using the mean molecular area of each modifier. The maximum, molar stationary phase concentration of methanol was found to exceed that of 1-hexanol under all experimental conditions; however, in each case the surface area coverage by hexanol was calculated to be larger.

The capacity factors of several substituted and unsubstituted aromatic hydrocarbons were determined in 0-1% (w/v) methanol modifier carbon dioxide. From the linearity of capacity factor *versus* modifier concentration plots, the ability of the solutes to compete with methanol for active column sites was determined. Unsubstituted aromatic hydrocarbons do not appear to compete with the modifier for direct adsorption onto modifier-sorbing active sites.

INTRODUCTION

Modifiers have been widely used in supercritical-fluid chromatography (SFC) to increase the solvent strength of the mobile phase, enhance selectivity, and improve peak shape and column efficiency^{1-12,14-16}. With packed columns, the effects of modifier addition on these parameters may result from changes in the nature of the stationary phase surface because of localized adsorption of the modifier onto active stationary phase sites, *e.g.*, silanols, or solvation of bonded phase moieties, as well as changes in the physical properties of the mobile phase. Localized adsorption on active sites is believed to be primarily responsible for the changes in retention and selectivity observed with packed columns at low mobile phase modifier concentrations^{6,7,11}. The extent of these changes depends on the type of solute, modifier and stationary phase examined. Several comparisons of methanol and hexanol as mobile phase modifiers in carbon dioxide have been reported. The retention of polycyclic aromatic and nitroaromatic hydrocarbons on ODS-modified silica columns was reported to be lower using 1-hexanol as the modifier in comparison to methanol at equivalent mobile phase concentrations⁷. This was attributed to better masking of active sites on the

silica surface by the longer, lipophilic chain of 1-hexanol. The retention of 4-nitroaniline on a cyano-modified silica column was also reported to decrease with increasing length of the alkyl chain of the alcohol modifier¹. This was suggested as being due to better access to active silanol sites and bonded cyano groups of the cyano column by the more lipophilic alcohols. Methanol, in contrast, was shown to decrease the retention of aromatic hydrocarbons on a diol-modified silica column more effectively than 1-hexanol³. This was thought to be the result of a more efficient interaction of the smaller methanol modifier with active column sites. Variations in temperature and mobile phase density can also have an effect on the degree to which a modifier interacts with an alters the stationary phase surface. The effect of mobile phase density on the adsorption of ethyl acetate modifier onto silica from supercritical carbon dioxide has been reported¹⁷.

In liquid chromatography, localized adsorption of the modifier has been shown to have a direct effect on the retention of solutes which compete with the modifier for active column sites¹⁸. Over the modifier concentration range in which localized surface coverage by the modifier is constant, the capacity factor of a solute can be related to the mobile phase modifier concentration using the equation

$$1/k' = a\phi + b \quad (1)$$

where k' is the capacity factor, ϕ is the concentration of modifier in the mobile phase, and a and b are constants. A plot of inverse capacity factor *versus* mobile phase modifier concentration is predicted to be linear. Over the modifier concentration range in which localized surface coverage by the modifier reaches completion, solutes that adsorb through localized interactions with active column sites but do not displace the adsorbed modifier from these sites will show a change in the slope of the line determined from the above equation. Non-linearity results because the interaction energy of the solute with the modified surface will be different than that of the solute with the unmodified surface. Snyder and Glajch¹⁹ have suggested that localized adsorption by the modifier is essentially complete at approximately 75% of the total surface coverage. Surface coverage beyond that point must involve delocalized adsorption due to steric restrictions. On the other hand, solutes which do not adsorb via localized interactions with active column sites and solutes which can displace the modifier from the stationary phase surface and interact directly with these active sites, should show linearity over the same concentration range.

In this work, the peak maxima method²⁰ was used to determine adsorption isotherms for methanol and hexanol modifiers onto silica from supercritical carbon dioxide as a function of mobile phase density and temperature. In addition the effects of low concentrations of methanol modifier (0–1%, w/w) on the retention of several substituted and unsubstituted aromatic hydrocarbons on silica from supercritical carbon dioxide were examined. From these results, the propensity of the solutes to compete with methanol for active column sites was also determined.

EXPERIMENTAL

Carbon dioxide was supercritical fluid grade from Scott Speciality Gases (Plumsteadville, PA, U.S.A.). The detector was a Varian Vari-Chrom multiwave-

length detector fitted with a high-pressure UV cell supplied by Hewlett-Packard. The recorder was a Spectra-Physics Model SP4290 integrator.

The experimental set-up used in the determination of adsorption isotherms was described earlier¹⁷. The column was 10 cm × 4.6 mm I.D. and packed with Whatman Partisil-10 using the upward slurry technique. Methanol was HPLC-grade from Mallinckrodt (Paris, KY, U.S.A.). 1-Hexanol (98%) was obtained from Aldrich (Milwaukee, WI, U.S.A.). Both solvents were dried over 3-Å molecular sieves and distilled. Detection wavelengths for both alcohols were 190 nm at modifier concentrations below 0.10% (g/ml) to achieve adequate sensitivity and 206 nm at higher concentrations to maintain a linear detector response.

Retention data was obtained at 50°C at a carbon dioxide density of 0.60 g/ml. The dual pumping system of a Hewlett-Packard Model 1082B modified liquid chromatograph was used to produce the necessary mobile phase mixtures of carbon dioxide and 1.0% (w/w) methanol in carbon dioxide (Scott Speciality Gases). Capacity factors were measured in the usual manner from retention time (t_R) and dead time (t_0) as $k' = (t_R - t_0)/t_0$, and were reproducible to ± 1.5%.

RESULTS

Adsorption isotherms for methanol and 1-hexanol were determined at four temperatures and three mobile phase densities as listed in Table I. Examples of these isotherms are shown in Fig. 1. The isotherm data was fitted to a linear equation derived from rearrangement of the Langmuir function for monolayer adsorption:

$$1/C_s = 1/(C_m K^o C_s') + 1/C_s' \quad (2)$$

Where C_s is the stationary phase modifier concentration, C_m is the mobile phase concentration, C_s' is the maximum stationary phase concentration, and K^o is the thermodynamic equilibrium constant for the distribution of the modifier between the adsorbed and non-adsorbed states. In all cases the correlation coefficient was not less

TABLE I

MAXIMUM MODIFIER CONCENTRATION AND SURFACE COVERAGE WITH TEMPERATURE AND DENSITY

Temperature (°C)	CO ₂ density (g/ml)	Maximum stationary phase concentration (%mol/g)		Maximum surface coverage ^a (m ² /g)	
		Methanol	Hexanol	Methanol	Hexanol
40	0.60	0.221	0.136	240	314
60	0.60	0.182	0.141	197	326
80	0.60	0.159	0.130	172	301
100	0.60	0.162	0.112	175	259
60	0.40	0.180	0.117	195	270
60	0.50	0.167	—	181	—
60	0.70	0.169	—	183	—
60	0.80	0.171	0.130	185	301

^a Mean molecular areas²¹: methanol = 18.0 Å²; 1-hexanol = 38.4 Å².

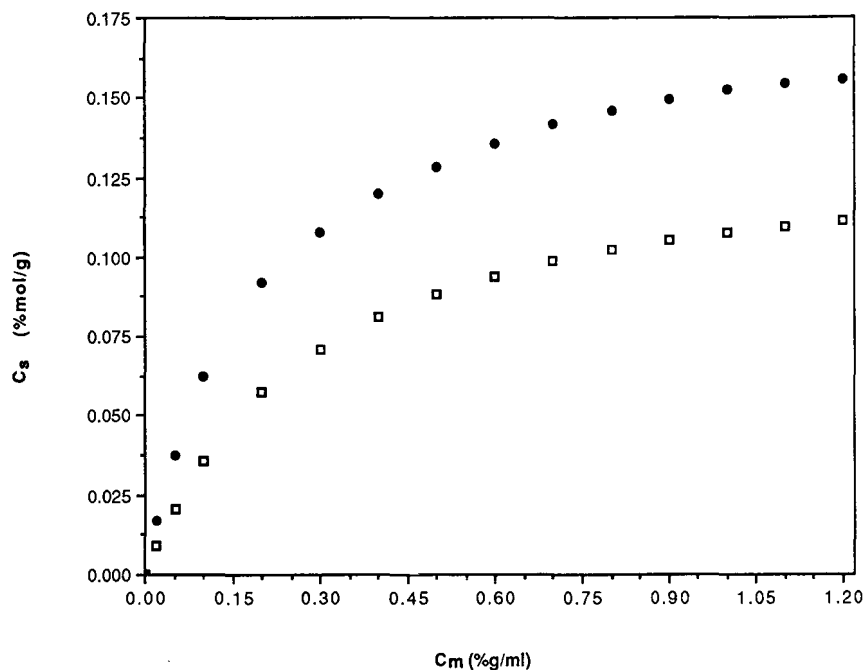


Fig. 1. Adsorption isotherms determined at 60°C at a CO_2 density of 0.60 (g/ml). Key: ● = methanol; □ = hexanol.

than 0.9998. The least-squares fits to these data were used to extrapolate the maximum surface coverage for each modifier. These results as well as the maximum surface area covered by the modifiers calculated from their mean molecular areas²¹ are listed in Table I. Under all temperature and density conditions examined, surface coverage by each modifier was more than 60% complete, based on the above calculations, at mobile phase concentrations of less than 1.5% (g/ml), and greater than 90% complete at this mobile phase concentration at 40°C. The importance of reporting concentration units in SFC work is overlooked in many published studies. This is especially important when comparing the effects of surface coverage on retention at low modifier concentrations, *e.g.*, comparing the isotherms in Fig. 1 at equivalent molar mobile phase concentrations, the stationary phase concentration of 1-hexanol increases more rapidly than that of methanol as determined by the difference in their molecular weights.

The surface coverage by each modifier was also examined as a function of temperature at constant mobile phase density. Plots of stationary phase modifier concentration *versus* temperature are shown in Fig. 2. The change in surface coverage was found to be linear with temperature at all mobile phase concentrations examined with correlation coefficients of 0.980–0.999. The rate of change in surface coverage with temperature at equivalent molar mobile phase concentrations was found to be the same for both modifiers.

Capacity factors were determined for several substituted and unsubstituted aromatic hydrocarbons as a function of mobile phase methanol concentration as

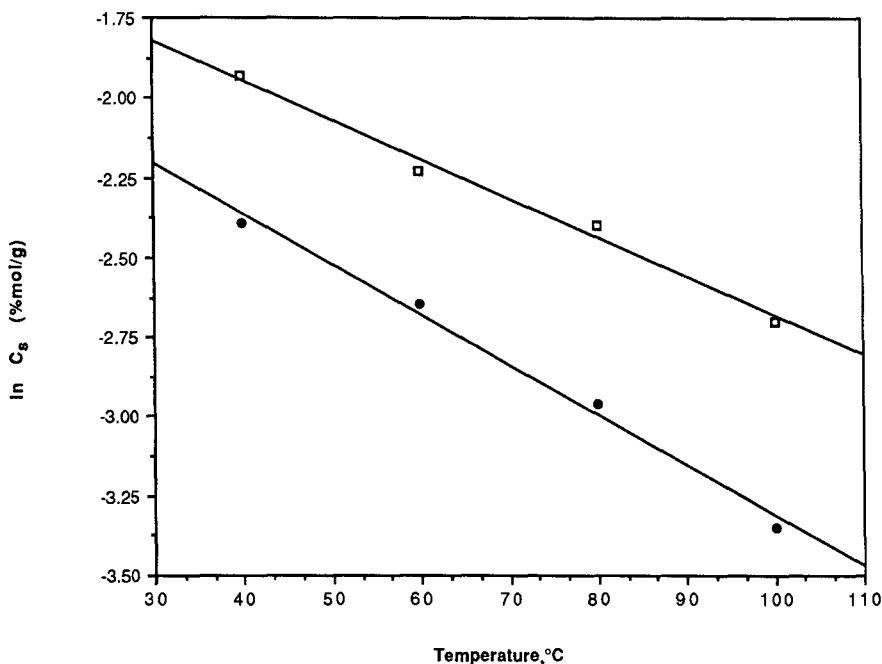


Fig. 2. Stationary phase coverage plotted *versus* temperature at a mobile phase concentration of 0.30% (g/ml) at a CO₂ density of 0.60 (g/ml). Key: □ = methanol, $r = 0.994$; ● = hexanol, $r = 0.995$.

shown in Table II. Plots of inverse capacity factor *versus* mobile phase modifier concentration are shown in Figs. 3–6. A linear least squares fit was made to the data using the four largest modifier concentrations measured, at which the surface coverage changes slowly relative to lower concentrations. Eqn. 1 was then used to predict the capacity factors at zero modifier concentration. The calculated values of the capacity factor for solutes that compete with the modifier for active column sites will be lower than the actual values. This is expected since the availability of silanols increases rapidly as the mobile phase modifier concentration approaches zero resulting in an increase in the interaction energy of the solute with the stationary phase. This type of retention behavior was exhibited by methoxynaphthalene and nitronaphthalene as shown in Fig. 3, and for chloromethylnaphthalene as shown in Fig. 4. For direct comparison of solute retention and modifier surface coverage, a methanol adsorption isotherm, determined under the same experimental conditions, is shown in Fig. 4 overlaid on the inverse capacity factor plot of chloromethylnaphthalene. In contrast to the above solutes, the calculated value of the capacity factor of chloronaphthalene in Fig. 5 is larger than the actual value with a resulting maximum in k' . Similar retention behavior has been observed in this laboratory for aromatic hydrocarbons on silica using ethyl acetate modifier in carbon dioxide, and has also been reported for aromatic hydrocarbons from tetrahydrofuran modified carbon dioxide on several stationary phases²². This behavior is likely the result of increased dispersive interactions with modifier covered silanols relative to free silanols, or lateral interactions of the adsorbed solute with the adsorbed modifier as has been suggested

TABLE II
SOLUTE CAPACITY FACTORS VERSUS MOBILE PHASE METHANOL CONCENTRATION

%Methanol (g/ml)	k'								
		Phenol	Chrysene	Naphthalene	1-Methoxy- naphthalene	2-Chloro- naphthalene	1-Nitro- naphthalene	1-Chloromethyl- naphthalene	Isobutyro- phenone
0.00	12.3		5.40	0.534	1.93	0.679	6.50	2.21	10.1
0.10	11.3		5.38	0.527	1.71	0.667	6.35	1.96	9.49
0.20	9.60		4.95	0.488	1.40	0.661	3.46	1.46	3.84
0.30	8.50		4.70	0.497	1.28	0.667	2.77	1.32	2.77
0.40	7.55		4.29	0.461	1.23	0.648	2.51	1.16	1.82
0.60	6.35		3.83	0.431	1.13	0.596	2.18	1.03	1.18
0.80	5.35		3.40	0.394	1.03	0.569	1.88	0.946	0.916
1.00	4.76		3.08	0.375	0.971	0.544	1.76	0.857	0.795

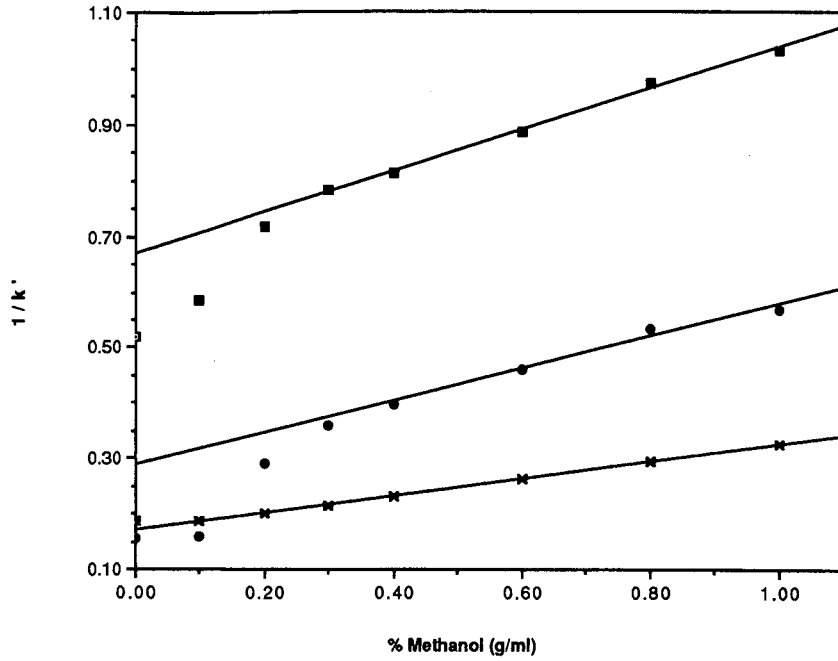


Fig. 3. Plots of inverse capacity factor of three solutes *versus* mobile phase methanol concentration at 50°C at a CO₂ density of 0.60 g/ml. Key: □ = methoxynaphthalene; ● = nitronaphthalene; × = chrysene.

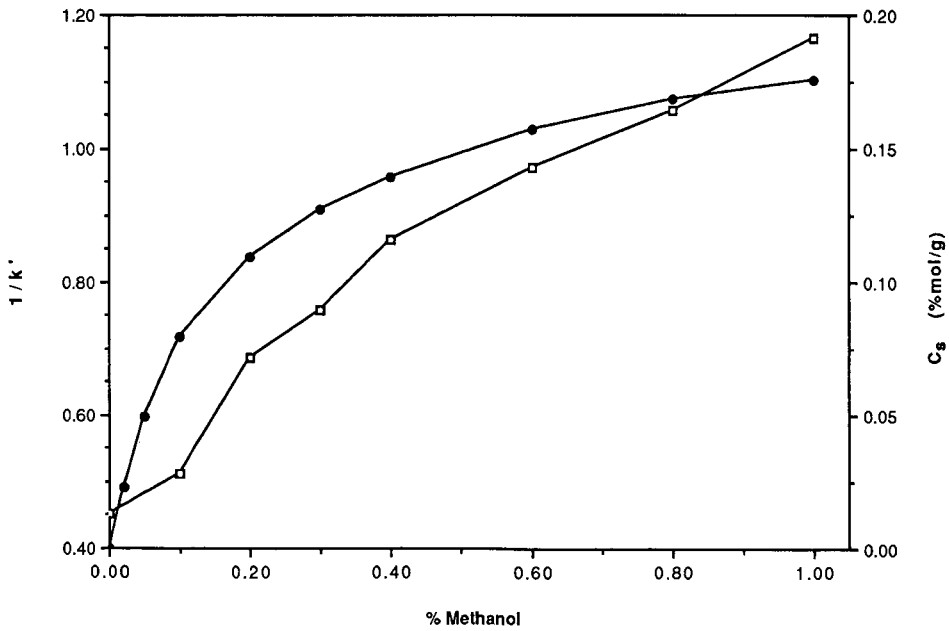


Fig. 4. Plot of inverse capacity factor of 1-chloromethylnaphthalene overlaid with an adsorption isotherm for methanol. Same conditions as in Fig. 3. Key: ● = C_s ; □ = $1/k'$.

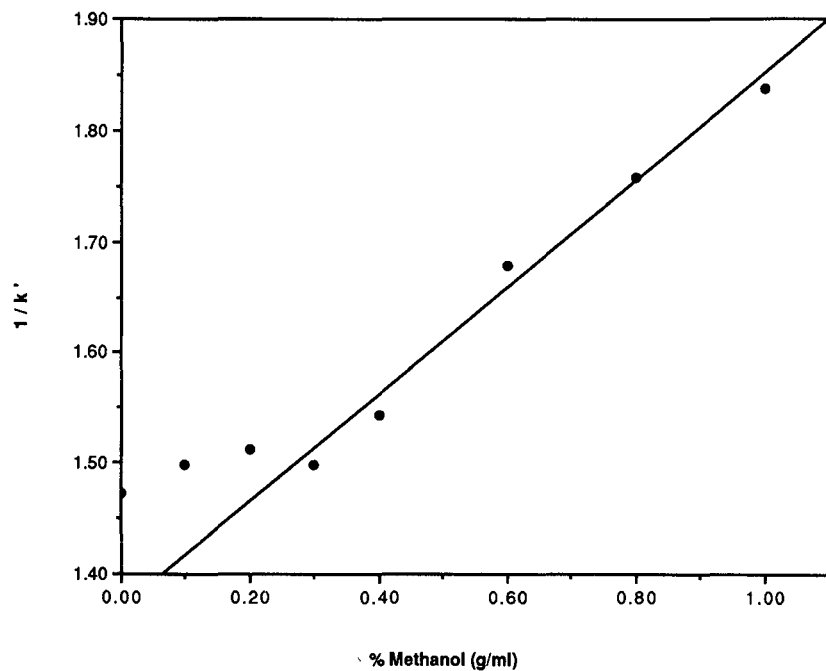


Fig. 5. Plot of inverse capacity factor of 2-chloronaphthalene *versus* mobile phase methanol concentration. Same conditions as in Fig. 3.

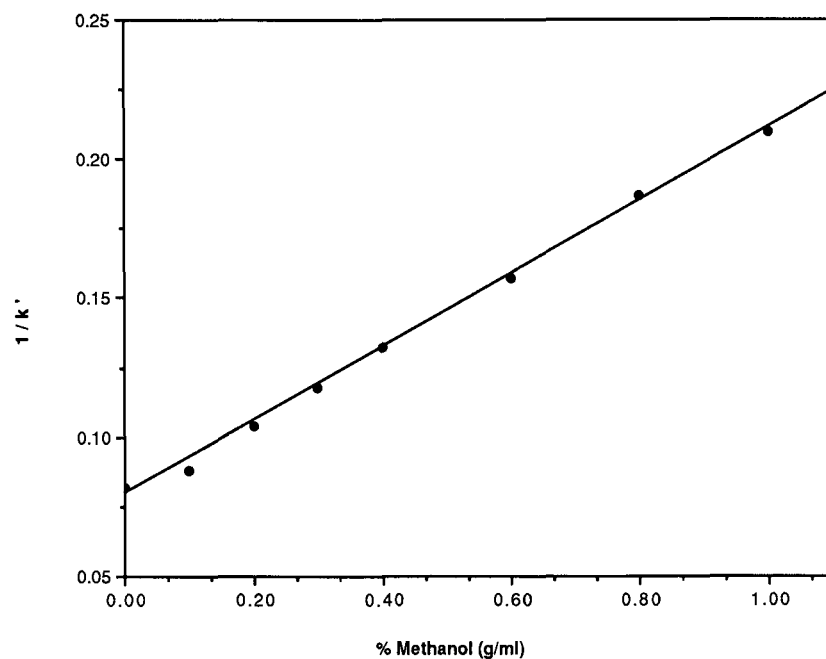


Fig. 6. Plot of inverse capacity factor of phenol *versus* mobile phase methanol concentration. Same conditions as in Fig. 3.

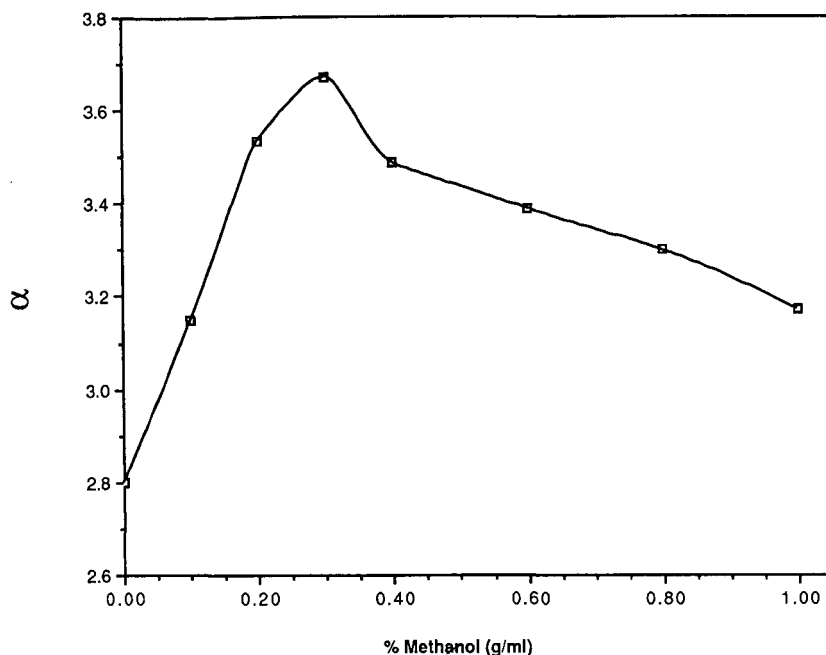


Fig. 7. Selectivity calculated for chrysene and 1-methoxynaphthalene plotted as a function of mobile phase methanol concentration.

for binary adsorption onto stationary phases in gas chromatography²³. The unsubstituted aromatics, which likely do not adsorb through localized interaction with the silanols, show linearity throughout this concentration range as indicated for chrysene in Fig. 3. Phenol, which is expected to interact strongly with the silanols as suggested by its relatively large capacity factor, exhibits linearity, as shown in Fig. 6, probably because of its ability to displace methanol rather than compete with it for active sites²¹.

The selectivity for a given solute pair can vary considerably over the modifier concentration range examined here. In the case of chrysene and methoxynaphthalene, in which one solute competes with the modifier for stationary phase active sites and the other does not, a maximum in selectivity is observed as shown in Fig. 7. As a result of its competition for active column sites, the capacity factor of methoxynaphthalene, which elutes first over this concentration range, decreases more rapidly than that of chrysene as the modifier is initially added to the mobile phase. As the active sites become covered with increasing modifier concentration, the capacity factor of chrysene decreases more rapidly than that of methoxynaphthalene with a resulting decrease in selectivity.

CONCLUSIONS

From the adsorption isotherms presented here and the values of surface coverage calculated from mean molecular surface area, 1-hexanol is apparently more

effective in masking stationary phase active sites than methanol. It must be noted, however, that the calculation of surface area coverage assumes that the molecules are spherical. This is probably a reasonable assumption for methanol, but the orientation of the adsorbed hexanol molecule, which has a greater length-to-breadth ratio, will have an effect on the apparent surface coverage. Orientation of the lipophilic chain away from the surface would increase its apparent coverage, while flat, horizontal, adsorption would have the opposite effect. Nevertheless, assuming that the actual orientation of the adsorbed hexanol molecules is somewhere between these extremes, calculations based on mean molecular area are a reasonable first approximation. The ability of 1-hexanol to restrict solute interaction relative to methanol will depend to some extent on the relative distribution of the modifiers between adsorbed and non-adsorbed states as a function of temperature and mobile phase density. The size, structure and functionality of the adsorbing solute, and its ability to intercalate between the longer lipophilic chains of 1-hexanol are also important.

The retention data presented here indicate that for certain solutes and functional groups competitive, solute-modifier, active site adsorption occurs in SFC with a carbon dioxide mobile phase. Non-substituted aromatics do not appear to interact directly with these alcohol-sorbing active sites under the conditions examined. The changes in retention for chrysene and naphthalene at low modifier concentrations are likely due to enhanced solubility of these solutes in the mobile phase and are not a response to the changing sorbent surface.

ACKNOWLEDGEMENT

The authors acknowledge the support of the National Science Foundation under Grant No. CHE-8500658.

REFERENCES

- 1 J. M. Levy and W. M. Richey, *J. Chromatogr. Sci.*, 24 (1986) 242.
- 2 D. Leyendecker, D. Leyendecker, F. P. Schmitz, B. Lorenschat and E. Klesper, *J. Chromatogr.*, 398 (1987) 105.
- 3 J. M. Levy and W. M. Richey, *J. High Resolut. Chromatogr. Chromatogr. Commun.*, 8 (1985) 503.
- 4 J. B. Crowther and J. D. Henion, *Anal. Chem.*, 57 (1985) 2711.
- 5 C. R. Yonker, D. G. McMinn, B. W. Wright and R. D. Smith, *J. Chromatogr.*, 396 (1987) 19.
- 6 J. E. Conaway, J. A. Graham and L. B. Rogers, *J. Chromatogr. Sci.*, 16 (1978) 102.
- 7 A. L. Blilie and T. Greibrokk, *Anal. Chem.*, 57 (1985) 2239.
- 8 A. L. Blilie and T. Greibrokk, *J. Chromatogr.*, 349 (1985) 317.
- 9 P. Mourier, P. Sassiati, M. Caude and R. Rosset, *J. Chromatogr.*, 353 (1986) 61.
- 10 P. A. Mourier, E. Eliot, M. H. Caude and R. H. Rosset, *Anal. Chem.*, 57 (1985) 2819.
- 11 B. W. Wright and R. D. Smith, *J. Chromatogr.*, 355 (1986) 367.
- 12 C. R. Yonker and R. D. Smith, *Anal. Chem.*, 59 (1987) 727.
- 14 F. P. Schmitz and E. Klesper, *J. Chromatogr.*, 388 (1987) 3.
- 15 S. Schmidt, L. G. Blomberg and E. R. Campbell, *Chromatographia*, 25 (1988) 775.
- 16 D. Leyendecker, F. P. Schmitz, D. Leyendecker and E. Klesper, *J. Chromatogr.*, 393 (1987) 155.
- 17 C. H. Lochmüller and L. P. Mink, *J. Chromatogr.*, 409 (1987) 55.
- 18 R. P. W. Scott and P. Kucera, *J. Chromatogr.*, 149 (1978) 93.
- 19 L. R. Snyder and J. L. Glajch, *J. Chromatogr.*, 214 (1981) 1.
- 20 A. W. J. de Jong, J. C. Kraak, H. Poppe and F. Nooitgedacht, *J. Chromatogr.*, 193 (1980) 181.
- 21 R. P. W. Scott and P. Kucera, *J. Chromatogr.*, 171 (1979) 37.
- 22 J. M. Levy, *Dissertation*, Case Western Reserve University, Cleveland, OH, 1986.
- 23 J. F. Parcher and K. Hyer-LoCoco, *J. Chromatogr. Sci.*, 21 (1983) 304.

CHROM. 21 305

AQUEOUS SIZE-EXCLUSION CHROMATOGRAPHY OF ANIONIC AND NON-IONIC WATER-SOLUBLE POLYMERS ON SILICA GEL WITH BONDED HYDROPHILIC GROUPS

SADAO MORI

Department of Industrial Chemistry, Faculty of Engineering, Mie University, Tsu, Mie 514 (Japan)

SUMMARY

The elution behaviour of sodium polystyrene sulphonates (NaPSS) and linear polysaccharides (pullulan) on a column packed with porous silica gel with bonded glyceropropyl groups was studied. Phosphate buffer solution of various concentrations was used as the mobile phase. Early elution of NaPSS relative to non-ionic polymers was observed at low concentrations. Calibration graphs of $\log [\eta]M$ vs. K_{SEC} of NaPSS ($[\eta]$ = intrinsic viscosity of the polymer in the mobile phase; M = molecular weight; K_{SEC} = distribution coefficient) converged to the pullulan calibration graph with increasing concentration, crossed it, and then diverged on the other side. Late elution regarding the calibration graph for pullulan was caused by the hydrophobic interactions. The addition of a simple electrolyte suppressed the ion-exclusion effect, but the addition of an excess did not suppress the hydrophobic interactions. It is not possible to conclude that "ideal SEC" is obtained when the calibration graph for NaPSS approaches that for pullulan. The retention volume of NaPSS results from a combination of three effects: size-exclusion, ion-exclusion and hydrophobic interactions.

INTRODUCTION

Aqueous size-exclusion chromatography (ASEC) has been used for the determination of molecular weights (MW) of proteins and water-soluble synthetic polymers. One of the packing materials used for ASEC is porous silica gel chemically treated with γ -glycidylxypropyltrimethoxysilane to form glyceropropyl groups on the surface¹. There are several commercially available supports of this type and most of them exhibit weak cation-exchange properties². These properties are due to electrostatic interactions with anionic polyelectrolytes, resulting in early elution relative to non-ionic water-soluble polymers³. The suppression of this electrostatic effect was observed at high ionic strength⁴, but "ideal SEC" (unperturbed by polymer-substrate interactions) cannot be achieved in this manner⁵.

Barth⁶ has summarized several problems associated with ASEC. Non-size-exclusion effects were divided into two types, ionic and adsorption effects. Ion-exchange, ion-exclusion, ion-inclusion and intramolecular electrostatic effects are ac-

counted for by ionic interaction between polyelectrolytes and substrate. Adsorption effects may arise from hydrogen bonding, hydrophobic and ionic interactions. Several studies have indicated that a mobile phase ionic strength of 0.2 is sufficient to eliminate these ionic interactions. However, the adsorption effects (hydrophobic interactions) of a number of proteins were observed by increasing the ionic strength of the mobile phase from 0.36 to 3.5 M ⁷. These hydrophobic interactions can be eliminated by the addition of ethylene glycol⁷ or an organic modifier (alcohol or glycol)⁸.

Several commercially available supports for ASEC have already been examined extensively^{2,4,6}, and were found to exhibit ion-exclusion, cation-exchange and hydrogen partitioning effects under certain conditions. Recently a silica gel with bonded glyceropropyl groups became commercially available, *i.e.* Shodex Protein WS (Showa Denko, Tokyo, Japan). This paper is concerned with the elution behaviour of non-ionic polymers such as polyethylene oxides (PEO) and polysaccharides (pullulan) and anionic polymers such as sodium polystyrene sulphonates (NaPSS) on Shodex Protein WS-803. Mainly the influence of the ionic strength of the mobile phase on retention volume and peak broadening was examined.

EXPERIMENTAL

ASEC measurements were performed on a Jasco TRIROTAR-V high-performance liquid chromatograph (Japan Spectroscopic, Tokyo, Japan) with a Model VL-611 loop injector. A UVIDEC-100V ultraviolet (UV) absorption detector was used at 254 nm for NaPSS samples and a Model SE-11 refractive index (RI) detector (Showa Denko) was used for other samples.

Shodex PROTEIN WS-803 was packed in a 50 cm \times 8 mm I.D. stainless-steel column. The number of theoretical plates (N) was determined to be 28 000 plates per 50 cm by injecting 0.025 ml of a 0.5% ethylene glycol (EG) solution at a flow-rate of 1 ml/min of deionized water.

Samples were PEO standards (Tosoh, Tokyo, Japan) (MW $2.5 \cdot 10^4$, $4.0 \cdot 10^4$, $7.3 \cdot 10^4$, $1.5 \cdot 10^5$, $2.8 \cdot 10^5$, $6.6 \cdot 10^5$ and $1.2 \cdot 10^6$), polyethylene glycols (PEG) (MW 300, 600, 1000, 3400 and 5000), pullulan standards (Showa Denko) (MW 5800, $1.22 \cdot 10^4$, $2.37 \cdot 10^4$, $4.80 \cdot 10^4$, $1.00 \cdot 10^5$, $1.86 \cdot 10^5$, $3.80 \cdot 10^5$ and $8.53 \cdot 10^5$) and NaPSS (Pressure Chemical, Pittsburgh, PA, U.S.A.) (MW 4000, 6500, $1.60 \cdot 10^4$, $3.10 \cdot 10^4$, $8.80 \cdot 10^4$, $1.77 \cdot 10^5$, $6.90 \cdot 10^5$ and $1.00 \cdot 10^6$) (henceforth the numbers given after the sample name represent the MW). These samples were dissolved in the solution used as the mobile phase at a concentration of 0.1% for NaPSS, 0.2% for PEO and pullulan and 0.5% for PEG. Sodium *p*-toluenesulphonate was also used as a model monomer sample of NaPSS. The sample injection volume was 0.025 ml in all experiments.

The mobile phase for non-ionic polymers was deionized water and that for NaPSS was made up from Na_2HPO_4 and NaH_2PO_4 to the desired concentration at pH 8.0. The flow-rate of the mobile phase was 1 ml/min.

RESULTS AND DISCUSSION

The retention volume of EG was 20.0 ml, which was assumed to be equivalent to the total permeation volume. Size-exclusion chromatograms of non-ionic, water-soluble polymers obtained with water as the mobile phase are shown in Fig. 1. All

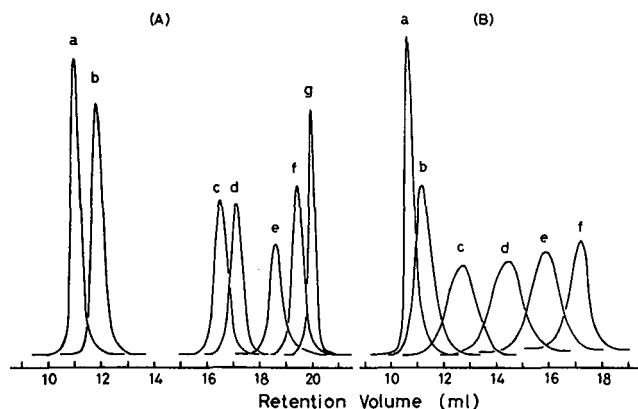


Fig. 1. Size-exclusion chromatograms of (A) PEO and PEG and (B) pullulan. Mobile phase, deionized water; detector, RI. Attenuation: (A)(a), (b) and (B), $\times 4$, (A)(c) – (g), $\times 16$. MW: (A)(a) $7.3 \cdot 10^4$, (b) $4.0 \cdot 10^4$, (c) 5000, (d) 3400, (e) 1000, (f) 600, (g) EG; (B)(a) $1.86 \cdot 10^5$, (b) $1.00 \cdot 10^5$, (c) $4.8 \cdot 10^4$, (d) $2.37 \cdot 10^4$, (e) $1.22 \cdot 10^4$, (f) 5800.

chromatograms are symmetrical and eluted before $V_R = 20$ ml, indicating that these polymers eluted mainly by size exclusion and no adsorption effects occurred.

The elution behaviour of anionic polymers, NaPSS, with water as the mobile phase was different from that of non-ionic polymers. Examples are shown in Fig. 2. Two peaks were observed for each sample, one at $V_R = 10.45$ ml and the other at $V_R = 20.3$ – 20.5 ml. The first peak corresponds to polystyrenesulphonic acid (PSSA) and the second to sodium hydroxide. These compounds originated from the NaPSS sample which separated into two components during elution by ion-exchange between ionic groups on the stationary phase and NaPSS. The packing material used in this experiment exhibits weak cation-exchange properties owing to the residual silanol groups. The Na^+ ions in NaPSS might undergo ion-exchange interactions with the

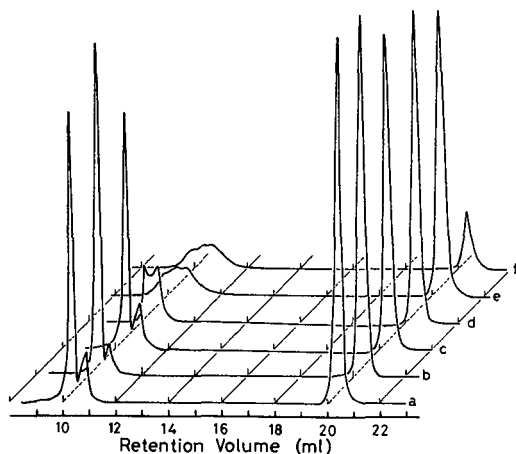


Fig. 2. Size-exclusion chromatograms of NaPSS in a mobile phase of deionized water. Detector, RI; attenuation, $\times 4$. MW: (a) 4000; (b) 6500; (c) 3.1×10^4 ; (d) $1.77 \cdot 10^5$; (e) $6.9 \cdot 10^5$; (f) $1.0 \cdot 10^6$.

H^+ ions of the silanol groups, and PSSA elutes at the retention volume corresponding to the exclusion volume owing to ion-exclusion interactions between $PSSA^-$ and SiO^- ions. The reasons why the first peak split into a large and a small peak and why the peaks of high-MW NaPSS such as $1.0 \cdot 10^6$ and $6.9 \cdot 10^5$ were broad are unclear; probably one represents PSSA and the other the residual NaPSS. However, when $1.15 \cdot 10^{-3} M$ phosphate buffer solution was used as the mobile phase, no splitting occurred and only one sharp peak was observed at the exclusion volume ($V_R = 10.45$ ml). The second peak at $V_R = 20.3\text{--}20.5$ ml also disappeared.

The retention volume of NaPSS increased with increasing phosphate buffer concentration in the mobile phase. Fig. 3 shows an example using NaPSS 6500, which eluted at the exclusion volume when the phosphate buffer concentration in the mobile phase was $1.15 \cdot 10^{-3} M$ and eluted after the exclusion volume at higher concentrations. The retention volume of NaPSS 6500 continued to increase with increasing phosphate buffer concentration in the mobile phase and finally the NaPSS peak almost disappeared above the total permeation volume. The negative peak near the total permeation volume may be due to the difference in concentration of phosphate ions between the mobile phase and the sample solution. Although this negative peak interrupted the NaPSS 6500 peak at high phosphate buffer concentrations in the mobile phase, it was obvious that NaPSS 6500 eluted after the total permeation volume and the peak became very broad, indicating the existence of secondary effects other than ion-exclusion when the phosphate buffer concentration in the mobile phase was $0.3 M$. The peak width of NaPSS 6500 also increased with increasing concentration of phosphate buffer in the mobile phase, mainly owing to the size-exclusion effect as it eluted between the size-exclusion volume and the total permeation volume.

Sodium *p*-toluenesulphonate can be assumed to be a model monomer compound of NaPSS. Its retention volume increased with increasing phosphate buffer concentration in the mobile phase, similarly to NaPSS. However, the peak of this compound was broad at low phosphate buffer concentrations in the mobile phase (below $1.0 \cdot 10^{-2} M$) and sharp at concentrations above $2.76 \cdot 10^{-2} M$. The results are

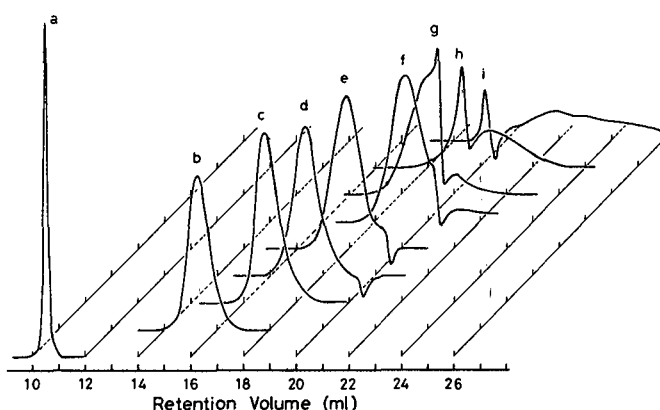


Fig. 3. Size-exclusion chromatograms of NaPSS 6500 in mobile phases with various phosphate buffer concentrations (M): (a) $1.15 \cdot 10^{-3}$; (b) $2.76 \cdot 10^{-2}$; (c) $6.0 \cdot 10^{-2}$; (d) $8.0 \cdot 10^{-2}$; (e) 0.10; (f) 0.12; (g) 0.15; (h) 0.20; (i) 0.30, UV attenuation: (a), (c), (d), $\times 0.16$; (b), (e)–(i), $\times 0.08$.

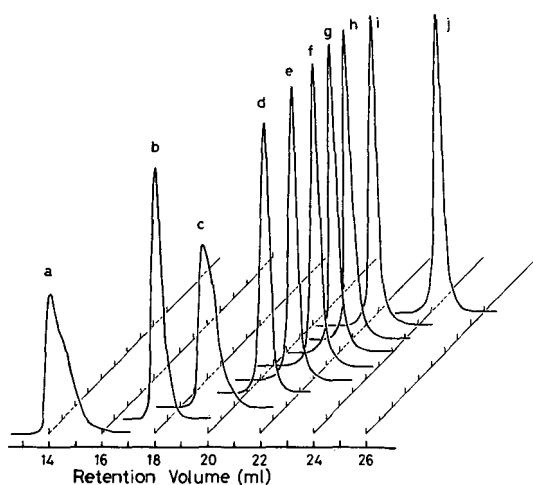


Fig. 4. Chromatograms of sodium *p*-toluenesulphonate. Concentration of phosphate buffer in the mobile phase (M): (a) $1.15 \cdot 10^{-3}$; (b) $5.0 \cdot 10^{-3}$; (c) $1.0 \cdot 10^{-2}$; (d) $2.76 \cdot 10^{-2}$; (e) $5.0 \cdot 10^{-2}$; (f) $6.0 \cdot 10^{-2}$; (g) 0.10; (h) 0.12; (i) 0.15; (j) 0.40 UV. attenuation: $\times 0.16$.

shown in Fig. 4. Peaks e–j eluted above the total permeation volume and were sharp as peak d eluted at the total permeation volume ($V_R = 20$ ml). The widths of peaks d–j were identical. The elution behaviours of the polymer and the monomer may differ.

An example of the size-exclusion chromatograms of several NaPSS in a mobile phase with a phosphate buffer concentration of 0.05 M is shown in Fig. 5. The peaks that eluted at the exclusion volume were sharp and those eluting between the exclusion volume and the total permeation volume were broad. This peak broadening may be due mainly to the size-exclusion effect and implies that the NaPSS samples have molecular weight distributions, although they were supposed to have narrow distri-

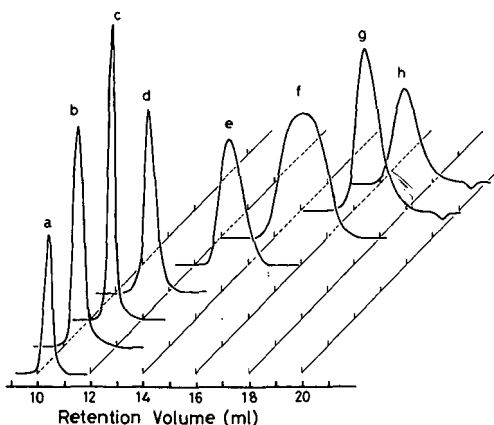


Fig. 5. Size-exclusion chromatograms of NaPSS in a mobile phase of 0.05 M phosphate buffer solution of pH 8.0. MW: (a) $1.0 \cdot 10^6$; (b) $6.9 \cdot 10^5$; (c) $1.77 \cdot 10^5$; (d) $8.8 \cdot 10^4$; (e) $3.1 \cdot 10^4$; (f) $1.6 \cdot 10^4$; (g) 6500; (h) 4000. UV attenuation: (a)–(d), $\times 0.16$; (e)–(h), $\times 0.08$.

butions. The pH of the mobile phase used here was 8.0; the same results were obtained at pH 4.7.

The retention volume, V_R , in SEC can be expressed by the equation

$$V_R = V_o + K_{SEC} V_i$$

where V_o is the interstitial volume (the exclusion volume) of the column, V_i is the inner volume of the packing material in the column and K_{SEC} is the distribution coefficient. V_o was taken as the retention volume of NaPSS in a mobile phase consisting of deionized water or phosphate buffer of concentration $1.15 \cdot 10^{-3} M$. The validity of this assumption was supported by observations that all the NaPSS tested in these two mobile phases appeared at $V_R = 10.45$ ml. V_i was measured as the difference between the retention volume of EG and V_o , and was 9.55 ml.

Fig. 6 shows plots of $\log M$ vs. K_{SEC} . Pullulan and PEO (and PEG) eluted according to their molecular weights and were not affected by the concentration of the mobile phase; their K_{SEC} values were between 0 and 1. K_{SEC} for NaPSS in deionized water was zero and increased with increasing phosphate buffer concentration in the mobile phase. The NaPSS peaks also broadened with increasing retention volume. NaPSS of MW $6.9 \cdot 10^5$ and $1.0 \cdot 10^6$ appeared at V_o and were not affected by the phosphate buffer concentration in the mobile phase. NaPSS 6500 and 4000 appeared near $V_o + V_i$ with a phosphate buffer concentration in the mobile phase of 0.15 M and were retained in the column with concentrations over 0.20. NaPSS above MW $1.6 \cdot 10^4$ appeared with phosphate buffer concentrations in the mobile phase of up to 0.30 M. At buffer concentrations above 0.40 M all NaPSS were retained in the

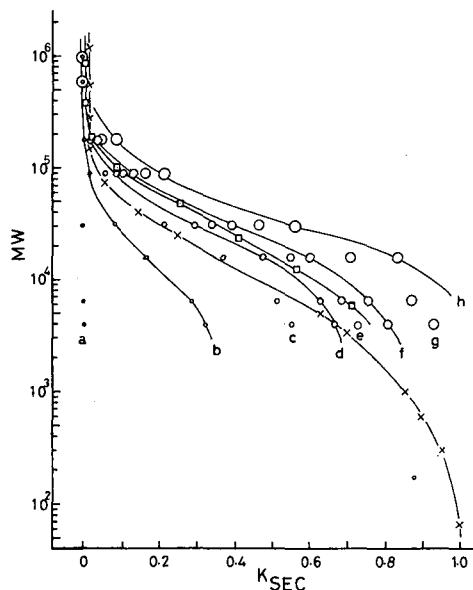


Fig. 6. Calibration graphs of $\log MW$ vs. distribution coefficient for (\square) pullulan, (\times) PEO and PEG and (\circ) NaPSS. Concentration of phosphate buffer in the mobile phase (M): (a) 0; (b) $1.0 \cdot 10^{-2}$; (c) $2.76 \cdot 10^{-2}$; (d) $5.0 \cdot 10^{-2}$; (e) $7.0 \cdot 10^{-2}$; (f) 0.10; (g) 0.15; (h) 0.20. The mobile phase for pullulan, PEO and PEG was deionized water.

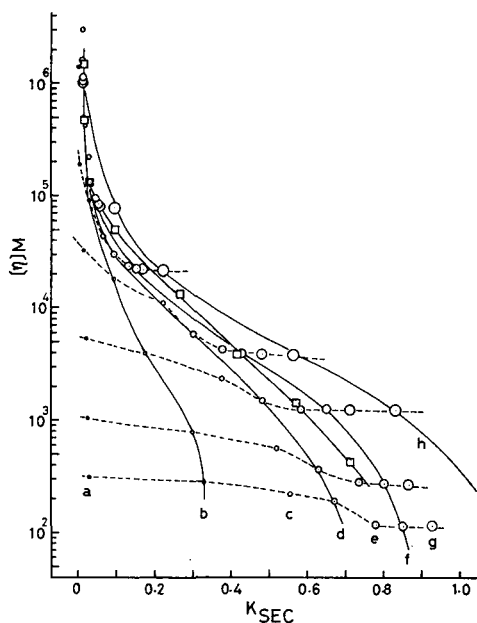


Fig. 7. Calibration graphs of $\log [\eta]M$ vs. distribution coefficient for (\square) pullulan and (\circ) NaPSS. Concentration of phosphate buffer in the mobile phase (M): (a) $1.15 \cdot 10^{-3}$; (b) $1.0 \cdot 10^{-2}$; (c) $2.76 \cdot 10^{-2}$; (d) $5.0 \cdot 10^{-2}$; (e) $9.0 \cdot 10^{-2}$; (f) 0.12; (g) 0.15; (h) 0.20. The mobile phase for pullulan was deionized water.

column and only sodium *p*-toluenesulphonate eluted; NaPSS are more hydrophobic than the latter.

NaPSS of MW $6.9 \cdot 10^5$ and $1.0 \cdot 10^6$ could not enter the pores of the packing material and their peak widths were unchanged until they were retained in the column. Other NaPSS showed broadened peaks when they could enter the pores. Peak broadening may be due mainly to the size-exclusion effect in mobile phases with low concentrations of phosphate buffer. Intramolecular chain expansion of polyelectrolytes leads to early elution relative to non-ionic polymers and this expansion can be suppressed by the addition of simple electrolytes³. To discuss the elution behaviour of NaPSS from the viewpoints of secondary effects, the variable of intramolecular chain expansion should be removed. The solution is to use the hydrodynamic volume parameter $[\eta]M$, where $[\eta]$ is the intrinsic viscosity of the polymer in the mobile phase and M is the molecular weight. Fig. 7 shows plots of $\log [\eta]M$ vs. K_{SEC} for pullulan standards and NaPSS. The hydrodynamic volume of NaPSS decreased rapidly with increasing concentration of phosphate buffer in the mobile phase up to $9.0 \cdot 10^{-2} M$. It is evident that retention volume of NaPSS of the same molecular size increased with increasing phosphate buffer concentration in the mobile phase.

It is possible to compare the retention volumes of NaPSS and pullulan of the same hydrodynamic volume by using Fig. 7. The retention volume of NaPSS converged to that of pullulan of the same molecular size with increasing concentration of phosphate buffer in the mobile phase and then diverged to the other side. The phosphate buffer concentration in the mobile phase at the crossing point of the pullulan calibration graph for low-MW NaPSS was $9.0 \cdot 10^{-2} M$ and that for high-MW

NaPSS was $1.2 \cdot 10^{-1} M$. The retention volume of NaPSS continued to increase and finally NaPSS was retained in the column.

In conclusion, it is evident that the early elution of NaPSS relative to non-ionic polymers was caused by the ion-exclusion effect and late elution after the pullulan calibration graph by hydrophobic interactions. A size-exclusion effect would occur after V_0 . The addition of a simple electrolyte suppressed the ion-exclusion effect. However, the addition of an excess of simple electrolyte (high concentration in the mobile phase) did not suppress the hydrophobic interactions, and it therefore cannot be said that "ideal SEC" will be obtained when the calibration graph for NaPSS approaches that for pullulan or when it overlaps that for pullulan. Elution between V_0 and $V_0 + V_i$ will be a combination of three effects: size-exclusion, ion-exclusion and hydrophobic interactions.

REFERENCES

- 1 K. K. Unger and J. N. Kinkel in P. L. Dubin (Editor), *Aqueous Size-Exclusion Chromatography*, Elsevier, Amsterdam, 1988, Ch. 8.
- 2 E. Pfannkoch, K. C. Lu, F. E. Regnier and H. G. Barth, *J. Chromatogr. Sci.*, 18 (1980) 430.
- 3 P. L. Dubin and M. M. Tecklenburg, *Anal. Chem.*, 57 (1985) 275.
- 4 A. L. Spatorico and G. L. Beyer, *J. Appl. Polym. Sci.*, 19 (1975) 2933.
- 5 P. L. Dubin, C. M. Speck and J. I. Kaplan, *Anal. Chem.*, 60 (1988) 895.
- 6 H. G. Barth, *J. Chromatogr. Sci.*, 18 (1980) 409.
- 7 D. E. Schmidt, Jr., R. W. Giese, D. Connor and B. L. Karger, *Anal. Chem.*, 52 (1980) 177.
- 8 S. Hjerstén, *J. Chromatogr.*, 87 (1973) 325.

CHROM. 21 299

OVERPRESSURED MULTI-LAYER CHROMATOGRAPHY

ERNÖ TYIHÁK*

Plant Protection Institute, Hungarian Academy of Sciences, P.O. Box 102, H-1525 Budapest (Hungary)
and

EMIL MINCSOVICS and TIBOR J. SZÉKELY

Labor-MIM, P.O. Box 280, H-1445 Budapest (Hungary)

SUMMARY

A new version of overpressured layer chromatography using two, three or more chromatoplates during one separation was developed. The admission of the eluent to the multi-layer system as a critical step is performed by making a perforation in the chromatoplates at the eluent inlet of a suitable size and shape. The technique, called overpressured multi-layer chromatography, is the most up-to-date version of layer liquid chromatography and is very attractive because a large number of samples (50–100 or more) can be separated during one development. It can be used effectively, *e.g.*, in plant breeding, clinical laboratories and industrial control laboratories and for the sequence analysis of proteins and nucleic acids.

INTRODUCTION

Conventional planar and non-planar and also thin- and thick-layer liquid chromatographic techniques require little equipment and are fairly simple. Among the planar layer liquid chromatographic techniques, paper chromatography (PC) and its variants were first developed in the 1940s by Martin and Syngé¹. Thin-layer chromatography (TLC) discovered by Izmailov and Shraiber², improved by Kirchner *et al.*³ and standardized and extended by Stahl *et al.*^{4,5}, contributed to the isolation and analysis of many natural and synthetic substances. The combination of the flame ionization detector with TLC resulted in a special non-planar layer liquid chromatographic technique (TLC–FID)⁶ with a thin layer of sorbent, *e.g.*, on a glass rod (open column).

Column and planar and non-planar layer liquid chromatographic techniques have developed together and it is not surprising that the rapid development of high-performance liquid chromatography (HPLC) entailed the need for a fundamental reappraisal of TLC as the most popular planar layer liquid chromatographic technique. It is also understandable that the latest efforts aimed at the further development of TLC have been characterized by the desire to introduce sophisticated instrumental techniques similar to those in HPLC. These efforts are in apparent contradiction with the advantages offered by the simplicity of the instruments and the

flexibility of the operational steps in conventional layer liquid chromatographic techniques.

The first successful attempt was the development of overpressured layer chromatography (OPLC) using a pressurized ultramicro chamber⁷⁻⁹. In this chamber system, the sorbent layer is completely covered with a flexible membrane under external pressure. Thus OPLC, which is a collective term for different versions of the technique, corresponds to HPLC on a column having a very thin but wide cross-section¹⁰.

Depending on the application, linear, circular (radial) and anticircular (triangular) development modes can be performed in OPLC and each has its own merits. In the linear development mode, one- and two-directional and two-dimensional developments are possible^{11,12}. It should be mentioned that the linear versions of OPLC require precoated chromatoplates whose edges are impregnated with a suitable impregnating liquid.

OPLC is suitable for both on-line and off-line sample application, separation and detection¹³⁻¹⁵. The OPLC system permits both analytical and preparative investigations¹⁶. The resolution and spot capacity of different versions of OPLC are considerably increased in comparison with conventional layer techniques^{17,18}.

These advantages of OPLC ensured progress in the field of layer liquid chromatography similarly to the development of HPLC in the field of column liquid chromatography.

However, because OPLC is theoretically and practically a planar layer version of HPLC and, at the same time, has further special advantages as a planar layer system, there are additional development possibilities.

With the apparatus used so far in OPLC, only one chromatoplate could be developed, but the efficiency of this technique could be significantly increased if more than one chromatoplate could be developed simultaneously. In this paper, we outline technical and theoretical aspects of the applicability of overpressured multi-layer chromatography (OPMLC), which seems to be a promising new version of the original technique.

EXPERIMENTAL

OPMLC was carried out with Chrompres 10 and Chrompres 25 OPLC chromatographs from Labor-MIM (Budapest, Hungary). The separations were performed with perforated and/or non-perforated silica gel 60F₂₅₄ TLC and HPTLC chromatoplates (Merck, Darmstadt, F.R.G.). Impregnation of the chromatoplates on two, three or four sides was performed with Impres polymer suspension from Labor-MIM. Densitograms were taken with Shimadzu (Kyoto, Japan) CS-920 and CS-930 scanners. Samples were applied with a Nanomat sample applicator (Camag, Muttenz, Switzerland) or with a Hamilton (Bonaduz, Switzerland) syringe.

A standard mixture of PTH-amino acids (Pierce, Rockford, IL, U.S.A.) was prepared by dissolution in the eluent to be used. Choline, betaine and trigonelline were purchased from Fluka (Buchs, Switzerland) and other chemicals from Merck (Darmstadt, F.R.G.) and Serva (Heidelberg, F.R.G.). The solvents used were LiChrosolv (Merck) and compounds of analytical-reagent grade.

RESULTS AND DISCUSSION

Technical aspects of the multi-layer system

The sorbent layer plays a central role in TLC and this is especially valid for OPLC. In order to achieve a linear chromatogram in OPLC, the edges of the sorbent layer on the chromatoplate must be suitably sealed by removing the sorbent from the edges of the sorbent layer and forming a polymer film by impregnation, *e.g.*, with a polymer suspension. Thus the eluent cannot escape as a result of the overpressure. However, this is not sufficient to provide an effective separation. The movement of the eluent with a linear solvent front can be ensured by placing a narrow plastic sheet on the layer or making a narrow channel in the layer ahead of the solvent inlet. In practice, a polythene or PTFE insert sheet with an eluent-leading channel is placed between the sorbent layer and the water cushion to protect the cushion and to direct the eluent as a linear front.

We have found that OPLC instruments are suitable for the development of several chromatoplates simultaneously if the plates are specially modified, *i.e.*, a hole of a suitable shape and size is made adjoining the eluent inlet. The eluent can travel almost unhindered among the sorbent layers, one on top of another, so the chromatograms can be developed simultaneously.

In practice, a hole has to be made in each plate except the lower one (as shown in Fig. 1a). This modification is made near the edge of the plate if linear one-directional development is to be carried out. The spreading of the eluent on the different plates, which is a condition of linear development, can be solved in different manners, *e.g.*, (i)

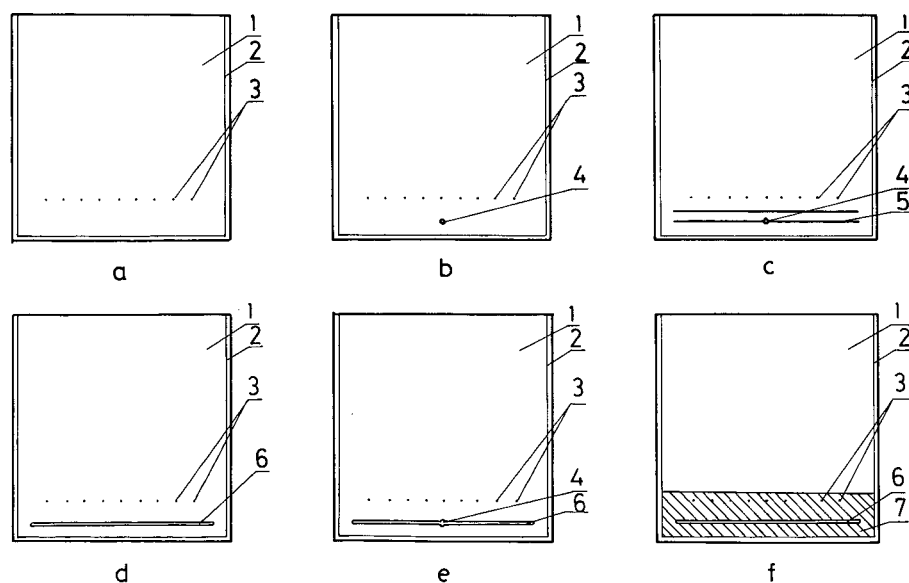


Fig. 1. Chromatoplates for one-directional linear OPMLC. (a) Basic chromatoplate; (b-e) with various perforations; (f) perforated chromatoplate with concentrating zone. 1, Sorbent layer; 2, impregnated edge; 3, sample application sites; 4, hole-like perforation; 5, directing channels in sorbent layer; 6, slit-like perforation; 7, inactive sorbent.

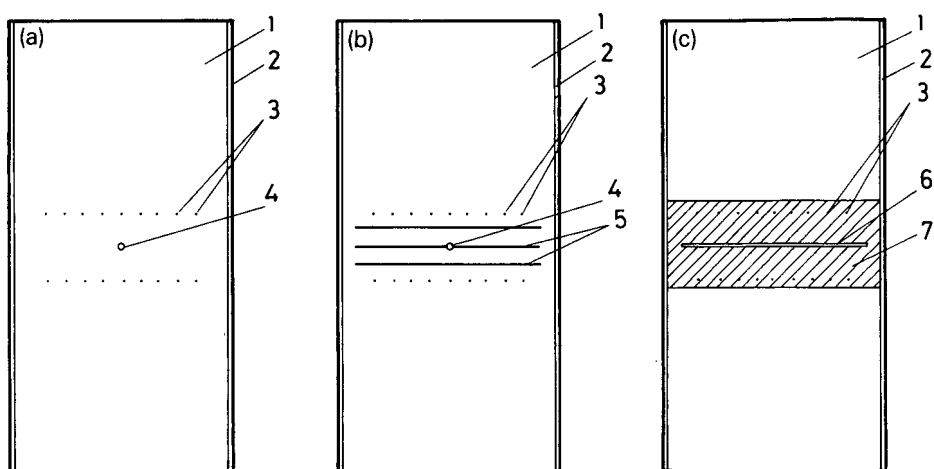


Fig. 2. Chromatoplates for two-directional linear OPMLC. 1, Sorbent layer; 2, impregnated edge; 3, sample application sites; 4, hole-like perforation; 5, directing channels in sorbent layer; 6, slit-like perforation; 7, inactive sorbent.

each sorbent layer can be covered with a perforated insert sheet supplied with leading channel; this is necessary in the situations shown in Fig. 1a and b; (ii) one or several channels leading the eluent can be cut into the sorbent layer (Fig. 1c); or (iii) the perforation is made at right-angles to the direction of the migration of the eluent and its shape is a longitudinal slit (Fig. 1d and e). One can also use chromatoplates having a concentrating zone (Fig. 1f) consisting of inactive sorbent.

If the hole was made in the middle of the plates after several have been placed on top of one another, these plates are suitable for circular multi-layer development. In this instance it is not necessary to impregnate the edges of the plate and to use channels to direct eluent.

If the development is two-directional, the hole is also made in the middle of the plate (as shown in Fig. 2a, b and c), but in this instance each sorbent layer can be covered with a perforated insert sheet supplied with a leading channel (Fig. 2a). Of course, the lower plate is not holed. Several channels leading the eluent can be also cut into the sorbent layer (Fig. 2b). Fig. 2c shows a combination of a longitudinal slit in the plate and a concentrating zone.

In practice one can place the holed plates with eluent-leading channels on the sorbent-free side on top of one another in the OPLC apparatus. The upper layer can be covered with a closure plate supplied with leading channels, while a conventional, hole-free plate as generally used in OPLC is fitted as the lower layer (as shown in Fig. 3). Therefore, although the cushion of the OPLC apparatus is applied to the topmost layer only, each plate serves as a cushion for the sorbent layer below it. Hence each sorbent layer is under pressure.

One can fasten a suitable number of holed covering plates with leading channels together, and several such units can be joined to each other (Fig. 4).

The eluent can be led out from the chromatoplates (sealed at all edges) similarly to the manner in which it is led in, through a hole on the opposite side to that for admission of the eluent. This gives the possibility of continuous development.

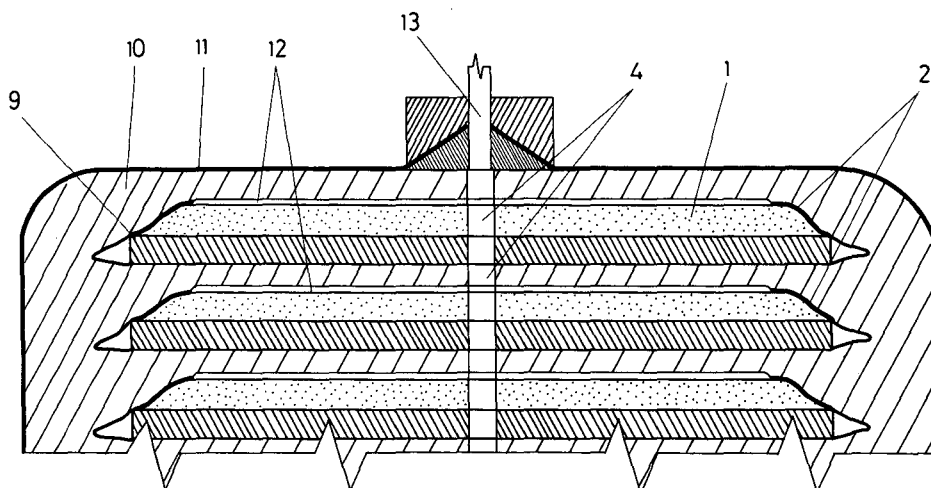


Fig. 3. Cover-plate system for OPMLC. 1, Sorbent layer; 2, impregnated edge; 4, hole-like perforation; 9, support plate; 10, cover-plate system for several plates; 11, cushion of Chrompres instrument; 12, eluent directing channel in cover-plate; 13, eluent inlet.

Theoretical aspects of OPMLC

In conventional layer chromatography, the relationship between the distance of visible eluent front (Z_t) and the development time (t) can be described by a quadratic equation¹⁹:

$$Z_t^2 = kt$$

where k is the velocity constant.

In OPLC, the eluent can be forced through the sorbent bed by means of a pump

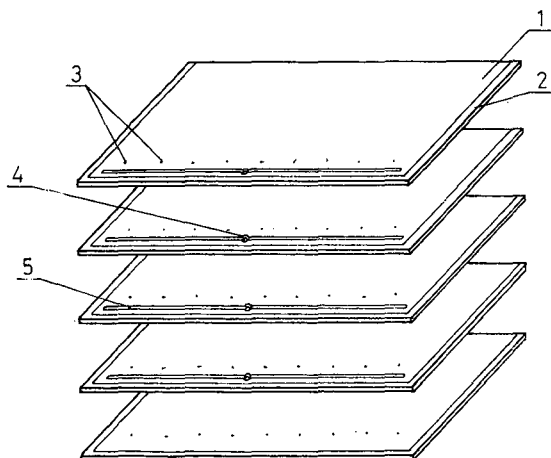


Fig. 4. Combination of plates. 1, Sorbent layer; 2, impregnated edge; 3, sample application sites; 4, hole-like perforation; 5, slit-like perforation (this latter perforation is also suitable for eluent direction).

system at a chosen flow-rate⁷. On feeding the eluent at constant velocity, the speed of the front depends on the cross-sectional area of the sorbent layer in the direction of development. It is obvious that in multi-layer system the cross-sectional area is correlated with the number of chromatoplates used or, more exactly, with the actual thickness of the sorbent layers.

In linear OPMLC, the basic flow equation is¹⁷

$$z_i = u_i t$$

where z_i is the migration distance of the i th component or the eluent front, u_i is the linear migration velocity of the i th component or the eluent and t is the time of development. In our experiences, there is almost no difference between the plates with regard to the retention data measured. Therefore, this basic flow equation is also suitable for describing the migration of eluent fronts in the multilayer system (or "layered sorbent column") in general. It should be pointed out that in linear OPMLC, similarly to linear OPLC, the velocity of the eluent front is constant along the plate, in contrast to the circular version of OPMLC, where the velocity of the front decreases along the radius with the developing time.

In classical fully off-line OPLC, in the zone which follows the α front (F_α) the

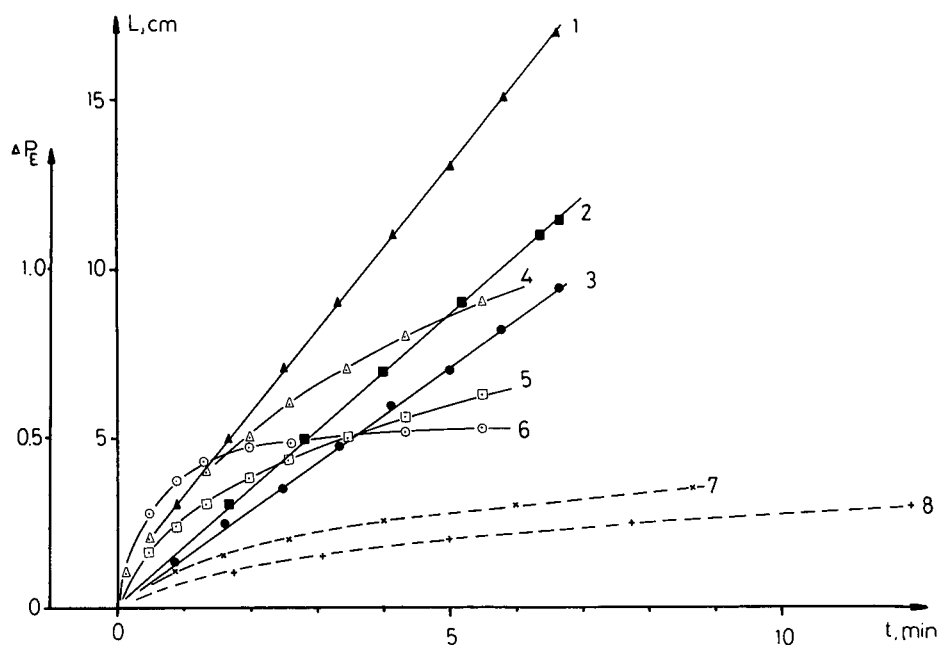


Fig. 5. Comparison of visual eluent front migration (F_α), front of total wetness ($F_{t,w}$) and eluent inlet pressure value (ΔP_E) in linear one-directional OPLC, circular OPLC and normal unsaturated (N_{us}) TLC chamber. Chromatographic conditions: Chrompres 10 OPLC instrument; HPTLC silica gel 60, $200 \times 200 \times 0.17$ mm; $P_{ext.}$, 1.5 MPa; eluent, carbon tetrachloride; flow-rate, $0.645 \text{ cm}^3/\text{min}$; temperature, 21°C . Linear one-directional OPLC: 1, F_α ; 2, $F_{t,w}$; 3, ΔP_E ; circular OPLC: 4, F_α ; 5, $F_{t,w}$; 6, ΔP_E ; normal TLC: 7, F_α , N_{us} ; 8, $F_{t,w}$, N_{us} .

spaces among the particles and within the pores are partially filled with both air and eluent and it was called the partially wetted zone (z_{pw})¹³. The next zone towards the eluent inlet is a totally wetted zone (z_{tw}), which is completely filled with eluent. The border between them is the front of total wetness (F_{tw}), which in most instances is not straight. On applying a constant flow-rate, F_z and F_{tw} are independent of the eluent (homologous alkyl alcohols), while the bed pressure drop or eluent inlet pressure increases with increasing homologue number, within experimental error²⁰. The pressure drop depends on the viscosity of the eluent, the particle size of the sorbent layer and the external pressure on the layer surface. Within experimental error, the "incompressible model" is in agreement with experiment and the velocities of the fronts are²⁰ $u_{F_z} = (1 + \alpha)u_{F_{tw}}$ and $\alpha = \varepsilon_p/\varepsilon_i$, where ε_i is the interstitial and ε_p the interparticulate porosity per total volume of the bed.

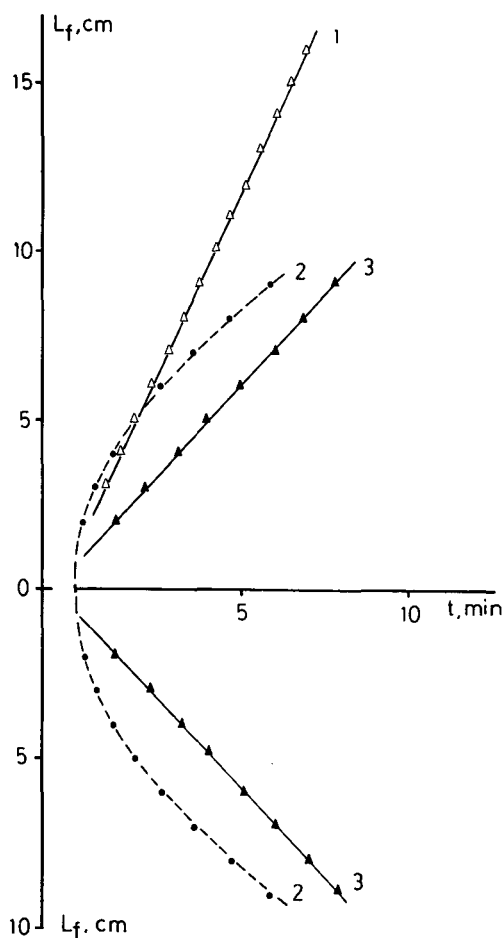


Fig. 6. Migration of visual eluent fronts measured on the top sorbent layer using different fully off-line overpressured three-layer chromatographic methods and a constant flow-rate. Chromatographic conditions: Chrompres 10 OPLC instrument; HPTLC silica gel 60; eluent, chloroform; temperature, 22.3°C; flow-rate on three sorbent layers, 1.575 cm³/min (i.e., 0.525 cm³/min on a single layer); $P_{ext.}$ 1.3 MPa. 1, Linear one-directional OPMLC; 2, circular OPMLC; 3, linear two-directional OPMLC.

Fig. 5 compares the changes in the migration of the fronts and the eluent inlet pressure in TLC and in OPLC. It can be seen that the pressure drop varies linearly with time of development and there is a fundamental difference among the conditions of eluent flow in conventional layer chromatography and linear and circular OPLC at a constant flow-rate.

Fig. 6 shows the migration of the eluent fronts measured on the top sorbent layer using different fully off-line OPLC on three sorbent layers and at a constant flow-rate. It can be seen that in the linear versions of OPMLC there is really a constant eluent front velocity, but in circular OPMLC this relationship is not valid. It is assumed that the migrations of the eluent fronts are the same on the second and third plates, but their measurement is technically impossible.

It is known that in conventional TLC the components of the eluent which are sorbed strongly by the sorbent sites can cause secondary fronts (F_{β} , F_{γ} , etc.)²¹. These fronts are independent of F_{tw} and can occur during adsorption and also during reversed-phase developments when the eluent consists of solvents of different strengths. The effect of this solvent demixing is stronger in a fully off-line OPLC system, owing to the total elimination of the vapour space, than in chambers with a small vapour space, *e.g.*, in sandwich chambers^{5,19}. These fronts divide the sorbent layer into zones of different eluting strength, within which the solvent polarity is almost the same, whereas at the fronts themselves there is a sudden increasing in eluent strength giving rise to "polarity steps". This phenomenon also occurs in circular and linear OPMLC.

The R_F of secondary fronts depends on the eluent composition. The eluent strength of a mixture can be calculated according to Snyder²² and it was correlated with the R_F , in the case of fully off-line OPLC, using silica gel 60 and different apolar and polar mixtures²³.

The location of F_{tw} can be altered by changing the flow-rate and the R_F value of F_{tw} can be increased or decreased by increasing or decreasing the flow-rate²⁰. Complete elimination of F_{tw} can be achieved by applying a pre-run prior to the separation in which the components to be analysed do not migrate and the air is removed from the sorbent layer. Eluents used in either TLC or HPLC can be applied in OPLC or OPMLC if the concentration of the polar constituent in the mixture is higher than 20%. On changing the apolar constituent to a more polar material both the $R_{F\beta}$ value and the eluent strength of Z_{β} will increase.

In HPLC there is a characteristic relationship between average theoretical plate height (H) and the eluent front velocity (u). It follows from the basic principles of OPLC that such a relationship can likewise be established^{24,25}. In conventional layer chromatography the height equivalent to a theoretical plate (HETP) can be calculated according to Guiochon and Siouffi²⁶ and it is also applicable to off-line OPLC systems⁸. For a given substance (i) the HETP (H) is given by

$$H_i = \frac{\sigma_i^2}{(L_f - s_0)R_{Fi}}$$

where σ_i is one-fourth of the width of the spot, L_f is the front distance, s_0 is the distance between the position of spotting and the trough of the eluent inlet and R_F is the retention factor.

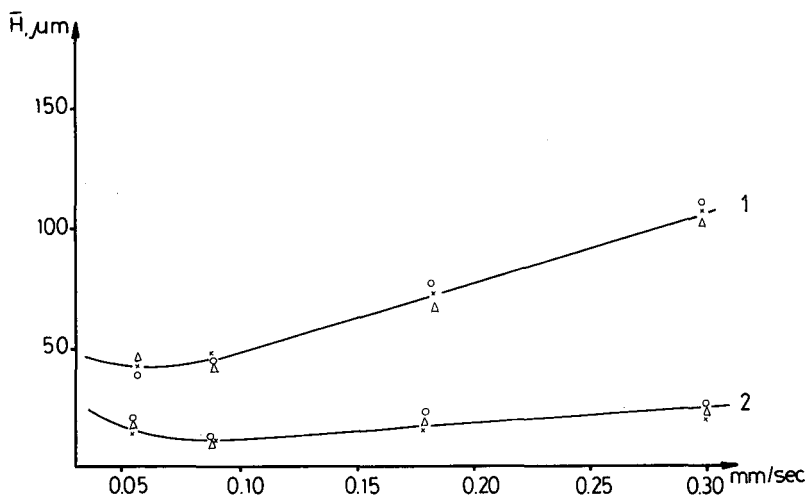


Fig. 7. Relationship between average theoretical plate height (\bar{H}) and eluent front velocity (u) in OPMLC on three sorbent layers for quaternary ammonium compounds. Chromatographic conditions: Chrompres 25 instrument; P_{ext} , 2.0 MPa; sorbent, HPTLC silica gel 60 F₂₅₄ with impregnated edges; eluent, isopropyl alcohol-methanol-0.9 M sodium acetate (20:3:30, v/v/v); reagent, Dragendorff. 1, Choline; 2, betaine. Δ , Upper plate; \times , second plate; \circ , lower plate.

Owing to the effect of focusing, an initial (starting) spot width may be defined that is different from the spot width deposited. The initial spot variance (σ_{0i}^*) of a given compound (i) is

$$\sigma_{0i}^* = \sigma_0^s(1 - R_{Fi}^E)R_{Fi}^s$$

where σ_0^s is the spot variance of the solvent deposited and R_{Fi}^s and R_{Fi}^E are the retention factors in the solvent and eluent, respectively.

In off-line OPMLC, the HETP may vary with the linear front velocity similarly to off-line OPLC (Fig. 7). It can be seen that the relationship between the HETP values and eluent front velocity does not differ significantly on the three sorbent layers in the case of two quaternary ammonium compounds.

It follows from these results that in OPMLC the maximum value of the spot capacity (n_M), which is the maximum number of compounds that can be separated with the system, is given separately for each plate by

$$n_M = \frac{1}{2} \cdot \frac{L}{H}$$

where L is the distance of development and H is the average HETP value of a compound under given conditions^{27,28}.

Applications of OPMLC

The application of several chromatoplates during one separation in same chamber is known in TLC^{5,19} and generates special advantages (*e.g.*, a large number of

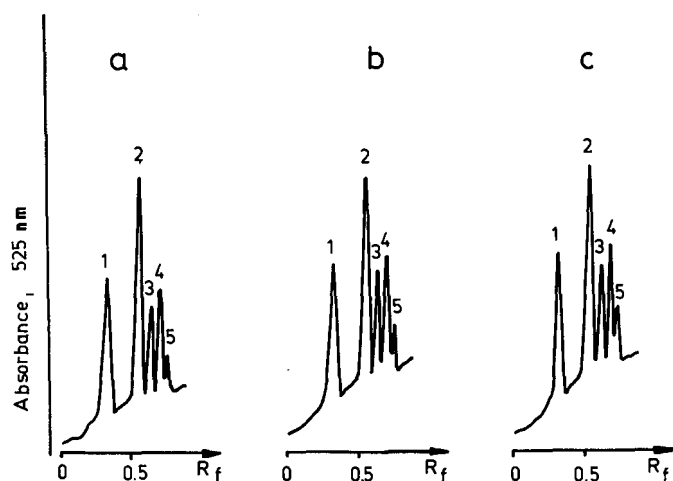


Fig. 8. Separation of quaternary ammonium compounds by circular OPMLC on three sorbent layers. Chromatographic conditions as in Fig. 7. Quantitative evaluation with Shimadzu CS-930 scanner. (a) Upper plate; (b) second plate; (c) lower plate. 1, *N*^ε-Trimethyl-L-lysine (TML); 2, choline; 3, carnitine; 4, trigonelline; 5, betaine.

samples can be used). However, the integration of a multilayer system in OPLC also exploits the advantages of a forced flow. OPMLC is qualitatively a new layer liquid chromatographic technique.

At the present stage of development of OPLC, 2–8 plates can be developed simultaneously, depending on the type of apparatus. The size of the plates and the direction of migration of the eluent (one-directional, two-directional, circular) can be chosen appropriately.

Inorganic (*e.g.*, silica gel, alumina, talc) or organic (*e.g.*, cellulose, polyamide) sorbents can be used on the plate. Siliceous marl and Celite can be employed as inactive sorbents.

Circular OPMLC is the simplest version of this attractive technique. In this mode we can use the plates without edge impregnation and eluent directing channels, but except for the lower plate we have to perforate the other plates in the middle where the eluent inlet point is also. Fig. 8 illustrates the separation of quaternary ammonium compounds by circular OPMLC on three silica gel layers, demonstrating only one densitogram from each chromatogram. It can be seen that the separation efficiency is very similar on each chromatogram.

Fig. 9 shows the separation of quaternary ammonium compounds by two-directional linear OPMLC, illustrating schematically only one densitogram from the two-directional three-layer chromatograms. Fig. 9 illustrates well the attraction of this operating mode.

Fig. 10 shows the determination of trigonelline with different $\text{NO}_3\text{-N}$ levels on tomato plants using repeated application of the samples in overpressured two-layer chromatography.

The Chrompres 10 OPLC instrument is also suitable for development over longer distances. Using a 30×20 cm fine-particle silica gel 60 layer (a gift from

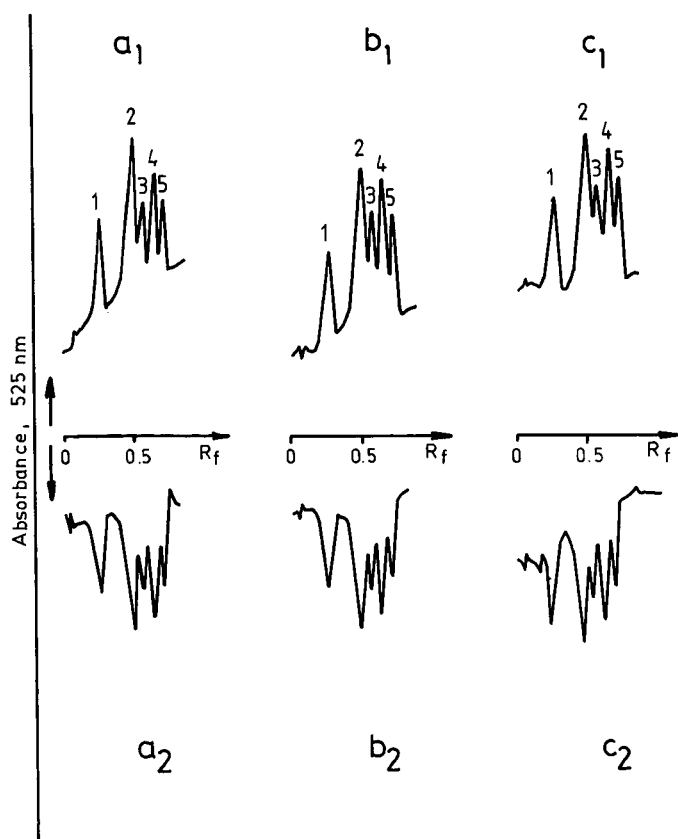


Fig. 9. Separation of quaternary ammonium compounds by two-directional linear OPMLC on three sorbent layers. Chromatographic conditions as in Fig. 7. (a_1 and a_2) Upper plate; (b_1 and b_2) second plate; (c_1 and c_2) lower plate. 1, TML; 2, choline; 3, carnitine; 4, trigonelline; 5, betaine.

Merck), the efficient separation of PTH-amino acids can be achieved by overpressured two-layer chromatography (Fig. 11).

Some special advantages of OPMLC are the following. Plates with different kinds of sorbent layers can be employed in a multi-plate system, so an eluent can be tested on several sorbent layers simultaneously and quickly. Conventional OPLC, as classical TLC or HPTLC, gives the possibility of using different specific colour reactions. In OPMLC there is a good possibility of using different colour reactions on the various plates, using the same sample on each plate.

To summarize, OPMLC is an attractive version of OPLC and 50–100 or more samples can be separated during one development. OPMLC can be used effectively, e.g., in plant breeding, clinical laboratories and industrial control laboratories, and for the sequence analysis of proteins and nucleic acids.

CONCLUSIONS

Preliminary experiences with OPMLC show that the combination of a multi-

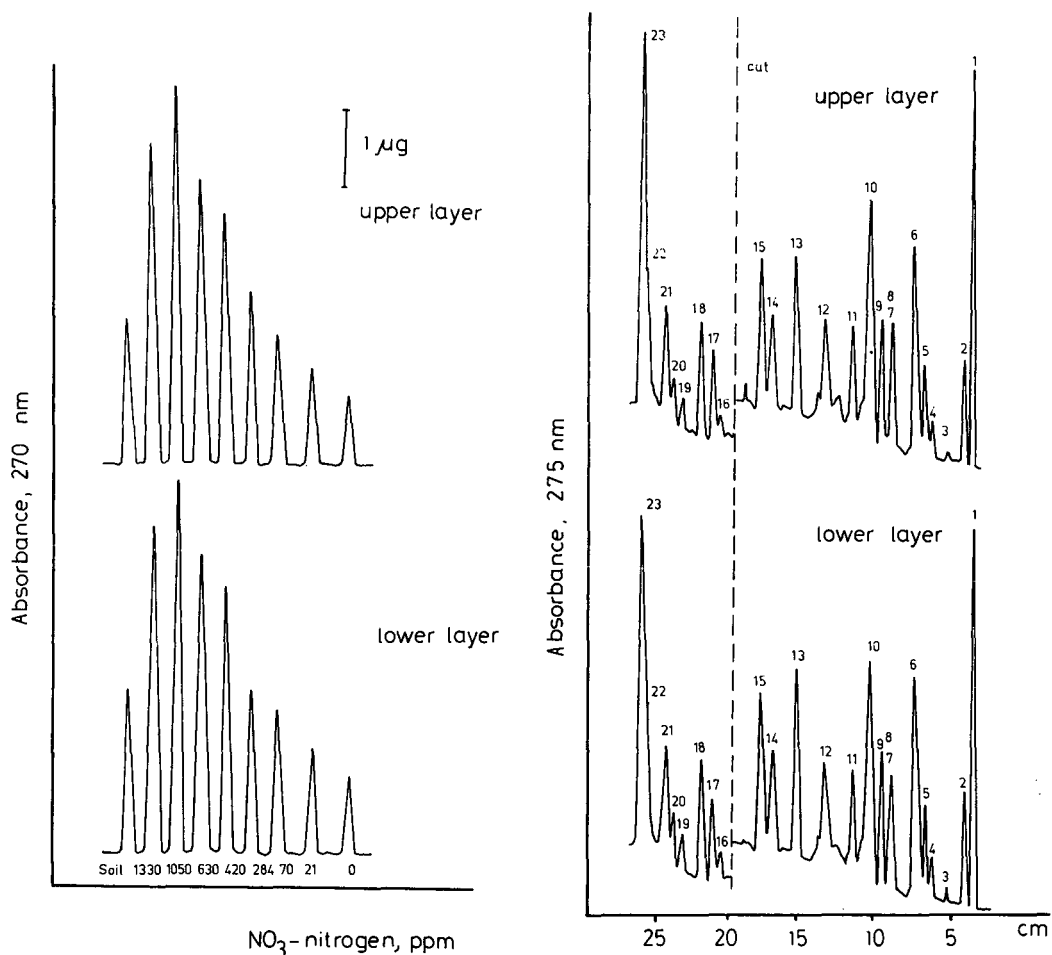


Fig. 10. Determination of trigonelline in tomato leaf extracts with different $\text{NO}_3\text{-N}$ levels by OPMLC on two sorbent layers. Chromatographic conditions as in Fig. 7, except quantitative evaluation at 270 nm with Shimadzu CS-930 scanner.

Fig. 11. Separation of PTH-amino acids by OPMLC on two sorbent layers simultaneously. Chromatographic conditions: Chrompres 10; HPTLC silica gel 60 F_{254} (20×30 cm, experimental plate) with impregnated edges; 1st eluent, chloroform-methanol-acetic acid (90:10:3, v/v/v); 2nd eluent, dichloromethane-ethyl acetate (90:10, v/v); sample, 400 ng of each PTH-amino acid; external pressure on the membrane in Chrompres 10 chamber, 1.4 MPa; absorbance, 275 nm using Shimadzu CS-920 scanner; 1st development time, 25 min at 19 cm; 2nd development time, 43 min (continuous development). The plate is cut for quantitative evaluation. 1, CySO_3K ; 2, His; 3, CH_3SO_2 ; 4, Asn; 5, Gln; 6, Asp; 7, Ser; 8, Glu; 9, Thr; 10, Lys; 11, Tyr; 12, Gly; 13, Trp; 14, Ala; 15, Met; 16, Phe; 17, Val; 18, Nle; 19, Ile; 20, Leu; 21, Pro; 22-23, eluent fronts.

layer system with a forced eluent flow complicates really to a certain extent the original simple and flexible TLC technique and also partly conventional Θ PLC. However, the result is an efficient and promising technique in the field of layer liquid chromatography which is applicable to analytical and preparative separations in various types of laboratories.

The development of OPMLC exploits unique possibilities of the layer liquid system which are absent from column liquid systems. The exploitation of the multi-layer system is carried out with the use of the modern column liquid chromatographic instrumentation, *e.g.*, a pump system for the admission of the eluent into the multi-layer system. The development of OPMLC makes a fundamental reassessment of densitometry desirable, with special emphasis on acceleration of measurement, sensitivity and resolution.

REFERENCES

- 1 A. J. P. Martin and R. L. Synge, *Biochem. J.*, 35 (1941) 138.
- 2 N. A. Izmailov and M. A. Shraiber, *Farmatsiya (Moscow)*, 3 (1938) 1.
- 3 I. G. Kirchner, M. J. Miller and I. G. Keller, *Anal. Chem.*, 23 (1951) 420.
- 4 E. Stahl, G. Schröter, G. Kraft and R. Renz, *Pharmazie*, 11 (1956) 633.
- 5 E. Stahl (Editor), *Thin-Layer Chromatography*, Springer, New York, 2nd ed., 1969.
- 6 T. Cotgreave and A. Lynes, *J. Chromatogr.*, 30 (1967) 117.
- 7 E. Tyihák, E. Mincsovcics and H. Kalász, *J. Chromatogr.*, 174 (1979) 75.
- 8 E. Mincsovcics, E. Tyihák and H. Kalász, *J. Chromatogr.*, 191 (1980) 293.
- 9 H. Kalász, J. Nagy, E. Tyihák and E. Mincsovcics, *J. Liq. Chromatogr.*, 3 (1980) 845.
- 10 E. Tyihák and E. Mincsovcics, *J. Planar Chromatogr.*, 1 (1988) 6.
- 11 E. Tyihák, E. Mincsovcics and F. Körmendi, *Hung. Sci. Instrum.*, 55 (1983) 33.
- 12 E. Tyihák and E. Mincsovcics, in R. E. Kaiser (Editor), *Proceedings of the Third International Symposium on Instrumental HPTLC*, Würzburg, Institut für Chromatographie, Bad Dürkheim, 1985, p. 442.
- 13 E. Mincsovcics, E. Tyihák and A. M. Siouffi, in E. Tyihák (Editor), *Proceedings of the International Symposium on TLC with Special Emphasis on OPLC*, Szeged, 1984, Labor-MIM, Budapest, 1986, p. 251.
- 14 P. Oroszlán, G. Verzár-Petri, E. Mincsovcics and T. J. Székely, in E. Tyihák (Editor), *Proceedings of the International Symposium on TLC with Special Emphasis on OPLC*, Szeged, 1984, Labor-MIM, Budapest, 1986, p. 343.
- 15 Sz. Nyiredy, C. A. J. Erdelmeier, K. Dallenbach-Toelke, K. Nyiredy-Mikita and O. Sticher, *J. Nat. Prod.*, 49 (1986) 885.
- 16 E. Tyihák, *J. Pharm. Biomed. Anal.*, 5 (1987) 191.
- 17 E. Tyihák, E. Mincsovcics, H. Kalász and J. Nagy, *J. Chromatogr.*, 211 (1981) 45.
- 18 E. Mincsovcics and E. Tyihák, *J. Planar Chromatogr.*, 1 (1988) 141.
- 19 F. Geiss, *Die Parameter der DC*, Vieweg, Braunschweig, 1972.
- 20 A. Velayudhan, B. Lillig and Cs. Horváth, *J. Chromatogr.*, 435 (1988) 397.
- 21 A. Niederwieser and M. Brenner, *Experientia*, 21 (1965) 50.
- 22 L. R. Snyder, *Principles of Adsorption Chromatography*, Marcel Dekker, New York, 1968.
- 23 E. Mincsovcics and E. Tyihák, in F. A. A. Dallas, H. Reid, R. J. Ruane and I. D. Wilson (Editors), *Recent Advances in Thin-Layer Chromatography*, Plenum Press, New York, 1988, p. 57.
- 24 H. Kalász and J. Nagy, *J. Liq. Chromatogr.*, 4 (1981) 985.
- 25 H. E. Hauck and W. Jost, *J. Chromatogr.*, 262 (1983) 113.
- 26 G. Guiochon and A. M. Siouffi, *J. Chromatogr. Sci.*, 16 (1978) 470.
- 27 G. Guiochon and A. M. Siouffi, *J. Chromatogr.*, 245 (1982) 1.
- 28 G. Guiochon, L. A. Beaver, M. F. Gonnord, A. M. Siouffi and M. Zakaria, *J. Chromatogr.*, 255 (1983) 415.

CHROM. 21 442

LASER MICROPROBE MASS SPECTROMETRY OF SELECTED COMPOUNDS DIRECTLY FROM NORMAL PHASE HIGH-PERFORMANCE THIN-LAYER PLATES

R. W. FINNEY and H. READ*

BP Research, Sunbury Research Centre, Chertsey Road, Sunbury-on-Thames, Middlesex TW16 7LN (U.K.)

SUMMARY

Direct analysis of high-performance thin-layer chromatography (HPTLC) plates by laser microprobe mass spectrometry has been demonstrated. A series of general organics and ionic surfactants were examined as reference materials and after application to normal-phase HPTLC plates. Spectra were generated, containing structurally significant ions and a contribution from the silica chromatography medium. After chromatography in a solvent system, spectra were weak but included sufficient compound-specific ions to permit structural confirmation. The identification of total unknowns by this means alone would at present be speculative but, supplemented by visualisation reagents and known chromatographic reference points, valuable information can be gained.

INTRODUCTION

Current mass spectrometry (MS) technology requires compounds of interest to be removed from the thin-layer plate prior to analysis. This may involve solvent elution or the scraping of the compound, along with the chromatographic support phase, from the plate.

Previous studies of direct analysis of thin-layer plates have incorporated desorption by various heat sources, followed by analysis of the desorbed species by thermal conductivity or flame ionisation detection^{1,2}, MS³, or by secondary ion mass spectrometry⁴. The use of lasers simply to desorb⁵ or both desorb and ionise species from thin-layer plates⁶ has been addressed. On-line mass analysis using both quadrupole and time-of-flight MS has been used.

Laser microprobe MS provides for the energy from a Nd:YAG laser to be directed onto a specimen retained at high vacuum. The ions produced are mass analysed by means of a time-of-flight mass spectrometer. Consequently, full mass spectra may be obtained from specific areas of the specimen.

The facility to examine compounds *in situ* on high-performance thin-layer chromatography (TLC) plates eliminates the possibility of chemically changing species during the elution process or losing trace components during scraping from the plate.

In addition, the spatial resolution of the laser is such that possible heterogeneity within a located spot on a plate may be examined.

The studies described herein were intended to determine the feasibility of examining HPTLC plates by this means, with reference to compounds selected from the categories of general organics and surfactants encountered in industrial detergent, fuel and oil formulations. Laser ionisation being a relatively recent development, few reference spectra for organic molecules are available. Consequently, laser spectra for those reference compounds chosen were determined prior to application to HPTLC media.

EXPERIMENTAL

Chromatographic procedure

All solvents and visualisation reagents were of analytical reagent grade (BDH, Poole, U.K.). Solvents were redistilled prior to use. Samples analysed were of technical grade from several commercial sources. The chromatography was carried out on pre-cleaned reactivated (120°C) aluminium backed HPTLC plates (Merck, BHD). Samples were applied as 3 μ l aliquots using the HPTLC spot applicator (Linomatt IV, Camag). The plates were developed in toluene-methanol (4:1).

The solvent front was allowed to migrate 150 mm up the plate, followed by drying in a stream of nitrogen. The spots were visualised using ultraviolet illumination at 254 and 365 nm, followed by iodine vapour visualisation prior to analysis by laser microprobe MS.

Sample presentation

Reference compounds were applied as powders or crystals to double-sided adhesive tape or as thin smears to the surface of aluminium foil. These were mounted onto an aluminium sample holder and retained with a stainless-steel grid which also assisted in residual charge dissipation.

Instrumental

The LIMA-4 laser microprobe (Cambridge Mass Spectrometry, Cambridge, U.K.) optically directs light at 266 nm from a Nd:YAG laser source, onto a specimen retained at ultra-high vacuum. The sample can be moved by means of a stepper-motor driven stage and viewed using an optical microscope-closed-circuit TV system.

Locations on the specimen can be specifically interrogated at high spatial resolution (*ca.* 1 μ m). Simultaneous information may be obtained relating to elemental, inorganic and organic components.

Ionised species produced by the laser impact are mass analysed by a time-of-flight mass spectrometer which provides for a simultaneous detection of all ions produced over a large mass range (*ca.* 10 000 daltons) and offers a sensitivity of detection in the order of 10 ppm for selected elemental species.

Specimens were examined in positive and negative ion modes and, in each case, laser power and beam focus were optimised to produce structurally significant mass spectra.

RESULTS AND DISCUSSION

Reference spectra were obtained for several general organic molecules. Fig. 1 shows the spectrum obtained for methoxybenzoic acid under negative ion conditions at optimal laser powers. The spectrum includes an abundant M^- at m/z 152 with an equally intense $[M-OH]^-$ at m/z 135. Structural ions at m/z 107 from the loss of COOH from the molecule and at m/z 93 the $[C_6H_5O]^-$ species were also noted.

The spectrum shown in Fig. 2 is of *p*-aminobenzoic acid, in the positive ion mode. Ions associated with the M^+ at m/z 137, the loss of NH_2 at m/z 121 and the elimination of COOH at m/z 92 were the most significant structure-related ions observed.

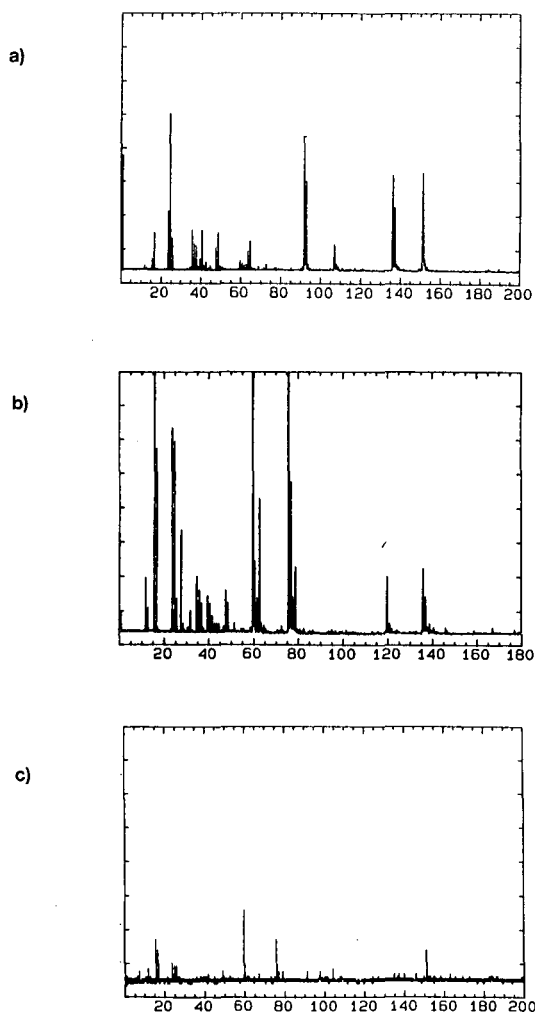


Fig. 1. Laser ionisation mass spectra of methoxy benzoic acid (negative ions). (a) Reference standard, solid; (b) HPTLC plate origin; (c) after chromatography in toluene-methanol (4:1).

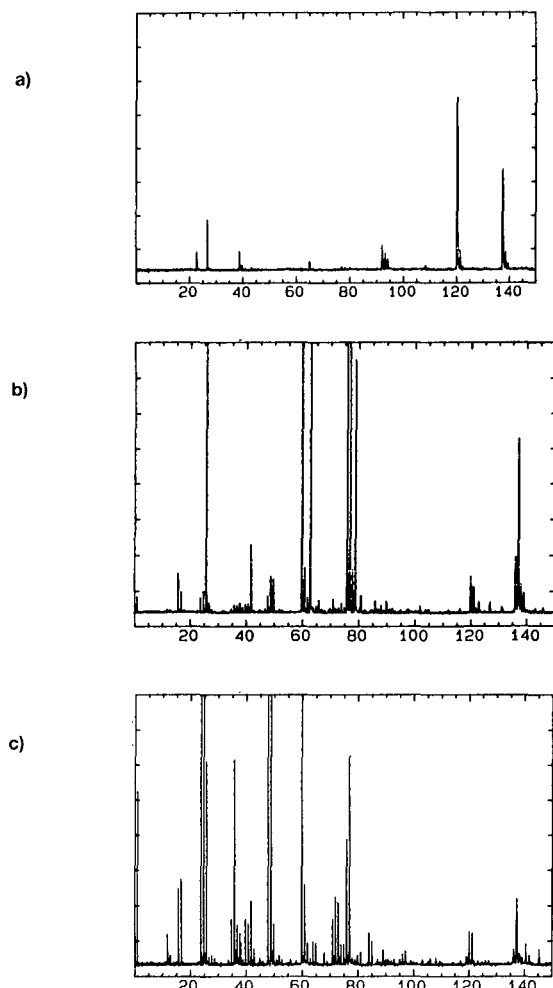


Fig. 2. Laser ionisation mass spectra of *p*-aminobenzoic acid. (a) Reference standard, solid (positive ions); (b) HPTLC plate origin (negative ions); (c) after chromatography in toluene-methanol (4:1) (negative ions).

Cetylpyridinium bromide is a cationic ionic surfactant used in fuels formulations. Its typical laser ionisation spectrum is shown in Fig. 3, with negative ions at m/z 380 $[M]^-$, m/z 301 $[M-Br]^-$, m/z 299 $[M-HBr]^-$, m/z 223 $[C_{16}H_{31}]^-$, m/z 159 $[C_5H_6NBr]^-$ and m/z 79/81 $[Br]^-$ evident.

The anionic surfactants sodium dodecylsulphate and sodium dodecylbenzenesulphonate were similarly examined. Figs. 4 and 5 show the negative ion spectra. Ions corresponding to $[M-Na]^-$ (m/z 265), $[NaSO_4]^-$ (m/z 119), $[NaSO_3]^-$ (m/z 103), $[SO_4]^-$ (m/z 96), $[SO_3]^-$ (m/z 80), $[SO_2]^-$ (m/z 64), $[SO]^-$ (m/z 48) and $[S]^-$ m/z 32/34 were noted in the former. In the latter, a strong response at m/z 184 was noted in a spectrum difficult to rationalise but totally reproducible.

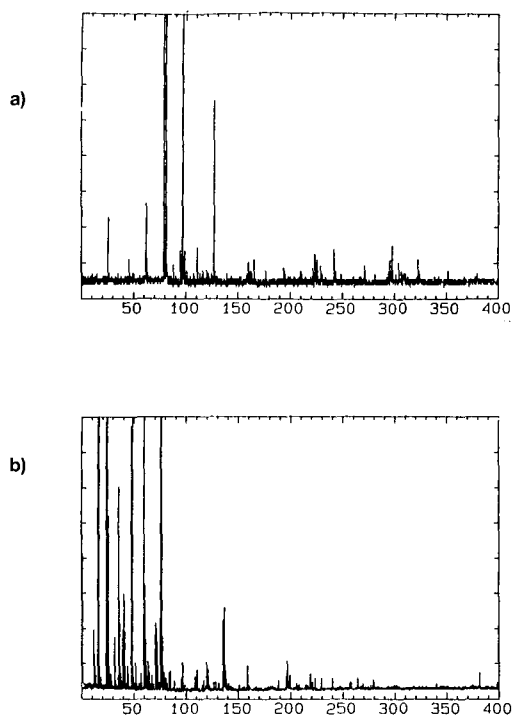


Fig. 3. Laser ionisation mass spectra of cetylpyridinium bromide (negative ions). (a) Reference standard, solid; (b) HPTLC plate origin.

With representative laser ionisation spectra for each compound to be studied available, each selected compound was spotted onto a thin-layer plate and its position of application noted. Sections of plate were removed and examined by laser ionisation mass analysis and spectra compared with those obtained previously.

Figs. 1–5 show the comparable spectra obtained directly by laser ablation and ionisation from normal-phase HPTLC plates. In most cases, the major spectral ions were similar to those obtained from pure reference materials. Generally, however, higher laser powers were required to desorb and ionise equivalent species from the chromatographic matrix.

The influence of the matrix is shown by an examination of Figs. 1 and 2. Methoxybenzoic acid as a solid reference material fragments to yield a strong M^- at m/z 152, with structural ions at m/z 135, 107 and 93, as previously described. When applied to the origin of an HPTLC plate, no molecular ion was evident, the most intense structurally specific ion being from the $[M-OH]^-$ at m/z 135.

p-Aminobenzoic acid yielded a strong positive ion spectrum when examined as a reference material. From the chromatography plate, however, the negative ion spectrum was found to provide more structural information, with prominent M^- and $[M-NH_2]^-$ being noted.

These differences in the qualitative nature of laser ionisation spectra from different matrices demands some caution to be exercised when comparing reference spectra with those from such media as that studied here.

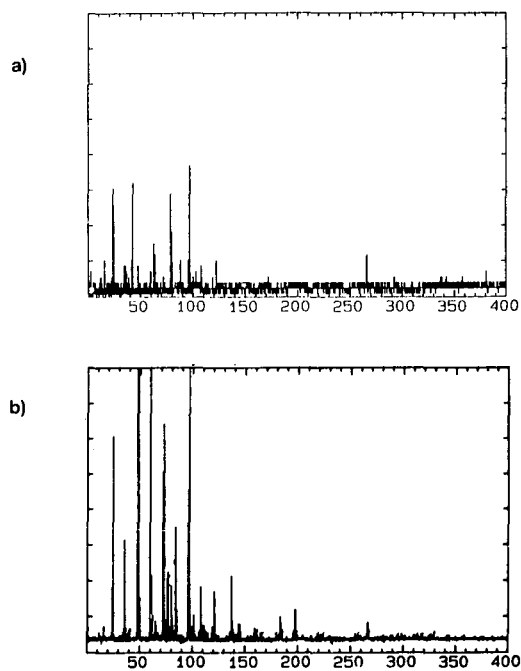


Fig. 4. Laser ionisation mass spectra of sodium dodecylsulphate (negative ions). (a) Reference standard, solid; (b) HPTLC plate origin.

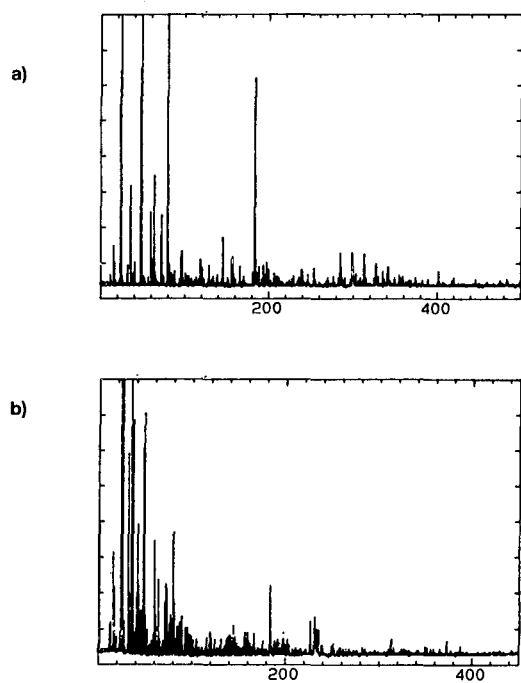


Fig. 5. Laser ionisation mass spectra of sodium dodecylbenzenesulphonate (negative ions). (a) Reference standard, solid; (b) HPTLC plate origin.

Several features of the laser ionisation process may influence spectral quality. Whilst the amount of laser energy incident onto the sample may be nominally similar, the proportion of that power absorbed by the specimen is determined by the chemical nature, morphology and topography of the specimen and matrix. The chromatographic support, being white in colour, tends to absorb heat less efficiently than does a darker medium. Possibly, more of the laser irradiation will be reflected and consequently proportionately less coupled to the sample. In addition, the surface of the HPTLC plate undulates on a micro scale and hence the focussing of the laser beam onto the surface is made more difficult. Also one must consider the effects of striking a matrix composed of potentially ionisable species and possible competitive effects.

The influence of the silica background was apparent in negative ion spectra. Major responses were m/z 60 $[\text{SiO}_2]^-$, m/z 76 $[\text{SiO}_3]^-$, m/z 72 $[\text{Si-O-Si}]^-$, with reduced contributions at m/z 88 $[\text{Si}_2\text{O}_2]^-$, m/z 104 $[\text{Si}_2\text{O}_3]^-$, m/z 120 $[\text{Si}_2\text{O}_4]^-$ and m/z 136 $[\text{Si}_2\text{O}_5]^-$. In some cases, minor silica-derived responses overlapped with major structural ions from the compounds being studied. These contributions were of sufficiently low intensity to be unlikely to compromise sample spectra.

Some of the selected samples were spotted as before onto normal-phase silica and chromatographed in toluene-methanol. Spectra are shown in Figs. 1 and 2 and can be seen to consist of major structural fragments and molecular species as were found in previous experiments.

In essence, the detection of target compounds after chromatography was shown to be feasible. Spectra were, however, weak due to the "smearing" effects of the chromatographic process. More recent studies of regions of HPTLC plates previously visualised with compound-specific reagents have shown the great enhancement of spectral quality to be derived by removing chromatographic phase outside the immediate area of interest. By exposing the aluminium backing around the "spot", the difficulties associated with sample charging can be reduced.

The identification of a total unknown compound by this means alone would be tentative. Additional information, relating to specific visualisation techniques, chromatographic reference points and specimen origin etc would, however, make possible the confirmation of the presence of specified compounds or compound-types. Also, an initial screening of the HPTLC plate by laser microprobe MS for components worthy of further study would be appropriate.

CONCLUSION

Structurally significant mass spectra have been obtained from selected reference compounds separated on HPTLC plates. Direct mass spectral analysis without removal of the component from the plate avoids potential problems of contamination or poor recovery of material by the elution process. Initial studies indicated that spectra were weak but by exposing the metal backing plate around the area of interest, spectral intensity and quality were improved.

The combination of HPTLC separation with laser ionisation and the high sensitivity of detection associated with a time-of-flight mass analyser, has been shown to produce meaningful spectra for low levels of separated components. Used in conjunction with retention and selective chemical visualisation information, the HPTLC-laser microprobe technique is an extremely useful aid to the structural confirmation

of separated components. The spatial resolution of the laser beam may also permit the examination of chemical heterogeneity within the same area of the thin-layer plate.

FURTHER WORK

Further work will include the study of more complex mixtures and establish the potential of the technique for problem-solving on real samples. Initial experiments in this direction are promising and useful information has already been provided. Comparisons with the fast atom bombardment MS-HPTLC technique⁷ will be pursued. In addition, some study of means of reducing sample charging after several laser pulses may go some way to improving the spectral intensity, particularly of positive ion species.

ACKNOWLEDGEMENTS

We thank Mr. A. Carter for providing the HPTLC specimens and the British Petroleum Company plc for permission to publish this research.

REFERENCES

- 1 T. Cotgreave and A. Lynes, *J. Chromatogr.*, 30 (1967) 117.
- 2 H. K. Mangold and K. D. Mukharjee, *J. Chromatogr. Sci.*, 13 (1975) 398.
- 3 R. Kaiser, *Chem. Br.*, 5 (1967) 54.
- 4 M. S. Stanley, K. L. Duffin, S. J. Doherty and K. L. Bush, *Anal. Chim. Acta*, 200 (1987) 447.
- 5 L. Ramaley, M. A. Vaughan and W. D. Jamieson, *Anal. Chem.*, 57 (1985) 353.
- 6 F. P. Novak and D. M. Hercules, *Anal. Lett.*, 18 (1985) 503.
- 7 K. J. Bare and H. Read, *Analyst (London)*, 112 (1987) 433.

CHROM. 21 294

DETERMINATION OF FREE AND ESTERIFIED STEROLS AND OF WAX ESTERS IN OILS AND FATS BY COUPLED LIQUID CHROMATOGRAPHY–GAS CHROMATOGRAPHY

KONRAD GROB* and MAURO LANFRANCHI

Kantonales Labor, P.O. Box, CH-8030 Zürich (Switzerland)

and

CARLO MARIANI

Via Scheiwiller 1, I-20139 Milan (Italy)

SUMMARY

A liquid chromatographic–gas chromatographic (LC–GC) method is described for the rapid determination of free sterols, esterified sterols and wax esters in oils and fats in a single GC run, circumventing saponification and any off-line preseparation. The free sterols are esterified with pivalic acid in the oil. The diluted oil is injected into the LC system and the fraction containing the above classes of compounds is transferred to the gas chromatograph (carried out by a fully automated LC–GC instrument). The information obtained with this analysis allows a better identification of oils and fats and a better characterization of the treatment of an oil (*e.g.*, distinguishing between cold-pressed and extraction oils and between different refining methods).

INTRODUCTION

Small-bore liquid chromatographic columns with silica

There is a new field, namely coupled liquid chromatography–gas chromatography (LC–GC), making wide use of the small-bore LC columns initiated by Scott and Kucera in 1976¹ and subsequently reviewed^{2,3}. In addition to other arguments brought forward by users of small-bore LC columns, in coupled LC–GC there is a strong interest in keeping the LC fraction volumes small in order to facilitate transfer, to shorten solvent evaporation times and to keep the peaks due to solvent impurities as small as possible. Column diameters down to 0.25 mm have been used⁴. Many applications, however, call for larger column diameters to provide the capacity required by the sample (*e.g.*, in the application considered below), and 2 mm I.D. LC columns have proved to be well suited. In addition to the small-bore LC columns, coupled LC–GC has profited from the work on silica gel carried out by Scott and Traiman⁵. As in sample preparation for conventional LC, normal-phase chromatography is far more important when using LC for sample preparation than for the final analytical determinations.

Sterol determination

As the fatty acid composition of fats and oils often does not allow one to distinguish between different oils or different qualities of a given oil, trace components are determined in order to obtain the information required. The most important groups of these compounds are the sterols and the triterpene alcohols. Their presence and concentrations vary over a far wider range than those of the fatty acids.

The sterol fraction is analysed for the identification of a fat or an oil (*e.g.*, to distinguish between sunflower oil and other oils of similar fatty acid composition^{6,7}), for the detection of the addition of non-declared cheap oils to more expensive oils (*e.g.*, rapeseed oil in olive oil) or to distinguish between different qualities of the same oil (*e.g.*, between virgin, *i.e.*, cold-pressed, and extraction olive oils⁸, or oils subjected to different treatments⁹). Wax ester contents are measured during the refining of certain oils^{10,11}, but also serve to distinguish between virgin and extraction olive oil¹². For the latter analysis an LC–GC method has been described¹³.

Considerable efforts have been made to develop rapid methods for the analysis of the sterol fraction. Nearly all methods start with the saponification of the triglycerides. The unsaponifiable matter is extracted and analysed directly (with considerable problems concerning interfering peaks) or after preseparation, classically carried out by thin-layer chromatography^{14–17}. Thin-layer chromatography can be replaced with chromatography on silica gel columns^{18,19} or by off-line high-performance liquid chromatography (LC)²⁰. Finally, adsorption on aluminium oxide has been used to circumvent the often tedious extraction of the saponified fat²¹.

We propose here a fundamentally new method, greatly reducing manual operations and providing more information at the same time. Saponification of the triglycerides is avoided; instead, the triglycerides are removed by LC. Simultaneously, interfering components are removed. Previous esterification of the free sterols (and other alcohols) with pivalic acid allows the determination of the free and the esterified sterols and of the wax esters within the same GC run. On-line coupling of LC to GC allows full automation of the analysis except for the derivatization carried out in the fat or oil.

CONCEPT OF THE METHOD

When simultaneously determining several components by coupled LC–GC, the major problem in LC concerns not separating these components at the maximum separation efficiency in order to obtain a narrow fraction containing the components of interest. This is often a problem. For instance, when determining sterols in an unsaponified fat, both free and esterified sterols should be isolated from the triglycerides and transferred to the GC system. However, free sterols elute from LC columns far removed from the sterol esters. Esterified sterols elute from silica gel columns nearly together with the wax esters. Hence, all three classes of compounds of interest, the free and esterified sterols and the wax esters, can be transferred to the GC system within the same fraction if we succeed in derivatizing the free sterols in such a way that their LC retention time corresponds to the esterified sterols and the wax esters.

Esterified sterols are eluted from apolar GC capillary columns at *ca.* 350°C, clearly separated from the wax esters. As they are split into several peaks (each sterol can be esterified with all the fatty acids available) and their quantitation is based on

the summed peak areas, this separation from the wax esters is important. The derivatized free sterols form a single GC peak for each sterol and should again be positioned such that no other peaks (wax ester peaks) interfere. To keep the maximum analysis temperature at an acceptable level, they should elute before the esterified sterols. As there is not sufficient "space" in the chromatogram between the wax esters and the sterol esters, this necessitates elution even before the wax esters.

Esterification of the free sterols with a short-chain acid (*e.g.*, acetylation) causes these components to be eluted from the GC capillary column well before the wax esters. However, their polarity is so high that in LC they are eluted excessively far behind the esterified sterols and wax esters. On elongating the chain length of the acid used for esterification, the situation improves in LC, but shifts the corresponding GC peaks into the zone where the wax ester peaks are located. To solve this problem, the free sterols were esterified with pivalic acid. The bulky apolar part of this 2,2-dimethylpropanoic acid protects the polar ester group, reducing the LC retention time. The molecular weight is still low enough to keep the GC retention time clearly below that of the wax esters.

EXPERIMENTAL

Derivatization of the free sterols

Sterols were derivatized with pivalic anhydride, primarily because pivalic chloride produces a strong odour. The conditions required for the derivatization were investigated using the following experiment. Sitosterol was added to an olive oil to increase its concentration to 1%. To 100 μl of this oil, 10–50 μl of pivalic anhydride were added. This mixture was heated at various temperatures for 15 min. Then the oil was diluted 1:100 with *n*-heptane and 0.3 μl of the mixture was injected on-column on to a 17 m \times 0.27 mm I.D. glass capillary column coated with SE-52 of 0.15- μm film thickness. Free sitosterol eluted clearly before the corresponding pivalate ester, allowing a rapid determination of the esterification yield.

In a first step, it was found that the addition of pyridine (10 μl) to the reaction mixture did not accelerate esterification. Nevertheless, pyridine was used as a solvent for adding the internal standard. The amount of anhydride and the reaction temperature required can be derived from Table I.

For the determination of the sterols, the following procedure was applied. To

TABLE I
YIELDS OF ESTERIFIED SITOSTEROL UNDER DIFFERENT CONDITIONS

Temperature (°C)	Pivalic anhydride (μl)	Yield (%)
120	10	35
120	50	92
140	20	82
140	50	100
160	10	62
160	20	95
160	50	100

100 mg of the oil to be analysed, weighed into a 10-ml screw-capped flask, 10 μ l of a 1% cholesterol solution in pyridine were added as an internal standard, representing a 0.1% concentration. Pivalic anhydride (50 μ l) was added and the mixture was heated at 150°C on a hot-plate. After 15 min, the flask was filled with *n*-heptane, resulting in a 1:100 dilution.

Instrumentation

LC-GC was performed on a prototype of the fully automated Carlo Erba LC-GC instrument²². This instrument included a 20-ml syringe pump (Phoenix 20), a fully automated valve system for the interface and the solvent vapour exit, and a GC oven equipped with a loop-type and an on-column interface.

LC conditions

LC prepreparation was carried out on a 10 cm \times 2 mm I.D. silica gel column (Spherisorb S-5-W) from Knauer, using *n*-hexane-dichloromethane (80:20) containing 0.05% of acetonitrile as the eluent. Volumes of 20 μ l were injected through a Valco six-port valve; detection was performed at 220 nm. Derivatized oils produced a small, broad peak (representing many compounds) at the position of the esters analysed Fig. 1). The fraction transferred to the GC system (750 μ l) was slightly extended towards higher retention times (as indicated in the chromatogram) to include all material of the originally free sterols (pivalate esters). The LC column was backflushed (first removing the triglycerides) with 1 ml of dichloromethane-acetonitrile (95:5), followed by normal eluent, 2 min after transfer of the ester fraction to the GC system. The backflush valve returned to stand-by 10 min later. There were 45 min between two injections. The regularity of this cycle ensured stable LC retention times.

LC-GC transfer

Concurrent eluent evaporation²³ was applied with the loop-type LC-GC interface²⁴. A solvent vapour exit was used at the column exit, diverting most of the

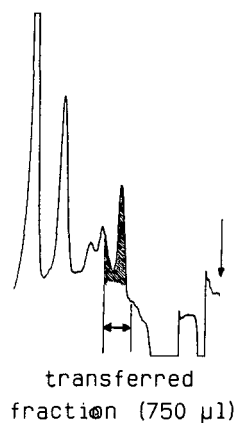


Fig. 1. Liquid chromatogram of an olive oil after esterification with pivalic anhydride. The fraction indicated was transferred to the GC system (Fig. 2). The triglycerides would be eluted later, but were removed by backflushing (not shown).

solvent before it entered the detector. The carrier gas inlet pressure behind the flow regulator was 3 bar; the regulated flow-rate 3 ml/min; GC column temperature during transfer 2.7 min after injection, 130°C. The sample and the carrier gas valves switched to transfer, and the solvent vapour exit opened at the same time. Then, 5 min later, the sample and the gas valve returned to stand-by and the GC oven was heated at 30°C/min to 200°C, then at 10°C/min to 350°C. With a delay of 40 s on the reduction of the inlet pressure at the end of the transfer, the solvent vapour exit automatically switched to a high resistance (2 m × 75 μm I.D. fused-silica capillary), leaving a small purge flow.

GC separation

GC separation was carried out on a 15 m × 0.32 mm I.D. glass capillary column coated with PS-225 (a methylsilicone) of 0.15-μm film thickness. This column was equipped with a 3 m × 0.32 mm I.D. fused-silica precolumn deactivated by phenyldimethylsilylation (connection: press-fit, after opening of the glass capillary butt²⁵). The column exit, equipped with a short piece of 0.32 mm I.D. fused-silica tubing, was mounted in the stainless-steel T-piece of the solvent vapour exit, which in turn was connected to the flame ionization detector through a 15 cm × 100 μm I.D. fused-silica capillary.

RESULTS

Fig. 2 shows the gas chromatogram obtained from the fraction of the olive oil shown in Fig. 1. The small peaks eluted before the cholesterol (internal standard) have not been identified, but probably represent originally free fatty alcohols (now esterified with pivalic acid). The group of the originally free sterols clearly shows the

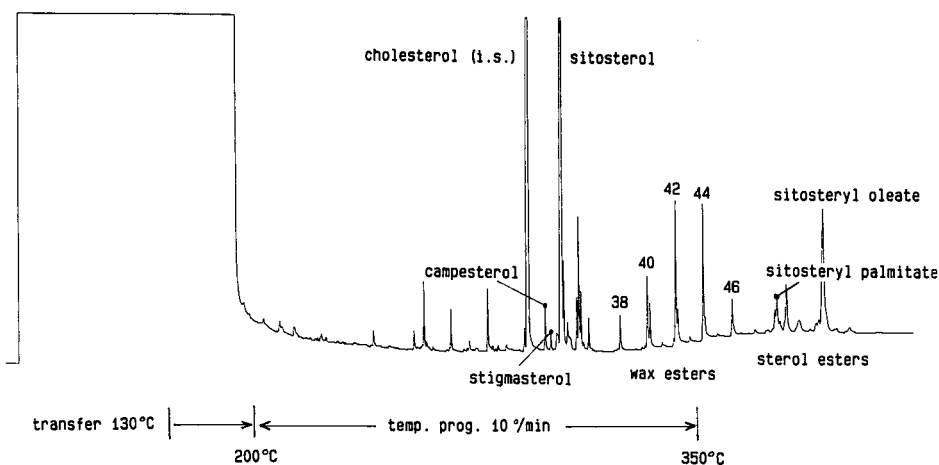


Fig. 2. Gas chromatogram of the olive oil fraction shown in Fig. 1. Cholesterol was added as an internal standard (0.1% referred to the oil). Wax esters are indicated by the total number of carbon atoms. The solvent peak has a width of 7.5 min. The analysis lasted 31 min. The olive oil shown, a commercial oil not declared as "extra virgin" (cold-pressed), contains some extraction oil, as shown by the moderately high concentration of the wax esters and by the fact that the wax esters 42 and 44 are most abundant. On the other hand, the concentration of free sitosterol (740 ppm) is low.

abundance of β -sitosterol (740 ppm) and the two much smaller campesterol and stigmasterol peaks typical of olive oil. The peaks immediately following sitosterol have not been identified. Next are the peaks of the wax esters, characterized by total carbon numbers. Finally, the sterol esters form a multiplet of peaks. The major peak represents sitosteryl oleate, combined with slightly later eluted sitosteryl stearate and the esters of avenastanol. Some tentative identifications suggested that there are some compounds other than sterol esters, forming peaks primarily between the C_{16} and C_{18} sitosteryl esters.

Available information

The following information is available from the described analysis:

(1) The total sterol content is calculated by addition of the concentrations of the originally free sterols and of the esterified sterols. We found good agreement with results obtained by the classical method involving saponification.

(2) The sterol composition (individual concentrations relative to the total sterol concentration, as commonly used for characterizing a fat or oil) is calculated from the free sterols, assuming that the compositions of the free and the esterified esters are identical (small deviations are negligible as the esterified sterols represent only small proportions of the total sterol content).

(3) The ratio of the (originally) free to the esterified sterols is probably a sensitive indicator of oil treatments. For instance, extraction oils contain considerably higher concentrations of free sterols than cold-pressed oils, whereas the esterified sterols are nearly completely recovered by the cold-pressed oil. Treatments such as filtration or crystallization affect the free and esterified sterols to different extents.

(4) The amounts and the composition of the wax esters are different for cold-

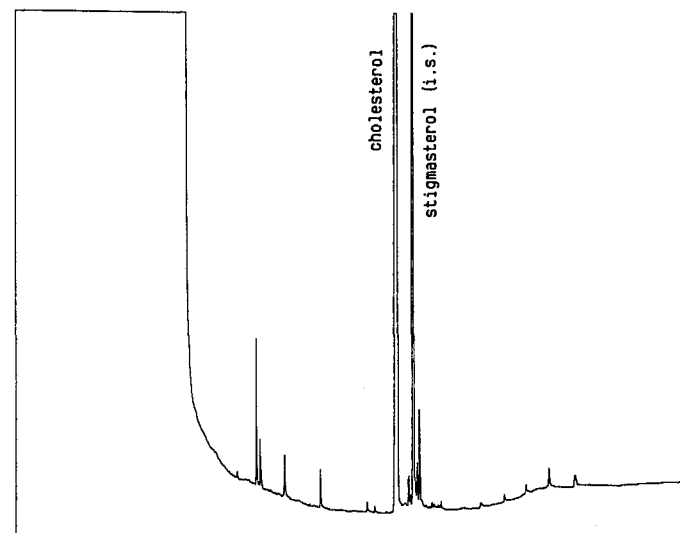


Fig. 3. Rapid determination of the cholesterol concentration in a butter fat, using stigmasterol as internal standard.

pressed (virgin) and extracted olive oil, and are again influenced by the methods applied for refining the oil.

Application of the new technique to routine analysis has only just started, and a more thorough study on the recognition of differently treated olive oils is in progress. Some preliminary results are given below.

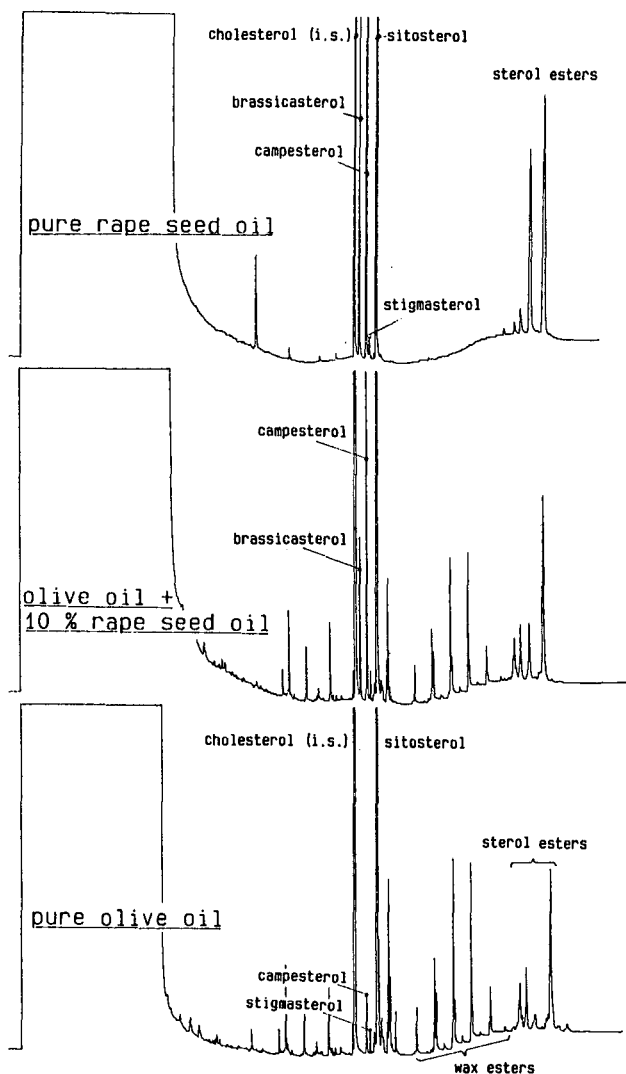


Fig. 4. Determination of rapeseed oil in olive oil. Rapeseed oil contains high concentrations of brassicasterol and campesterol (top chromatogram), whereas these sterols are absent or present at only low concentration in olive oil (bottom chromatogram). The detection limit for rapeseed oil in olive oil is below 1% (middle chromatogram).

Butter fat

Butter fat produced the simplest chromatogram of the fats analysed (Fig. 3). Stigmasterol (0.1%) was added as an internal standard (instead of the cholesterol added to the plant fats and oils). Most of the peaks near this stigmasterol peak represent impurities in the stigmasterol. Hence, cholesterol (present at a concentration of 0.28%) is almost the only peak in the chromatogram. There is no significant concentration of esterified cholesterol. The small peaks at the rear of the chromatogram were not identified, but eluted at higher retention times than the wax esters found in plant fats and oils.

Rape seed oil in olive oil

Fig. 4 shows the sterols and wax esters of a rapeseed oil, an olive oil and an olive oil containing 10% rapeseed oil. Rapeseed oil is characterized by a high total sterol

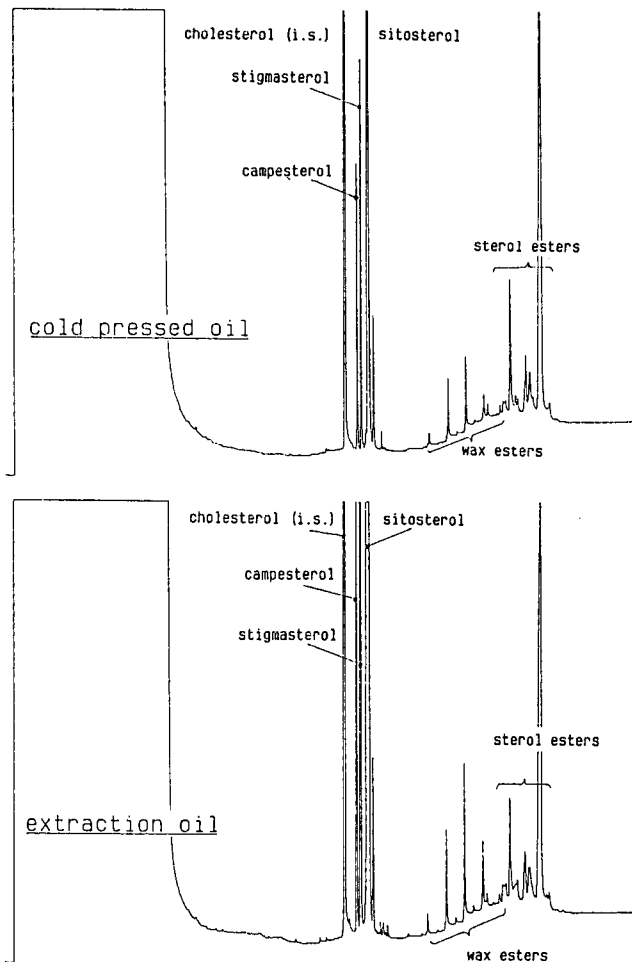


Fig. 5. Differentiation between cold-pressed and extracted sunflower oil.

content (0.43% for our oil), a high concentration of campesterol and the presence of brassicasterol. This is the basis for the classical method used for detecting rapeseed oil in olive oil. With the method described above, the analysis becomes rapid and easy. Rapeseed oil additions below 1% can be detected.

Cold-pressed versus extracted sunflower oil

Fig. 5 compares the chromatograms obtained from a cold-pressed and an extracted sunflower oil. The sterol ester concentrations are almost identical, which indicates that the sterol esters pressed out of the seeds at about the same yield as the oil. The concentrations of free sterols, however, are more than doubled in the extraction oil (as for olive oil²⁶). Wax ester concentrations also increased, although much less than for extracted olive oil. The distribution of the individual wax esters is shifted slightly towards higher molecular weight.

REFERENCES

- 1 R. P. W. Scott and P. Kucera, *J. Chromatogr.*, 125 (1976) 251.
- 2 R. P. W. Scott, *Adv. Chromatogr.*, 22 (1983) 247.
- 3 R. P. W. Scott, *J. Chromatogr. Sci.*, 23 (1985) 233.
- 4 H. J. Cortes, C. D. Pfeiffer and B. E. Richter, *J. High Resolut. Chromatogr. Chromatogr. Commun.*, 8 (1985) 469.
- 5 R. P. W. Scott and S. Traiman, *J. Chromatogr.*, 196 (1980) 193.
- 6 E. Homberg, *Dtsch. Lebensm.-Rdsch.*, 81 (1985) 12.
- 7 F. Mordret, A. Prévot and J.-P. Wolff, *Ann. Falsif. Expert. Chim.*, 70 (1977) 87.
- 8 D. Firestone, K. L. Carson and R. J. Reina, *J. Am. Oil Chem. Soc.*, 65 (1988) 788.
- 9 C. Gertz, *Fat Sci. Technol.*, 90 (1988) 45.
- 10 C. Mariani, A. Lanzani and E. Fedeli, *Riv. Ital. Sostanze Grasse*, 64 (1987) 13.
- 11 V. Paganuzzi, *Riv. Ital. Sostanze Grasse*, 60 (1983) 489.
- 12 C. Mariani and E. Fedeli, *Riv. Ital. Sostanze Grasse*, 63 (1986) 3.
- 13 K. Grob and T. Läubli, *J. High Resolut. Chromatogr. Chromatogr. Commun.*, 9 (1986) 593.
- 14 G. Morchio and R. De Andreis, *Riv. Ital. Sostanze Grasse*, 60 (1983) 427.
- 15 G. Lercker and M. F. Caboni, *Riv. Ital. Sostanze Grasse*, 62 (1985) 193.
- 16 G. Amelotti, A. Griffini, M. Bergna and P. Montofano, *Riv. Ital. Sostanze Grasse*, 62 (1985) 459.
- 17 G. Bonaga, A. Antonelli, L. S. Conte and G. Lercker, *Riv. Ital. Sostanze Grasse*, 63 (1986) 583.
- 18 R. E. Worthington and H. L. Hitchcock, *J. Am. Oil Chem. Soc.*, 61 (1984) 1085.
- 19 P. Horstmann and A. Montag, *Fette-Seifen-Anstrichm.*, 88 (1986) 262.
- 20 M. C. Iatrides, J. Artaud and M. Derbesy, *Analisis*, 12 (1984) 205.
- 21 E. Homberg, *Fat Sci. Technol.*, 89 (1987) 215.
- 22 F. Munari and K. Grob, *J. High Resolut. Chromatogr. Chromatogr. Commun.*, 11 (1988) 172.
- 23 K. Grob, Ch. Walder and B. Schilling, *J. High Resolut. Chromatogr. Chromatogr. Commun.*, 9 (1986) 95.
- 24 K. Grob and J.-M. Stoll, *J. High Resolut. Chromatogr. Chromatogr. Commun.*, 9 (1986) 518.
- 25 B. Schilling, K. Grob, P. Pichler, R. Dubs and B. Brechbühler, *J. Chromatogr.*, 435 (1988) 204.
- 26 C. Mariani, E. Fedeli and V. Bovio, *Riv. Ital. Sostanze Grasse*, in press.

CHROM. 21 289

RETENTION BEHAVIOUR OF β -CARBOLINES IN NORMAL-PHASE CHROMATOGRAPHY

SILICA AND AMINO PHASES IN HIGH-PERFORMANCE AND THIN-LAYER CHROMATOGRAPHY

M. C. PIETROGRANDE* and F. DONDI

Department of Chemistry, Analytical Chemical Laboratory, University of Ferrara, Via L. Borsari 46, 44100 Ferrara (Italy)

P. A. BOREA

Pharmacology Institute, University of Ferrara, Ferrara (Italy)

and

C. BIGHI

Department of Chemistry, Analytical Chemical Laboratory, University of Ferrara, Ferrara (Italy)

SUMMARY

The retention behaviour of a series of β -carbolines in normal-phase chromatography was studied. Silica and amino phases in high-performance liquid (HPLC) and thin-layer chromatographic (TLC) systems were analyzed. The Snyder–Soczewinski approach was used to interpret the retention mechanism in relation to different solute, solvent and stationary phase characteristics. Amino and silica stationary phases, TLC and HPLC techniques and various solvent selectivities were compared. The molecular structure–retention relationship was also studied by means of the group contributions to retention and the electronic constant.

INTRODUCTION

The chromatographic retention behaviour of polar solutes in normal-phase (NP) systems is determined by specific solute–stationary and mobile phase interactions^{1–4}. The semiempirical adsorption model of Snyder^{5,6} has proved to be a valuable tool in investigating how the solute molecular structure, the mobile phase composition and the stationary phase structure affect retention in both thin-layer (TLC) and high-performance liquid chromatographic (HPLC) systems. Studies on the retention behaviour of various solute classes in different chromatographic systems may be helpful to clarify the rôle each interaction plays in the retention mechanism. For this purpose, TLC seems to be a very promising technique because of its speed and applicability to a wide range of solute and solvent types^{5,7,8}. Therefore it is very important to estimate TLC as a pilot technique replacing HPLC.

In this study the retention of β -carbolines (β CCs) on NP systems was analyzed and TLC and HPLC systems were compared. β CCs are a class of drugs, chemically

unrelated to benzodiazepine, able to interact to various degrees with the benzodiazepine receptors in the mammal central nervous system^{9,10}. In a previous work the retention of β CCs, in reversed-phase (RP) systems, particularly in an ion-pairing system, was studied in order to determine their lipophilic character¹¹. In the present work the Snyder approach was applied. The slopes and intercepts of the linear relationships between retention and mobile phase composition are discussed in relation to the solute, solvent and stationary phase characteristics in order to obtain information about the retention mechanism and the structure-retention relationships.

EXPERIMENTAL

The HPLC measurements were performed with a Waters 600 multisolvent delivery system equipped with a Waters 990 photodiode array detector. A Wisp Model 712 was used to inject 10 μ l of the standard solutions. The columns used were 30 cm \times 3.9 mm I.D. μ Porasil and μ Bondapak NH₂ from Waters Assoc.

The TLC measurements were carried out using Merck HPTLC NH₂ and silica plates. A Camag Nanomat was used to spot about 100 nl of the β CC solutions on the plates. HPLC grade 2-propanol, ethyl acetate, dioxane, tetrahydrofuran (THF), acetonitrile, *n*-hexane and dichloromethane were obtained from Rudi Pont. For each chromatographic system, a minimum of seven different compositions of mixtures with *n*-hexane as the diluent (or dichloromethane for acetonitrile) were studied. The only exception to this was ethyl acetate on HPLC NH₂ where only the measurements with 100% solvent were possible.

The β CCs, obtained from Sigma Chemicals (St. Louis, MO, U.S.A.), were dissolved in 2-propanol or in 2-propanol-water mixtures in a concentration range between 100 and 500 μ g/ml. The molecular structures of the β CCs studied are shown in Fig. 1.

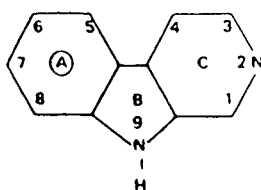
RESULTS AND DISCUSSION

Both the Snyder and the Soczewinski approaches^{5,12} draw a linear relationship between retention (as $\log k'$ or R_M values) and the mobile phase composition (as X_S = mole fraction of the strong solvent)

$$\log k' = R_M = c - n \log X_S \quad (1)$$

from the intercept, c , of which it is possible to estimate the strength of the solute interaction with the stationary phase, while the slope, n (as the ratio between the molecular area of the solute and solvent at the adsorbent surface), indicates the number of active solute molecule adsorption sites interacting with the stationary phase.

The validity of eqn. 1 was experimentally confirmed for all stationary and mobile phases examined: the correlation coefficients were excellent for HPLC (mean 0.996 ± 0.0016) and satisfactory for TLC (mean 0.984 ± 0.100). The values of the intercept and slope are presented in Tables I and II for amino and silica HPLC and TLC stationary phases when 2-propanol and ethyl acetate were the strong solvents. A comparison of the intercept values calculated for the different chromatographic



Cpd	Name	R ₁	R ₃	R ₄	R ₅	R ₆	R ₇	Ring C
1	Nor-harman	H	H	H	H	H	H	Arom.
2	Harman	CH ₃	H	H	H	H	H	Arom.
3	Harmine	CH ₃	H	H	H	H	OCH ₃	Arom.
4	Harmol	CH ₃	H	H	H	H	OH	Arom.
5		CH ₂ OH	H	H	H	H	H	Arom.
6	-CCM	H	COOCH ₃	H	H	H	H	Arom.
7	-CCE	H	COOC ₂ H ₅	H	H	H	H	Arom.
8	PR-CC	H	COOC ₃ H ₇	H	H	H	H	Arom.
9	DMCM	H	COOCH ₃	C ₂ H ₅	H	OCH ₃	OCH ₃	Arom.
10	ZK 91296	H	COOC ₂ H ₅	CH ₂ OCH ₃	OCH ₂ C ₆ H ₅	H	H	Arom.
11	ZK 93426	H	COOC ₂ H ₅	CH ₃	OiC ₃ H ₇	H	H	Arom.
12		H	COONHCH ₃	H	H	H	H	Arom.
13	Harmaline	CH ₃	H	H	H	H	OCH ₃	Non ar.
14	Harmalol	CH ₃	H	H	H	H	OH	Non ar.
15	ZK 93423	H	COOC ₂ H ₅	CH ₂ OCH ₃	H	OCH ₂ C ₆ H ₅	H	Arom.

Fig. 1. Molecular structures of the β CCs studied.

systems shows that for this series of solutes the amino phase is more retentive than silica. This pattern is more evident from the data calculated from measurements with ethyl acetate as the strong solvent. As predicted theoretically, when ethyl acetate was used as the strong solvent, larger slopes and intercepts were obtained. Table III reports the linear relationships calculated when the intercept values with ethyl acetate and 2-propanol are correlated with one another for the different systems (eqns. 2-4). The poor correlations may be interpreted in terms of solvent selectivity according to the relative importance of hydrogen bonding vs. dipole interaction. 2-Propanol, as a strong proton acceptor and donor, exhibits different specific interactions toward

TABLE I
INTERCEPT, c , AND SLOPE, n , OF EQN. 1 ON HPLC AND TLC AMINO PHASES

	<i>2-Propanol</i>				<i>Ethyl acetate</i>		
	<i>HPLC</i>		<i>TLC</i>		<i>HPLC</i>	<i>TLC</i>	
	c	n	c	n	c^a	c	n
1	-0.381	0.811	-0.544	1.497	0.92	0.351	2.219
2	-0.446	0.982	-0.526	1.468	0.90	0.368	2.138
3	-0.284	1.043	-0.471	1.612	1.09	0.531	2.984
4	-0.079	2.690	0.117	2.601	—	—	—
5	-0.308	2.296	-0.245	2.335	—	1.107	3.332
6	-0.342	0.994	-0.239	1.268	1.00	1.042	2.832
7	-0.368	0.834	-0.277	1.222	0.98	0.946	3.306
8	-0.402	0.781	-0.328	1.281	0.90	0.914	2.629
9	-0.225	1.330	-0.197	1.867	1.26	1.306	3.992
10	-0.503	1.073	-0.374	1.689	0.85	0.851	3.673
11	-0.583	1.120	-0.435	1.281	0.71	0.684	3.303
12	-0.335	1.595	-0.328	2.422	0.90	0.741	3.165
13	-0.372	1.069	-0.335	1.636	1.15	0.990	2.703
14	-0.145	2.839	0.050	2.791	—	—	—
15	-0.475	1.121	-0.379	1.480	0.72	0.755	3.635

^a Only experimental measurements with 100% ethyl acetate were possible.

TABLE II
INTERCEPT, c , AND SLOPE, n , VALUES OF EQN. 1 ON HPLC AND TLC SILICA PHASES

	<i>2-Propanol</i>		<i>Ethyl acetate</i>			
	<i>HPLC</i>		<i>HPLC</i>		<i>TLC</i>	
	c	n	c	n	c	n
1	-0.413	0.981	0.549	2.145	0.871	1.386
2	-0.463	1.041	0.511	2.346	0.854	1.526
3	-0.317	1.092	0.906	2.501	1.252	1.767
4	-0.109	2.687	1.044	3.162	1.46 ^a	—
5	-0.331	2.375	0.729	3.194	1.278	3.705
6	-0.376	1.073	0.520	2.507	0.714	2.084
7	-0.409	0.943	0.458	2.286	0.569	2.399
8	-0.468	0.887	0.297	2.179	0.418	2.190
9	-0.254	1.407	0.685	3.591	1.103	2.276
10	-0.683	1.391	0.147	3.644	0.365	3.552
11	-0.695	1.460	0.143	2.958	0.353	2.359
12	-0.425	1.871	0.343	3.832	0.615	2.839
13	-0.375	1.084	0.868	1.981	1.248	1.705
14	-0.009	2.365	1.021	2.711	1.46 ^a	—
15	-0.642	1.391	0.160	3.481	0.416	3.337

^a Only experimental measurements with 100% ethyl acetate were possible.

TABLE III

CORRELATIONS BETWEEN INTERCEPT VALUES, c , OBTAINED FOR 2-PROPANOL AND ETHYL ACETATE (EQNS. 2-4) AND IN CORRESPONDING TLC AND HPLC SYSTEMS (EQNS. 5-7)

$n = 12$	$c(2\text{-propanol}) = -0.887 (\pm 0.093) + 0.521 (\pm 0.096) c(\text{ethyl acetate})$ $r = 0.863$ $s = 0.052$ $F = 29.19$	HPLC NH ₂	(2)
$n = 13$	$c(2\text{-propanol}) = -0.664 (\pm 0.026) + 0.374 (\pm 0.030) c(\text{ethyl acetate})$ $r = 0.966$ $s = 0.030$ $F = 151.93$	TLC NH ₂	(3)
$n = 15$	$c(2\text{-propanol}) = -0.711 (\pm 0.045) + 0.560 (\pm 0.070) c(\text{ethyl acetate})$ $r = 0.911$ $s = 0.082$ $F = 63.13$	HPLC Si	(4)
$n = 11$	$c(\text{TLC}) = 0.130 (\pm 0.049) + 1.093 (\pm 0.131) c(\text{HPLC})$ $r = 0.935$ $s = 0.063$ $F = 68.28$ (cpds. 4-15)	NH ₂ 2-propanol	(5)
$n = 8$	$c(\text{TLC}) = -0.021 (\pm 0.141) + 0.949 (\pm 0.153) c(\text{HPLC})$ $r = 0.908$ $s = 0.029$ $F = 43.61$ (cpds. 6-13 and 15)	NH ₂ ethyl acetate	(6)
$n = 15$	$c(\text{TLC}) = 0.148 (\pm 0.050) + 1.284 (\pm 0.078) c(\text{HPLC})$ $r = 0.977$ $s = 0.091$ $F = 268.15$	Si ethyl acetate	(7)

β CC solutes when compared to ethyl acetate, a solvent characterized by strong dipole interactions and lower proton donor and acceptor strength^{13,14}. The worst correlation obtained with data on the HPLC amino phase (eqn. 2) may be due to the fact that experimental ethyl acetate measurements were related to calculated 2-propanol intercept values.

TLC-HPLC correlation

By comparing the intercept values reported in Tables I and II the correlation between retention values in the corresponding TLC and HPLC systems was calculated (eqn. 5-7 in Table III). Eqns. 5 and 6 show that for the amino phase the slope of the TLC-HPLC correlation does not differ from unity, thus suggesting that the same retention mechanism occurs in both TLC and HPLC. Moreover, the equality of the parameters for both 2-propanol and ethyl acetate solvents may suggest this similarity is independent of eluent type. The linear relationship between R_M and $\log k'$ values is statistically significant only when compounds 1-3 (which do not contain an ester or hydroxyl group) are excluded from the correlation. In Fig. 2 one may note that these compounds deviate most from the straight line, thus showing that the HPLC system exerts a specific, stronger retention towards them. The different solute selectivities of the systems may be explained by the different distribution of the mobile phase over the stationary phase and by some specific effects of the stationary phase⁷⁻¹⁵. When the silica phase is considered (eqn. 7 in Table III), the slope value 1.3 may suggest some differences in the retention properties of the TLC and HPLC silica systems. However, the statistical parameters of eqn. 7 are very good, thus excluding any evident specific selectivity of the two systems towards particular solutes. Since the TLC data on silica are very highly correlated with those of HPLC for all the β CCs studied, silica plates were chosen to study solvent selectivity effects.

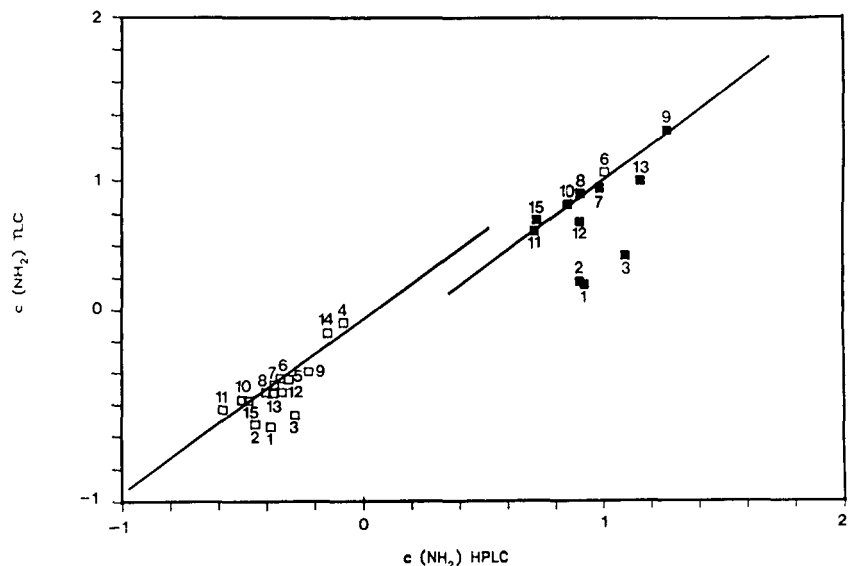


Fig. 2. Relationships between R_M and $\log k'$ (both as intercept values of eqn. 1) on the amino stationary phase with 2-propanol (\square , eqn. 5, Table III) or ethyl acetate (\blacksquare , eqn. 6, Table III) as the strong solvent.

TABLE IV

CORRELATIONS BETWEEN THE INTERCEPT, c , AND SLOPE, n , OBTAINED IN CORRESPONDING SILICA AND AMINO SYSTEMS

$c(\text{Si}) = -0.013 (\pm 0.042) + 1.490 (\pm 0.114) c(\text{NH}_2)$ $n = 15 \quad r = 0.958 \quad s = 0.056 \quad F = 146.12$	HPLC 2-propanol	(8)
$n(\text{Si}) = 0.333 (\pm 0.095) + 0.829 (\pm 0.065) n(\text{NH}_2)$ $n = 15 \quad r = 0.964 \quad s = 0.160 \quad F = 172.95$	HPLC 2-propanol	(9)
$c(\text{Si}) = -0.858 (\pm 0.252) + 1.396 (\pm 0.262) c(\text{NH}_2)$ $n = 12 \quad r = 0.860 \quad s = 0.140 \quad F = 28.45$ (cpds. 1-3, 6-13 and 15)	HPLC ethyl acetate	(10)
$c(\text{Si}) = -0.636 (\pm 0.138) + 1.072 (\pm 0.148) c(\text{NH}_2)$ $n = 8 \quad r = 0.947 \quad s = 0.069 \quad F = 52.27$ (cpds. 6-12 and 15)	HPLC ethyl acetate	(10')
$c(\text{Si}) = -0.925 (\pm 0.326) + 1.610 (\pm 0.319) c(\text{NH}_2)$ $n = 4 \quad r = 0.963 \quad s = 0.069 \quad F = 25.33$ (cpds. 1-3 and 13)	HPLC ethyl acetate	(10'')
$c(\text{Si}) = -0.414 (\pm 0.235) + 1.086 (\pm 0.254) c(\text{NH}_2)$ $n = 8 \quad r = 0.867 \quad s = 0.135 \quad F = 18.25$ (cpds. 6-12 and 15)	TLC ethyl acetate	(11')
$c(\text{Si}) = 0.732 (\pm 0.208) + 0.580 (\pm 0.338) c(\text{NH}_2)$ $n = 4 \quad r = 0.771 \quad s = 0.174 \quad F = 2.94$ (cpds. 1-3 and 13)	TLC ethyl acetate	(11'')

Amino-silica comparison

The silica and amino phases show very similar selectivities when 2-propanol is the strong solvent, according to the statistical parameters of the correlations reported in Table IV (eqns. 8 and 9). The quality of the relationship is lower with ethyl acetate (eqn. 10). Nonetheless, a statistically significant improvement is achieved when two groups of compounds are considered: one containing ester, amide or hydroxyl groups and the other without them (eqns. 10' and 10'' in Table IV). The TLC stationary phases exhibit the same behaviour, however the quality of the correlations is worse (eqns. 11' and 11'' in Table IV). This behaviour may be interpreted assuming that the amino phase exerts a strong specific retention towards the carbonyl and the hydroxyl functions present in the solute molecules.

Structure-retention relationship

Similarly to the intercept values, the slopes increase in the order of solute polarity. This order, apparently similar to the solute hydrogen-bonding ability, is therefore, about the same on both the phases. When ethyl acetate is the strong solvent, the slope assumes values of about 2 for compounds 1 and 2; *i.e.*, either these β CC molecules contain two groups which are strongly adsorbed on the stationary phase, or a single β CC molecule is able to interact simultaneously with two silanol or amino groups. This value may be due to the binding of the β CC molecule to the column by the two hydrogen-bonding acceptor aliphatic N atoms in positions 2 and 9. When one or more ester or ether substituents are present in the molecule (compounds 3, 6-11, 13 and 15) the slope increases by about 0.3 (on silica) or 0.5 (on amino) for each group, indicating the partial adsorption of these groups. Moreover, when a larger number of functional groups are present in the solute molecule, the values of c and n are smaller than the simple sums of the corresponding values for monofunctional compounds. This scattering effect may be due to very specific solute-solvent interactions. When an hydroxyl or an amide group is present in the molecule (compounds 4, 5, 12 and 14) the slope increases by about 1, thus indicating that these hydrogen-bonding donor and acceptor groups are one more active site for β CC adsorption. When 2-propanol is the strong solvent, the solutes containing an OH group (4, 5 and 14) show exceptionally high slopes (2.3-2.8). This behaviour reflects the solvent solvation properties: 2-propanol strongly manifests its electron donor properties relative to proton donor groups, thus determining specific solvation interactions with solutes containing such groups^{13,16,17}.

Group contributions

In order to correlate the retention behaviour with molecular structure, the contribution of different substituents to retention was calculated as Δc and Δn . The intercept and slope contributions increased approximately in the same order, while a clearer trend was evident for the Δn values. The slope increased in the order



for the amino phase, and



for the silica phase. These values are in accord with the literature data, with the exception of the unusually low increment for the ester group, particularly on silica¹⁸⁻²⁰. This behaviour may be determined by a shielding effect, probably due to the resonance of the conjugated double bond system going from C=O to N₉ through N₂, as confirmed by the crystal structure of β -CCM²¹. Support for this hypothesis is also provided by the pattern of the linear free energy correlation between the electronic constant and chromatographic retention. As widely reported for NP chromatographic systems^{22,23}, this relationship is expressed by:

$$\log k' = a + \rho\sigma \quad (12)$$

The linearity is confirmed for this class of β CCs in HPLC systems when the electronic constant is expressed as the Taft inductive constant, σ_i ²⁴ (Table V). However, Fig. 3 evidences the presence of two approximately parallel straight lines where the one corresponding to an ester function (or substituents in β CCs containing an ester group) is shifted to lower retention values. This behaviour is consistent with the previous hypothesis that intramolecular interactions systematically decrease the adsorptive strength of β CC solutes containing an ester group. The substituent interaction effect on retention reflects mainly the influence of substituents on the hydrogen-bonding ability of the solute molecule with the stationary phase. Therefore, the positive ρ value in eqn. 12 indicates that the β CC molecule, as a whole, acts as a proton acceptor in hydrogen-bonding interactions with the silica and amino stationary phases.

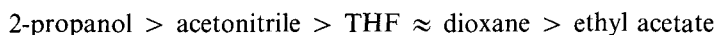
TABLE V

SUBSTITUENT CONTRIBUTIONS, CALCULATED AS $\log k'$ WITH 2-PROPANOL, AND INDUCTIVE ELECTRONIC CONSTANT, σ_i

Substituents	$\log k'$ on silica	$\log k'$ on amino	σ_i
(A) CH ₃	-0.03	-0.06	-0.04
(B) CH ₂ OH	0.08	0.07	0.05
(C) OCH ₃	0.15	0.16	0.23
(D) OH	0.35	0.37	0.31
(E) COOR	-0.01	0.01	0.31
(F) CONHCH ₃	-0.01	0.05	0.33
(G) OC ₃ H _{7-iso} + CH ₃	-0.32	-0.21	0.23
(H) CH ₂ OCH ₃ + OCH ₂ C ₆ H ₅	-0.25	-0.12	0.26
(I) C ₂ H ₅ + 2 OCH ₃	0.12	0.11	0.43

Modifier selectivity

In order to study the solvent effects on β CC retention on silica, the TLC measurements were extended to acetonitrile, dioxane and tetrahydrofuran as strong solvents. The Snyder-Soczewinski relationship (eqn. 1) was obeyed by these solvents as well. Table VI reports the intercept, c , and slope, n , values. The elution strength (evaluated in terms of the intercept values) shows the decreasing order:



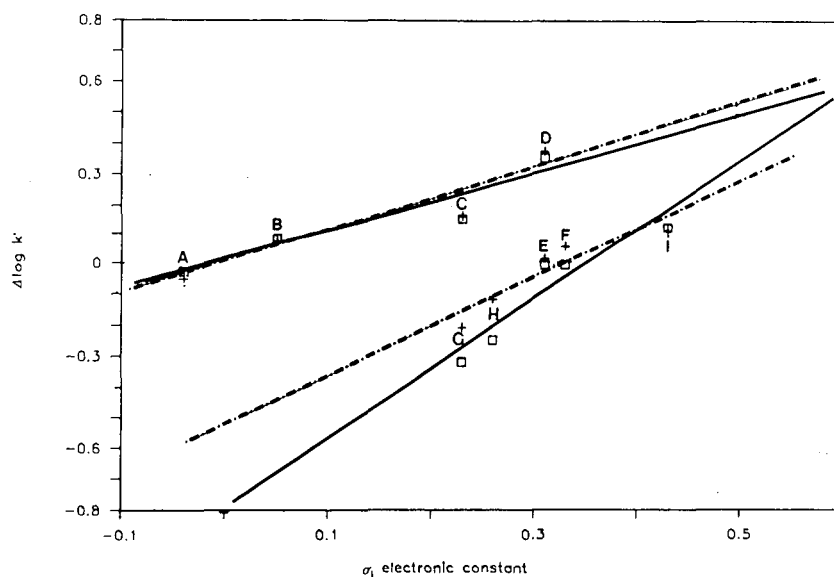


Fig. 3. Relationships between substituent contributions ($\Delta \log k'$ with 2-propanol) and the electronic constant σ_1 . \square , Silica; +, amino.

This sequence closely parallels the eluotropic series, except for the unusually low strength of ethyl acetate. Table VII reports the correlations between the intercept values with the different solvents and ethyl acetate as a reference. The slope being quite close to unity in eqns. 13 and 14 may be interpreted by these solvents (THF, dioxane

TABLE VI
INTERCEPT, c , AND SLOPE, n , OF EQN. 1 ON THE TLC SILICA PHASE WITH ACETONITRILE, DIOXANE AND THF AS STRONG SOLVENTS

Acetonitrile		Dioxane		THF		
c	n	c	n	c	n	
1	0.540	1.400	0.176	1.603	0.216	3.153
2	0.558	1.343	0.151	1.798	0.171	3.050
3	1.14 ^a	—	0.381	2.019	0.412	3.608
4	1.34 ^a	—	0.663	3.418	0.664	4.754
5	1.20 ^a	—	0.479	3.364	0.475	4.733
6	-0.259	0.743	-0.091	1.919	0.170	3.466
7	-0.498	0.752	-0.200	1.780	0.003	4.007
8	-0.572	0.676	-0.297	1.706	-0.130	4.185
9	-0.045	0.752	0.090	2.103	0.201	4.096
10	-0.773	1.058	-0.339	2.100	-0.285	4.708
11	-0.797	1.233	-0.282	2.026	-0.271	3.975
12	-0.409	2.238	-0.263	2.567	-0.028	5.049
13	1.03 ^a	—	0.476	2.189	0.476	3.107
14	1.34 ^a	—	0.701	3.530	0.674	4.591
15	-0.570	1.667	-0.248	2.277	-0.244	4.363

^a Only measurements with 100% acetonitrile were possible.

TABLE VII

CORRELATIONS BETWEEN INTERCEPT VALUES, c , OBTAINED IN TLC ON SILICA FOR DIFFERENT SOLVENTS

$n = 15$	$c(\text{THF}) = -0.451 (\pm 0.097) + 0.734 (\pm 0.083) c(\text{ethyl acetate})$ $r = 0.981 \quad s = 0.045 \quad F = 78.21$	TLC Si (13)
$n = 15$	$c(\text{dioxane}) = -0.674 (\pm 0.055) + 0.887 (\pm 0.058) c(\text{ethyl acetate})$ $r = 0.973 \quad s = 0.088 \quad F = 234.41$	TLC Si (14)
$n = 15$	$c(\text{acetonitrile}) = -1.467 (\pm 0.165) + 1.944 (\pm 0.174) c(\text{ethyl acetate})$ $r = 0.952 \quad s = 0.264 \quad F = 125.35$	TLC Si (15)

and ethyl acetate) exerting very similar effects on β CC retention. On the other hand, the slope value for acetonitrile and for 2-propanol (1.9 and 0.6, respectively) may suggest that these solvents exert some specific solvent-solute and/or solvent-stationary phase interactions compared to ethyl acetate.

When the correlations between retention values for different solvent pairs are calculated, the smallest values of the correlation coefficient, r , must be associated with the maximum differences in solvent selectivity. Snyder *et al.*²⁵ considered this effect to be a result of interactions produced by solvent and solute localization, *e.g.*, direct interaction of a polar solute molecule with a corresponding adsorption site on the adsorbent surface. The results of these correlations are summarized in Table VIII. THF, dioxane and ethyl acetate show good correlation with each other, implying an absence of solvent-specific localization for these mobile phases. According to the Snyder classification of solvent properties¹³, polarity index and selectivity parameters—indicating the relative importance of hydrogen bonding *vs.* dipole interaction—are all quite similar for these three solvents. The pairs acetonitrile-ethyl acetate and acetonitrile-THF exhibit lower r values suggesting specific solvent-solute-stationary phase interactions most likely due to the high polarity of acetonitrile (dipole moment 4.0²⁶). Snyder *et al.*²⁵ calculated a much higher solvent selectivity parameter, related to the polarity or adsorption energy of the solvent molecule, for acetonitrile than for ethyl acetate and THF. However, this hypothesis contrasts with the high r value calculated for the correlation between acetonitrile and dioxane. Strong solute-solvent localization may also explain the low slope, n , values (Table VI) calculated for acetonitrile. Fig. 4 shows that the selectivity of acetonitrile results in a particularly strong silica retention of those β CC molecules which do not contain an ester group (compounds 1-3, 5 and

TABLE VIII

CORRELATION COEFFICIENTS, r , BETWEEN INTERCEPT VALUES OBTAINED FOR DIFFERENT SOLVENT PAIRS

	THF	Dioxane	Ethyl acetate	Acetonitrile
THF	1	0.970	0.979	0.954
Dioxane	0.970	1	0.978	0.980
Ethyl acetate	0.979	0.978	1	0.952
Acetonitrile	0.954	0.980	0.952	1

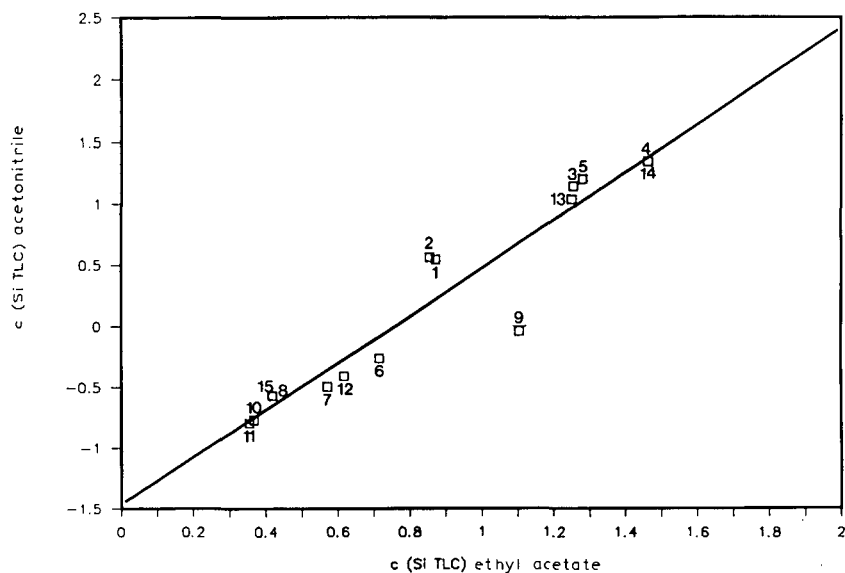


Fig. 4. Relationship between retention (as intercept c values) for acetoneitrile and ethyl acetate (eqn. 15, Table VII).

13). The quite good correlation between dioxane and THF confirms that for both these solvents the competition for silanol between the solute and modifier molecule is the predominant adsorption mechanism¹⁴. However, some specific selectivity of dioxane vs. THF is seen in the plot in Fig. 5. The points corresponding to solutes with only one

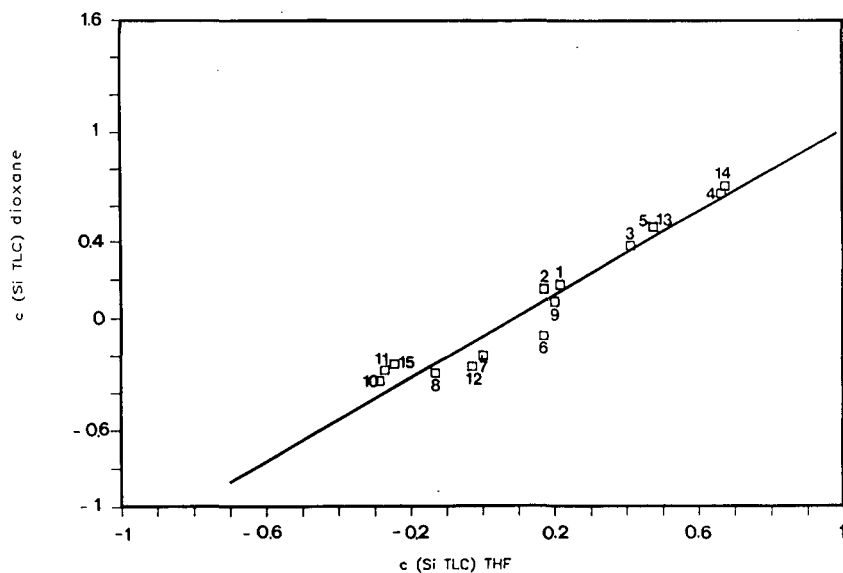


Fig. 5. Relationship between retention (as intercept values) for dioxane and tetrahydrofuran (see Table VIII).

carbonyl group (compounds 6–8 and 12) are shifted down in relation to the line, thus indicating a relatively weaker adsorption in the dioxane system. This effect may be produced by the more complex adsorption mechanism, *e.g.*, coadsorption which takes place when the solute and exposed ether oxygens of the dioxane molecules interact, the latter being adsorbed as a monolayer on the silica surface^{27,28}.

The substituent contributions to retention were calculated for TLC systems with all the solvents studied and related to σ_i values. In general, the TLC data are more scattered than HPLC ones and therefore the quality of the Δc vs. σ_i relationship is lower. Two approximately parallel straight lines were found for all solvents. Moreover, mean slope value (1.53 ± 0.49) is in accord with the HPLC value (1.49 ± 0.59). This result further confirms that the interactions (particularly specific electronic effects) controlling the retention mechanism are all quite similar in both TLC and HPLC systems.

CONCLUSIONS

The Snyder–Soczewinski approach seems a suitable tool for interpreting the retention mechanism of β CCs in NP chromatographic systems. Since retention is related to hydrogen-bonding ability, it is possible to identify the active sites in the β CC molecule which determine their adsorption on the silica and amino surfaces. The comparison between TLC and HPLC data suggests the possible use of TLC as a pilot technique replacing the more precise but time-consuming HPLC. The selectivity effects shown by different modifier and stationary phases evidence that specific intramolecular interactions play a significant rôle in determining retention. Complex equilibria, such as competitive solvation, displacement of the solvent molecule and coadsorption of the solute molecule, simultaneously affect solute retention.

REFERENCES

- 1 R. J. Hurtubise, A. Hussain and H. F. Silver, *Anal. Chem.*, 53 (1981) 1993.
- 2 R. P. W. Scott and P. Kucera, *J. Chromatogr.*, 149 (1978) 93.
- 3 Y. I. Yashin, *J. Chromatogr.*, 251 (1982) 269.
- 4 B. Oscik-Mendyk and J. K. Rozylo, *Chromatographia*, 25 (1988) 300.
- 5 L. R. Snyder, *Principles of Adsorption Chromatography*, Marcel Dekker, New York, 1968.
- 6 L. R. Snyder and T. C. Schunk, *Anal. Chem.*, 54 (1982) 1764.
- 7 S. Hara, *J. Chromatogr.*, 137 (1977) 41.
- 8 E. Soczewinski, in R. E. Kaiser (Editor), *Planar Chromatography*, Hüthig, Heidelberg, 1986, p. 149.
- 9 P. A. Borea and V. Ferretti, *Biochem. Pharm.*, 35 (1986) 2836.
- 10 P. A. Borea, G. Gilli, V. Bertolasi and V. Ferretti, *Mol. Pharm.*, 31 (1987) 334.
- 11 M. C. Pietrogrande, P. A. Borea, G. Lodi and C. Bigli, *Chromatographia*, 23 (1987) 713.
- 12 E. Soczewinski, *Anal. Chem.*, 41 (1969) 179.
- 13 L. R. Snyder, *J. Chromatogr. Sci.*, 16 (1978) 223.
- 14 T. Dzido and E. Soczewinski, *J. Chromatogr.*, 395 (1987) 489.
- 15 J. K. Rozilo, J. Gross, M. Poniewaz, R. Lodkowski and B. Buszewski, *J. Liq. Chromatogr.*, 7 (1984) 1301.
- 16 E. Soczewinski and T. Dzido, *Chromatographia*, 22 (1986) 25.
- 17 M. L. Bieganowska and K. Glowmiak, *Chromatographia*, 25 (1988) 111.
- 18 S. Hara, Y. Fujii, M. Hirasawa and S. Miyamoto, *J. Chromatogr.*, 149 (1978) 143.
- 19 M. Petrovic, L. Kolarov, E. S. Fraljić and J. Petrovic, *Anal. Chem.*, 54 (1982) 934.
- 20 J. Thomas, *J. Chromatogr.*, 404 (1987) 73.
- 21 V. Bertolasi, V. Ferretti, G. Gilli and P. A. Borea, *Acta Crystallogr., Sect. C*, 40 (1984) 1981.

- 22 Y. L. Mokrosz and L. Ekiert, *Chromatographia*, 18 (1984) 401.
- 23 M. C. Spanjer and C. L. de Ligny, *Chromatographia*, 120 (1985) 20.
- 24 N. B. Chepman and J. Shorter, *Correlation Analysis in Chemistry*, Plenum, New York, 1978.
- 25 L. R. Snyder, J. L. Glajch and J. J. Kirkland, *J. Chromatogr.*, 218 (1981) 299.
- 26 A. L. McClellan, *Tables of Experimental Dipole Moments*, Freeman, San Francisco, CA, 1963.
- 27 T. Dzido and E. Soczewiński, *J. Chromatogr.*, 388 (1987) 99.
- 28 M. Verzele, F. Van Damme, C. Dewaele and M. Chijs, *Chromatographia*, 24 (1987) 302.

CHROM. 21 276

ZONE BROADENING DUE TO SAMPLE INJECTION IN CAPILLARY ZONE ELECTROPHORESIS

ELI GRUSHKA*^a and R. M. McCORMICK

E.I. du Pont de Nemours & Company, Inc., Central Research and Development Department, Experimental Station, P.O. Box 80228, Wilmington, DE 19880-0228 (U.S.A.)

SUMMARY

A new source of zone broadening in capillary zone electrophoresis (CZE) associated with electrokinetic and hydrostatic injection techniques has been identified. The actual insertion of the capillary into or withdrawal of the capillary from the sample solution results in the extraneous injection of sample into the capillary. Examination of the sample plug resulting from this extraneous injection indicates that its length can exceed the maximum value permitted to realize the high separation efficiency of CZE. Experiments show that this mode of injection is present even under conditions where hydrostatic flow should occur from the capillary back into the sample vial.

INTRODUCTION

Capillary zone electrophoresis (CZE) is fast becoming a popular separation technique due to its inherently high separation efficiency in terms of plate numbers. This promise of high efficiency has spurred a large number papers on applications of CZE.

Surprisingly few studies can be found in the literature on the effect of operating conditions on CZE efficiency. Martin and co-workers^{1,2} discussed cases where the plug flow is distorted by the walls of the capillary. Lukacs and Jorgenson³ experimentally examined the effect of capillary inner diameter, capillary length, and solute concentration on the plate number. Sepaniak and co-workers⁴ experimentally investigated the effects of sample injection, applied voltage, column dimensions and buffer concentration on the efficiency in micellar electrokinetic capillary chromatography⁵. Knox and Grant⁶ as well as Grushka *et al.*⁷ derived an expression for the mass transfer contribution to the plate height due to temperature effects arising from Joule heating. Walbroehl⁸ has examined theoretically some of the band broadening effects in CZE.

Many experimental parameters can adversely affect solute zone broadening in CZE; these include hydrostatic flow superimposed on electroporetic mobility, radial temperature gradients in the capillary, and solute adsorption onto the capillary wall.

^a Permanent address: Department of Inorganic and Analytical Chemistry, The Hebrew University, Jerusalem, Israel.

This communication deals specifically with zone broadening associated with an artifact of sample introduction.

Ideally, the sample should be introduced into the CZE capillary as an infinitely narrow zone. The two most popular sample introduction techniques are electrokinetic and hydrostatic injection. In the former method, one end of the capillary is removed from the buffer reservoir and immersed in a buffer containing the sample and an electrode from the power supply. Voltage is applied momentarily across the capillary, during which time the sample is "pumped" into the capillary by electrophoretic and/or electroosmotic migration. The voltage is then turned off and the capillary end is moved from the sample vial back to pure buffer. The voltage is turned on again and the electrophoretic analysis begins.

In the second injection method, one end of the capillary is removed from the buffer reservoir and inserted into a sample solution which is elevated above the capillary outlet. Hydrostatic pressure causes the sample to siphon into the capillary. After a predetermined length of time, the capillary is returned to the buffer reservoir and the analysis proceeds as in the previous case. Although there are other methods of sample introduction (see, for example, refs. 9 and 10), the preceding two techniques are used most frequently because of their simplicity.

Some information on the effect of the injection process on CZE efficiency can be found in the literature^{4,8,9}. In the electrokinetic injection, the sample is assumed to enter the capillary as a square plug. According to Sternberg¹¹, the contribution of a plug injection to the total height equivalent to theoretical plate (HETP) is:

$$\sigma_{inj}^2 = \frac{l_{inj}^2}{12} \quad (1)$$

where σ_{inj}^2 is the variance due to the injection and l_{inj} indicates the length of the plug. This equation permits the calculation of the acceptable length of the injected sample plug for a given loss in efficiency. Using the Sternberg expression in eqn. 1 and the following plate equation¹² for CZE

$$H = \frac{2D}{U} \quad (2)$$

the injection length can be approximated as:

$$l_{inj} = (24DEt)^{\frac{1}{2}} \quad (3)$$

where D is the solute's diffusion coefficient, U is the solute's velocity, t is the elution time, and E is the acceptable increase in H relative to the theoretical minimum HETP of the system (from eqn. 2). For example, for protein as a solute (diffusion coefficient of $1 \cdot 10^{-6}$ cm²/s), the theory predicts that at a migration velocity of 0.1 cm/s, the minimum plate height should be 0.2 μ m. If the increase in HETP due to the injection is to be less than 10% of this HETP value (*i.e.*, $E = 0.1$), then for a 10-min analysis time, the length of the injection plug should be less than 380 μ m. For a smaller molecule having a diffusion coefficient of $1 \cdot 10^{-5}$ cm²/s and identical experimental conditions as

above, the allowed injection plug length for a 10% decrease in efficiency is about 1.2 mm. These calculations are based on the assumption that eqn. 2 defines the plate height of the CZE system. Eqn. 2 is pertinent when diffusion is the major band-broadening mechanism in the CZE separation; if other mechanisms are active, then eqn. 2 does not strictly apply and the stringency of the injection plug lengths is somewhat alleviated relative to the values calculated from eqn. 3.

The realization that the injection plug should be less than 400 μm for a large solute molecule, coupled with the fact that measured efficiencies in CZE are routinely well below the theoretical values, prompted us to examine carefully the injection process. Our studies revealed that when a capillary is inserted into the sample vial, a volume of sample penetrates into the capillary even under experimental conditions where hydrostatic flow is from the capillary back into the sample vial. We describe here some experiments which demonstrate this mode of unwanted, but ubiquitous, injection. To the best of our knowledge, the existence of this source of zone broadening has not been previously reported.

EXPERIMENTAL

Instrumentation

A detailed description of the electrophoretic system is given elsewhere¹³. In the present system, the power supply was changed to a Glassman Series EH high-voltage unit. The dimensions of the fused-silica capillary were 110 cm length; 60 cm separation distance; 50 μm I.D.; 375 μm O.D.

Penetration of liquid into the capillary was observed with a Micromaster Model E microscope (Fisher Scientific, King of Prussia, PA, U.S.A.). For these experiments, the CZE capillary was mounted on a glass microscope slide and the glass tube (1 mm I.D.) containing the dye was held in a micromanipulator designed in-house from optical bench parts. An x-y-z translation stage was used to manipulate the dye tube into contact with the capillary, which was filled with 150 mM Na_2HPO_4 (pH 8).

Chemicals

Phenol was used as the solute for the electrophoresis runs. The buffer in the capillary was a pH 6 phosphate buffer prepared by dissolving 150 mmol of NaH_2PO_4 in 100 ml of water and adjusting the pH with concentrated NaOH. The dye used in the injection study was bromophenol blue dissolved at a concentration of 20 mg/ml in pH 8 phosphate buffer.

Procedure

The sample injection was accomplished using the electrokinetic or the hydrostatic method. To study the sample penetration into the capillary, the liquid in the sample vial was placed 2 cm below the level in the reservoir at the other end of the capillary.

RESULTS AND DISCUSSION

Allowable injection plug length

Eqn. 3 in the Introduction allows us to examine the allowable injection length as

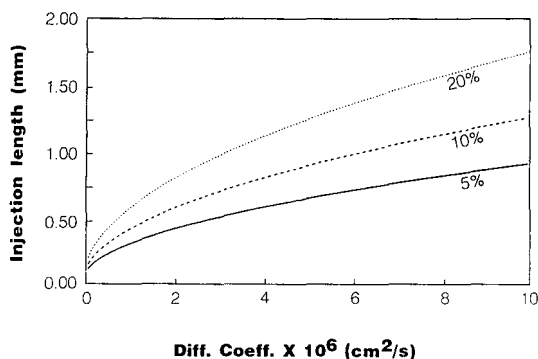


Fig. 1. The allowed injection plug length as a function of the solute's diffusion coefficient. The analysis time was assumed to be 10 min. Each line corresponds to a different allowable loss in the efficiency (increasing H).

a function of the diffusion coefficient (or molecular weight) of the solute and of the elution time from the system. Fig. 1 shows plots of injection length as a function of the solute's diffusion coefficient for specified losses in separation efficiency. A 10-min analysis time was assumed in the calculations. Three different cases are given: 5%, 10% and 20% loss in efficiency. Not surprisingly, the restriction on the injection plug length is rather stringent for large molecules (small diffusion coefficients); this arises primarily because the small D for these solutes imparts a high inherent efficiency (small H , large N) to the CZE system for these solutes.

Fig. 2 shows the injection length as a function of the analysis time. In this case, the diffusion coefficient was constant at $1 \cdot 10^{-6} \text{ cm}^2/\text{s}$. Again, each of the curves depicts the behavior for a different acceptable loss in efficiency. In terms of injection length requirements, a longer analysis time appears to be more advantageous, primarily because band broadening due to diffusion during the separation becomes more significant and thus reduces the stringency of the injection process.

Extraneous injection

The preceding discussion indicates that the injection procedure should be controlled tightly in terms of injection voltages and times to avoid peak broadening. In

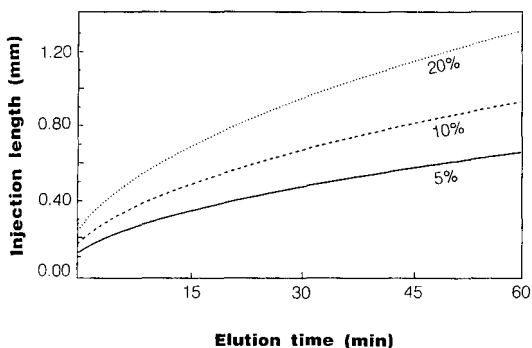


Fig. 2. The allowed injection plug length as a function of the analysis time. The diffusion coefficient was taken as $1 \cdot 10^{-6} \text{ cm}^2/\text{s}$. Each line corresponds to a different allowable loss in the efficiency.

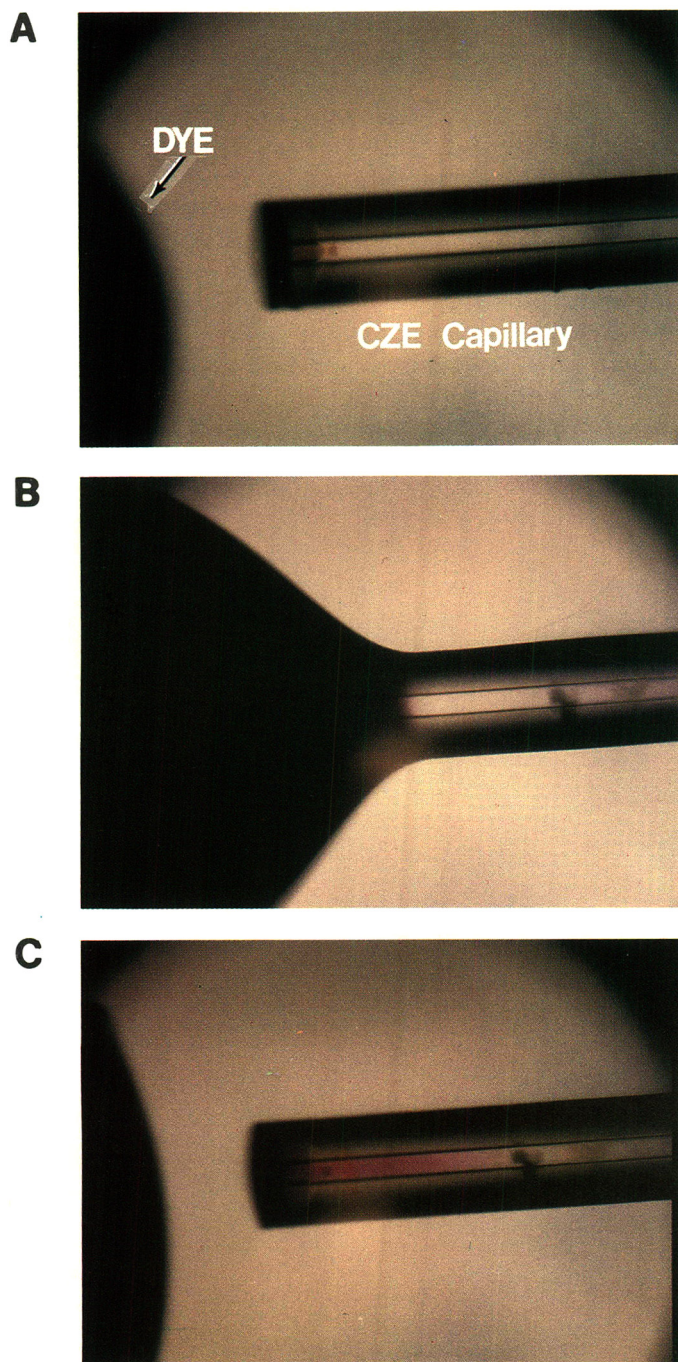


Fig. 3. (A) The CZE capillary (on the right) before contact with the dye pool (on the left). (B) The CZE capillary touching the dye pool. (C) After contact between the capillary and dye. The dye inside the CZE capillary is clearly visible.

our studies it soon became apparent that an additional source of peak broadening in which the sample enters the capillary in an uncontrolled manner is associated with the injection process.

Fig. 3A shows a photograph of a CZE capillary (on the right of the photograph) just before touching a larger tube containing a dye solution (on the left). The other end of the CZE capillary (1 m length) was elevated 5 cm relative to the end inserted into the dye. Fig. 3B shows a photograph of the CZE capillary touching the dye in the other tube. As a result of surface tension, there is considerable wetting of the CZE capillary by the dye. Fig. 3C shows the capillary after contact with the dye was broken. This sequence of photographs reveals that some dye solution penetrated into the CZE capillary. The length of the dye zone in the capillary is about 700 μm . This plug size can cause a serious deterioration in the system performance in the case of large solutes, such as proteins (see Fig. 1).

Frequently, the sample penetrates into the capillary not only upon withdrawal

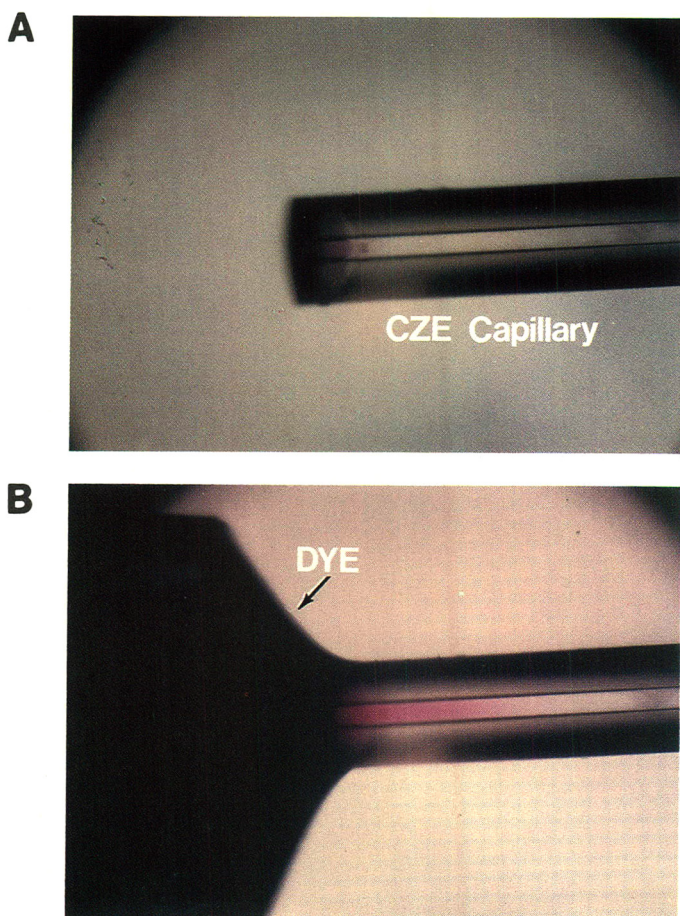


Fig. 4. (A) The CZE capillary (on the right) before contact with the dye pool. (B) The CZE capillary immediately after touching the dye pool. The dye inside the CZE capillary is clearly visible.

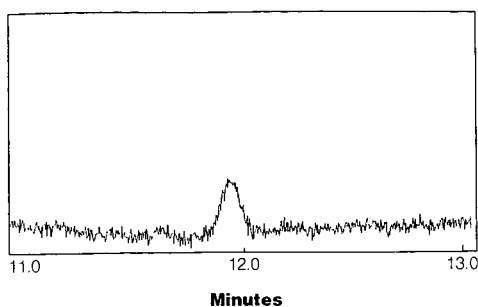


Fig. 5. An electropherogram resulting from an extraneous injection.

from the dye solution, but also upon contact. Fig. 4 shows a photograph of a CZE capillary immediately after contact with the dye. The dye inside the CZE capillary (on the right) is evident. The length of the dye zone in the capillary is again about $700\ \mu\text{m}$. The injection end of the capillary was lowered 5 cm relative to the elution end of the capillary. Similar results were obtained when the elution end of the CZE capillary was at the same height as the injection end.

These photographs demonstrate that the actual insertion (or withdrawal) of the capillary into (from) the sample vial can cause an extraneous injection of solute into a CZE capillary. Fig. 5 shows an electropherogram showing a phenol peak resulting from such an extraneous injection. In this case, the liquid level in the sample vial was about 2 cm lower than that in the buffer vial at the elution end of the capillary. In addition, the capillary was left in the sample vial for 2 min, during which time hydrostatic flow should have been in the direction from the capillary back into the sample vial. Still, enough sample entered the capillary to result in a peak. The peak is quite broad, yielding a plate number which is much less (48% of N_{theor}) than the theoretical value.

This experiment was repeated several times for several insertion intervals: 20, 30, 60, 120 and 300 s. Though experiments at each insertion interval resulted in a peak, no clear trends, either with respect to peak height or HETP values, could be found. The lack of a clear pattern in the peak heights or widths is due to the random nature of sample penetration because, in any given experiment, insertion, withdrawal, or both actions can result in sample penetration into the capillary. This mode of extraneous injection will be superimposed on the electrokinetic or hydrostatic injections resulting in total injection plug sizes which can be unacceptable in terms of plate heights.

Three mechanisms may be responsible for the extraneous sample injection: (a) insertion of the capillary into the sample solution may displace a small volume of the sample into the capillary; (b) viscosity, surface tension, and/or density differences between the sample solution and the buffer could cause a convective outflow of some buffer and subsequent inflow of sample into the CZE capillary; (c) diffusion of the solute into the capillary may occur. Initial experiments indicate that density differences between the sample and the buffer play a major part in this extraneous injection. This undesired mode of injection is rather ubiquitous, and it may be operative under a wide range of experimental conditions without operator awareness. Further research is now underway to elucidate the exact cause of sample penetration, as well as to develop alternative approaches to sample introduction into CZE systems.

REFERENCES

- 1 M. Martin and G. Guiochon, *Anal. Chem.*, 56 (1984) 614–620.
- 2 M. Martin, G. Guiochon, Y. Walbroehl and J. W. Jorgenson, *Anal. Chem.*, 57 (1985) 559–561.
- 3 K. D. Lukacs and J. W. Jorgenson, *J. High Resolut. Chromatogr. Chromatogr. Commun.*, 8 (1985) 407–411.
- 4 D. E. Burton, M. J. Sepaniak and M. P. Maskarinec, *Chromatographia*, 21 (1986) 583–586.
- 5 M. J. Sepaniak and R. O. Cole, *Anal. Chem.*, 59 (1987) 472–476.
- 6 J. H. Knox and I. H. Grant, *Chromatographia*, 24 (1987) 135–143.
- 7 E. Grushka, R. M. McCormick and J. J. Kirkland, *Anal. Chem.*, 61 (1989) 241–246.
- 8 Y. Walbroehl, *Ph. D. dissertation*, University of North Carolina, Chapel Hill, NC, 1986.
- 9 R. A. Wallingford and A. G. Ewing, *Anal. Chem.*, 59 (1987) 678–681.
- 10 D. J. Rose and J. W. Jorgenson, *Anal. Chem.*, 60 (1988) 642–648.
- 11 J. C. Sternberg, *Adv. Chromatogr.*, 2 (1966) 205–270.
- 12 J. W. Jorgenson and K. D. Lukacs, *J. High Resolut. Chromatogr. Chromatogr. Commun.*, 4 (1981) 230–231.
- 13 R. M. McCormick, *Anal. Chem.*, 60 (1988) 2322–2328.

CAPILLARY ZONE ELECTROPHORETIC SEPARATIONS OF PROTEINS IN POLYETHYLENE GLYCOL-MODIFIED CAPILLARIES

G. J. M. BRUIN, J. P. CHANG^a, R. H. KUHLMAN, K. ZEGERS, J. C. KRAAK and H. POPPE*
Laboratory for Analytical Chemistry, University of Amsterdam, Nieuwe Achtergracht 155, 1018 WV Amsterdam (The Netherlands)

SUMMARY

Fused-silica capillaries were wall modified with γ -glycidoxypropyltrimethoxy-silane and polyethylene glycol 600 in order to decrease the influence of wall adsorption in capillary zone electrophoretic separations of proteins. It is shown that a significant decrease in adsorption is obtained and electro-osmotic flow is also diminished. For the proteins studied, symmetrical peaks were obtained in the pH range 3–5. However, some adsorption still occurs as the plate numbers are below theoretical expectations. At higher pH values appreciable peak deformations and drastic decreases in resolving power are observed. The procedure allows the rapid and efficient separation of protein mixtures suitable for separation in the indicated pH range, and the coating shows a good stability.

INTRODUCTION

Capillary zone electrophoresis (CZE) has been shown to be a separation technique with a very high resolving power for charged substances. The technique is less laborious than conventional gel electrophoresis with respect to quantitation because the preparation of the gel and staining/destaining procedures for band detection are absent in CZE.

Although CZE has frequently been applied to the separation of small molecules such as amino acids¹, peptides² and organic³ and inorganic ions⁴, a main interest is in its application to the separation and characterization of proteins. Especially proteins with molecular weights between 5000 and hundreds of thousands are suitable for analysis by CZE. In liquid chromatography (LC), highly efficient separations of proteins are very limited owing to the small diffusion coefficients, which lead to slow mass transfer. In contrast to LC, small diffusion coefficients are desirable in CZE as the efficiency (N) increases according to²

$$N = \mu_{0,i}V/2D_i \quad (1)$$

^a Present address: Shanghai Institute of Materia Medica, Chinese Academy of Sciences, 319 Yuyang Road, Shanghai 200031, China.

where V is the applied voltage and $\mu_{0,i}$ is the overall mobility and D_i the molecular diffusion coefficient of a sample component i . This simple relationship was derived by Jorgenson and DeArman Lukacs² under the assumption of diffusion-limited band broadening. However, in practice, it will be difficult to realize this ideal situation, owing to the occurrence of additional band broadening caused by thermal gradients in the capillary system and perturbations in the local electric field within a sample zone due to conductivity changes. However, these additional band-broadening effects are small compared with the band broadening that occurs when large molecules distribute between the liquid and the wall, which will destroy the efficiency. As has been shown by Martin and Guiochon⁵, the slightest adsorption will cause an appreciable decrease in efficiency, while moderate adsorption can lead to completely destroyed peaks shapes and poor reproducibility. Therefore, it is of paramount importance that adsorption is absent in order to exploit the full benefit of the separation of CZE.

Several approaches have been employed to eliminate wall adsorption of proteins. One of these, described by Lauer *et al.*⁶, is based on adjustment of the pH of the buffer system to a value above the iso electric point (pI) of the proteins. Under such circumstances, both proteins and the silanol groups on the wall are negatively charged and repulsive forces result in strongly diminished adsorption. Highly efficient separations have been demonstrated using this approach⁶. Also, very low pH values, where electrical wall charges are small, have been applied⁷. However, in biopolymer separations it is of great importance to retain the pH as a freely adjustable parameter for various reasons: the stability of the sample materials may be involved; the pH is the predominant parameter governing the separation properties of the solutes; high pH values lead to a high electro-osmotic flow, which impairs the resolving power; and too large pH-pI differences may cause structural changes in the proteins.

An approach of more general scope is to bond chemically a neutral, hydrophilic coating to the capillary surface in order to shield the silanol groups so that a broad range of proteins can be separated with high resolution at various pH values. Moreover, the shielding of the silanol groups reduces the ζ -potential. It will be shown that the coating has a strong beneficial influence on the electro-osmotic flow and the extent of adsorption.

Various chemical modifications of the capillary have already been employed in CZE, such as with polyacrylamide⁸, glycol groups⁹, polysiloxanes⁷ and a glyceroglycidoxypopyl coating⁷. However, especially for protein separations, there is still a need for wall modification schemes that satisfy the following requirements: effective suppression of adsorption; reproducibility in the preparation of capillaries; long lifetime of the capillaries and preservation of the inertness and efficiency over that lifetime; and applicability over a wide pH range.

This work involves the application of a simple procedure to modify fused-silica capillaries with polyethylene glycol (PEG) chains in order to create a suitable hydrophilic surface structure, while the chemical epoxy-based bonding used favours long-term stability.

EXPERIMENTAL

Apparatus

A 0–60 kV d.c. high voltage delivered by a power supply (Wallis, Worthing,

U.K.) drove the electrophoretic separations. Platinum electrodes were used for the connection of the supply with the buffer reservoirs located at each end of the capillary. The total set-up was placed in a Plexiglas box; opening the box automatically shut off the high voltage. Fused-silica capillaries (SGE, North Melbourne, Australia) of 50 or 100 μm I.D. were used for the separations.

Detection was carried out at the cathodic side partly using a fluorescence detector (RF-530, Shimadzu, Kyoto, Japan) slightly modified for on-column detection at an excitation wavelength of 280 nm and an emission wavelength of 340 nm. For most of the measurements, a UV detector (Kratos 757) with a modified cell arrangement for on-column work was used. This new arrangement facilitated the positioning of the capillary and of an adjustable slit in front of the capillary for focusing the light beam on the inner part of the capillary. The wavelength was set at 205 nm. The signal from the detectors was fed to a chart recorder (Type BD40, Kipp and Zonen, Delft, The Netherlands).

The current in the system was measured over a 10-k Ω resistance in the return circuit of the power supply by means of a battery-powered electrical service meter. The temperature in the Plexiglas box was constant to within 1°C (25–26°C) during the separations.

Samples were injected by means of the electromigration technique¹⁰ at constant voltage (5–10 kV) at the positive side for a fixed period of time (10–30 s). The protein samples were dissolved at a concentration of 1 mg/ml in phosphate buffer of the appropriate pH and concentration and could be stored for a few days at 4°C.

Reagents

All proteins were obtained from Sigma (St. Louis, MO, U.S.A.). Polyethylene glycol was purchased from Merck (Darmstadt, F.R.G.) and γ -glycidoxypropyl-trimethoxysilane from Serva (Heidelberg, F.R.G.). The other reagents and solvents used were of analytical-reagent grade. Distilled water was used to prepare the buffers.

Capillary modification

The coating procedure is shown schematically in Fig. 1. The capillary (50 or 100 μm I.D.) was first etched with 1 M potassium hydroxide solution for 3 h at room temperature and rinsed with water for 10 min. Next the capillary was flushed with 0.1

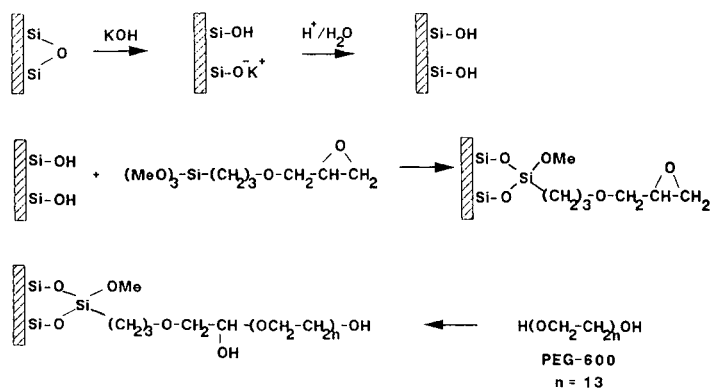


Fig. 1. Scheme of the procedure for the deactivation of the silica wall. Me = methyl.

M hydrochloric acid to remove K^+ ions from the wall and to produce free silanol groups at the surface of the wall. The capillary was dried at 200°C for 3 h with gentle flushing with helium. The dried capillary was then coated with the coupling reagent γ -glycidoxypolytrimethoxysilane by pumping through a solution of the reagent in dried toluene (10%, v/v) at 110°C for 3 h at an inlet pressure of 0.5 MPa. Subsequently the unbound reagent was flushed from the capillary with toluene. Next the epoxide group was opened by a reaction carried out in the same manner with a solution of 20% polyethylene glycol 600 and 2% boron trifluoride etherate in dioxane for 1 h at 100°C. Finally, the capillary was rinsed with distilled water.

This standard procedure was applied to 50 and 100 μm I.D. capillaries with a length of approximately 1 m.

RESULTS AND DISCUSSION

Fig. 2 shows separations of protein mixtures obtained with (A) an untreated and (B) a PEG-600 treated capillary in 0.01 *M* phosphate buffer at pH 6.8. In both separations the same mixture, *i.e.*, lysozyme, trypsin and chymotrypsinogen, was injected. Most of the constituents do not elute at all in the untreated capillary, whereas in the PEG-treated tube a good separation is obtained. Lysozyme and chymotrypsinogen are invisible in Fig. 2A. The one peak in Fig. 2A corresponds to trypsin, as was established in a separate experiment (not shown). It can be safely assumed that wall adsorption impedes the successful separation in Fig. 2A.

Fig. 2C shows a separation with a PEG-treated tube under the same conditions but with more optimized conditions in terms of pH and buffer concentration. This electropherogram is typical of the efficiency obtained during this work. Plate numbers between 80 000 and 150 000, depending on the species, pH, buffer concentration and capillary diameter, can be achieved routinely.

In experiments such as that in Fig. 2B, the proteins elute in the order expected on the basis of their isoelectric points (see Table I). Lysozyme, which has the highest *pI*

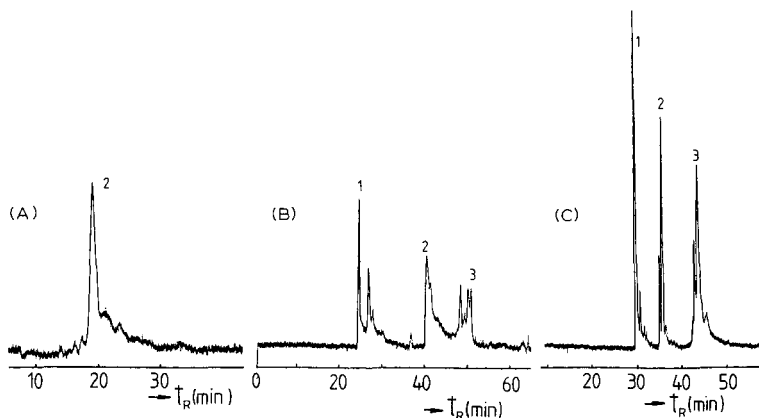


Fig. 2. Separation of a mixture of proteins (A) in an untreated and (B and C) in treated capillaries with fluorescence detection. Injection: (1) lysozyme, (2) trypsin and (3) chymotrypsinogen. (A) Untreated fused-silica capillary; buffer, 0.01 *M* KH_2PO_4 , pH = 6.8. (B) PEG-coated capillary; buffer, 0.01 *M* KH_2PO_4 , pH = 6.8. (C) PEG-coated capillary; buffer, 0.05 *M* KH_2PO_4 , pH = 4.1.

TABLE I
ISOELECTRIC POINTS (*pI*) AND MOLECULAR WEIGHTS OF THE PROTEINS USED¹¹

<i>Protein</i>	<i>pI</i>	<i>MW</i>
Cytochrome <i>c</i>	10.8	12 200
Lysozyme	10.0	14 000
Myoglobin	7.5	17 500
Trypsin	9.3	23 300
Ribonuclease	8.7	13 500
Trypsinogen	8.7	24 500
Chymotrypsinogen	8.7	21 600

value, has the highest charge of the three proteins at $\text{pH} < 6$ and elutes first. These results indicate that a substantial decrease in the adsorption activity of the wall for these proteins has been achieved.

Although the observed plate numbers are large, they are still low when compared with theoretical predictions. For instances, by means of eqn. 1 and using a value for the diffusion coefficient, D_i , of $10^{-10} \text{ m}^2/\text{s}$, a value for the mobility, $\mu_{0,i}$, of $2 \cdot 10^{-8} \text{ m}^2/\text{V} \cdot \text{s}$ and an applied voltage of 25 kV, a theoretical plate number of approximately $2.5 \cdot 10^6$ can be calculated, roughly a factor of 15 higher than the observed values. Although it was found to be possible to obtain higher plate numbers by improving the experimental set-up (cooling, injection), it can be assumed that the observed extra band broadening is still mainly caused by residual adsorption. As shown by Martin and Guiochon⁵, a very small distribution towards the wall, such that it would not be noticed via deviations in the mobilities, can seriously impair the efficiency.

Effect of pH of the buffer solution

Operation at pH values below the isoelectric points of the proteins ensures that the three model proteins all have a net positive charge and as a result they migrate in the direction of the negative electrode.

Fig. 3 shows the dependence of the mobility of three proteins, lysozyme, trypsin and chymotrypsinogen, on the pH of phosphate solutions. The mobilities reported are "overall" values, *i.e.*, they include the osmotic flow of the liquid, *i.e.* $\mu_{0,i} = \mu_{el,i} + \mu_{ec}$. It must be noted that the electrophoretic and electro-osmotic flow are both directed towards the negative electrode in this instance and thus have the same sign. There is a decrease in the mobility (except for lysozyme) on going from pH 3.0 to 5.1. Because the positive charge on the proteins decreases at higher pH , there is a reduction in electrophoretic mobility. This reduction is stronger for trypsin and chymotrypsinogen because of their lower iso-electric points (see Table I).

At a pH of *ca.* 6, peaks in the electropherogram with strong tailing were observed. This may be caused by increasing adsorption of the proteins on the wall, either by interaction with residual surface silanols or by interaction of the less protonated proteins with the neutral, hydrophilic PEG chains.

Effect of concentration of the buffer solution

Fig. 4 illustrates the relationship between the observed mobilities, $\mu_{0,i}$, of the three proteins and the phosphate buffer concentration over the range 0.01–0.08 *M* at pH 3.8.

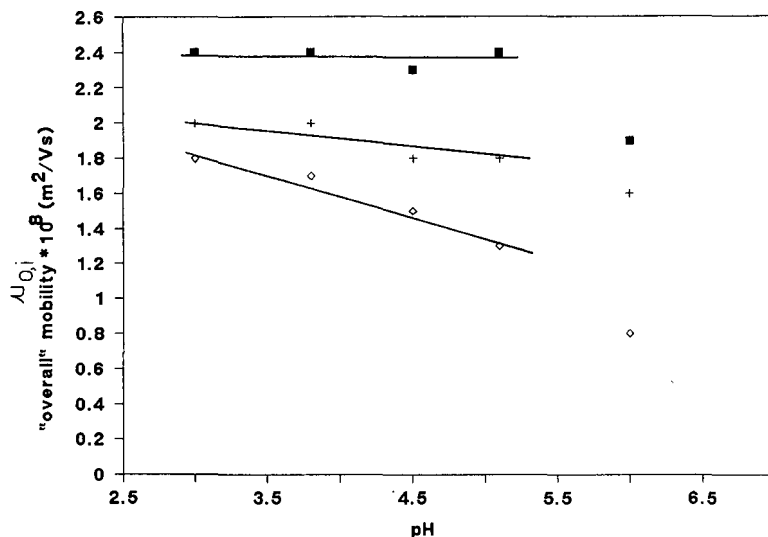


Fig. 3. Mobility, $\mu_{0,i}$, of the three model proteins as a function of pH at a KH_2PO_4 concentration of 0.05 M. Separation voltage, 20 kV; injection, 10 s, 10 kV. $L = 0.59$ m, $l_{\text{inj.-det.}} = 0.35$ m. (■) Lysozyme; (+) trypsin; (◇) chymotrypsinogen.

It shows that the mobilities decrease on going from 0.01 M to 0.08 M KH_2PO_4 solution. This may be partly due to a changing effective charge (ζ -potential) of the proteins. However, the effect is mainly due to a strong reduction of the electro-osmotic flow.

The dependence of osmotic flow on buffer concentration, as measured with β -naphthol as a neutral marker, is shown in Fig. 5. The contribution of electro-osmotic

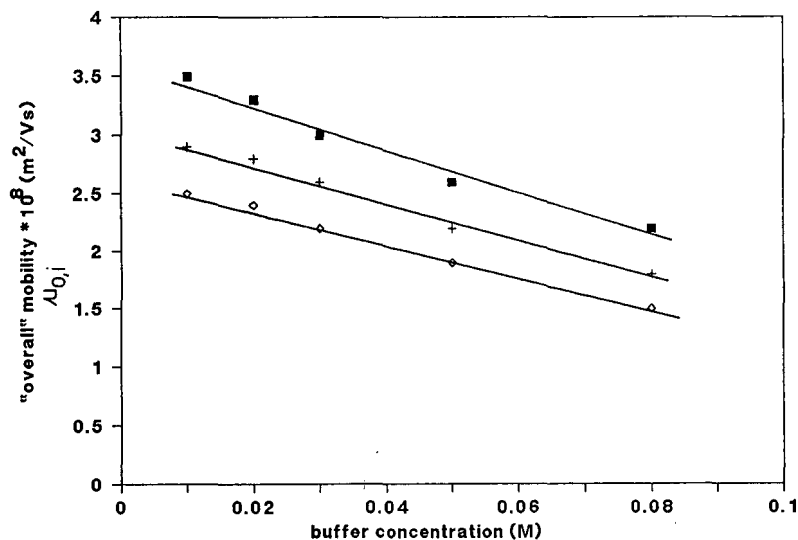


Fig. 4. Mobility, $\mu_{0,i}$, as a function of KH_2PO_4 concentration at pH 3.8. Separation voltage, 20 kV; injection, 10 s, 10 kV. $L = 0.63$ m, $l_{\text{inj.-det.}} = 0.37$ m. (■) Lysozyme; (+) trypsin; (◇) chymotrypsinogen.

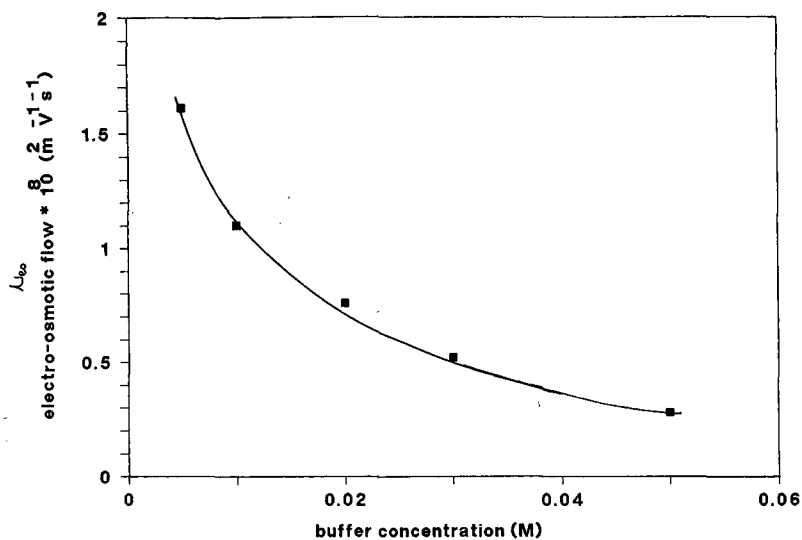


Fig. 5. Electro-osmotic mobility, μ_{eo} , as a function of KH_2PO_4 concentration at pH 3.8. $L = 0.59$ m, $l_{inj-dct.} = 0.35$ m. Neutral marker: β -naphthol.

flow to the overall mobilities of the proteins is significant (10–70%), especially at buffer concentrations below 0.02 M. Working with buffer concentrations between 0.03 and 0.08 M resulted in a large reduction in the electro-osmotic flow.

It should be noted that these electro-osmotic velocities were observed to be much smaller than those in untreated capillaries, in agreement with earlier observations on modified silica tubes^{3,7,12}. This again is an indication of the good coverage of the active sites of the fused-silica wall by PEG. At concentrations higher than 0.08 M, one can observe strongly tailing peaks for the three proteins. This can be attributed to interactions between the PEG chains and the proteins, the charge of the latter being partly shielded by the phosphate groups at higher concentrations.

An example of the speed of this CZE system with the PEG-modified wall is shown in Fig. 6. Seven proteins are separated in less than 9 min.

Effect of applied voltage on the separations

As pointed out by Jorgenson and DeArman Lukacs², the reciprocal of the elution time should be linearly proportional to the applied voltage. In practice, the inverse elution time is not a linear function of voltage, as can be seen in Fig. 7. The increased temperature in the capillary at higher applied voltages reduces the viscosity of the buffer, which increases the lysozyme mobility.

Stability

The prepared wall-modified capillaries were found to be stable over several months. When not in use for a long period (months) they were stored after drying with a gentle stream of helium. They withstood treatment with dilute hydrochloric acid (0.01 M) applied after accidental irreversible adsorption of sample material, e.g., at high pH.

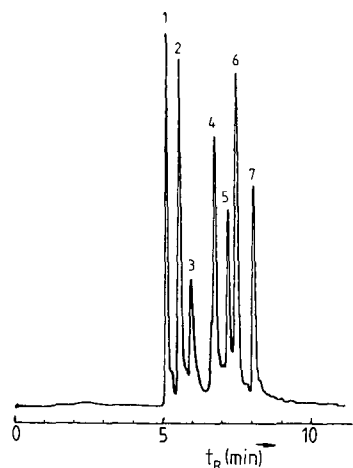


Fig. 6. Electropherogram of a mixture of seven proteins. Injection, 10 s, 10 kV. KH_2PO_4 concentration, 0.03 M, pH = 3.8. 1 = Cytochrome *c*; 2 = lysozyme; 3 = myoglobin; 4 = trypsin; 5 = ribonuclease; 6 = trypsinogen; 7 = chymotrypsinogen.

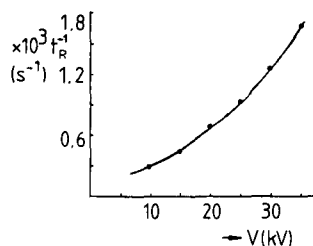


Fig. 7. Reciprocal of lysozyme retention time as a function of the applied voltage. $L = 0.89$ m, $l_{\text{inj.-det.}} = 0.65$ m. Buffer: concentration 0.05 M, pH = 3.8.

CONCLUSIONS

Deactivation of the wall of a fused-silica capillary with polyethylene glycol to avoid adsorptive interactions between the proteins and the wall is successful at low pH. The capillaries can be used for several months without a noticeable decrease in separation efficiency. However, it can be concluded that PEG-600-modified capillaries are not useful in the more interesting intermediate pH range between 5 and 8. Further work on fused-silica deactivation procedures, *e.g.*, with carbohydrate moieties, for the separation of proteins is in progress.

REFERENCES

- 1 E. Gassmann, J. E. Kuo and R. N. Zare, *Science (Washington, D.C.)*, 230 (1985) 813.
- 2 J. W. Jorgenson and K. DeArman Lukacs, *J. Chromatogr.*, 218 (1981) 209.
- 3 T. Tsuda, K. Nomura and G. J. Nakagawa, *J. Chromatogr.*, 248 (1982) 241.
- 4 T. Tsuda, K. Nomura and G. J. Nakagawa, *J. Chromatogr.*, 264 (1983) 385.
- 5 M. Martin and G. Guiochon, *Anal. Chem.*, 56 (1984) 614.
- 6 H. H. Lauer and D. McManigill, *Anal. Chem.*, 58 (1986) 166.
- 7 R. M. McCormick, *Anal. Chem.*, 60 (1988) 2322.
- 8 S. Hjertén, *J. Chromatogr.*, 347 (1985) 191.
- 9 J. W. Jorgenson, *Trends Anal. Chem.*, 3 (1984) 51.
- 10 D. J. Rose and J. W. Jorgenson, *Anal. Chem.*, 60 (1988) 642.
- 11 P. G. Righetti and T. Caravaggio, *J. Chromatogr.*, 127 (1976) 1.

Note

Picolinic acid: a mobile phase additive for improved chromatography of metal-chelating heterocyclic acids and β -diketones

D. W. ROBERTS, R. J. RUANE and I. D. WILSON*

ICI Pharmaceuticals PLC, Mereside, Alderley Park, Macclesfield, Cheshire SK10 4TG (U.K.)

During the course of the development of high-performance liquid chromatographic (HPLC) analytical methods for some metal-chelating compounds from two distinct chemical series, one series containing a heterocyclic acid, the other a β -diketone (see Fig. 1 for general structures), severe problems were encountered due to poor chromatographic peak shapes. Thus, using reversed-phase HPLC, peaks from these compounds were characterised by excessive tailing, peak asymmetry and, in the worst cases, "chair"-shaped peaks. These problems were clearly a property of the compounds under investigation and did not reflect deficiencies in the instrumentation.

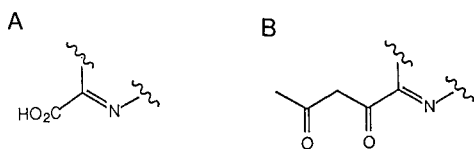


Fig. 1. Part structures of (A) the heterocyclic acid series and (B) the β -diketone series of metal-chelating compounds.

A number of strategies were therefore investigated in an attempt to eliminate this problem. However, improvements in peak shape were only obtained when the analytes themselves were added to the solvent. This resulted in a dramatic improvement and suggested that the poor peak shape was a result of a specific, saturable, interaction of the analytes with the chromatographic system.

In some ways the results obtained by us for these metal-chelating compounds are similar to those reported by a number of groups engaged in the analysis of tetracyclines¹⁻³. These workers have shown that on reversed-phase systems the tetracyclines can be subject to poor chromatographic efficiencies and irreversible adsorption of trace amounts of the analytes. In order to eliminate this problem several investigators^{1,4} have added related compounds to the mobile phase in order to deactivate the packing material. Another approach has been to add EDTA to the mobile phase to prevent complexation of the tetracyclines with metal ions in the chromatographic system⁵⁻¹⁰.

Here experiments designed to further improve the chromatographic behaviour of these β -diketones and heterocyclic acids are described.

MATERIALS AND METHODS

Apparatus

The HPLC system consisted of an LC-XPD pump (Pye Unicam Cambridge, U.K.), a Rheodyne 7125 loop injector (Rheodyne, Berkley, CA, U.S.A.) fitted with a 50- μ l loop, a Spectromonitor 3000 variable-wavelength UV detector (Milton Roy, Stone, U.K.) operating at 300 nm and a Model BS 273 chart recorder (Bryans Southern Instruments, Mitcham, U.K.).

Reagents. Acetonitrile and tetrahydrofuran were HPLC grade (Fisons, Loughborough, U.K.). Orthophosphoric acid (85%) and butylamine were analytical grade (Fluka, U.K.). Picolinic acid (pyridine-2-carboxylic acid), nicotinic acid (pyridine-3-carboxylic acid) and picoline (2-methylpyridine) were supplied by BDH (Poole, U.K.). Water for HPLC was produced using an Elga Spectrum ROI system (Elga, High Wycombe, U.K.).

Chromatography

Heterocyclic acid series. For the chromatography of compounds from the heterocyclic acid series stainless-steel columns (15 cm \times 0.46 mm I.D.) were used packed with either 5 μ m Zorbax C₈ silica (Jones Chromatography, Galmorgan, U.K.) or 5 μ m Spherisorb C₁ silica (Capital HPLC Specialists, West Lothian, U.K.).

β -Diketone series. Compounds from the β -diketone series were chromatographed on a stainless-steel column (15 cm \times 4.5 mm I.D.) packed with a polymer-based resin, 5 μ m, 100A PLRP-S: macroporous polystyrene-divinylbenzene (Polymer Laboratories, U.K.).

Mobile phases. The mobile phase was prepared by mixing varying proportions (see figure captions) of acetonitrile with 0.1 M phosphoric acid–butylamine buffer. The buffer was prepared by adding *ca.* 7.0 g of orthophosphoric acid to 1 l of water followed by sufficient butylamine to give a pH of *ca.* 2 for the heterocyclic acid and between 7.5 and 10.5 for the β -diketone series.

Picolinic acid, nicotinic acid or picoline were added to the mobile phase to give a final concentration of 1 mM. Solvent was delivered at a flow-rate of 1.5–2.0 ml min⁻¹.

In the case of the β -diketone series the column was maintained at a temperature of 50°C. Otherwise chromatography was carried out at ambient temperatures.

Analytes were dissolved in the HPLC mobile phase for injection.

RESULTS AND DISCUSSION

Heterocyclic acids

When an otherwise unmodified mobile phase consisting only of acetonitrile–phosphoric acid–butylamine buffer was used, the peak corresponding to the analyte demonstrated excessive tailing as illustrated in Fig. 2A and B for a typical example on C₈ and C₁ columns, respectively. This phenomenon was initially assumed to be due to interaction of the analyte with residual silanols remaining on the surface of the silica-based packing materials. This type of interaction can usually be overcome by the addition of organic bases (*e.g.* butylamine or hexylamine), pH control, incorporation of ion-pair reagents into the mobile phase or the use of other packing materials *e.g.*

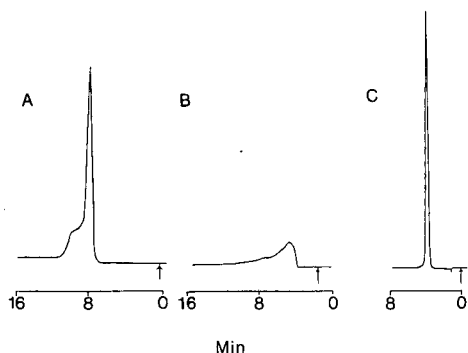


Fig. 2. (A) Typical chromatogram obtained for a member of the heterocyclic acid series on a Zorbax C₈ column using an unmodified mobile phase of acetonitrile–phosphoric acid–butylamine buffer (pH 2.5) (1:1, v/v). Flow rate 1.5 ml min⁻¹ at ambient temperature. (B) The same conditions as (A) using Spherisorb C₁. Chromatographic conditions as for (A). (C) Conditions as for (A) with the addition of 1 mM picolinic acid to the mobile phase.

LiChrosorb RP-select, and non-silica-based materials such as the PRP1 resins. However, our attempts to overcome the peak asymmetry problems exhibited by these compounds by using such alternative approaches was unsuccessful with either poor peak shape or non-elution of the analytes from the columns. We also attempted to use EDTA as a mobile phase additive but observed no improvement in the peak shape of these analytes.

As it seemed clear that the analytes were interacting strongly with some component in the system we added the compounds themselves to the mobile phase (*ca.* 1 mM) in order to saturate the binding. This resulted in a dramatic improvement in the peak shape on subsequent injections of the analytes themselves, together with a corresponding increase in the UV background provided by the solvent. To reduce this baseline noise sufficiently to be able to employ the system for trace analysis a number of structurally related substances with maximum values for UV absorbance well below those of the analytes were studied as mobile phase additives. The first of those to be investigated was picolinic acid (pyridine-2-carboxylic acid) resulting in the chromatogram shown in Fig. 2C. Here, addition of the picolinic acid resulted in the production of excellent symmetrical peaks enabling trace analysis of the compound of interest at the ppm level. The use of mobile phase additives such as either nicotinic acid, the pyridine-3-carboxylic acid analogue of picolinic acid, or picoline (2-methyl pyridine) at similar concentrations to picolinic acid was without effect. The difference between picolinic and nicotinic acids suggest that the observed interaction was relatively specific for carboxylic acids adjacent to heterocyclic nitrogens. Injection of the analytes in the mobile phase was essential as failure to do this resulted in system peaks.

β-Diketone series

Initially we attempted to overcome the similar problems of poor peak shape associated with the *β*-diketone series using the approach developed for the heterocyclic acids. However, these attempts were completely unsuccessful. It was felt that the very broad tailing peaks observed with these compounds might, in addition to

problems associated with metal chelation, perhaps also be due to keto-enol tautomerism as these β -diketones were likely to be in the enol form under the conditions employed for analysis.

Such compounds can be stabilised by the use of solvents of sufficiently high pH and to enable the use of such solvents without adverse effect on the column a polymer-based packing material (PLRP-S) was adopted. This enabled the use of solvents with pH values greater than 9, and in addition also eliminated any possible silanol interactions. An example of the chromatographic behaviour of a typical β -diketone compound from this series is shown in Fig. 3A. The peak shape obtained by using such a system was still not acceptable. As seen with the heterocyclic acids the addition of EDTA to the mobile phase also proved ineffective in improving peak shape. Given that it was quite likely that these compounds were interacting with metal ions in the system, we examined the effect of adding excess ferric ions to the mobile phase. It has been shown in the case of the tetracyclines that metal ions in the mobile phase can exert a strong influence on chromatography and, for example, Reeuwijk and Tjaden noted a large increase in the capacity ratio of tetracyclines in the presence of ferric ions¹¹. A similar effect on the chromatography of β -diketones was noted by us when the effect of ferric ions in the mobile phase was studied but the chromatographic result was still unacceptable.

However, addition of picolinic acid once again resulted in a dramatic improvement in chromatography (Fig. 3B). Once again it was necessary to inject the analyte as a solution in the HPLC mobile phase to avoid system peaks.

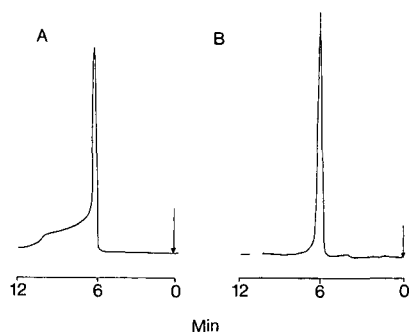


Fig. 3. (A) Typical chromatogram obtained for a member of the β -diketone series on a PLRP-S polymer column using an unmodified mobile phase of acetonitrile-phosphoric acid-butylamine buffer (pH 8.5) (30:70, v/v). Flow-rate 1.5 ml min^{-1} at 50°C . (B) Conditions as for (A) with the addition of 1 mM picolinic acid to the mobile phase.

To explain these observations for both the acid and β -diketone series some saturable interaction with a component of the chromatographic system seems likely. This interaction may be with the stationary phase, the solvent or, given the metal-chelating properties of these compounds, with the stainless-steel tubing and frits present in the system.

It is therefore probable that the mechanism by which the picolinic acid in the mobile phase causes the observed improvement in peak shape is that it saturates these active sites by effectively masking them, and thus prevents their interaction with the

analytes. It seems most unlikely that the residual silanols are responsible for the observed results as similar poor peak shape was observed on polymer-based packings from which silanols are absent. It is also unlikely that the observed dramatic improvements in peak shape are due to the action of picolinic acid as an ion-pair reagent as conventional ion-pair reagents were singularly ineffective in improving peak shape.

Whilst we are currently unable to provide complete structures for any of the compounds discussed here, we would like to emphasise that the poor chromatographic properties described here were seen in a wide range of compounds containing the part structures shown in Fig. 1 and were not significantly affected by changes elsewhere in the molecule. However, this phenomenon may be quite common for strongly metal-chelating compounds as we have subsequently been able to effect a considerable improvement in the peak shape of several structurally unrelated compounds by using a similar approach.

Further studies to understand the mechanism underlying our observations are continuing.

ACKNOWLEDGEMENTS

The comments and advice of E. R. H. Walker, H. Tucker and R. Dowell are gratefully acknowledged.

REFERENCES

- 1 R. Böcker, *J. Chromatogr.*, 187 (1980) 439.
- 2 S. Eksborg, *J. Chromatogr.*, 208 (1981) 78.
- 3 J. H. Knox and J. Jurand, *J. Chromatogr.*, 110 (1975) 103.
- 4 J. P. Sharma and R. P. Bevil, *J. Chromatogr.*, 166 (1978) 213.
- 5 J. H. Knox and J. Jurand, *J. Chromatogr.*, 186 (1979) 763.
- 6 J. Hermansson, *J. Chromatogr.*, 232 (1982) 385.
- 7 S. Eksborg, H. Ehrsson and U. Lönnroth, *J. Chromatogr.*, 185 (1979) 583.
- 8 H. J. C. F. Nelis and A. P. De Leenheer, *J. Chromatogr.*, 195 (1980) 35.
- 9 H. Poiger and C. H. Schlatter, *Analyst*, 101 (1976) 808.
- 10 E. R. White, M.A. Carroll and J. E. Zarembo, *J. Antibiot.*, 30 (1977) 811.
- 11 H. J. E. M. Reeuwijk and U. R. Tjaden, *J. Chromatogr.*, 353 (1986) 339.

Note

Trace/ultratrace analyses of unstable compounds

Investigations on hydrazobenzene and azobenzene^a

S. AHUJA*, G. THOMPSON and J. SMITH

Development Department, Pharmaceuticals Division, CIBA-GEIGY Corporation, Suffern, NY 10901 (U.S.A.)

Trace analysis generally entails determination at ppm or $\mu\text{g/g}$ level. Analyses performed at trace or lower levels (ultratrace) are difficult to carry out for several reasons. The difficulties relate to obtaining a representative sample, avoiding loss or contamination during sample preparation, finding a suitable method for resolving the component of interest without significant loss, and, finally, having sufficient detectability in the range of interest to assure reliable quantitation. These problems are further compounded when one is dealing with compounds such as hydrazobenzene and azobenzene. Discussed below is a method developed to analyze these compounds and which circumvent some of the problems encountered with them.

EXPERIMENTAL

A sample weight anticipated to contain *ca.* 10 ppm of hydrazobenzene or azobenzene is weighed accurately and shaken with 30 ml of pH 9.2 tris(hydroxymethyl) aminomethane (THAM) buffer. This is followed by extraction with 10 ml of *n*-hexane. After centrifugation, 5 ml of the *n*-hexane layer are evaporated to dryness at room temperature with nitrogen and the residue is solubilized in 1.0 ml of acetonitrile. A 25- μl sample is immediately injected into a high-performance liquid chromatography (HPLC) apparatus equipped with a Partisil 10 μm C₈ column (25 cm \times 4.6 mm I.D.) and a dual-channel detector (254 and 313 nm). Elution is carried out with a mobile phase composed of acetonitrile–acetate buffer, pH 4.1 (11:14, v/v). Both hydrazobenzene and azobenzene standards are treated similarly.

RESULTS AND DISCUSSION

A review of the literature revealed that a normal-phase HPLC method has been reported for the analysis of hydrazobenzene and azobenzene¹. The method entails extraction of these compounds into *n*-hexane from 1M NaOH followed by analysis on Partisil-10 PAC column with a mobile phase containing 2.5% absolute ethanol.

^a Presented in part at the *Symposium on Trace Analyses — Accomplishments, Goals, Challenges*, National Bureau of Standards, Gaithersburg, MD, September 28, 1987.

TABLE I
STABILITY OF HYDRAZOBENZENE AND AZOBENZENE

Medium	Time (min)	% Loss	
		Hydrazobenzene	Azobenzene
0.1M NaOH	30	82.9 ^a	4.6 ^b
pH 9.2 buffer	30	0.9 ^c	0 ^d

^a Original concentration in 10% acetonitrile, 11.8 μg hydrazobenzene/ml.

^b Original concentration in 10% acetonitrile, 15.7 μg azobenzene/ml.

^c Original concentration in 10% acetonitrile, 3.55 μg hydrazobenzene/ml.

^d Original concentration in 10% acetonitrile, 2.59 μg azobenzene/ml.

The published method suffers from the following shortcomings: Hydrazobenzene and azobenzene show significant instability in 1M NaOH (Table I); azobenzene can occur as *cis*- and *trans*- isomers. Their separation is not demonstrated or accounted for in the method; parent compound (I) can degrade directly or indirectly into hydrazobenzene and azobenzene (Fig. 1)²; selectivity of transformation products given in Fig. 1 is not demonstrated.

The properties of hydrazobenzene and azobenzene are given in Fig. 2. Hydrazobenzene is known to be an unstable compound; it oxidizes easily to azobenzene and other compounds and has $t_{1/2}$ of 15 min in wastewater⁵. Azobenzene, on the other hand, can isomerize or sublime even at 30°C³.

To assure that the methodology would be reliable at *ca.* 10 ppm, suitable methods were developed for detecting these compounds at levels ≤ 1 ppm, *i.e.* ultratrace levels. To further assure reliability of analyses, an effort was made to meet the following requirements for ultratrace analysis⁶: Sample used for analysis was representative of the whole lot; methodology incorporated optimum separation and detection techniques; component of interest was allowed to suffer a minimum loss during various analytical operations; adequate steps were incorporated in the analytical method to account for losses that might occur due to sample preparation or degradation. Furthermore, to assist other researchers in evaluating whether these methods could be useful for their investigations, the following analytical parameters were included:

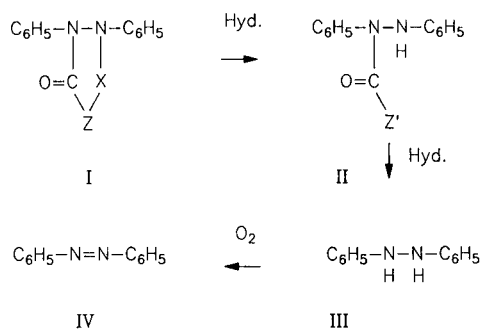


Fig. 1. Degradation pathway of parent compound².

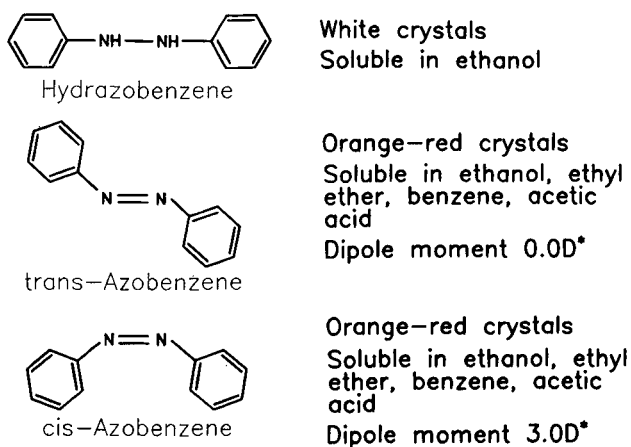


Fig. 2. Physical properties of hydrazobenzene and azobenzene³. For dipole moment see ref. 4.

amount present in original sample (APIOS); minimum amount detected in g (MAD); minimum amount quantitated in g (MAQ).

Investigations revealed that the optimum pH for extraction for both hydrazobenzene and azobenzene is 9.2. At this pH, these compounds can be easily extracted from the parent compound and are also quite stable (Table I). The *cis*- and *trans*-isomers of azobenzene and hydrazobenzene can be resolved well with the reversed-phase HPLC method (Fig. 3). Previous investigations had confirmed the selectivity of

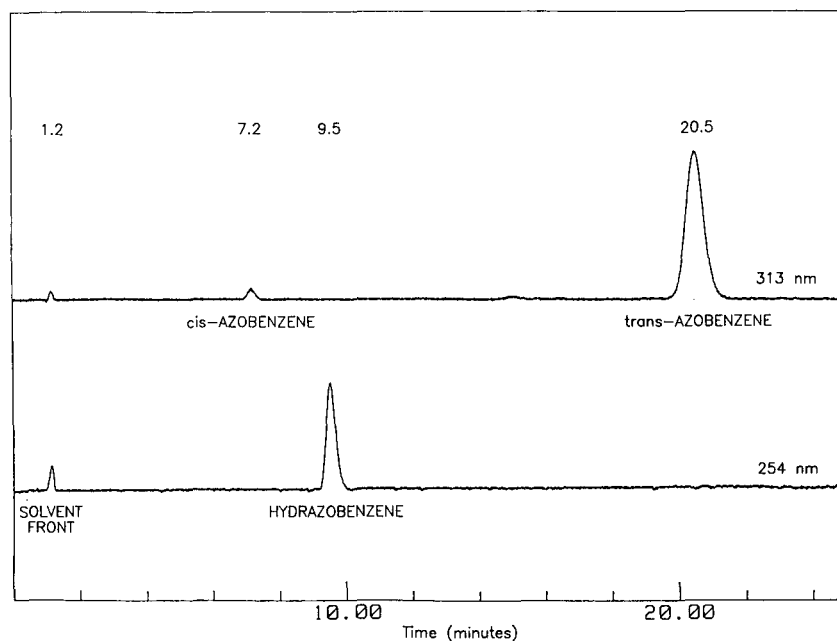


Fig. 3. Chromatograms of *cis*- and *trans*-azobenzene and hydrazobenzene. A 0.05- μ g sample of each compound was injected and monitored at 313 and 254 nm.

TABLE II
RECOVERY DATA OF SPIKED SAMPLES

Apios: ≤ 10 $\mu\text{g/g}$ of parent compound.

Sample	Hydrazobenzene found	Azobenzene found
Parent compound (%)	89.0 ± 8.6 ($n = 7$)	123 ± 2.6 ($n = 6$)
Capsules (%)	89.6 ± 10.8 ($n = 5$)	98.7 ± 10.2 ($n = 3$)
Tablets (%)	95.8 ± 5.4 ($n = 3$)	121 ± 4.2 ($n = 3$)
Average (%)	91	114
R.S.D. (%)	$\pm 5 - 11$	$\pm 3 - 10$
MAD (μg)	0.006	0.007
MAQ ($\mu\text{g/g}$)	≤ 1	≤ 1

this method as it resolves compound I ($t_R \approx 11$ min) from other transformation products⁷. Data on spiked samples are given in Table II. An average recovery of 91 and 114% was obtained for hydrazobenzene and azobenzene, respectively with relative standard deviation (R.S.D.) of 3–11%. The methods were found useful for quantitating ≤ 1 $\mu\text{g/g}$ of these compounds with respect to the parent compound (MAD = 6–7 ng). The high recovery obtained for azobenzene is partly due to conversion of hydrazobenzene to azobenzene (*ca.* 9%). Further improvements are being investigated.

CONCLUSIONS

Selective methods have been developed for analysis of hydrazobenzene and azobenzene.

The instability of hydrazobenzene in aqueous and organic solvents is well known. This problem has been effectively dealt with in that an average recovery of 91% was obtained for the active ingredient, capsules and tablets.

It was found that azobenzene is susceptible to isomerization and sublimation. The developed procedure provides an average recovery of 114% for the active ingredient, capsules and tablets. The high values are partly due to conversion of hydrazobenzene into azobenzene (*ca.* 9%).

The developed methods provide reliable values (3–11% R.S.D.) for hydrazobenzene and azobenzene at a concentration of ≤ 10 $\mu\text{g/g}$ (≤ 10 ppm) in terms of the parent compound.

REFERENCES

- 1 F. Matsui, E. G. Lovering, N. M. Curran and J. R. Watson, *J. Pharm. Sci.*, 72 (1983) 1223.
- 2 S. Ahuja, in J. Touchstone (Editor), *Techniques and Applications of TLC*, Wiley, New York, 1985.
- 3 R. C. Weast, *Handbook of Chemistry and Physics*, CRC Press, Boca Raton, FL, 1985, pp. C-91, C-314, C-664.
- 4 J. Janssen, *J. Chem. Educ.*, 46 (1969) 117.
- 5 R. M. Riggan and C. C. Howard, *Anal. Chem.*, 51 (1979) 210.
- 6 S. Ahuja, *Ultratrace Analysis of Pharmaceuticals and Other Compounds of Interest*, Wiley, New York, 1986, p. 1.
- 7 S. Ahuja, S. Shiramani, G. Thompson and J. Smith, personal communication, March 2, 1984.

Letter to the Editor

On some nomenclature in chromatography

Sir,

Our present-day chromatographic nomenclature has resulted from intensive discussions among various groups in many countries over a number of years. The nomenclatures of gas and liquid chromatography and their variants, developed and published by the British Standards Institution, the American Society for Testing and Materials and the International Union of Pure and Applied Chemistry were excellently reviewed by Ettre¹⁻³ with special emphasis on its evolution and recommendations by early *ad hoc* Committees. He gave numerous valuable proposals for consideration in future revisions of chromatography nomenclature.

However, two broad areas of classification, namely, inverse chromatography and reversed-phase chromatography, seem to need attention. To my knowledge, the first term was not included in the recommended chromatography nomenclature when it was felt necessary to reconsider the latter term. They are discussed in this letter and a more scientific nomenclature is proposed for possible inclusion in future revisions of chromatography nomenclature.

Inverse chromatography

The first use of the term "inverse chromatography" is attributed to Davis and Petersen⁴, who applied the technique to the determination of the degree of oxidation of asphalt. Since then, the technique has been applied by many workers, especially by Guillet⁵ in the study of synthetic polymers.

In conventional gas chromatography, the properties of an unknown sample in the mobile phase are determined by interaction with a known stationary phase. An inverse sequence of information is obtained in inverse gas chromatography, where the properties of an unknown stationary phase are determined by its interaction with selected probe molecules in the mobile phase. The vaporizable molecules in the gas phase were designated "probe" molecules by Guillet⁵. In my opinion, it is inappropriate to classify chromatography on the basis of the sequence of information obtainable and call it "inverse chromatography". It is therefore suggested that it be given a special name, "molecular probe chromatography" (MPC). The technique is used in both gas and liquid chromatography. Hence MPC may be defined as a branch of chromatography where the properties of an unknown stationary phase are studied by interaction with probe molecules in the mobile phase. The term MPC has been used previously^{6,7} in studies on coal.

Reversed-phase chromatography

Chromatography has been subdivided on the basis of a number of principles. Subdivision on the basis of the relative polarities of the two phases is particularly important in liquid chromatography. Unlike gas chromatography, the mobile phase

in liquid chromatography represents an additional component influencing the separation mechanism. In practical liquid chromatography these subdivisions can be put into two variants. In the first, the stationary phase is more polar than the mobile phase while in the second case the opposite is true. The first variant is called normal-phase chromatography and the second reversed-phase chromatography.

In normal-phase chromatography specific interactions occur between the solute and the stationary phase and the retention of compounds depends mainly on the type of functional groups present in the molecule. On the other hand the solute – stationary phase interactions in reversed phase chromatography is due to a kind of hydrophobic sorption by means of non-specific dispersion forces. The hydrophobic part of the solute is preferentially sorbed on the hydrophobic surface of the stationary phase and the hydrophilic part of the solute is oriented towards the polar mobile phase. The sorption process is modified when the balance of the hydrophobic – hydrophilic effects of the solute and/or solvent is changed. The behaviour in the mobile phase is therefore predominant here.

Reversed-phase chromatography was originally introduced in 1950 by Howard and Martin⁸ and was widely used in paper chromatography in those days. To-day it has become the most widely used variant of liquid chromatography, accounting for as many as 70% of modern high-performance liquid chromatographic applications⁹.

Nevertheless, the expression reversed-phase is confusing. It is not the phase that is reversed but the polarity of the phase. It is, therefore, proposed to call it “reversed-polarity chromatography” and the former “normal-polarity chromatography”.

*Central Fuel Research Institute,
P.O. FRI, Dt. Dhanbad, Bihar,
Pin-828 108 (India)*

O. K. GUHA

1 L. S. Ettre, *J. Chromatogr.*, 165 (1979) 235.

2 L. S. Ettre, *J. Chromatogr.*, 220 (1981) 29.

3 L. S. Ettre, *J. Chromatogr.*, 220 (1981) 65.

4 T. C. Davis and J. C. Petersen, *Anal. Chem.*, 38 (1966) 1938.

5 J. E. Guillet, in H. Purnell (Editor) *New Developments in Gas Chromatography*, Vol. II, Wiley, New York, 1973, p. 187.

6 O. K. Guha and J. Roy, *Fuel*, 64 (1985) 1164.

7 O. K. Guha and J. Roy, *Fuel Proc. Technol.*, 11 (1985) 113.

8 G. A. Howard and A. J. P. Martin, *Biochem. J.*, 46 (1950) 532.

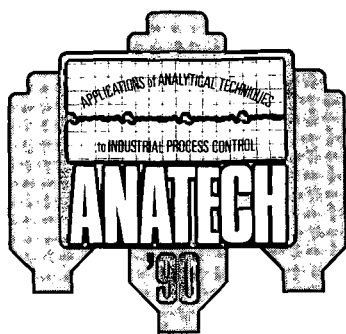
9 R. E. Majors, in C. Horváth (Editor), *High Performance Liquid Chromatography: Advances and Perspectives*, Vol. I, Academic Press, New York, 1980, p. 76.

Author Index

- Ahuja, S
—, Thompson, G. and Smith, J.
Trace/ultratrace analyses of unstable compounds. Investigations on hydrobenzene and azobenzene 443
- Akapo, S. O.
—, Furst, A., Khong, T. M. and Simpson, C. F.
Chromatographic evaluation of oligomeric C₆ reversed phases for the use in high-performance liquid chromatography 283
- Apps, P. J.
— and Pretorius, V.
Comparison between the conditions for solute focussing by the static and dynamic solvent effects under ideal conditions 81
- Asano, T., see Takeuchi, T. 297
- Audunsson, A., see Nilvé, G. 151
- Bartle, K. D.
—, Boddington, T., Clifford, A. A., and Shilstone, G. F.
Effect of pressure drop across the column on average densities and capacity factors in supercritical fluid chromatography 347
- Bertsch, W., see Green, L. S. 113
- Betz, W. R.
— and Supina, W. R.
Determination of the gas chromatographic performance characteristics of several graphitized carbon blacks 105
- Bighi, C., see Pietrogrande, M. C. 407
- Boddington, T., see Bartle, K. D. 347
- Boesten, W. H. J., see Duchateau, A. 263
- Borea, P. A., see Pietrogrande, M. C. 407
- Brinkman, U. A. Th., see Lipschitz, C. 321
- Bruin, G. J. M.
—, Chang, J. P., Kuhlman, R. H., Zegers, K., Kraak, J. C. and Poppe, H.
Capillary zone electrophoretic separations of proteins in polyethylene glycol-modified capillaries 429
- Chang, J. P., see Bruin, G. J. M. 429
- Clifford, A. A.
Theory of open-tube chromatography: an exact proof of Golay's equations 61
—, see Bartle, K. D. 347
- Crombach, M., see Duchateau, A. 263
- Damme, G., Van, see Verzele, M. 335
- De Jong, G. J., see Lipschitz, C. 321
- Dimov, N.
—, and Mekenyan, Ov.
Quantitative relationships between the structure of alkylbenzenes and their gas chromatographic retention on stationary phases with different polarity 227
- Dondi, F., see Pietrogrande, M. C. 407
- Drawert, F., see Nitz, S. 173
- Duchateau, A.
—, Crombach, M., Kamphuis, J., Boesten, W. H. J., Schoemaker, H. E. and Meijer, E. M.
Determination of the enantiomers of α -H- α -amino acids, α -alkyl- α -amino acids and the corresponding acid amides by high-performance liquid chromatography 263
- Engewald, W., see Maurer, T. 245
- Evans, M. B.
— and Haken, J. K.
Dispersion and selectivity indices in gas chromatography. Part II. Studies of homologous carbonyl and carboxyl compounds 217
- Farkaš, P.,
—, Soják, L., Kováč, M. and Janák, J.
Interface adsorption and reproducibility of retention indices in glass capillary columns with dimethylpolysiloxane stationary phases cross-linked by γ -irradiation 251
- Feltl, L., see Kohoutová, A. 139
- Fernández-Díaz, M., see García-Raso, A. 205
- Finney, R. W.
— and Read, F.
Laser microprobe mass spectrometry of selected compounds directly from normal phase high-performance thin-layer plates 389
- Frei, R. W., see Lipschitz, C. 321
- Furst, A., see Akapo, S. O. 283
- García-Raso, A.
—, Fernández-Díaz, M. Páez, M. I., Sanz, J. and Martínez-Castro, I.
Gas chromatographic retention of carbohydrate trimethylsilyl ethers. III. Keto-hexoses 205
- Gehrke, C. W.
— and Guo, C. K.
Ribonucleoside analysis by reversed-phase high-performance liquid chromatography 3
- Green, L. S.
— and Bertsch, W.
Characteristics of glass based packings as a support in chromatography 113

- Grob, K.
 —, Lanfranchi, M. and Mariani, C.
 Determination of free and esterified sterols and wax esters in oils and fats by coupled liquid chromatography-gas chromatography 397
- Grushka, E.
 — and McCormick, R. M.
 Zone broadening due to sample injection in capillary zone electrophoresis 421
- Guha, O. K.
 On some nomenclature in chromatography 448
- Guo, C. K., see Gehrke, C. W. 3
- Haken, J. K., see Evans, M. B. 217
- Heybey, J., see Mohnke, M. 37
- Horká, M., see Janák, K. 237
- Ioffe, B. V., see Vitenberg, A. G. 55
- Irth, H., see Lipschitz, C. 321
- Ishii, D., see Takeuchi, T. 297
- Janák, J., see Farkaš, P. 251
- Janák, K.
 —, Horká, M. and Tesařík, K.
 Effect of repeated cross-linking of SE-54 stationary phase film on the chromatographic properties of capillary columns 237
- Janeček, M.
 — and Šlais, K.
 Simultaneous photometric and conductivity detection for microcolumn liquid chromatography 303
- Jönsson, J. Å., see Nilvé, G. 151
- Jong, G. J. de, see Lipschitz, C. 321
- Kamphuis, J., see Duchateau, A. 263
- Katsanos, N. A.
 — and Vassilakos, Ch.
 New method for measuring obstructive factors and porosity using gas chromatographic instrumentation 123
- Kersten, B. R., see Poole, S. K. 91
- Khong, T. M., see Akapo, S. O. 283
- Kohoutová, A.
 —, Smolková-Keulemansová, E. and Feltl, L.
 Use of gas chromatography for a study of crown ethers 139
- Kollmannsberger, H., see Nitz, S. 173
- Kováč, M., see Farkaš, P. 251
- Kraak, K., see Bruin, G. J. M. 429
- Kuhlman, R. H., see Bruin, G. J. M. 429
- Kuksis, A., see Myher, J. J. 187
- Lanfranchi, M., see Grob, K. 397
- Lipschitz, C.
 —, Irth, H., De Jong, G. J., Brinkman, U. A. Th. and Frei, R. W.
 Trace enrichment of pyrimidine nucleobases, 5-fluorouracil and bromacil on a silver-loaded thiol stationary phase with on-line reversed-phase high-performance liquid chromatography 321
- Lochmüller, C. H.
 — and Mink, L. P.
 Adsorption isotherms on silica for methanol and 1-hexanol modifiers from supercritical carbon dioxide 357
- Lyne, P. M.
 — and Philips, C. S. G.
 Isomerization of propyne to propadiene. Studies by gas chromatography 145
- McCormick, R. M., see Grushka, E. 421
- McCune, J. E., see Pirkle, W. H. 271
- Mariani, C., see Grob, K. 397
- Martínez-Castro, I., see García-Raso, A. 205
- Martire, D. E.
 Application of a unified molecular theory to gas-liquid chromatography 71
- Maurer, T.
 —, Welsch, Th., and Engewald, W.
 Non-linearity of the plot of log(adjusted retention time) versus carbon number for *n*-alkanes in series-coupled gas chromatographic columns 245
- Meijer, E. M., see Duchateau, A. 263
- Mekenyan, Ov., see Dimov, N. 227
- Mincovic, E., see Tyihák, E. 375
- Mink, L. P., see Lochmüller, C. H. 357
- Mohnke, M.
 — and Heybey, J.
 Gas-solid chromatography on open-tubular columns: an isotope effect 37
- Mori, S.
 Aqueous size-exclusion chromatography of anionic and non-anionic water-soluble polymers on silica gel with bonded hydrophilic groups 367
- Myher, J. J.
 — and Kuksis, A.
 Reative gas-liquid chromatographic retention factors of trimethylsilyl ethers of diradylglycerols on polar capillary columns 187
- Nilvé, G.
 —, Audunsson, A. and Jönsson, J. Å.
 Sample preparation by means of a supported liquid membrane for the determination of chlorophenoxyalkanoic acids 151

- Nitz, S.
—, Kollmannsberger, H. and Drawert, F.
Determination of sensorial active trace compounds by multi-dimensional gas chromatography combined with different enrichment techniques 173
- Noda, H., see Tsuda, T. 311
- Onuska, F.
— and Terry, K. A.
Quantitative high-resolution gas chromatography and mass spectrometry of toxaphene residues in fish 161
- Páez, M. I., see García-Raso, A. 205
- Phillips, C. S. G., see Lyne, P. M. 145
- Pietrogrande, M. C.
—, Dondi, F., Borea, P. A. and Bigli, C.
Retention behaviour of β -carbolines in normal-phase chromatography. Silica and amino phases in high-performance and thin-layer chromatography 407
- Pirkle, W. H.
— and McCune, J. E.
Improved chiral stationary phase for the separation of the enantiomers of chiral acids as their anilide derivatives 271
- Poole, C. F., see Poole, S. K. 91
- Poole, S. K.
—, Kersten, B. R. and Poole, C. F.
Comparison of solvent models for characterizing stationary phase selectivity in gas chromatography 91
- Poppe, H., see Bruin, G. J. M. 429
- Pretorius, V., see Apps, P. J. 81
- Read, F., see Finney, R. W. 389
- Roberts, D. W.
—, Ruane, R. J. and Wilson, I. D.
Picolinic acid: a mobile phase additive for improved chromatography of metal-chelating heterocyclic acids and β -diketones 437
- Ruane, R. J., see Roberts, D. W. 437
- Sanz, J., see García-Raso, A. 205
- Schoemaker, H. E., see Duchateau, A. 263
- Schuddink, G., see Verzele, M. 335
- Shilstone, G. F., see Bartle, K. D. 347
- Šlais, K., see Janeček, M. 303
- Smith, J., see Ahuja, S. 443
- Smolková-Keulemansová, E., see Kohoutová, A. 139
- Soják, L., see Farkaš, P. 251
- Supina, W. R., see Betz, W. R. 105
- Székely, T. J., see Tyihák, E. 375
- Takeuchi, T.
—, Asano, T. and Ishii, D.
Mass detection limits achieved with a commercially available fluorimeter in micro high-performance liquid chromatography 297
- Terry, K. A., see Onuska, F. 161
- Tesařík, K., see Janák, K. 237
- Thompson, G., see Ahuja, S. 443
- Tsuda, T.
— and Noda, H.
Effects of the position of the laser beam focal point on a capillary flow-through cell on the signal-to-noise ratio for a fluorimetric detector in capillary column liquid chromatography 311
- Tyihák, E.
—, Mincovic, E. and Székely, T. J.
Overpressured multi-layer chromatography 375
- Van Damme, G., see Verzele, M. 335
- Vassilakos, Ch., see Katsanos, N. A. 123
- Verzele, M.
—, Van Damme, G., Schuddink, G. and Vyncke, P.
Quantitative microscale liquid chromatography of piperine in pepper and pepper extracts 335
- Vitenberg, A. G.
— and Ioffe, B. V.
Basic equations in continuous gas extraction and their application to headspace analysis 55
- Vyncke, P., see Verzele, M. 335
- Welsch, Th., see Maurer, T. 245
- Wilson, I. D., see Roberts, D. W. 437
- Zegers, K., see Bruin, G. J. M. 429



ANATECH '90

Second International Symposium on Applications of Analytical Techniques to Industrial Process Control

Noordwijkerhout, The Netherlands,
3-5 April 1990

SCOPE OF THE SYMPOSIUM

The importance of analytical techniques for the control of industrial processes is continuously increasing. The development of chemical types of process analysers from laboratory instruments to on-line/in-line measuring devices requires the cooperation of analytical chemists as well as process and system engineers. Like its predecessor, this second symposium is aimed at an interdisciplinary audience of analytical chemists with an academic or industrial background, and those involved in process analytical chemistry and process control. The organisation of the scientific sessions, as well as the congress facilities, will ensure that participants are given the opportunity for the exchange of views in conducive working surroundings.

Speakers will focus on recent developments in analytical techniques and applications in process control. Particular attention will be paid to sampling problems, sample preparation, in-line and on-line measurements and remote sensing. The scientific programme will comprise invited as well as submitted papers (oral and posters). Time will also be reserved for roundtable discussion sessions on selected topics. The official language of the symposium will be English.

LOCATION

The symposium will be held at the Leeuwenhorst Congress Centre in Noordwijkerhout, The Netherlands. This centre, which is quietly situated between flowering bulb fields and the dunes, is approximately 25 km from Amsterdam and Schiphol Airport, and 20 km from The Hague. The congress centre is within walking distance of the sea. Participants will be accommodated in the centre.

For further information contact:

Symposium Secretariat ANATECH '90

Professor W.E. van der Linden,
Laboratory for Chemical Analysis-CT,
Twente University of Technology
P.O. Box 217, NL-7500 AE Enschede, The Netherlands
Telephone: (053) 892629. Fax: (053) 356024

Do you have access to...

CARBOHYDRATE RESEARCH

An International Journal

Editors: L. Anderson, *Madison, WI, USA*
D.C. Baker, *Tuscaloosa, AL, USA*
A.B. Foster, *London, UK*
D. Horton, *Columbus, OH, USA*
R.W. Jeanloz, *Charlestown, MA, USA*
J.M. Webber, *Birmingham, UK*

Since its inception in 1965, *Carbohydrate Research* has gained a reputation for its high standard and wide scope which includes all aspects of carbohydrate chemistry and biochemistry. Articles published in the journal cover sugars and their derivatives (also cyclitols, and model compounds for carbohydrate reactions), oligo- and polysaccharides, nucleosides, nucleotides, and glycoconjugates. These systems are considered from the viewpoints of:

- * **chemical synthesis**
- * **the study of structures and stereochemistry**
- * **reactions and their mechanism**
- * **isolation of natural products**
- * **physicochemical studies**
- * **macromolecular dynamics**
- * **analytical chemistry**
- * **biochemistry (biosynthesis, metabolism, degradation, etc.)**
- * **action of enzymes**
- * **immunochemistry**
- * **technological aspects.**

The journal publishes normal-length research papers, notes, preliminary communications and book reviews together with notices of meetings concerned with carbohydrates.

Subscription Information

1989: Vols. 185-197 (26 issues); US\$ 1592.50 / Dfl. 3185.00 incl. postage
ISSN 0008-6215

If your library does not yet receive this journal, ask for a free sample copy now!



For details of other Elsevier journals, write to:

ELSEVIER SCIENCE PUBLISHERS

P.O. Box 211, 1000 AE Amsterdam, The Netherlands

P.O. Box 882, Madison Square Station, New York, NY 10159, USA

PUBLICATION SCHEDULE FOR 1989

Journal of Chromatography and Journal of Chromatography, Biomedical Applications

MONTH	J	F	M	A	M	J	J	A	S	O	N	D
Journal of Chromatography	461 462 463/1	463/2 464/1	464/2 465/1 465/2	466 467/1 467/2	468 469 470/1 470/2	471 472/1 472/2 473/1	The publication schedule for further issues will be published later					
Bibliography Section		486/1		486/2		486/3		486/4				
Biomedical Applications	487/1	487/2	488/1 488/2	489/1 489/2	490/1 490/2	491/1	491/2	492/1	492/2 493			

INFORMATION FOR AUTHORS

(Detailed *Instructions to Authors* were published in Vol. 445, pp. 453–456. A free reprint can be obtained by application to the publisher, Elsevier Science Publishers B.V., P.O. Box 330, 1000 AH Amsterdam, The Netherlands.)

Types of Contributions. The following types of papers are published in the *Journal of Chromatography* and the section on *Biomedical Applications*: Regular research papers (Full-length papers), Notes, Review articles and Letters to the Editor. Notes are usually descriptions of short investigations and reflect the same quality of research as Full-length papers, but should preferably not exceed six printed pages. Letters to the Editor can comment on (parts of) previously published articles, or they can report minor technical improvements of previously published procedures; they should preferably not exceed two printed pages. For review articles, see inside front cover under Submission of Papers.

Submission. Every paper must be accompanied by a letter from the senior author, stating that he is submitting the paper for publication in the *Journal of Chromatography*. Please do not send a letter signed by the director of the institute or the professor unless he is one of the authors.

Manuscripts. Manuscripts should be typed in double spacing on consecutively numbered pages of uniform size. The manuscript should be preceded by a sheet of manuscript paper carrying the title of the paper and the name and full postal address of the person to whom the proofs are to be sent. Authors of papers in French or German are requested to supply an English translation of the title of the paper. As a rule, papers should be divided into sections, headed by a caption (*e.g.*, Summary, Introduction, Experimental, Results, Discussion, etc.). All illustrations, photographs, tables, etc., should be on separate sheets.

Introduction. Every paper must have a concise introduction mentioning what has been done before on the topic described, and stating clearly what is new in the paper now submitted.

Summary. Full-length papers and Review articles should have a summary of 50–100 words which clearly and briefly indicates what is new, different and significant. In the case of French or German articles an additional summary in English, headed by an English translation of the title, should also be provided. (Notes and Letters to the Editor are published without a summary.)

Illustrations. The figures should be submitted in a form suitable for reproduction, drawn in Indian ink on drawing or tracing paper. Each illustration should have a legend, all the *legends* being typed (with double spacing) together on a *separate sheet*. If structures are given in the text, the original drawings should be supplied. Coloured illustrations are reproduced at the author's expense, the cost being determined by the number of pages and by the number of colours needed. The written permission of the author and publisher must be obtained for the use of any figure already published. Its source must be indicated in the legend.

References. References should be numbered in the order in which they are cited in the text, and listed in numerical sequence on a separate sheet at the end of the article. Please check a recent issue for the layout of the reference list. Abbreviations for the titles of journals should follow the system used by *Chemical Abstracts*. Articles not yet published should be given as "in press" (journal should be specified), "submitted for publication" (journal should be specified), "in preparation" or "personal communication".

Dispatch. Before sending the manuscript to the Editor please check that the envelope contains three copies of the paper complete with references, legends and figures. One of the sets of figures must be the originals suitable for direct reproduction. Please also ensure that permission to publish has been obtained from your institute.

Proofs. One set of proofs will be sent to the author to be carefully checked for printer's errors. Corrections must be restricted to instances in which the proof is at variance with the manuscript. "Extra corrections" will be inserted at the author's expense.

Reprints. Fifty reprints of Full-length papers, Notes and Letters to the Editor will be supplied free of charge. Additional reprints can be ordered by the authors. An order form containing price quotations will be sent to the authors together with the proofs of their article.

Advertisements. Advertisement rates are available from the publisher on request. The Editors of the journal accept no responsibility for the contents of the advertisements.

Eight Books for the Professional

ANALYTICAL ARTIFACTS: GC, MS, HPLC, TLC and PC by B.S. Middleditch

(Journal of Chromatography Library, 44)

An easy-to-use, encyclopaedic catalogue of the pitfalls and problems encountered by analysts when using various common analytical techniques. Emphasis is on impurities, by-products, contaminants and other artifacts and more than 1100 entries are included. The book is designed to be used. It is destined to spend more time on the workbench than on the library shelf.

1989 1058 pages US\$ 260.50 / Dfl. 495.00
0-444-87158-6

EXPERIMENTAL DESIGN: A Chemometric Approach

by S.N. Deming and S.L. Morgan

(Data Handling in Science and Technology, 3)

Now also in paperback, this is "an excellent addition to the collection of every analytical chemist. I recommend it with great enthusiasm. Deming and Morgan should be given high praise for bringing the principles of experimental design to the level of the practicing analytical chemist.. an exceptionally lucid, easy-to-read presentation." (Analytical Chemistry).

1987 1st repr. 1988 300 pages
US\$ 118.50 / Dfl. 225.00 0-444-42734-1
Paperback: US\$ 65.75 / Dfl. 125.00
0-444-43032-6

OPTIMIZATION OF CHROMATOGRAPHIC SELECTIVITY: A Guide to Method Development

by P.J. Schoenmakers

(Journal of Chromatography Library, 35)

"...an important contribution by a worker who has been in the field almost from its inception and who understands that field as well as anyone. If one is serious about method development, particularly for HPLC, this book will well reward a careful reading and will continue to be useful for reference purposes." (LC-GC, Mag. Liquid and Gas Chromatography)

1986 1st repr. 1988 362 pages
US\$ 113.25 / Dfl. 215.00; 0-444-42681-7

CHEMOMETRICS: A Textbook

by D.L. Massart, B.G.M. Vandeginste, S.N. Deming, Y. Michotte and L. Kaufman

(Data Handling in Science and Technology, 2)

"... the book is the most comprehensive available on chemometrics. Beginners and those more familiar with the field will find it a great benefit... will be the standard text on the subject for some time." (Trends in Analytical Chemistry)

1988 500 pages US\$ 92.00 / Dfl. 175.00
0-444-42660-4

ADVANCED SCIENTIFIC COMPUTING IN BASIC WITH APPLICATIONS IN CHEMISTRY, BIOLOGY AND PHARMACOLOGY

by P. Valkó and S. Vajda

(Data Handling in Science and Technology, 4)

A practical introduction to numerical methods with BASIC subroutines for real-life computations in chemistry, biology, and pharmacology. The authors show how to extract useful information from measurements via modelling, simulation, and statistical data evaluations. The subroutines given in the book are also available on a diskette.

1989 340 pages US\$ 100.00 / Dfl. 190.00
0-444-87270-1
5.25" Diskette: US\$ 58.00 / Dfl. 110.00
0-444-87271-X

FOURIER TRANSFORMS IN NMR, OPTICAL, AND MASS SPECTROMETRY: A User's Handbook

by A.G. Marshall and F.R. Verdun

"...a useful user's handbook and an excellent textbook for students performing research in one of the various types of FT spectroscopy." (N.M.M. Nibbering)

1989 ca. 420 pages US\$ 115.75 / Dfl. 220.00
0-444-87360-0
Paperback: US\$ 49.95 / Dfl. 95.00*
0-444-87412-7

INTRODUCTION TO INDUCTIVELY COUPLED PLASMA ATOMIC EMISSION SPECTROMETRY

by G.L. Moore

(Analytical Spectroscopy Library, 3)

Today, atomic emission spectroscopy is a well-established technique with widespread application which no-one involved in chemical analysis can afford to ignore. This book provides a much-needed introduction to the analytical techniques of atomic emission spectroscopy, outlining the principles, history and applications.

Written in an easy-to-understand way, it will be invaluable for tertiary-level students and for newcomers to the field.

1989 352 pages US\$ 100.00 / Dfl. 190.00
0-444-43029-6

QUANTITATIVE GAS CHROMATOGRAPHY for laboratory analyses and on-line process control

by G. Guiochon and C.L. Guillemin

(Journal of Chromatography Library, 42)

This is a book which no chemical analyst should be without! It explains how quantitative gas chromatography can – or should – be used for accurate and precise analysis. All the problems involved in the achievement of quantitative analysis by GC are covered, whether in the research laboratory, the routine analysis laboratory or in process control. The theory is kept to essentials and presented in a way simple enough to be understood by all analytical chemists, while being complete and up-to-date. A book which should be in the library of universities, instrument companies and any laboratory or plant where gas chromatography is used.

1988 780 pages US\$ 165.75 / Dfl. 315.00
0-444-42857-7

For full details on these
books, write to



Elsevier Science Publishers

P.O. Box 211, 1000 AE Amsterdam, The Netherlands
P.O. Box 882, Madison Square Station, New York,
NY 10159, USA